

TECHNICAL REPORT



PROJECTIONS FOR AUSTRALIA'S NRM REGIONS



Australian Government
Department of the Environment
Bureau of Meteorology

-20° -10° 0° 10° 20° 30° 40° 50°



MACDONNELL RANGES, NORTHERN TERRITORY, ISTOCK

-20° -10° 0° 10° 20° 30° 40° 50°



TECHNICAL REPORT



PROJECTIONS FOR AUSTRALIA'S NRM REGIONS

-20° -10° 0° 10° 20° 30° 40° 50°

© CSIRO 2015

**CLIMATE CHANGE IN AUSTRALIA
TECHNICAL REPORT**

BIBLIOGRAPHY
ISBN 9781921232947 (PDF)

CONTACTS
E: enquiries@csiro.au
T: 1300 363 400

ACKNOWLEDGEMENTS

This scientific assessment and new research has been funded by the Australian Government Department of the Environment, the Commonwealth Scientific and Industrial Research Organisation and the Australian Bureau of Meteorology. The work has benefited from a high degree of cooperation between these agencies and the project stakeholders.

LEAD SCIENTIST AND EDITOR

Penny Whetton

EDITORS

Marie Ekström, Chris Gerbing, Michael Grose, Jonas Bhend, Leanne Webb and James Risbey.

CHAPTER AUTHORS

- CHAPTER 1** Penny Whetton, Paul Holper
- CHAPTER 2** John Clarke, Leanne Webb, and Kevin Hennessy
- CHAPTER 3** Rob Colman, Aurel Moise, Scott Power, Karl Braganza and Ian Watterson
- CHAPTER 4** Karl Braganza, Brad Murphy, Bertrand Timbal, Pandora Hope, Andrew Dowdy, Kevin Hennessy, Jonas Bhend and Dewi Kirono
- CHAPTER 5** Aurel Moise, Jonas Bhend, Ian Watterson and Louise Wilson
- CHAPTER 6** Jonas Bhend, Ian Watterson, Michael Grose, Marie Ekström and Penny Whetton
- CHAPTER 7**
- 7.1 Ian Watterson, Tony Rafter, Louise Wilson, Jonas Bhend and Craig Heady
- 7.2 Penny Whetton, Aurel Moise, Dewi Kirono, Tony Rafter, Louise Wilson, Kevin Hennessy, Jonas Bhend, Pandora Hope, Bertrand Timbal, Andrew Dowdy, Ian Watterson, Michael Grose, Sugata Narsey and Janice Bathols
- 7.3 Kathy McInnes, Aurel Moise, Debbie Abbs, Bertrand Timbal, Pandora Hope, Andrew Dowdy and Louise Wilson
- 7.4, 7.5 & 7.6 Dewi Kirono and Louise Wilson

7.7 Freddie Mpelasoka, Francis Chiew, Ian Watterson, Jonas Bhend and Louise Wilson

7.8 Chris Lucas

CHAPTER 8

Kathy McInnes, Didier Monselesan, John Church, Andrew Lenton and Julian O'Grady

CHAPTER 9

Kevin Hennessy, Leanne Webb and John Clarke

CHAPTER 10

Paul Holper and Penny Whetton

APPENDIX A

Ian Watterson

PROJECTIONS ANALYSIS SUPPORT

Janice Bathols, Tim Bedin, Tim Erwin, Craig Heady, Yun Li and Louise Wilson

PROJECT COORDINATION

Paul Holper, Kevin Hennessy, Carol Grossman and Mandy Hopkins

PEER REVIEW

David Karoly (University of Melbourne), Andrew Tait (National Institute of Water and Atmospheric Research, New Zealand) and Michael Hutchinson (Australian National University)

DESIGN AND LAYOUT

Alicia Annable, Liz Butler and Siobhan Duffy

EDITORIAL SUPPORT

Stephanie Baldwin

We acknowledge the World Climate Research Programme's Working Group on Coupled Modelling, which is responsible for CMIP, and we thank the climate modelling groups (listed in Table 5.2.2 of this Report) for producing and making available their model output. For CMIP, the U.S. Department of Energy's Program for Climate Model Diagnosis and Intercomparison provides coordinating support and leads development of software infrastructure in partnership with the Global Organization for Earth System Science Portals.

CITATION

CSIRO and Bureau of Meteorology 2015, Climate Change in Australia Information for Australia's Natural Resource Management Regions: Technical Report, CSIRO and Bureau of Meteorology, Australia

DISCLAIMER

No responsibility will be accepted by CSIRO or the Bureau of Meteorology for the accuracy of the projections in or inferred from this Report, or for any person's reliance on, or interpretations, deductions, conclusions or actions in reliance on, this Report or any information contained in it.

TABLE OF CONTENTS

EXECUTIVE SUMMARY.....	5
CHAPTER 1 INTRODUCTION.....	11
CHAPTER 2 USER NEEDS AND REGIONALISATION	14
2.1 Assessing user needs.....	14
2.2 Meeting user needs.....	15
2.3 Sub-dividing Australia.....	16
CHAPTER 3 GLOBAL CLIMATE CHANGE SCIENCE	23
3.1 Factors driving climate variability and change.....	23
3.1.1 Internal (“unforced”) climate variability.....	23
3.1.2 External forcing factors	24
3.2 Emissions scenarios and climate models.....	25
3.2.1 Future scenarios of greenhouse gas concentrations	25
3.2.2 Global climate models	27
3.3 Introduction to climate model ensembles and to the CMIP5 ensemble.....	28
3.3.1 The Coupled Model Intercomparison Project Phase 5 (CMIP5).....	28
3.4 Observed global trends and their attribution.....	32
3.5 Global climate change projections	34
3.6 Comparison of CMIP3 and CMIP5 global projections.....	36
3.6.1 Global sensitivity of the CMIP3 and CMIP5 models.....	36
3.6.2 Model responses to global warming in the Asia-Pacific region.....	37
CHAPTER 4 UNDERSTANDING RECENT AUSTRALIAN CLIMATE	40
4.1 Australian climate variability	40
4.1.1 Tropical modes	40
4.1.2 Extra-tropical modes	41
4.2 Observed trends and attribution in the Australian region.....	42
4.2.1 Temperature	42
4.2.2 Rainfall.....	43
4.2.3 Changes in circulation in the Australian region and their possible association with rainfall trends	46
4.2.4 Drought.....	48
4.2.5 Snow	49
4.2.6 Surface winds over continental Australia.....	49

4.2.7	Tropical cyclones	49
4.2.8	East coast lows	49
4.2.9	Solar radiation	50
4.2.10	Surface humidity	50
4.2.11	Pan evaporation	50
4.2.12	Fire weather	51
CHAPTER 5 EVALUATION OF CLIMATE MODELS		53
5.1	Introduction	53
5.2	Evaluation based on climatological characteristics	53
5.2.1	Assessment of historical mean climatologies: temperature, rainfall and mean sea level pressure	54
5.2.2	Assessment of spatial structure of historical mean climatologies: M-scores for rainfall and temperature	59
5.2.3	Assessment of annual cycles of historical climate: rainfall and temperature	61
5.2.4	Assessment of additional climate features and associated skill scores	63
5.3	Evaluation of simulated rainfall and temperature trends	70
5.4	Evaluation of extremes in climate models	72
5.5	Evaluation of downscaling simulations	73
5.6	Synthesis of model evaluation	74
CHAPTER 6 CLIMATE CHANGE PROJECTION METHODS		78
6.1	Limitations and uncertainties in climate change data	78
6.1.1	Sources of uncertainty	78
6.1.2	Interpretation of ranges of change in projections	79
6.2	Regional projection methods	80
6.2.1	Overview and comparison of existing regional projection methods	80
6.2.2	Projection methods used in this Report	82
6.2.3	Comparison with climate change in Australia 2007	83
6.3	Downscaling	85
6.3.1	What is downscaling?	85
6.3.2	Combining insights from downscaling and GCM projections	86
6.3.3	Statistical and dynamic downscaling methods used	87
6.3.4	Pros and cons of statistical and dynamical downscaling	87
6.3.5	Areas of greatest potential added value	87
6.3.6	Availability	88
6.4	Assessing confidence in projections	88

CHAPTER 7 PROJECTIONS: ATMOSPHERE AND THE LAND	91
7.1 Surface temperature	91
7.1.1 Average temperature	91
7.1.2 Extreme temperature	95
7.2 Rainfall	99
7.2.1 Projected mean rainfall change	99
7.2.2 Projected extreme rainfall change	118
7.2.3 Drought	119
7.2.4 Snow	123
7.3 Winds, storms and weather systems	125
7.3.1 Mean and extreme winds	125
7.3.2 Synoptic systems	129
7.4 Solar Radiation	131
7.5 Humidity	133
7.6 Potential evapotranspiration	134
7.7 Soil Moisture and runoff	136
7.7.1 Projected changes in soil moisture	136
7.7.2 Projected changes in runoff	137
7.8 Fire weather	139
CHAPTER 8 PROJECTIONS (AND RECENT TRENDS): MARINE AND COASTS	143
8.1 Sea level rise	143
8.1.1 Factors contributing to sea level change	143
8.1.2 Historical global mean sea level change	143
8.1.3 The Australian coastline	144
8.1.4 Global projections	146
8.1.5 Regional projections for Australia for the 21st century	148
8.1.6 Caveats	152
8.1.7 Beyond 2100	153
8.2 Extreme sea levels	153
8.3 Sea surface temperature	157
8.4 Sea surface salinity	160
8.5 Ocean acidification	162

CHAPTER 9 USING CLIMATE CHANGE DATA IN IMPACT ASSESSMENT AND ADAPTATION PLANNING.	167
9.1 Introduction	167
9.2 Conducting a climate change impact assessment.	168
9.2.1 Establishing the context.	168
9.2.2 Risk identification.	168
9.2.3 Risk analysis.	169
9.2.4 Risk evaluation and risk treatment	175
9.3 Information products for risk identification and analysis	175
9.3.1 Climate change in Australia website	175
9.3.2 Decision tree	175
9.3.3 Report-ready projected change information	177
9.3.4 Climate data	177
9.3.5 Climate analogue tool	183
9.3.6 Links to other projects	183
CHAPTER 10 RESEARCH DIRECTIONS	186
10.1 Understanding climatic variability and monitoring change	186
10.2 New climate model ensembles.	187
10.3 Targeted projection products and communication	187
10.4 Conclusions	187
APPENDIX A COMPARISON OF CMIP3 AND CMIP5 CHANGES OVER AUSTRALIA	188
REFERENCES.	192
NRM GLOSSARY OF TERMS	212
GLOSSARY REFERENCES	216

EXECUTIVE SUMMARY

INTRODUCTION

This Report provides an assessment of observed climate change in Australia and its causes, and details projected future changes over the 21st century. This document, produced by CSIRO and the Australian Bureau of Meteorology, underpins extensive climate change projections for Australia provided as part of a larger package of products developed with funding from the Commonwealth Government's Regional Natural Resource Management (NRM) Planning for Climate Change Fund.

The projections are based on our understanding of the climate system, historical trends and model simulations of the climate response to global scenarios of greenhouse gas and aerosol emissions. Simulations come from the archive of global climate models (GCMs) developed by modelling groups from around the world through the Coupled Model Intercomparison Project phase 5 (CMIP5) which also underpins the science of the *Fifth Assessment Report* of the Intergovernmental Panel on Climate Change (IPCC).

These projections supersede those released by CSIRO and the Bureau of Meteorology in 2007. Although the findings are similar to those of the 2007 projections, note that these and the 2007 projections are not always directly comparable due to different baselines, emissions scenarios and periods of consideration.

Extensive engagement with users has led to the production of a range of communication tools that support the projections, including guidance material, regional information, animations, webinars, a video and a web site at www.climatechangeinaustralia.gov.au.

Projected changes have been prepared for four Representative Concentration Pathways (RCPs) used by the latest IPCC assessment, which represent different scenarios of emissions of greenhouse gases, aerosols and land-use change. These RCPs include RCP2.6, requiring very strong emission reductions from a peak at around 2020 to reach a carbon dioxide (CO₂) concentration at about 420 parts per million (ppm) by 2100, RCP4.5 with slower emission reductions that stabilise the CO₂ concentration at about 540 ppm by 2100, and RCP8.5 which assumes increases in emissions leading to a CO₂ concentration of about 940 ppm by 2100 (Section 3.2). This range of emissions scenarios is broader than those used for the 2007 projections.

Climate change projections are presented for eight regions (some further sub-divided) covering the entire nation (Section 2.3, Box 2.1).

Confidence ratings for the projections are based on the judgement of the authors derived from multiple lines of evidence. These include physical theory and understanding of processes driving the change, agreement amongst climate model simulations of the future, model evaluation both with respect to current mean climate and recent observed climate change, and consistency of global climate model results with downscaled, high-resolution simulations (Section 6.4).

GLOBAL CHANGES

Global mean near-surface air temperature has risen by around 0.85 °C from 1880 to 2012 and at 0.12 °C per decade since 1951 (Section 3.4 and IPCC). The IPCC (2013) concluded, "It is extremely likely that human influence has been the dominant cause of the observed warming since the mid-20th century" and "Human influence has been detected in warming of the atmosphere and the ocean, in changes in the global water cycle, in reductions in snow and ice, in global mean sea level rise, and in changes in some climate extremes." Natural forcings (e.g. solar variations and volcanic aerosols) and intrinsic climate variability have had little effect on the warming since 1951 (Section 3.4 and IPCC).

Global mean temperatures are projected to rise from 0.3-1.7 °C under RCP2.6 to 2.6-4.8 °C under RCP8.5 by 2081-2100, compared to the climate of 1986-2005 (Section 3.5 and IPCC). Warming is projected to be stronger over land than oceans and strongest over the Arctic (Section 3.5 and IPCC). Hot days and heat waves are projected to become more frequent and cold days less frequent (Section 3.5 and IPCC).

Projected changes in rainfall are much less spatially uniform than projected warming. Rainfall is generally projected to increase at high latitudes and near the equator and decrease in regions of the sub-tropics, although regional changes may differ from this pattern (Section 3.5 and IPCC). Rainfall extremes are projected to become more intense and more frequent in most regions (Section 3.5 and IPCC).

Global mean sea level is projected to increase by 26-55 cm for RCP2.6 and 45-82 cm for RCP8.5 by 2080-2100 relative to 1986-2005 (Section 8.1). Global sea level rise is driven mainly by ocean thermal expansion and melting from glaciers and ice caps.

-20° -10° 0° 10° 20° 30° 40° 50°



AUSTRALIAN CLIMATE VARIABILITY AND CHANGE

AUSTRALIA HAS BEEN WARMING AND WILL WARM SUBSTANTIALLY DURING THE 21ST CENTURY

Australian average surface air temperature has increased by 0.9 °C since 1910, and increasing greenhouse gases have contributed to this rise (Section 4.2.1). Climate models are able to reproduce the observed warming over the 20th century (Sections 5.2, 5.3, 7.1.1).

In recent decades anomalously warm months have occurred more often than anomalously cold months (Section 4.2.1). Many heat-related records were broken in the summer of 2012-13 and in the year of 2013, including Australia's hottest day, week, month and year averaged across Australia (Section 4.2.1). Extreme summer temperatures during 2012-13 were unlikely to have been caused by natural variability alone, and such temperatures are now five times more likely due to the enhanced greenhouse effect (Section 4.2.1).

There is *very high confidence* in continued increases of mean, daily minimum and daily maximum temperatures throughout this century for all regions in Australia. This takes into account the observed warming, strong agreement on the direction and magnitude of change among models, downscaling results and the robust understanding of the driving mechanisms of warming (Section 7.1.1). The magnitude of the warming later in the century is strongly dependent on the emission scenario.

Warming will be large compared to natural variability in the near future (2030) (*high confidence*) and very large compared to natural variability late in the century (2090) under RCP8.5 (*very high confidence*). By 2030 (the period 2020-2039), Australian annual average temperature is projected to increase by 0.6-1.3 °C above the climate of 1986-2005 under RCP4.5 with little difference in warming between RCPs (Section 7.1.1). The projected temperature range by 2090 (the period 2080-2099) shows larger differences between RCPs, with increases of 0.6 to 1.7 °C for RCP2.6, 1.4 to 2.7 °C for RCP4.5 and 2.8 to 5.1 °C for RCP8.5 (Section 7.1.1).

Mean warming is projected to be greater than average in inland Australia, and less in coastal areas, particularly in southern coastal areas in winter (Section 7.1.1).

MORE FREQUENT AND HOTTER HOT DAYS AND FEWER FROST DAYS ARE PROJECTED

Since 2001, the number of extreme heat records in Australia has outnumbered extreme cool records by almost 3 to 1 for daytime maximum temperatures and almost 5 to 1 for night-time minimum temperatures (Section 4.2.1). Heat waves have increased in duration, frequency, and intensity in many parts of the country (Section 4.2.1).

Strong model agreement and our understanding of the physical mechanisms of warming mean that there is *very high confidence* the projected warming will result in more frequent and hotter hot days and warmer cold extremes

and *high confidence* in reduced frost. Notably, the projected temperature increase for the hottest day of the year on average and the hottest day in 20 years on average is very similar to the projected increase in mean temperature (Section 7.1.2).

For example, in Perth, the average number of days per year above 35 °C or above 40 °C by 2090 is projected to be 50 % greater than present under median warming for RCP4.5. The number of days above 35 °C in Adelaide also increases by about 50 % by 2090, while the number of days above 40 °C more than doubles (Section 7.1.2).

Locations where frost occurs only a few times a year under current conditions are projected to become nearly frost-free by 2030. Under RCP8.5, coastal areas are projected to be free of frost by 2090 while frost is still projected to occur inland (Section 7.1.2).

MID-LATITUDE WEATHER SYSTEMS ARE PROJECTED TO SHIFT SOUTH IN WINTER AND THE TROPICS TO EXPAND

Observed large-scale circulation changes can be characterised by an expansion of the tropics and a contraction of the mid-latitude storm tracks to higher southern latitudes. Correspondingly, an intensification of the subtropical ridge (the high pressure belt over Australia), an expansion of the Hadley Cell (a circulation in the north-south direction connecting tropical and mid-latitude areas), and a trend to a more positive Southern Annular Mode (a hemispheric mode of variability associated with weaker than normal westerly winds and higher pressures over southern Australia) have all been observed. These changes have been linked to a reduction in rainfall in southern Australia (Section 4.2.3).

The observed intensification of the subtropical ridge and expansion of the Hadley Cell circulation are projected to continue in the 21st century (*high confidence*; Section 7.3.2).

In winter, mid-latitude weather systems are projected to shift south and the westerlies are projected to strengthen (*high confidence*; Section 7.3.2). Concurrent and related changes in the mid-latitude circulation are projected, including a more positive Southern Annular Mode (SAM), a decrease in the number of deep lows affecting south-west Western Australia and a decrease in the number of fronts in southern Australia (Section 7.3.2).

Projected changes to mid-latitude circulation in summer are less clear (Section 7.3.2). There are competing influences, with increasing greenhouse gases leading to a more positive SAM and projected stratospheric ozone recovery leading to a less positive SAM (Section 7.3.2).

Climate models underestimate the observed changes in mid-latitude circulation and southern Australian rainfall (Section 4.2.3). It is unclear whether this is due to natural variability, additional climate influences unaccounted for in the models or due to the models underestimating the true response (Section 4.2.3).



COOL-SEASON RAINFALL IS PROJECTED TO DECLINE IN SOUTHERN AUSTRALIA; OTHER CHANGES TO AVERAGE RAINFALL ARE UNCERTAIN

Australian average rainfall has been increasing since the 1970s, mainly due to an increase in wet season rain in northern Australia (Section 4.2.2). During the cooler months, rainfall has declined in the south-east and south-west of the continent (Section 4.2.2). The rainfall decline in southern Australia has been linked to circulation changes in the southern hemisphere that are influenced by increasing greenhouse gases and reductions in stratospheric ozone (Section 4.2.2).

In southern Australia, cool season (winter and spring) rainfall is projected to decrease (*high confidence*), though increases are projected for Tasmania in winter (*medium confidence*; Section 7.2.1). The cool season rainfall decline is driven by the southward movement of winter storm systems (Section 7.2.1). The winter decline may be as great as 50 % in south-western Australia under RCP8.5 by 2090 (Section 7.2.1). The direction of change in summer and autumn rainfall in southern Australia cannot be reliably projected, but there is *medium confidence* in a decrease in south-western Victoria in autumn and in western Tasmania in summer (Section 7.2.1).

In eastern Australia, there is *high confidence* that in the near future (2030) natural variability will predominate over trends due to greenhouse gas emissions. For late in the century (2090), there is *medium confidence* in a winter rainfall decrease related to the southward movement and weakening of winter storm systems (Section 7.2.1). Otherwise, there is *low confidence* in the direction of seasonal rainfall change due to strongly contrasting results from global climate models and downscaling approaches (Section 7.2.1). The large uncertainty in this region is likely to be related to the range of rainfall drivers and competing influences on rainfall change as well as their relationship to topographical features such as the Great Dividing Range and Eastern Seaboard (Section 7.2.1).

In northern Australia and northern inland areas, there is *high confidence* that in the near future (2030), natural variability will predominate over trends due to greenhouse gas emissions. There is *low confidence* in the direction of future rainfall change by late in the century (2090), but substantial changes to wet-season and annual rainfall cannot be ruled out (Section 7.2.1). Confidence in rainfall projections is low due to the lack of model agreement (Section 7.2.1), and limitations of models in reproducing features of the observed rainfall climate and important drivers of rainfall variability in the region (Section 5.2).

EXTREME RAIN EVENTS ARE PROJECTED TO BECOME MORE INTENSE

Heavy daily rainfall has accounted for an increased proportion of total annual rainfall over an increasing fraction of the Australian continent since the 1970s (Section 4.2.3). Record rainfall totals occurred in many areas during 2010 and 2011, attributable in part to the presence of strong La Niña conditions and higher than average sea surface temperatures to the north of Australia (Section 4.2.2).

Throughout most of Australia, extreme rainfall events (wettest day of the year and wettest day in 20 years) are projected to increase in intensity with *high confidence* due to our understanding of physical mechanisms (increasing moisture-holding capacity of a warmer atmosphere), strong model agreement and a wealth of previous research (Section 7.2.2). However, there is only *medium confidence* in increased rainfall intensity for south-western Western Australia, because of the large projected reduction in mean rainfall in this region (Section 7.2.2).

TIME IN DROUGHT IS PROJECTED TO INCREASE IN SOUTHERN AUSTRALIA, WITH A GREATER FREQUENCY OF SEVERE DROUGHTS

The time in drought, as measured by the Standardised Precipitation Index, is projected to increase over southern Australia with *high confidence* (Section 7.2.3). This is consistent with the projected decline in mean rainfall. Time in drought is projected to increase with *medium or low confidence* in other regions. The nature of droughts is also projected to change, with a greater frequency of extreme droughts, and less frequent moderate to severe drought projected for all regions (*medium confidence*) (Section 7.2.3).

SNOWFALL IN THE AUSTRALIAN ALPS IS PROJECTED TO DECREASE, ESPECIALLY AT LOW ELEVATIONS

Average snow depths have decreased at a number of Australian sites since the 1950s. There is *very high confidence* that as warming progresses there will be a decrease in snowfall, an increase in snowmelt and thus reduced snow cover. These trends will be large compared to natural variability and most evident at low elevations (Section 7.2.4).

SMALL CHANGES IN WIND SPEED

Mean wind speeds are projected to decrease in southern mainland Australia in winter and increase in Tasmania

By 2030, changes in near-surface wind speeds are projected to be small compared to natural variability (*high confidence*). By 2090, wind speeds are projected to decrease in southern mainland Australia in winter (*high confidence*) and south-eastern mainland Australia in autumn and spring. Winter decreases are not expected to exceed 10 % under RCP8.5. Wind speed is projected to increase in winter in Tasmania (Section 7.3.1). Projected changes in extreme wind speeds are generally similar to those for mean wind (Section 7.3.1).



TROPICAL CYCLONES MAY OCCUR LESS OFTEN, BECOME MORE INTENSE, AND MAY REACH FURTHER SOUTH

There is some observational evidence for a decrease in the occurrence of tropical cyclones (Sections 4.2.1, 4.2.7). However, the short period of consistent observational records and high year to year variability make it difficult to discern clear trends in tropical cyclone frequency or intensity (Section 4.2.7).

Based on global and regional studies, tropical cyclones are projected to become less frequent with a greater proportion of high intensity storms (stronger winds and greater rainfall) (*medium confidence*). A greater proportion of storms may reach south of latitude 25 degrees South (*low confidence*; Section 7.3.2).

MORE SUNSHINE IS PROJECTED IN WINTER AND SPRING, WITH LOWER RELATIVE HUMIDITY AND HIGHER EVAPORATION RATES THROUGHOUT THE YEAR

There is *high confidence* in little change in solar radiation over Australia in the near future (2030). Late in the century (2090), there is *medium confidence* in an increase in winter and spring in southern Australia (Section 7.4). The increases in southern Australia may exceed 10 % by 2090 under RCP8.5 (Section 7.4).

Relative humidity is projected to decline in inland regions and where rainfall is projected to decline (Section 7.5). By 2030, the decreases are relatively small (*high confidence*). By 2090, there is *high confidence* that humidity will decrease in winter and spring as well as annually, and there is *medium confidence* in declining relative humidity in summer and autumn (Section 7.5).

There is *high confidence* in increasing potential evapotranspiration (atmospheric moisture demand) closely related to local warming, although there is only *medium confidence* in the magnitude of change (Section 7.6).

SOIL MOISTURE IS PROJECTED TO DECREASE AND FUTURE RUNOFF WILL DECREASE WHERE RAINFALL IS PROJECTED TO DECREASE

Soil moisture and runoff projections are strongly influenced by projected changes in rainfall (Sections 7.7.1, 7.7.2), but tend toward decrease because of projected increases in potential evapotranspiration. Changes in runoff are generally 2-3 times larger than the relevant rainfall change (Section 7.7.2).

There is *high confidence* in decreasing soil moisture in the southern regions (particularly in winter and spring) driven by the projected decrease in rainfall and higher evaporative demand (Section 7.7.1). There is *medium confidence* in decreasing soil moisture elsewhere in Australia where evaporative demand is projected to increase but the direction of rainfall change is uncertain (Section 7.7.1).

Decreases in runoff are projected with *high confidence* only in south-western Western Australia and southern South Australia, and with *medium confidence* in far south-eastern Australia, where future rainfall is projected to decrease. The direction of change in future runoff in the northern half of Australia cannot be reliably projected because of the uncertainty in the direction of rainfall change (Section 7.7.2).

SOUTHERN AND EASTERN AUSTRALIA ARE PROJECTED TO EXPERIENCE HARSHER FIRE WEATHER; CHANGES ELSEWHERE ARE LESS CERTAIN

Extreme fire weather days have increased at 24 out of 38 Australian sites from 1973-2010, due to warmer and drier conditions.

Projected warming and drying in southern and eastern Australia will lead to fuels that are drier and more ready-to-burn, with increases in the average forest fire danger index and a greater number of days with severe fire danger (*high confidence*; Section 7.8).

In northern Australia and inland areas, the primary determinant of bushfires is fuel availability, which depends strongly on year to year rainfall variability (Section 7.8). There is *medium confidence* that there will be little change in fire frequency in tropical and monsoonal northern Australia. There is *low confidence* in projections of fire risk in the arid inland areas where fire risk is dependent on availability of fuel, which is driven by episodic rainfall.

SEA LEVELS WILL CONTINUE TO RISE THROUGHOUT THE 21ST CENTURY AND BEYOND; EXTREME SEA LEVELS WILL ALSO RISE

For 1966 to 2009, the average rate of relative sea level rise from observations along the Australian coast was 1.4 ± 0.2 mm/year, and 1.6 ± 0.2 mm/year when the sea level variations directly correlated with the Southern Oscillation Index (SOI) are removed (Section 8.1.3).

In line with global mean sea level, Australian sea levels are projected to rise through the 21st century (*very high confidence*), and are very likely to rise at a faster rate during the 21st century than over the past four decades, or the 20th century as a whole, for the range of RCPs considered (*high confidence*). Sea level projections for the Australian coastline by 2090 (the average of 2080 to 2100) are comparable to, or slightly larger than (by up to about 6 cm) the global mean sea level projections of 26-55 cm for RCP2.6 and 45-82 cm for RCP8.5 (*medium confidence*; Section 8.1.5). These ranges of sea level rise are considered likely (at least 66 % probability), and if a collapse in the marine based sectors of the Antarctic ice sheet were initiated, the projections could be up to several tenths of a metre higher by late in the century. Regional projections for 2100 (a single year) are not given because of the effect of interannual to decadal variability on regional sea levels. However, for all scenarios, global averaged sea level in 2100 will be higher than in 2090 and sea level is projected to continue to rise beyond 2100.



Taking into account uncertainty in sea level rise projections and the nature of extreme sea levels along the Australian coastline, an indicative extreme sea level ‘allowance’ is calculated. This allowance is the minimum distance required to raise an asset to maintain current frequency of breaches under projected sea level rise. Along the Australian coast, these allowances are comparable to the upper end of the range of the respective sea level projections (*medium confidence*; Section 8.2). The main contribution to increasing extreme sea levels is from the rise in mean sea level (*medium confidence*). Contributions to extreme sea levels from changes in weather events are projected to be small or negative (*low confidence*; Section 8.2).

OCEANS AROUND AUSTRALIA WILL WARM AND BECOME MORE ACIDIC. SALINITY MAY ALSO CHANGE

There is *very high confidence* that sea surface temperatures around Australia will rise, with the magnitude of the warming dependent on the RCP (Section 8.3). Near-coastal sea surface temperature rise around Australia is typically around 0.4-1.0 °C by 2030 and around 2-4 °C by 2090 under RCP8.5 compared to current (1986-2005) (Section 8.3).

Changes in sea surface salinity reflect changes in rainfall (Section 7.2) and may affect ocean circulation and mixing. A net reduction in the salinity of Australian coastal waters is projected, but this projection is of *low confidence* (Section 8.4). For some southern regions, models indicate an increase in sea surface salinity, particularly under higher emissions (Section 8.4).

The oceans are absorbing more than 25 % of current carbon dioxide emissions (Section 8.5). In the oceans, carbon dioxide dissolves and leads to a reduction in carbonate concentration and seawater pH. This is known as ocean acidification (Section 8.5). There is *very high confidence* that around Australia the ocean will become more acidic, with a net reduction in pH (Section 8.5). There is also *high confidence* that the rate of ocean acidification will be proportional to carbon dioxide emissions (Section 8.5). There is *medium confidence* that long-term viability of corals will be impacted under RCP8.5 and RCP4.5, and that there will be harm to marine ecosystems from the projected reduction in pH under RCP8.5 (Section 8.5).

MODEL EVALUATION AND PROJECTION METHODS

The climate models used for making future climate projections were evaluated by examining their simulation of the present climate of the Australian region (Chapter 5). This evaluation contributes to assessment of confidence in model-simulated future climate changes (see Chapter 6, Section 6.4) and to assessment of the adequacy of any model or models for particular applications.

The ability of individual CMIP5 models to simulate Australian climate depends on the climatic variable, region and season under consideration. Observed climate for

broad-scale temperature, rainfall and surface wind is well captured by global climate models, although deficiencies are found in finer details around pronounced topography and coastlines such as in Tasmania or the Cape York Peninsula (Sections 5.2).

Global climate models are also able to reproduce the major climate systems, including sources of year to year variability, which affect Australia. However, there are deficiencies in simulating aspects of the El Niño – Southern Oscillation (ENSO) and its connection to Australian rainfall. Some models also do not simulate monsoon onset well (Section 5.2.4).

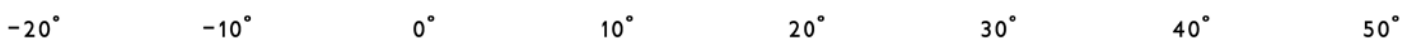
The projections presented here are based on all the available simulations since no subset of climate models was found to perform well across all metrics, and methods that did allow for model performance did not lead to different projection results (Section 6.2). However, information about consistently poorly performing models is used in model selection for some more specific applications (Sections 9.2.3, 9.3.4, Box 9.1).

Projections are presented as ranges of change for different 20-year time periods in the future with respect to the reference period (1986–2005). Generally, the 10th to 90th percentile range of the distribution of CMIP5 global climate model results is used to characterise the projections (Section 6.2.2).

In addition, time series of simulated climate change from 1910 to 2090 against a 1950 to 2005 baseline are shown together with observations to illustrate the interplay of the slowly emerging climate change signal and natural internal variability (Section 6.2.2, Box 6.2.2).

USING CLIMATE CHANGE DATA IN IMPACT ASSESSMENT AND ADAPTATION PLANNING

Climate change data provide an essential input to the impact assessment process (Section 9.2). The framework for impact assessment includes context setting, impact identification and impact analysis, the latter incorporating consideration of planning horizons and relevant climate data input. Methods for generating, presenting and selecting data are described, along with information to help users find data and research tools on the Climate Change in Australia website (Section 9.3). This website includes a decision tree to guide users to the most relevant material; report-ready images and tables; climate change data (described as, for example, a 10 percent decrease in rainfall relative to 1986-2005); and application-ready data (where projected changes have been applied to observed data for use in detailed risk assessments) (Section 9.3.4). Links are also provided to other projects that supply climate change information (Section 9.3.6).



CHAPTER ONE

INTRODUCTION

SUNSET, OUTBACK AUSTRALIA, ISTOCK

-20° -10° 0° 10° 20° 30° 40° 50°

CHAPTER 1 INTRODUCTION

This Technical Report provides an up to date description and assessment of observed climate change in Australia and its causes, and details likely future changes over the 21st century. It provides information for assessing exposure, risks and opportunities that may flow from regional climate change due to global warming.

A range of products have been designed with the end users in mind. There has been extensive stakeholder consultation in order to assess information and data needs and the desired approaches to obtaining these. Hence, this Report is part of a suite of products that includes datasets, regional information, and guidance for users. The Climate Change in Australia website (www.climatechangeinaustralia.gov.au) provides ready access to the wealth of available material.

This Report underpins extensive climate change projections for Australia provided as part of a larger package of products developed with funding from the Commonwealth Government's Regional Natural Resource Management Planning for Climate Change Fund. This fund was established to support regional Natural Resource Management (NRM) organisations to update their plans to account for likely climate change impacts and to maximise the environmental benefits of carbon farming projects. Thus, this Report has a focus on science relevant to planning how best to manage the impact of climate change on Australia's natural resources, and on regional areas more generally.

The scientific context for new climate change projections includes the relevant conclusions of the latest Intergovernmental Panel on Climate Change (IPCC) report, recent climate trends in Australia and their causes, climate model results and regional projection methods. It presents projections for a range of simulated climate variables (*e.g.* temperature, rainfall, wind) and derived variables (*e.g.* indices of climatic extremes, fire weather, soil moisture), and concludes with guidance on a range of issues that arise when using climate projection information.

This Report links strongly to findings of the IPCC *Fifth Assessment Report*, but it provides the detail for Australia that cannot be provided by the IPCC's global perspective. This Report also draws upon relevant research from CSIRO, the Australian Bureau of Meteorology and Australian Universities, including the Australian Climate Change Science Programme. This Programme was undertaken by CSIRO and the Bureau of Meteorology in association with the Department of the Environment.

CSIRO has taken a major role in providing information about regional climate change for Australia over the past two decades. Information products were released in 1992, 1996, 2001 (CSIRO, 1992; 1996; 2001) and jointly with the Bureau of Meteorology in 2007 (CSIRO and BOM, 2007).

The new projections differ from those released in 2007 in a number of important ways:

- They are based on the latest global climate model archive (known as the Coupled Model Intercomparison Project phase 5 (CMIP5)). This contains simulations from more than 40 global climate models, representing the state of the art in climate modelling.
- The role of high resolution downscaling is enhanced.
- Levels of confidence are developed and attached to all key projection statements.
- In addition to providing 10th to 90th percentile ranges of change for most variables, the needs of risk assessment are better supported through the provision of application-ready data sets.

The functionality of the projections for decision-makers and planners has also been improved:

- The *Australian Climate Futures* tool has been developed (and made available online) to further support impact assessments. This tool helps in the development of future climate scenarios appropriate to applications and in the selection of climate model results to populate those scenarios. The tool also provides much improved capacity for users to set previous regional projection products in the context of the latest science.
- The capacity and functionality of the Climate Change in Australia website has been greatly enhanced to support users in understanding what information they need, what is available and how they can obtain it.

The structure of this Technical Report is as follows: Chapter 2 addresses the context of the projections and describes user needs, Chapter 3 covers global climate change science, Chapter 4 surveys observed Australian climate variability and climate changes and their possible causes, and Chapter 5 examines how well CMIP5 models simulate the Australian climate. Chapter 6 presents projection methods that are used in Chapter 7 to describe projected future climate change for a range of atmospheric and terrestrial variables, emission scenarios, and time periods to the end of the century. Chapter 8 provides observed trends and projections for a range of marine variables. Chapter 9 explains how climate projection information can be used in impact assessments. Finally, Chapter 10 explores future directions for climate change

projections research and communication. Appendix A compares findings from CMIP3 models with those from the latest CMIP5 assessments.

Climate change information is presented on a regional basis. The regionalisation is based on eight 'clusters' of NRM regions. The separate Cluster Reports each contain a description of the relevant biophysical and climatological features in each cluster. Readers primarily interested in regional climate change projections and less interested in the technical details surrounding their production should consult the Cluster Reports and Brochures.

Electronic copies of this Report, the Cluster Reports, and other related publications, are available at the Climate Change in Australia website (www.climatechangeinaustralia.gov.au). Further information on the projection products prepared for this project is given in Box 1.1.

The climate change projections described here contribute to the work of nine allied teams undertaking impacts and adaptation research projects. There is a team for each of the eight clusters, and one team focussed nationally. The above website contains information on each of these projects.

BOX 1.1: CLIMATE CHANGE IN AUSTRALIA – PRODUCTS

This Report is part of a suite of Climate Change in Australia (CCIA) products prepared as part of the Australian Government's Regional Natural Resource Management Planning for Climate Change Fund. These products provide information on climate change projections and their application.

CLUSTER BROCHURES

Purpose: key regional messages for everyone

A set of brochures that summarise key climate change projections for each of the eight clusters. The brochures are a useful tool for community engagement.

CLUSTER REPORTS

Purpose: regional detail for planners and decision-makers

The Cluster Reports are to assist regional decision-makers in understanding the important messages deduced from climate change projection modelling. The Cluster Reports present a range of emissions scenarios across multiple variables and years. They also include relevant sub-cluster level information in cases where distinct messages are evident in the projections.

TECHNICAL REPORT

Purpose: technical information for researchers and decision-makers

A comprehensive report outlining the key climate change projection messages for Australia across a range of variables. The report underpins all information found in other products. It contains an extensive set of figures

and descriptions on recent Australian climate trends, global climate change science, climate model evaluation processes, modelling methodologies and downscaling approaches. The report includes a chapter describing how to use climate change data in risk assessment and adaptation planning.

WEB PORTAL

URL: www.climatechangeinaustralia.gov.au

Purpose: one stop shop for products, data and learning

The CCIA website is for Australians to find comprehensive information about the future climate. This includes some information on the impacts of climate change that communities, including the natural resource management sector, can use as a basis for future adaptation planning. Users can interactively explore a range of variables and their changes to the end of the 21st century. A 'Climate Campus' educational section is also available. This explains the science of climate change and how climate change projections are created.

Information about climate observations can be found on the Bureau of Meteorology website (www.bom.gov.au/climate). Observations of past climate are used as a baseline for climate projections, and also in evaluating model performance.



CHAPTER TWO

USER NEEDS AND REGIONALISATION



COURTESY OF NORTH EAST CMA, VICTORIA

-20° -10° 0° 10° 20° 30° 40° 50°

CHAPTER 2 USER NEEDS AND REGIONALISATION

To maximise the utility of climate change projections, user needs should be considered while ensuring the projections are scientifically robust and regionally applicable. This chapter describes an assessment of user needs undertaken to inform the projections contained in this Report. The users consulted were primarily from the natural resource management (NRM) sector of Australia, due to the strong linkages between this work and regional NRM planning. This chapter also compares the results with similar international studies. The regionalisation used throughout this Report and associated products is described and explained here. This includes the eight clusters and additional sub-clusters.

2.1 ASSESSING USER NEEDS

Throughout its history of developing climate projections for Australia and elsewhere, CSIRO has worked closely with a variety of partners and end users to deliver climate projections information that can be used in planning and impact assessments. In the 1990s, reports and maps were suitable for awareness-raising and broad-scale general assessments that were prevalent at the time. Since then however, the requirements of end users of climate projections have progressively increased in complexity and sophistication.

This requirement for increasingly detailed projections information has led to a growth in demand from researchers, private sector entities, governments, and non-government organisations undertaking impact assessments, as well as long-term strategic planning exercises. These users require information about the likelihood and magnitude of future climate change for many variables of interest. Community level information is also often required to assist in building relevant knowledge and capability among constituents.

In response to the increasing needs of users, new products and services were required. A computer-based (and later, online) projections tool called *OzClim* (Page and Jones, 2001, Ricketts and Page, 2007) was developed to provide access to climate model data on a 25 km grid. The *Climate Change in Australia* website, underpinning the technical report and brochure of the same name (CSIRO and BOM, 2007), provided users with access to more detailed results. A climate projections liaison service was initiated in 2009 to deliver tailored projections information, advice and data.

Uptake of these products and services has increased over time. Users have undertaken impact assessments that range from simple to complex, with significant and varying data requirements. The ability to service these requests has evolved as methodologies, data sharing arrangements, data formatting and impact assessment options have matured. An increasing need for both climate change data (*i.e.* the projected change values from climate models) and also application-ready data (*i.e.* 'synthetic' future climate information that is calculated by applying projected change values from climate models to observed climate data) has been identified.

Organisations that have a role in community engagement and education about future climate require more than data provision. Tailored regional messages, or narratives, about the projected changes are required for a range of different stakeholders. Local-scale approaches (within the limitations of the spatial scale of climate model output) are often well received, and assist in increasing the relevance of engagement and communication activities.

In 2011, stakeholder workshops were held in seven Australian capital cities to seek feedback on the utility of the projections published in 2007 (CSIRO and BOM, 2007) and identify needs for future projections. The feedback included a number of common user requirements:

- Ensure legitimacy, credibility and relevance;
- Provide information about climate model reliability;
- Convey information in ways that are easy to understand;
- Represent uncertainty and provide guidance on how to deal with it;
- Supply an appropriate level of spatial and temporal detail;
- Generate projections for 20-year periods centred on 2030, 2050, 2070 and 2090;
- Include information on year to year variability and extreme events;
- Provide easy access to data, support, guidance material and case studies;
- Supply information in different formats, *e.g.* text summaries, GIS data, tables, maps, graphs, PowerPoint slides, animations, etc.

This aligns well with the experience of others around the world. For example, in their evaluation of the United Kingdom Climate Impacts Program, Steynor *et al.* (2012) recognized the need to:

- Establish an understanding of user requirements;
- Manage tensions that exist between meeting user requirements and developing credible climate science;
- Help users incorporate inherent uncertainty into decision-making;
- Solicit a wide range of users' views about presentation and delivery, including projections themselves, delivery interface, guidance materials and training;
- Support sustained user engagement.



In addition to this, CSIRO collaborated with the Bureau of Meteorology to undertake a range of stakeholder engagement activities in Australia from 2012 to 2014. This engagement was primarily with the NRM sector, reflecting the Australian Government's alignment of projections research in assisting the sector to understand and plan for future climate change.

A major component of this engagement was the Climate Projections User Panel, comprised of key NRM stakeholders, which was established to enhance the two-way exchange of views about data and information needs, use and accessibility of online tools, guidance materials and training requirements. Stakeholder workshops and interviews were also conducted to delve into how users had previously interacted with climate change projections information and data, and to understand the future potential uses (referred to hereafter as Use Cases).

These interactions facilitated a shared understanding amongst scientists and stakeholders about what was needed and what could be delivered with the available resources while maintaining adequate scientific rigour.

The Use Cases revealed a number of common themes:

Simple exploration of the future climate involves basic searches for information, most often in map form, in responses to general queries about key variables within a location and time period, or under a certain emissions scenario.

Retrieval of data from a user-defined area or point involves accessing information regarding a specific region, or uploading data points, to facilitate impact studies associated with particular points within a landscape.

Selecting and downloading climate projection data describes accessing appropriate data file types for use in impact studies which match other systems (e.g. GIS formats), are suitable for batch download, and can be included in robust metadata.

Comparing historical climate information with projections describes linking climate projections with historical observation data, which can be compared through combined data sets and displayed graphically.

Quantitative exploration of future climate involves more detailed use of projection information in sophisticated mapping and tabular formats regarding climate thresholds, time series, extreme event occurrences, coastal impacts and the like.

The Use Cases also provided information about the objectives or motivations for projection information usage. These include:

Estimating future impacts – in plant productivity, plant mortality, species distributions, biodiversity and water supply by modelling or projecting plant growth (invasive, native and crop species), soil and sediment erosion, fire occurrences, sea levels, fresh and salt water interactions, drought and catchment water balance.

Identifying adaptation strategies – by working with different sectors (e.g. tourism, primary production, water) to develop plans. This involves identifying vulnerable sites or locations where crops and species will survive, considering alternative options regarding water supply or plant varieties, managing remnant vegetation and conservation planting, and deciding water allocations.

Communicating and educating about adaptation – by developing information materials to assist different sectors, strategies to change public water use attitudes and behaviours, guidance to help planners shift from a focus on mitigation and single scenarios, and advice to facilitate conversations between NRM groups and the community about climate change.

2.2 MEETING USER NEEDS

Projections are provided for many climate variables at national, regional and sub-regional scales in this Report and the companion Cluster Reports and brochures. Access to this information and associated datasets is also provided through the *Climate Change in Australia* website. Information regarding how to use these data in impact assessments is detailed in Chapter 9.

Specific products and services provided on the website to support users of these projections include:

- A decision tree to guide the selection of projection methods and products to use for different applications (*i.e.* fit for purpose);
- Guidance material, such as step-by-step guides to assist the appropriate use of the data;
- Online training;
- A service to assist users and respond to requests for data not readily obtainable from the reports or the website.

Important issues such as addressing uncertainty in projections (Section 6.1) and climate model reliability (Chapter 5) are addressed in this Report as well as on the website. NRM regional staff, researchers and members of local groups, societies and education facilities are tasked with the role of communicating climate change information to the broader community. To assist them, a range of useful and targeted resources and links to additional material are available on the *Climate Change in Australia* website. These resources include an extensive climate information site (called 'Climate Campus'), slide packs, a guide to communicating about climate change and access to informative graphics.

2.3 SUB-DIVIDING AUSTRALIA

For the purposes of this Report and associated products, Australia has been considered at three levels of detail to suit specific purposes.

The regionalisation scheme, developed in consultation with the Department of the Environment, defines eight natural resource management (NRM) clusters. This subdivision was informed by logical groupings of recent past climatic conditions (e.g. Stern *et al.* 2000), biophysical

factors and expected broad patterns of climate change (e.g. CSIRO and BOM, 2007). Where possible, the cluster boundaries were aligned with existing boundaries of 56 NRM regions (Department of Agriculture, 2013, Department of the Environment, 2013) – these are described in Box 2.1. The clusters are shown in Figure 2.1 and a summary of selected characteristics of each cluster is provided in Table 2.1. There is a Cluster Report describing the climate change projections for each cluster available on the *Climate Change in Australia* website.

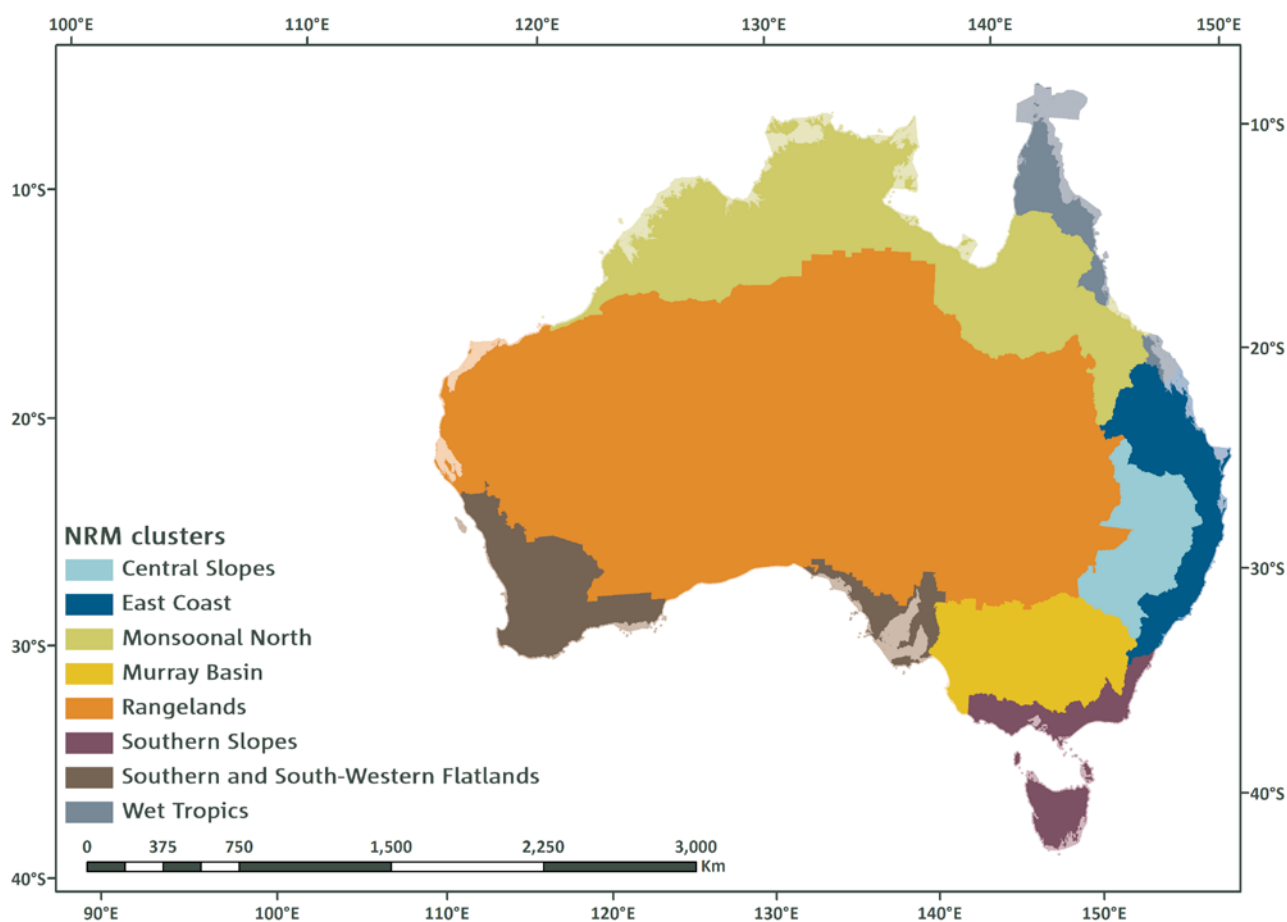


FIGURE 2.1: NATURAL RESOURCE MANAGEMENT (NRM) CLUSTERS (LIGHTER SHADES DENOTE COASTAL WATERS INCLUDED IN THE CLUSTERS TO ENCOMPASS OFFSHORE ISLANDS).



Recent studies (e.g. Grose *et al.* 2010) and preliminary analysis of the model results in the early stages of this work suggested further sub-division was needed in some cases to better capture the important patterns of projected change. In light of this, five of the eight clusters were sub-divided (Figure 2.2). Projections at this scale, called sub-clusters, are also more useful for impact assessment and adaptation planning.

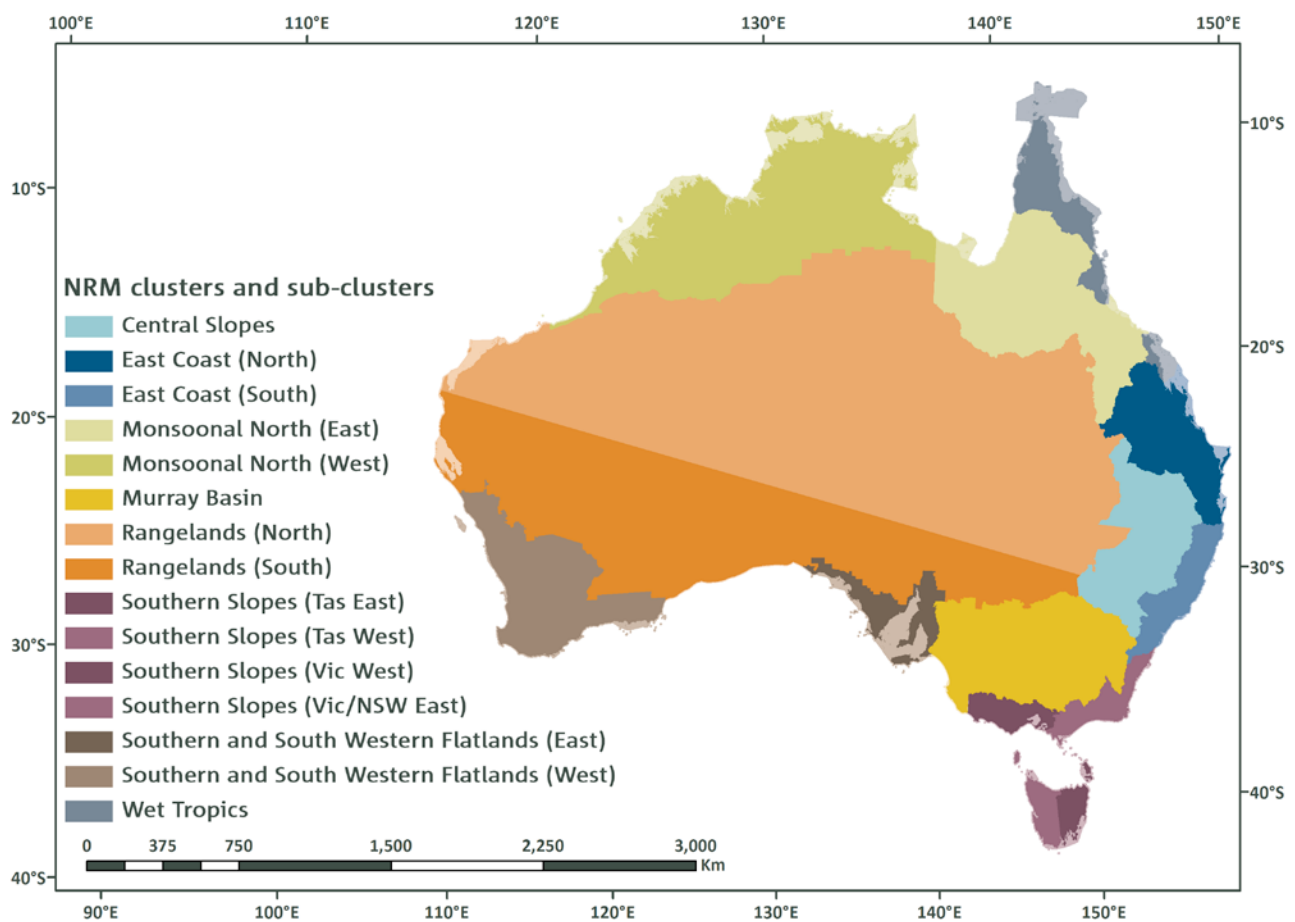


FIGURE 2.2: NRM CLUSTERS AND SUB-CLUSTERS (LIGHTER SHADES DENOTE COASTAL WATERS INCLUDED IN THE CLUSTERS TO ENCOMPASS OFFSHORE ISLANDS).

TABLE 2.1: CLIMATIC ZONES (STERN *ET AL.* 2000); ECOREGIONS (SEWPAC, 2013); APPROXIMATE AREA, POPULATION AND TOP THREE LAND USES BY AREA (AUSTRALIAN BUREAU OF STATISTICS, 2013) FOR THE EIGHT NRM CLUSTERS.

CLUSTER (APPROX. AREA 1000 KM ²)	APPROX. POP. (X1000)	CLIMATIC ZONES (SEE NOTES)	ECOREGIONS (SEE NOTES)	MAIN LAND USES (% OF AREA)
CENTRAL SLOPES (372)	566	A (mainly north) D (south east) E (west)	4 (south east) 5 (west) 6 (north and central)	Agricultural (94) Parkland (5) Residential (0.5)
EAST COAST (395)	9,080	C (north) D (south)	4 (south) 6 (north)	Agricultural (79) Parkland (18) Residential (2)
MONSOONAL NORTH (1,906)	462	B (north) C (far east) E (south)	6	Agricultural (94) Parkland (5) Residential (0.2)
MURRAY BASIN (510)	1,557	D (south) E (north)	2 (west) 4 (east and south) 5 (central)	Agricultural (85) Parkland (14) Residential (0.6)
RANGELANDS (4,888)	226	E (scattered) F (majority)	1 (majority) 2 (south west & far south) 5 (east) 6 (north east)	Agricultural (95) Parkland (4) Residential (0.03)
SOUTHERN AND SOUTH-WESTERN FLATLANDS (754)	3,480	C (west coast) D (inland) E (coastal)	2	Agricultural (89) Parkland (9) Residential (0.6)
SOUTHERN SLOPES (200)	5,685	D	3 (patches) 4 (majority)	Agricultural (51) Parkland (45) Residential (2)
WET TROPICS (178)	390	A (north) B (north) C (south)	6 (northern) 7 (southern)	Agricultural (79) Parkland (20) Residential (<1)

CLIMATIC ZONES

- A. Equatorial
- B. Tropical
- C. Subtropical
- D. Temperate
- E. Grassland
- F. Desert

ECOREGIONS

- 1. Deserts and xeric shrublands.
- 2. Mediterranean forests, woodlands and scrubs.
- 3. Montane grasslands and shrublands.
- 4. Temperate broadleaf and mixed forests.
- 5. Temperate grasslands, savannas and shrublands.
- 6. Tropical and subtropical grasslands, savannahs and shrublands.
- 7. Tropical and subtropical moist broadleaf forests.

-20° -10° 0° 10° 20° 30° 40° 50°

We have also developed a broad-scale regionalisation of Australia by amalgamating the NRM clusters into four super-clusters: Northern Australia, Eastern Australia, Southern Australia and Rangelands (Figure 2.3). This regionalisation is used within this Report (particularly in Chapter 7) to

describe climate changes at national-scale while permitting representation of differing projected climate changes for the major climatic zones. The relationship between the three levels of sub-division is shown in Table 2.2.

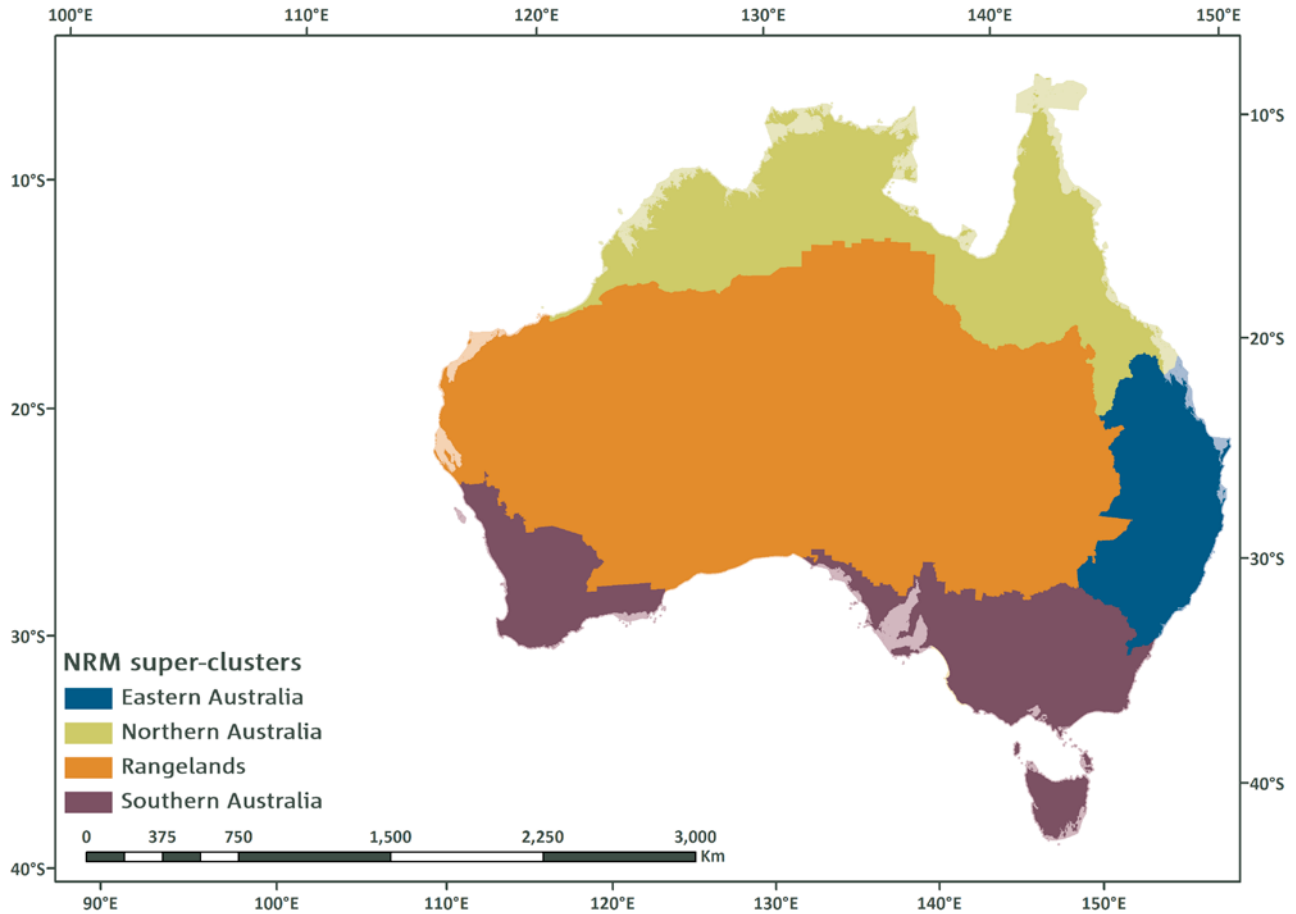


FIGURE 2.3: NRM SUPER-CLUSTERS (LIGHTER SHADES DENOTE COASTAL WATERS INCLUDED IN THE CLUSTERS TO ENCOMPASS OFFSHORE ISLANDS).

TABLE 2.2: THE SUPER-CLUSTERS, CLUSTERS AND SUB-CLUSTERS USED THROUGHOUT THIS REPORT.

SUPER-CLUSTER	CLUSTER(S)	SUB-CLUSTERS
EASTERN AUSTRALIA	East Coast	East Coast – North
		East Coast – South
	Central Slopes	Not subdivided
NORTHERN AUSTRALIA	Monsoonal North	Monsoonal North – East
		Monsoonal North – West
	Wet Tropics	Not subdivided
RANGELANDS	Rangelands	Rangelands – North
		Rangelands – South
SOUTHERN AUSTRALIA	Murray Basin	Not subdivided
	Southern & South Western Flatlands (SSWF)	SSWF – East
		SSWF – West
	Southern Slopes (SS)	SS – Tasmania East
		SS – Tasmania West
		SS – Victoria East
		SS – Victoria West

While a wide range of projections information has been provided as cluster, super-cluster and sub-cluster averages, finer scale data are available for users with a particular need. Chapter 9 gives a full explanation of the projections data available, the spatial scales, and notes on how to use them appropriately.



BOX 2.1: NRM REGIONS

Australia is divided up into 56 natural resource management (NRM) regions based on catchments or bioregions. These regions facilitate the development and implementation of strategic NRM plans, and regional bodies play a key role in delivery of government NRM programmes, including the National Landcare Programme. These regions are determined by the Commonwealth, State and Territory governments, with revisions from time to time.

For these projections, a regionalisation scheme using the NRM regional boundaries has been used. The main projections regions are called clusters. To allow time for the extensive analyses required to develop the results presented in this Report (and associated products) it was necessary to settle on the cluster boundaries and retain those boundaries for the life of the project. The boundaries were fixed on 1 January 2013. In early 2014, the New South Wales government realigned their NRM regional boundaries. This affects the East Coast, Southern

Slopes and Murray Basin clusters, and to a lesser extent the Rangelands cluster (see the relevant Cluster Reports for details).

In most cases, the definition of clusters was based on NRM regional boundaries. However, the whole of the Northern Territory is a single NRM region as is northern Western Australia. It was important in the definition of cluster boundaries to recognise the distinct climatic and biophysical character of the far northern monsoonal areas. As such, the Northern Territory and northern Western Australia were split along their sub-regional boundaries delineating the Monsoonal North and the Rangelands clusters. In addition, the Cape York Cooperative Management Area was used to delineate part of the boundary between the Wet Tropics and Monsoonal North clusters. Figure B2.1 shows the NRM regions and other boundaries used as the basis for the regionalisation described in this chapter.

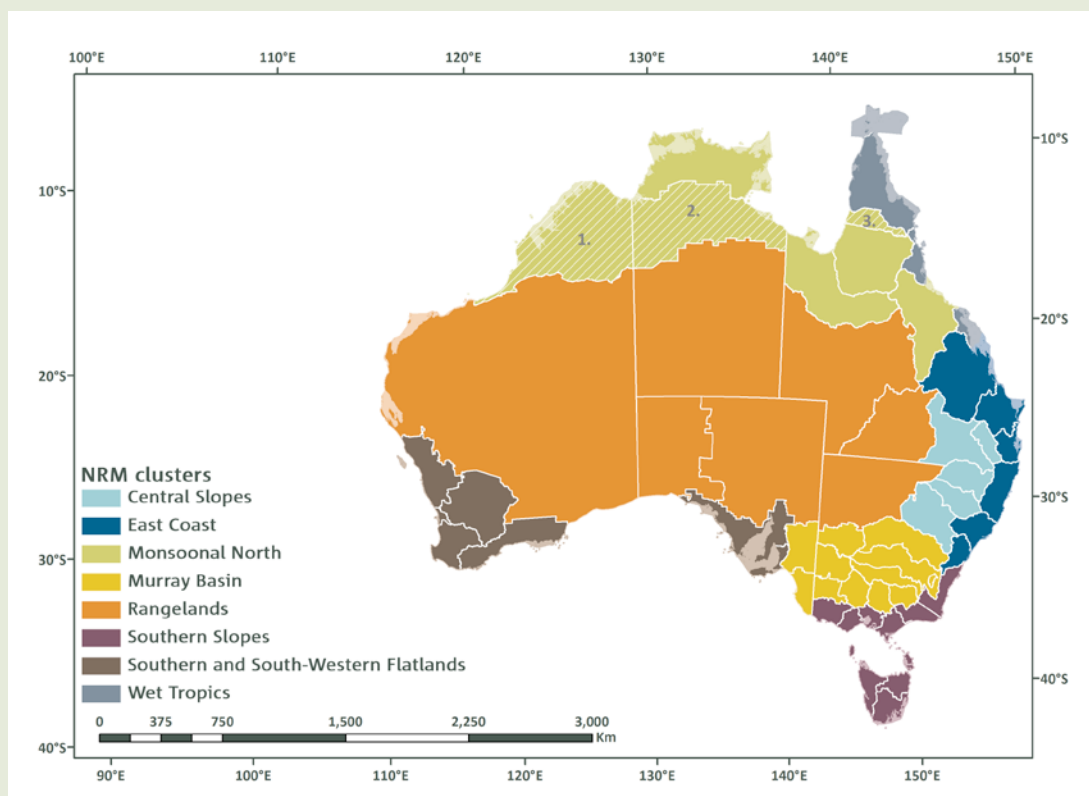


FIGURE B2.1 THE NRM REGIONS USED TO DEVELOP THE REGIONALISATION FOR THIS REPORT AND ASSOCIATED PRODUCTS, IN CONSULTATION WITH THE DEPARTMENT OF THE ENVIRONMENT. NOTE THAT SOME BOUNDARIES ARE DEFINED BY NRM SUB-REGIONS (1 AND 2), AND THE COOPERATIVE MANAGEMENT AREA ON CAPE YORK (3).

Note that NRM Regions are reviewed from time to time by the relevant State agencies (e.g. the NSW regions were revised in early 2014). To facilitate the extensive analyses required for this project, the boundaries were fixed on 1 January 2013.

CHAPTER THREE

GLOBAL CLIMATE CHANGE SCIENCE



FLOODED ROAD, WESTERN AUSTRALIA, ISTOCK

-20° -10° 0° 10° 20° 30° 40° 50°

CHAPTER 3 GLOBAL CLIMATE CHANGE SCIENCE

This chapter introduces the global climate system, how it varies naturally, and the concept of external forcing of the climate system, global trends and their causes. It also introduces global climate models and the external forcing scenarios that are used to run climate model experiments that are the basis for many of the results presented in this Report.

3.1 FACTORS DRIVING CLIMATE VARIABILITY AND CHANGE

Climate variability occurs naturally within the climate system, due to the ‘internal’ interaction of physical processes, for example through chaotic processes or through exchanges of heat within, and between the atmosphere and ocean.

A second source of influences on the climate arises from changes in factors ‘external’ to the climate system. Examples of these are changes to atmospheric composition from volcanic activity or anthropogenic (human) activities, or changes in output of the Sun (solar radiation) or changes in the Earth’s orbit around the Sun. What these have in common is that they alter the balance of radiation of the Earth/atmosphere system, by changing the absorbed or reflected solar radiation or by changing the absorption characteristics of the radiation emitted by the Earth. In simple terms, the Earth must then respond by further changing these fluxes to restore radiative balance.

The effects of ‘naturally occurring’ external factors (principally the solar cycle and volcanic activity) can be considered part of the natural climate variability.

‘Climate change’ refers to long-term (typically decades or longer) changes in the properties of the climate, such as the mean or variability. Climate change can arise from both internal processes and from external factors, natural and anthropogenic.

‘Anthropogenic climate change’, in particular, is that which originates from the Earth’s response to the long-term ‘external’ radiative imbalance caused by human activities.

The measure of the imbalance imposed by external factors is termed ‘radiative forcing’, as it ‘forces’ an adjustment to the Earth’s natural balance of incoming and outgoing radiation. Radiative forcing (sometimes called ‘climate forcing’) is the net measure of incoming and outgoing radiation and is measured at the tropopause or top of the atmosphere. A negative forcing acts to cool the climate system, whereas positive forcing has a warming impact.

3.1.1 INTERNAL (“UNFORCED”) CLIMATE VARIABILITY

Natural oscillations and variations occur within the climate system across the full range of spatial and temporal timescales. Variations occur from daily synoptic timescales, involving the passage of high and low pressure systems (‘weather’), through to seasonal variations such as monsoon systems and interannual variations due to processes such as El Niño Southern Oscillation (ENSO) and the Indian Ocean Dipole (IOD) (see Chapter 4), and to decadal variability from processes such as the Interdecadal Pacific Oscillation (IPO).

Typically, climate variability involves the exchange of heat, moisture and momentum between or within the atmosphere, ocean and land surface, marked by transient changes to the total heat within the climate system. By contrast, climate change is characterised by changes to the long-term storage or redistribution of heat. The vast heat capacity of the ocean acts as both the ‘buffer’ associated with very long (*e.g.* decadal) timescale climate variability and as the long-term accumulator of heat under climate change (Church *et al.* 2005).

Although climate variability occurs on all scales, its magnitude becomes larger as spatial scales decrease. For example regional rainfall variability is greater than continental scale variability, which is greater in turn than that at global scales. Furthermore, variability has different characteristics for different features. For example rainfall is highly spatially and temporally variable, relative to mean values. It will be seen below that these features of variability have important implications for the detection and attribution of climate change, as climate variability can often ‘mask’ climate change, particularly at regional or local scales (see Chapter 4). Long- and short-term variability can additionally oppose or reinforce future climate changes (refer Chapter 6) and must be factored into the ‘envelope’ of projected changes.



3.1.2 EXTERNAL FORCING FACTORS

Estimates of anthropogenic and natural external forcing are presented in Figure 3.1.1. For each gas, the forcing is shown as a function of its emissions rather than its final atmospheric concentrations.

Greenhouse gases produce positive forcing from increased trapping of outgoing longwave radiation, along with some additional absorption of solar radiation. Water vapour is an important greenhouse gas, however, its residence time in the atmosphere is short, and water vapour amounts are not directly affected by humans. Rather, water vapour concentrations respond to temperature increases arising from initial forcing by the long lived greenhouse gases, thereby further reinforcing (amplifying) the warming that occurs.

The best estimate of the forcing from changes in the long-lived greenhouse gases (carbon dioxide, methane, nitrous oxide and halocarbons) is around 3.0 W/m^2 (watts per square metre) (Figure 3.1.1). Carbon dioxide is the largest contributor, at around 1.7 W/m^2 . Isotopic evidence, carbon dioxide concentration distributions and a measured decrease in atmospheric oxygen together provide overwhelming evidence that human activities have been responsible for these changes in greenhouse gas concentrations (IPCC, 2013).

These gases are ‘long-lived’ in the atmosphere, and as a consequence their geographical concentrations are relatively homogeneous (*i.e.* evenly spread). Carbon dioxide lifetime in the atmosphere is hard to quantify simply, because it is a result of many different cycles and processes, with a wide range of timescales. Around half the emitted carbon dioxide is currently being absorbed by the ocean and terrestrial biosphere (IPCC, 2013, Chapter 6), with the remainder contributing to increased atmospheric CO_2 concentrations. The ‘adjustment time’ (*i.e.* the time taken to permanently remove the increased CO_2 concentration from the atmosphere) is of the order of centuries.

Land use changes have produced a small net negative forcing globally, mainly due to the clearing of (low reflectivity) forests, and their replacement by (higher reflectivity) crop or pastureland, and the difference in snow characteristics over cleared versus forested terrain (IPCC, 2013). Land use changes can also potentially have impacts on regional temperatures and rainfall, such as in south-west Western Australia (Pitman *et al.*, 2004, Timbal and Arblaster, 2006). Land-use change also impacts on the carbon budget, and globally have significantly increased carbon levels in the atmosphere (IPCC, 2013).

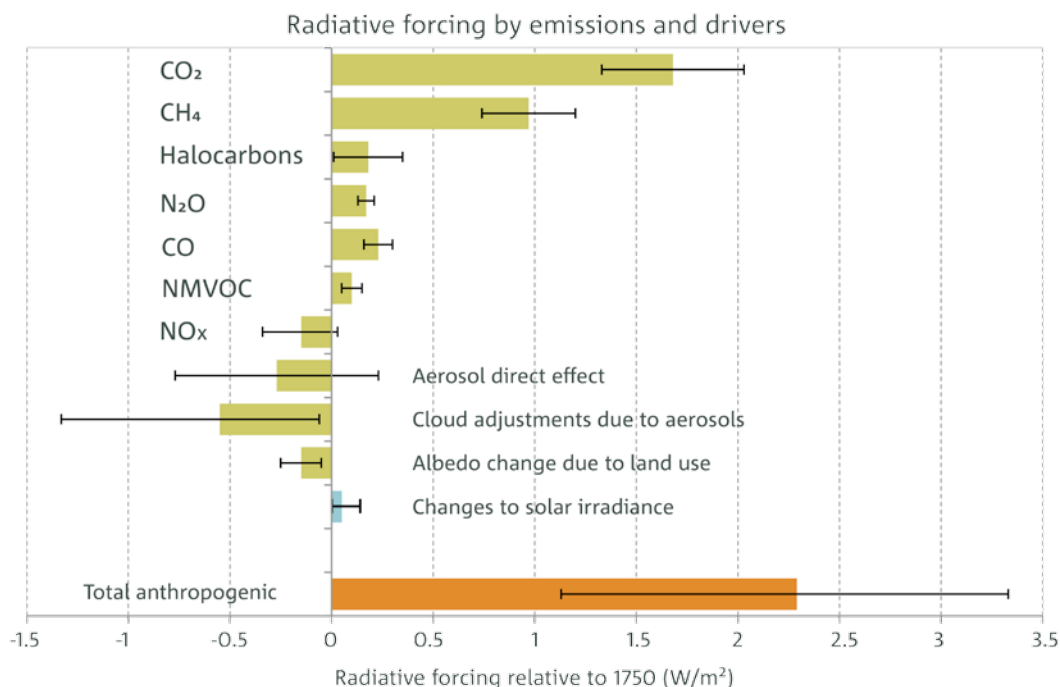


FIGURE 3.1: RADIATIVE FORCING ESTIMATES IN 2011 WITH RESPECT TO PRE-INDUSTRIAL CONDITIONS (1750) FROM EMISSIONS AND DRIVERS. FOR EACH GAS, THE FORCING IS SHOWN AS A FUNCTION OF ITS EMISSIONS RATHER THAN ITS FINAL CONCENTRATIONS. FOR EXAMPLE THE IMPACT OF EMITTED HALOCARBONS ON REDUCING STRATOSPHERIC OZONE CONCENTRATIONS AND CONSEQUENT RADIATIVE FORCING IS INCLUDED UNDER HALOCARBONS, GREEN BARS SHOW ANTHROPOGENIC EMISSIONS AND DRIVERS, BLUE ARE NATURAL, AND THE ORANGE BAR SHOWS THE TOTAL ANTHROPOGENIC FORCING. BARS REPRESENT THE 90 % CONFIDENCE RANGE. NMVOC REPRESENTS NON-METHANE VOLATILE ORGANIC COMPOUNDS SUCH AS BENZENE AND ETHANOL (ADAPTED FROM: FIGURE SPM.5 IN IPCC, 2013).



Solar cycles or changes in the orbit of the Earth can affect the amount of incoming solar radiation. Variability of the sun is imperfectly understood, but the well-established 11 year sunspot cycle alters total solar output by around 0.08 % (IPCC 2013, Chapter 8), which has only minor impact on climate (Meehl *et al.* 2009). The best estimate for net solar output change from 1750 to present, derived from several proxies, is for a forcing of 0.05 W/m² (Figure 3.1.1). Direct measurements from space over the last 30 years suggest a small reduction in forcing for this period of -0.04 W/m². Forcing from solar changes is dwarfed by those from anthropogenic sources, indicating the Sun has played little role in observed changes (Section 3.4).

Ozone in the stratosphere results from ultraviolet interaction with oxygen. In the troposphere it results from chemical transformation of other gases such as carbon monoxide or nitrous oxide. Ozone concentration changes have a varying impact depending on their location within the atmosphere. Increases in the lower atmosphere (troposphere) have caused a warming, due to their trapping of outgoing radiation. Stratospheric decreases in ozone (due to destruction by chlorofluorocarbons (CFCs), and related to the ‘ozone hole’) have resulted in a negative forcing from decreased absorption of outgoing radiation. Forcing for ozone is not shown explicitly in Figure 3.1.1, but is included under its precursor emissions (CFCs, carbon monoxide, nitrous oxide).

Aerosols are tiny solid or liquid particles suspended in the atmosphere. They have a ‘direct’ impact on radiation by reflecting incoming solar radiation back to space. They additionally have an ‘indirect’ impact on radiation by affecting the distribution, lifetime and type of clouds through their role as cloud condensation nuclei (*i.e.* particles on which water vapour can condense, as part of the process in forming water droplets). Forcing from aerosol changes is highly uncertain, with the best estimate of around -0.9 W/m² (IPCC, 2013). Aerosol characteristics differ dramatically from greenhouse gases, in that their lifetimes in the atmosphere are short (of the order days to weeks) and their distribution is not uniform within the atmosphere, with large concentrations downwind of industrial areas. There are additionally large natural sources of aerosols, including dust from arid inland regions of Australia (Mitchell *et al.* 2013) and sea salt particles arising from the oceans (any trends in these are not explicitly included in Figure 3.1.1)

Volcanic eruptions can deposit large amounts of dust and sulphate aerosols into the atmosphere, increasing the reflection of incoming solar radiation, producing a negative (cooling) forcing. Most volcanoes have only minor radiative impact, but large explosive volcanoes can inject aerosols directly into the stratosphere, where they can persist for months or years causing significant forcing. It is estimated

that Mount Pinatubo induced a short-term cooling of around 0.5 °C, peaking a year or so after eruption (Soden *et al.* 2002). The carbon dioxide emitted by volcanoes, however, is negligibly small compared to anthropogenic emissions (Morner and Etiope, 2002). Volcanoes are not included in Figure 3.1.1, as they provide only transient forcing, and there is no evidence that volcanic activity has changed since pre-industrial times.

Urban heat island effects describe the warming influence on urban regions from their built environment. They operate in all seasons, and are usually greater at night (Trewin, 2010). They are included in Figure 3.1.1 under land use changes but their global impact is relatively small. They may however, have significant local impacts, and must be considered for urban projections. Stations that have experienced the urban heat island effect have been removed from the temperature record for detection and attribution purposes (see Section 4.2).

Net forcing describes the best estimate of anthropogenic global net forcing and is assessed to be around 2.3 W/m² since 1750. This value dwarfs natural external forcing (Figure 3.1.1).

3.2 EMISSIONS SCENARIOS AND CLIMATE MODELS

3.2.1 FUTURE SCENARIOS OF GREENHOUSE GAS CONCENTRATIONS

The future of anthropogenic greenhouse gas and aerosol emissions (and hence their resultant radiative forcing) is highly uncertain, encompassing substantial unknowns in population and economic growth, technological developments and transfer, and political and social changes. The climate modelling community has developed Representative Concentration Pathways (RCPs) to explore credible future options.

The four RCPs used in this Report represent the distillation of a much larger number of potential futures discussed in the literature (van Vuuren *et al.* 2011, Meinshausen *et al.* 2011). Each prescribes internally self-consistent ‘representative’ concentrations of greenhouse gases and aerosols, as well as land use changes. They were developed by a group of experts in areas spanning atmospheric modelling, chemistry and the carbon cycle and social scientists working in economics, policy and impacts (Moss *et al.* 2010). They are used in the fifth Climate Model Intercomparison Project (CMIP5) (refer Section 3.3) and the latest IPCC Assessment Report (2013).

The (estimated) carbon emissions and the corresponding radiative forcing for the four RCPs are shown in Figure 3.2.1.



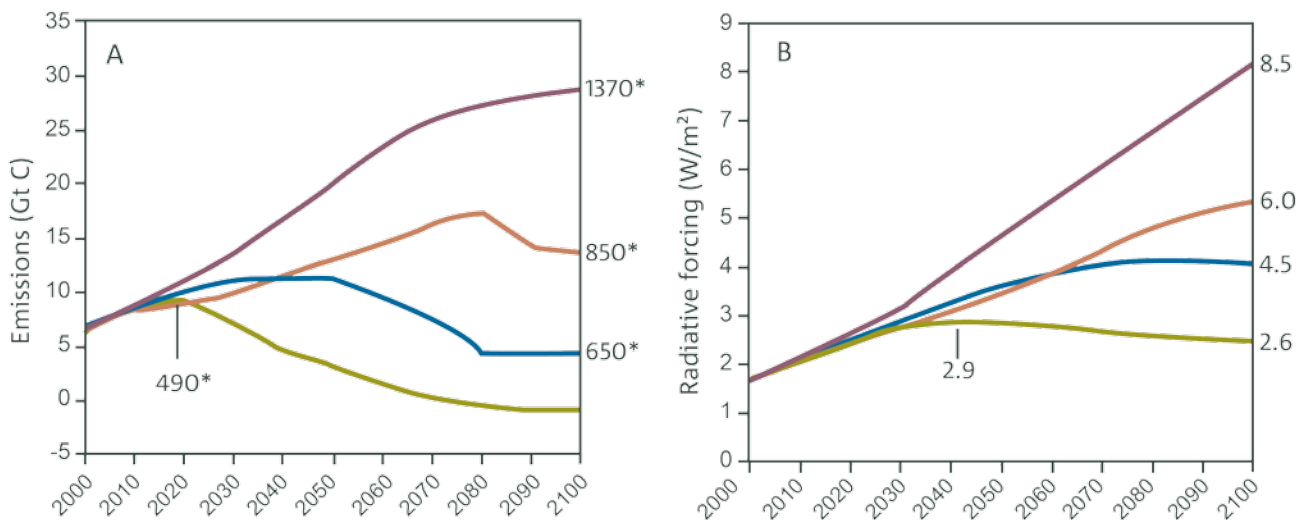


FIGURE 3.2.1: (A) EMISSIONS OF CARBON, IN GIGATONS FOR THE DIFFERENT RCP SCENARIOS USED IN THIS REPORT. THE ASTERISKED NUMBERS SHOW THE ATMOSPHERIC CO₂ EQUIVALENT¹ LEVELS IN PARTS PER MILLION (PPM). (B) RADIATIVE FORCING (SEE SECTION 3.1 FOR DEFINITION) FOR THE DIFFERENT SCENARIOS. THE NUMBERS ON THE RIGHT HAND AXIS SHOW THE FINAL FORCING (W/M²) AND EQUATE TO THE NAMES OF THE RCP SCENARIOS. DRAWN FROM DATA AVAILABLE AT [HTTP://WWW.PIK-POTSDAM.DE/~MMALTE/RCPS/](http://www.pik-potsdam.de/~mmalte/rcps/).

RCPs differ from the Special Report on Emissions Scenarios (SRES) scenarios (Nakicenovic and Swart, 2000) used in the previous Climate Change in Australia (CSIRO and BOM, 2007) projections report and in the IPCC (2007) report). A comparison of carbon dioxide concentrations for the two sets of scenarios is shown in Figure 3.2.2. The

RCPs represent a wider set of futures than SRES, and now explicitly include the effect of mitigation strategies. As with SRES, no particular scenario is deemed more likely than the others, however, some require major and rapid change to emissions to be achieved.

CO₂ concentrations in SRES and RCP scenarios

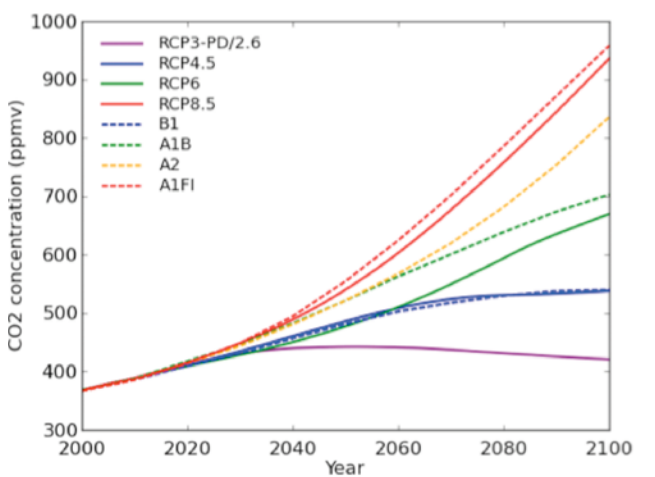


FIGURE 3.2.2: A COMPARISON OF RCPs AND SRES: CO₂ CONCENTRATIONS. NOTE THAT THESE ARE CO₂ ALONE, NOT THE “CO₂ EQUIVALENT” CONCENTRATIONS SHOWN ON THE RIGHT HAND AXIS OF FIGURE 3.2A. DRAWN FROM DATA AVAILABLE AT [HTTP://WWW.PIK-POTSDAM.DE/~MMALTE/RCPS/](http://www.pik-potsdam.de/~mmalte/rcps/).

1 CO₂ equivalent is the carbon dioxide concentration that would cause the same level of radiative forcing from all greenhouse gasses in the atmosphere (including methane, nitrous oxide and halocarbons).



RCP8.5 represents a future with little curbing of emissions, with a CO₂ concentration continuing to rapidly rise, reaching 940 ppm by 2100. Resultant forcing is close to that of SRES A1FI (Figure 3.2.2). RCP6.0 represents lower emissions, achieved by application of some mitigation strategies and technologies (van Vuuren *et al.* 2011). This scenario results in the CO₂ concentration rising less rapidly than RCP8.5, but still reaching 660 ppm by 2100 and total radiative forcing stabilising shortly after 2100. RCP4.5 concentrations are slightly above those of RCP6.0 until after mid-century, but emissions peak earlier (around 2040), and the CO₂ concentration reaches 540 ppm by 2100. Carbon dioxide concentrations under RCP4.5 closely mimic those of SRES scenario B1, the lowest emission scenario considered in the previous report (Figure 3.2.2). RCP2.6 (which can also be referred to as RCP3-PD for ‘peak and decline’) is the most ambitious mitigation scenario, with emissions peaking early in the century (around 2020), then rapidly declining. Such a pathway would require early participation from all emitters, including developing countries, as well as the application of technologies for actively removing carbon dioxide from the atmosphere (IGBP, 2010). The CO₂ concentration reaches 440 ppm by 2040 then slowly declines to 420 ppm by 2100. There was no equivalent scenario under SRES.

There are implications for projection uncertainties from the change in scenarios from the last report. RCPs begin with concentration levels, rather than with socio-economic assumptions followed by inferred emissions. As a result, uncertainties due to the response of the carbon cycle did not need to be factored into climate projections, as they do with the use of SRES scenarios. Consequently uncertainties due to the carbon cycle are not included in the projections in this Report. Instead, those uncertainties must now be factored into the mitigation strategies required to achieve particular concentration pathways (Rogelj *et al.* 2012). Such mitigation uncertainties lie outside the scope of this Report but are discussed and evaluated at length in IPCC (2014).

3.2.2 GLOBAL CLIMATE MODELS

Future climate changes cannot be simply extrapolated from past climate and further, and will depend on future concentration pathways. The best tools for climate change projections are general circulation models also called global climate models (GCMs). These are mathematical representations of the climate system run on powerful computers. Their fundamentals are based on the laws of physics, including conservation of mass, energy and momentum. GCMs are closely related to models used by the Bureau of Meteorology to produce Australia’s weather forecasts.

GCMs represent the atmosphere and ocean as three-dimensional grids, with a typical atmospheric resolution of around 200 km, and 20 to 50 levels in the vertical. Models explicitly represent large-scale synoptic features of the atmosphere, such as the progression of high and low pressure systems, and large-scale oceanic currents and overturning. However many important physical processes occur at finer spatial scales. Examples include radiation and

precipitation processes, cloud formation and atmospheric and oceanic turbulence. The impacts of such processes are included in ‘parameterisations’, whereby their effects are expressed in approximate form on the coarser model grid. Parameterisations are typically the result of intensive theoretical and observational study, and essentially represent an additional detailed physical modelling within the climate model itself.

Climate models have undergone continuous development for the last three decades, and now incorporate interactions between the atmosphere, oceans, sea ice and land surface. The schematics of a typical GCM are shown in Figure 3.2.3.

Some latest generation models can additionally represent the interactions between oceanic, atmospheric and land surface carbon cycles, including interactive atmospheric chemistry and vegetation (depicted in Figure 3.2.3). These models are evolving towards full ‘Earth System Models’. For the RCP scenario experiments used in this Report however, all models were run with specified atmospheric trace gas concentrations.

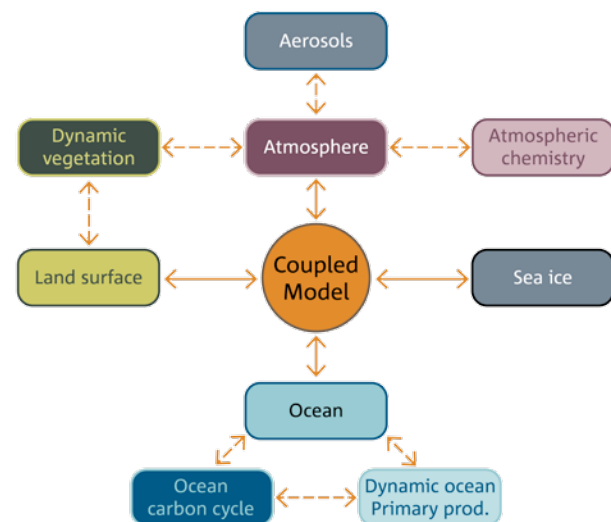


FIGURE 3.2.3: SCHEMATIC OF A GLOBAL COUPLED MODEL (GCM). CONTINUOUS LINES SHOW INTERACTIONS WITH COMPONENTS IN ALL COUPLED MODELS USED IN THIS REPORT. DASHED LINES SHOW INTERACTIONS INCLUDED IN SOME COUPLED MODELS.

Confidence in the use of models for projections comes from their basis in fundamental physical principles and from their ability to represent important features of the current and past climate (see Chapter 5). Over several generations of model development, GCMs have shown a substantial and robust warming due to increases in greenhouse gases. However, uncertainties in the details and timing of changes arise. These differences arise from uncertainties in how to represent some processes in models, and the resulting confidence in projections is greater for some variables

(e.g. temperature) than others (e.g. rainfall). These uncertainties are partly reflected in the ranges presented for projections in this Report. Also, while most models perform reasonably well, there is no single “best” model or subset of models, and climate projections differ between models.

Although model resolution has improved since the 2007 Australian projections, grid scales of global models limit representation of some important regional and local scale features of topography and coastline. These can be important for the local distribution of rainfall, for example. To better represent such features, techniques for downscaling can be applied, whereby finer resolution regional models are embedded within a global model, or where statistical relationships between local-scale climate and broad-scale climate features are exploited. Downscaling methods used in this Report, and their implications for projections, are discussed in Section 6.3.

3.3 INTRODUCTION TO CLIMATE MODEL ENSEMBLES AND TO THE CMIP5 ENSEMBLE

In order to support a systematic evaluation of climate models and their simulated future climate, a standardised set of model simulations (often also called experiments) is necessary. Since a large group of modelling centres around the world run this suite of simulations, the details of model performance can be assessed more readily. Some of the simulations are aimed at testing each model’s ability to simulate the observed climate (called historical simulations) in order to assess confidence in climate model performance as a whole. Sets of additional simulations allow comparison of climate change under standard scenarios of future emission scenarios or concentrations pathways.

The international Model Intercomparison Projects (MIPs) have provided this experimental setup over the past two decades and the latest intercomparison is the Coupled Model Intercomparison Project Phase 5 (CMIP5; see <http://cmip-pcmdi.llnl.gov/cmip5/> for more specific details). Simulations of future climate use the RCPs introduced in Section 3.2). The recently published Working Group One (WGI) report of the IPCC Fifth Assessment (IPCC, 2013) made extensive use of experiments from both CMIP5 and the previous intercomparison project (CMIP3) (Meehl *et al.* 2007).

There are several advantages in using a standard benchmark of experiments, including:

- The possibility to compare historical simulations with observations (exploring model skill)
- The possibility to compare model projections with each other (exploring the range of future climates)
- To isolate common strengths and weaknesses of each model
- To identify systematic errors (e.g. similar errors occurring in many models) from single model errors (to inform future model selection for impact assessment and model development and improvement)

The projections presented in this Report are based on analysis of the CMIP5 ensemble, and this ensemble is described in more detail in the next section.

3.3.1 THE COUPLED MODEL INTERCOMPARISON PROJECT PHASE 5 (CMIP5)

This section gives an overview of the current status of the CMIP5 model ensemble with respect to its overall properties and how it compares to CMIP3 – the previous generation of global climate models. There will be a more detailed examination of the capability of CMIP5 models to simulate the current climate, especially the Australian climate, in Chapter 5.

Table 3.3.1 provides a summary of the ocean-atmosphere general circulation models that were utilised in CMIP5 and CMIP3, including the horizontal grid resolution for the ocean and atmosphere components (in degrees) and the size of a single atmosphere grid cell (in km). There were simulations from 23 GCMs available from the CMIP3 experiments, which have now increased to 48 for the CMIP5 experiments. The archived data amount is extremely large and the analysis will take several years by the global science community since only a fraction of the overall data has been collected worldwide. However, a large group of models have already lodged data sets from the historical period and the future emission scenarios in the archive.

At the time of writing, CMIP5 was still active and model data were still being submitted to the CMIP5 archive. As such, the analysis contributing to this Report has been limited to the set of models in Table 3.3.1. Not all these models currently provide data for all variables of interest and thus it is necessary to use a smaller set of models in many individual analyses. In Table 3.3.2 the list of atmospheric monthly and daily variables from the different experiments used in this Report is shown for five experiments (one historical and four future experiments using the RCPs) along with the number of models used for the standard projection results for each of the variables.



TABLE 3.3.1: LIST OF CMIP5 AND CMIP3 OCEAN-ATMOSPHERE GENERAL CIRCULATION MODELS INCLUDING THE GRID RESOLUTION FOR THE OCEAN AND ATMOSPHERE COMPONENTS (IN DEGREES) AND THE SIZE OF A SINGLE ATMOSPHERE GRID CELL (IN KM). MODELS USED AS INPUT INTO DOWNSCALING STUDIES ARE MARKED (DOWNSCALING BY # BUREAU OF METEOROLOGY STATISTICAL DOWNSCALING MODEL, * CUBIC CONFORMAL ATMOSPHERIC MODEL (SEE SECTION 6.3)).

CMIP5 MODEL ID	INSTITUTE AND COUNTRY OF ORIGIN	OCEAN HORIZONTAL RESOLUTION (°LAT X °LON)	ATMOSPHERE HORIZONTAL RESOLUTION (°LAT X °LON)	ATMOSPHERE RESOLUTION (AT THE EQUATOR)	
				LATITUDE (KM)	LONGITUDE (KM)
ACCESS-1.0 # *	CSIRO-BOM, Australia	1.0×1.0	1.9×1.2	210	130
ACCESS-1.3 #	CSIRO-BOM, Australia	1.0×1.0	1.9×1.2	210	130
BCC-CSM1-1	BCC, CMA, China	1.0×1.0	2.8×2.8	310	310
BCC-CSM1-1-M #	BCC, CMA, China	1.0×1.0	1.1×1.1	120	120
BNU-ESM #	BNU, China	0.9×1.0	2.8×2.8	310	310
CanCM4	CCCMA, Canada	1.4×0.9	2.8×2.8	310	310
CanESM2 #	CCCMA, Canada	1.4×0.9	2.8×2.8	310	310
CCSM4 # *	NCAR, USA	1.1×0.6	1.2×0.9	130	100
CESM1-BGC	NSF-DOE-NCAR, USA	1.1×0.6	1.2×0.9	130	100
CESM1-CAM5	NSF-DOE-NCAR, USA	1.1×0.6	1.2×0.9	130	100
CESM1-FASTCHEM	NSF-DOE-NCAR, USA	1.1×0.6	1.2×0.9	130	100
CESM1-WACCM	NSF-DOE-NCAR, USA	1.1×0.6	2.5×1.9	275	210
CMCC-CESM	CMCC, Italy	2.0×1.9	3.7×3.7	410	410
CMCC-CM	CMCC, Italy	2.0×1.9	0.7×0.7	78	78
CMCC-CMS #	CMCC, Italy	2.0×2.0	1.9×1.9	210	210
CNRM-CM5 # *	CNRM-CERFACS, France	1.0×0.8	1.4×1.4	155	155
CNRM-CM5-2	CNRM-CERFACS, France	1.0×0.8	1.4×1.4	155	155
CSIRO-Mk3-6-0 #	CSIRO-QCCCE, Australia	1.9×0.9	1.9×1.9	210	210
EC-EARTH	EC-EARTH, Europe	1.0×0.8	1.1×1.1	120	120
FIO-ESM	FIO, SOA, China	1.1×0.6	2.8×2.8	310	310
GFDL-CM2p1	NOAA, GFDL, USA	1.0×1.0	2.5×2.0	275	220
GFDL-CM3 *	NOAA, GFDL, USA	1.0×1.0	2.5×2.0	275	220
GFDL-ESM2G #	NOAA, GFDL, USA	1.0×1.0	2.5×2.0	275	220
GFDL-ESM2M #	NOAA, GFDL, USA	1.0×1.0	2.5×2.0	275	220
GISS-E2-H	NASA/GISS, NY, USA	2.5×2.0	2.5×2.0	275	220
GISS-E2-H-CC	NASA/GISS, NY, USA	1.0×1.0	1.0×1.0	110	110
GISS-E2-R	NASA/GISS, NY, USA	2.5×2.0	2.5×2.0	275	220
GISS-E2-R-CC	NASA/GISS, NY, USA	1.0×1.0	1.0×1.0	110	110
HadCM3	MOHC, UK	1.2×1.2	3.7×2.5	410	280
HadGEM2-AO	NIMR-KMA, Korea	1.0×1.0	1.9×1.2	210	130
HadGEM2-CC #	MOHC, UK	1.0×1.0	1.9×1.2	210	130
HadGEM2-ES	MOHC, UK	1.0×1.0	1.9×1.2	210	130
INMCM4	INM, Russia	0.8×0.4	2.0×1.5	220	165
IPSL-CM5A-LR #	IPSL, France	2.0×1.9	3.7×1.9	410	210
IPSL-CM5A-MR #	IPSL, France	1.6×1.4	2.5×1.3	275	145
IPSL-CM5B-LR #	IPSL, France	2.0×1.9	3.7×1.9	410	210
MIROC4h	JAMSTEC, Japan	0.3×0.2	0.56×0.56	60	60

-20° -10° 0° 10° 20° 30° 40° 50°

MIROC5 #	JAMSTEC, Japan	1.6×1.4	1.4×1.4	155	155
MIROC-ESM #	JAMSTEC, Japan	1.4×0.9	2.8×2.8	310	310
MIROC-ESM-CHEM #	JAMSTEC, Japan	1.4×0.9	2.8×2.8	310	310
MPI-ESM-LR #	MPI-N, Germany	1.5×1.5	1.9×1.9	210	210
MPI-ESM-MR #	MPI-N, Germany	0.4×0.4	1.9×1.9	210	210
MPI-ESM-P	MPI-N, Germany	1.5×1.5	1.9×1.9	210	210
MRI-CGCM3 #	MRI, Japan	1.0×0.5	1.1×1.1	120	120
MRI-ESM1	MRI, Japan	1.0×0.5	1.1×1.1	120	120
NorESM1-M # *	NCC, Norway	1.1×0.6	2.5×1.9	275	210
NorESM1-ME	NCC, Norway	1.1×0.6	2.5×1.9	275	210

CMIP3 MODEL ID	INSTITUTE AND COUNTRY OF ORIGIN	OCEAN HORIZONTAL RESOLUTION (°LAT X °LON)	ATMOSPHERE HORIZONTAL RESOLUTION (°LAT X °LON)	ATMOSPHERE RESOLUTION (AT THE EQUATOR)	
				LATITUDE (KM)	LONGITUDE (KM)
bccr-bcm2-0	BCCR, Norway	1.0×1.0	2.8×2.8	310	310
cccma-cgcm3-1	CCCMA, Canada	1.9×1.9	3.7×3.7	410	410
cccma-cgcm3-1-t63	CCCMA, Canada	1.4×0.9	2.8×2.8	310	310
cnrm-cm3	CNRM, France	2.0×1.0	2.8×2.8	310	310
csiro-mk3-0	CSIRO, Australia	1.9×0.9	1.9×1.9	210	210
csiro-mk3-5	CSIRO, Australia	1.9×0.9	1.9×1.9	210	210
gfdl-cm2-0	NOAA, GFDL, USA	1.0×1.0	2.5×2.0	275	220
gfdl-cm2-1	NOAA, GFDL, USA	1.0×1.0	2.5×2.0	275	220
giss-aom	NASA/GISS, USA	4.0×3.0	4.0×3.0	440	330
giss-model-e-h	NASA/GISS, USA	1.0×1.0	5.0×4.0	550	440
giss-model-e-r	NASA/GISS, USA	5.0×4.0	5.0×4.0	550	440
iap-fgoals1-0-g	IAP, China	1.0×1.0	2.8×2.8	310	310
ingv-echam4	INGV, Italy	1.0×1.0	1.1×1.1	120	120
inmcm3-0	INM, Russia	2.5×2.0	5.0×4.0	550	440
ipsl-cm4	IPSL, France	2.0×1.0	3.7×2.5	410	280
miroc3-2-hires	CCSR, Japan	1.2×0.6	1.1×1.1	120	120
miroc3-2-medres	CCSR, Japan	1.4×0.9	2.8×2.8	310	310
miub-echo-g	MIUB, Germany/Korea	2.8×2.3	3.7×3.7	410	410
mpi-echam5	MPI-M, Germany	1.0×1.0	1.9×1.9	210	210
mri-cgcm2-3-2a	MRI, Japan	2.5×2.0	2.8×2.8	310	310
ncar-ccsm3-0	NCAR, CO, USA	1.1×0.5	1.4×1.4	155	155
ncar-pcm1	NCAR, CO, USA	1.0×1.0	2.8×2.8	310	310
ukmo-hadcm3	MOHC, UK	1.2×1.2	3.8×2.5	420	280

-20° -10° 0° 10° 20° 30° 40° 50°



TABLE 3.3.2: LIST OF AVAILABLE SIMULATIONS FROM CMIP5 OCEAN-ATMOSPHERE GENERAL CIRCULATION MODELS FOR NINE MONTHLY (TOP SECTION) AND EIGHT DAILY (EXTREMES; BOTTOM SECTION) CLIMATE VARIABLES FROM 5 DIFFERENT EXPERIMENTS. THE CLIMATE VARIABLES ARE: *HURS* = SURFACE RELATIVE HUMIDITY; *PR* = PRECIPITATION; *PSL* = SURFACE PRESSURE; *RSDS* = SURFACE DOWNWARD SOLAR RADIATION; *TAS* = SURFACE AIR TEMPERATURE; *TASMIN* AND *TASMAX* = MINIMUM AND MAXIMUM SURFACE AIR TEMPERATURE; *UAS* AND *VAS* = SURFACE ZONAL AND MERIDIONAL WINDS; *RX1DAY* = ANNUAL MAXIMUM 1-DAY RAINFALL; *RX1DAY-RV20* = 20 YEAR RETURN VALUE FOR *RX1DAY*; *TXX* = ANNUAL MAXIMUM DAILY MAXIMUM TEMPERATURE; *TXX-RV20* = 20 YEAR RETURN VALUE FOR *TXX*; *TNN* = ANNUAL MINIMUM DAILY MINIMUM TEMPERATURE; *TNN-RV20* = 20 YEAR RETURN VALUE FOR *TNN*; *SFCWINDMAX* = ANNUAL MAXIMUM SURFACE WIND SPEED; *SFCWINDMAX-RV20* = 20 YEAR RETURN VALUE OF *SFCWINDMAX*.

MONTHLY fields	hurs	pr	psl	rsds	tas	tasmax	tasmin	uas	vas
HISTORICAL	37	47	46	45	46	42	42	19	19
RCP4.5	31	38	38	37	38	36	36	23	23
RCP8.5	30	39	39	39	37	37	36	24	24
RCP6.0	18	21	21	21	21	20	19	13	13
RCP2.6	20	28	27	26	28	24	24	18	18

DAILY fields (extremes)	rx1day	rx1day-RV20	txx	txx-RV20	tnn	tnn-RV20	sfcWind max	sfcWind max-RV20
HISTORICAL	25	25	27	27	27	27	22	22
RCP4.5	21	22	23	24	23	23	18	15
RCP8.5	24	24	25	26	26	26	18	17
RCP6.0	-	-	-	-	-	-	3	3
RCP2.6	-	-	-	-	-	-	12	12

Not all modelling centres made the same data fields available and there are (at the time of writing) gaps in the data archive globally. For example, while there are monthly rainfall data from 48 models, the maximum 1-day rainfall is only available from 31 models, highlighting the fact that different modelling centres have different priorities with respect to which model output they can contribute.

The climate models that participated in the CMIP3 experiment have been widely described in the literature over the last five years (e.g. Randall *et al.* 2007). Some of the modelling institutes have since improved the resolution in their models from CMIP3 to CMIP5 (e.g. CNRM, GISS, INM and MRI, see Table 3.3.1 for details). Overall, the average resolution has significantly improved from CMIP3 to CMIP5 and is shown for the atmospheric grid cells in Figure 3.3.1. The median size of an atmospheric grid cell has decreased from (300 x 300 km) to (200 x 200 km) and there are now global models in CMIP5 with sub-100 km grid cell size, which is approaching values usually seen in regional climate models.

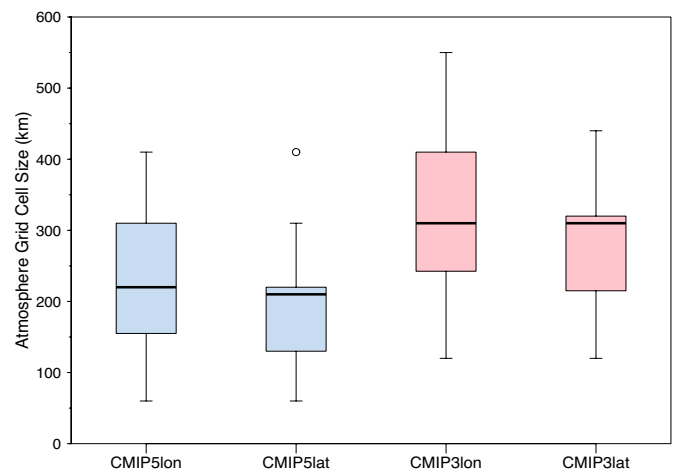


FIGURE 3.3.1: BOX-WHISKER PLOT OF GRID CELL SIZE (IN KM) IN GLOBAL CLIMATE MODEL'S ATMOSPHERE FOR CMIP5 MODELS (BLUE, FOR LONGITUDES AND LATITUDES; N=46) AND CMIP3 MODELS (PINK, N=23). THE BOX DISPLAYS THE MIDDLE 50% OF THE MODELS WHILE THE WHISKERS SHOW THE RANGE. THE CENTRE LINE IS THE MEDIAN GRID CELL SIZE. THE CIRCLE REPRESENTS AN OUTLIER MODEL (E.G. A MODEL WITH MUCH LOWER RESOLUTION COMPARED TO THE OTHER MODELS).

From CMIP3 to CMIP5, a large number of additional experiments have been included and a more detailed description can be found in Taylor *et al.* (2012). Some of the new experiments now include a biogeochemical component accounting for carbon cycles in the land, atmosphere, and ocean (Earth System Models, see “ESM” in model names of Table 3.3.1).

Most of the CMIP3 and CMIP5 models have repeated historical (and future) experiments to form an ensemble with different initial conditions (the initial state is taken in different points of the pre-industrial simulation). This provides insight into the influence of natural variability on the simulations.

A subset of CMIP5 simulations are used to examine future greenhouse gas and aerosol scenarios called representative concentration pathways or RCPs in CMIP5 (see section 3.2). The size of this subset is given by the number of models that have simulated both the current and future climate for each forcing scenario (and for all variables of interest; see Table 3.3.2). For the majority of the projection results presented in this Report, RCP2.6, RCP4.5 and RCP8.5 are used as the contribution of model runs are more complete for these scenarios (Table 3.3.2).

There are far more models and more simulations in CMIP5 than there were in CMIP3. All model data have been accessed using the global Earth System Grid (ESG), which had been setup to facilitate the movement of large data amounts across many institutes (see <https://www.earthsystemgrid.org/about/overview.htm> for details about the ESG). The main archive in Australia – which is only a subset of all the CMIP5 data available across the ESG – is located in Canberra at the National Computing Infrastructure (NCI) facility (a collaboration between ANU, CSIRO, the Bureau of Meteorology and Geoscience Australia; see <http://nci.org.au/> for details about the NCI facility) and has reached a size of over 284 terabytes – comprising over 730,000 climate data files. This is more than eight times the volume of data that was collected for CMIP3 analysis. Analysing such large data amounts requires specialised frameworks. The *Pipeline Framework* has been developed at the Centre for Australian Climate and Weather Research (CAWCR) and has been used for much of the CMIP5 processing and analysis for this Report (see <https://trac.nci.org.au/trac/cawcr/wiki/pipeline/> for more information about the Pipeline Framework).

3.4 OBSERVED GLOBAL TRENDS AND THEIR ATTRIBUTION

The latest report of the IPCC WGI (2013) concluded that “warming of the climate system is unequivocal, and since the 1950s, many of the observed changes are unprecedented over decades to millennia. The atmosphere and ocean have warmed, the amounts of snow and ice have diminished, sea level has risen, and the concentrations of greenhouse gases have increased”. Figure 3.4.1 (from IPCC, 2013) shows the observed global mean temperature record from 1850. Observed global mean temperature has risen by around 0.85 °C from 1880 to 2012, at a rate of around 0.12 °C per decade since 1951 (IPCC, 2013).

Increasing greenhouse gases have been the dominant cause of these observed changes to the climate system, along with smaller contributions from natural and other human influences.

Formal attribution has typically been based on research that uses a combination of climate modelling, instrumental climate observations, physical understanding and sometimes palaeoclimate reconstructions (use of proxies such as tree rings and ice cores to establish climate over Earth’s history) to investigate cause and effect in a climate change context.

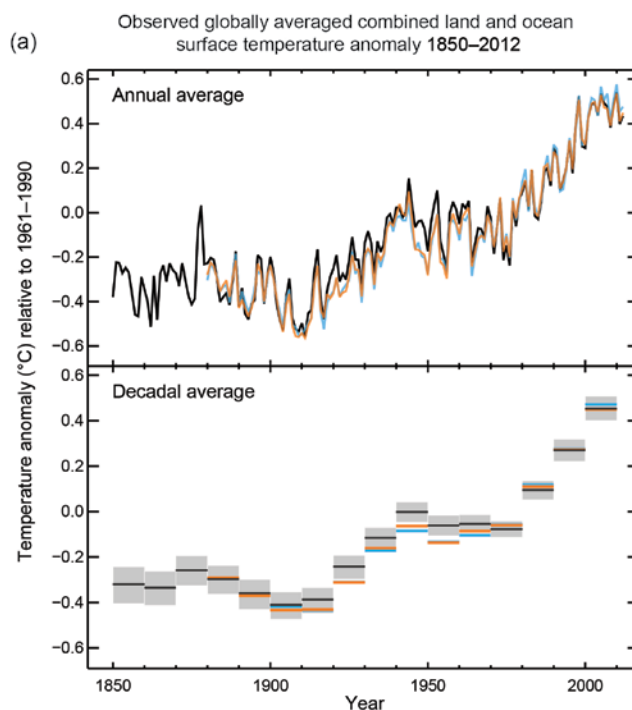


FIGURE 3.4.1: OBSERVED GLOBAL MEAN COMBINED LAND AND OCEAN SURFACE TEMPERATURE ANOMALIES (RELATIVE TO 1961–1990), FROM 1850 TO 2012 FROM THREE DATA SETS, WITH THE TOP PANEL GIVING ANNUAL MEAN VALUES AND THE LOWER PANEL DECADAL MEANS WITH AN UNCERTAINTY IN GREY FOR ONE DATA SET (SOURCE: FIGURE 5PM.1A IN IPCC, 2013).



Specifically, climate models are used to characterise both natural internal climate variability as well as changes to the climate system that are driven by changes in one or more forcing mechanisms, such as changes in greenhouse gases, changes in solar radiation and changes in volcanic aerosols. This process determines climate change ‘signals’ (or ‘responses’) associated with changes in forcing parameters that are preferably unique to those parameters. A detailed comparison of observed changes with climate model derived signals, also known as climate change fingerprints, forms the basis of formal attribution studies.

Using a variety of methods, climate change attribution also seeks to clearly distinguish intrinsic modes of climate variability such as the El Niño-Southern Oscillation, from externally forced climate change and determine the dominant causes of the observed climate change over the last century or more.

For the Second and Third IPCC WGI Assessment Reports (IPCC, 1995, IPCC, 2001), robust attribution was mostly limited to global climate change metrics. The Second Assessment Report in 1995 concluded, “The balance of evidence suggests a discernible human influence on climate”. For the Third Assessment report, optimal fingerprints of climate change (or four-dimensional spatio-temporal climate indicators) provided “new and stronger evidence that most of the warming observed in the last 50 years is attributable to human activities”.

This evidence strengthened in the two subsequent IPCC Reports. The Fifth IPCC Assessment Report (IPCC, 2013) concluded that it is extremely likely that human influence has been the dominant cause of the observed warming since the mid-20th century.

Of the observed global mean temperature increase of around 0.85 °C from 1880 to 2012 increasing greenhouse gases were likely responsible for between 0.5 °C and 1.3 °C of warming since 1951, an amount likely offset by other anthropogenic influences (mostly aerosols) responsible for temperature forcing of between -0.6 °C and 0.1 °C (IPCC, 2013). Natural forcings and intrinsic climate variability were determined to have had little influence on recent warming trends.

The Fourth and Fifth IPCC Assessment Reports included additional regional attribution studies. In general, regional attribution is much more difficult than attribution of global changes, since the signal-to-noise ratio (or the magnitude of climate change signals in comparison to intrinsic variability) is much smaller at the regional scale, where the influence of intrinsic climate modes of variability can be very large (Stott *et al.* 2010).

Similarly, while attribution of regional warming can be reasonably expected to be consistent with attribution of global warming, this is not the case for all climate variables. In the Australian context in particular, attributing rainfall

changes is a difficult task due to the strong influence of natural drivers such as the El Niño-Southern Oscillation, and the inherently large range of Australian rainfall variability.

While these considerations continue to hamper efforts to firmly attribute observed regional changes, more recent studies have demonstrated that regional attribution is increasingly possible, as the signal of warming grows larger over time (Stott *et al.* 2010). Several studies have shown a substantial anthropogenic contribution to warming over every continent except Antarctica (Hegerl *et al.* 2007, Morice *et al.* 2012, Jones *et al.* 2013). The IPCC *Fifth Assessment Report* (IPCC, 2013) noted that further evidence has accumulated for the attribution of regional climate change. Large observational uncertainties continue to impact on the ability to firmly attribute the warming observed in Antarctica.

In addition to surface and tropospheric warming, the *Fifth Assessment Report* concludes that a human influence has also been detected on a number of other climate variables. It is very likely that human influences have made a substantial contribution to upper-ocean warming (above 700 m) and global mean sea level rise since the 1970s. Anthropogenic forcing is also very likely to have influenced Arctic sea-ice loss, reduction in ice sheets and glaciers, and reduction in Northern Hemisphere snow cover. A human influence is also increasingly detected on the global water cycle since 1960 (IPCC, 2013). In a warming climate, the atmosphere can hold more water vapour, around 7 % more for every degree of global warming. Such a change represents an intensification of the hydrological cycle, expressed as increased heavy rainfall and potential evaporation in climate models. There is emerging evidence, in regions with good quality observational data, that global warming has contributed to a global-scale intensification of heavy precipitation over the second half of the 20th century (Donat *et al.* 2013b).

The *Fifth Assessment Report* also finds strengthening evidence for human influence on temperature extremes since the IPCC’s *Fourth Assessment Report and Special Report on Managing the Risks of Extreme Events and Disasters to Advance Climate Change Adaptation* (SREX) (IPCC, 2012). A recent analysis of northern hemisphere heatwaves has shown that very hot summers have increased in frequency approximately 10 fold since the 1950s (Hansen *et al.* 2012), and that a number of recent summer heatwaves (such as the European 2003 and Moscow 2010 heatwaves) have been so extreme that their probability of occurrence without global warming would be close to zero (Otto *et al.* 2012, Rahmstorf and Coumou, 2011, Stott *et al.* 2004).



3.5 GLOBAL CLIMATE CHANGE PROJECTIONS

In this section we describe global scale projections of climate change based largely on the recently released IPCC WGI *Fifth Assessment Report* (see Chapter 11, 12 and 14 in IPCC, 2013; also SPM in IPCC, 2013). The ENSO projections described below are updated in light of more recent literature (Power *et al.* 2013, Santoso *et al.* 2013)

The global average surface air temperature over the period 1850–2100 from the CMIP5 models is depicted in Figure 3.5.1. The values presented are anomalies relative to the average over the period 1986–2005. IPCC (2013) concluded that global mean surface air temperatures for 2081–2100 relative to 1986–2005 are likely to be in the following ranges: 0.3 to 1.7 °C for RCP2.6, 1.1 to 2.6 °C for RCP4.5, 1.4 to 3.1 °C for RCP6.0, and 2.6 to 4.8 °C for RCP8.5.

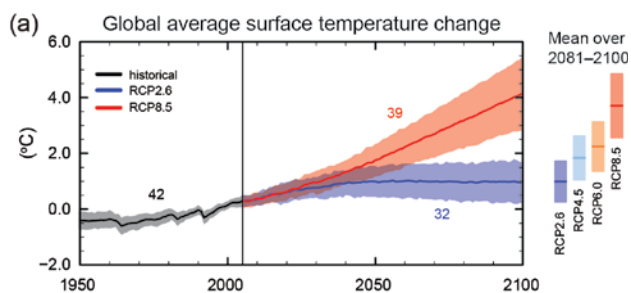


FIGURE 3.5.1: CHANGE IN GLOBAL ANNUAL MEAN SURFACE TEMPERATURE RELATIVE TO 1986–2005 AS SIMULATED BY CMIP5 MODELS. SHOWN IS THE TIME SERIES OF PROJECTIONS (BOLD LINES) AND UNCERTAINTY (SHADING) FOR SCENARIOS RCP2.6 (BLUE) AND RCP8.5 (RED). BLACK (GREY SHADING) IS THE MODELLED HISTORICAL EVOLUTION OF TEMPERATURE USING HISTORICAL RECONSTRUCTED FORCINGS. ON THE RIGHT HAND SIDE THE MEAN AND ASSOCIATED UNCERTAINTIES AVERAGED OVER 2081–2100 ARE GIVEN FOR ALL RCP SCENARIOS AS COLOURED VERTICAL BARS. THE NUMBERS OF CMIP5 MODELS USED TO CALCULATE THE MULTI-MODEL MEAN IS INDICATED (SOURCE: FIGURE SPM.7A IN IPCC, 2013).

It is important to realise that temperature changes could be higher than those depicted in Figure 3.5.1. For example, greenhouse gas concentrations might end up being larger than those assumed under the RCP8.5 scenario. Higher values might arise through the release of carbon dioxide or methane to the atmosphere from, for example, thawing permafrost from Arctic and sub-Arctic peat bogs over the 21st century. Some thawing has already occurred over Alaska, Canada and northern Russia and further thawing is expected. However, the magnitude of the increase in emissions from thawing over the 21st century is very uncertain. The latest IPCC report gave a range of 50 to 250 GtC (gigatons of carbon) over this century under the RCP8.5 scenario, but stated that confidence in this range is low. The global oceans will continue to remove anthropogenic CO₂ from the atmosphere independent of the future concentration pathway, which will lead to rising acidification of the oceans. The oceans will also continue to remove heat from the atmosphere in deeper ocean layers – a long-term process that will continue to warm the oceans for centuries (IPCC, 2013, Chapter 6).

REGIONAL CONTRASTS IN WARMING AND PRECIPITATION CHANGE

Global warming is not spatially uniform. This is illustrated in Figure 3.5.2, which shows the projected warming over the globe in 2081–2100 relative to 1986–2005 under the RCP2.6 and RCP8.5 scenarios. Under both scenarios warming tends to be greater over land than over the ocean, and warming tends to be greater over the Arctic than elsewhere. Warming tends to be weaker over several oceanic regions.

Precipitation patterns are projected to change. This is illustrated in Figure 3.5.2 (b) which shows the projected precipitation change over the globe in 2081–2100 relative to 1986–2005 under the RCP2.6 and RCP8.5 scenarios. Under both scenarios precipitation tends to increase at high latitudes and near the equator, with reductions projected to the south-west of Australia, South America and Africa, and over a band reaching from the Mid-Atlantic into the Mediterranean region.

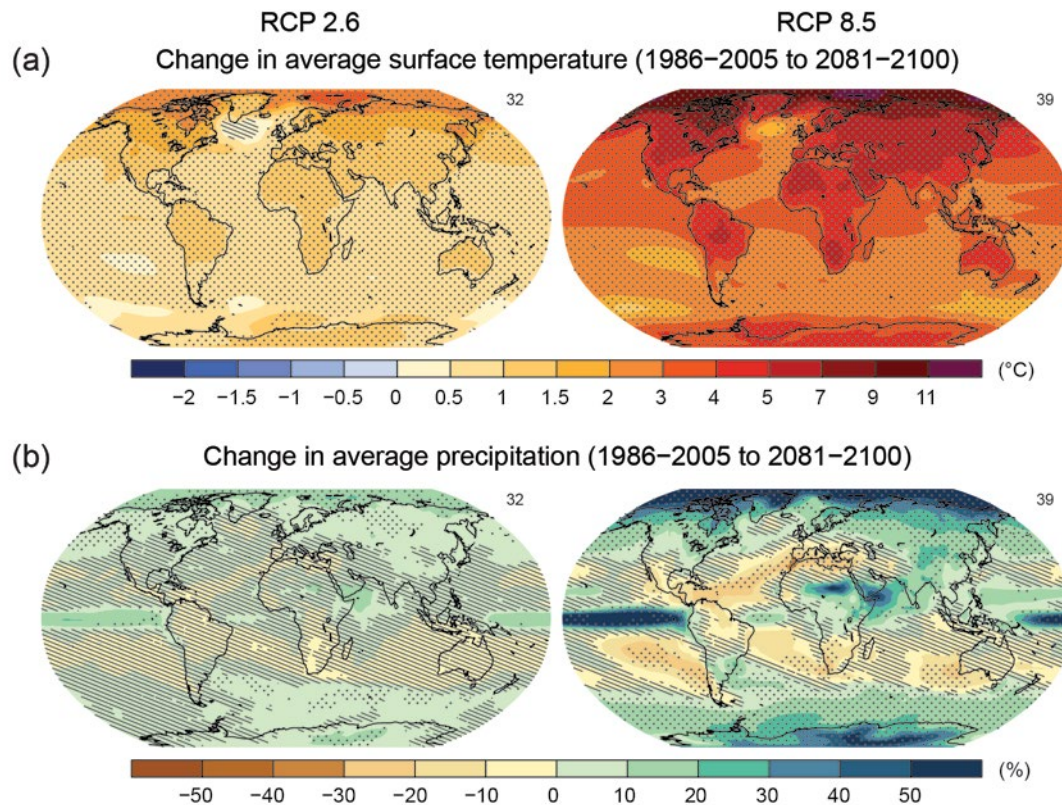


FIGURE 3.5.2: MAPS OF CMIP5 MULTI-MODEL MEAN RESULTS FOR THE SCENARIOS RCP2.6 AND RCP8.5 IN 2081-2100 OF (A) ANNUAL MEAN SURFACE TEMPERATURE CHANGE AND (B) AVERAGE PER CENT CHANGE IN ANNUAL MEAN PRECIPITATION. CHANGES ARE SHOWN RELATIVE TO 1986-2005. THE NUMBER OF CMIP5 MODELS USED TO CALCULATE THE MULTI-MODEL MEAN IS INDICATED IN THE UPPER RIGHT CORNER OF EACH PANEL. HATCHING INDICATES REGIONS WHERE THE MULTI-MODEL MEAN IS SMALL COMPARED TO INTERNAL VARIABILITY (*I.E.* LESS THAN ONE STANDARD DEVIATION OF INTERNAL VARIABILITY IN 20-YEAR MEANS). STIPPLING INDICATES REGIONS WHERE THE MULTI-MODEL MEAN IS LARGE COMPARED TO INTERNAL VARIABILITY (*I.E.* GREATER THAN TWO STANDARD DEVIATIONS OF INTERNAL VARIABILITY IN 20-YEAR MEANS) AND WHERE 90 % OF MODELS AGREE ON THE SIGN OF CHANGE (SOURCE: FIGURE SPM.8 IN IPCC, 2013).

Projected changes in temperature and precipitation for the next few decades show spatial patterns of change similar to those projected for the late 21st century described above, but with smaller magnitude. Internal variability will continue to be a major influence on climate, particularly in the near-term and at the regional scale.

PROJECTED CHANGES IN SELECTED CLIMATE FEATURES

The IPCC (2013) states that global warming will cause more hot and fewer cold days and seasons over most land areas (*virtually certain* in their assessment) and that heat waves will occur with a higher frequency and duration (*very likely* in their assessment). Occasional cold winter extremes will continue to occur. Additionally, extreme precipitation events over most of the mid-latitude land masses and over wet tropical regions will become more intense and more frequent by the end of this century, as global mean surface temperature increases (*very likely* assessment in IPCC, 2013). This increase stems mostly from the greater moisture holding capacity of a warmer atmosphere (IPCC, 2013) as

well as a potential for increased vertical velocity of air masses under enhanced greenhouse warming (O’Gorman and Schneider, 2009).

The global monsoon system contributes greatly to the water cycle on Earth. The relevant regional monsoon system for Australia is described in more detail in Section 4.1, with projections in Chapter 7. On the global scale, however, the region affected by the monsoons is projected to increase over the 21st century, together with monsoon rainfall and intensity (IPCC, 2013, Chapter 12). These increases are understood to be related to the increases in atmospheric moisture under enhanced warming. At the same time, monsoon winds are projected to weaken due to the slowing of the global tropical circulation (IPCC, 2013, Chapter 12). Monsoon onset dates are projected to become earlier or not to change much, while monsoon retreat dates are projected to be delayed, resulting in lengthening of the monsoon season in many regions (IPCC, 2013, Chapter 12).

The IPCC report (Chapter 12 in IPCC, 2013) also concluded that “there is *high confidence* that the El Niño-Southern Oscillation (ENSO, see Section 4.1 for a more detailed

description) will remain the dominant mode of year to year variability in the tropical Pacific, with global effects in the 21st century. Due to the increase in moisture availability, ENSO-related precipitation variability on regional scales will *likely* intensify. Natural variations of the amplitude and spatial pattern of ENSO are large and thus *confidence* in any specific projected change in ENSO and related regional phenomena for the 21st century remains *low*". Additionally, more recent work concluded that global warming will intensify El Niño-driven drying in the western equatorial Pacific and further increase El Niño driven rainfall increases in the central and eastern Pacific during El Niño (Power *et al.* 2013, Cai *et al.* 2014).

The Indian Ocean Dipole (IOD, see Section 4.1 for a more detailed description) is associated with droughts in Indonesia, reduced rainfall over parts of Australia, intensified Indian summer monsoon, floods in East Africa, hot summers over Japan, and anomalous climate in the extra-tropical Southern Hemisphere (IPCC, 2013). Positive IOD has led to below average winter and spring rainfall across central and southern Australia. The overall frequency of IOD events (positive and negative) is not projected to change (Ihara *et al.* 2008, IPCC, 2013, Cai *et al.* 2013).

Changes in the Southern Annular Mode (SAM, see Section 4.1 for more detail) have an influence on the climate of Antarctica, Australasia, southern South America and South Africa (Watterson, 2009, Thompson *et al.* 2011 and references therein). In the past few decades the SAM index (describing the phase of this mode) has exhibited a positive trend in southern summer and autumn (Marshall, 2007, Jones *et al.* 2009b), a change attributed to the effects of ozone depletion and the increase in greenhouse gases (Thompson *et al.* 2011, IPCC, 2013). These two factors will continue to be the principal drivers into the future (assessed as likely in Chapter 14 in IPCC, 2013).

3.6 COMPARISON OF CMIP3 AND CMIP5 GLOBAL PROJECTIONS

The IPCC (2013, Chapter 12) provides a general comparison of CMIP3 and CMIP5 projections, but it is particularly worthwhile to compare the projections for Australia using the method applied in used in CSIRO and BOM (2007). As described further in Section 6.2 (and in Watterson, 2008), the comparison assumes that 'pattern scaling' applies, *i.e.* that there is a dominant climate change response pattern, and each location has a sensitivity or change 'per degree of global warming'. Consistent with this, it is assumed that a 'probability density function' (PDF) for change in a variable at a certain time and location can be obtained by combining a distribution for the global warming for that time with a distribution for the local sensitivity to warming. Maps of changes over Australia calculated using CMIP5 results are presented in later sections, and a comparison with maps from CMIP3 is made in Appendix A. The focus of this section is the difference between CMIP3 and CMIP5 on the larger scale, including the global warming.

3.6.1 GLOBAL SENSITIVITY OF THE CMIP3 AND CMIP5 MODELS

The probability distribution for the global warming used in the pattern scaling method provides a convenient representation of the global warming from the models. Given that the range of global surface warming from a model ensemble tends to be proportional to the median warming at the time (see for example CMIP5 results in Figure 3.5.1) it is assumed that a single shape of distribution holds for that ensemble. The shape has been derived from the near-linear trends during the 21st century projected under RCP8.5. The 100-year trend results from 40 CMIP5 models are shown in Figure 3.6.1. Three distributions for the change, which have the same mean and standard deviation as the ensemble, are shown. The beta form (a standard theoretical distribution), which also matches the range, is used as the global warming PDF. This CMIP5 PDF has a similar relative spread to the CMIP3 PDF (illustrated in CSIRO and BOM, 2007, Figure 4.6), with the ratio of the standard deviation to the mean being 19 % for CMIP5, compared to 21 % for CMIP3.

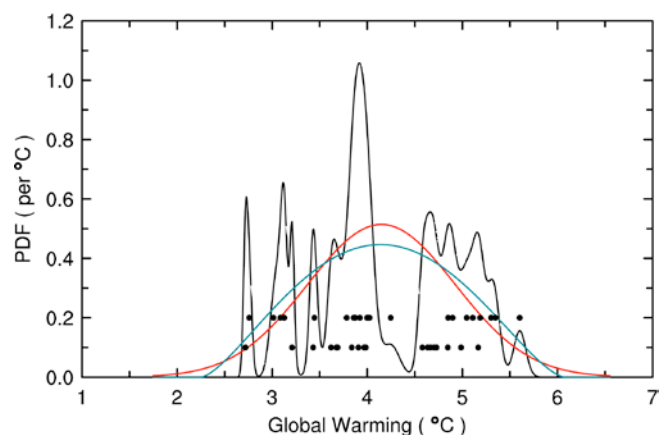


FIGURE 3.6.1: GLOBAL MEAN WARMING TRENDS (X 100 YEARS) OVER 2001–2100 FOR 40 CMIP5 MODELS, UNDER RCP8.5, SHOWN AS DOTS, WITH EARTH SYSTEM MODELS BEING THE UPPER SET. THE AVERAGE OF THE INDIVIDUAL PDFS (CENTRED ON EACH TREND, ALLOWING FOR STATISTICAL UNCERTAINTY) IS THE BLACK LINE. THE NORMAL DISTRIBUTION WITH THE SAME MEAN AND STANDARD DEVIATION IS RED. THE BETA FIT USED AS THE GLOBAL WARMING PDF IS BLUE.

The climate change from 1986–2005 to 2080–2099 under the RCP8.5 scenario is used as a standard case for presentation. The global warming from the multi-model mean is 3.7 °C, and the beta PDF has been scaled to have this mean. The 5th to 95th percentile range of the PDF is then 2.6 to 4.8 °C, which matches the range for this case given by the IPCC *Fifth Assessment Report* (IPCC, 2013).

The actual warming projected by a model depends on the forcing and the global sensitivity to it. Direct comparison of the CMIP3 and CMIP5 sensitivities is hampered by the different scenarios used (section 3.5). However, based on a range of studies and methods, the *Fifth Assessment Report* found that there is 'no fundamental difference' in the



overall sensitivities of the two ensembles. For the purpose of comparison in Appendix A, the beta PDF used in 2007 has been scaled to the same mean value of 3.7 °C.

The accuracy of the CMIP5 ensemble as representing the possible response of the real world has been assessed at length by the IPCC in the *Fifth Assessment Report* (IPCC, 2013), with particular consideration of the implications of the slower rate of warming in the past decade in estimates of the (real-world) global mean surface temperature. This is an active area of research with some recent work highlighting natural variability as likely to be the major cause of the difference between CMIP5 models' surface temperature and that observed in the past decade. England *et al.* (2014) found that an observed variation in winds over the Pacific Ocean, not captured by models, has led to enhanced uptake of heat by the subsurface ocean. They noted that if the winds returned to their usual state, there could potentially be a rapid upturn in surface temperature trends, similar to that which occurred after 1975.

However, given uncertainties in future ocean heat uptake, carbon cycle feedbacks and other processes not well represented in models (section 3.2.1), the *Fifth Assessment Report* authors assessed the existing CMIP5 range of global warming for 2080–2099 as a 'likely' range (more than 66 % probability), rather than the 90 % range from the PDF used here. A similar position was taken by the *Fourth Assessment Report*, in relation to the CMIP3 range, as used in the 2007 projections (IPCC, 2007).

3.6.2 MODEL RESPONSES TO GLOBAL WARMING IN THE ASIA-PACIFIC REGION

The local sensitivity to global warming used in the pattern scaling method is determined from the individual responses or 'change per degree' fields from models (see definition above). These are determined from yearly values over the whole 21st century. The fields from the CMIP3 and CMIP5 ensembles are compared here for the Asia-Pacific region that is especially important to Australian climate.

The ensemble mean and standard deviations for the temperature response (a non-dimensional ratio of local to global warmings) from CMIP3 and CMIP5 are shown in Figure 3.6.2. The patterns for both statistics are very similar. Over all land except for some coasts, the mean warming is larger than the global mean (as indicated by a value over one). The equatorial Pacific Ocean has relatively high values, but they are a little lower in CMIP5. High values also hold in the western Tasman Sea for both ensembles, while the Southern Ocean warms less. For both ensembles, the standard deviation over Australia and the central Pacific is double that of the regional ocean, except farther south. In fact, the variation in the 'NINO3.4' region (5°S–5°N, 170°W–120°W) is even larger in CMIP5. However, the result for CMIP5 is strongly affected by a single model (FGOALS-g2) that displays an unusual projection in this region.

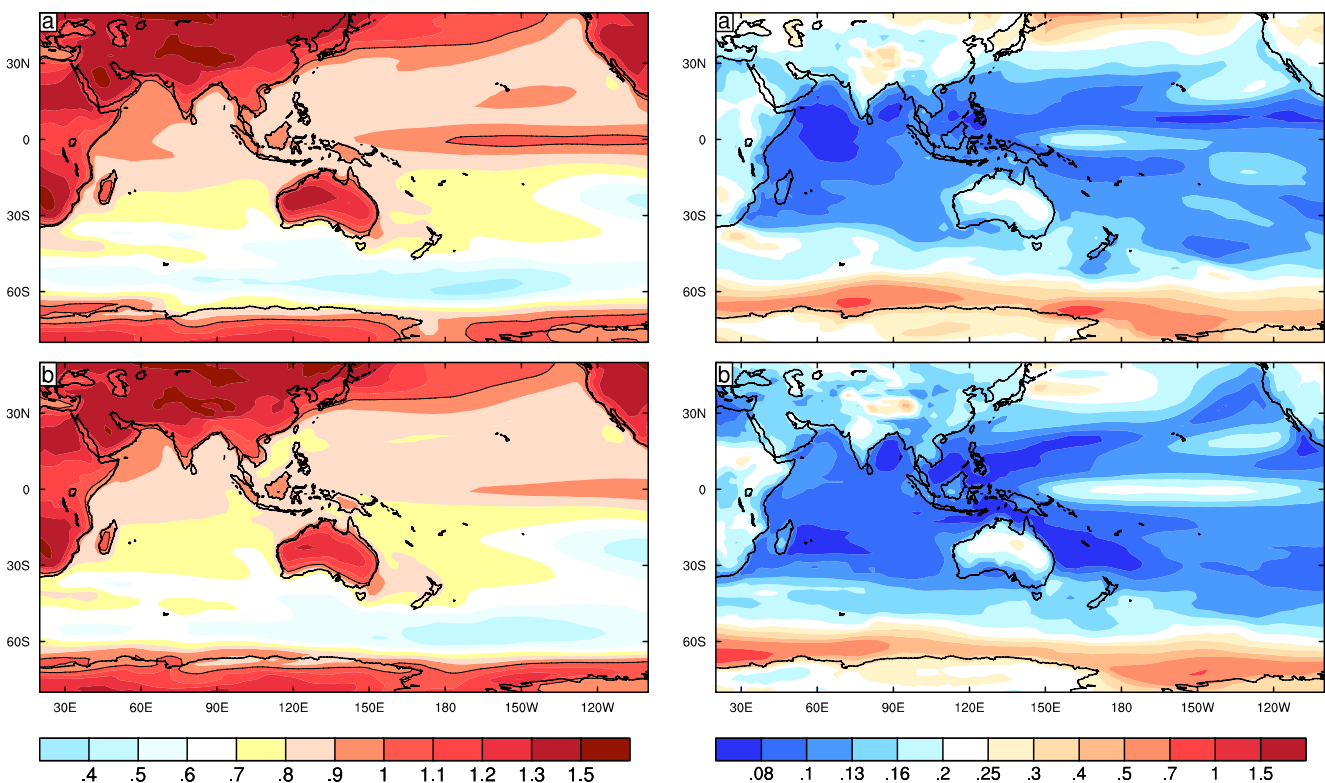


FIGURE 3.6.2: LEFT: ENSEMBLE MEANS OF THE TEMPERATURE 'CHANGE PER DEGREE' FIELDS (NON-DIMENSIONAL): (A) CMIP3 (24 MODELS) AND (B) CMIP5 (40 MODELS). RIGHT: THE ENSEMBLE STANDARD DEVIATIONS (A) CMIP3 AND (B) CMIP5.

-20° -10° 0° 10° 20° 30° 40° 50°

Change per degree fields for rainfall, determined as a percentage of the present climate means of each model, have been evaluated, and again are similar in the two ensembles, as seen in Figure 3.6.3. Declines in the ensemble means occur in most of the sub-tropics, especially in the south-west of Australia. The decline in central and eastern Australia is smaller in CMIP5. Over most subtropical regions the standard deviation across each ensemble is relatively large, and changes of both signs occur in individual models.

These local sensitivities in temperature, rainfall and other variables, explain much of the spatial variation in the future changes. Furthermore, as shown by Watterson (2012) for CMIP3, much of the range of change over Australia can be linked to the range in the low-latitude ocean temperature changes, through ENSO and IOD-like patterns. With the ensemble mean warming in the NINO3.4 region being larger than in surrounding oceans (Figure 3.6.2b), the pattern in the mean change has often been described as ‘El Niño-like’. Given the usual pattern of interannual variability in ENSO, the small mean drying over eastern Australia in the ensemble means (Figure 3.6.3b) could be interpreted as being a consequence of the El Niño-like change (see Section 4.1 for more detail on how these global modes of variability affect Australian climate). The range of the warming in the NINO3.4 region across the CMIP5 models, as inferred from Fig.3.6.2d, can likewise be inferred as driving part of the range in Australian future changes in rainfall and other variables.

The effect of this tropical sea surface temperature (SST) driver can be demonstrated by forming an index by area-averaging the individual annual change per degree fields (determined from the RCP8.5 simulations) over the NINO3.4 region. The correlation coefficient between the index values from 40 models with the Australian mean of the rainfall changes (in % per degree) from the models is -0.79 . Correlations between the index and rainfall changes at most locations in eastern Australia are nearly as large. Thus models with a higher than average change in the index simulate a larger than average decline in rainfall. For CMIP3, Watterson (2012) found that an alternative tropical ocean index that quantified the difference between the western Pacific and east Indian Ocean temperature trends was even more effective. SST anomalies in these two regions tend to drive opposite directions of change in Australian rainfall. Even for CMIP5, this ‘Pacific Indian Dipole’ index has a correlation with Australian rainfall trends of -0.78 . The variation in the east Indian region is smaller in CMIP5 (comparing Figures 3.6.2 a and b), but the dipole index still provides a simple description of the tropical SST driver: models that warm more/less in the Pacific than the Indian tend to have declining/increasing Australian rainfall. Ideally, assessments of mechanisms (such as that of Weller and Cai, 2013b) might provide insight into the possible realism of trends in such mode indices, and hence rainfall.

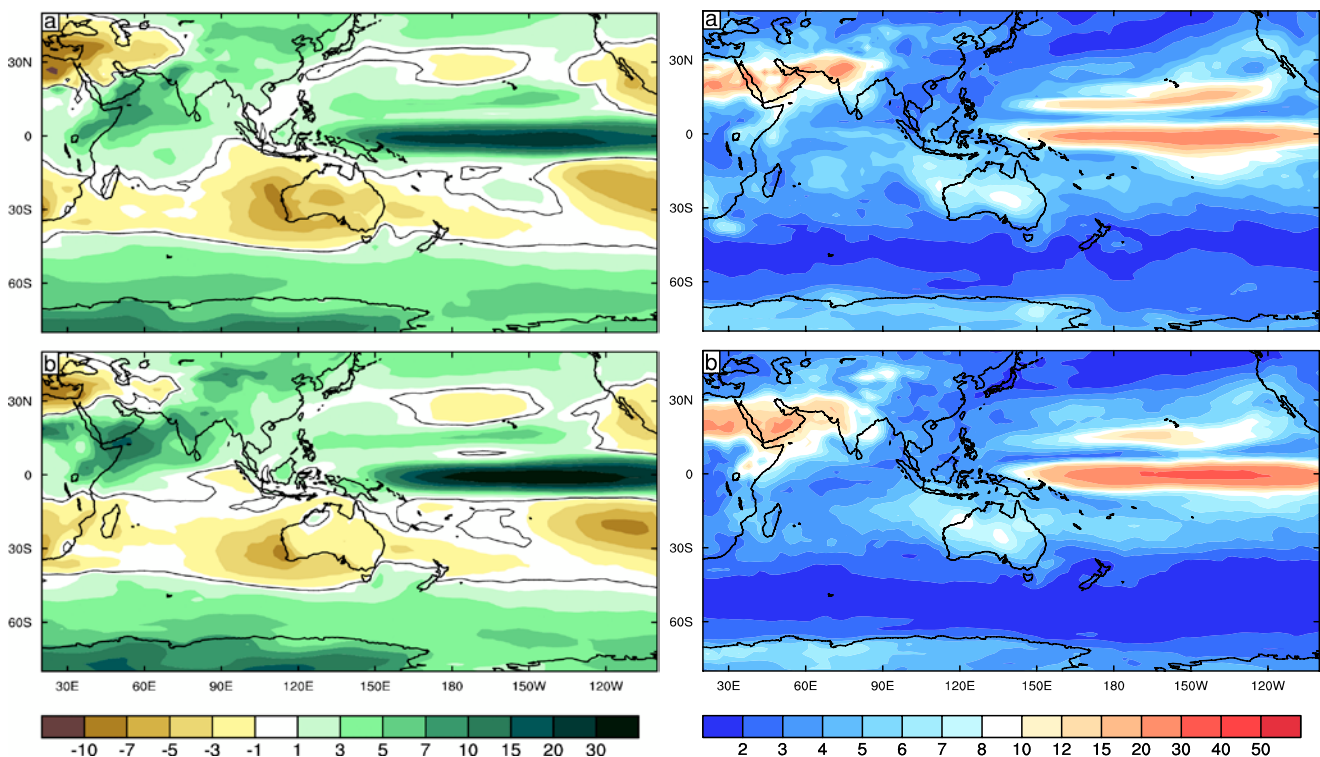


FIGURE 3.6.3: LEFT: ENSEMBLE MEANS OF THE RAINFALL ‘CHANGE PER DEGREE (OF GLOBAL WARMING)’ FIELDS (AS A PERCENTAGE OF PRESENT CLIMATE): (A) CMIP3 (24 MODELS) AND (B) CMIP5 (40 MODELS). RIGHT: THE ENSEMBLE STANDARD DEVIATIONS (A) CMIP3 AND (B) CMIP5.



CHAPTER FOUR

UNDERSTANDING RECENT AUSTRALIAN CLIMATE

FALLEN ARM AFTER FIRE, VICTORIA, ISTOCK

-20° -10° 0° 10° 20° 30° 40° 50°



CHAPTER 4 UNDERSTANDING RECENT AUSTRALIAN CLIMATE

This chapter describes current climate variability over Australia and its drivers (Section 4.1), and observed climate trends and potential causes. The understanding presented in this chapter contributes to the interpretation of the GCM-simulated climate projections and assessing our confidence in the projections (Chapters 5 and 7). Note that this chapter only deals with observed aspects of atmospheric and terrestrial variables. Observations of sea level and the marine climate are discussed in Chapter 8 alongside projections in those variables.

4.1 AUSTRALIAN CLIMATE VARIABILITY

The Australian continent spans over 30° of latitude, from the tropics in the north to the mid-latitudes in the south. As a result, Australia is affected by many different weather systems and climate variability is driven by many significant climate features. Tropical systems affect the north, where there are two main seasons defined by very distinct mean rainfall: the wet season from November to April and the dry season from May to October. To the south the influence of the tropical systems decreases and extra-tropical weather and climate features become dominant. The annual cycle in rainfall becomes weaker but the temperature contrast between winter and summer increases and four distinct seasons exist.

The many different weather and climate features that affect Australia are summarised in Figure 4.1.1 (from Risbey *et al.* 2009b). The main tropical weather features (modes) and their influences are described in section 4.1.1 and the extra-tropical modes are described in Section 4.1.2.

4.1.1 TROPICAL MODES

On the seasonal time-scale most of the northern tropics experience distinct wet and dry seasons, their contrast increasing further north as the influence of the Australian monsoon increases. The monsoon has the strongest influence in northern Australia from late December, when the prevailing easterly winds turn westerly, until March, when it retreats to the north (following the sun) and easterly winds and dry conditions return. The monsoon is driven by the summer heating of the Australian continent and the resulting change in land-sea temperature gradients. It brings high rainfall for much of November to April, but the wet season consists of active (wet) and break (dry) periods of one to several weeks.

The monsoon breaks are partly determined by the phases of the Madden-Julian Oscillation (MJO). The MJO is an eastward moving tropical disturbance of high convection and rainfall with a mean frequency of 40-50 days. As the MJO moves across Australian longitudes it brings enhanced

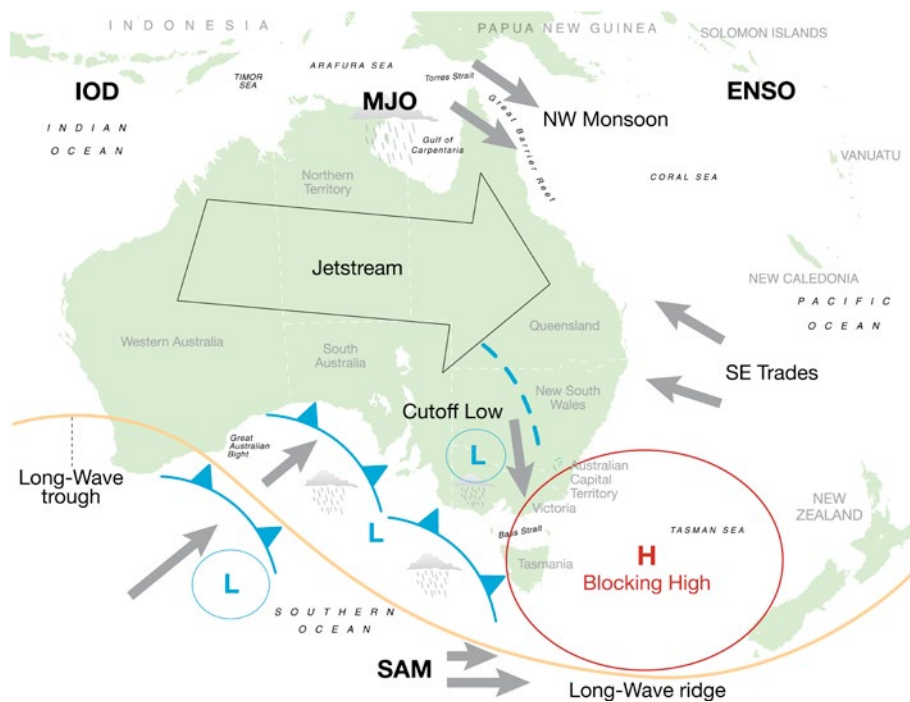


FIGURE 4.1.1: SCHEMATIC SHOWING THE MAIN WEATHER AND CLIMATE FEATURES AFFECTING AUSTRALIAN CLIMATE VARIABILITY (SOURCE: RISBEY *ET AL.* 2009B).

rainfall, and each of its phases have been found to be associated with preferred rainfall anomalies over the continent (Wheeler *et al.* 2009).

The northern wet season is also the tropical cyclone (TC) season in Australia. Most TCs occur between November and April, with a mean of 11 TCs affecting the Australian continent per year during the period from the 1981/1982 wet season to the 2012/2013 wet season (Dowdy *et al.* 2014).

The above weather and climate features are modulated from year to year by the main modes of natural tropical climate variability, namely the El Niño Southern Oscillation (ENSO) and the Indian Ocean Dipole (IOD). ENSO originates in the Pacific Ocean and is the major driver of global interannual climate variability (Ropelewski and Halpert, 1989). Its link to Australian climate variability has long been known

(*e.g.* McBride and Nicholls, 1983). ENSO is a coupled ocean-atmosphere mode, with strong interaction between the tropical atmospheric circulation and the Pacific Ocean (Philander, 1990). Under normal conditions (the ENSO “neutral” phase), the trade winds and Pacific sea surface temperatures (SST) are in balance. The easterly equatorial trade winds feed into the strong convection over the West Pacific Warm Pool, which in summer brings moisture and rainfall to the tropics. In some years the trade winds weaken or reverse, the Warm Pool expands eastward and convection moves away from Australian longitudes. During these ‘El Niño’ conditions, SSTs are warmer in the eastern Pacific and cooler around northern Australia compared to neutral conditions. As a result rainfall is often below average over much of eastern Australia and TCs are less likely in the Coral Sea. In some other years, the trade winds strengthen, the eastern Pacific cools and SST around northern Australia are warmer than average, leading to enhanced convection over northern Australia and TCs are more likely to form close to Australia. During these ‘La Niña’ conditions the enhanced convection leads to increased moisture availability and so rainfall is often above average over eastern Australia. Australia’s wettest two-year period on record, 2010–11, was associated with a strong, prolonged La Niña in addition to a strong negative phase of SAM (see 4.1.2) (Hendon *et al.* 2014). The effects of ENSO in northern Australia are direct, through changes in SST around Australia and the enhancement or suppression of convection. As ENSO affects SST and surface winds, its phases drive interannual variability in the timing of the onset of the monsoon, and the movement of the MJO. The strongest influences of ENSO on Australian rainfall are in spring and summer. El Niño and La Niña events are natural variations in the climate system and occur on average every 4–7 years, but ENSO and its impacts display significant variability on decadal time scales (Power and Colman, 2006).

The IOD is active in the tropical Indian Ocean but influences interannual climate variability across tropical and extra-tropical Australia. The IOD is characterised by changes in SST off the Sumatra coast in the eastern Indian Ocean basin and changes of the opposite sign in the west of the

basin (Saji *et al.* 1999). Low SST in the east (and high in the west) is known as the positive phase of the IOD (see also section 3.5) and comes about when south-east winds off the north-west of Australia induce upwelling in the eastern Indian Ocean (England *et al.* 2006). The IOD is usually active from May to November and is often terminated by the wind reversal accompanying the arrival of the monsoon in northern Australia. A positive IOD has been found to cause heavy rains in eastern Africa and droughts over Indonesia (Yamagata *et al.* 2004), and it can also lead to below average rainfall in winter and spring over central and southern Australia (Risbey *et al.* 2009b). Those regions can receive above average rainfall during the negative phase of IOD, when eastern Indian Ocean SSTs are above average.

Many of the Australian impacts of the IOD are independent of ENSO, but certain ENSO and IOD phases tend to occur concurrently. Meyers *et al.* (2007) found that positive IOD events are more likely during El Niño years and negative IOD events were more frequent during La Niña. They found that a negative IOD event had never been observed during an El Niño.

4.1.2 EXTRA-TROPICAL MODES

Not all climate variability in Australia is due to modes of tropical variability like ENSO and the IOD. The southern part of the Australian continent is affected by a number of extra-tropical weather features and modes of variability in the mid-latitudes. This region is located under the descending (dry) branch of the Hadley circulation, resulting in relatively dry air and little rainfall and the formation of high pressure systems.

The high pressure centres are the predominant extra-tropical weather features and their averaged signature on the climatic time-scale is a band of high pressure: the subtropical ridge (STR). The STR is weaker and located further south in summer but stronger and further north in winter (Drosowsky, 2005).

A band of strong westerly winds and storms encircles Antarctica (‘the Roaring 40s and 50s’; Sturman and Tapper, 2006), and while the preferred tracks of the centres of the storms (the “storm track”) are generally south of Australia (Simmonds and Keay, 2000), the fronts associated with these storms have a major impact. They are most significant for southern Australian rainfall and temperatures during winter and spring when the STR and the storm track are located furthest north. During summer, they bring the classic ‘cool change’ and the associated strong winds, fire danger (Mills, 2005) and dust events (Trewin, 2002). They, along with cut-off lows, are a major source of rainfall across southern Australia (Risbey *et al.* 2009a,b, Pook *et al.* 2012). Two recent climatologies (Berry *et al.* 2011, Simmonds *et al.* 2012) indicate the prevalence of fronts, particularly cold fronts, across southern Australia.

The northern extent of the westerlies can shift north and south on a range of timescales, influencing rainfall variability across southern Australia. The north-south shift in the westerlies and the low pressure systems is also



part of the hemispheric mode of variability known as the Southern Annular Mode (SAM) (Thompson and Wallace, 2000). The SAM reflects the variability in the hemispheric pattern of low pressure around Antarctica and high pressure over Australia. Higher values of the SAM index mean higher pressures over Australia, and a southward shift of the band of westerlies and storm track. The impact of SAM varies with location and season (Hendon *et al.* 2007). In winter in southern Australia a positive SAM phase has low pressure systems shifted to the south, thus shifting rainfall away from south-eastern Australia. In spring and summer a positive SAM phase shifts the westerlies southward so easterly winds are more common over the Eastern Seaboard, bringing above average rainfall. Over recent decades there have been trends towards the positive phase of SAM (primarily in summer), principally due to stratospheric ozone depletion (Arblaster and Meehl, 2006) and a more intense and further southward located STR (primarily during the cooler half of the year: Timbal and Drosowsky, 2013). These trends have affected rainfall in the south of the country, particularly in the south-west and the south-east where cool season rainfall has fallen significantly since the early 1970s (south-west) and 1990s (south-east). See section 4.2 for more details.

Low pressure systems sometimes develop in the region to the north of the westerlies and the storm track. Known as 'cut-off lows', these bring large rainfall totals to southern Australia (Pook *et al.* 2012). On the eastern Australia coast, cut-off lows are commonly referred to as East Coast Lows. These storms are responsible for some of the most damaging natural disasters in Australia's history due to the extreme winds, waves and rainfall (McInnes *et al.* 2002; Mills *et al.* 2010; Dowdy *et al.* 2014). East Coast Lows can also have positive impacts on the Eastern Seaboard of Australia, being responsible for major inflows to water catchments (Pepler and Rakich, 2010, Dowdy *et al.* 2013b). Large-scale atmospheric and oceanic variability (including ENSO, SAM, the intensity of the subtropical ridge and the strength of the East Australian Current, but excluding blocking) do not appear to have a significant influence on East Coast Low occurrence (Dowdy *et al.* 2013c). The climate of the Eastern Seaboard of Australia is distinct from the rest of eastern Australia in that it is not affected by large-scale environmental influences (such as ENSO) in the same way as other parts of eastern Australia (Risbey *et al.* 2009b; Timbal and Hendon, 2011). Eastern Australia is also a favoured location for the formation of extra-tropical cyclones, as indicated by frequent upper-tropospheric disturbances over this region (Dowdy *et al.* 2013c). These are likely related to phenomena such as persistent high pressure systems known as atmospheric blocking (Pook *et al.* 2013) and a prevalent split in the subtropical jet over eastern Australia during winter (Grose *et al.* 2012).

4.2 OBSERVED TRENDS AND ATTRIBUTION IN THE AUSTRALIAN REGION

4.2.1 TEMPERATURE

AVERAGE SURFACE TEMPERATURE

Australian temperatures have warmed by 0.9 °C since 1910, with more warming in night time minimum temperature than daytime maximum temperature based on the homogenised daily Australian Climate Observation Reference Network – Surface Air Temperature (ACORN-SAT) data (Trewin, 2013, Fawcett *et al.* 2012). Figure 4.2.1 shows mean temperature (the average of maximum and minimum temperature) changes across Australia from 1950 to 2013. Warming has been apparent in all seasons and all States and Territories. 2013 was Australia's warmest year since records began in 1910 (BOM, 2014b).

Regional climate change attribution studies have shown significant consistency between observed increases in Australian temperatures and those from climate models forced with increasing greenhouse gases (Hegerl *et al.* 2007, Karoly and Braganza, 2005). By extension, many aspects of warming over Australia are also attributable to the enhanced greenhouse effect.

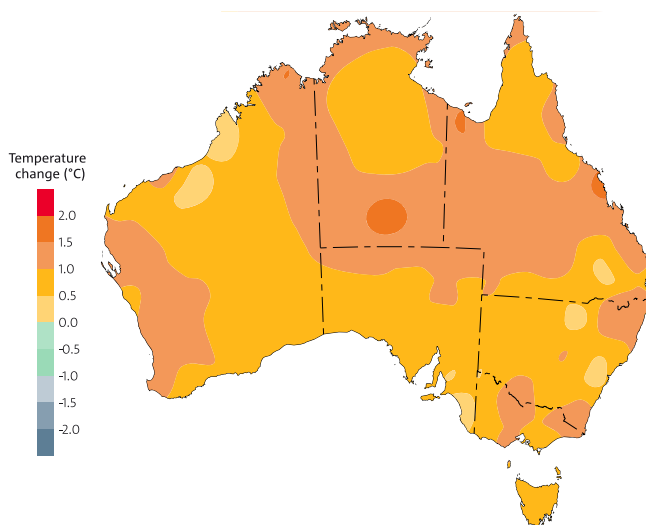


FIGURE 4.2.1: LINEAR TREND IN AUSTRALIAN MEAN TEMPERATURE FROM THE AUSTRALIAN CLIMATE OBSERVATIONS REFERENCE NETWORK (ACORN-SAT) CALCULATED FOR THE ENTIRE PERIOD 1910 TO 2013 (SOURCE: BOM, 2014A).



TEMPERATURE EXTREMES

The mean temperature changes have been accompanied by a large increase in extreme temperatures. Since 2001, the number of extreme heat records in Australia has outnumbered extreme cool records by almost 3 to 1 for daytime maximum temperatures, and almost 5 to 1 for night-time minimum temperatures (Trewin and Vermont, 2010, Trewin and Smalley, 2013). Very warm months (those with monthly averaged temperature above the second standard deviation of monthly temperatures from a 1951-1982 reference period) have increased five-fold in the past 15 years. The frequency of very cool months has declined by around a third over the same period (Fawcett *et al.* 2013). Figure 4.2.2 shows trends in days above 35 °C across Australia, while Figure 4.2.3 shows trends in the temperature of the coldest night since 1950.

The changes in the frequency of temperature extremes have been shown to be directly related to warming trends. These changes include recent, significant increases in the frequency of high-temperature extremes and decreases in the frequency of low temperature extremes (Trewin and Vermont, 2010, Trewin and Smalley, 2013), and increases in the duration, frequency and intensity of heatwaves in many parts of the country (Perkins *et al.* 2012; Alexander and Arblaster, 2009; Alexander *et al.* 2006).

Extreme heat was experienced during the Australian summer of 2012-2013. Near-surface air temperatures and regional sea-surface temperatures for the December to February period were the highest on record for Australia. This period also included Australia's area-averaged hottest month, hottest week and hottest day on record, and the longest and most spatially extensive national heatwave on record (BOM, 2013a). Analysis with forced and unforced climate model simulations show that increasing greenhouse gases lead to a five-fold increase in the odds of Australia recording the temperatures experienced in January 2013 (Lewis and Karoly, 2013; 2014).

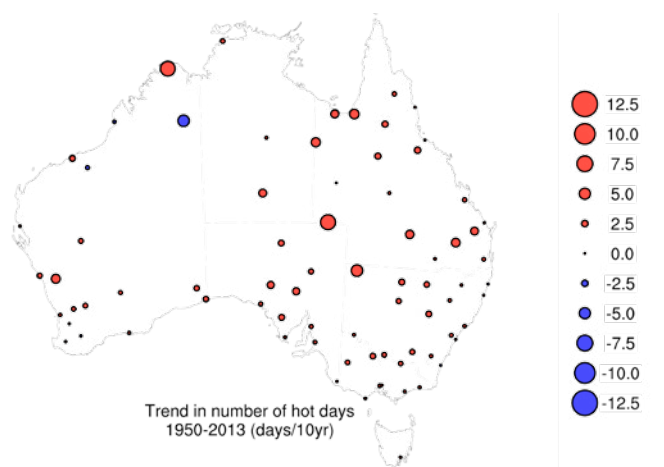


FIGURE 4.2.2: TRENDS IN THE NUMBER OF HOT DAYS (GREATER THAN 35 °C) IN AUSTRALIAN MEAN TEMPERATURE FROM THE AUSTRALIAN CLIMATE OBSERVATIONS REFERENCE NETWORK OF SURFACE AIR TEMPERATURE (ACORN-SAT) FROM 1950 TO 2013 (SOURCE: BUREAU OF METEOROLOGY).

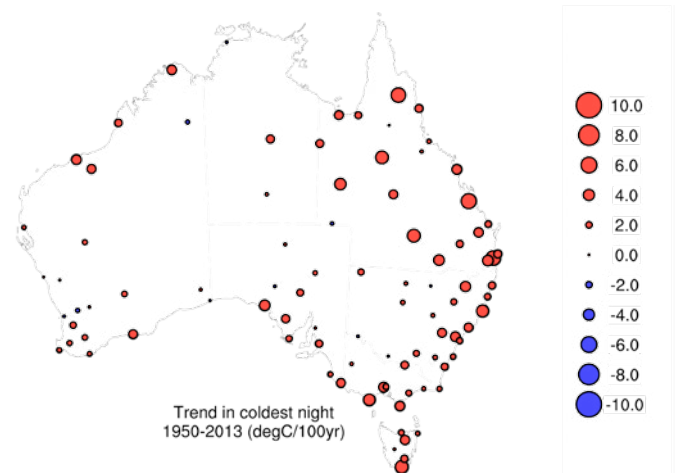


FIGURE 4.2.3: TRENDS IN THE COLDEST NIGHT (°C) IN AUSTRALIAN MEAN TEMPERATURE FROM THE AUSTRALIAN CLIMATE OBSERVATIONS REFERENCE NETWORK OF SURFACE AIR TEMPERATURE (ACORN-SAT) FROM 1950 TO 2013 (SOURCE: BUREAU OF METEOROLOGY).

4.2.2 RAINFALL

Attributing observed regional rainfall changes is a more difficult task than attributing temperature changes. This is especially so in the Australian region, where intrinsic rainfall variability on year to year and decade to decade timescales is large. The following sections cover rainfall in the warmer months (the wet season in northern Australia), the cooler months (the wetter season in much of southern Australia) and heavy rainfall throughout the year. Deciles for the recent period 1997-2013 are shown to illustrate recent changes (linear trends in various seasons and through various periods can be explored at the Bureau of Meteorology Tracker - <http://www.bom.gov.au/climate/change>).

AUSTRALIAN WARM SEASON RAINFALL

Northern Australian wet season (October to April) rainfall has shown wet and dry decades through the 20 century but with a slight increase indicated in the linear trend in 1900-2012. In recent decades, increases are discernible across northern and central Australia, with the increase in summer rainfall most apparent since the early 1970s (Figure 4.2.4; Braganza *et al.* 2011), and has been large enough to increase total Australian rainfall (averaged over the entire continent) by about 50 mm when comparing the 1900 to 1960 period with 1970 to 2013. Rainfall during the months of October to April from 1997 to 2013 was very much above average over large parts of the continent (Figure 4.2.5). The period 2010 to 2012 recorded the highest 24-month rainfall totals for Australia as a whole, in conjunction with two strong La Niña events. The statistical significance of trends in monsoonal rainfall is difficult to determine due to high intrinsic variability in the summer monsoon.

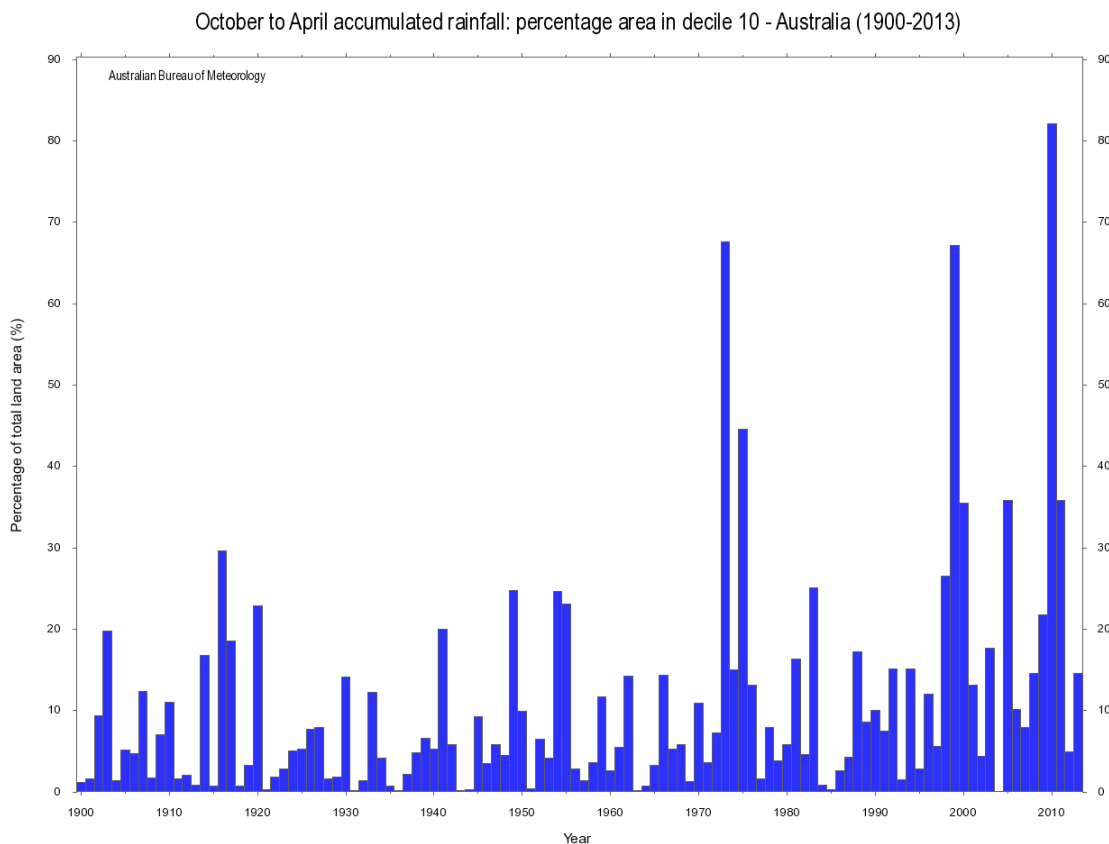


FIGURE 4.2.4: PERCENTAGE OF AUSTRALIA RECEIVING RAINFALL IN DECILE 10 (GREATER THAN 90TH PERCENTILE) DURING WARMER MONTHS OF THE YEAR (DEFINED HERE AS OCTOBER TO APRIL) ACCUMULATED SINCE 1900 (SOURCE: BUREAU OF METEOROLOGY).

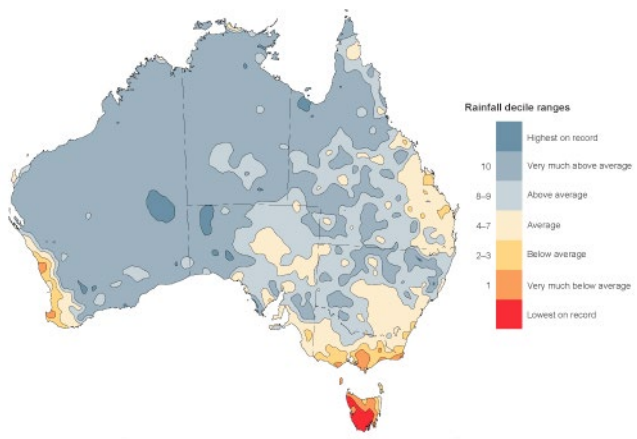


FIGURE 4.2.5: RAINFALL DECILES FOR OCTOBER TO APRIL (THE NORTHERN WET SEASON) 1997 TO 2013, RELATIVE TO THE REFERENCE PERIOD 1900–2013, BASED ON AWAP DATA (SOURCE: BOM, 2014A).

AUSTRALIAN COOL SEASON RAINFALL

Northern Australia is seasonally dry in the cooler months, so the focus here is on southern Australia. Rainfall declines in the south-west and south-east of the continent are apparent over cooler months of the year. These are most significant for the south-west of Western Australia, where a decrease is seen in the linear trend in rainfall over the entire 20th century. Decreases in some regions of south-east Australia are seen in the linear trend in rainfall through the whole century, with many other regions experiencing a decrease since around 1960. Outside of the tropics, rainfall is the major limiting factor for agriculture and water resource management in the Australian environment, and particular attention is paid here to describing the causes of southern rainfall declines.

The southern drying trends are characterised by a 10-20 percent reduction (expressed as a step change or series of step-changes) in cool season (April–September) rainfall across the south of the continent. The rainfall declines have persisted since around 1970 in the south-west and since the mid-1990s in the south-east (Braganza *et al.* 2011).

These regions typically receive most of their rainfall during the cooler months of the year, and the rainfall declines have occurred in late autumn to early winter in the south-east, and in winter in the south-west (Figure 4.2.6). In



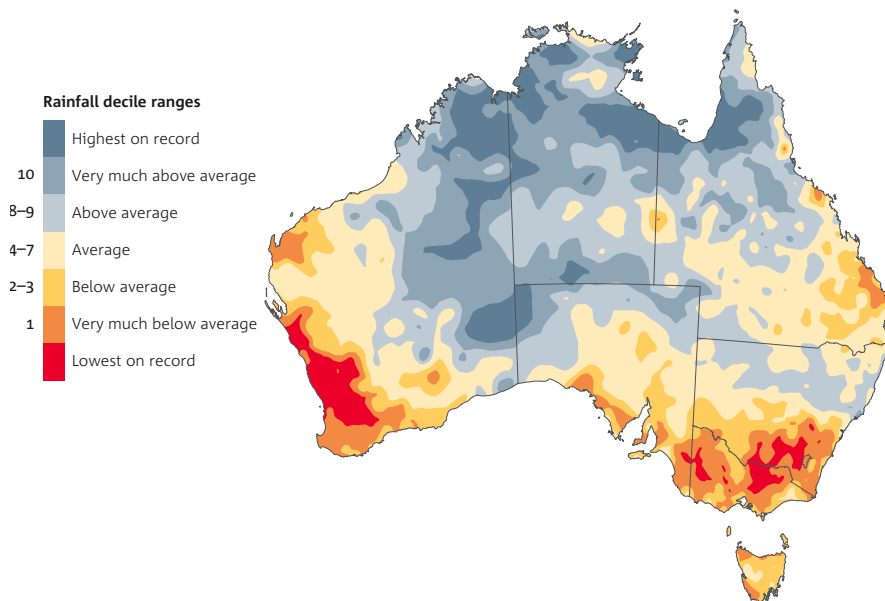


FIGURE 4.2.6: RAINFALL DECILES FOR APRIL TO SEPTEMBER 1997-2013, RELATIVE TO THE REFERENCE PERIOD 1900-2013, BASED ON AWAP DATA (SOURCE: BOM, 2014A).

some regions of the south-west, the decline in cool season rainfall is as much as 40 % over the past fifty years (Cai and Cowan, 2008) with larger decreases in runoff (CSIRO, 2012).

Mean rainfall, and rainfall variability, is dominated by cut-off low pressure systems and cold fronts (Risbey *et al.* 2009a). It has now been reasonably established that the decline in rainfall has been associated with both fewer rain-bearing systems, and less rainfall from those systems that do cross the region (Hope *et al.* 2006, Pook *et al.* 2012, Risbey *et al.* 2013a,b).

Studies have implicated a range of possible drivers of drying trends across southern Australia. To date, this literature could be classified as mostly implied attribution, relying on inferred causality from the attribution of large-scale drivers. More formal model-based attribution has also been attempted; however definitive causes have yet to be firmly established due to a range of uncertainties.

In general, the causes of the rainfall decline can be separated into proximate (local) and ultimate (global atmosphere and ocean) drivers (Nicholls, 2010). While natural variability of Australian rainfall is large, and strongly connected to well-known intrinsic modes of climate variability, it seems likely from the literature to date that drying across southern Australia cannot be explained by natural variability alone. The most notable proximate driver is the frequency and impact of sea-surface temperature variability associated with the El Niño-Southern Oscillation (ENSO) and the Indian Ocean Dipole (IOD). Specifically, a lack of negative-phase IOD events has been identified as a contributing factor to drying and drought in the south-east since the 1990s (Ummenhofer *et al.* 2009).

There is some uncertainty regarding the degree to which variability in Indian Ocean drivers are separate from ENSO variability in the Pacific, though it is notable that Indian Ocean sea surface temperatures have warmed in recent years over a very wide area of the basin. There is also

uncertainty as to whether IOD variability can exert much influence on autumn rainfall declines, since both the IOD and ENSO have limited influence on autumn rainfall in south-east Australia (Murphy and Timbal, 2008). The IOD is most important in the June–October period (Risbey *et al.* 2009b). Other studies have suggested that the true forcing by persistent SST is weak, and would account for only a fraction of the observed rainfall trends (Watterson, 2010), while Nicholls (2010) indicates that that long-term rainfall deficiencies do not seem related to changes in the behaviour of ENSO or the IOD.

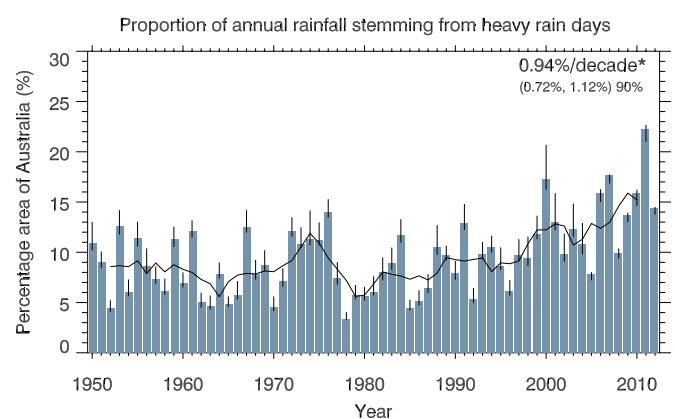


FIGURE 4.2.7: PERCENTAGE AREA OF AUSTRALIA EXPERIENCING A SIGNIFICANT PROPORTION (GREATER THAN 90 %) OF ANNUAL PRECIPITATION ACCUMULATION STEMMING FROM HEAVY ONE-DAY EVENTS. A HEAVY RAIN DAY IS DEFINED AS A DAY WHERE THE RAINFALL TOTAL EXCEEDS THE 90TH PERCENTILE (SOURCE: GALLANT *ET AL.* 2014).

AUSTRALIAN HEAVY RAINFALL

There is recent evidence that extremes of intense precipitation, over various time intervals, are increasing in more places around the globe than not (see for example Donat *et al.* 2013a). Consistent with global studies, an increase in the proportion of heavy rainfall has been detected over Australia. The fraction of Australia receiving a high proportion (greater than the 90th percentile) of annual rainfall from extreme rain days (greater than the 90th percentile for 24 hour rainfall) has been increasing since the 1970s (Figure 4.2.7; Gallant *et al.* 2013). Significant regional variability exists, with the east coast region experiencing a significant decrease in extreme rain events since 1950 (Gallant *et al.* 2014). There is also an increase in the fraction of Australia receiving summer (December to February, accumulated) rainfall that is above the 90th percentile (BOM, 2013b). Detection of changes in heavy rainfall in Australia tends to be sensitive to the indices and thresholds chosen to monitor change over time.

The period 2010 through to 2013 has also seen widespread, individual very-heavy rainfall events, particularly through the warmer months of the year. Based on the linear relationship between Southern Oscillation Index (SOI) values and Australian rainfall (Power *et al.* 2006), the El Niño Southern Oscillation (ENSO) remains the dominant driver of changes in rainfall extremes in Australia (King *et al.* 2013). However the extent to which record rainfall totals during the period 2010 to 2011 are due to natural variability is difficult to determine, since global warming can be expected to influence ENSO itself (*e.g.* Power *et al.* 2013). The La Niña event of 2010-2011 was record breaking as measured by the SOI.

Attribution studies have also found that the warming trend in sea surface temperatures to the north of Australia may have contributed to the magnitude of recent heavy rainfall in 2010-11 in eastern Australia — contributing around 10 to 20 percent of the heavy rainfall anomalies (Hendon *et al.* 2014, Evans and Bouyer-Sochet, 2012). Another study found that the warm SSTs increased the chances of above average rainfall in eastern Australia in March 2012 by 5-15 % (Christidis *et al.* 2013).

4.2.3 CHANGES IN CIRCULATION IN THE AUSTRALIAN REGION AND THEIR POSSIBLE ASSOCIATION WITH RAINFALL TRENDS

Studies have also looked to the larger, global and hemispheric circulation changes as providing ultimate causality of cool season rainfall declines in Australia. It seems likely that broader-scale circulation changes that are decoupled from local sea-surface temperature variability and trends are the dominant contributing factors to the observed rainfall declines.

In general, the large-scale circulation changes can be described through various dynamical features, each of which share a considerable amount of common variance and dynamical organisation at the hemispheric scale. These can be characterised as expansion of the tropics

and a tendency for a contraction of mid-latitude storm tracks toward higher southern latitudes, or movement of the subtropical and polar jet streams. Such a change in circulation would be characterised by a mean decrease in rainfall in mid-latitude regions, and a mean increase in higher latitudes. In the Australian region, this is broadly consistent with cool season rainfall declines described above, and evidence of increased rainfall over the Southern Ocean (Durack *et al.* 2012)

Most studies of changes to these circulation patterns form an inferred attribution of Australian rainfall changes, since this circulation controls changes in the predominant cut-off lows and frontal systems, or storm track, across the south. The basic dynamical reasoning for changes in the Southern Hemisphere circulation is that warming expands the tropics, or Hadley Cell circulation, toward the pole. This is supported by studies of reanalysis and radiosonde data, which show an expansion of the southern Hadley Circulation over the last 30 years (Nguyen *et al.* 2013; Lucas *et al.* 2012).

Warming also reduces the temperature gradient (or baroclinicity) between the equator and pole, reducing the amount of energy available to mid-latitude weather systems. A contraction of mid-latitude weather systems toward the pole, associated with a more positive Southern Annular Mode (SAM), has been attributed to both anthropogenic greenhouse gas warming and springtime Antarctic stratospheric ozone depletion (*e.g.* Arblaster and Meehl, 2006).

While rainfall declines in the south-west have occurred for longer than those in the south-east, and the rainfall regimes in the two regions are not identical, enough similarity between the two regions exists during cooler months to allow some extension of attribution results in one region to be cautiously applied to the other (Hope *et al.* 2010).

For south-west Western Australia, synoptic typing techniques have shown a marked decline in the frequency of troughs associated with rainfall since 1975, along with an increase in weather patterns associated with higher pressure and dry conditions. The decrease in the number of rain-bearing systems accounts for about half of the rainfall decline, while the reduction in rainfall from rain-bearing systems accounts for further drying (Hope *et al.* 2006). These changes are consistent with a general decrease in baroclinicity.

This is consistent with studies showing increased intensity (higher pressure) in the subtropical ridge (STR) in the wider Australian region (Timbal and Drosowsky, 2013). This is a potentially important attribution step in the research, since the regions of long-term rainfall deficits correspond to those regions where rainfall is well correlated with STR variability during March to October; with increasing pressure potentially explaining two-thirds of the rainfall decline in those regions (Timbal and Drosowsky, 2013). Figure 4.2.8 shows the correlation between the strength of the STR in the Australian region and January to December rainfall since 1900. There is inconclusive or no evidence



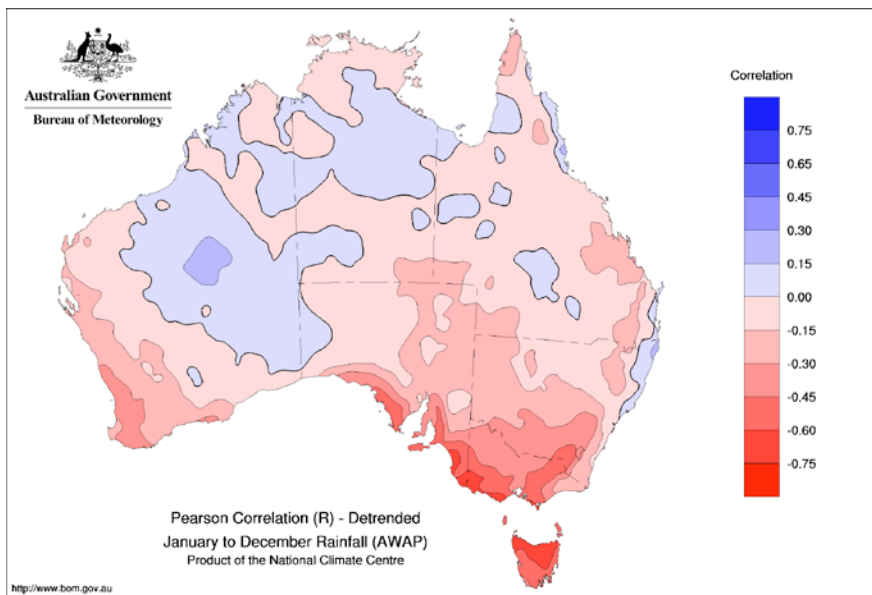


FIGURE 4.2.8: CORRELATION BETWEEN THE STRENGTH OF THE SUBTROPICAL RIDGE (STR) IN THE AUSTRALIAN REGION AND THE JANUARY TO DECEMBER RAINFALL FROM THE AUSTRALIAN WATER AVAILABILITY PROJECT (AWAP, 1900 TO PRESENT) (SOURCE: BUREAU OF METEOROLOGY).

for a poleward shift in the mean position of the STR (Drosowsky, 2005). Such a shift might be reasonably expected, associated with trends toward a more positive phase of the SAM and expansion of the Hadley circulation. This result does not imply that the storm track across southern Australia has remained constant over time.

Modelling studies have shown a reduction in storm formation in the Australian region since the mid 1970s, and particularly for the period 1997-2006, with storm activity moving from the subtropical jet to the polar jet (Frederiksen *et al.* 2011). This is consistent with a southward movement of the storm track and reduced storminess in the region.

Attribution of the changes in Southern Hemisphere atmospheric circulation has been attempted by several studies. Each of these attribution studies show inconsistencies between climate models and the real world, mostly related to the magnitude of the observed circulation and rainfall changes as well as the seasonality of the relationships between circulation and rainfall changes.

While poleward expansion of the Hadley circulation is consistent with anthropogenic forcing simulations, comparison between those experiments and reanalysis data show observed changes are much larger, as a function of latitudinal movement per decade, than the models (Hu *et al.* 2013, Lucas *et al.* 2014). Similarly, observed increases in the intensity of the subtropical ridge are consistent with anthropogenic simulations and inconsistent with natural variability, but very much less than pressure increases that have been observed in the Australian region (CSIRO, 2012).

The southward contraction of SAM (or trend toward an increasingly positive phase) in the last several decades has been associated with both greenhouse gas increases and stratospheric ozone decreases. The majority of studies have

found that stratospheric ozone depletion is the biggest contributor to the poleward contraction of SAM during summer in the second half of the twentieth century (Polvani *et al.* 2011, Son *et al.* 2010, Arblaster and Meehl, 2006, Gillett and Thompson, 2003). Increases of greenhouse gases are also likely to be a factor, and are necessary for the simulation of the observed trends at the surface. Since the 1950s, the greenhouse gas driven contribution to total SAM changes is estimated to be two to three times smaller than the contribution ozone reductions in summer, but larger than ozone contributions during winter (Arblaster and Meehl, 2006). More recent studies in the Northern Hemisphere show that increased atmospheric aerosols may also play a part in poleward movement of storm tracks (Allen *et al.* 2012; Lucas *et al.* 2014). It is important to note that stratospheric ozone depletion may be expected to stabilise and possibly recover in coming decades, but that greenhouse gas forcing is likely to increase.

While the connection between anthropogenic forcing and circulation changes is relatively clear, seasonality issues remain in connecting changes in the SAM and rainfall declines over southern Australia. The influence of Southern Hemisphere ozone depletion and trends in the SAM at the surface are most apparent in summer (Thompson *et al.* 2011), while declining rainfall trends occur in autumn and winter. Timbal *et al.* (2010) find that the trend in the SAM can account for rainfall declines during May, June and July in the south-east, but that the mechanism could only account for around half of the observed drying.

Complicating that comparison is the fact that the local surface pressure signal from trends in SAM is largest prior to the period of observed rainfall decline (Timbal *et al.* 2010). However modelling studies (Cai and Cowan, 2006) show the possibility that a SAM-south-west Western

Australia relationship exists in winter, with anthropogenic forcing contributing to about 50 % of the observed rainfall decline since the late 1960s.

Simulations of rainfall changes over the south-west of Western Australian and south-eastern Australia consistently show declines during cooler months of the year. The largest modelled declines, in response to increasing greenhouse gases, occur in winter and spring rather than autumn and winter. Similar to other atmospheric variables discussed here, rainfall simulations from climate models also show changes that are much smaller than those observed. For drying over Australia, observed changes are around two to five times larger than model simulations for a 1 °C global warming.

There are a range of potential reasons for the discrepancy in the magnitude of observed and modelled response. It is possible that natural variability superimposed on anthropogenic forced changes is causing larger, transient changes in the real world. Similarly, it is possible that unaccounted forcings are present and of a similar direction to anthropogenic forced changes. It is also possible that the model response is too small compared to the real world. The discrepancy between observed rainfall and modelled rainfall locally in southern Australia is consistent with some global studies suggesting that the models underestimate the amplification of the hydrological cycle under the enhanced greenhouse effect (see for example Durack *et al.* 2012 and Wentz *et al.* 2007).

While much discussion of rainfall variability and trends focuses on zonal mean (north-south) changes, it should be noted that zonal asymmetries (east-west differences in circulation) also play a role in setting rainfall variability and trends across southern Australia.

For many parts of south-east Australia, rainfall variability and trends are more strongly determined by variation in rain from cut-off low systems than from frontal systems (Risbey *et al.* 2013b). The frontal component of rainfall declines is associated with north-south shifts in the storm tracks as discussed above. However, the cut-off low contribution reflects both north-south shifts in the storm tracks and east-west shifts in the zones of preferred blocking. The Millennium Drought (section 4.2.4) in the south-east was at least partly associated with a reduction in cut-off rainfall and blocking activity in the Tasman Sea region (Risbey *et al.* 2013a).

In south-west Australia the rainfall reductions are more strongly driven by frontal rain than cut-off rain, but variations in blocking and cut-off rain also play a role there (Pook *et al.* 2012). A fuller understanding of the causes of rainfall changes in southern Australia needs to account for longitudinal as well as latitudinal shifts in the preferred storm track regions (Risbey *et al.* 2013b).

4.2.4 DROUGHT

Australia has experienced three major dry periods over the last century or more, including the “Federation drought” (1895-1903), the “World War II drought” (1939-1945), and the so-called “Millennium drought” (1996-2010). These major droughts have been related to variability of large-scale drivers including ENSO, the monsoonal circulation over northern Australia, Indian Ocean sea surface temperatures, and the large-scale circulation in the Southern Hemisphere (*e.g.* Risbey *et al.* 2003, Timbal and Hendon, 2011). On the decadal scale, the Interdecadal Pacific Oscillation (IPO) may modulate droughts by changing the regional impact of ENSO (Power *et al.* 1999, Verdon-Kidd and Kiem, 2009).

Assessment of changes in the behaviour of droughts over time is complex, with the IPCC *Fifth Assessment Report* finding that results varied greatly between studies, depending on the drought indicator used (in particular, whether it was purely rainfall-based or incorporated other variables) and the timescale of drought considered (IPCC, 2013). Major studies in Australia include those of Hennessy *et al.* (2008), which considered rainfall and soil moisture below the 5th percentile at the 12-month timescales, and Gallant *et al.* (2013), which considered rainfall and soil moisture below the 10th percentile over rolling 3-month periods. Observed trends in the areal extent and frequency of exceptionally low rainfall years over Australia are highly dependent on the period of analysis due to large variability between decades, with those trends which exist superimposed on those decadal-scale variations (Hennessy *et al.* 2008).

The recent period has included a significant drought that coincided with seasonal rainfall declines in the south-east (described above). The Millennium Drought, running from about 1996 to 2010, saw a reduction of annual rainfall associated with declines in autumn and winter months, and a lack of significant rainfall outside of those months. The Millennium Drought is likely the result of coincident timing of separate, but potentially correlated, climate drivers. These include the drivers of the cool-season rainfall decline (discussed above), including the decline of cyclone frequency, (McGrath *et al.* 2012).

A comparison of the Millennium Drought with previous drought in the Murray Darling Basin has shown that the most recent dry period was larger in spatial extent, and that the depth of the drought during late autumn and winter was more severe, perhaps influenced by coincident rainfall trends (Timbal and Drosowsky, 2013, Timbal and Fawcett, 2013). However, little evidence for trends in episodic drought has been found for Australia, using a variety of metrics (Hennessy *et al.* 2008). Amongst the most robust trends has been an increase in various drought-related variables in the south-west of Western Australia, where there has been an increase in the frequency of exceptionally low rainfall totals covering large areas, particularly in winter (Hennessy *et al.* 2008, Gallant and Karoly, 2010); although this is again conflated with a long-term seasonal rainfall decline. A significant increase in the area of south-east Australia experiencing exceptionally low rainfall during



autumn was largely due to a substantial increase since the turn of the 21st century (Gallant and Karoly, 2010). On the other hand, many other parts of the continent, particularly in the tropics, show a decrease in drought frequency and intensity at various timescales since the early 20th century (Gallant *et al.* 2013), although the exact nature of these results is sensitive to the period used for analysis, with the 1900–1920 period having a particularly high frequency of droughts in many regions.

4.2.5 SNOW

In 2003, CSIRO and the Australian National University published a report titled *The impact of climate change on snow conditions in mainland Australia* (Hennessy *et al.* 2003). One of the key findings was that snow depths at four alpine sites (Rocky Valley Dam, Spencers Creek, 3-Mile Dam and Deep Creek) have declined from the 1950s to 2001. In 2012, an updated analysis of snow measurements at Rocky Valley Dam in Victoria from 1954–2011 (Bhend *et al.* 2012) indicated an ongoing trend to lower maximum snow depths and an earlier end of the snow season. The long-term changes are superimposed on considerable year to year variability. The variability in maximum snow depth can be well explained by maximum temperature and precipitation from June to August. The earlier end of the snow season is dependent on changes in temperature.

4.2.6 SURFACE WINDS OVER CONTINENTAL AUSTRALIA

Wind fields across Australia are associated with large-scale circulation patterns and their seasonal movement. Across the southern half of Australia, average wind conditions are influenced by the seasonal movement of the subtropical high pressure belt which separates the mid-latitude westerly winds to the south and the south-east trade winds to the north. From November to March, the Asian-Australian monsoon interrupts the trade winds, bringing a north-westerly flow across northern Australia.

Trends in terrestrial near-surface winds (2 to 10 metres above the ground) determined from anemometers over recent decades have been found to be declining in the tropics and mid-latitudes globally (Vautard *et al.* 2010, McVicar *et al.* 2012) and this has been attributed mainly to an increase in land surface roughness arising from increased vegetation cover (Vautard *et al.* 2010). Over Australia, the trend at 2 m is of the order -0.01 m/s/year or metres per second per year (McVicar *et al.* 2008). However at 10 m, an increasing trend of the order of 0.03 m/s/year has been detected (Troccoli *et al.* 2012). Over the oceans, increasing trends have been found in mean and extreme 10 m wind speeds based on two decades of satellite altimeter data (Young *et al.* 2011). Wind trends in the Australian region are related to the poleward shift in the Hadley circulation. This has been associated with a declining trend in pressure in the sub-tropics and an increasing trend in mean sea level pressure (MSLP) in the mid-latitudes over 1989–2006 in the NCEP–NCAR reanalysis (Troccoli *et al.* 2012).

Due to the sparseness of long-term, high quality wind measurements from terrestrial anemometers, a high quality gridded data set for wind is not available over Australia (Jakob, 2010). Therefore 10 m winds from reanalysis products are commonly used as a baseline against which climate model winds are compared. Although constrained by observations, reanalysis products are also derived from models and so may contain biases. For example, McInnes *et al.* (2011) found that average wind speeds between the NCEP–DEO AMIP-II (Kanamitsu *et al.* 2002) and ERA40 (Uppala *et al.* 2005) reanalysis products over 1981–2000 exhibited spatial differences between each other that were greater than the differences between these products and some CMIP3 climate models. This was particularly the case in the southern hemisphere in winter (McInnes *et al.* 2011).

4.2.7 TROPICAL CYCLONES

Tropical cyclones are relatively small-scale weather phenomena that affect the tropical coasts of Western Australia, the Northern Territory and Queensland from late November through to April. The most severe impacts of tropical cyclones in Australia are characterised by catastrophic wind speeds, storm surges and extreme heavy rainfall and flooding. Natural variability in the number of tropical cyclones making landfall in Australia is strongly influenced by ENSO, with more tropical cyclones during La Niña years and fewer in El Niño years.

The relatively short time span of consistent records, combined with high year to year variability, makes it difficult to discern any clear trends in tropical cyclone frequency or intensity for the Australian region. For the period 1981 to 2007, no statistically significant trends in the total numbers of cyclones, or in the proportion of the most intense cyclones, have been found in the Australian region, South Indian Ocean or South Pacific Ocean (Kuleshov *et al.* 2010). However, observations of tropical cyclone numbers from 1981–82 to 2012–13 in the Australian region show a decreasing trend that is significant at the 93–98 % confidence level when variability associated with ENSO is accounted for (Dowdy, 2014). Only limited conclusions can be drawn regarding tropical cyclone frequency and intensity in the Australian region prior to 1981, due to a lack of data. However, a long-term decline in numbers on the Queensland coast has been suggested (Callaghan and Power, 2010).

4.2.8 EAST COAST LOWS

Observational studies provide some indication of a small decreasing trend in the number of East Coast Lows, based on reanalysis data (Dowdy *et al.* 2013c). There is a strong connection between heavy rainfall and East Coast Low occurrence in the eastern Australian region (Pepler *et al.* 2014, Dowdy *et al.* 2013b) and a decrease in extreme rain events along the east coast has been observed since 1950 (Gallant *et al.* 2007). East Coast Lows are also the primary cause of large ocean waves in NSW coastal regions (Dowdy *et al.* 2014).



4.2.9 SOLAR RADIATION

The downward solar radiation at the Earth's surface is a key parameter for the Earth-atmosphere climate system. It also plays an important role in many physical, chemical and biological processes. Its variation relates to factors including cloud cover, air pollution, latitude and the season. In Australia, there is a close connection, or covariability, at continental scales between rainfall, cloudiness, temperature and solar radiation at the surface.

Estimates of solar radiation from a cloud-based model using data from 29 stations across Australia from 1967 to 2004 show no significant changes at the majority of stations, with only eight stations showing significant decreases and two stations showing significant increases (Nunez and Li, 2008). Specifically, the notable changes in solar radiation over time are concentrated over the south of the continent. High quality cloud observations show that the Australian mean annual total cloud amount is characterised by high year to year variability, with a weak increase over the 1957 – 2007 period (Jovanovic *et al.* 2011). Attribution of small changes in solar radiation over time is difficult, due to the range of complex influences. These include changes in cloud associated with high rainfall variability in the Australian region and the direct and indirect effect of changes in aerosols.

4.2.10 SURFACE HUMIDITY

Humidity describes the relative amount of water vapour in an air parcel. Surface humidity in Australia is an important component of local weather. Very high or low humidity is associated with ecological and agricultural impacts, the severity of fire weather and the impact of heat waves on human health.

Changes in humidity across Australia are closely connected to rainfall variability, and are not well described by linear trends over time. Instead, large interannual and decadal variability is apparent in Australian dewpoint temperatures (the saturation temperature for an air parcel cooled at a constant pressure and moisture content). However most sites across Australia have shown increases in dewpoint temperature from 1957 to 2003, with the largest increases in the interior of the continent (Figure 4.2.9) (Lucas, 2010a). Specific attribution of these changes has not been performed.

4.2.11 PAN EVAPORATION

Pan evaporation is a direct measurement of the evaporative loss from a uniform (standard) small body of water placed within the environment at the surface. Pan evaporation is mostly utilized for estimating evapotranspiration, or the transfer of water vapour from vegetation and the land surface. Evapotranspiration is a key variable in determining the water balance of a system.

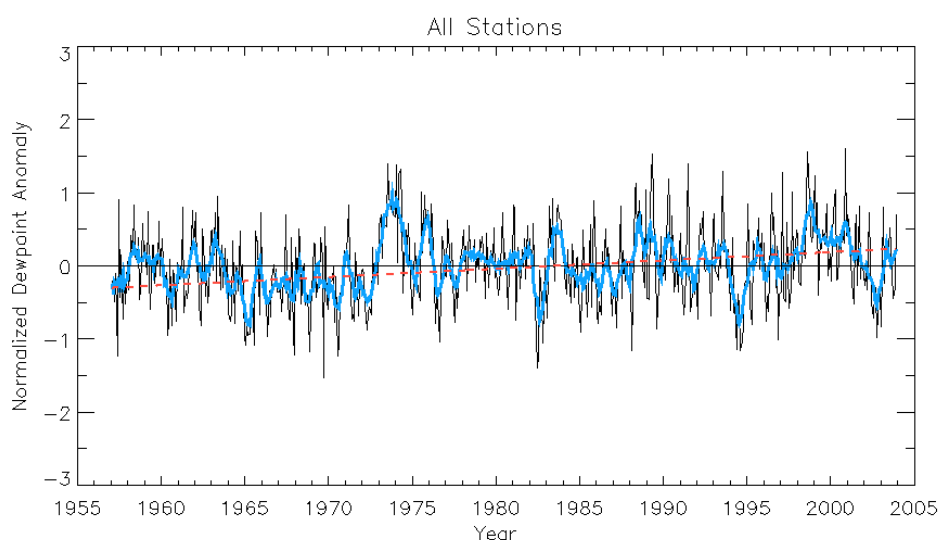


FIGURE 4.2.9: AVERAGE MONTHLY NORMALIZED DEWPOINT ANOMALY ACROSS ALL 58 HIGH QUALITY STATIONS OVER AUSTRALIA. BLUE LINE IS THE 7-MONTH SMOOTHED VALUE (SOURCE: LUCAS, 2010A).



There are no clear changes observed in pan evaporation across Australia in data available since 1970 (Jovanovic *et al.* 2008). Uncertainties in pan evaporation changes over time are largely due to sensitivity to wind speed at pan height, which in turn is highly sensitive to changes in site exposure. There is a broad-scale pattern of decreases in pan evaporation across northern Australia in regions which have seen recent increases in monsoonal rainfall.

4.2.12 FIRE WEATHER

Australia is one of the most fire prone regions in the world. The fire season is distinctly different for different parts of the continent; during the dry season for northern Australia, spring and summer for the sub-tropics and middle to late summer for southern regions. Fire potential at a given place depends on four 'switches': 1) ignition, either human-caused or from natural sources such as lightning; 2) fuel abundance or load (a sufficient amount of fuel must be present); 3) fuel dryness, where lower moisture contents are required for fire, and; 4) suitable weather conditions for fire spread, generally hot, dry and windy (Bradstock, 2010). The settings of the switches depend on meteorological conditions across a variety of time scales, particularly the fuel conditions.

Fire weather is monitored using a McArthur Forest Fire Danger Index (FFDI), which is calculated from daily temperature, wind speed, humidity and a drought factor, at sites with consistent data across Australia (Lucas, 2010b). An increase in the annual (July-June) cumulative FFDI is observed across all 38 sites analysed in Australia from 1973 to 2010, and is statistically significant at 16 of those sites. (Figure 4.2.10; Clarke *et al.* 2013), particularly in the south-eastern part of the country. This increase across south-east Australia is characterised by an extension of the fire season further into spring and autumn (Clarke *et al.* 2013). There has also been an increase in high FFDI values (90th percentile) from 1973–2010 at all 38 sites, with a statistically significant increase at 24 sites, indicating that extreme fire weather days have become more frequent over time (Clarke *et al.* 2013).

The FFDI increases are partly driven by temperature increases that are attributable to climate change. Similarly, temperature changes alone have been shown to contribute significantly to evaporation and surface evapotranspiration in drier catchments of the Murray Darling Basin (McVicar *et al.* 2012). However, no studies explicitly attributing the Australian increase in fire weather to climate change have been performed at this time.

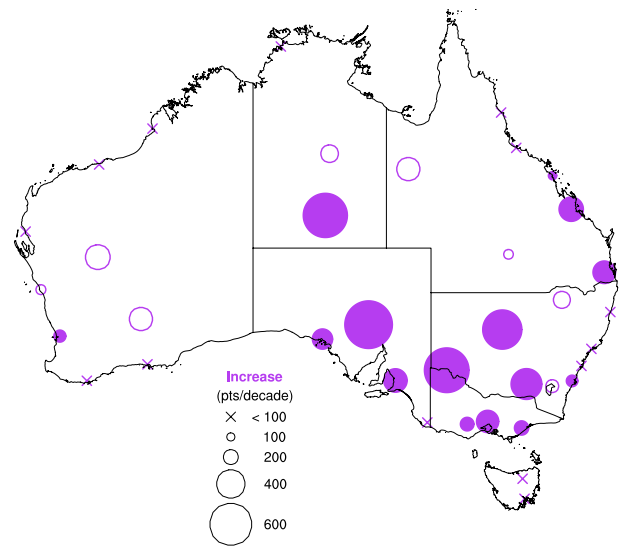
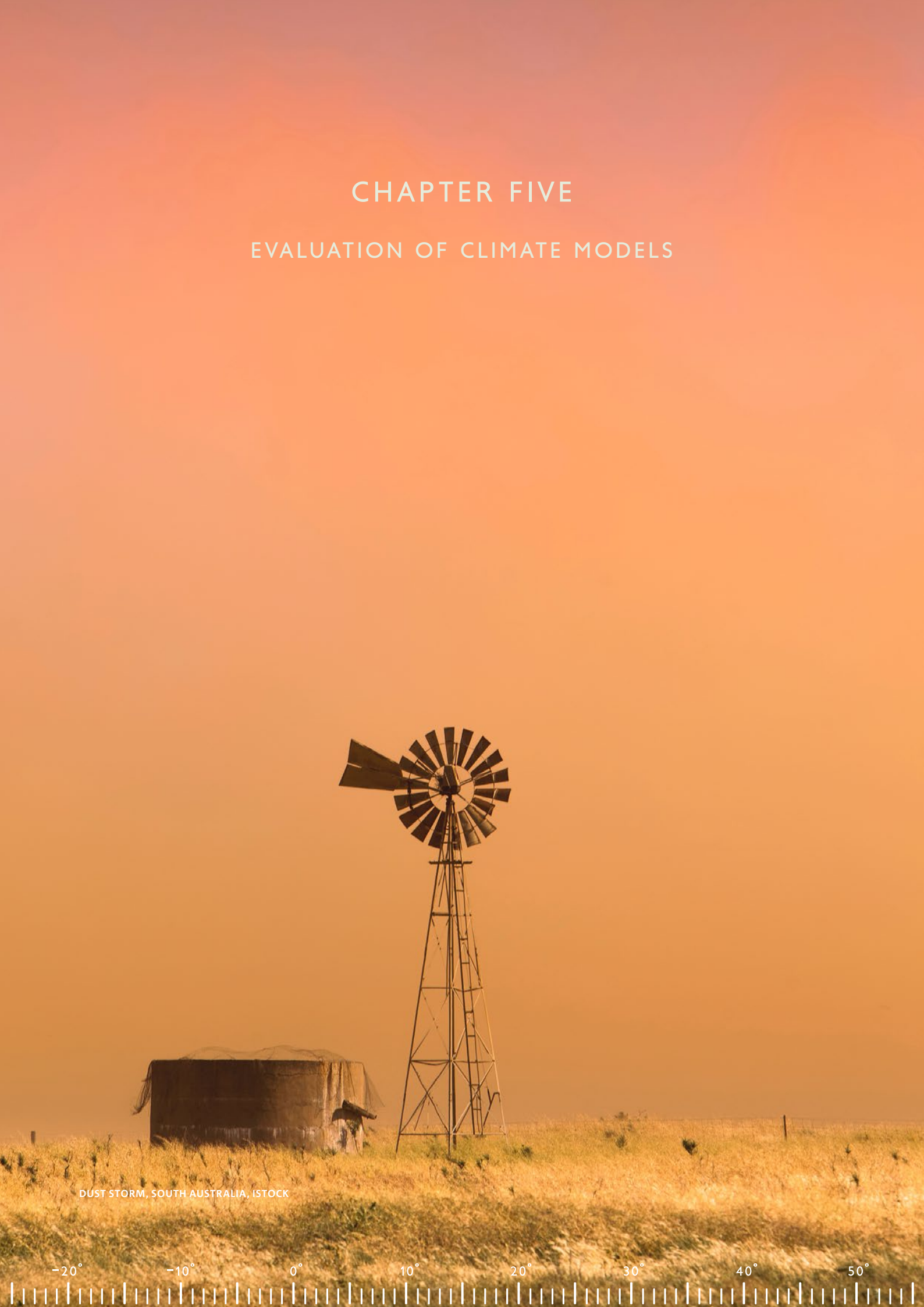


FIGURE 4.2.10: MAP OF TREND IN ANNUAL 90TH PERCENTILE FFDI. MARKER SIZE IS PROPORTIONAL TO THE MAGNITUDE OF TREND. REFERENCE SIZES ARE SHOWN IN THE LEGEND. FILLED MARKERS REPRESENT TRENDS THAT ARE STATISTICALLY SIGNIFICANT. THE MARKER FOR LAVERTON HAS BEEN MOVED WEST TO AVOID OVERLAP WITH MELBOURNE AIRPORT (SOURCE: CLARKE *ET AL.* 2013).

CHAPTER FIVE

EVALUATION OF CLIMATE MODELS



DUST STORM, SOUTH AUSTRALIA, ISTOCK

-20° -10° 0° 10° 20° 30° 40° 50°

CHAPTER 5 EVALUATION OF CLIMATE MODELS

5.1 INTRODUCTION

In this Chapter climate models are evaluated by using measures of agreement between model simulations and observations of the present climate of the Australian region. The results of this model evaluation contribute to our assessment of confidence in model-simulated future climate changes (see Section 6.4) and also to the assessment of the adequacy of any model, or models in general, for particular applications. Recent IPCC Assessment Reports also use model evaluation to guide confidence in projections of future climate (IPCC, 2007; 2013).

The ability of individual CMIP5 models to simulate the Australian climate can vary depending on which aspect of a model simulation is considered. There is a wide range of climate features that have been included in this evaluation (see also Section 4.1.2 for details on the processes and features) in order to capture the complexity of the climate system as well as satisfy the interests of stakeholders. While this makes it difficult to identify a group of best performing models, it is possible to identify a small subset of models that perform consistently poorly across many aspects of the climate, or that perform poorly on critical aspects of the climate. Such information on poorly performing individual models is relevant when users are choosing a subset of models for application in impact assessment (*e.g.* through the Climate Futures approach – see Chapter 9). Similarly, the results from the model evaluation are very important when choosing host models for dynamical downscaling (see Section 6.3.3).

At the core of every model evaluation is a set of high quality observations to which model simulations can be compared. The high quality data set from the Australian Water Availability Project (AWAP, Jones *et al.* 2009a, Raupach *et al.* 2009, 2012) is used for the evaluation of rainfall and temperature over the Australian continent. These provide an excellent indicator of mean climate across Australia. For the assessment of trends in temperature a recently updated high-quality reference station data set is used (ACORN-SAT – Trewin, 2013). For several climate fields (including rainfall and temperature) there are multiple global data sets available, which allows for an extension of the evaluation over a wider region including ocean regions surrounding Australia, and an estimate of the uncertainty in observations when multiple data sets are used for the same climate field. The various observational datasets used in this chapter are described in Table 5.2.1 and the global climate models (from CMIP3 and CMIP5) are described in Table 3.3.1, including the model labels used throughout this Report.

Features of global climate models, such as resolution and representation of physical processes, and details of the CMIP5 suite of experiments are discussed in Chapter 3.

Most analysis in this chapter is carried out with respect to the historical experiments described in Section 3.3.1. The performance of global climate models with respect

to climatological characteristics, features and processes is evaluated in Section 5.2. The simulation of observed regional climate trends is evaluated in Section 5.3. The simulation of climatic extremes is evaluated in Section 5.4 and downscaling simulations are discussed in Section 5.5, before we conclude in Section 5.6.

5.2 EVALUATION BASED ON CLIMATOLOGICAL CHARACTERISTICS

Global climate models are designed to simulate large-scale processes well. On a smaller regional scale, the spatial and temporal details of these processes are simulated with much more varying capacity. On even smaller scales, processes might not be directly simulated by global climate models at all (*i.e.* tropical cyclones).

Climate model resolution will give a rough indication of the spatial extent as to what of features and processes these models may simulate realistically. Table 3.3.1 shows the CMIP5 model ensemble and the resolution of both the atmospheric and ocean components of the models. CMIP5 is overall an improved set of global climate models compared to CMIP3 in terms of model formulation. The improvements arise from the increase in horizontal and vertical resolution; an improved representation of processes within the climate system (*i.e.* aerosol-cloud interactions, and the carbon cycle in the subset that are Earth-System-Models, ESMs) and also the availability of a larger number of ensemble members improves statistics overall (Chapter 9 in IPCC, 2013).

On a continental and global scale, this has also led to an improved ability to simulate historical climate. Some examples of this ability are reported by IPCC (2013) and include the representation of:

- Global mean surface temperature, including trends over the recent decades
- Long-term global mean large-scale rainfall patterns (but less well than temperature)
- Regional mean surface temperature (sub-continental scales)
- Annual cycle of Arctic sea ice extent (and recent trends)
- Trends in ocean heat content



- ENSO simulation
- Extreme events, especially temperature related ones
- Recent ozone trends

Beside these improvements, certain areas have not improved since the previous IPCC Assessment in 2007. This includes important systematic errors and biases such as the “cold tongue” bias (*e.g.* the sea surface temperature difference between East and West equatorial Pacific are too large in models, leading to a cold bias in the Western Pacific), problems in simulating the diurnal cycle of rainfall, the Madden-Julian Oscillation, and more. In many cases, there is a large inter-model spread leading to enhanced uncertainty, however amongst the models that do not include carbon cycle these are reduced compared to CMIP3 (IPCC, 2013).

Apart from spatial resolution, models also employ different physical schemes representing atmospheric and oceanic

processes (such as clouds and convection schemes). One of the main aims of model evaluation is to assess the skill of these models through standardised inter-comparisons. The CMIP5 experiments allow for such a comparison. Following is an overview of an assessment for the Australian region.

5.2.1 ASSESSMENT OF HISTORICAL MEAN CLIMATOLOGIES: TEMPERATURE, RAINFALL AND MEAN SEA LEVEL PRESSURE

Figures 5.2.1 and 5.2.2 show a comparison of annual and seasonal climatologies (long-term averages) of temperature and rainfall for Australia. The left column in both figures shows the reference observational data set (AWAP, Jones *et al.* 2009a, Raupach *et al.* 2009; 2012) while the middle column shows an average of a selection of other observational data sets and reanalyses (see Table 5.2.1 for an overview of these) and the right column displays the CMIP5 ensemble mean.

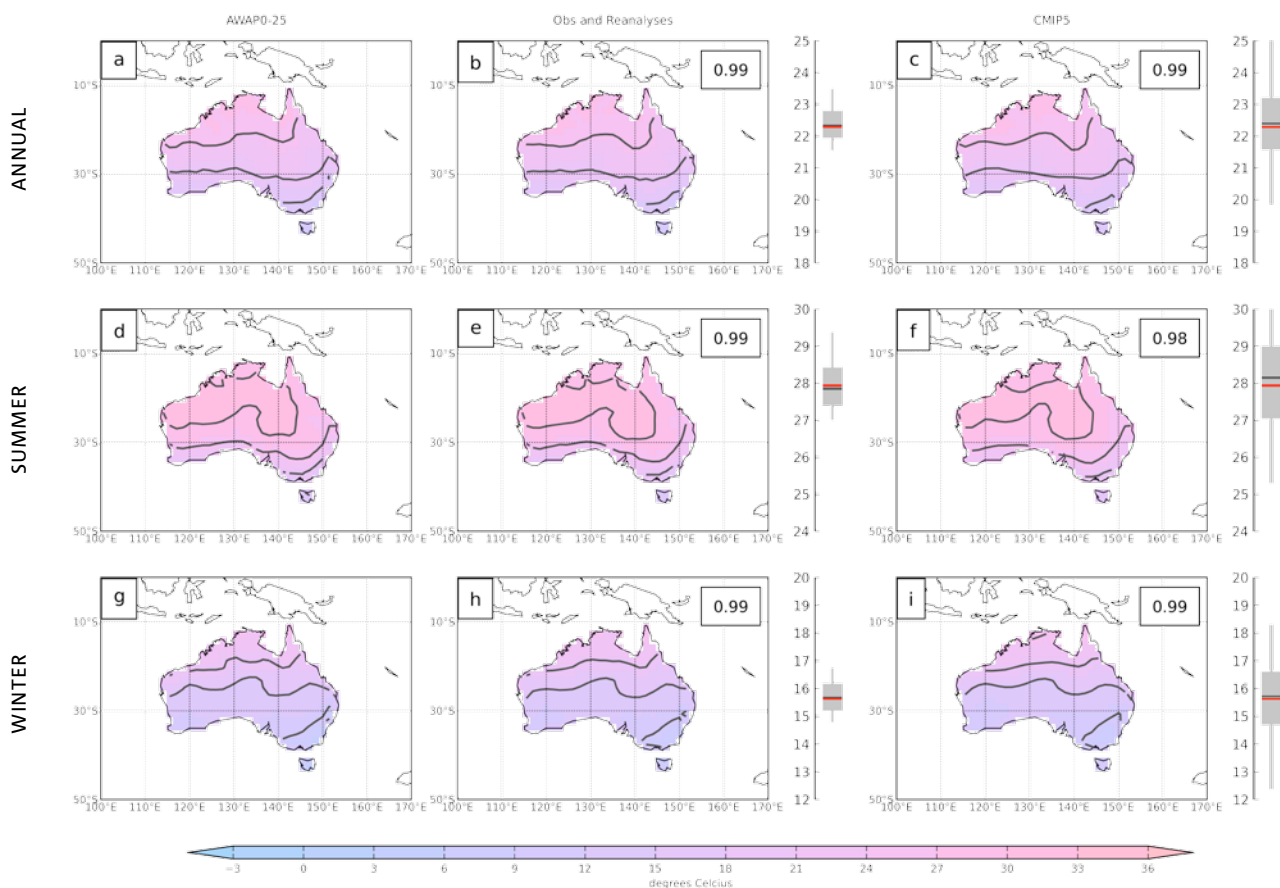


FIGURE 5.2.1: CLIMATOLOGICAL MEAN SURFACE AIR TEMPERATURE FROM AWAP (A, D, G, THE REFERENCE DATA SET), THE AVERAGE OF A SELECTION OF OTHER OBSERVATIONAL DATA SETS (B, E, H, SEE TABLE 5.2.1) AND THE CMIP5 MEAN MODEL (C, F, I) FOR ANNUAL (TOP ROW), SUMMER (DEC-FEB, MIDDLE ROW) AND WINTER (JUN-AUG, BOTTOM ROW) SURFACE AIR TEMPERATURE. THE AVERAGING PERIOD IS 1986–2005 AND THE UNITS ARE DEGREES CELSIUS (°C). THE CONTOURS HIGHLIGHT THE 9, 15, 21, 27 AND 33 °C THRESHOLDS FOR BETTER COMPARISON. THE NUMBER IN THE TOP RIGHT CORNER INDICATES THE SPATIAL CORRELATION BETWEEN THE CORRESPONDING DATA AND AWAP. THE SPREAD IN THE DATA SETS IS INDICATED BY THE BOX-WHISKER TO THE RIGHT OF EACH SUBPLOT: EACH SHOWS THE AUSTRALIA-AVERAGED SURFACE AIR TEMPERATURE WHERE THE GREY BOX REFERS TO THE MIDDLE 50 % OF THE DATA AND THE WHISKERS SHOW THE SPREAD FROM MINIMUM TO MAXIMUM. THE THICK BLACK LINE IS THE MEDIAN OF THE UNDERLYING DATA AND THE RED LINE IS AWAP.



TABLE 5.2.1: LIST OF GLOBAL GRIDDED OBSERVATIONAL (BLUE) AND REANALYSIS DATA SETS (GREEN), THEIR CLIMATE FIELDS USED, TIME COVERAGE, ORIGIN AND REFERENCE. THE AWAP AND ACORN-SAT REFERENCE DATA SETS FOR SURFACE AIR TEMPERATURE AND RAINFALL OVER AUSTRALIA ARE SHOWN IN ORANGE. THE ABBREVIATION PR REFERS TO PRECIPITATION; TAS: SURFACE AIR TEMPERATURE; MSLP: MEAN SEA LEVEL PRESSURE.

GRIDDED DATA SET		PERIOD	ORIGIN	REFERENCES
NAME	FIELDS			
AWAP	PR	1900-2012	Australian Water Availability Project, Bureau of Meteorology and CSIRO	Jones <i>et al.</i> 2009a; Raupach <i>et al.</i> 2009 and 2012
ACORN-SAT	TAS	1910-2012	Australian Climate Observations Reference Network – Surface Air Temperature, Bureau of Meteorology	Trewin 2013
CMPA	PR	1979-2008	Climate Prediction Centre Merged Analysis of Precipitation	Xie & Arkin, 1997
GPPC	PR	1901-2010	Global Precipitation Climatology Centre (GPPC)	Rudolf <i>et al.</i> 2005; Beck <i>et al.</i> 2005
GPCP	PR	1979-2008	Global Precipitation Climatology Project 2	Huffman <i>et al.</i> 2009; Adler <i>et al.</i> 2003
CRU	TAS	1901-2006	Climate Research Unit temperature database	Harris <i>et al.</i> 2013
GISS	TAS	1850-2006	NASA Goddard Institute for Space Sciences (GISS) Surface Temperature Analysis	GISTEMP; Hansen <i>et al.</i> 2010
HADCRU	TAS, PR	1901-2008	Met Office Hadley Centre and Climate Research Unit	HadCRUT3; Brohan <i>et al.</i> 2006
COREv2	PR, TAS, MSLP	1958-2006	CLIVAR Working Group on Ocean Model Development (WGOMD) Coordinated	Large & Yeager, 2009 & 2004
HOAPS	PR, FLUXES	1987-2005	Hamburg Ocean Atmosphere parameters and fluxes satellite	Fennig <i>et al.</i> , 2012; Andersson <i>et al.</i> 2010
HadISST	SST	1870-2010	Hadley Centre Sea Ice and Sea Surface Temperature dataset	HadISST2; Rayner <i>et al.</i> 2003
HadSLP2	MSLP	1850-2004	Hadley Centre Sea Level Pressure dataset	Allan and Ansell 2006
CFSR	PR, WINDS, MSLP, TAS	1979-2009	NCEP Climate Forecast System Reanalysis	Saha <i>et al.</i> 2010
Merra	PR, WINDS, MSLP, TAS	1979-2011	Modern Era Retrospective-analysis for Research and Applications	Rienecker <i>et al.</i> 2011
ERA40	PR, WINDS, MSLP, TAS	1958-2002	European 40-year reanalysis	Uppala <i>et al.</i> 2005
ERA_INT	PR, WINDS, MSLP, TAS	1979-2011	ERA-interim	Dee <i>et al.</i> 2011
NCEP	PR, WINDS, MSLP, TAS	1948-2011	NCEP/NCAR reanalysis 1	Kalnay <i>et al.</i> 1996
NCEP2	PR, WINDS, MSLP, TAS	1979-2011	NCEP/DOE reanalysis 2	Kanamitsu <i>et al.</i> 2002
JRA25anl	PR, WINDS, MSLP, TAS	1979-2010	Japanese 25-year reanalysis	Onogi <i>et al.</i> 2007

On average, the CMIP5 models capture the climatological temperature distribution across the continent very well. The north-south gradient in temperature is correctly simulated as well as the coastal versus inland differences during summer (middle row in Figure 5.2.1) although the ensemble mean model climate is cooler than AWAP across northern parts over Western Australia. During winter (Jun-Aug) the model ensemble mean model is slightly too warm over

northern Australia as well as coastal regions in the south-east and Tasmania. Pattern correlations are generally very high for the mean model distribution of temperature.

There is a substantial spread in the Australia-averaged temperature amongst the CMIP5 models, as indicated by the spread in the box-whiskers in Figure 5.2.1. While 50 per cent of the models are within $\pm 1^\circ\text{C}$ of the AWAP reference data, some of the models are several degrees warmer or



colder. The box-whiskers belonging to the middle column in Figure 5.2.1 additionally indicate that there is some discrepancy amongst the other observational data sets and reanalysis data sets with respect to temperature across Australia. However, this discrepancy is generally less than half of the spread seen in the CMIP5 models.

Some of the model differences in temperature are driven by their differences in the simulation of the hydrological cycle. Mean rainfall differences are shown in Figure 5.2.2. There is a general tendency for the models to simulate too much rainfall across north-western Australia and reaching too far into the interior of the continent (summer and annual case). North-eastern regions show somewhat less summer rainfall in the models compared to AWAP.

The winter rainfall regime (across southern coastal regions of Australia) on the other hand is generally too dry as simulated by the climate models, especially in Tasmania. This could be caused by insufficient global model resolution of two kinds: (a) some model resolutions are too coarse to simulate the correct land-sea contrast over Tasmania; (b) even if global models have information over Tasmania it is usually not enough to correctly simulate the topographically driven high rainfall regimes particularly over western regions of Tasmania. Therefore the pattern correlations are lower for rainfall compared to temperature and the model spread for summer rainfall is very large.

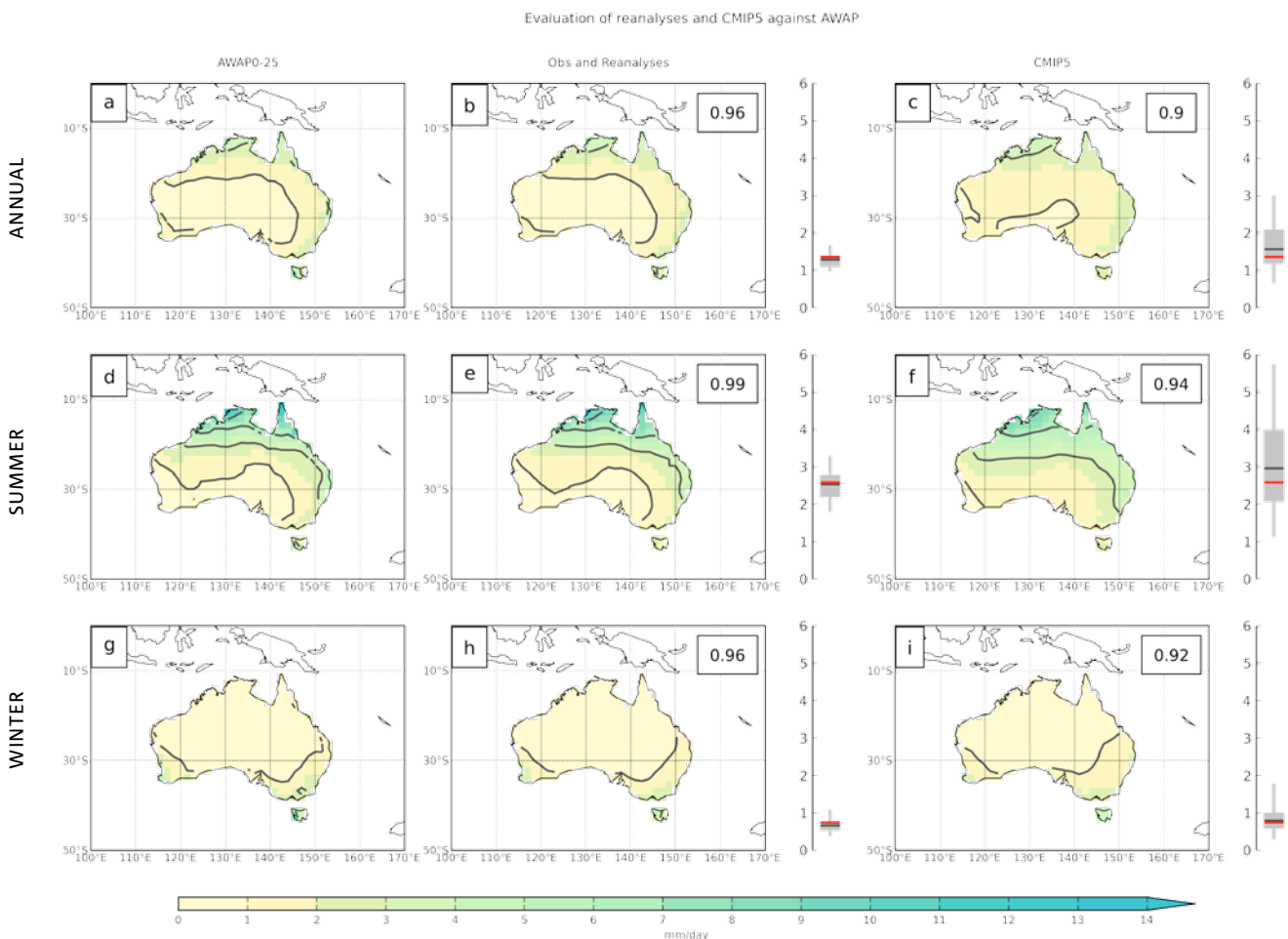


FIGURE 5.2: CLIMATOLOGICAL MEAN RAINFALL FROM AWAP (A, D, G, THE REFERENCE DATA SET), THE AVERAGE OF A SELECTION OF OTHER OBSERVATIONAL DATA SETS (B, E, H, SEE TABLE 5.2.1) AND THE CMIP5 MEAN MODEL (C, F, I) FOR ANNUAL (TOP ROW), SUMMER (DEC-FEB, MIDDLE ROW) AND WINTER (JUN-AUG, BOTTOM ROW) RAINFALL. THE AVERAGING PERIOD IS 1986-2005 AND THE UNITS ARE MM PER DAY. THE CONTOURS HIGHLIGHT THE 1, 3, 6, AND 9 MM/DAY THRESHOLDS. THE NUMBER IN THE TOP RIGHT CORNER INDICATES THE SPATIAL CORRELATION BETWEEN THE CORRESPONDING DATA AND AWAP. THE SPREAD IN THE DATA SETS IS INDICATED BY THE BOX-WHISKER TO THE RIGHT OF EACH SUBPLOT: EACH SHOWS THE AUSTRALIA-AVERAGED RAINFALL WHERE THE GREY BOX REFERS TO THE MIDDLE 50 % OF THE DATA AND THE WHISKERS SHOW THE SPREAD FROM MINIMUM TO MAXIMUM (FOR CMIP5 DATA ONLY). THE THICK BLACK LINE IS THE MEDIAN OF THE UNDERLYING DATA AND THE RED LINE IS AWAP.

Figures 5.2.3 and 5.2.4 show the cluster-based assessment of the CMIP5 model biases in seasonal surface air temperature and rainfall climatologies. In general, the CMIP5 models are able to capture seasonal temperatures much better than rainfall.

During summer, the model simulated median temperatures (Figure 5.2.3) are very close to AWAP reference values, particularly for the warmer regions across northern and central Australia (Monsoonal North and Rangelands clusters for example). While the temperature range within the model ensemble can be as large as 3 °C (with some models showing an even larger cold bias in southern regions and Tasmania), the majority of the models are within ± 1 °C of the observed values.

During winter, the majority of climate models have warm biases over some regions of south-eastern Australia (Southern Slopes cluster). Most other cluster regions are very well simulated with the median temperatures often within 1 °C of the AWAP values. Noteworthy is the large overall spread between the models, which can reach more than 4 °C between the warmest and coldest model for a particular cluster.

Overall, the biases in temperature point towards a deficiency in some models in capturing the north-south temperature gradient across Australia in either the summer or winter season.

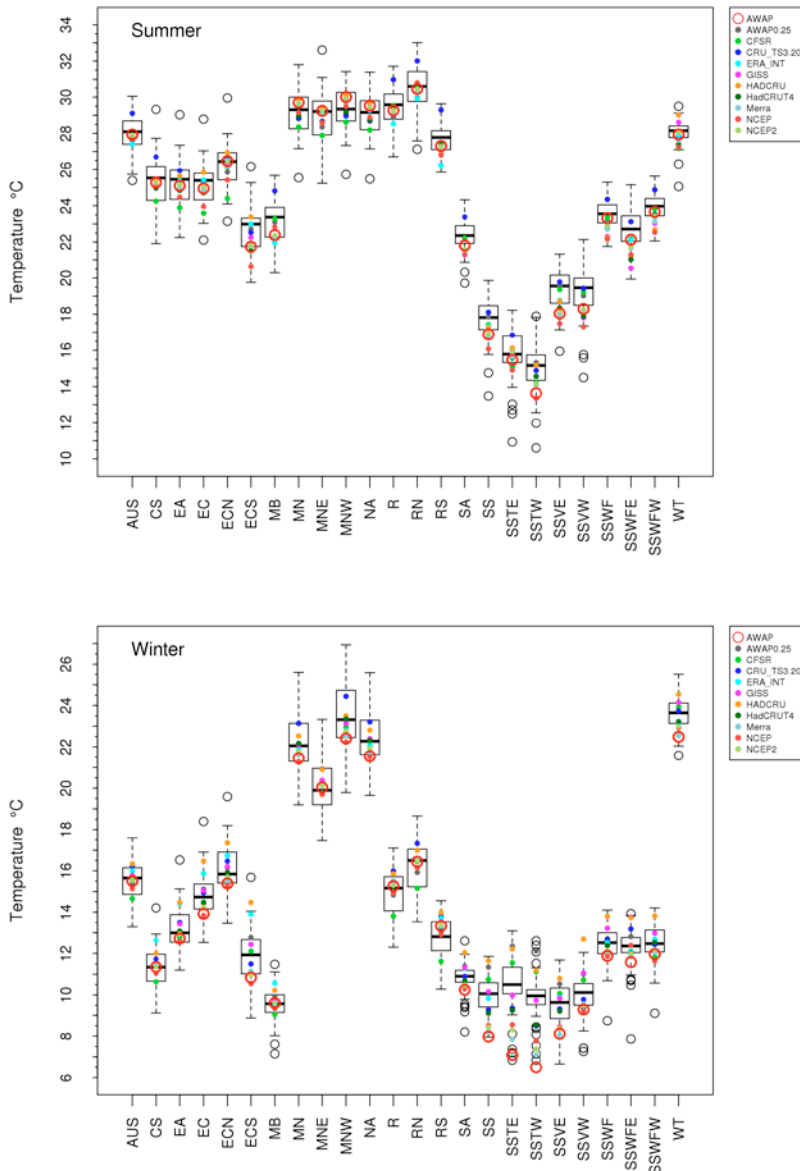


FIGURE 5.2.3: CLUSTER AVERAGED MEAN SURFACE AIR TEMPERATURE (UNITS: °C) FOR SUMMER (DEC-FEB, TOP) AND WINTER (JUN-AUG, BOTTOM) FROM ALL CMIP5 MODELS (REPRESENTED BY BOX-WHISKER BARS), AWAP (RED CIRCLE) AND SEVERAL OTHER OBSERVATIONS AND RE-ANALYSIS DATA SETS (COLOURED DOTS). THE BOX-WHISKERS DISPLAY THE MIDDLE 50 % OF THE CMIP5 MODELS (BOX, INCLUDING THE MEDIAN OF THE CMIP5 MODELS AS THICK BLACK LINE) AND THE RANGE (WHISKERS) WHILE OUTLIER MODELS ARE SHOWN AS BLACK CIRCLES (*I.E.* THEY ARE MORE THAN 1.5 TIMES THE BOX WIDTH AWAY FROM THE MEDIAN). THE TIME PERIOD USED IS 1986–2005.



Cluster-based rainfall biases are shown in Figure 5.2.4 for summer and winter. The skill of models in simulating climatological rainfall varies strongly across Australia: for example during summer, models capture rainfall amounts over regions with moderate to high seasonal rainfall totals such as the monsoon regions (except the Wet Tropics) and along the East Coast (except the East Coast South sub-cluster), but show more variable skill elsewhere.

While there is a fairly large model spread (particularly over the monsoon affected regions), the median rainfall is close to the AWAP data in summer. Along the tropical east coast (Wet Tropics cluster), models show a substantial dry bias. Further south and inland, there is a general tendency for models to overestimate summer rainfall (*i.e.* Rangelands, Southern Slopes, Murray Darling Basin, Central Slopes

clusters) with wet biases of up to 20 mm/month. Further south (Tasmania), the model biases are reversed with strong dry biases of around 20 mm/month for the entire region.

During winter (*e.g.* the main rainfall period for southern clusters), the model ensemble shows a dry bias over most of the higher rainfall regions (Southern Slopes and Murray Basin clusters), except for the East Coast cluster where the GCM ensemble median rainfall is a good match to the observed rainfall. The dry bias is particularly large in Tasmania where almost all models underestimate winter rainfall. For the large Rangelands cluster, winter rainfall is slightly overestimated. The models capture lower rainfall totals well along the tropical regions (Wet Tropics and Monsoonal North clusters) and also the higher winter rainfall of the East Coast cluster. Dry biases are common

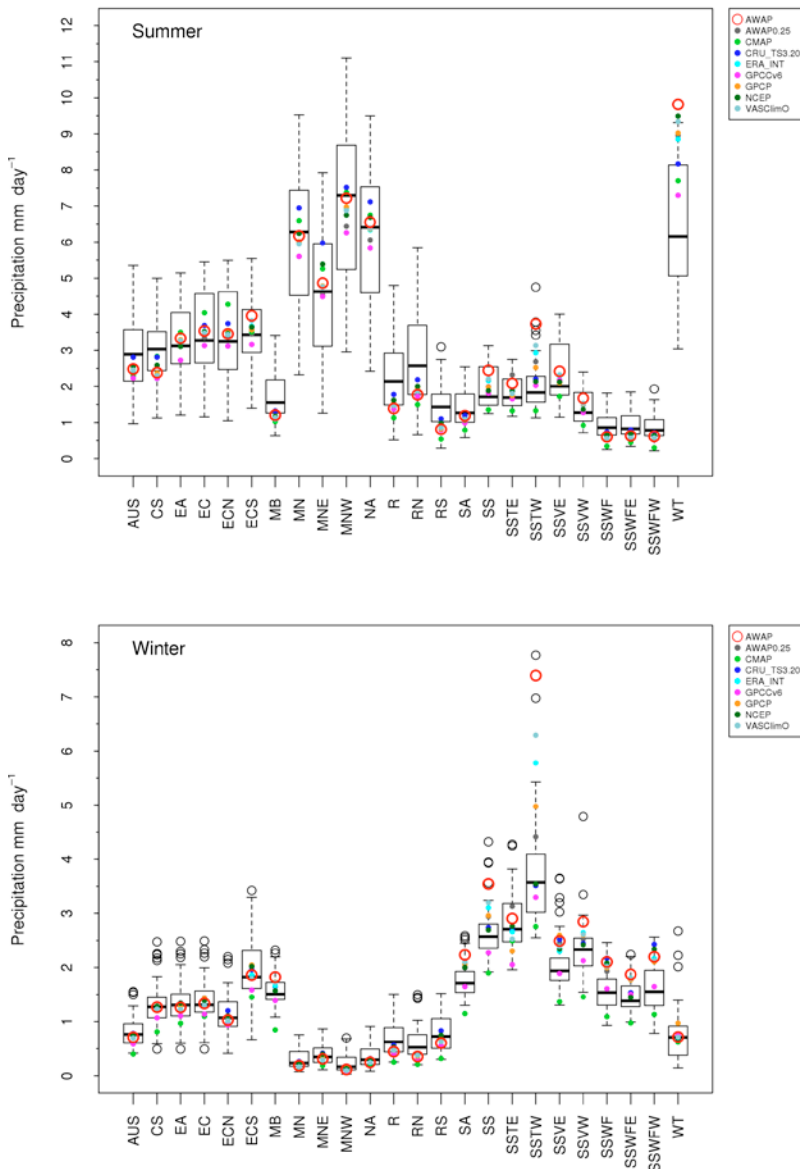


FIGURE 5.2.4: CLUSTER AVERAGED RAINFALL (UNITS: MM PER DAY) FOR SUMMER (DEC-FEB, TOP) AND WINTER (JUN-AUG, BOTTOM) FROM ALL CMIP5 MODELS (REPRESENTED BY BOX-WHISKER BARS), AWAP (RED CIRCLE) AND SEVERAL OTHER OBSERVATIONS AND RE-ANALYSIS DATA SETS (COLOURED DOTS). THE BOX-WHISKERS DISPLAY THE MIDDLE 50% OF THE CMIP5 MODELS (BOX, INCLUDING THE MEDIAN OF THE CMIP5 MODELS AS THICK BLACK LINE) AND THE RANGE (WHISKERS) WHILE OUTLIER MODELS ARE SHOWN AS BLACK CIRCLES (*i.e.* THEY ARE MORE THAN 1.5 TIMES THE BOX WIDTH AWAY FROM THE MEDIAN). THE TIME PERIOD USED IS 1986–2005.



in mountainous regions, which is likely due to model resolution being insufficient to simulate local orographic enhancement of rainfall.

Figure 5.2.5 shows the comparison of annual and seasonal climatologies of mean sea level pressure for the wider region around Australia from observations and the ensemble mean. The middle and bottom rows display the shift between summer and winter pressure climatologies. During summer, the monsoonal low over north-west Western Australia dominates with high pressure systems pushed south of the continent. During winter, the high pressure system over the continent dominates. On average, the CMIP5 models capture these patterns very well (high spatial correlations), but the heat low during summer across the 'Top End' is too deep and broad. The model spread is several hectopascals (hPa) either side of the mean sea level pressure.

5.2.2 ASSESSMENT OF SPATIAL STRUCTURE OF HISTORICAL MEAN CLIMATOLOGIES: M-SCORES FOR RAINFALL AND TEMPERATURE

The correct representation of climatological seasonal rainfall is a very important test for climate models. Questions such as how well the models capture the southward extent of the monsoon are a typical example addressing this issue. Similarly important and somewhat related is the representation of temperature distribution across Australia. There are several methods that can be used to evaluate spatial characteristics from climate models. Here we applied the M-Statistic (see Box 5.1; Watterson, 1996) which has also been used for the previous *Climate Change in Australia* projections (CSIRO and BOM, 2007).

Two recent studies have made use of skill scores based on the M statistic for seasonal climatologies of selected climatic variables. Watterson *et al.* (2013a) used a simple test for overall skill in basic surface climate (calculating M-scores for each model) and Watterson *et al.* (2013b)

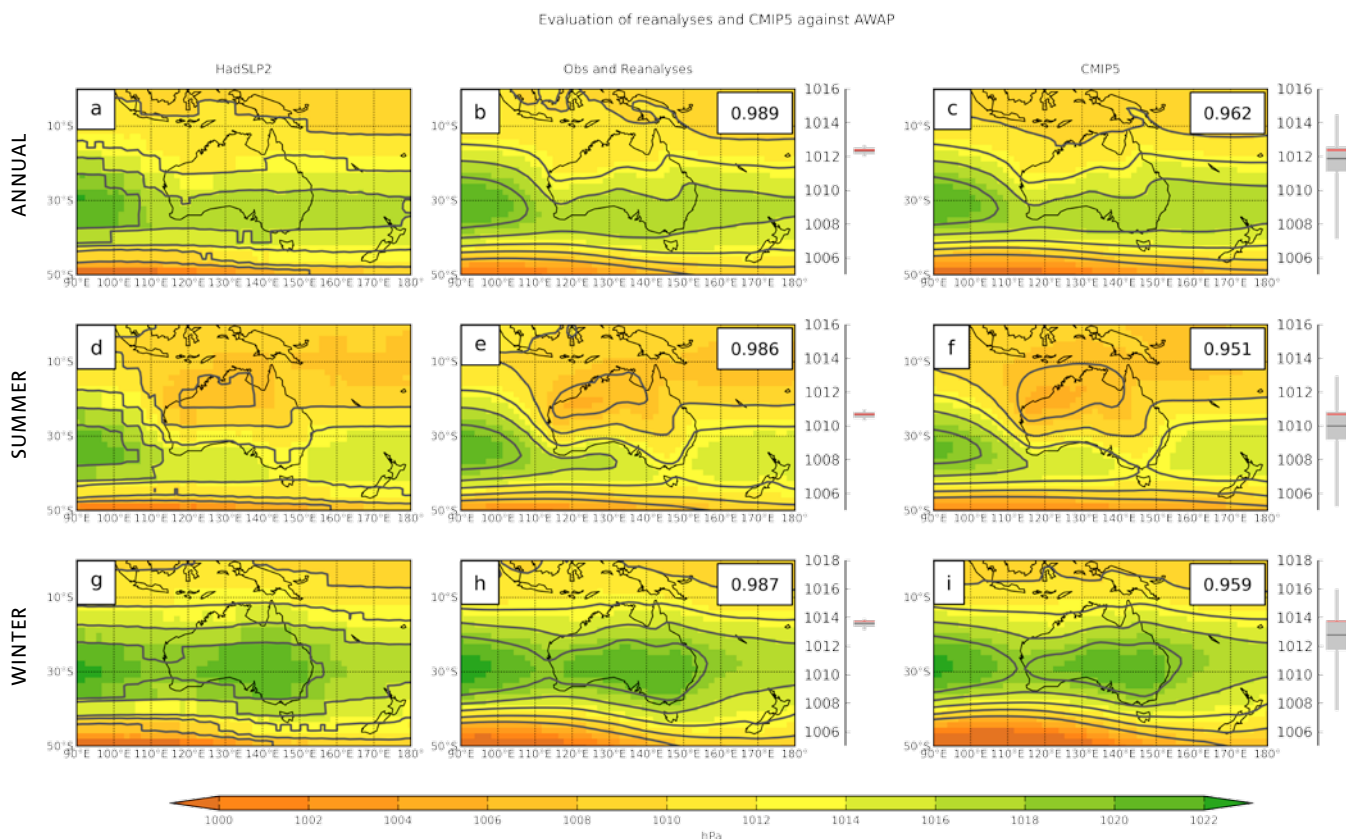


FIGURE 5.2.5: CLIMATOLOGICAL MEAN SEA LEVEL PRESSURE FROM HADSLP2 (A, D, G, USED AS THE REFERENCE DATA SET, SEE TABLE 5.1), THE AVERAGE OF A SELECTION OF OTHER OBSERVATIONAL DATA SETS (B, E, H, SEE TABLE 5.2.1) AND THE CMIP5 ENSEMBLE MEAN OF THE MODELS (C, F, I) FOR ANNUAL (TOP ROW), SUMMER (DEC-FEB, MIDDLE ROW) AND WINTER (JUN-AUG, BOTTOM ROW) MEAN SEA LEVEL PRESSURE. THE AVERAGING PERIOD IS 1986-2005 AND THE UNITS ARE HECTOPASCALS (HPA). THE X1, X2, AND X3 CONTOURS ARE HIGHLIGHTED FOR BETTER COMPARISON. THE NUMBER IN THE TOP RIGHT CORNER INDICATES THE SPATIAL CORRELATION BETWEEN THE CORRESPONDING DATA AND HADSLP2 (WITH VALUES CLOSER TO ONE INDICATING A BETTER CORRELATION). THE SPREAD IN THE DATA SETS IS INDICATED BY THE BOX-WHISKER TO THE RIGHT OF EACH SUBPLOT: EACH SHOWS THE AUSTRALIA-AVERAGED MEAN SEA LEVEL PRESSURE WHERE THE GREY BOX REFERS TO THE MIDDLE 50 % OF THE DATA AND THE WHISKERS SHOW THE SPREAD FROM MINIMUM TO MAXIMUM. THE THICK BLACK LINE IS THE MEDIAN OF THE UNDERLYING DATA AND THE RED LINE IS HADSLP2.

applied tests of various features of climate (such as the subtropical jet).

The calculations were done for the super-cluster regions (see Figure 2.3) used in this assessment: Southern Australia (SA), Eastern Australia (EA), Northern Australia (NA), and the Rangelands (R). The overall average of the M-scores (for three variables and four seasons) for each region and each model are given in Table 5.2.2. The score is out of a maximum of 1000. Most CMIP5 models show considerable skill in each region. The scores tend to be lower in smaller regions that have less spatial variation. The top scoring model for the full Australian region (AUS) is ACCESS1.0, but others do best for other regions.

Given the continuing use and validity of CMIP3 results, there is interest in how the two ensembles compare. Watterson *et al.* (2013a) gave results for 24 models in CMIP3. The top results are a little lower than for CMIP5, with differences from 14 to 111 points, as can be seen in Table 5.2.2. The means show a consistent, and larger, improvement for CMIP5, by 57 points for AUS. In fact, several CMIP3 models have poor scores, lowering the CMIP3 mean considerably.

The best performing models on these scores are: ACCESS1-0, bcc-csm1-1-m, EC-EARTH, HadGEM2-ES, MPI-ESM-LR and MPI-ESM-MR. The worst performing models are BNU-ESM, CESM1-WACCM, CMCC-CESM, GISS-E2-H, GISS-E2-H-CC, MIROC-ESM and MIROC-ESM-CHEM.

BOX 5.1: M STATISTIC FOR AGREEMENT

The *M* statistic or skill score is used as a metric for agreement between simulated and observed climatological fields over a particular region (Watterson, 1996). For the model field *X* and observed field *Y*, the *M* score is given by

$$M = (2/\pi) \arcsin[1 - mse / (V_x + V_y + (GX - G_y)^2)],$$

with *mse* the mean square error between *X* and *Y*, and *V* and *G* the spatial variance and regional mean, respectively, of the fields (as subscripted).

Like the correlation coefficient, *M* is non-dimensional and varies between +1 and -1, with 0 signifying no agreement. However, with *M*, 1 is reached only for identical fields (*mse* = 0), and *M* approaches 1 more slowly (for instance, global temperature fields typically correlate at *r* = 0.99, while *M* is 0.90). Tabulated values are multiplied by 1000. Averages of *M*-scores for the four seasons, for individual variables over the Australian region, are given in Table 5.2.2. Note that the *M* statistic is x1000. The average of scores for the three standard variables temperature, precipitation and pressure gives the score for overall skill in simulating the present climate for each model in Table 5.2.2. This overall score was used as a weight for each model in calculating projections by the 2007 method (see Section 6.2). Watterson *et al.* (2013a) further compares scores from CMIP5 and CMIP3 models over all continents.

TABLE 5.2.2: OVERALL SKILL SCORES FOR 40 CMIP5 MODELS OVER FIVE AUSTRALIAN DOMAINS. THE VALUES ARE THE AVERAGE M SCORE, TIMES 1000, FOR TEMPERATURE, RAINFALL AND MEAN SEA LEVEL PRESSURE, AND THE FOUR SEASONS. THE TOP VALUES ARE HIGHLIGHTED IN RED AND LOWEST VALUES IN BLUE. ALSO SHOWN ARE THE OVERALL AVERAGES AND TOP MODEL SCORE FOR THE CMIP5 ENSEMBLE AS WELL AS FOR CMIP3 FOR COMPARISON.

MODEL	AUS	SA	EA	NA	R
ACCESS1-0	727	575	514	540	677
ACCESS1-3	691	492	463	532	583
bcc-csm1-1	684	464	447	513	604
bcc-csm1-1-m	711	573	490	525	611
BNU-ESM	564	388	260	400	462
CanESM2	706	542	447	544	616
CCSM4	642	519	429	492	533
CESM1-BGC	653	518	471	488	543
CESM1-CAM5	659	589	640	475	511
CESM1-WACCM	555	360	429	410	442
CMCC-CESM	549	355	240	283	479
CMCC-CM	663	583	416	532	554
CMCC-CMS	672	471	408	553	568
CNRM-CM5	706	587	450	537	584
CSIRO-Mk3-6-0	613	431	362	467	500
EC-EARTH	711	636	569	499	587
FGOALS-g2	653	518	398	417	551
FIO-ESM	641	480	347	451	546
GFDL-CM3	676	546	571	465	542
GFDL-ESM2G	638	467	499	389	527
GFDL-ESM2M	607	383	396	393	515
GISS-E2-H	586	458	426	358	432
GISS-E2-H-CC	581	473	405	344	430
GISS-E2-R	575	516	406	350	445
GISS-E2-R-CC	614	543	459	394	477
HadGEM2-AO	711	499	499	541	634
HadGEM2-CC	698	533	472	538	628
HadGEM2-ES	720	556	506	554	674
inmcm4	657	455	423	434	569
IPSL-CM5A-LR	581	395	299	512	532
IPSL-CM5A-MR	612	477	360	556	527
IPSL-CM5B-LR	625	424	307	498	569
MIROC5	644	488	431	499	521
MIROC-ESM	549	434	321	379	451
MIROC-ESM-CHEM	561	450	344	386	456
MPI-ESM-LR	720	542	520	567	650
MPI-ESM-MR	705	513	513	587	625
MRI-CGCM3	659	511	482	434	559
NorESM1-M	604	480	471	368	505
NorESM1-ME	594	475	455	362	488
CMIP5 Average	643	492	434	464	543
CMIP3 Average	586	442	383	407	473
CMIP5 Top model	727	636	640	587	677
CMIP3 Top model	706	587	529	573	625



5.2.3 ASSESSMENT OF ANNUAL CYCLES OF HISTORICAL CLIMATE: RAINFALL AND TEMPERATURE

The annual cycle is one of the main climate features which, particularly for temperature and rainfall, is a crucial element to simulate correctly. Figure 5.2.6 shows the surface air temperature annual cycles for Australia and the super-cluster regions. In general there is very good

agreement, but with some model spread around the mean. For most regions (and months) the multi-model average is within half a degree of the AWAP value. One exception is the Southern Slopes cluster (Figure 5.2.6 bottom right) where models are too warm year round, but most of the differences there are related to biases over Tasmania (which is often poorly resolved) and not over the Victorian region within Southern Slopes.

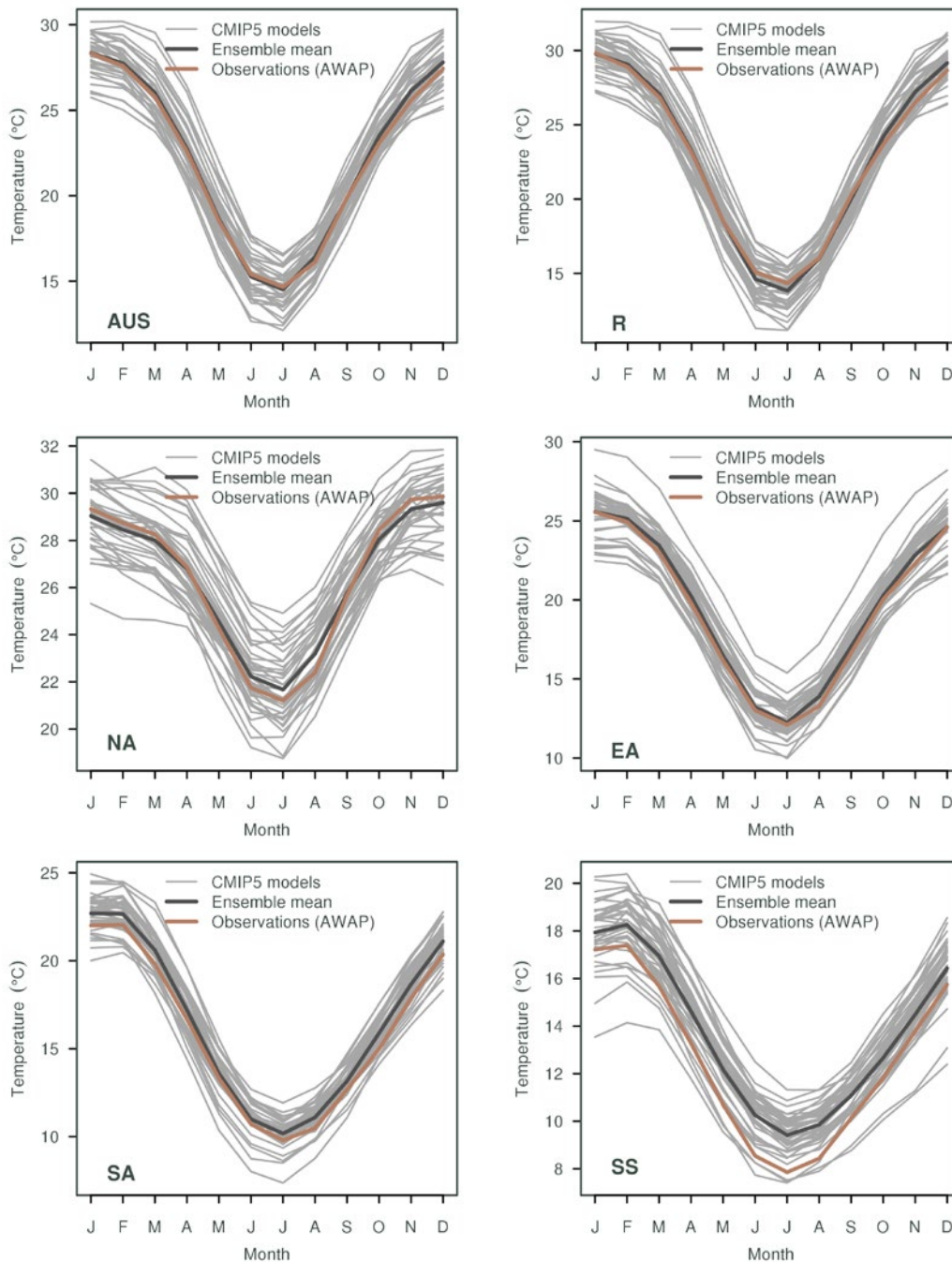


FIGURE 5.2.6: AVERAGE ANNUAL CYCLES OF SURFACE AIR TEMPERATURE FOR AUSTRALIA (TOP LEFT) AND SELECTED REGIONS (EAST AUSTRALIA - EA, NORTH AUSTRALIA - NA, RANGELANDS - R, SOUTHERN AUSTRALIA - SA, AND SOUTHERN SLOPES - SS) FROM CMIP5 MODELS. EACH GREY LINE REPRESENTS A MODEL SIMULATION, THE BLACK LINE BEING THE ENSEMBLE MEAN AND OBSERVATIONS (AWAP) SHOWN AS A BROWN LINE. THE AVERAGING PERIOD IS 1986–2005.

Figure 5.2.7 shows the corresponding rainfall annual cycles for the same regions. Because of the small-scale processes involved in rainfall simulation, it is more difficult to correctly simulate rainfall, particularly across small regions such as some of the clusters.

Regions with a pronounced annual rainfall cycle, such as monsoon dominated Northern Australia, show good model skill with the multi-model average matching the AWAP cycle – albeit with large inter-model spread. Other regions show more varying model skill and while the average might still be close to AWAP there is significant departure by some models. In the example of a fairly “flat” annual rainfall cycle (Southern Slopes cluster, Figure 5.2.7 bottom right), some models show even a reversed annual cycle (also see Figure 7.2.7).

The spatial-temporal root-mean-square-error (STRMSE) is used as a skill measure for the 1986–2005 annual-average rainfall cycle (following Gleckler *et al.* 2008). It combines spatial deviations from observed patterns for each month, thereby reflecting also the skill of simulating the annual cycle. This error measure is portrayed in Figure 5.2.8 as a relative error by normalizing the result by the median error of all model results. For example, a value of 0.20 indicates that a model’s STRMSE is 20 % larger than the median CMIP5 error for that variable, whereas a value of -0.20 means the error is 20 % smaller than the median error. For Australia, the median STRMSE for the CMIP5 models is close to 1 mm/day. The group of models that show significantly lower STRMSE values for rainfall are: MPI-ESM-MR, HadCM3, MPI-ESM-LR, IPSL-CM5B-LR, MRI-CGCM3, MIROC4h and CNRM-CM5. Those that have at least 30 % higher STRMSE than the median error are: CESM1-BGC, CCSM4, NorESM1-ME, NorESM1-M, CESM1-WACCM and CMCC-CMS.

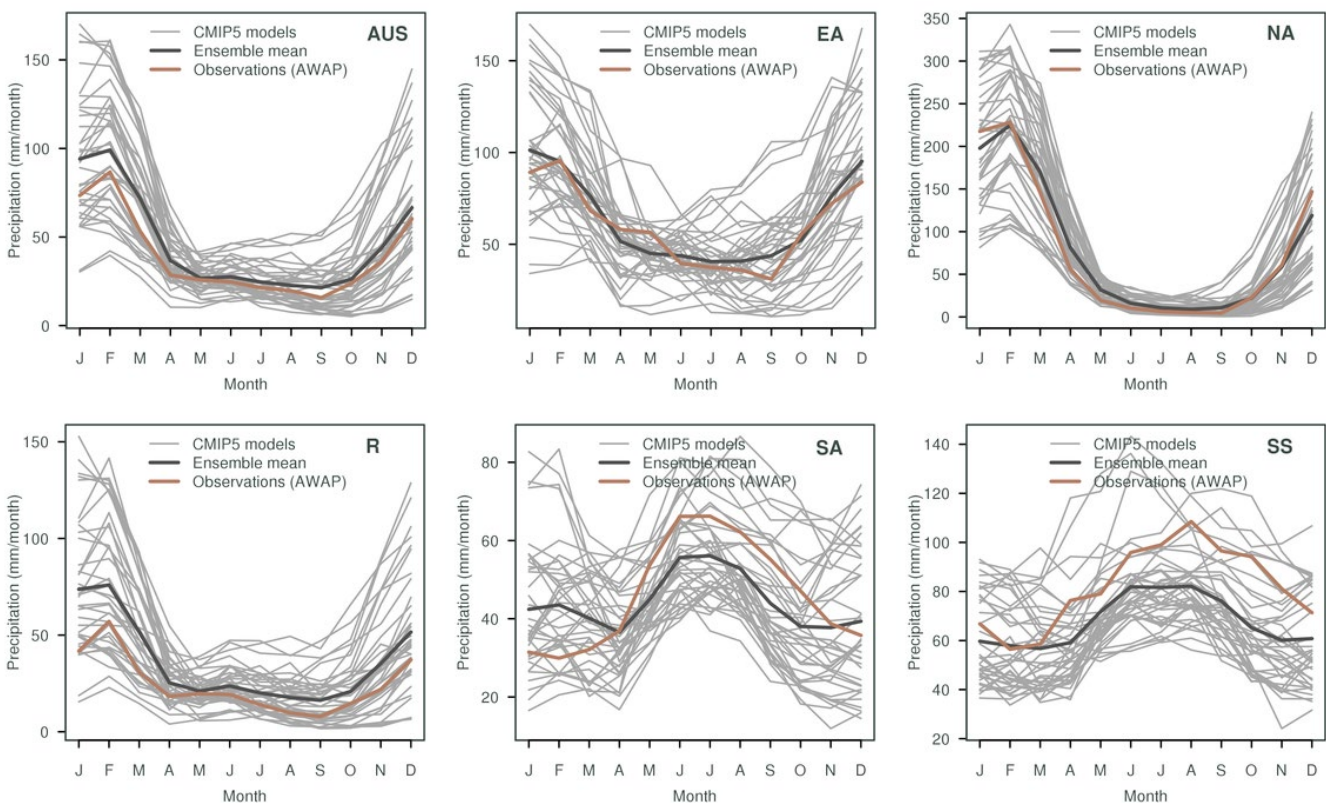


FIGURE 5.2.7: AVERAGE ANNUAL CYCLES OF RAINFALL FOR AUSTRALIA (TOP LEFT) AND SELECTED REGIONS (EAST AUSTRALIA - EA, NORTH AUSTRALIA - NA, RANGELANDS - R, SOUTHERN AUSTRALIA - SA, AND SOUTHERN SLOPES - SS) FROM CMIP5 MODELS. EACH GREY LINE REPRESENTS A MODEL SIMULATION, THE BLACK LINE BEING THE ENSEMBLE MODEL MEAN AND OBSERVATIONS (AWAP) SHOWN AS A BROWN LINE. THE AVERAGING PERIOD IS 1986–2005.



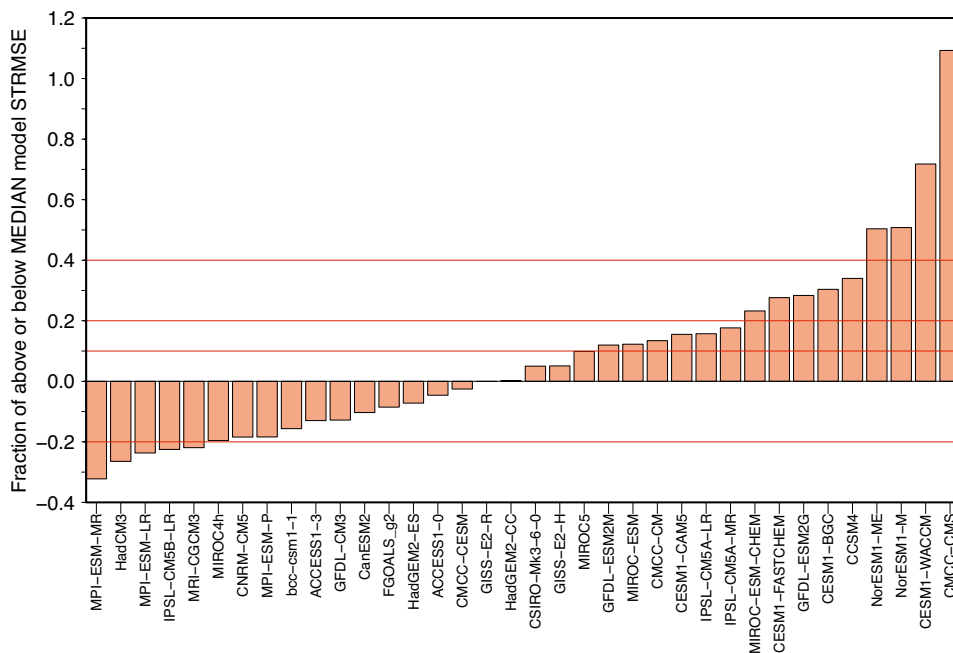


FIGURE 5.2.8: SPACE-TIME ROOT MEAN SQUARE ERROR OF CMIP5 MODELS RAINFALL ACROSS AUSTRALIA. THE ERROR IS SCALED TO SHOW THE FRACTIONAL ERROR HIGHER OR LOWER THAN THE MEDIAN MODEL ERROR. VALUES BELOW ZERO INDICATE BETTER THAN MEDIAN ERROR AND VALUES ABOVE ZERO HIGHER THAN MEDIAN ERROR. THE RED DOTTED LINES DISPLAY THRESHOLDS OF 10, 20 AND 40 % ABOVE THE MEDIAN ERROR (1.13 MM/DAY).

5.2.4 ASSESSMENT OF ADDITIONAL CLIMATE FEATURES AND ASSOCIATED SKILL SCORES

INTRODUCTION

As part of the UK Met Office's CAPTIVATE project (Scaife *et al.* 2011; stands for Climate Processes, Variability and Teleconnections), an evaluation of simulated Australian climate features was used. The tests were initially applied to the three Australian CMIP5 models (ACCESS 1.0, ACCESS 1.3 and CSIRO Mk3.6), with the results described in Watterson *et al.* (2013b). Here we consider only the tests for climatological features, which have been somewhat modified to suit the available data and NRM interests.

Again, the M statistic is used to quantify the agreement between each model and the observations, in each season. The variable and domains depend on the test, as outlined in Table 5.2.3. The variables surface air temperature (tas) and precipitation (pr), without being averaged as in Table 5.2.2, are tested and the domain is that of the Australian land area. The domain for the variable sea level pressure (psl) is over the larger region, as described in Table 5.2.3 in order to capture the pressure systems extending past the continent. Also tested over Australian land are incoming solar radiation (rsds) and the diurnal temperature range (DTR; using maximum and minimum temperature). Data for DTR are missing for 3 models (CMCC-CM, MPI-SEM-MR and NorESM1-ME).

TABLE 5.2.3: OVERVIEW OF TESTS FOR NINE FEATURES OF AUSTRALIAN CLIMATE, WITH VARIABLES AND DOMAIN GIVEN. ALL TESTS ARE DONE ACROSS THE FOUR SEASONS, EXCEPT FOR 'MONSOON ONSET', WHICH IS OVER SON AND DJF ONLY.

FEATURE	FIELDS- CMIP5 NAME	DOMAIN
1.5m Temperature	tas	Australia – land only
Rainfall	pr	Australia – land only
Solar radiation	rsds	Australia – land only
Diurnal temperature range	DTR	Australia – land only
Zonal and meridional winds at 850 hPa height	ua, va 850hPa	Region (longitude: 105 °E–165 °E; latitude: 0 °S–50 °S)
Zonal and meridional winds at 200 hPa height	ua, va 200hPa	Region (longitude: 105 °E–165 °E; latitude: 0 °S–50 °S)
Sea level pressure	psl	Region (longitude: 105 °E–165 °E; latitude: 0 °S–40 °S)
Subtropical jet	ua, 850, 500, 200 hPa	East Australia (longitude: 140 °E–150 °E; latitude: 15 °S–40 °S)
Monsoon onset	ua, va 1000 hPa ua 850hPa	North Australia (longitude: 120 °E–150 °E; latitude: 10 °S–20 °S)

-20° -10° 0° 10° 20° 30° 40° 50°

The diurnal temperature range is an important indicator for models' representation of extreme cold and warm temperatures, and therefore contributes to the skill in representing temperature extremes. Table 5.2.4 shows a very large spread along M-skill scores for DTR in CMIP5 models (from 94 to 496), which indicates that (a) the simulation of DTR is the least skillful of all features listed in Table 5.2.3 and (b) the spread of skill is largest amongst the CMIP5 models for DTR compared to the other features.

The ERA-Interim data set is again used as representing the observations for rsds (although given some doubt about its representation of cloud cover, the corresponding scores from the rsds field may not be reliable). For DTR, the AWAP data set is used.

The four other tests use wind data in zonal (east-west) and meridional (north-south) direction, which are available from 20 of the 40 models. The tests for wind at 850 hPa and 200 hPa are over the larger region (see Table 5.2.3) and are representative measures for skill in capturing the larger atmospheric circulation both closer to the surface (850 hPa) and further aloft (200 hPa). The tests for 'Subtropical Jet' and 'Monsoon Onset' are very simplified tests of winds over smaller rectangular regions (see Table 5.2.3 for domain details). Wind data from ERA-Interim are used as representing the observations.

The scores for the nine tests are given in Table 5.2.4. Quantities with smaller spatial variation tend to have smaller scores, in particular DTR. Even the best score for DTR, from ACCESS1.0, is only 496.

The top six models (averaged over the nine tests) are: ACCESS-1.0, CMCC-CM, CNRM-CM5, HadGEM2-CC, HadGEM2-ES, and MPI-ESM-MR. Note that three out of these six have the same atmosphere model. The worst performing models are: BNU-ESM, CESM1-WACCM, GISS-E2-H-CC, GISS-E2-R, GISS-E2-R-CC, IPSL-CM5A-LR, MIROC-ESM and MIROC-ESM-CHEM.

The main purpose of the scores is to support the NRM project by providing information about the quality of the models being used for projections. Naturally, these tests are only for the climate of the past decades, and the link between such skills and the reliability of climate changes is not well established. Nevertheless, skill in simulating the features of climate through the four seasons can add confidence in a model's ability to simulate changes that follow from global warming. This confidence is part of the overall assessment of projected changes in Australia's climate (see Section 6.4). The scores for the nine features add to the information available for assessment. It is important to note that both versions of ACCESS are well ranked in most of these tests.

THE EL NIÑO–SOUTHERN OSCILLATION

The El Niño–Southern Oscillation (ENSO) phenomenon is the dominant driver of climate variability on seasonal to interannual time scales for Australia (see for example Risbey *et al.* 2009b, Wang *et al.* 2004a, see also Section 4.1). While there has been an improvement in the simulation of ENSO in climate models from CMIP3 to CMIP5 (see for example Guilyardi *et al.* 2009; Chapter 14 in IPCC, 2013), some systematic errors remain and impact to some extent on the simulation of the relationship between ENSO and Australian rainfall (Watanabe *et al.* 2012, Weller and Cai, 2013a). However, there are improvements in the multi-model mean which is mostly due to a reduced number of poor-performing models (Flato *et al.* 2013).

The ENSO–rainfall teleconnection involves mechanisms similar to those related to the rainfall response to global warming (Neelin *et al.* 2003) and therefore provides a valuable insight into each model's rainfall response. While CMIP5 models display a slightly better skill in Australian rainfall reductions associated with El Niño (Neelin, 2007, Cai *et al.* 2009, Coelho and Goddard, 2009, Langenbrunner and Neelin, 2013), there is not much additional improvement over CMIP3. There is also little change in their abilities to represent the correlations between the equatorial Pacific sea surface temperatures (Niño 3.4 region) and north Australian sea surface temperatures (Catto *et al.* 2012a, 2012b) with models failing to adequately capture the strength of the negative correlations during the second half of the year. In general, the evolution of sea surface temperatures in the north Australian region during El Niño and La Niña is still problematic for models to simulate.

The teleconnection patterns from ENSO to rainfall over Australia are reasonably well simulated in the key September–November season (Cai *et al.* 2009, Weller and Cai, 2013b) in the CMIP3 and CMIP5 multi-model mean. Figure 5.2.9 shows the ranked list of the skill of this relationship in both CMIP3 and CMIP5 models. While there is clearly a majority of CMIP5 models towards the more skillful end of the list, there are a few CMIP5 models showing very little correlation (CSIRO-Mk3-6-0, IPSL-CM5A-MR, IPSL-CM5A-LR, HadCM3) or only small correlation (CanESM2, MIROC-ESM, INMCM4, and GFDL-ESM2G).



TABLE 5.2.4: SKILL SCORES FOR 40 CMIP5 MODELS FOR NINE FEATURES OF AUSTRALIAN CLIMATE. THE VALUES ARE THE AVERAGE M SCORE, TIMES 1000. THE TOP VALUES ARE HIGHLIGHTED IN RED AND LOWEST VALUES IN BLUE. WHERE THERE WAS SOME MISSING DATA, THE SCORE COULDN'T BE CALCULATED AND ARE INDICATED BY 'XXX'.

MODEL	TAS	PR	RSDS	DTR	WIND850	WIND200	PSL	ST JET	MONS ONS
ACCESS1-0	832	552	604	496	760	750	834	798	645
ACCESS1-3	792	544	606	198	690	678	798	738	496
bcc-csm1-1	780	499	699	295	657	684	716	687	543
bcc-csm1-1-m	766	525	744	365	xxx	xxx	811	xxx	xxx
BNU-ESM	755	451	534	120	xxx	xxx	615	xxx	xxx
CanESM2	824	492	705	426	717	718	812	712	500
CCSM4	816	379	602	172	720	758	802	744	611
CESM1-BGC	824	400	645	184	xxx	xxx	801	xxx	xxx
CESM1-CAM5	806	493	544	188	xxx	xxx	815	xxx	xxx
CESM1-WACCM	743	281	337	94	xxx	xxx	673	xxx	xxx
CMCC-CESM	641	479	644	289	xxx	xxx	481	xxx	xxx
CMCC-CM	794	486	698	xxx	xxx	xxx	757	xxx	xxx
CMCC-CMS	729	564	725	358	xxx	xxx	673	xxx	xxx
CNRM-CM5	742	602	770	485	xxx	xxx	863	xxx	xxx
CSIRO-Mk3-6-0	744	482	601	400	691	666	657	647	658
EC-EARTH	687	701	xxx	315	xxx	xxx	765	xxx	xxx
FGOALS-g2	755	535	725	235	667	737	586	625	624
FIO-ESM	817	424	705	141	xxx	xxx	636	xxx	xxx
GFDL-CM3	781	564	790	172	741	724	731	623	653
GFDL-ESM2G	716	472	617	122	712	724	798	771	593
GFDL-ESM2M	728	469	630	118	745	740	731	726	589
GISS-E2-H	661	490	271	228	662	647	738	748	486
GISS-E2-H-CC	610	501	269	181	xxx	xxx	769	xxx	xxx
GISS-E2-R	651	461	286	272	xxx	xxx	760	xxx	xxx
GISS-E2-R-CC	731	472	279	265	xxx	xxx	779	xxx	xxx
HadGEM2-AO	808	600	644	496	xxx	xxx	797	xxx	xxx
HadGEM2-CC	800	541	723	474	737	718	782	781	638
HadGEM2-ES	807	561	715	457	730	735	801	744	602
inmcm4	681	524	730	290	657	683	815	635	439
IPSL-CM5A-LR	796	403	414	118	622	659	507	473	390
IPSL-CM5A-MR	825	404	406	100	674	688	612	531	446
IPSL-CM5B-LR	760	596	519	128	xxx	xxx	559	xxx	Xxx
MIROC5	793	432	805	338	xxx	xxx	778	xxx	Xxx
MIROC-ESM	790	342	710	271	519	561	488	552	319
MIROC-ESM-CHEM	790	333	695	265	517	574	516	560	300
MPI-ESM-LR	830	593	812	232	xxx	xxx	743	xxx	xxx
MPI-ESM-MR	808	640	799	xxx	xxx	xxx	704	xxx	xxx
MRI-CGCM3	726	599	652	350	xxx	xxx	743	xxx	xxx
NorESM1-M	730	347	558	162	699	699	779	774	627
NorESM1-ME	724	343	559	xxx	676	699	752	785	623

-20° -10° 0° 10° 20° 30° 40° 50°

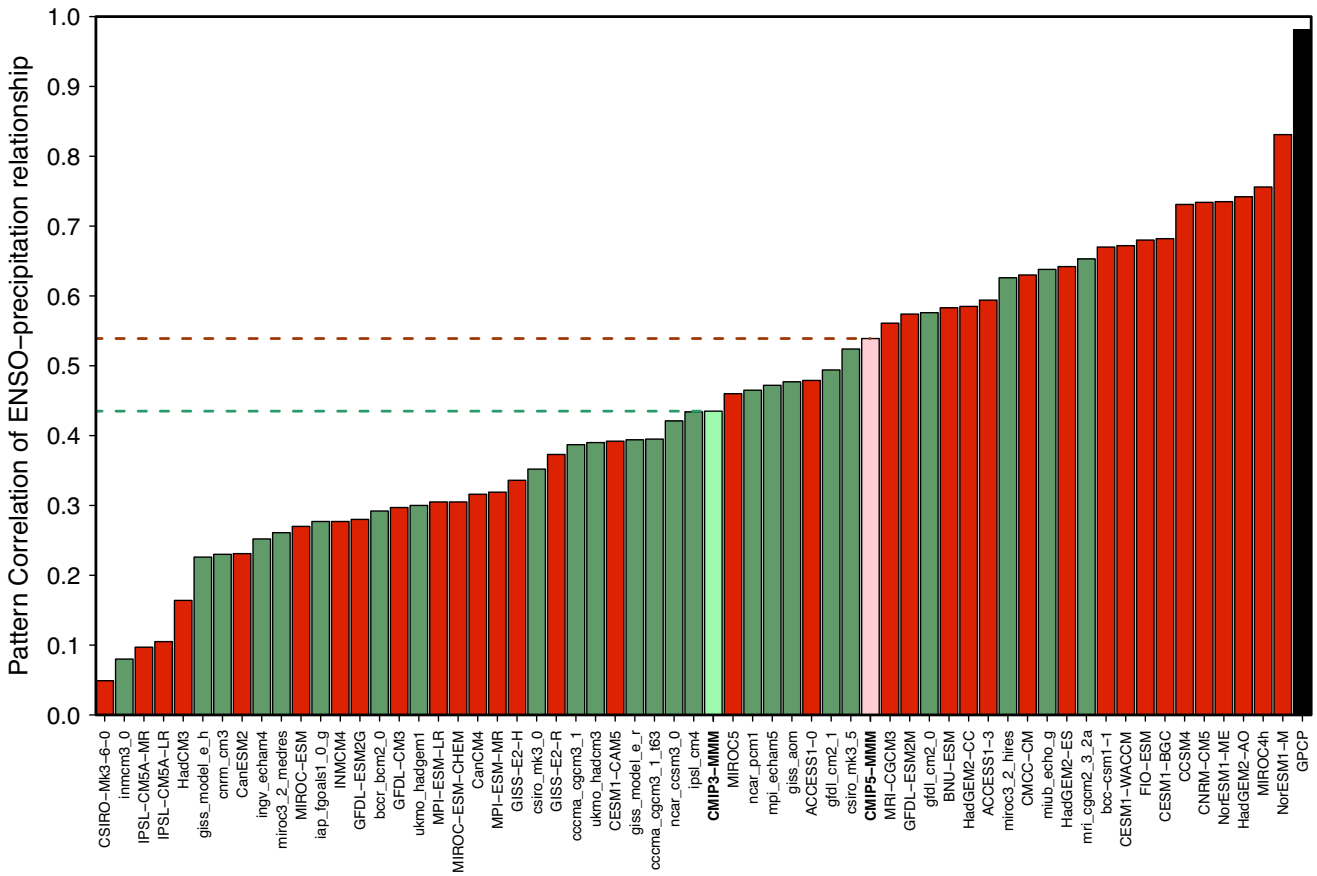


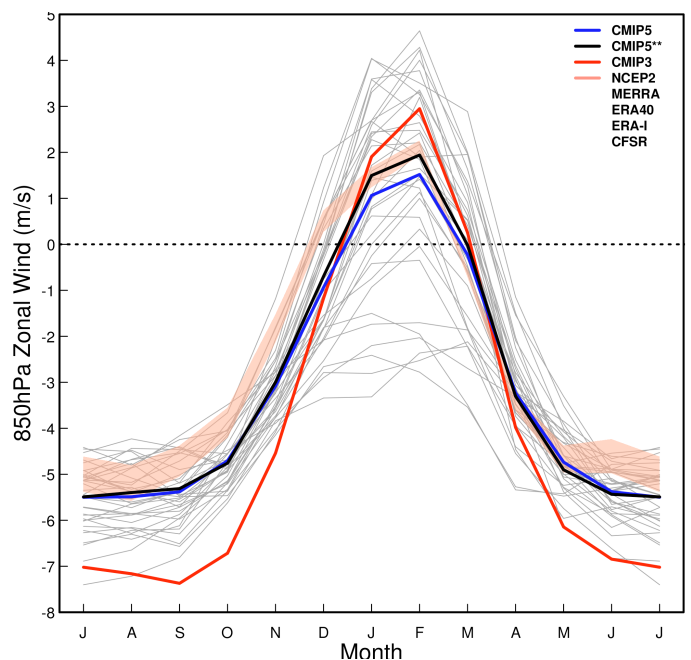
FIGURE 5.2.9: PATTERN CORRELATIONS (AGAINST THE CMAP-HADISST REFERENCE PATTERN) OF THE ENSO-AUSTRALIAN-RAINFALL TELECONNECTION PATTERN FOR EACH CMIP5 (RED) AND CMIP3 MODEL (GREEN). A SECOND OBSERVED DATA SET (GPCP-HADISST, BLACK BAR) IS SHOWN ON THE RIGHT WHILE THE MODELS ARE ORDERED IN INCREASING SKILL TOWARDS THE RIGHT. THE ENSEMBLE MEAN OF THE MODELS ARE SHOWN IN PINK (FOR CMIP5) AND LIGHT GREEN (FOR CMIP3).

THE AUSTRALIAN MONSOON

The Australian monsoon is the main driver of annual variation in the tropical regions (Trenberth *et al.* 2000, Wang and Ding, 2008, Moise *et al.* 2012) and therefore is an important feature for climate models to correctly simulate. This will also enhance confidence in future projections of mean changes and associated impacts (Colman *et al.* 2011).

The monsoon is characterised by an annual reversal of the low level winds and well defined dry and wet seasons (Moise *et al.* 2012, Wang and Ding, 2008), and its variability is primarily connected to the Madden-Julian Oscillation (MJO) and ENSO. Most CMIP3 models

FIGURE 5.2.10: MONTHLY SEASONAL CLIMATOLOGY OF 850 HPA ZONAL WIND (1986-2005), AVERAGED OVER 120–150°E, 10–20°S LAND ONLY FOR 37 CMIP5 MODELS, 5 REANALYSIS PRODUCTS (CFSR, MERRA, NCEP2, ERA40 AND ERA-INT; FORMING THE PINK SHADED BAND) AND THE ENSEMBLE MEAN OF THE MODELS OF CMIP3 (RED) AND CMIP5 (BLUE). THE THICK BLACK LINE REPRESENTS THE ENSEMBLE MEAN OF CMIP5 EXCLUDING MODELS NOT SIMULATING MONSOON WESTERLIES OVER THIS REGION.



poorly represent the characteristics of the monsoon and monsoon teleconnections (Randall *et al.* 2007), with some improvement in CMIP5 with respect to the mean climate, seasonal cycle, intraseasonal, and interannual variability (Sperber *et al.* 2013; also see Figure 5.2.7 top right for Northern Australia). Figure 5.2.10 shows the annual cycle of low level zonal winds for CMIP5 models and several reanalysis data sets. On average the models reversal to westerlies starts later than in the reanalysis, but has a similar timing in the switch to easterlies in March. Several models fail to simulate monsoon westerlies over northern Australia altogether: GISS-E2-H, GISS-E2-H-CC, GISS-E2-R, IPSL-CM5A-LR, IPSL-CM5A-MR, MIROC-ESM, INMCM4, ACCESS1-3 and MIROC-ESM-CHEM.

While the entire annual rainfall cycle has been assessed earlier using the spatial-temporal root-mean-square error (STRMSE, see Figure 5.2.8) here we focus on the wet season only and assess the spatial distribution of wet season rainfall from the models over the tropical Australia domain. Figure 5.2.11 shows the ranked list of the skill of Australian tropical rainfall distribution in both CMIP3 and CMIP5 models. While there is clearly a majority of CMIP5 models towards the more skilful end of the list, there are a few CMIP5 models showing very little skill (MIROC-ESM, MIROC-

ESM-CHEM, MPI-ESM-LR, MPI-ESM-MR, MPI-ESM-P) or only small skill (GFDL-ESM2G, MIROC5, and HadCM3).

With respect to the onset of the Australian monsoon, Table 5.2.4 also includes the M-score for skill in monsoon onset for CMIP5 models. While better models reach a score above 600, several models score below 400 and both MIROC-ESM and MIROC-ESM-CHEM are close to 300.

ATMOSPHERIC BLOCKING

The climate along the Australian mid-latitudes is predominantly affected by weather regimes such as east-west moving pressure systems or East Coast Lows, and blocking weather regimes are often associated with extreme rainfall events (see Section 4.1.2 and also Risbey *et al.* 2009a). During blocking, the prevailing mid-latitude westerly winds and storm systems are interrupted by a local reversal of the zonal flow resulting in enhanced rainfall events. The strongest correlation between blocking (using a blocking index) and Australian rainfall is during autumn, but also in winter. It affects mainly south-eastern regions of the continent (Risbey *et al.* 2009a).

Climate models in the past have universally underestimated the occurrence of blocking. As in CMIP3, most of the CMIP5

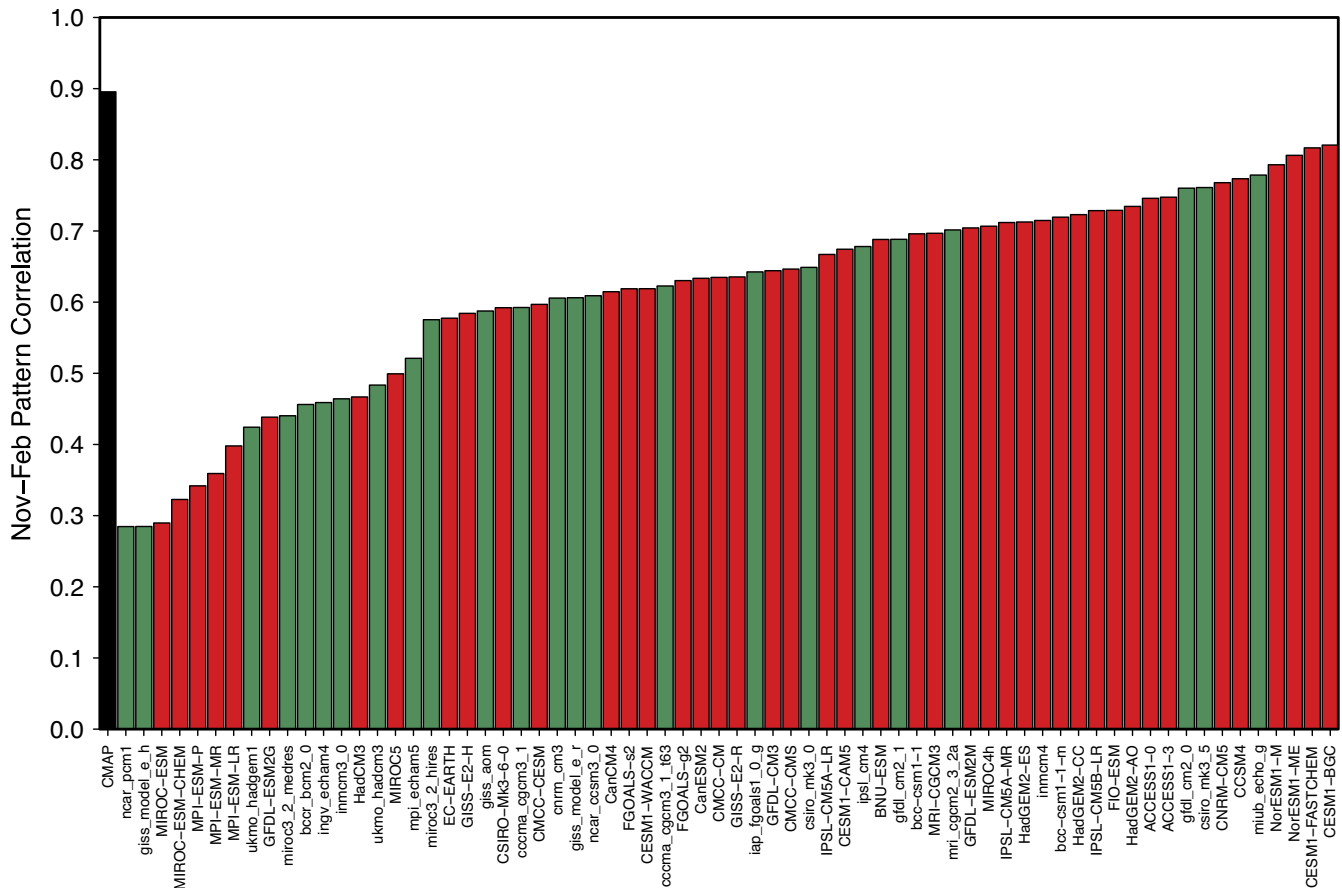


FIGURE 5.2.11: WET SEASON (NOV-FEB) RAINFALL PATTERN CORRELATIONS (AGAINST GPCP REFERENCE DATA SET) FOR CMIP5 (RED) AND CMIP3 MODELS (GREEN) OVER TROPICAL AUSTRALIA. A SECOND OBSERVED DATA SET (CMAP, BLACK BAR) IS SHOWN ON THE LEFT WHILE THE MODELS ARE ORDERED IN INCREASING SKILL TOWARDS THE RIGHT.

-20° -10° 0° 10° 20° 30° 40° 50°

models still significantly underestimate blocking (Dunn-Sigouin and Son, 2013). Increasing model resolution is expected to improve model representation of blocking significantly (IPCC, 2013, Chapter 14).

During atmospheric blocking the upper tropospheric westerly air stream typically splits into two sections. The strength of this split can be assessed through a combination of the upper air zonal wind field (at 500hPa) at different latitudes integrated into a simple Blocking Index (BI, Pook and Gibson, 1999 see also Risbey *et al.* 2009a, Grose *et al.* 2012):

$$BI = 0.5(u_{a_{25}} + u_{a_{30}} - u_{a_{40}} - 2u_{a_{45}} - u_{a_{50}} + u_{a_{55}} + u_{a_{60}})$$

Where u_{ax} is the zonal wind at 500hPa at latitude x (degrees south). The BI is calculated here at longitude 140°E which represents the region over Australia where blocking is typically observed. The CMIP5 models were evaluated with respect to the seasonal correlations of the Blocking Index in autumn and winter to rainfall across relevant south-eastern cluster regions (Central Slopes, East Coast South, Murray Basin, Southern Slopes) (results not shown). Almost half of the models assessed showed reasonable correlations across several clusters. Models that showed very low skill in reproducing this relationship include ACCESS1-3, CanCM4, GFDL-ESM2G, GISS-E2-R and GISS-E2-H.

SOUTHERN ANNULAR MODE

The Southern Annular Mode (SAM) is the most dominant driver for large-scale climate variability in the mid- and high-latitudes of the Southern Hemisphere (Thompson and Solomon, 2002) – describing the alternation of atmospheric mass between high- and mid-latitudes. This alternation affects pressure and wind patterns across southern parts of Australia and therefore also impacts on rainfall in these regions (for more detail, see Section 4.1.2 and also Hendon *et al.* 2007, Risbey *et al.* 2009b). When SAM is in its high phase there are higher pressures over southern Australia, wind anomalies are predominantly easterly and rainfall is reduced on west-facing coastlines, but enhanced on east-facing regions.

CMIP3 and CMIP5 models are able to produce a clear Southern Annular Mode (Raphael and Holland, 2006, Zheng *et al.* 2013, Barnes and Polvani, 2013), but there are relatively large differences between models in terms of the exact shape and orientation of this pattern.

THE INDIAN OCEAN DIPOLE

Similar to ENSO, the Indian Ocean dipole mode (IOD) (see Section 4.1.2) is an ocean-atmosphere phenomenon located in the tropical Indian Ocean. The main period of impact on Australian rainfall is spring (Sep–Nov) and depending on the phase of the IOD, the ENSO impact can be enhanced over Australia. If the IOD is in its positive phase, El Niños can result in stronger reduction of rainfall and if the IOD is in its negative phase, La Niñas show further enhanced rainfall (Risbey *et al.* 2009b).

Most CMIP3 and CMIP5 models are able to reproduce the general features of the IOD, but show a large spread in the strength of the IOD (Saji *et al.* 2006, Liu *et al.* 2011, Cai and Cowan, 2013). Most models also show a location bias in the westward extension of the IOD. No substantial improvement is seen in CMIP5 compared to CMIP3 (Weller and Cai, 2013a).

A majority of CMIP3 and CMIP5 models also simulate the observed correlation between IOD and ENSO. The magnitude of this correlation varies substantially between models, but seems independent of each model's simulation of ENSO (Saji *et al.* 2006, Jourdain *et al.* 2013).

The teleconnection patterns from both ENSO and IOD to precipitation over Australia are reasonably well simulated in the key September–November season (Cai *et al.* 2009, Weller and Cai, 2013b) in the CMIP3 and CMIP5 multi-model mean.

One way to assess the spatial structure of the IOD is by computing the Taylor statistics (Taylor, 2001) of the tropical Indian Ocean sea surface temperatures where the IOD occurs as shown in Figure 5.2.12. These statistics (spatial correlation; spatial root-mean-square error and spatial standard deviation) can highlight non-temporal deficiencies in the simulation of this feature. Most CMIP5 models simulated very high spatial correlations. Combining the statistics into a skill score as proposed by Taylor (2001) we find that while most CMIP5 models show very high spatial correlations (above 0.95), the main difference between more skilful and less skilful models lies in their simulation of the spatial variability of sea surface temperatures (horizontal spread of letters in Figure 5.2.12). In particular, MRI-CGCM3 and CSIRO-MK3-6-0 have a much reduced variability and GFDL-CM3, IPSL-CM5B-LR, ACCESS1-0 and HadCM3 show a far too strong variability (furthest right from the reference dashed line).

THE MADDEN–JULIAN OSCILLATION

During summer the eastward propagating feature of enhanced and diminished convection from the Indian Ocean into the western Pacific known as the Madden-Julian Oscillation (MJO; Madden and Julian, 1972; 1994) mainly affects the tropics north of 15°S. It is one of the dominating features of intra-seasonal variability (60–90 days) and plays a major role in the onset of the Australian monsoon (Wheeler *et al.* 2009; see Section 4.1).

Various diagnostics have been used to assess the skill of simulating the MJO in climate models (Waliser *et al.* 2009, Xavier, 2012). The main model errors in representing the MJO relate to the skill in the model convection schemes and their mean state biases (Kim *et al.* 2012, Mizuta *et al.* 2012, Inness *et al.* 2003).

Sperber and Kim (2012) provided a simplified metric synthesising the skill of CMIP3 and CMIP5 model results. Some of the more skilful models are those with higher resolution (CNRM-CM5, CMCC-CM) while several models



showed very low coherence in the propagation of the convection: MIROC-ESM-CHEM, INM-CM4, IPSL-CM5A-MR, IPSL-CM5A-LR, MIROC-ESM, GFDL-ESM2G and HadGEM2-ES.

While Sperber and Kim (2012) show that the simulation of the MJO is still a challenge for climate models (see also Lin *et al.* 2006, Kim *et al.* 2009, Xavier *et al.* 2010), there has been some improvement in CMIP5 in simulating the eastward propagation of the summer MJO convection (Hung *et al.* 2013). Further improvements have been reported for the MJO characteristics in the east Pacific (Jiang *et al.* 2013). In general, CMIP5 models have improved compared to previous generations of climate models with respect to the MJO (Waliser *et al.* 2003, Lin *et al.* 2006, Sperber and Annamalai, 2008).

WINDS AND ATMOSPHERIC CIRCULATION

Wind fields across Australia are associated with large-scale circulation patterns and their seasonal movement. Across the southern half of Australia, average wind conditions are influenced by the seasonal movement of the subtropical high pressure belt which separates the mid-latitude westerly winds to the south and the south-east trade winds to the north (see Section 4.1.2 for more information on subtropical ridge). Across the north of Australia, from about November to March the Asian-Australian monsoon interrupts the trade winds bringing a north-westerly flow across northern Australia (see Figure 4.1.1).

The evaluation of winds in climate models therefore mainly focuses on these two large-scale seasonal changes: the north-south shift across the southern half of Australia and the east-west reversal of winds across tropical Australia. Due to the sparseness of long-term, high quality wind

measurements from terrestrial anemometers, a high quality gridded data set for wind is not available over Australia (Jakob, 2010). Therefore 10 m winds from reanalysis products are commonly used as a baseline against which climate model winds are compared (see Table 5.2.1 for overview of reanalysis data sets). The annual cycle in the pressure and latitude of the subtropical high pressure belt known as the subtropical ridge (STR) is fairly well represented in the CMIP3 mean, but each model has some biases in position and intensity (Kent *et al.* 2013). This means there are typically some biases in the northern boundary of the westerly circulation. Also, the relationship between the STR and rainfall variability is poorly simulated in some models and trends in the pressure of the ridge are underestimated by all CMIP3 models (Kent *et al.* 2013, Timbal and Drosowsky, 2013). Preliminary results indicate that results are similar in CMIP5 models (not shown).

The path of westerly weather system generally to the south of the subtropical ridge is known as the ‘storm track’ and is a crucial feature of rainfall variability in southern Australia. The representation of the storm track, and its connection to processes such as ENSO, has improved from CMIP3 to CMIP5, but certain models still show poor performance (Grainger *et al.* 2014).

Regarding the wind reversal over tropical Australia during the monsoon season, Figure 5.2.10 shows the annual cycle of low level zonal winds for CMIP5 models and several reanalysis data sets. As mentioned above, on average the models’ reversal to westerlies starts later compared to the reanalysis, but has a similar timing in the switch back to easterlies in March. As noted earlier, several models fail to simulate monsoon westerlies over northern Australia altogether.

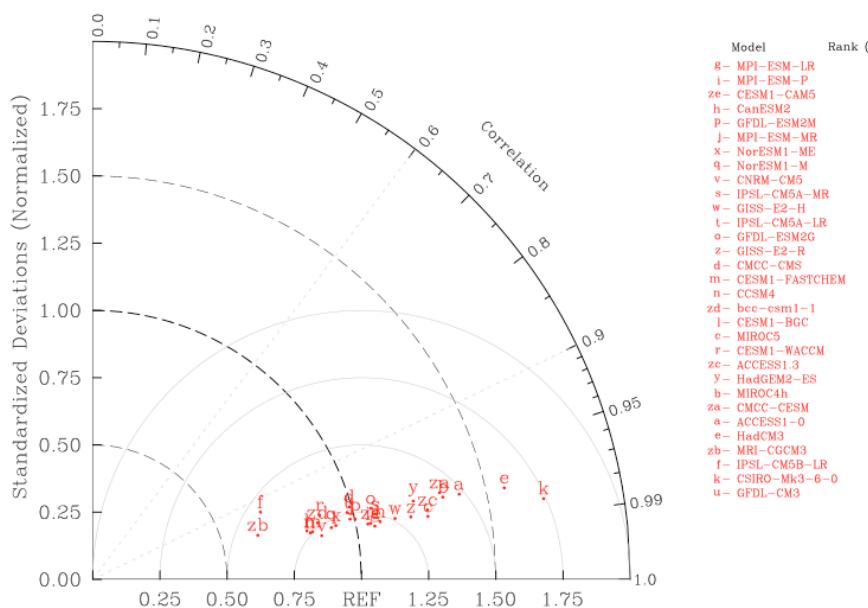


FIGURE 5.2.12: TAYLOR PLOT OF SPATIAL STATISTIC OF SEA SURFACE TEMPERATURES FROM CMIP5 MODELS OVER THE TROPICAL EASTERN INDIAN OCEAN AGAINST HADISST OBSERVED SEA SURFACE TEMPERATURES (REF POINT AT HORIZONTAL AXIS). EACH LETTER REPRESENTS ONE CMIP5 MODEL’S SIMULATION AVERAGED OVER THE PERIOD (1986-2005).



5.3 EVALUATION OF SIMULATED RAINFALL AND TEMPERATURE TRENDS

In addition to the long-term climatology and the annual cycle (see previous section), climate models are also evaluated with respect to how well they are able to reproduce observed climate change. Aspects of climate change have been extensively evaluated at global to continental scales and the simulated warming is found to agree well with observations (Stone *et al.* 2009). Changes in global precipitation, on the other hand, are less well reproduced in simulations (Zhang *et al.* 2007). Recently, global climate models have also been evaluated against observed regional climate change (van Oldenborgh *et al.* 2009, van Haren *et al.* 2012, van Oldenborgh *et al.* 2013, Bhend and Whetton, 2013)

Recent regional trends in seasonal mean daily maximum and minimum temperature and rainfall have been evaluated (Bhend and Whetton, 2013). Simulated trends in the historical experiment from the CMIP5 ensemble are compared to the observed trends. Climate models used here have been run with a comprehensive set of observed and reconstructed boundary conditions including the changing atmospheric concentrations of greenhouse gases, aerosols, and ozone as well as solar irradiance changes. The models thus produce a realistic - within model limitations - representation of recent climate change.

It is important to note, however, that a portion of the observed and simulated recent change is due to natural internal variability in the climate system. This part of climate change differs between observations and simulations, as the simulations are not constrained to exhibit internal variability that is in phase with the observed internal variability. The remainder of the change – the signal – is due to changes in external forcing mechanisms and therefore in principle reproducible in long-term simulations (see Section 3.1 for further discussion). Only this deterministic, forced component of climate change can be used for evaluation of climate models. Therefore, being able to separate signal from noise (internal variability) is crucial when evaluating transient behaviour in climate models and a multitude of methods to achieve this exists (Bindoff *et al.* 2013). For simplicity, we assume here that the regional signal in both temperature and rainfall over the period from 1956 to 2005 is approximately linear.

Simulated seasonal rainfall and daily maximum and minimum temperature trends from 42 global climate models in the CMIP5 ensemble (see Table 3.3.1) are compared with observed trends in the station-based gridded datasets. ACORN-SAT (Trewin, 2013) and CRU TS3.20 (Harris *et al.* 2013) were used for temperature, and AWAP (Jones *et al.* 2009a, Raupach *et al.* 2009; 2012) and CRU TS3.20 for precipitation (listed in Table 5.2.1 under CRU). We compute linear trends from 1956 to 2005 using ordinary least squares regression.

The observed trends in seasonal mean daily maximum temperature from 1956 to 2005 show significant warming in eastern and southern Australia and widespread cooling (some of which is statistically significant) in the summer half-year in north-western Australia (Figure 5.3.1a-d). The ensemble median simulated trends for the same period show consistent warming and less than 10 per cent of the simulations reproduce the cooling in spring (SON) and summer (DJF) in north-western Australia (Figure 5.3.1e-h). While the trend biases are locally significant (at 90 per cent level based on a simple estimate of internal variability in observations and model time series) in the majority of the climate models, the area where significant differences are found is generally not larger than what one would expect due to internal variability alone. Results for trends in seasonal mean daily minimum temperatures are qualitatively similar (not shown).

The picture is similar for rainfall. The area where significant differences are found between observed and simulated rainfall trends is generally not larger than what one expects due to internal variability alone (Figure 5.3.2a-d). Less than 10 per cent of the models reproduce the significant wetting in north-western Australia in summer (DJF), the drying in south-eastern Australia in autumn (MAM) and the wetting in north-eastern Australia in spring (SON). Additional analyses reveal that the majority of the models significantly (at the 10 per cent level) underestimate the observed wetting in north-western Australia in summer and the observed drying in south-eastern Australia in spring (not shown.) (i.e. due to random chance).

In conclusion, areas where the CMIP5 ensemble fails to reproduce observed trends from 1956-2005 in seasonal mean daily maximum and minimum temperature and seasonal rainfall are evident. The extent of the areas for which these discrepancies exist, however, is generally not larger than expected due to the pronounced variability on inter-annual to decadal scales. Therefore, there is no conclusive evidence that CMIP5 models fail to reproduce recent observed trends in daily maximum and minimum temperature and rainfall. Nevertheless, confidence in rainfall projections is inevitably reduced where consistency is low, particularly north-western Australia in summer and south-eastern Australia in autumn.



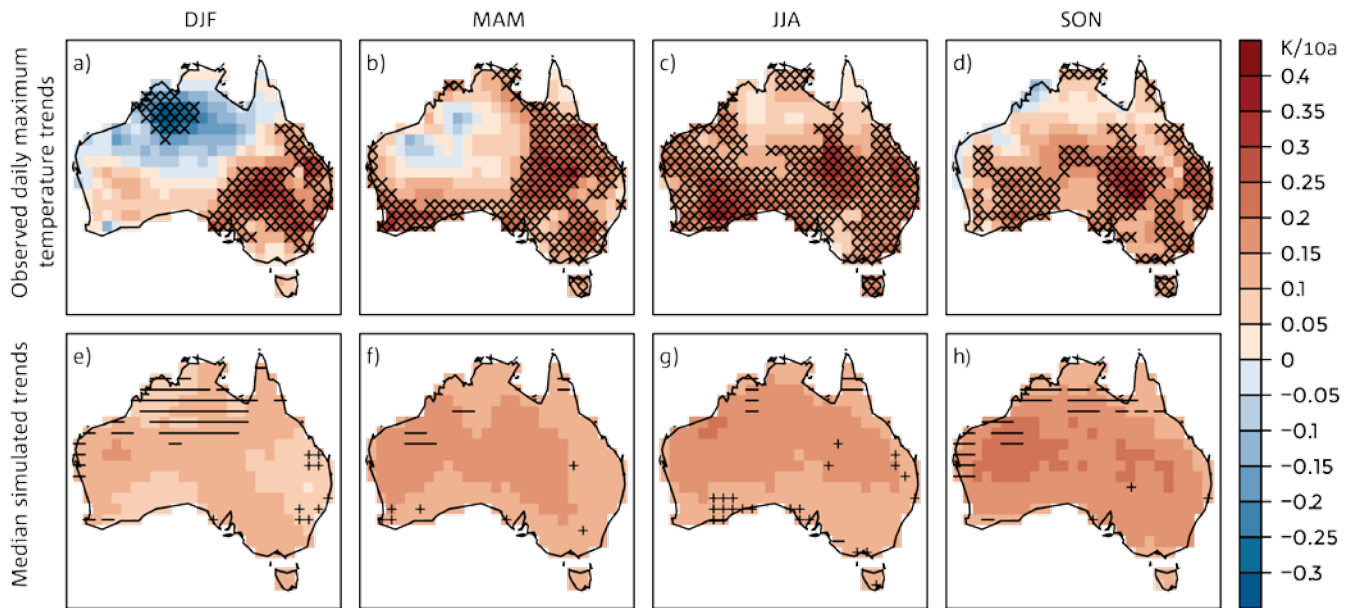


FIGURE 5.3.1: OBSERVED TREND IN SEASONAL MEAN DAILY MAXIMUM TEMPERATURE FROM 1956 TO 2005 (A-D) AND MEDIAN OF SIMULATED TRENDS FROM 42 CMIP5 MODELS (E-H). CROSSES IN A-D DENOTES AREAS WHERE THE OBSERVED TREND IS SIGNIFICANTLY DIFFERENT FROM ZERO AT THE 10 % LEVEL. CROSSES (DASHES) IN E-H DENOTE AREAS WHERE LESS THAN 10 % OF THE SIMULATED TRENDS ARE AS LARGE (SMALL) AS THE OBSERVED TREND.

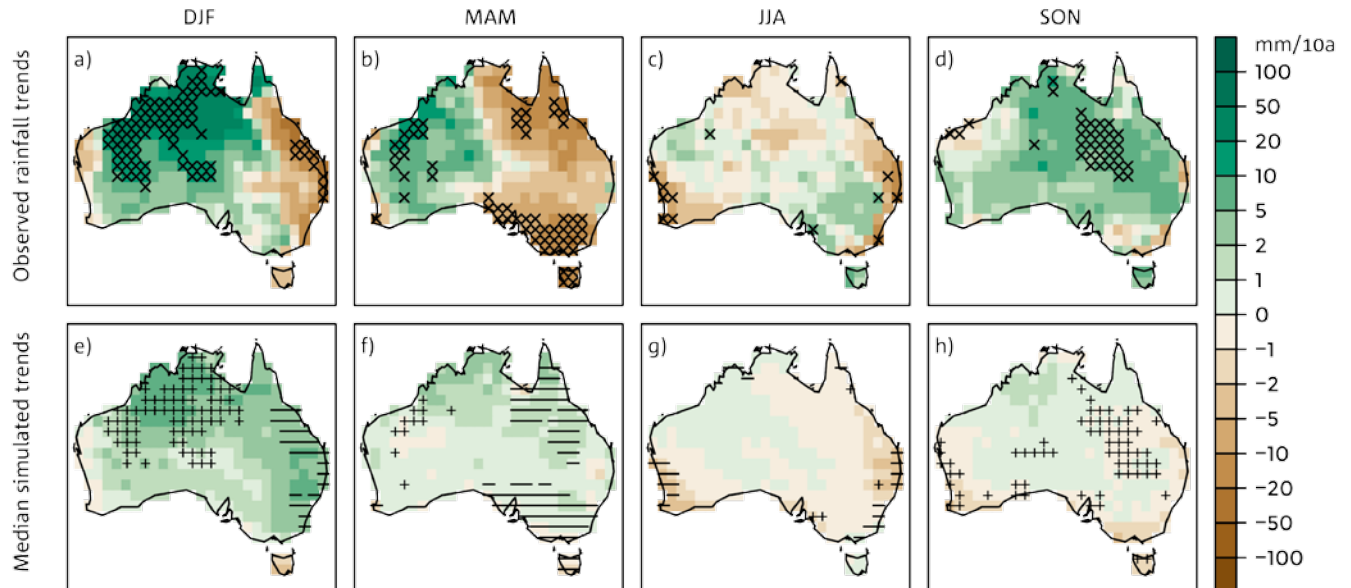


FIGURE 5.3.2: AS IN FIGURE 5.3.1 BUT FOR SEASONAL RAINFALL IN MM PER DECADE.

-20° -10° 0° 10° 20° 30° 40° 50°

5.4 EVALUATION OF EXTREMES IN CLIMATE MODELS

Extreme events refer to weather and climate events near the ‘tail’ of the probability distribution. They are in general difficult to realistically represent in climate models. The 2007 IPCC *Fourth Assessment Report* concluded that models showed some considerable skill in simulating the statistics of extreme events (especially for temperature extremes) given their coarse resolution (Randall *et al.* 2007). In a separate report, the IPCC has conducted an assessment of extreme events in the context of climate change: the Special Report on Managing the Risks of Extreme Events and Disasters to Advance Climate Change Adaptation (SREX) (IPCC, 2012). Although climate model evaluation with respect to extreme events was not done in a consistent manner in SREX, model performance was taken into account when projections uncertainty was assessed.

The evaluation of the simulation of extremes in climate models is important because the impacts of climate change will be experienced more profoundly in terms of the frequency, intensity or duration of extreme events (*e.g.* heat waves, droughts, extreme rainfall events).

The recently published IPCC *Fifth Assessment Report* (Working Group 1) (IPCC, 2013) summarised that the global distribution of temperature extremes are represented well by CMIP5 models. Furthermore, it reported that CMIP5

models tend to simulate more intense and thus more realistic precipitation extremes than CMIP3, which could be partly due to generally higher horizontal resolution. Also, CMIP5 models are able to better simulate aspects of large-scale drought.

Specifically for Australia, we have assessed the bias in three of the extreme indices from the CMIP5 model ensemble: annual and seasonal maximum of daily maximum temperature (T_{xx}); annual and seasonal minimum of daily minimum temperature (T_{nn}) and the annual and seasonal maximum 1-day rainfall event (rx1day). Additionally, the 20-year return value of these quantities has been compared to observed values. There are currently two global observation-based data sets available to assess climate extreme indices: the GHCNDEX (Donat *et al.* 2013a, Fischer and Knutti, 2014) and the HadEX2 (Donat *et al.* 2013b) data set, with the latter having less spatial coverage, particular across northern Australia.

A comparison between CMIP5 model daily maximum rainfall and observations is shown in Figure 5.4.1 for seasons and annually for two example clusters; Monsoonal North (MN) and Southern Slopes (SS). With less data coverage in tropical Australia for the Monsoonal North we focus on how the models are placed compared to the GHCNDEX data points (red downward triangles in Figure 5.4.1). Overall the observed daily maximum rainfall amounts here are mostly captured

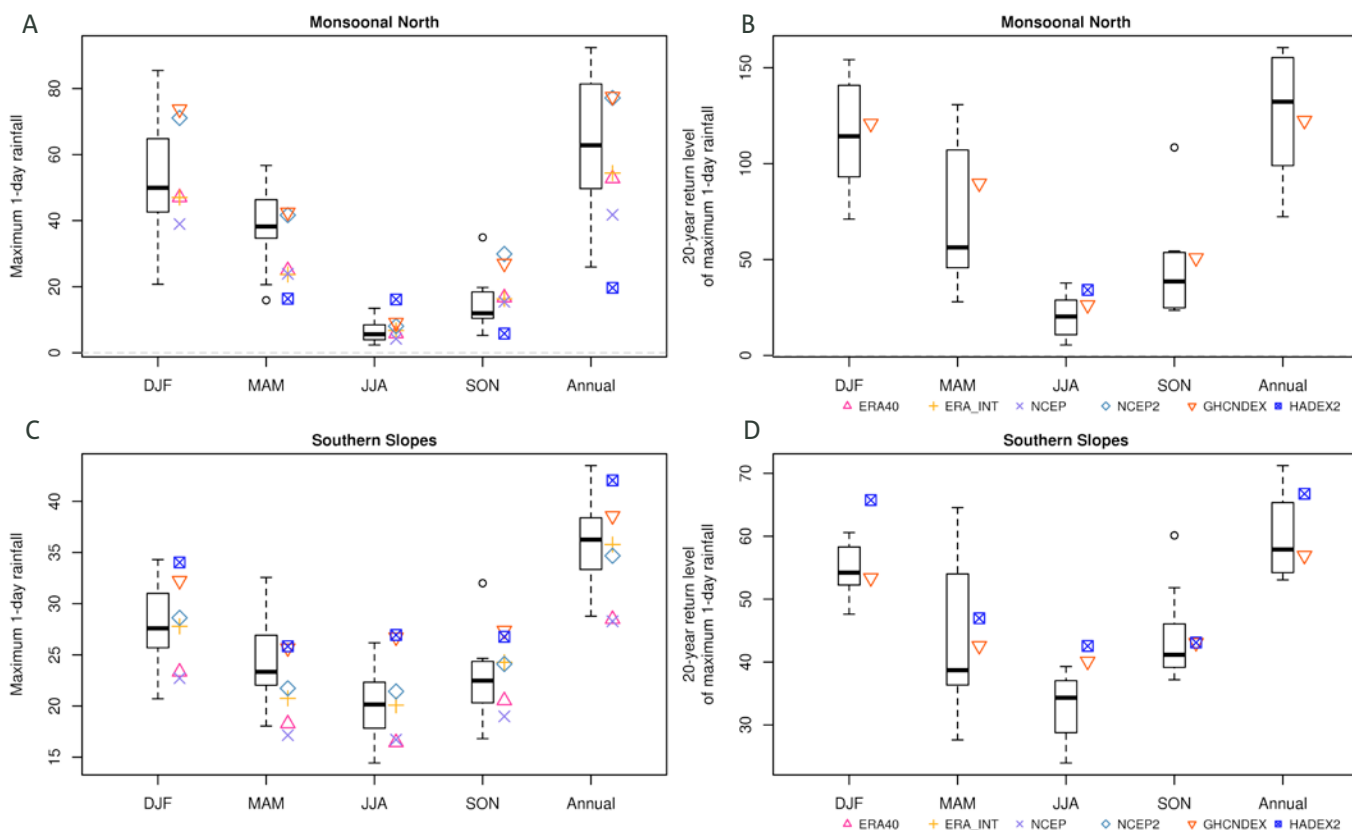


FIGURE 5.4.1: DAILY EXTREME RAINFALL (LEFT COLUMN: FOR DAILY MAXIMUM RAINFALL PER YEAR; ((A) FOR CLUSTER MN AND (C) FOR CLUSTER SS); FOR DAILY MAXIMUM RAINFALL IN 20 YEARS ((B) FOR CLUSTER MN AND (D) FOR CLUSTER SS) ACROSS SEASONS AND ANNUALLY (UNITS ARE MM/DAY). CMIP5 MODELS ARE REPRESENTED BY THE BOX-WHISKER WHILE COLOURED SYMBOLS REPRESENT REANALYSIS PRODUCTS (SEE TABLE 5.2.1) AND TWO GRIDDED OBSERVATIONAL DATA PRODUCTS (SEE TEXT).

-20° -10° 0° 10° 20° 30° 40° 50°

by the Interquartile Range (middle 50 % of CMIP5 model simulations) of the model ensemble. This is true for both the maximum daily rainfall event within a year (Figure 5.4.1a) as well as the maximum daily rainfall event over a 20 year period (Figure 5.4.1b). For summer and averaged over the entire Monsoonal North cluster, the latter event is around 120 mm in the observations and very close to the ensemble median. The spread is fairly substantial – particular towards the lower end with some models showing less than half the observed rainfall during the maximum event.

For the Southern Slopes cluster, the CMIP5 models have a tendency to underestimate the maximum 1-day rainfall event during a year (Figure 5.4.1c), but are still within range. The 20-year event (Figure 5.4.1d) is somewhat better captured. Noteworthy is the fact that despite on average receiving more rainfall during winter (JJA), the maximum one-day rainfall events are stronger in the summer months.

Other clusters show very similar results quantitatively: fairly large model spread around median maximum rainfall values that are not too far from that observed.

However, it should be noted that this assessment is for rain events averaged at large spatial scales, whereas many extreme rainfall events in the real world occur at a far smaller spatial scale. These events are included not as single small-scale events, but aggregated over each larger grid cell.

Annual and 20 year daily maximum and minimum temperatures show similar biases to mean temperature: a slight cold bias for maximum and slight warm bias for minimum temperatures. As with rainfall, the model spread is fairly large (up to 10 degrees for some seasons for both daily maximum and minimum temperature).

In summary, the CMIP5 models are able to capture the annual maximum 1-day rainfall event reasonably well. Additionally, they are able to simulate both annual and seasonal daily maximum and minimum temperatures with some skill.

5.5 EVALUATION OF DOWNSCALING SIMULATIONS

This Report includes regional climate change projections information from two downscaling methods (described in detail in later in Section 6.3). Therefore it is necessary to also provide some information about how well these simulations perform over the historical period.

Each of the two methods used here have important aspects that bring them closer to observations. For the statistical downscaling method, observed relationships between local synoptic situations and the large-scale climate are used to build the statistical model. This usually leads to a very close representation of the observed climate in the statistical downscaling model, (almost) independent of the choice of host global climate model. A set of 22

global climate models have been used as hosts and the resulting statistical downscaling model simulations are all very similar over the historical period (1986-2005). For the dynamical downscaling method, the monthly sea surface temperature data used as input from each global climate model simulation are initially adjusted to match the observed mean climate before being used to build the dynamical downscaling simulation. This means the resulting dynamically downscaled simulations are again fairly similar to each other and to the observations over the historical period (1986-2005). Not surprisingly then, for the mean climate we find that all performance metrics are very high for temperature and rainfall, as well as for mean sea level pressure in the dynamical downscaling simulations (not shown).

We also assessed two measures of temporal variability for rainfall: the annual cycle (through the spatial-temporal root mean square error, STRMSE following Gleckler *et al.* (2008) as above) and the inter-annual variability of rainfall – both at cluster level. Figure 5.5.1 shows the comparison of the STRMSE for both ensembles across the cluster regions and the entire continent. Even though the dynamical downscaling ensemble only has 6 members (compared to 22 for the statistical downscaling ensemble), the spread in performance is quite similar for both. Apart from the Southern Slopes (SS) and Murray Basin (MB) clusters, the size of the error is comparable between the two ensembles as well. The dynamical downscaling shows larger STRMSE than the statistical downscaling for SS and MB clusters. For all other non-tropical clusters, the median STRMSE is mostly below 0.5 mm/day. The larger inter-model spread is seen for the tropical cluster regions (Wet Tropics and Monsoonal North) where climatological rainfall is very high and seasonal differences are also very pronounced.

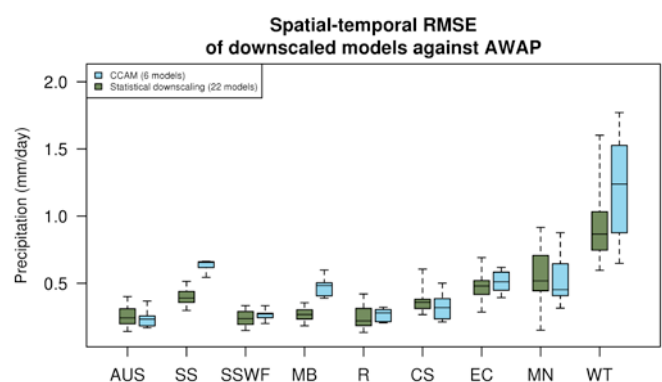


FIGURE 5.5.1: BOX-WHISKER PLOT OF THE SPATIAL-TEMPORAL ROOT MEAN SQUARE ERROR (STRMSE; LARGER VALUES INDICATE LARGER ERRORS COMPARED TO OBSERVATIONS) FOR RAINFALL FROM TWO DOWNSCALED ENSEMBLES AGAINST AWAP RAINFALL FOR AUSTRALIA AND THE EIGHT CLUSTER REGIONS. THE DOWNSCALED ENSEMBLES ARE THE BOM-SDM STATISTICAL DOWNSCALED ENSEMBLE (GREEN) AND THE CCAM DYNAMICAL DOWNSCALED ENSEMBLE (BLUE).



The year to year variability of rainfall is an important feature of the climate within each of the clusters and Figure 5.5.2 shows a comparison of the two downscaling ensembles against various observational data sets (including AWAP) for the period 1986–2005. In the observations, the inter-annual variability is fairly modest except along the East Coast and over tropical Australia where the impact of monsoonal rainfall is strong. The statistical downscaling ensemble is able to capture the extra-tropical inter-annual rainfall variability well, whereas the dynamical downscaling ensemble shows especially good skill over the tropical clusters and the Rangeland cluster.

It should be noted that whereas downscaling generally involves processes that bring the simulation of the current climate further in line with observations, the downscaling simulations inherit much of the climate change ‘signal’ from the host model. Therefore the set of excellent evaluation metrics shown above does not lead to a proportional increase in the confidence in the projections from downscaling compared to GCMs. They do however show that both downscaling methods achieved their aim: to produce higher resolution outputs with smaller biases than GCMs (compare 1.13 mm/day median STRMSE across Australia in GCMs (Figure 5.2.8) to around 0.25 mm/day in downscaled simulations here) that may then reveal regional detail in the climate change signal at finer scale than GCMs can (see further discussion of these points in Sections 6.3 and 7.2).

5.6 SYNTHESIS OF MODEL EVALUATION

Model evaluation is an important tool to help rate confidence in climate model simulations. This can add to the overall confidence assessment for future projections of the Australian climate. Additionally it can highlight significant model deficiencies that may affect the selection of a subset of models for use in impact assessment.

ATMOSPHERIC VARIABLES

The CMIP5 models are able to capture the broad-scale characteristics of the 1986–2005 average surface air temperature, rainfall and surface wind climatology. However they display some important deficiencies in simulating the finer details, especially for rainfall. Sometimes model skill can be impacted by large-scale biases in the models. For example in some models the so-called ‘cold-tongue’ bias in the central Pacific Ocean influences the ENSO teleconnection to Australian rainfall and therefore results in an additional bias in the annual rainfall cycle. There are also biases in the representation of the seasonal wind reversal across tropical Australia around the onset of the monsoon.

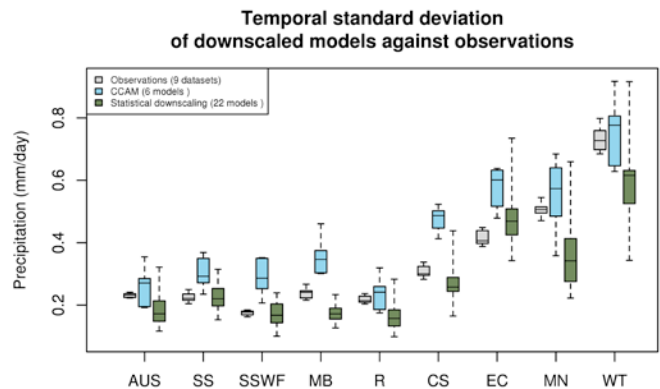


FIGURE 5.5.2: BOX-WHISKER PLOT OF THE TEMPORAL STANDARD DEVIATION OF ANNUAL RAINFALL (1986–2005) FROM TWO DOWNSCALED ENSEMBLES AND GRIDDED OBSERVATIONAL RAINFALL FOR AUSTRALIA AND THE EIGHT CLUSTER REGIONS. THE DOWNSCALED ENSEMBLES ARE THE BOM-SDM STATISTICAL DOWNSCALED ENSEMBLE (GREEN) AND THE CCAM DYNAMICAL DOWNSCALED ENSEMBLE (BLUE). THE OBSERVATIONAL DATA INCLUDES AWAP.

The GISS-E2 models (GISS-E2-H, GISS-E2-H-CC and GISS-E2-R) and MIROC-ESM models (MIROC-ESM MIROC-ESM-CC) provide consistently poorer simulations of the average climate across all atmospheric variables examined. Additionally, IPSL-CM5A-LR shows deficient simulations for several fields and both NorESM1-M models are particularly deficient for rainfall across Australia.

REGIONS AND CLUSTERS

Some regions and clusters are more difficult to simulate than others (for temperature and rainfall). This is typically the case when (a) the region or cluster is quite small and therefore only a few grid cells contribute to the statistics; and (b) where topography and coastlines play a major role. For example, the skill of simulation of rainfall is acutely linked to surface fields such as topography, coastlines and land surface cover. This is one of the reasons why rainfall varies strongly at regional scales. Therefore higher resolution models can potentially better resolve these processes. The Wet Tropics region is a good example for both. Others are the Southern Slopes sub-clusters in Tasmania and the East Coast cluster.

For rainfall, the two models CESM1-WACCM and CMCC-CESM show particularly poor simulations across regions in Australia and GISS models GISS-E2-H, GISS-E2-H-CC and GISS-E2-R are similarly deficient mainly over the Wet Tropics and Rangelands regions (Table 5.2.2). A few other models showing deficiencies only over some regions include BNU-ESM (for Southern and Eastern Australia); GFDL-ESM2M (for Southern Australia); IPSL-CM5A-LR and IPSL-CM5B-LR (for Eastern Australia); and MIROC-ESM (scoring the lowest for the entire continent).



CLIMATE FEATURES AND PATTERNS OF VARIABILITY

Most of the CMIP5 global climate models are able to reproduce the major climate features (SAM, monsoon, pressure systems, subtropical jet, circulation – see Table 5.2.4 and Section 5.2.4) and modes of variability (seasonal cycle, ENSO, Indian Ocean Dipole). Three models (IPSL-CM5A-MR, IPSL-CM5A-LR and CSIRO-MK3-6-0) show unusually low skill with respect to the ENSO-rainfall teleconnection. This is partly due to their bias in the equatorial sea surface temperatures. The following models do not simulate the reversal to monsoon westerlies across tropical Australia during the monsoon season: GISS-E2-H, GISS-E2-H-CC, GISS-E2-R, IPSL-CM5A-LR, IPSL-CM5A-MR, MIROC-ESM, INMCM4, ACCESS1-3 and MIROC-ESM-CHEM.

RECENT OBSERVED TRENDS

There is no conclusive evidence that CMIP5 models fail to reproduce 1956-2005 observed trends in daily maximum and minimum temperature and rainfall. The extent of the areas where discrepancies exist are generally not larger than expected due to the pronounced variability on inter-annual to decadal scales. Nevertheless, confidence in rainfall projections is inevitably reduced where consistency is low, particularly north-western Australia in summer and south-eastern Australia in autumn.

EXTREMES

CMIP5 models are able to capture the annual maximum 1-day rainfall events across different clusters reasonably well. Additionally, they are able to simulate both annual and seasonal daily maximum and minimum temperatures with some skill.

DOWNSCALING SIMULATIONS

Because of the inherent nature of the downscaling methods applied here, the rainfall and temperature climatology is simulated very well. Some differences between the statistical and dynamical method are seen when evaluating climate variability, with the dynamical scheme showing better ability to simulate higher inter-annual variability (in the tropics) while the statistical scheme shows better ability across the southern half of Australia.

CMIP5 MODEL RELIABILITY AND IMPLICATION FOR PROJECTIONS

Despite some models performing poorly across multiple evaluation metrics, the approach adopted for generating climate change projections for Australia has been to equally weight all participating CMIP5 models. As will be seen in Section 6.2, in forming ranges of projected change using CMIP5, factoring in model performance (by different methods weighting or model elimination) does not have a strong affect, and is not done routinely in the ranges of projected change presented in Chapter 7 (although there are some exceptions noted in that chapter). Nevertheless

the model performance results are used in two other important ways. First, they are considered in formulating the confidence rating that is attached to the CMIP5 projections (see Section 6.4 and Chapter 7). Secondly, poor performing models are flagged in the Climate Futures tool (Chapter 9), to guard against these models being selected when forming a small set of models for use in impact assessment.

From the results of the analysis presented in the individual sections of this chapter, the following models were identified as poor performing models, for the reasons outlined (see also Table 5.6.1). All of these models should be used with caution in any projection work in regions or for variables, where the noted model deficiencies are likely to be particularly relevant. The models are:

- MIROC-ESM and MIROC-ESM-CHEM don't simulate temperature and rainfall over Australia well. They also do not produce monsoon westerlies during the monsoon season and therefore show deficient wet season rainfall (spatial distribution). Both models score low on the simple MJO skill (propagating convection into tropical region). MIROC-ESM additionally shows deficient ENSO-rainfall teleconnection for Australia.
- GISS-E2H, GISS-E2H-CC and GISS-E2R show low scores for temperature and rainfall across Australia. They also simulate low scores averaged across various climate features and don't produce monsoon westerlies during the wet season over tropical Australia. Two of the three GISS models do not show a correlation between blocking and rainfall over Australia.
- IPSL-CM5A-MR and IPSL-CM5A-LR show unusually low skill with respect to the ENSO-rainfall teleconnection over Australia. These two IPSL models also have deficient simulation of larger circulation (no monsoon westerlies) and propagating convection (low MJO related skill) across tropical Australia.
- CESM1-WACCM and BNU-ESM are equally low in skill for temperature and rainfall simulations across Australia and averaged over nine climate features important for Australia. Additionally, CESM1-WACCM shows deficiencies in simulating the annual cycle of rainfall while BNU-ESM has lower skill in the spatial representation of wet season rainfall.
- Similar to the IPSL models mentioned above, the INMCM4 model has low skill in representing the ENSO-rainfall relationship for Australia and does not produce monsoon westerlies during the wet season over tropical Australia. Additionally, there is low MJO related skill.
- GFDL-ESM-2G has low skill in representing the ENSO-rainfall relationship for Australia and does not show a correlation between blocking and rainfall over Australia. Additionally, there is low MJO related skill.



TABLE 5.6.1: SUMMARY OF MODELS SCORING LOW ON VARIOUS SKILL METRICS USED THROUGHOUT THE MODEL EVALUATION PROCESS. FOR EACH EVALUATION THE LOWEST 6-8 MODELS ARE INCLUDED. THE COLUMN ON THE RIGHT GIVES THE OVERALL SUM OF HOW OFTEN A MODEL FELL INTO THE LOWER GROUP.

MODEL	Low M-Score for PR and TAS	Low STRMSE	Low score for climate features	Low ENSO – rainfall tele connection	No Monsoon westerlies	Wet season rainfall not good spatially	Rainfall relationship to Blocking not good	IOD spatial variability too low or too high	Simple MJO skill not good	
ACCESS1-0								X		1
ACCESS1-3					X		X			2
BNU-ESM	X		X			X				3
CanCM4							X			1
CanESM2				X						1
CCSM4		X								1
CESM1-BGC		X								1
CESM1-WACCM	X	X	X							3
CMCC-CESM	X									1
CMCC-CMS		X								1
CSIRO-Mk3-6-0				X				X		2
GFDL-CM3								X		1
GFDL-ESM2G				X			X		X	3
GISS-E2-H	X		X		X		X			4
GISS-E2-H-CC	X		X		X					3
GISS-E2-R			X		X		X			3
HadCM3				X				X		2
HadGEM2-ES									X	1
INMCM4				X	X				X	3
IPSL-CM5A-LR				X	X				X	3
IPSL-CM5A-MR				X	X				X	3
IPSL-CM5B-LR								X		1
MIROC-ESM	X			X	X	X			X	5
MIROC-ESM-CHEM	X				X	X			X	4
MPI-ESM-LR						X				1
MPI-ESM-MR						X				1
MPI-ESM-P						X				1
MRI-CGCM3								X		1
NorESM1-M		X								1
NorESM1-ME		X								1

CHAPTER SIX

CLIMATE CHANGE PROJECTION METHODS



MACQUARIE RIVER, TASMANIA, ISTOCK

-20° -10° 0° 10° 20° 30° 40° 50°

CHAPTER 6 CLIMATE CHANGE PROJECTION METHODS

The Australian climate change projections are based on the full body of knowledge of the climate system and the most up to date view of how the current climate may change under enhanced greenhouse gas emissions. This view of future climate is informed by sophisticated global climate models, simulating the climate response to a range of plausible scenarios of how greenhouse gases and aerosols may change throughout the 21st century. This chapter outlines the methods for producing projections and accompanying confidence ratings. Note that methods unique to the marine projections will be covered where those projections are presented in Chapter 8.

The key sources of uncertainties in climate change data from global climate models are discussed in Section 6.1, followed by a description of the method used to summarise their outputs (Section 6.2). An outline of downscaling and how it is used to provide additional and complementary insights to global climate model simulations is described in Section 6.3. The final section describes how model evaluation, process understanding, attribution of observed trends and consistency with simulated recent changes, and downscaled projections are used to derive confidence statements for climate change projections. These confidence statements give guidance about the robustness of the projections, and act to support users when implementing these projections in further analysis, impact assessment and adaptation planning.

6.1 LIMITATIONS AND UNCERTAINTIES IN CLIMATE CHANGE DATA

6.1.1 SOURCES OF UNCERTAINTY

Uncertainties in regional climate change projections can be grouped into three main categories: scenario uncertainty, due to the uncertain future emissions and concentrations of greenhouse gases and aerosols; response uncertainty, resulting from limitations in our understanding of the climate system and its representation in climate models; and natural variability uncertainty, the uncertainty stemming from unperturbed variability in the climate system. Figure 6.1.1 illustrates the relative contributions of these three broad sources of uncertainty to regional climate projections as estimated from 28 CMIP5 simulations for two variables, mean temperature and rainfall in winter (Hawkins and Sutton, 2009). The plot shows the contribution to uncertainty for a projection of decadal mean climate for different times in the future. Please note that the relative contributions also depend on the climatic variable, spatio-temporal aggregation and location (see discussion below).

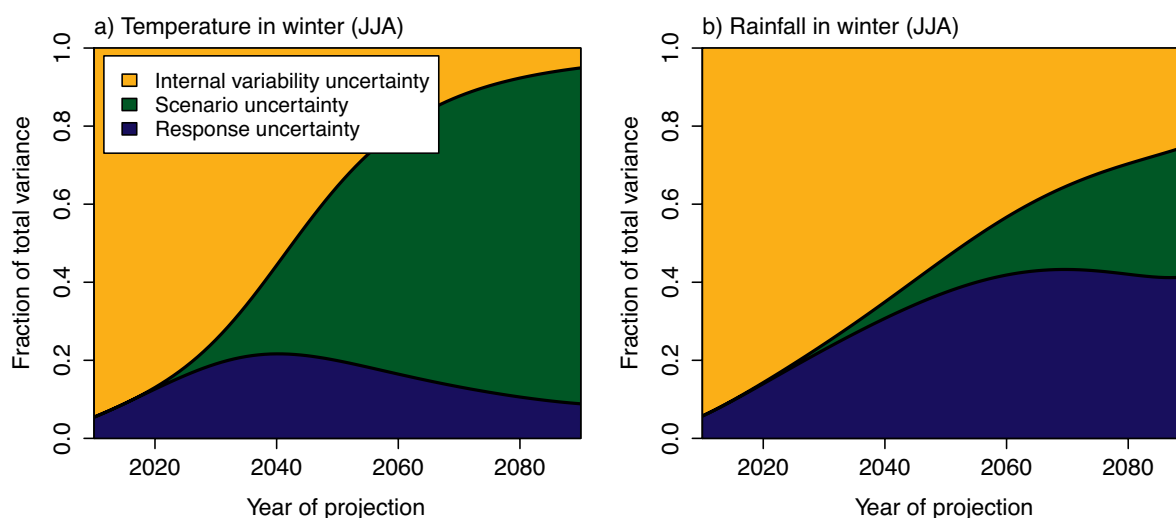


FIGURE 6.1.1: FRACTIONAL CONTRIBUTION OF INTERNAL VARIABILITY (ORANGE), SCENARIO (GREEN), AND RESPONSE UNCERTAINTY (BLUE) TO TOTAL UNCERTAINTY IN PROJECTED CHANGE IN TEMPERATURE (A) AND PRECIPITATION (B) IN SOUTHERN AUSTRALIA IN WINTER (JJA) BASED ON 28 CMIP5 MODELS (PRODUCED USING THE METHODS OF HAWKINS AND SUTTON, 2009).



Scenario uncertainty results from the range of possible, but also unknown, future concentrations of greenhouse gases and aerosols in the atmosphere, due to emission rates by human activities, and their complex interactions with the biosphere and hydrosphere. This source of uncertainty is commonly characterised by simulating the climate change response to a range of concentration scenarios that encompass different possible futures. In these projections, scenario uncertainty is considered through the use of Representative Concentrations Pathways (RCPs, see also Section 3.2). Each of the RCPs considered here represent a different pathway of greenhouse gas concentrations and associated enhanced greenhouse effect, but all are treated as plausible. Up to around 2030, greenhouse gas concentrations in the various RCPs differ only marginally and therefore scenario uncertainty is small. Its relative contribution to the total uncertainty increases over the future decades, becoming the dominant source of uncertainty for temperature by the end of the 21st century (green shading in Figure 6.1.1).

Response uncertainty results from limitations in our understanding of the climate system, our ability to simulate it and how it may evolve under different RCPs. While climate models are all based on the same physical laws, they have different configurations and use somewhat different components and parameterisations, which lead to differences in their simulation of climate feedbacks and in long-term changes (also see Section 3.2 and 3.3). The largest differences between models are from cloud feedbacks and the impact of aerosols on clouds and precipitation (Myhre *et al.* 2013), oceanic heat uptake (Kuhlbrodt and Gregory, 2012) and carbon cycle feedbacks (Friedlingstein *et al.* 2014). Further, uncertainty in future changes in the Greenland and Antarctic ice sheets is particularly important for sea level projections (Church *et al.* 2011b). We estimate response uncertainty from examining the range of climate simulations from global climate models with different, but equally acceptable, model configurations for a given RCP. While response uncertainty increases over the 21st century its relative contribution to total uncertainty generally peaks or plateaus around the middle of the century (blue shading in Figure 6.1.1).

Projected change in mean climate will be superimposed on natural climate variability. Natural variability uncertainty stems both from internal climate variability (*e.g.* the state of ENSO, see also Section 3.1.1) and natural external forcing mechanisms including future volcanic eruptions and changes in incoming solar radiation. Natural forcing mechanisms such as volcanic eruptions are typically not predictable into the future and are not included in simulations of the future so their contribution to the total projection uncertainty is not quantified in this Report. Similarly, internal variability (*e.g.* the timing of El Niño events) cannot be predicted beyond a few months into the future. Model simulations do include these sources of natural variability, but their timing is not tied to those in observations. Instead, natural internal variability contributes to the total projection uncertainty and

we quantify and display its contribution. This internal variability uncertainty is estimated from model experiments with varying initial conditions to reflect the range of possible future combinations of forced change and internal variability (see also Section 6.2). The relative importance of internal variability uncertainty generally decreases with time, as response and scenario uncertainty increase (Figure 6.1.1, orange shading). However, the relative contribution of internal variability uncertainty strongly depends on the location, on the spatio-temporal aggregation, and on the climatic variable analysed. In particular, internal variability uncertainty is generally larger at smaller spatial scales and for shorter averaging periods. Consequently, for regional climate change and variables with pronounced internal variability such as rainfall, internal variability uncertainty is always the largest source of uncertainty from one year to the next and can remain an important source of uncertainty for the long-term change (*e.g.* 10-year average) even at the end of the 21st century (Figure 6.1.1b).

6.1.2 INTERPRETATION OF RANGES OF CHANGE IN PROJECTIONS

In this Report, ranges of projected climate change for a given RCP are reported to indicate the range of plausible future outcomes. It is important to note, however, that not all sources of uncertainty are captured in the CMIP5 ensemble, and the ensemble does not sample *response uncertainty* in a systematic way (Parker, 2013). Also, climate change projections are made for late in the century, for unobserved (novel) states of the atmosphere, which means that it is not possible to demonstrate their reliability. The ranges of change reported in this Report therefore do not relate directly to the probability of the real world changing under a given RCP. Rather, the projected range of change from model simulations can often give an indication of a lower bound of uncertainty, as not all sources of uncertainty are quantified. However, in some particular cases where certain aspects of *response uncertainty* are uncertain the range of model changes may be larger than the physically plausible range of change. Additional lines of evidence, including model evaluation (Chapter 5) and processes driving change are used to assess the confidence in the model range, as a guide to future change for a given scenario (Section 6.4).



6.2 REGIONAL PROJECTION METHODS

6.2.1 OVERVIEW AND COMPARISON OF EXISTING REGIONAL PROJECTION METHODS

Climate projections are typically based on the output of climate models combined with knowledge about climate processes that help to contextualise and supplement the climate model outputs. Combining several model simulations into a model ensemble allows for an assessment of uncertainty (as outlined in previous section). However, several approaches exist to convert an ensemble of model simulations into climate change projections; some using model selection/weighting (based on model evaluation against observations) in an attempt to produce more 'reliable' projections. Many recent studies based on CMIP3 models have attempted to reduce uncertainty in projected climate change in Australia by only focusing on the better performing models (Charles *et al.* 2007, Perkins *et al.* 2007, Suppiah *et al.* 2007, Maxino *et al.* 2008, Moise and Hudson, 2008, Watterson, 2008, Chiew *et al.* 2009b, Grose *et al.* 2010, Kirono and Kent, 2011, Smith and Chandler, 2010, Vaze *et al.* 2011). There is an assumption that the better performing models will give a narrower and more plausible range of projected change than the entire ensemble. However, there is considerable disagreement regarding the relative merits of the various models (Chiew *et al.* 2009b, Smith and Chandler, 2010), making it difficult to justify a reduced set (Vaze *et al.* 2011).

There are some cases where researchers have selected a set of strong performing CMIP3 models based on a particular evaluation metric, with the range of uncertainty in projections narrowed in a potentially robust way. For example, Perkins *et al.* (2009) found less warming of extreme temperatures in models with stronger skill. However, sometimes different preferred models can provide opposing signals of climate change, *e.g.* where Smith and Chandler (2010) found a tendency for stronger rainfall decrease in the Murray-Darling Basin in better performing models, but Cai *et al.* (2011) and Pitman and Perkins (2008) found tendencies for increase when using a different set of preferred models. Other studies demonstrate cases where model selection had limited impact on the range of projected changes (Chiew *et al.* 2009b, Kirono and Kent, 2011).

An alternative to picking the best few models is to reject the models that have particularly poor performance. There is, for example, some agreement on a small set of CMIP3 models with consistently poor performance across a range of studies and metrics (Smith and Chandler, 2010, Cai *et al.* 2011, Frederiksen *et al.* 2011, Vaze *et al.* 2011). For CMIP5, some poor-performing models have been identified for Australia (Chapter 5).

For Australia, we can consider the impact on projections when excluding models identified as poor performers (Table 5.6.1 of Chapter 5). Figure 6.2.1 illustrates the effect for rainfall projections for the four large super-clusters.

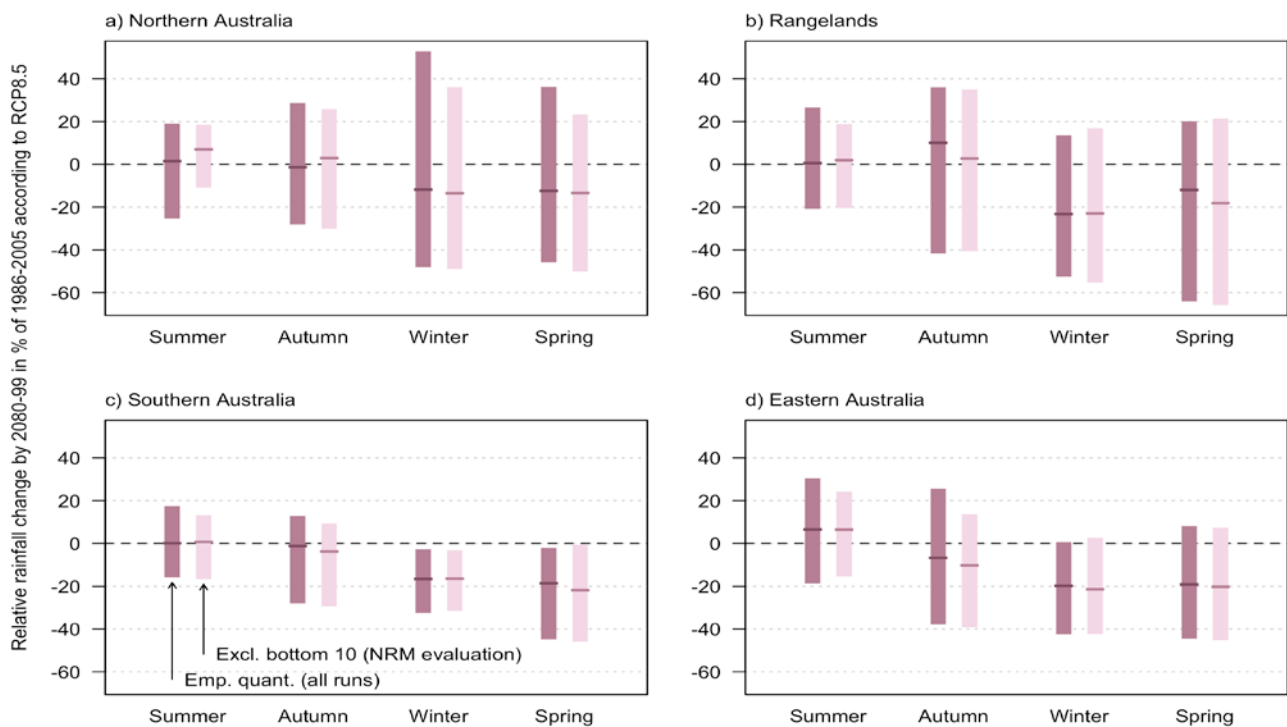


FIGURE 6.2.1: COMPARISON OF PROJECTED SEASONAL RAINFALL CHANGES ACCORDING TO RCP8.5 FOR FOUR SUPER-CLUSTERS IN AUSTRALIA WITH THE EMPIRICAL QUANTILES (EMP. QUANT.) OF THE FULL SET OF CMIP5 GCMs (DARK SHADED BARS) AND THE SUBSET EXCLUDING THE 10 MODELS THAT SCORE LOW ON A VARIETY OF EVALUATION METRICS IDENTIFIED IN CHAPTER 5 (LIGHT SHADED BARS).

Projections using the empirical quantiles (median and percentiles of the model range) of the full set of CMIP5 models are compared with projections from the better performing models (10 models being excluded due to low scores on at least 3 different evaluation metrics; no projections data are available for CESM1-WACCM) (Fig. 6.2.1). Noteworthy differences are a somewhat reduced occurrence of strong rainfall increases in summer and autumn in Eastern Australia (and to a lesser extent in Southern Australia), and less evidence for strong summer drying in Northern Australia in the reduced set of models.

However, overall differences between projections, including and excluding low-scoring models, are slight in most regions and seasons. Perhaps most importantly, selecting a subset of better performing models in this instance did not provide more clarity on the direction of the expected rainfall response.

In addition, performance-based weighting of models in regional projections has been widely used (Christensen *et al.* 2010). In many cases, however, performance in the current climate and future projections are only

BOX 6.2.1: THE EFFECT OF DIFFERENT PROJECTION METHODS

Projections can be generated using several different methods. Figure B6.2.2 demonstrates the effects of some of these methods, namely that of:

1. Spatial resolution: projections in some regions depend on the spatial resolution of the climate models. This applies in particular to the smaller regions with complex terrain, such as Tasmania, for which coarse resolution GCMs cannot represent potential small-scale differences in the climate change signal. The importance of spatial resolution is further analysed in this Report using downscaled data (see Section 6.3).
2. Selecting the 'best' models: selecting a subset of 'best' models can have an impact on regional climate change projections, but the effect strongly depends

on the metric and feature used to evaluate the models (see also Figure 6.2.1). For example, the 10 models that best represent the average rainfall, surface temperature and mean sea level pressure in Australia (Watterson *et al.* 2013a) indicate stronger drying for southern Australia, whereas the 10 models that best represent important modes of circulation variability in the southern hemisphere (Grainger *et al.* 2013, 2014) indicate less drying.

3. Constrained by observations: the effect of using observations (climatology or trends) as constraints is mostly small at the regional scale or is dependent on the specifics of the weighting method used.

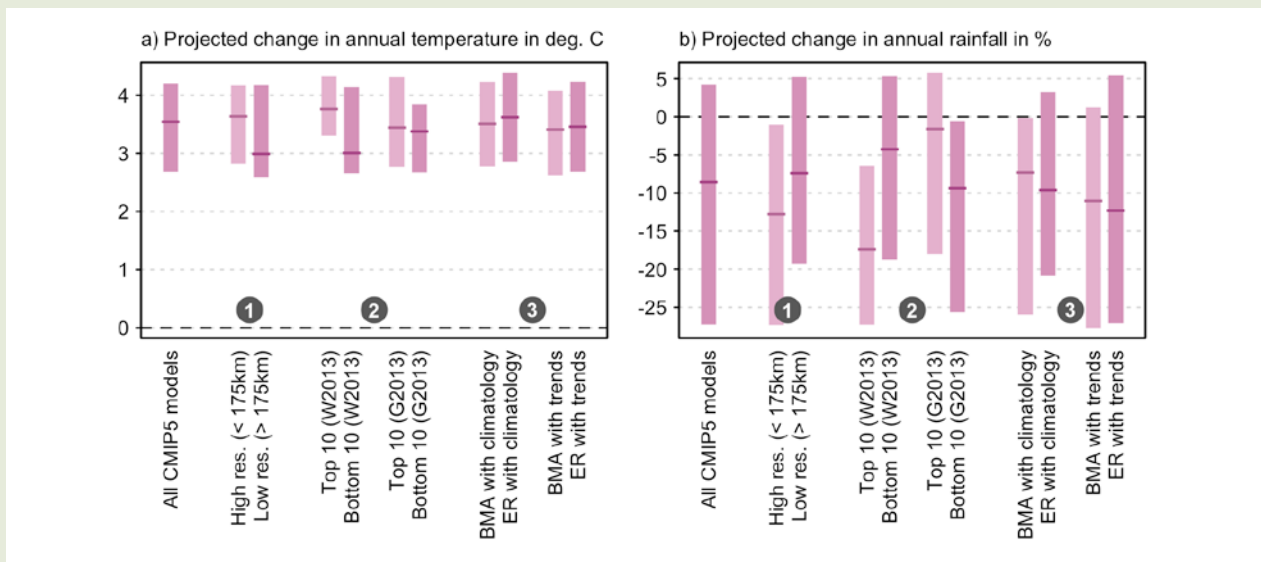


FIGURE B6.2.2: COMPARISON OF DIFFERENT METHODS TO PRODUCE PROJECTED CHANGES IN SOUTHERN AUSTRALIAN (A) ANNUAL TEMPERATURE AND (B) ANNUAL RAINFALL FOR 2080-99 WITH RESPECT TO 1986-2005 ACCORDING TO THE HIGHEST EMISSION SCENARIO (RCP8.5). FROM LEFT TO RIGHT THE PROJECTIONS USE ALL CMIP5 MODELS, HIGH- AND LOW-RESOLUTION MODELS ONLY, THE 10 TOP AND BOTTOM SCORING MODELS ACCORDING TO AN EVALUATION OF WATTERSON *ET AL.* (2013, DENOTED W2013) AND AFTER GRAINGER *ET AL.* (2013, DENOTED G2013), AND WEIGHTED BY HOW CLOSELY THE MODELS REPRESENT THE ANNUAL TEMPERATURE AND RAINFALL CLIMATOLOGY AND RECENT TRENDS FROM 1956-2005 RESPECTIVELY. IN THE LATTER CASES, TWO DIFFERENT WEIGHTING SCHEMES HAVE BEEN USED NAMELY BAYESIAN MODEL AVERAGING (BMA: MIN *ET AL.* 2007) AND ENSEMBLE REGRESSION (ER: BRACEGIRDLE AND STEPHENSON, 2012).

weakly related (Knutti *et al.* 2010), and therefore using performance-based weights will have little effect on projections. Using non-optimal weights is more often than not worse than not weighting models at all (Weigel *et al.* 2010).

Against this background, a number of scientists are taking the view that using the full range of available models, rather than a performance-based selection or weighting, is the most appropriate course of action for regional applications (Chiew *et al.* 2009b, Kirono *et al.* 2011a). Model evaluation results, however, may influence the choice of individual models in some applications (Chapter 9).

Attempts have been made to infer a probability distribution of future climate change from projections of multiple models. Such probabilistic projections for Australia have been prepared using the 'Reliability Ensemble Averaging' (REA) approach (Moise and Hudson, 2008) and using a fitted Beta-distribution (Watterson, 2008, Watterson and Whetton, 2013), where Watterson's approach (Section 6.2.3) was used in *Climate Change in Australia* 2007 (CSIRO and BOM, 2007). Other approaches have been used to produce regional probabilistic projections elsewhere. These include fully probabilistic statistical models used to interpret the diversity of projected changes in multi-model ensembles, such as CMIP3 and CMIP5 (Tebaldi *et al.* 2005, Buser *et al.* 2009, Smith *et al.* 2009, Chandler, 2013). Indeed the growing number of methods to produce probabilistic projections reflects the lack of consensus on how best to interpret diversity in model results (Parker, 2013).

In the absence of clear guidance on how best to form probabilistic projections from multiple climate models, and because the effect of different projection methods is generally small (Box 6.2.1), we adopt a simple method to produce the projections presented in this Report. The specific choices and details are discussed in the following section. In the interest of comparing model results using the CMIP3 and CMIP5 models across Australia, the method used to generate the 2007 projections (based on the CMIP3 models) is further applied to the CMIP5 dataset (Section 6.2.3).

6.2.2 PROJECTION METHODS USED IN THIS REPORT

Climate refers to the statistics of weather and therefore long-term averages are often used to characterise climate for a specific period and location. In this Report, 20-year averages of CMIP5 outputs are used to characterise change in the future climate.

The model-based projections are generally presented as the model ensemble median (50th percentile) and the 10th to 90th percentile range (see Box 6.2.2). That is, less than 10 per cent of the models project changes that are smaller than the lower bound (10th percentile) and less than 10 per cent project changes that are larger than the upper bound (90th percentile). The median projected change (50th percentile) is the middle value of the simulated changes with half the models showing changes larger/smaller than the median.

In accordance with results reported in the latest Assessment Report of the Intergovernmental Panel on Climate Change (IPCC, 2013), the primary reference period used in this Report is 1986-2005. This period is used to demonstrate change in bar charts, maps, and tables; note that this is different from the 1980-1999 period used in *Climate Change in Australia* 2007 (CSIRO and BOM, 2007). The more recent period is chosen partly because this period has more comprehensive observational data sets (aided by satellite measurements), which is important as the CMIP5 models are run with observed forcings as opposed to forcings based on different RCPs from 2005 onwards. It is important to note, however, that natural internal variability does not fully average out in 20-year averages, as some sources of natural variability manifest on time scales greater than 20 years. This has to be taken into account when relating simulations (or projected change) to recent observations.

The time series plots, however, use a different reference period, 1950-2005. The selection of a different reference period is due to technical reasons in producing a visually representative time series plot where simulations of the historical and future time periods are merged into one long series. The use of a longer reference period more

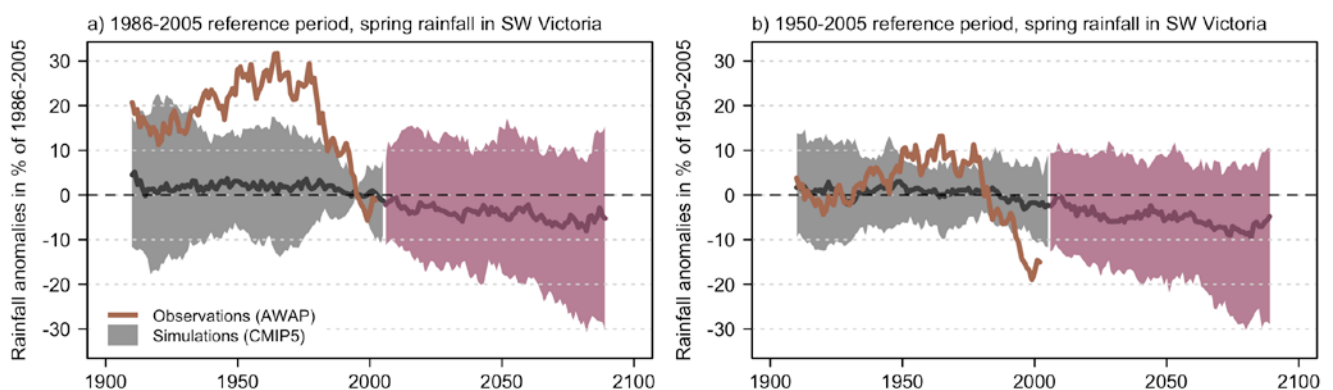


FIGURE 6.2.3: THE EFFECT OF USING DIFFERENT REFERENCE PERIODS WHEN RELATING SIMULATED AND OBSERVED CLIMATE TIME SERIES ILLUSTRATED WITH SPRING (MAM) RAINFALL IN SOUTH-WESTERN VICTORIA (SSVW). 20-YEAR AVERAGES OF SIMULATED AND OBSERVED RELATIVE ANOMALIES IN PER CENT OF THE 1986-2005 MEAN (A) AND OF THE 1950-2005 MEAN (B) ARE SHOWN. SHADING INDICATES THE 10TH TO 90TH PERCENTILE RANGE OF THE CMIP5 SIMULATIONS, THE SOLID LINE INDICATES THE MEDIAN.

-20° -10° 0° 10° 20° 30° 40° 50°

truthfully reflects our scientific understanding how these periods relate to each other. For example, the longer reference period is particularly important in cases when natural internal variability leads to a large deviation of the 1986–2005 mean from the ‘underlying’ (but unknown) climate (e.g. spring rainfall in western Victoria as shown in Figure 6.2.3). In this situation, the observations may appear to lie outside the simulated range for most of the 20th century with a 1986–2005 reference period, whereas adopting a long reference period highlights the anomaly of the recent past with respect to the long-term mean. The change to a longer reference period is also necessary to avoid the false impression that the climate in 1986–2005 is known exactly and thereby much more certain than the climate in 20-year periods earlier in the 20th century (Figure 6.2.3). As a consequence of the different reference periods, quantitative changes in time series plots differ slightly from the corresponding changes reported in tables and bar plots. This difference illustrates the influence of the choice of reference period in climate change projections.

WEIGHTING OF CLIMATE MODELS

Since there is no strong evidence to weight models, the possible detrimental effects of weighting and the small impact of model rejection (see above), we do not weight or exclude models.

NATURAL INTERNAL VARIABILITY

Projected regional warming has been shown to differ considerably across simulations when using different initial conditions (Deser *et al.* 2012a, b). Hence, natural internal variability is an important contributor to the spread of projected climate change (see also Figure 6.1.1). The contribution of natural internal variability is illustrated in this Report by showing the range (10th to 90th percentile) of changes due to natural internal variability only (e.g. right-hand panel in Figure B6.2.4). This range is estimated from the spread of simulations for the 2080–99 time period using different initial conditions (i.e. simulations that differ only in their state of internal variability). All available simulations are used to estimate projected change. Some models provided multiple simulations, each with different initial conditions and a distinct natural variability. To ensure that models get equal weight in the final projection, individual simulations of the same model are weighted with the inverse of the number of simulations.

MAPS OF PROJECTED CLIMATE CHANGE

Chapter 7 also uses maps, showing the 10th, 50th, and 90th percentile of projected climate change. Instead of using empirical quantiles, the method based on pattern scaling used in *Climate Change in Australia 2007* (CSIRO and BOM, 2007) has been adopted to illustrate the spatial pattern in projected climate change (Watterson, 2008). The two different approaches are compared in the following section.

6.2.3 COMPARISON WITH CLIMATE CHANGE IN AUSTRALIA 2007

The *Climate Change in Australia 2007* (CSIRO and BOM, 2007) approach for generating probability density functions (PDFs) for climate change relies on ‘pattern scaling’ based on the assumption that the local change (on the scale resolved by the GCMs) is proportional to the amount of global warming. To represent uncertainty, a PDF for both the global warming (for each scenario and time in the future) and the local sensitivity to the warming (for each variable) is derived. The PDF for the global warming is derived from RCP8.5 simulations over the 21st century; consistent with the *Fifth Assessment Report’s* assessment for global warming, as noted in Section 3.6. The local PDF is derived by regression of values of the variable against the global mean temperature, using yearly data from the RCP8.5 simulation for CMIP5 (or scenario A1B for CMIP3). For consistency with the 2007 report, the overall skill scores for Australia presented in Table 5.2.2 are used as model weights using the baseline period 1986–2005 for both CMIP3 and CMIP5 projections. This provides a ‘change per degree’ field for each model, variable, season, and grid cell, which is then interpolated to a common 1-degree grid over Australia. The product of the global and local PDFs gives the combined PDF for the forced local change from which percentile changes are estimated.

The pattern scaling approach has been further developed by Watterson and Whetton (2011) to include the contribution of natural decadal variability to the forced signal, and by Watterson and Whetton (2013) to allow for a time series representation of forced and random components matched to a long-term observed series. This is illustrated for the case of eastern Victorian temperature, shown in Figure 6.2.5b. It can be compared to the equivalent time series for the Southern Slopes Victoria East (SSVE) cluster in (a), derived using the present method (described in Box 6.2.2) from GCM simulated change. The span in (b) for the forced or underlying climate is similar to the shaded band in (a), and in this respect the PDFs provide similar results. Differences may indicate local effects of aerosols (included in (a) but not (b) as the PDFs are scaled from the long-term forced change) or limitations to the pattern-scaling theory. In this case the CMIP5 models are well calibrated in that each observed series falls within the 10th to 90th percentile ranges approximately 80 per cent of the time. In (b), an indication of how the observed series may link to the future span is provided, and a similar inference could be made in (a).

-20° -10° 0° 10° 20° 30° 40° 50°

BOX 6.2.2: PRESENTATION OF PROJECTED AREA-AVERAGE CHANGES

Time series plots and bar plots both illustrate projected climate change and how the simulated change relates to

the current climate. The following paragraphs explain how to interpret each of the two plot types.

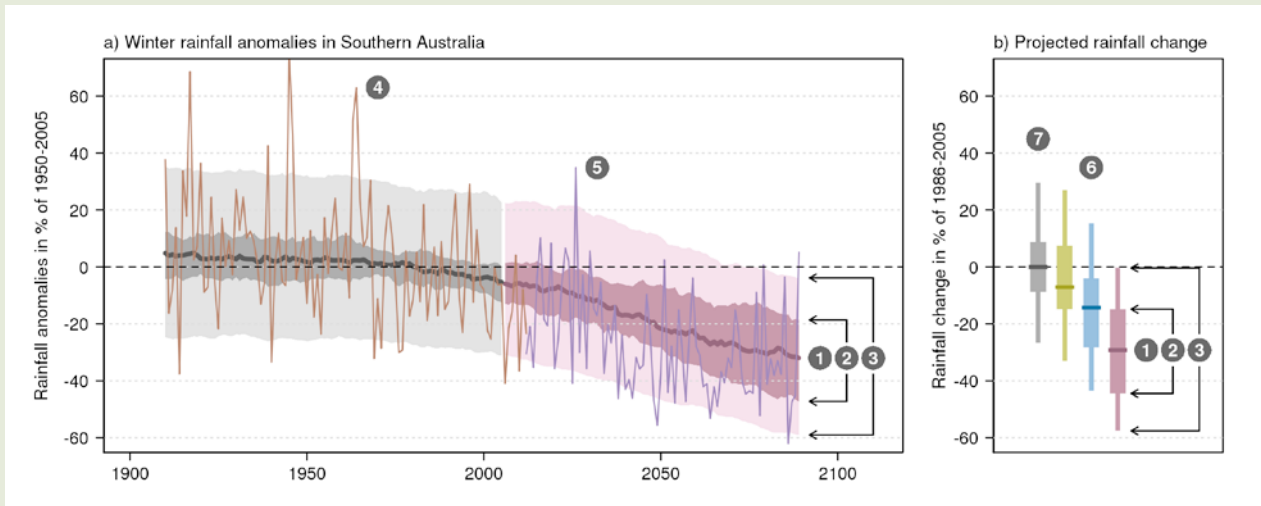


FIGURE B6.2.4: TIME SERIES OF OBSERVED AND SIMULATED CHANGE (A) AND PROJECTED CHANGE ACCORDING TO DIFFERENT SCENARIOS (B) FOR WINTER (JJA) RAINFALL IN SOUTHERN AUSTRALIA. PLEASE NOTE THE DIFFERENT REFERENCE PERIODS USED IN A AND B (SEE DISCUSSION IN SECTION 6.2.2). FOR EXPLANATIONS REGARDING THE KEY ELEMENTS SEE TEXT BELOW.

Time series plots: the range of model results is summarised using the median (1) and 10th to 90th percentile range of the projected change (2) in all available CMIP5 simulations. The change in mean climate is shown as 20-year moving averages (Figure B6.2.4a). Dark shading (2) indicates the 10th to 90th percentile range for 20-year averages, while light shading (3) indicates change in the 10th to 90th percentile for individual years. Where available, an observed time series (4) is overlaid to enable comparison between observed variability and simulated model spread. When CMIP5 simulations reliably capture the observed variability, the overlaid observations should fall outside the light-shaded range in about 20 per cent of the years. To illustrate one possible future time series and the role of year to year variability, the time series of one model simulation is superimposed onto the band representing the model spread (5). Note 20-year running average series is plotted only from 1910 to 2090.

Bar plots: similar to time series plots, bar plots also summarise model results using the median (1) and 10th to 90th percentile range of the projected change (2) in all available CMIP5 simulations. The extent of bars (2)

indicates the 10th to 90th percentile range for difference in 20-year averages (reference period to a future period), while line segments (3) indicate change in the 20-year average of the 10th and 90th percentile, as calculated from individual years. The projection bar plots enable comparison of model responses to different RCPs (6), where RCP2.6 is green, RCP4.5 is blue and RCP8.5 is purple (Figure B6.2.4b). The range of natural internal variability without changes in the concentration of atmospheric greenhouse gases and aerosols as prescribed by the RCP scenarios (see Section 6.2.2) is shown in grey (7). This range is estimated from the spread in projections for the period 2080-99 amongst simulations differing only in their initial conditions. In the above case, the median projection in all RCPs is for a decrease in winter rainfall. The models agree well on the magnitude of the decrease and therefore the spread in projected changes (coloured bars) is only slightly larger than due to natural internal variability alone (grey bar). In cases where the models do not agree on the magnitude and/or sign of the projected change, the range of projections is much larger than that due to natural internal variability.



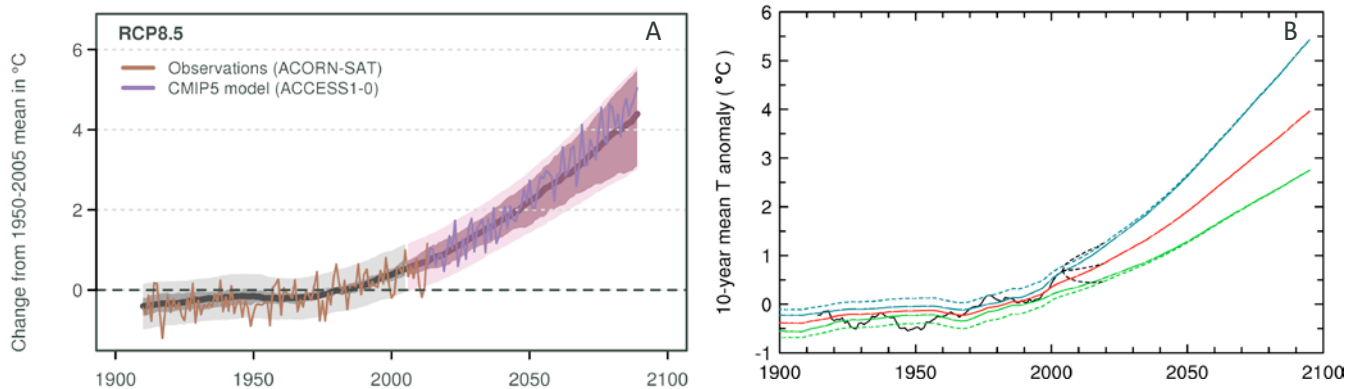


FIGURE 6.2.5: ANNUAL TEMPERATURE CHANGE FOR SSVE SHOWN AS TIME SERIES BASED ON THE PROJECTION METHOD FOR TIME SERIES USED IN THIS REPORT (A) AND THE PROJECTION METHOD USED IN *CLIMATE CHANGE IN AUSTRALIA 2007* (CSIRO AND BOM, 2007). THE DARK SHADED AREA IN (A) INDICATES THE 10TH TO 90TH PERCENTILE RANGE OF MOVING 20-YEAR AVERAGES, THE SOLID LINE IS THE MEDIAN OF THE CMIP5 SIMULATIONS. OVERLAID ARE THE OBSERVATIONAL SERIES AND MODELLED SERIES (AS IN BOX 6.2.2). THE BLACK LINE IN (B) IS THE DECADAL MEAN OBSERVED VALUES FOR EASTERN VICTORIA. THE OTHER SOLID LINES ARE THE 10TH, 50TH (MEDIAN) AND 90TH PERCENTILE SERIES FOR THE 'UNDERLYING' CLIMATE, BOTH IN THE PAST AND INTO THE FUTURE, AS FORCED BY RCP85, AND USING CMIP5 SENSITIVITY RANGES. THE DASHED LINES SHOW THE CORRESPONDING RANGE WHEN TAKING INTO ACCOUNT NATURAL INTERNAL VARIABILITY OF DECADAL MEANS IN ADDITION TO FORCED CHANGES.

Under pattern scaling, the projected changes for a specific time depend on the global warming and hence the RCP. In CSIRO and BOM, (2007), projections were given for forced change in 2030, 2050 and 2070, under the SRES scenarios. This Report uses mainly the periods 2020-2039 and 2080-2099, under the RCPs (estimates for other times will be available from the corresponding website, see Chapter 9). There is also a six-year difference in the base period (the 2007 projections using the 1980-1999 period). Typically, a later base period results in a slightly smaller projected change (see Figure 6.2.5). As a result of these various differences, the 2007 projections cannot be directly compared with those presented here. However, with regard to the response to global warming, scaling allows a comparison of the Australian projections based on the CMIP3 and CMIP5 ensembles under a common global warming case, as described further in Appendix A.

6.3 DOWNSCALING

This section gives a brief introduction to methods of downscaling, their advantages and limitations, how these methods are used in the report, where in Australia downscaling might provide most additional insight to complement global climate model (GCM) projections, and advice on availability of downscaled datasets in Australia. For more information about downscaling principles and practice, there are several useful reviews (Giorgi and Mearns, 1999, Wang *et al.* 2004b, Fowler and Wilby, 2007, Foley, 2010, Maraun *et al.* 2010, Rummukainen, 2010, Feser *et al.* 2011, Paeth and Mannig, 2013), and guidance material on selection and evaluation of downscaling methods for impact and adaptation planning is given in Ekström *et al.* (accepted).

6.3.1 WHAT IS DOWNSCALING?

Downscaling as it is applied here is the process by which GCM outputs, with a typical spatial resolution of 100-200 km, are translated into finer resolution climate change projections. There are a number of reasons for downscaling, the most common ones being:

- GCMs may not be able to adequately represent the current climate of a particular region, or the change to the regional climate (*e.g.* because landscape features or weather systems are not well represented by GCMs),
- there may be an interest in studying potential impacts on atmospheric processes that are not well resolved by GCMs (*e.g.* convective storms),
- because of a desire for climate change projections with greater detail and fine spatial resolution in impact assessments, guidance for decision making or adaptive planning.

There are many different ways in which GCM outputs can be translated to finer resolutions or even point locations. Some methods are nearly as complex as the GCMs themselves, while others merely involve adding the mean change, as given by the GCM, to observed data. As a general guide, downscaling methods can typically be categorised into three groups: *dynamical downscaling*, *statistical downscaling* and *change factor methods*. Dynamical downscaling means running a dynamical model also known as a Regional Climate Model (RCM) using output from a GCM as input, and statistical downscaling is doing the same but with a statistical model. Change factor methods are techniques of combining the change signal from GCM outputs with observed datasets and are therefore a simple form of downscaling.

Dynamical and statistical downscaling produce a projection with new information in the simulation of climate processes and the pattern of climate change (termed the climate change ‘signal’). Change factor methods don’t produce new information in the climate change signal (so don’t meet the somewhat stricter definition of downscaling). Downscaling will almost certainly create datasets that more closely match observations at the local scale (what we term *climate realism*). Depending on the method used, the downscaling method may also produce new information in the climate change signal that is more physically plausible than the host GCM (what we term *physically plausible change*) (Ekström *et al.* submitted). While *climate realism* is important in terms of practical applicability, *physically plausible change* is the crucial requirement for credible projections (Figure 6.3.1). Note, high *climate realism* does not equate with ability to show *physically plausible change*.

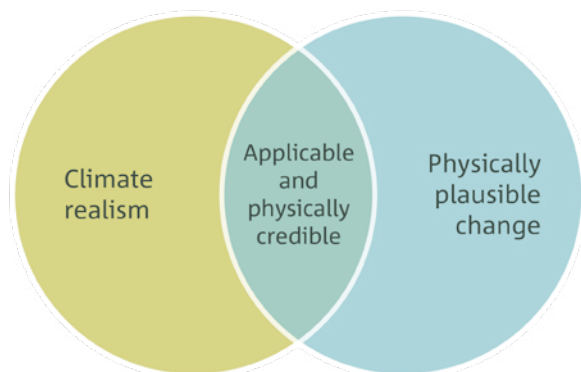


FIGURE 6.3.1: THE REALMS OF DOWNSCALING. IDEALLY, A DOWNSCALING METHOD SHOULD BE SKILFUL IN TERMS OF GENERATING DATA WITH HIGH CLIMATE REALISM AND HIGH PHYSICALLY PLAUSIBLE CHANGE, PRODUCING DATA SETS THAT ARE APPLICABLE TO REAL WORLD STUDIES AND PHYSICALLY CREDIBLE.

The merits of downscaling must be assessed in the context of what information about change is inherited from the host models (in this case, global climate models), and what is added. The degree of *climate realism* can be assessed by comparing downscaled data to observed climate characteristics, and downscaling often performs very well in this regard. However, assessing physically plausible change is more challenging and comprises an assessment of the plausibility of large-scale change inherited from the host GCM and the regional-scale change produced in the downscaling. The physical plausibility that may be added by downscaling can be broken down into approach capability and approach bias, where the former represents the theoretical ability of a particular approach to estimate certain aspects of change and the latter concerns the approach-specific bias that any particular method may exhibit due to its theoretical formulation (Ekström *et al.* accepted) (Figure 6.3.2).

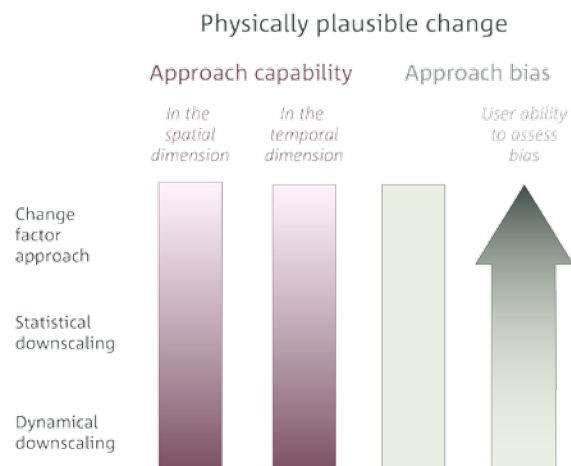


FIGURE 6.3.2: CONCEPTUAL MODEL SHOWING THE RELATIONSHIP BETWEEN DOWNSCALING APPROACHES OF DIFFERENT COMPLEXITY WITH APPROACH CAPABILITY AND APPROACH BIAS. DARKER SHADING DENOTES HIGHER CAPABILITY/ABILITY (EKSTRÖM *ET AL.* ACCEPTED).

It would be reasonable to expect increasing ability to depict physically plausible change in the spatial and temporal dimension for downscaling methods of higher complexity. Unfortunately, while more complex methods may give richer information about climate change, a user’s ability to assess presence and characteristics of approach bias becomes much more difficult simply due to the vast number of ways in which data can interact with model dynamics and parameterisation schemes (a similar argument could be made for more complex statistical methods). To avoid over-reliance on any particular method and minimise exposure to potential approach biases, users of downscaling data are often asked to consider a range of different downscaling methods when possible and to give the context from the GCM projections at the scale of the intended application. The process of choosing downscaling methods is discussed further in Chapter 9.

6.3.2 COMBINING INSIGHTS FROM DOWNSCALING AND GCM PROJECTIONS

A set of GCM projections is an informal ‘ensemble’, and the range of results between acceptable models gives some measure of the uncertainty in the projected climate change signal (see also Section 6.2). Downscaling may reveal additional regional detail in the climate change signal, but different methods of downscaling produce different results, so in fact reveal further uncertainty within climate change projections. Also, since many forms of downscaling are computationally demanding or require specific inputs, they are often run with a limited subset of GCMs and emissions scenarios. Therefore, to fully sample the uncertainties from all available global modelling and downscaling, some systematic experimental design is required.

Such a design should use multiple downscaling methods and adequately sample emission scenarios and the range of GCM projections. This has been attempted in the upcoming



set of projections in the North American Regional Climate Change Assessment Program (NARCCAP), sampling a representative set of runs from a GCM-RCM ‘matrix’ (Mearns *et al.* 2009). A similar approach was taken in the European ENSEMBLES program (Christensen *et al.* 2009, Kendon *et al.* 2010). Of regional interest is the Coordinated Regional Climate Downscaling Experiment project (CORDEX) for Australasia (<http://wcrp-cordex.ipsl.jussieu.fr/>), which will provide a sampling of a GCM-downscaling ‘matrix’ (both dynamical and statistical) for all of Australia when complete (Evans, 2011).

There is currently no set of systematically produced GCM-RCM climate projections available that covers the entire continent. However, two different downscaled projections were produced for this project and there are several regional climate change studies that have produced valuable insights (listed below). These outputs do not represent a systematic sampling of GCM and downscaling uncertainty. Therefore the CMIP5 ensemble is the primary tool for examining projected climate change in Australia in this Report, and downscaling data is used as a complementary source of information; reported only where and when it is felt that it provides compelling ‘added value’ about the climate change signal. We particularly look for cases where the downscaling shows higher *physical plausible* change than GCMs due to regional influences.

Most of the content in this Report discusses the regional insights that downscaling provides under a high emissions scenario (RCP8.5) for the end of the century, when the climate change signal is at its strongest. This emphasises the regional scale patterns that are revealed by downscaling, which is useful for qualitative interpretations. However, currently there is no fully representative and complete GCM-RCM dataset suitable for quantitative analysis to accompany these regional insights.

6.3.3 STATISTICAL AND DYNAMIC DOWNSCALING METHODS USED

Statistical downscaling is not a change factor method of the variable itself, it refers to a model that utilises a statistical relationship between the local-scale variable of interest and larger-scale atmospheric fields. This is achieved through regression methods (e.g. multiple regression statistics, principal component or canonical correlation analysis, neural networks), weather typing or through the use of weather generators calibrated to the large atmospheric fields. We report results from the Bureau of Meteorology analogue-based Statistical Downscaling Model (SDM) for Australia (Timbal *et al.* 2009).

Dynamical downscaling is the use of a numerical climate model operating at a finer spatial resolution (compared to GCMs), using the broad-scale climate change from a GCM as input. There are various configurations of dynamical downscaling models, but most are atmosphere-only models (using the SSTs from the ‘host’ GCM), and have fine resolution only over the area of interest. There are two main types used for downscaling in Australia: variable resolution global models and limited area models. We

report on results from the CCAM variable resolution global model (McGregor and Dix, 2008) plus other downscaled outputs where available.

6.3.4 PROS AND CONS OF STATISTICAL AND DYNAMICAL DOWNSCALING

Statistical downscaling (such as the BOM-SDM) will almost certainly produce greater *climate realism* than the host model, but may still have some level of approach bias compared to an observed dataset, both in spatial and temporal distributions. In terms of *physically plausible* change, statistical downscaling is likely to produce more spatial and temporal detail in the climate change signal compared to the GCM. This change signal could be more plausible compared to that of the host model, especially around areas of important topography and coastlines. The outputs may also have greater *physically plausible change* in the simulation of temporal distributions, both in the current climate and in the projected change in variability. However, many statistical techniques are not suited to simulating extremes, especially those extremes for which there are no historical precedent. Also, statistical downscaling does not produce a full suite of internally-consistent variables; it is generally done for a limited set of variables (typically temperature and rainfall).

Dynamical downscaling produces a suite of internally-consistent variables that have the potential to show a complete spatial and temporal response in the climate to the scenario, including events without historical precedent. The *climate realism* in dynamical models can be relatively high, but outputs will contain some inevitable approach biases compared to observations. This means that the outputs are not suitable for direct use into sophisticated impact analysis models and therefore require bias correction. Dynamical downscaling has great potential to produce *physically plausible* change on the regional-scale, in terms of spatial distribution (particularly in areas with a strong influence of topography or coastlines on the climate), and in temporal distribution, including extremes (*i.e.* the method has high approach capability). However, this potential for extra realism in the change signal needs to be critically assessed in the actual outputs for any region.

6.3.5 AREAS OF GREATEST POTENTIAL ADDED VALUE

In Australia, there are a few compelling cases where downscaling may produce more *physically plausible* change compared to the GCM hosts. Hence there is an argument for using downscaled data in preference to GCM outputs for impact analysis at the regional scale in these cases. These are the regions with the greatest influence of topography and coastlines, and also the regions where there are distinct climatic zones within a relatively small area. These areas include Tasmania, south-east mainland Australia, the Australian Alps, the Eastern Seaboard between the coast and the Great Dividing Range and south-east Queensland, as well as some regions within southern South Australia and south-west Western Australia. For example, downscaling was shown to reveal different projected rainfall changes in



western compared to eastern Tasmania in some seasons, according to plausible regional climate boundaries based on the relationships of rainfall to mean westerly circulation (Grose *et al.* 2013). For climate change projections in the tropics, the largest source of uncertainty is often from processes such as convection and clouds, therefore a different projection in downscaling may be due to a different simulation of convection and clouds and can be harder to attribute to finer resolution of surface features. Without such a firm basis to identify the added value, we place less emphasis on downscaling in the tropics, but emphasise the 'added value' from downscaling primarily in southern Australia.

6.3.6 AVAILABILITY

This project has produced two sets of downscaled climate projections for Australia that are reported on here. These outputs are produced using the CCAM model using six CMIP5 host GCMs as input (ACCESS-1.0, CCSM4, CNRM-CM5, GFDL-CM5, GFDL-CM3, MPI-ESM-LR and NorESM1-M). These six models were chosen to cover a representative range of projected changes for Australia and the wider region, chosen from the better performing set of CMIP5 models. CCAM data will be available through the *Climate Change in Australia* website. We also report on outputs from the Bureau of Meteorology Analogue-based SDM of Timbal *et al.* (2009) with 22 CMIP5 GCMs as input (see Table 3.3.1 for models used). Outputs are produced for RCP4.5 and the RCP8.5. Along with this new downscaling work, reference is made to regional studies that produced downscaled projections for particular sub-regions of Australia, including:

- Climate Futures for Tasmania (<http://www.acecrc.org.au/Research/Climate%20Futures>) and further work on the Australian Alps to be released in 2015
- South Eastern Australian Climate Initiative (SEACI; <http://www.seaci.org/>)
- Queensland Climate Change Centre of Excellence project for South-east Queensland
- Indian Ocean Climate Initiative (IOCI, <http://www.ioci.org.au/>)
- Goyder Institute South Australia (<http://goyderinstitute.org/>)
- Consistent climate scenarios project (Burgess *et al.* 2012) (<http://www.longpaddock.qld.gov.au/climateprojections/about.html>)
- NSW and ACT Regional Climate Modelling (NARCLIM, <http://www.crc.unsw.edu.au/NARCLiM/>)

Please note that while these sites provide information about the relevant data, it may not necessarily provide access to datasets.

6.4 ASSESSING CONFIDENCE IN PROJECTIONS

Assessing climate projections is quite different to assessing weather forecasts. Weather forecasts are initialised with current observations and provide predictions of the next 1-10 days that can be continually assessed against observations. Climate is the average weather. Climate projections are simulations that are largely independent of the initial conditions, designed to show the long-term response of the climate system to hypothetical, but plausible, scenarios of external forcings into the future. Climate projections are not expected to give accurate predictions of individual weather events into the far future.

However, it is expected that the projections will show a plausible change to multi-decadal climate statistics if a particular RCP is followed and natural climate variability is taken into account. Confidence in projections can be assessed by comparing simulations of the current climate and past climate changes with observations, assessing the agreement between climate model simulations, and by considering our understanding of the physical processes driving projected changes (see Chapter 5). In reality, projections for 2030 and beyond can never be fully assessed against observations, the concentrations of greenhouse gases in the atmosphere will probably not play out exactly as specified any one RCP, and there is likely to be unpredictable natural forcing factors such as volcanic eruptions. These factors affect what constitutes confidence in climate projections, and how it is assessed.

Confidence in a climate projection statement represents the authors' assessment of its reliability. Confidence comes from multiple lines of evidence including physical theory, past climate changes and climate model simulations. Here confidence language specified by the IPCC for their *Fifth Assessment Report* is used (see Mastrandrea *et al.* 2010), which considers factors along two dimensions; evidence (type, amount, quality and consistency), and agreement between those lines of evidence (Figure 6.4.1) to assign a confidence rating using calibrated language based on expert judgment of the various lines of evidence. As in IPCC (2013), confidence is expressed using the qualifiers 'very high', 'high', 'medium', 'low' and 'very low'. Though in practice, only four qualifiers were used as 'very low' confidence was never assigned to a variable.



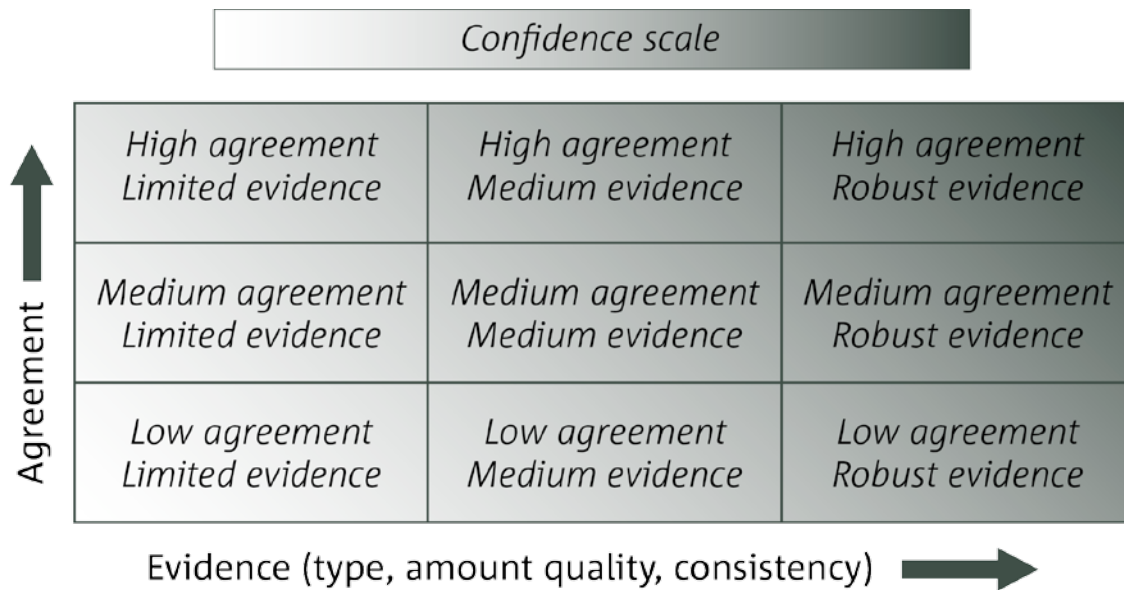
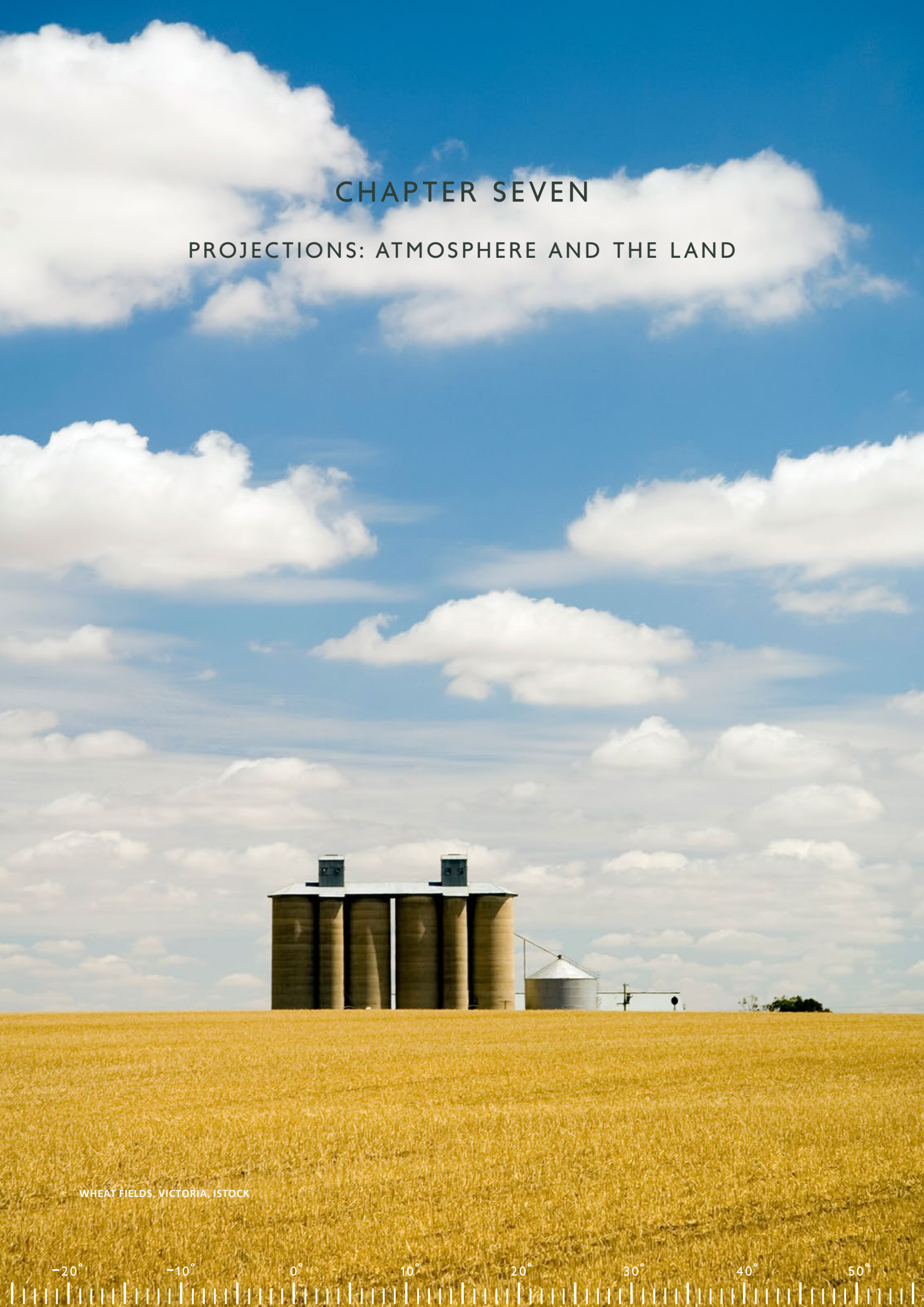


FIGURE 6.4.1: A DEPICTION OF EVIDENCE AND AGREEMENT STATEMENTS AND THEIR RELATIONSHIP TO CONFIDENCE. CONFIDENCE INCREASES TOWARDS THE TOP RIGHT CORNER AS SUGGESTED BY THE INCREASING STRENGTH OF SHADING. GENERALLY, EVIDENCE IS MOST ROBUST WHEN THERE ARE MULTIPLE, CONSISTENT INDEPENDENT LINES OF HIGH QUALITY EVIDENCE (ADAPTED FROM: MASTRANDREA ET AL. 2010).

In setting confidence for projections in this Report, the simulated range of change from CMIP5 models and any consistency on the simulated direction of change was considered. This is supplemented by the following lines of evidence: model reliability at simulating relevant aspects of the current climate, results from relevant downscaled projections, evidence for a plausible process driving the simulated changes, and the level of consistency with emerging trends in the observations. For rainfall change, all of these lines of evidence were considered in some detail (see Section 7.2, Table 7.2.2). Some other variables did not always permit or require this full approach, but in all cases confidence is assessed, and reasons and evidence are given.

CHAPTER SEVEN

PROJECTIONS: ATMOSPHERE AND THE LAND



WHEAT FIELDS, VICTORIA, ISTOCK

-20° -10° 0° 10° 20° 30° 40° 50°



CHAPTER 7 PROJECTIONS: ATMOSPHERE AND THE LAND

This chapter presents projected changes to Australia's climate based on the results of the CMIP5 models and other relevant information. For changes to mean temperature, rainfall, wind speed, solar radiation, relative humidity and potential evapotranspiration (PE), ranges of regional average change are presented based on 10-90th percentiles of the empirical distribution of the CMIP5 models using the approach described in the previous chapter. Changes are presented for 20 year time slices centred on 2030 and 2090 relative to the simulated climate of 1986–2005 and for selected RCPs (usually RCP2.6, RCP4.5 and RCP8.5). The changes can then be applied to observed climate data for use in impact assessments.

Aspects of projected changes to extremes for temperature (hot days and frosts), rainfall (heavy rainfall events and droughts) and winds are also examined, along with changes to runoff, soil moisture and fire weather derived from offline calculations. Observed changes in these variables are discussed only where these are relevant to assessment of the projections, as the main discussion of trends in observed atmospheric variables is in Section 4.2. For the atmospheric and terrestrial variables, the primary focus in this Report is on area average results for the four large super-clusters: Southern Australia, Northern Australia, Eastern Australia and the Rangelands. Some results are also given at the cluster level, but more detailed results for clusters are available in the Cluster Reports.

7.1 SURFACE TEMPERATURE

This Section presents projections for air temperature near the surface (nominally at 2 m height), followed by changes for seasonal and annual average daily mean, maximum and minimum temperatures, concluding with annual and 20-year extremes.

AUSTRALIA WILL WARM SUBSTANTIALLY DURING THE 21ST CENTURY

There is *very high confidence* in continued increases of mean, daily minimum and daily maximum temperatures throughout this century for all regions in Australia. The magnitude of the warming later in the century is strongly dependent on the emission scenario.

Warming will be large compared to natural variability in the near future (2030) (*high confidence*), and very large compared to natural variability late in the century (2090) under RCP8.5 (*very high confidence*). By 2030, Australian annual average temperature is projected to increase by 0.6-1.3 °C above the climate of 1986–2005 under RCP4.5 with little difference between RCPs. The projected temperature range by 2090 shows larger differences between RCPs, with 0.6 to 1.7 °C for RCP2.6, 1.4 to 2.7 °C for RCP4.5 and 2.8 to 5.1 °C for RCP8.5.

Mean warming is projected to be greater than average in inland Australia, and less in coastal areas, particularly in southern coastal areas in winter.

7.1.1 AVERAGE TEMPERATURE

Figure 7.1 shows simulated temperature change from 1910 to 2090 (see Box 6.2.2 for guidance on reading these plots). The figure includes the median and range of the change averaged over Australia from all models under both historical forcing and three future scenarios. Future yearly values from a representative CMIP5 model show similar variability to that in the observations. In this, and similar plots for the various cluster regions, the observational data usually lie within the spread of the model values, indicating consistency between the real-world and modelled series. The median temperatures from CMIP5 models also match closely the observed climatology for the 1986–2005 base period (Section 5.2.1).

Similar to the change in global mean temperature shown in Figure 3.5.1, the median Australian warming (Figure 7.1.1) increases steadily in the RCP8.5 scenario. The range of change broadens into the future because of both the range of global warming from the models and the range of local sensitivity to that warming, according to the interpretation presented in Section 6.2 and by Watterson and Whetton (2013). For the RCP4.5 scenario the median warming plateaus after around 2060. The RCP2.6 warming peaks earlier, around 2045. These warmings mirror those projected globally (Chapter 3) and thus represent the regional expression of global warming. They are also similar to the previous projections for Australia (CSIRO and BOM, 2007) (see further discussion below and in Appendix A).

-20° -10° 0° 10° 20° 30° 40° 50°

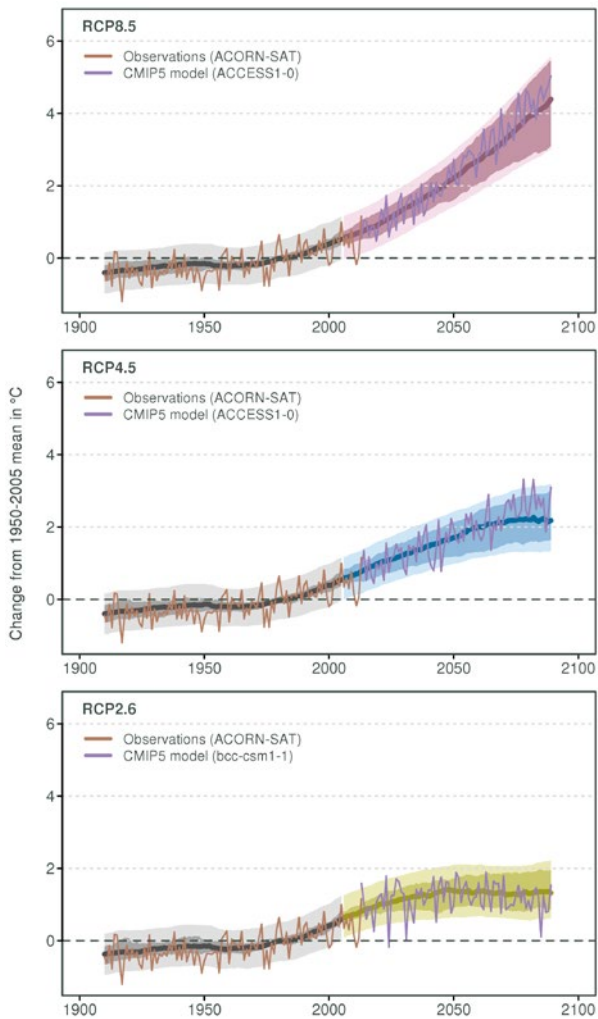


FIGURE 7.1: TIME SERIES FOR AUSTRALIAN AVERAGE TEMPERATURE FOR 1910–2090 AS SIMULATED IN CMIP5, RELATIVE TO THE 1950–2005 MEAN. THE CENTRAL LINE IS THE MEDIAN VALUE, AND THE SHADING IS THE 10TH AND 90TH PERCENTILE RANGE OF 20-YEAR RUNNING MEANS (INNER) AND SINGLE YEAR VALUES (OUTER). THE GREY SHADING INDICATES THE PERIOD OF THE HISTORICAL SIMULATION, WHILE THREE FUTURE SCENARIOS ARE SHOWN WITH COLOUR-CODED SHADING: RCP8.5 (PURPLE), RCP4.5 (BLUE) AND RCP2.6 (GREEN). ACORN-SAT OBSERVATIONS ARE SHOWN IN BROWN AND A SERIES FROM A TYPICAL MODEL ARE SHOWN INTO THE FUTURE IN LIGHT PURPLE (SEE BOX 6.2.2 FOR MORE EXPLANATION OF PLOT).

Figure 7.1.2 shows the range of mean warming for 2090 (the period 2080–2099) relative to 1986–2005 in each season, with results for the daily maximum and minimum also shown (the annual results are shown later). Overall the median warming is similar in each season and for each quantity. The warming is largest in spring for RCP8.5, and smallest in winter in the RCP2.6 case.

Spatial variation in the warming is evident from the regional values for RCP8.5 shown in Figure 7.1.3 (see Table 2.2 for description). Median projected temperature increases are typically 4 °C by 2090, while those in the north-east and far south are 3 °C or less. The climatological annual temperatures for the base period 1986–2005 averaged over each region are also shown. Generally similar changes occur for the maximum and minimum temperatures (not shown). However, increases in daily maximum temperature are around 0.5 °C greater than those for minimum temperature in the southern regions.

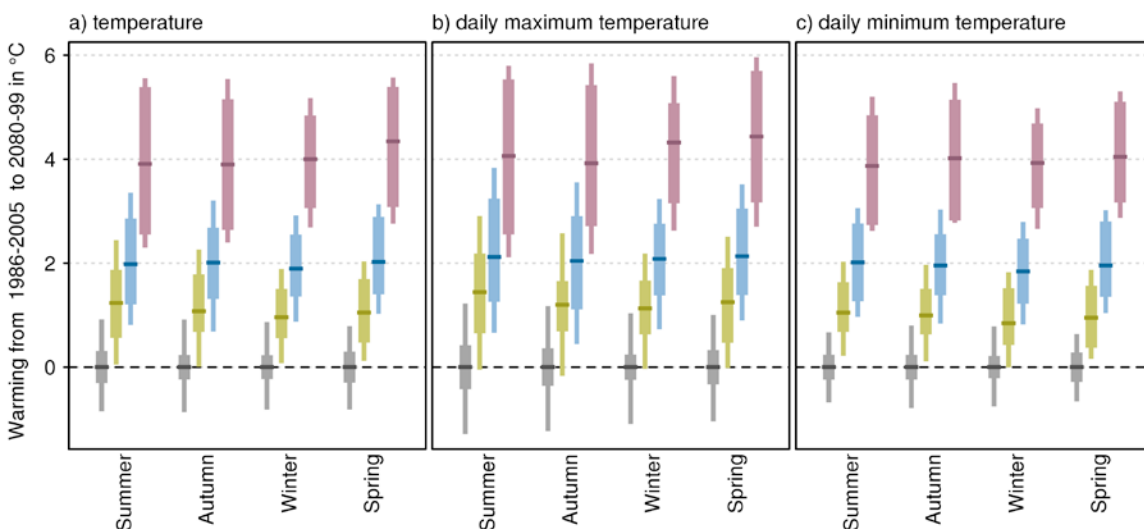


FIGURE 7.1.2: MEDIAN AND 10TH TO 90TH PERCENTILE RANGE OF PROJECTED AUSTRALIAN SEASONAL TEMPERATURE CHANGE FOR 2080–2099 RELATIVE TO THE 1986–2005 PERIOD (GREY BAR) FOR RCP2.6 (GREEN), RCP4.5 (BLUE) AND RCP8.5 (PURPLE). FINE LINES SHOW THE RANGE OF INDIVIDUAL YEARS AND SOLID BARS FOR TWENTY YEAR RUNNING MEANS FOR (A) MEAN TEMPERATURE, (B) DAILY MAXIMUM TEMPERATURE, AND (C) DAILY MINIMUM TEMPERATURE.



Table 7.1.1 presents medians and ranges averaged over Australia and four super-cluster regions for four cases. For 2030, the Australian average warming range is 0.6 to 1.3 °C (10th and 90th percentile) under RCP4.5 (and differs little for other scenarios). Later in the century, the scenario choice has a large effect on the projected warming. The projected Australian average temperature ranges for 2090 are 0.6 to 1.7 °C for RCP2.6, 1.4 to 2.7 °C for RCP4.5 and 2.8 to 5.1 °C for RCP8.5. Warming ranges in the super-clusters are similar, with slighter greater warming in the predominantly inland Rangelands (e.g. 2.9 to 5.3 °C in 2090 for RCP8.5), and slightly less warming in Southern Australia (e.g. 2.7 to 4.2 °C in 2090 for RCP8.5).

The spatial variation in the warming, on the scale resolved by the models, is evident from the median warming calculated using the ‘pattern scaling’ approach of the 2007 projections for a 1-degree common grid of points over Australia. Figure 7.1.4 presents results for each season under

RCP8.5. The median estimate for mean warming in the interior is some 20 % larger than the best estimate of the global mean value, which is 3.7 °C for this case. Warming is lower along most coasts, particularly in the south in the winter. In Appendix A, Figure A1 shows that there is little difference in the CMIP5 results relative to those inferred from CMIP3, although the warming in the north-west in the warmer seasons was greater in the earlier projections.

As for the cluster averages in Figure 7.1.3, there is a considerable range of possible warming at locations, determined using the scaling approach and shown in the maps of Figure A1, even for a single scenario. Much of the range relates to the range in global warming (Section 3.6). Some of the local range, and its seasonal variation, is associated with the influence of changes in atmospheric circulation and rainfall and hence with the external drivers of those changes (see Watterson (2012), Section 3.6, and Box 7.1).

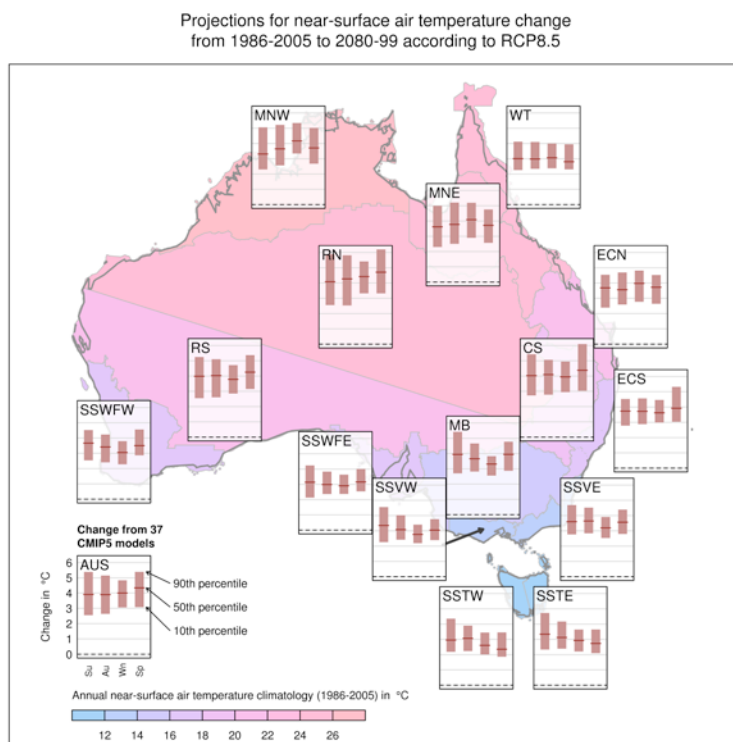


FIGURE 7.1.3: MEDIAN AND 10TH TO 90TH PERCENTILE RANGE OF PROJECTED CHANGE IN SEASONAL TEMPERATURE FROM 37 CMIP5 GCMS FOR 2080–2099 RELATIVE TO 1986–2005 FOR RCP8.5 FOR 20-YEAR MEANS. THE CHARTS FOR 15 REGIONS OVERLIE A MAP WITH EACH REGION COLOURED TO INDICATE ITS BASE CLIMATE AVERAGE (SEE SCALE). THE AUSTRALIAN AVERAGE RESULT IS IN THE BOTTOM LEFT.

TABLE 7.1.1: MEDIAN AND 10TH TO 90TH PERCENTILE RANGE OF PROJECTED TEMPERATURE CHANGE (IN °C) FOR AUSTRALIA, AND FOUR SUPER-CLUSTER REGIONS, RELATIVE TO THE 1986–2005 PERIOD. FOUR FUTURE CASES ARE GIVEN, WITH 2030 INDICATING THE PERIOD 2020–2039, AND 2090, BEING 2080–2099, FOR THREE RCPS.

	2030 RCP4.5	2090 RCP2.6	2090 RCP4.5	2090 RCP8.5
AUSTRALIA	0.9 (0.6 to 1.3)	1.0 (0.6 to 1.7)	1.9 (1.4 to 2.7)	4.1 (2.8 to 5.1)
NORTHERN AUSTRALIA	0.9 (0.6 to 1.3)	0.9 (0.5 to 1.6)	1.7 (1.3 to 2.6)	3.7 (2.7 to 4.9)
RANGELANDS	1.0 (0.6 to 1.4)	1.1 (0.6 to 1.8)	2.1 (1.5 to 2.9)	4.3 (2.9 to 5.3)
EASTERN AUSTRALIA	0.9 (0.6 to 1.2)	1.0 (0.6 to 1.6)	1.9 (1.3 to 2.6)	3.9 (2.8 to 5)
SOUTHERN AUSTRALIA	0.8 (0.5 to 1)	0.9 (0.5 to 1.4)	1.7 (1.2 to 2.1)	3.5 (2.7 to 4.2)



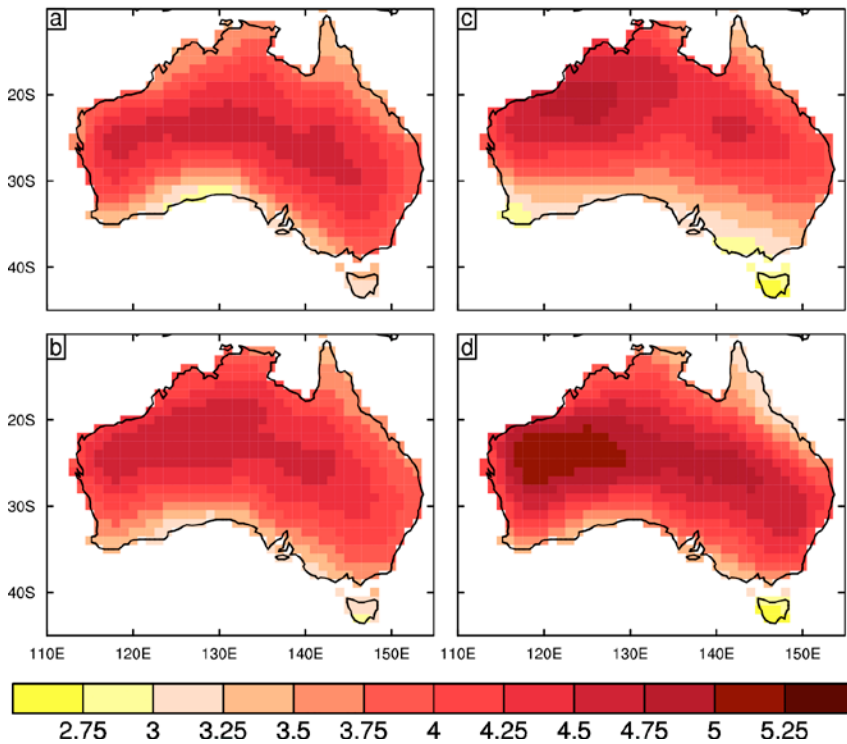


FIGURE 7.1.4: MEDIAN PROJECTED CHANGES IN TEMPERATURE (IN °C) IN EACH SEASON, FOR 2080–2099 RELATIVE TO 1986–2005 UNDER RCP8.5, USING CMIP5 GCMS (METHOD OF CSIRO AND BOM, 2007) (A) DJF, (B) MAM, (C) JJA AND (D) SON.

The mean temperature changes at most locations are anticipated to be fairly similar to those averaged over the spatial scale represented by global models. For finer scale variations, and to allow for processes that may not be well represented in the CMIP5 ensemble (see Chapter 3), results are considered from dynamical and statistical (SDM) downscaling. Figure 7.1.5 presents regional mean changes in daily maximum temperature for each season. The ranges from SDM can be compared directly with those from the 22 GCMs for which the analysis has been applied. The changes are broadly similar from the two methods. However, there are differences in some regions and seasons. Overall, the SDM increase in summer is lower than in the GCMs. This holds throughout the year in the east coast. However, the summer difference is questionable given that analogues for the most extreme future temperatures have not been observed. Simulations by CCAM, providing dynamical downscaling of six models, show little difference in mean temperature for summer from those simulated by global climate models. Generally, downscaling moderates warming along the coast, as a result of the smaller warming over the ocean than the land (see Timbal *et al.* 2011).

Estimates of temperatures for 2090 have been inferred by adding the GCM-scale projected median changes calculated using the 2007 method at each location over Australia, to the higher-resolution (0.25 °) observational mean temperature field from 1986–2005. In Figure 7.1.6 panel (a) the observed field is shown with coloured shading. Three contours are highlighted using solid lines, crossing the north, centre and south-east. Base temperatures are shown in much greater detail than those in Figure 7.1.3, with the lower temperatures evident over high orography.

Projections for GCM and downscaled daily maximum near-surface air temperature change from 1986–2005 to 2080–99 according to RCP8.5

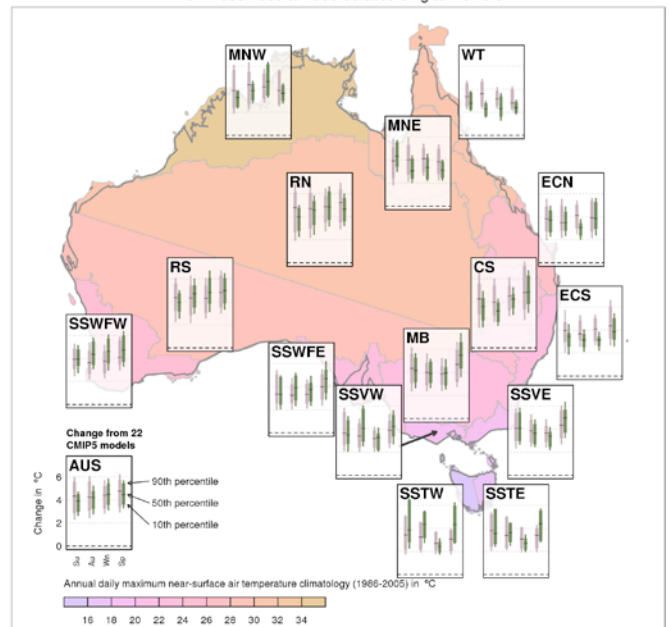


FIGURE 7.1.5: MEDIAN AND 10TH TO 90TH PERCENTILE PROJECTED CHANGES TO DAILY MAXIMUM TEMPERATURE FOR SUB-CLUSTERS IN 22 CMIP5 GCMS, AND FOR THE SAME 22 MODELS DOWNSCALED USING THE BOM SDM DOWNSCALING SYSTEM, FOR 2080–2099 RELATIVE TO 1986–2005 FOR RCP8.5. FINE LINES SHOW THE RANGE OF INDIVIDUAL YEARS AND SOLID BARS FOR TWENTY YEAR RUNNING MEANS. EACH PAIR OF BARS HAS THE CHANGES FROM THE GCMS ON THE LEFT (PURPLE) AND THE CHANGES FROM THE DOWNSCALING ON THE RIGHT (GREEN), EACH AVERAGED OVER THE REGION. THE AUSTRALIAN AVERAGE IS IN THE BOTTOM LEFT.



The temperatures for 2090 under RCP8.5 are shown in panel (b), using the same colours. A deep red area, indicating a very warm average, extends over a larger part of the continent in 2090. Blue, cooler areas have contracted. These changes are evident also from the shifts in the highlighted contours. The previous positions of the three are indicated by dashed lines. There is a southward movement across the interior of typically 8 ° latitude (about 900 km). The 15 °C line has retreated to the highlands of the south-east and southern Tasmania. Temperature analogues of the climate can be related to the original position of the new contour.

Adding the projected change from coarse model outputs to a detailed base temperature map is a simple form of downscaling (as discussed further in Chapter 6.3). More detail in the changes themselves, particularly on the coast, may be available from downscaled results on a fine grid. The coastal land is likely to be more strongly affected by maritime influences, which could mean slightly lower temperatures than shown in Figure 7.1.6(b).

In summary, continued increases in mean, daily maximum and daily minimum temperatures are projected for Australia with very *high confidence*, taking into account the strong agreement on the direction and magnitude amongst GCMs, downscaling results and the robust understanding of the driving mechanisms of warming. The magnitude of the warming later in the century is strongly dependent on the emission scenario. These warmings will be large compared to natural variability in the near future (2030) (*high confidence*), and very large compared to natural variability late in the century (2090) under RCP8.5 (*very high confidence*). Mean warming is projected to be greater than average in inland Australia, and less in coastal areas, particularly in southern coastal areas in winter.

7.1.2 EXTREME TEMPERATURE

MORE FREQUENT AND HOTTER HOT DAYS AND FEWER FROST DAYS ARE PROJECTED

Projected warming will result in more frequent and hotter hot days and warmer cold extremes (*very high confidence*) and reduced frost (*high confidence*).

Hot days are projected to occur more frequently. For example, in Perth, the average number of days per year above 35 °C or above 40 °C by 2090 is projected to be 50 % greater than present under RCP4.5. The number of days above 35 °C in Adelaide also increases by about 50 % by late in the century, while the number of days above 40 °C more than doubles.

Locations where frost occurs only a few times a year under current conditions are projected to become nearly frost-free by 2030. Under RCP8.5 coastal areas are projected to be free of frost by 2090 while frost is still projected to occur inland.

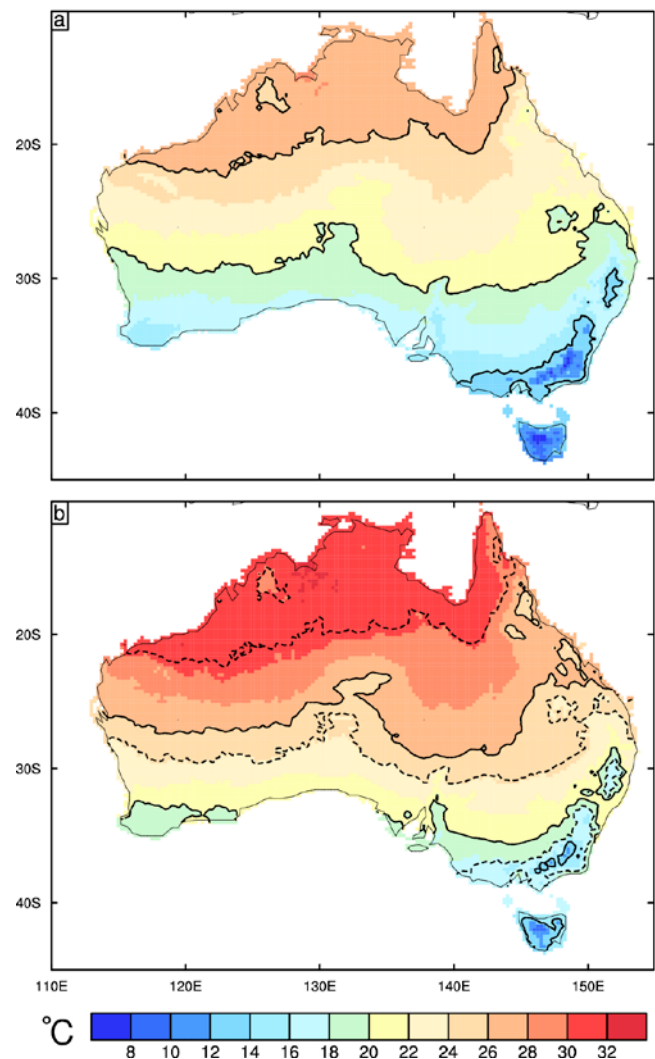


FIGURE 7.1.6: ANNUAL MEAN TEMPERATURE (IN °C), FOR THE PRESENT CLIMATE (A), AND FOR LATE 21ST CENTURY (B). THE FUTURE CASE IS CALCULATED BY ADDING THE MEDIAN (P50) WARMING FROM 1986–2005 TO 2080–2099 UNDER RCP8.5 TO THE MEAN TEMPERATURE OF THE PRESENT CLIMATE. IN EACH PANEL THE 14 °C, 20 °C, AND 26 °C CONTOURS ARE SHOWN WITH SOLID BLACK LINES. IN (B) THE SAME CONTOURS FROM THE ORIGINAL CLIMATE ARE PLOTTED AS DOTTED LINES. TO PROVIDE THE clearest DEPICTION OF THE SHIFTS IN CONTOURS, THE LONGER PERIOD 1950–2008 BOM DATASET IS USED FOR THE PRESENT CLIMATE, ON A 0.25° GRID.

Climate impacts of temperature are often felt through extremes, which are quantified here through the indices described by Karl *et al.* (1999). The extreme temperature indices have been calculated using daily data from the 24 CMIP5 models for which these values could be obtained, and the focus here is on the annual extremes. The Australian average for changes by 2090 under two RCPs is shown in Figure 7.1.7 (a). The changes for the ‘hottest day of the year’ are similar to those for the annual mean of daily maximum (and also for the average summer daily maximum increase (not shown)), as seen in Figure 7.1.2. For example, this means hot days would be around 3-5 degrees warmer in 2090 under RCP8.5. To examine changes in very rare daily maximum temperatures, extreme value theory was used to infer 1-in-20 year return values. The Generalised Extreme Value distribution was fitted to the annual maximum temperature at each location for the 20-year period centred on 2090, and the expected 20-year extreme was calculated and compared to that for 1986-2005. Again, the Australian average changes by a similar amount to the annual value, while the contrast between the scenarios is maintained. The panel in Figure 7.1.7(b) gives the increase in number of days per year that fall within ‘warm spells’, defined as six or more days above the 90th percentile value for daily temperatures over 1961 – 1990. This warm spell metric increases dramatically by 2090, with RCP8.5 showing more than 100 additional warm spell days each year.

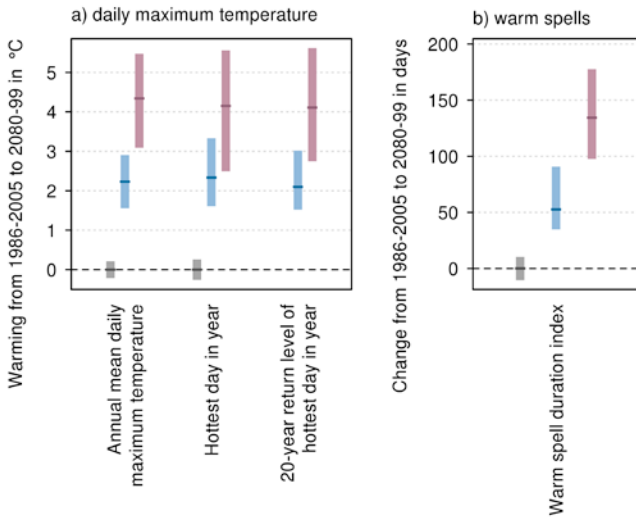


FIGURE 7.1.7: (A) MEDIAN AND 10TH TO 90TH PERCENTILE RANGE OF PROJECTED CHANGE IN MEAN AND EXTREME DAILY MAXIMUM TEMPERATURE AVERAGED OVER AUSTRALIA FOR 2080–2099 RELATIVE TO THE 1986–2005 PERIOD (GREY BAR), FOR RCP4.5 (BLUE) AND RCP8.5 (PURPLE). CHANGES IN DAILY MAXIMUM TEMPERATURES ARE SHOWN FOR ANNUAL MEAN (LEFT), HOTTEST DAY OF THE YEAR (CENTRE), AND 20-YEAR RETURN LEVEL (RIGHT). (B) CHANGES IN NUMBER OF DAYS PER YEAR WITHIN WARM SPELLS (DEFINED AS PERIODS OF 6 OR MORE CONSECUTIVE DAYS ABOVE THE 90TH PERCENTILE OF DAILY TEMPERATURES FOR THE 1961–1990 PERIOD).

Projections for daily maximum near-surface air temperature change from 1986-2005 to 2080-99 according to RCP8.5 for both the annual mean and annual extremes

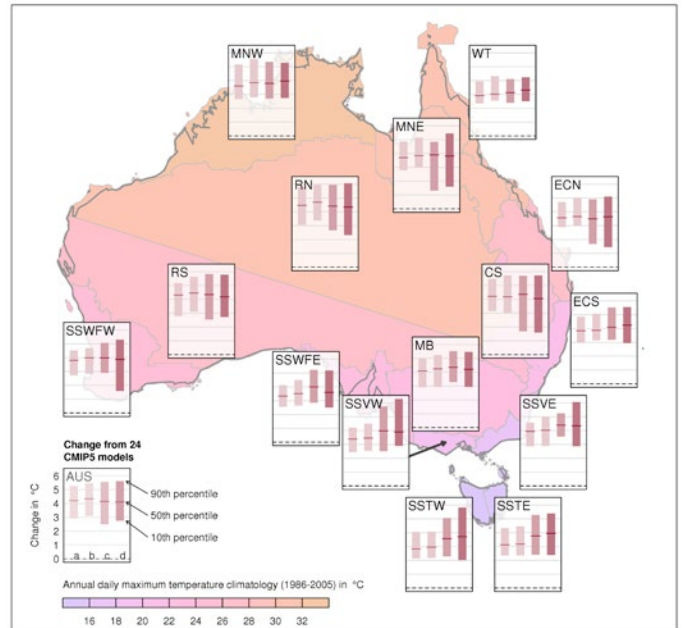


FIGURE 7.1.8: MEDIAN AND 10TH TO 90TH PERCENTILE RANGE OF PROJECTED CHANGE IN DAILY MAXIMUM TEMPERATURE IN SUB-CLUSTERS FOR 2080–2099 RELATIVE TO 1986–2005 FOR RCP8.5. SHOWN IN EACH BOX FROM LEFT TO RIGHT IS (A) THE ANNUAL DAILY MEAN FOR THE LARGER SET OF 37 MODELS, (B) THE ANNUAL DAILY MEAN, (C) THE ANNUAL DAILY MAXIMUM, AND THE (D) 20 YEAR RETURN LEVEL OF ANNUAL DAILY MAXIMUM TEMPERATURE FROM A CONSISTENT SUBSET OF 24 MODELS. THE AUSTRALIAN AVERAGE RESULT IS SHOWN AT BOTTOM LEFT.

Figure 7.1.8 and Figure 7.1.9 show the regional results for extreme temperatures under the RCP8.5 scenario for daily maxima and minima, respectively. In both figures, for each region the median and ranges of the annual mean determined from the full set of CMIP5 models (the first bar) are similar to that from the subset of 24 models (the second bar from the left). As with the mean temperatures, there is some variation around the continent. In Figure 7.1.8, in the warmer regions, there is little difference between changes in the magnitude of annual extremes when compared to changes in 1-in-20 year extremes. The increases in the annual and 1-in-20 year maximums are a little higher than for the means in the southern coastal regions. This seems consistent with the effect of hot winds from the interior providing an even greater temperature contrast to those from across the ocean under the warmer climates, as examined by Watterson *et al.* (2008). Smaller simulated warming of the Southern Ocean may account for a less pronounced temperature rise in cool extremes experienced in southern regions (Figure 7.1.9). Moreover, there tends to be reduced cloud cover in winter (as evidenced by seasonal changes in solar radiation and humidity, Sections 7.4 and 7.5), which can lead to relatively cool minima.



Projections for daily minimum near-surface air temperature change from 1986-2005 to 2080-99 according to RCP8.5 for both the annual mean and annual extremes

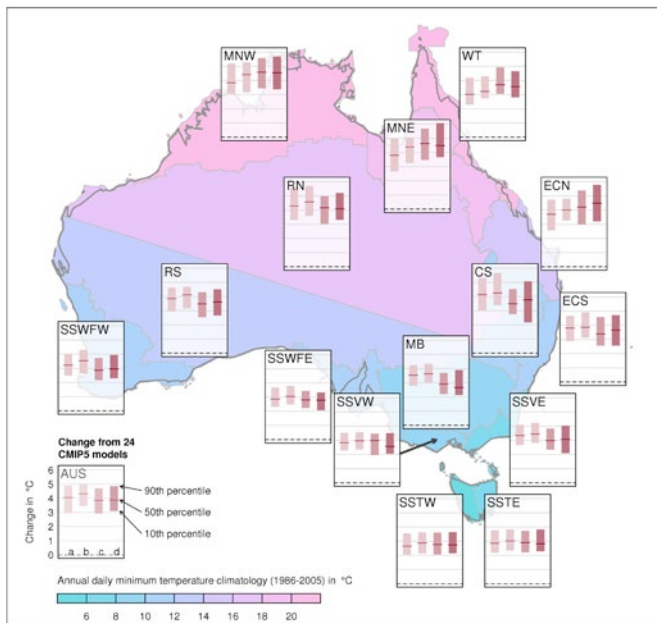


FIGURE 7.1.9: MEDIAN AND 10TH TO 90TH PERCENTILE RANGE OF PROJECTED CHANGE IN DAILY MINIMUM TEMPERATURE IN SUB-CLUSTERS FOR 2080–2099 RELATIVE TO 1986–2005 FOR RCP8.5. SHOWN IN EACH BOX FROM LEFT TO RIGHT IS (A) THE ANNUAL MEAN FOR THE LARGER SET OF 36 MODELS, (B) THE ANNUAL MEAN, (C) THE ANNUAL MINIMUM, AND (D) THE 20 YEAR RETURN LEVEL OF ANNUAL DAILY MINIMUM TEMPERATURE FROM A CONSISTENT SUBSET OF 24 MODELS. THE AUSTRALIAN AVERAGE RESULT IS SHOWN AT BOTTOM LEFT.

Given the similarity of the rises in extreme high daily maximum temperatures and those in the mean daily maximum temperature, an estimate of actual daily maximum temperatures in a future climate can be made by adding the average projected changes for daily maximums to observational values – the scaling factor method (Chapter 6). This has been done using seasonal changes (medians and 10th/90th percentiles) for the region in which the location falls (see Figure 7.1.8), although this approach may not account for local effects. If ‘hot’ days are defined using a simple threshold, then tallies of these are readily made. Table 7.1.2 presents the results for 15 cities and regional centres. This calculation does not take into account any change to heat island effects in the future. The results from the recent 30 years (1981–2010 or ‘1995’) for the 35 °C threshold tend to be a little higher than those given in the CSIRO and BOM, (2007) report (Table 5.2) for 1971–2000. Projected numbers are given for the four future cases included in Table 7.1.1 (i.e. 2030 under RCP4.5, and 2090 under RCP2.6, RCP4.5 and RCP8.5, based on model changes for 2020–2039 and 2080–2099 relative to 1986–2005). In 2030 under RCP4.5, the numbers increase considerably, particularly in the northern centres and at some inland sites with larger warming, e.g. Canberra (airport). The increases for the other scenarios are similar in this period (not shown). Numbers of days above 35 °C in the period centred on 2090 are mostly similar to those in 2030 for RCP2.6, but numbers increase further for the other two scenarios.

For example, in Perth, the number of days above 35 °C or above 40 °C by 2090 is 50 % greater than the period centred on 1995 under RCP4.5. The number of days above 35 °C in Adelaide also increases by about 50 % by 2090, whereas the number of days above 40 °C more than doubles.

Maximum temperatures over 40 °C (Table 7.1.2) also occur in most years at most sites by 2090, and could become normal for a summer day in Alice Springs and Wilcannia.

Changes in the frequency of surface frost have significant implications for agriculture and the environment. Assessing frost occurrence directly from global model output is not reliable, in part because of varying biases in land surface temperatures. However, an indication of future changes in frost can be obtained using a similar approach to that used for hot days. For most regions, the rise in the low extreme temperature (Figure 7.1.9) is similar to that for the means for the winter season (not shown). Therefore, adding the average seasonal change in daily minimum temperatures to an observational record of daily minimum temperatures provides a plausible representation of the series of minimums for the future. On frosty mornings, when the land surface temperature is below 0 °C, the air temperature is typically 2 °C warmer (see the Bureau of Meteorology web pages on potential frost occurrence). This temperature thus provides a suitable criterion to represent the potential for frost to occur, based on the usual (air) temperature data. Table 7.1.3 presents the average annual number of potential frost days calculated using this approach for representative sites (omitting those with zero values). Locations where frost occurs only a few times a year at present are likely by 2030 to be nearly frost free on average. Coastal mainland cities will be frost free on average by 2090 under RCP8.5. Inland locations, even Alice Springs, will retain some frost days. The actual occurrence of frost will depend on many local factors. Downscaling can be used to provide more detailed information (e.g. see Murray Basin cluster report), however assessment of available (regionally restricted) results did not show changes substantially different from those presented here.

In summary, strong model agreement and the understanding of the physical mechanisms of warming indicate more frequent and hotter hot days and warmer cold extremes (*very high confidence*) and reduced frost (*high confidence*).

TABLE 7.1.2: CURRENT (FOR THE 30-YEAR PERIOD 1981–2010) AVERAGE NUMBER OF DAYS PER YEAR WITH MAXIMUM TEMPERATURE ABOVE 35 °C (TOP) AND 40 °C (BOTTOM) FOR VARIOUS LOCATIONS BASED ON ACORN-SAT (TREWIN, 2013). ESTIMATES FOR THE FUTURE ARE CALCULATED USING THE MEDIAN CMIP5 WARMING OF MAXIMUM TEMPERATURES FOR 2030 AND 2090, AND WITHIN BRACKETS THE 10TH AND 90TH PERCENTILE CMIP5 WARMING FOR THESE PERIODS, APPLIED TO THE 30-YEAR ACORN-SAT STATION SERIES. (LOCATION LEGEND: 1 CBD, 2 AIRPORT, 3 AMBERLEY RAAF BASE (INLAND FROM BRISBANE), 4 BATTERY POINT, 5 OBSERVATORY HILL, THE ROCKS).

THRESHOLD 35 °C	1995	2030 RCP4.5	2090 RCP2.6	2090 RCP4.5	2090 RCP8.5
ADELAIDE ¹	20	26 (24 to 29)	28 (24 to 31)	32 (29 to 38)	47 (38 to 57)
ALICE SPRINGS ²	94	113 (104 to 122)	119 (104 to 132)	133 (115 to 152)	168 (145 to 193)
AMBERLEY ³	12	18 (15 to 22)	18 (14 to 30)	27 (21 to 42)	55 (37 to 80)
BROOME ²	56	87 (72 to 111)	95 (70 to 154)	133 (94 to 204)	231 (173 to 282)
CAIRNS ²	3	5.5 (4.4 to 7.9)	5.5 (4.4 to 14)	11 (7.4 to 22)	48 (24 to 105)
CANBERRA ²	7.1	12 (9.4 to 14)	13 (10 to 16)	17 (13 to 23)	29 (22 to 39)
DARWIN ²	11	43 (25 to 74)	52 (24 to 118)	111 (54 to 211)	265 (180 to 322)
DUBBO ²	22	31 (26 to 37)	34 (26 to 43)	44 (36 to 54)	65 (49 to 85)
HOBART ⁴	1.6	2.0 (1.9 to 2.1)	2.0 (1.8 to 2.5)	2.6 (2.0 to 3.1)	4.2 (3.2 to 6.3)
MELBOURNE	11	13 (12 to 15)	14 (12 to 17)	16 (15 to 20)	24 (19 to 32)
MILDURA ²	33	42 (37 to 46)	44 (39 to 50)	52 (45 to 61)	73 (60 to 85)
PERTH ²	28	36 (33 to 39)	37 (33 to 42)	43 (37 to 52)	63 (50 to 72)
ST. GEORGE ²	40	54 (48 to 62)	58 (47 to 69)	70 (59 to 87)	101 (79 to 127)
SYDNEY ⁵	3.1	4.3 (4.0 to 5.0)	4.5 (3.9 to 5.8)	6.0 (4.9 to 8.2)	11 (8.2 to 15)
WILCANNIA	47	57 (53 to 62)	60 (54 to 66)	67 (59 to 75)	87 (72 to 100)

THRESHOLD 40 °C	1995	2030 RCP4.5	2090 RCP2.6	2090 RCP4.5	2090 RCP8.5
ADELAIDE ¹	3.7	5.9 (4.7 to 7.2)	6.5 (5.2 to 8.5)	9.0 (6.8 to 12)	16 (12 to 22)
ALICE SPRINGS ²	17	31 (24 to 40)	37 (24 to 51)	49 (33 to 70)	83 (58 to 114)
AMBERLEY ³	0.8	1.2 (1.1 to 1.6)	1.2 (1.1 to 2.5)	2.1 (1.5 to 3.9)	6.0 (2.9 to 11)
BROOME ²	4.1	7.2 (6.0 to 9.3)	7.7 (5.7 to 13)	11 (7.7 to 22)	30 (17 to 61)
CAIRNS ²	0	0.1 (0.1 to 0.2)	0.1 (0.1 to 0.3)	0.3 (0.2 to 0.4)	0.7 (0.5 to 2.0)
CANBERRA ²	0.3	0.6 (0.4 to 0.8)	0.7 (0.5 to 1.3)	1.4 (0.8 to 2.8)	4.8 (2.3 to 7.5)
DARWIN ²	0	0.0 (0.0 to 0.0)	0.0 (0.0 to 0.0)	0.0 (0.0 to 0.2)	1.3 (0.2 to 11)
DUBBO ²	2.5	3.9 (3.2 to 5.6)	5.0 (3.2 to 8.0)	7.8 (5.1 to 12)	17 (9.9 to 26)
HOBART ⁴	0.1	0.2 (0.2 to 0.4)	0.2 (0.1 to 0.4)	0.4 (0.2 to 0.5)	0.9 (0.5 to 1.4)
MELBOURNE	1.6	2.4 (2.1 to 3.0)	2.7 (2.3 to 3.7)	3.6 (2.8 to 4.9)	6.8 (4.6 to 11)
MILDURA ²	7.2	10 (8.8 to 12)	11 (9.4 to 14)	15 (12 to 20)	27 (19 to 35)
PERTH ²	4	6.7 (5.4 to 7.5)	6.9 (5.6 to 9.0)	9.7 (6.9 to 13)	20 (12 to 25)
ST. GEORGE ²	5.1	8.2 (6.3 to 11)	10 (6.1 to 16)	15 (11 to 23)	31 (20 to 49)
SYDNEY ⁵	0.3	0.5 (0.5 to 0.8)	0.7 (0.5 to 0.9)	0.9 (0.8 to 1.3)	2.0 (1.3 to 3.3)
WILCANNIA ¹	11	16 (14 to 20)	18 (15 to 25)	23 (18 to 31)	40 (27 to 53)



TABLE 7.1.3: CURRENT (FOR THE 30-YEAR PERIOD 1981–2010) AVERAGE NUMBER OF POTENTIAL FROST DAYS PER YEAR FOR VARIOUS LOCATIONS BASED ON ACORN-SAT (TREWIN, 2013). ESTIMATES FOR THE FUTURE ARE CALCULATED USING THE MEDIAN CMIP5 WARMING OF MINIMUM TEMPERATURES FOR 2030 AND 2090, AND WITHIN BRACKETS THE 10TH AND 90TH PERCENTILE CMIP5 WARMING FOR THESE PERIODS, APPLIED TO THE 30-YEAR ACORN-SAT STATION SERIES. THE CRITERION USED FOR POTENTIAL FROST IS 2 °C. (LOCATION LEGEND: 1 CBD, 2 AIRPORT, 3 AMBERLEY RAAF BASE (INLAND FROM BRISBANE), 4 BATTERY POINT).

	1995	2030 RCP4.5	2090 RCP2.6	2090 RCP4.5	2090 RCP8.5
ADELAIDE ¹	1.1	0.5 (0.8 to 0.4)	0.4 (0.8 to 0.3)	0.2 (0.4 to 0.1)	0.0 (0.0 to 0.0)
ALICE SPRINGS ²	33	24 (28 to 19)	24 (30 to 17)	13 (20 to 8.4)	2.1 (6.0 to 0.8)
AMBERLEY ³	22	16 (18 to 14)	17 (20 to 12)	11 (14 to 7.4)	3.1 (6.8 to 0.7)
CANBERRA ²	91	81 (87 to 76)	80 (87 to 71)	68 (75 to 61)	43 (52 to 35)
DUBBO ²	39	30 (34 to 27)	31 (35 to 22)	21 (26 to 13)	6.0 (10 to 2.4)
HOBART ⁴	9.1	5.8 (6.9 to 3.7)	5.3 (7.7 to 2.3)	2.1 (4.1 to 1.1)	0.3 (0.6 to 0.1)
MELBOURNE	0.9	0.6 (0.8 to 0.4)	0.5 (0.7 to 0.2)	0.2 (0.3 to 0.1)	0.0 (0.0 to 0.0)
MILDURA ²	19	14 (16 to 12)	13 (16 to 9.4)	9.0 (11 to 6.7)	3.0 (4.9 to 1.2)
PERTH ²	3.4	2.1 (2.5 to 1.4)	1.9 (2.5 to 1.0)	0.9 (1.3 to 0.7)	0.1 (0.4 to 0.0)
ST. GEORGE ²	17	12 (15 to 11)	13 (15 to 8.7)	8.3 (11 to 5.5)	1.5 (3.5 to 0.5)
WILCANNIA	20	14 (17 to 11)	14 (16 to 9.7)	9.4 (12 to 6.3)	2.4 (4.4 to 1.0)

7.2 RAINFALL

This section considers changes to average rainfall conditions, as well as indices of extreme rainfall, drought occurrence and snow. The evidence considered is based mainly on CMIP5 GCM results, but various downscaled data sets are also considered. As part of considering the plausible processes driving the simulated rainfall changes, the section also considers changes to some patterns of atmospheric circulation.

7.2.1 PROJECTED MEAN RAINFALL CHANGE

COOL-SEASON RAINFALL IS PROJECTED TO DECLINE IN SOUTHERN AUSTRALIA; CHANGES ARE UNCERTAIN ELSEWHERE

Southern Australia: Cool season (winter and spring) rainfall is projected to decrease (*high confidence*), though little change or increases in Tasmania in winter are projected (*medium confidence*). The winter decline may be as great as 50 % in south-western Australia in the highest emission scenario (RCP8.5) by 2090. The direction of change in summer and autumn rainfall in southern Australia cannot be reliably projected, but there is *medium confidence* in a decrease in south-western Victoria in autumn and in western Tasmania in summer.

Eastern Australia: There is *high confidence* that in the near future (2030), natural variability will predominate over trends due to greenhouse gas emissions. For late in the century (2090), there is *medium confidence* in a winter rainfall decrease.

Northern Australia and northern inland areas:

There is *high confidence* that in the near future (2030) natural variability will predominate over trends due to greenhouse gas emissions. There is *low confidence* in the direction of future rainfall change for late in the century (2090), but substantial changes to wet-season and annual rainfall cannot be ruled out.

There is a range of dominant drivers of change in the different regions of Australia, and projected changes to some of these are well understood and robust among models (see also Section 4.2). For example, one consistent finding is that an increase in pressure in the sub-tropics, poleward shifts in the storm tracks, expansion of the Hadley Cell and positive trends in the Southern Annular Mode are leading to a general drying of the sub-tropics and southern continental Australia - especially in winter. Other changes, including those in the tropics are less consistent in theory and models. Therefore, this Report focuses primarily on rainfall changes and the reasons behind them for sub-regions of Australia rather than the nation as a whole.

GCM-BASED RAINFALL PROJECTIONS

Global climate models can resolve rainfall changes due to shifts in atmospheric circulation, storm tracks and extra-tropical cyclones as well as integrate the results of changes to thermodynamic processes to create projections of rainfall change. Global climate models vary in their simulation of circulation change and other processes over Australia, and this implies a range of projected changes in rainfall. The report focuses on the range between models as a measure of the uncertainty in the response in atmospheric circulation and rainfall processes, rather than on a single model or the multi-model mean.

To give a broad overview of the rainfall projections from CMIP5, Figure 7.2.1 gives the model simulated annual rainfall for 1910 to 2090 for each of the Northern Australian (NA), Southern Australian (SA), Eastern Australian (EA) and Rangelands (R) super-clusters. Table 7.2.1 gives results in numerical form for 2030 (RCP4.5) and 2090 (RCP2.6, RCP4.5 and RCP8.5). The table also indicates levels of agreement amongst models on increase, decrease etc, using the categories defined in Section 6.4.

It is immediately clear from the time series (Figure 7.2.1) that natural variability of rainfall remains significant compared to any climate change signal out to 2090. Indeed, under the RCP2.6 and RCP4.5 scenarios it is difficult to detect any marked change in many cases. This is particularly the case in the Australia wide average results (not shown). This is in marked contrast to the results for temperature reported in the previous section.

Nevertheless, under RCP8.5 there is an emerging drying trend clearly evident in Southern and Eastern Australia, and in Southern Australia this is also evident under the lower RCPs. This is in line with the global-scale patterns of rainfall decrease in the mid-latitudes and is consistent with theory, knowledge of climate dynamics and previous model results (e.g. CSIRO and BOM, 2007). The expanding uncertainty with time that is visible in all cases under RCP8.5, and to a lesser extent under the lower RCPs, is indicative of the fact that there are differing forced responses for at least some models, even in cases where the model median indicates little change. As indicated in Table 7.2.1 there is medium agreement amongst models on a substantial annual decrease in Eastern and Southern Australia, whereas in the Rangelands and Northern Australia there is low agreement on the direction of change.

By 2090, the projected changes are larger for the higher emission scenario, consistent with the understanding of climate forcings. The magnitude of the ranges of projected change in rainfall in 2030 relative to 1995 (under RCP4.5) are around -10 % to little change in Southern Australia, and -10 to +5 % in the other regions (see Table 7.2.1). In 2090 under RCP8.5 the projected rainfall changes -25 to +5 % in Southern Australia, around -25 to +10 % in Eastern Australia, around -30 to +20 % in the Rangelands and -25 to +25 % for Northern Australia. Changes are generally much more moderate in 2090 under RCP2.6.



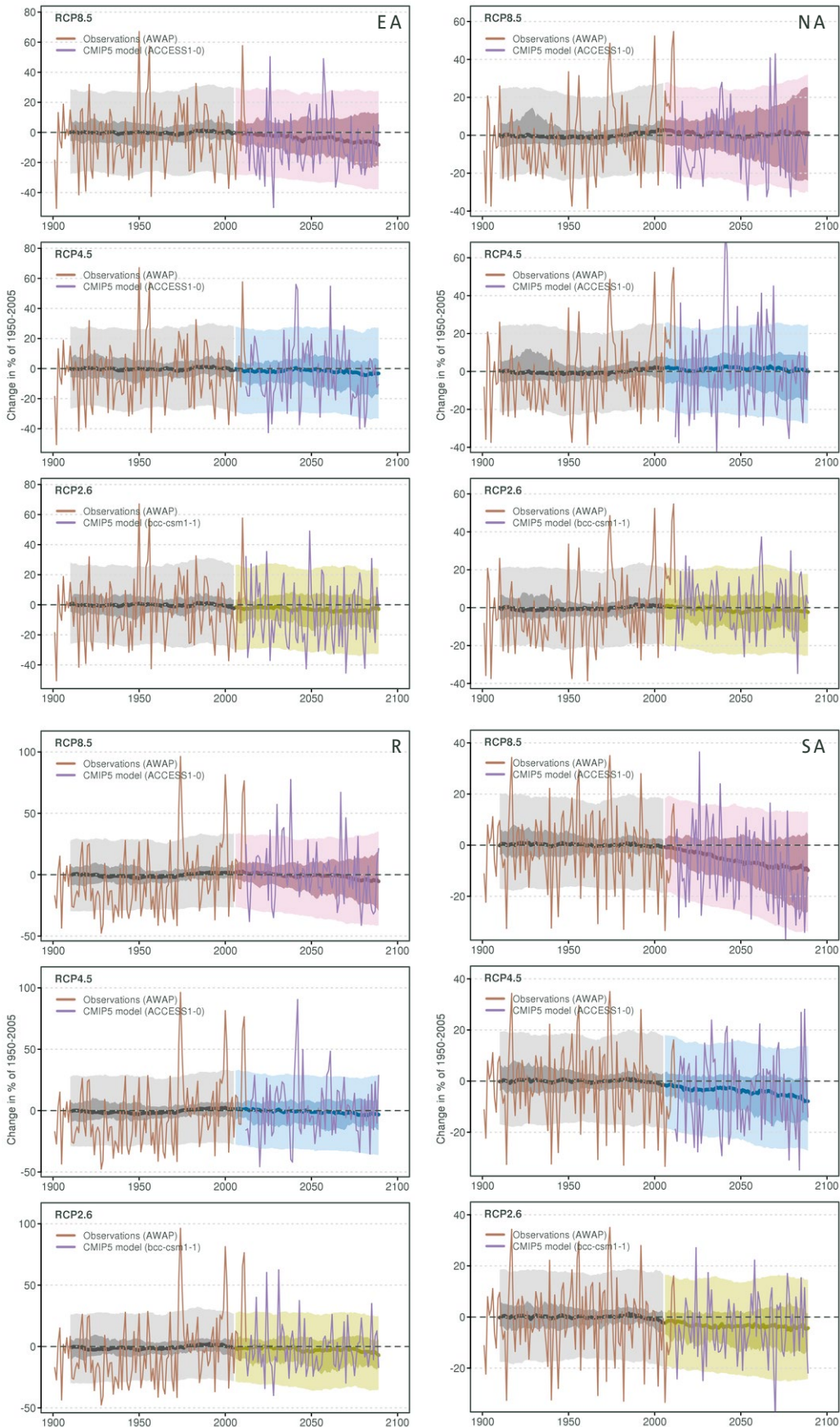


FIGURE 7.2.1: RAINFALL FOR 1910–2090 AS SIMULATED IN CMIP5 FOR EACH OF THE EASTERN AUSTRALIAN (EA; TOP LEFT), NORTHERN AUSTRALIAN (NA; TOP RIGHT), RANGELANDS (R; BOTTOM LEFT) AND SOUTHERN AUSTRALIAN (SA; BOTTOM RIGHT) SUPER-CLUSTERS. THE CENTRAL LINE IS THE MEDIAN VALUE, AND THE SHADING IS THE 10TH AND 90TH PERCENTILE RANGE OF 20-YEAR MEANS (INNER) AND SINGLE YEAR VALUES (OUTER). THE GREY SHADING INDICATES THE PERIOD OF THE HISTORICAL SIMULATION, WHILE THREE FUTURE SCENARIOS ARE SHOWN WITH COLOUR-CODED SHADING: PURPLE RCP8.5, BLUE RCP4.5 AND GREEN RCP2.6. AWAP OBSERVATIONS ARE SHOWN IN BROWN AND A SERIES FROM A TYPICAL MODEL ARE SHOWN INTO THE FUTURE IN LIGHT PURPLE (SEE BOX 6.2.2 FOR MORE EXPLANATION OF PLOT).

TABLE 7.2.1: MEDIAN AND 10TH TO 90TH PERCENTILE RANGE OF PROJECTED RAINFALL CHANGE (PERCENT) FOR NORTHERN AUSTRALIA, EASTERN AUSTRALIA, RANGELANDS AND SOUTHERN AUSTRALIA SUPER-CLUSTERS (COMPARED TO 1986–2005 BASELINE). MODEL AGREEMENT ON PROJECTED CHANGES IS SHOWN FOR 2090 AND RCP8.5 (WITH ‘MEDIUM’ BEING MORE THAN 60% OF MODELS, ‘HIGH’ MORE THAN 75%, ‘VERY HIGH’ MORE THAN 90%, AND ‘SUBSTANTIAL’ A CHANGE OUTSIDE THE 10 TO 90% RANGE OF MODEL NATURAL VARIABILITY).

SEASON	2030 RCP4.5	2090 RCP2.6	2090 RCP4.5	2090 RCP8.5	MODEL AGREEMENT 2090 RCP8.5 (PERCENTAGES SHOW FRACTION OF MODELS)
RAINFALL CHANGE IN NORTHERN AUSTRALIA (%)					
ANNUAL	0 (-9 to +4)	-4 (-12 to +3)	-1 (-14 to +6)	0 (-26 to +23)	<i>Low agreement in direction of change</i> (51% decrease), but substantial decrease (37%) & increase (32%) possible.
DJF	-1 (-8 to +8)	-2 (-16 to +4)	-1 (-18 to +8)	+2 (-24 to +18)	<i>Low agreement in direction of change</i> (56% increase), but substantial increase (42%) & decrease (29%) possible.
MAM	0 (-17 to +7)	-4 (-18 to +11)	-2 (-17 to +12)	-2 (-30 to +26)	<i>Medium agreement in little change</i> (37% of models), but substantial decrease (33%) and increase (31%) possible.
JJA	-5 (-26 to +16)	-8 (-41 to +16)	-14 (-35 to +20)	-15 (-48 to +46)	<i>Medium agreement in decrease</i> (67%).
SON	-4 (-26 to +20)	-7 (-32 to +13)	-7 (-32 to +27)	-13 (-44 to +44)	<i>Medium agreement in decrease</i> (64%).
RAINFALL CHANGE IN EASTERN AUSTRALIA (%)					
ANNUAL	-1 (-13 to +5)	-4 (-19 to +6)	-7 (-16 to +6)	-10 (-25 to +12)	<i>Medium agreement in substantial decrease</i> (52%), but substantial increase possible (21%).
DJF	-2 (-12 to +13)	-6 (-20 to +13)	-2 (-15 to +13)	+4 (-16 to +28)	<i>Medium agreement in little change</i> (61%), but substantial increase (27%) and decrease (13%) possible.
MAM	-4 (-22 to +13)	-8 (-25 to +15)	-7 (-28 to +18)	-8 (-33 to +26)	<i>Medium agreement in little change</i> (55%), but substantial decrease (28%) & increase (17%) possible.
JJA	-3 (-19 to +9)	-4 (-24 to +9)	-10 (-25 to +8)	-16 (-40 to +7)	<i>Medium agreement in substantial decrease</i> (53%).
SON	-2 (-18 to +11)	-3 (-26 to +11)	-10 (-27 to +9)	-16 (-41 to +8)	<i>Medium agreement in substantial decrease</i> (57%).
RAINFALL CHANGE IN RANGELANDS (%)					
ANNUAL	-2 (-11 to +6)	-6 (-21 to +3)	-5 (-15 to +7)	-4 (-32 to +18)	<i>Low agreement in direction of change</i> (59% decrease), but substantial decrease (41%) and increase (22%) possible.
DJF	-1 (-16 to +7)	-6 (-22 to +8)	-2 (-16 to +10)	+3 (-22 to +25)	<i>Low agreement in direction of change</i> (52% increase), but substantial decrease (36%) and increase (33%) possible.
MAM	+0 (-23 to +21)	-6 (-26 to +18)	0 (-23 to +27)	+9 (-42 to +32)	<i>Medium agreement in little change</i> (54%), but substantial increase (28%) and decrease (19%) possible.
JJA	-7 (-20 to +14)	-4 (-31 to +12)	-11 (-34 to +7)	-20 (-50 to +18)	<i>Medium agreement in substantial decrease</i> (61%), but substantial increase possible (14%).
SON	-3 (-21 to +19)	-5 (-32 to +15)	-10 (-26 to +11)	-11 (-50 to +23)	<i>Medium agreement in decrease</i> (68%).
RAINFALL CHANGE IN SOUTHERN AUSTRALIA (%)					
ANNUAL	-4 (-9 to +2)	-3 (-15 to +3)	-7 (-16 to +2)	-8 (-26 to +4)	<i>Medium agreement in substantial decrease</i> (69%)
DJF	-1 (-17 to +9)	-5 (-22 to +6)	-2 (-13 to +8)	+1 (-13 to +16)	<i>High agreement in little change</i> (71%), but substantial increase (18%) & decrease (11%) possible.
MAM	-2 (-18 to +8)	-5 (-17 to +11)	-2 (-19 to +10)	-1 (-25 to +13)	<i>Medium agreement in little change</i> (57%), but substantial decrease (28%) & increase (15%) possible.
JJA	-4 (-12 to +3)	-3 (-9 to +4)	-9 (-19 to +2)	-17 (-32 to -2)	<i>High agreement in substantial decrease</i> (80%).
SON	-4 (-13 to +5)	-5 (-23 to +4)	-10 (-23 to +1)	-18 (-44 to -3)	<i>High agreement in substantial decrease</i> (79%).

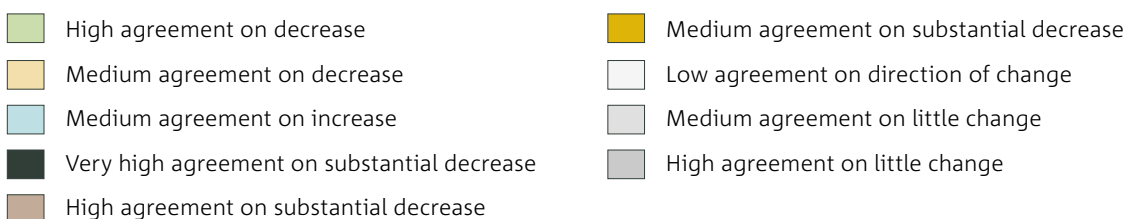
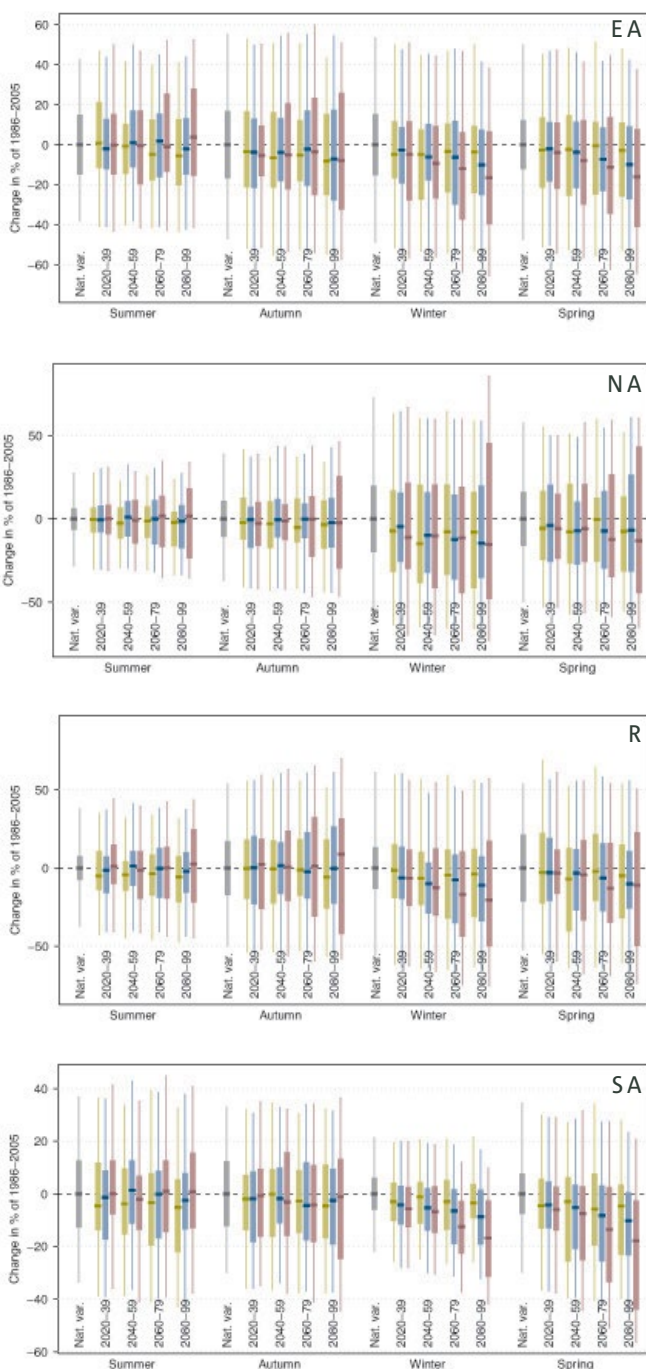


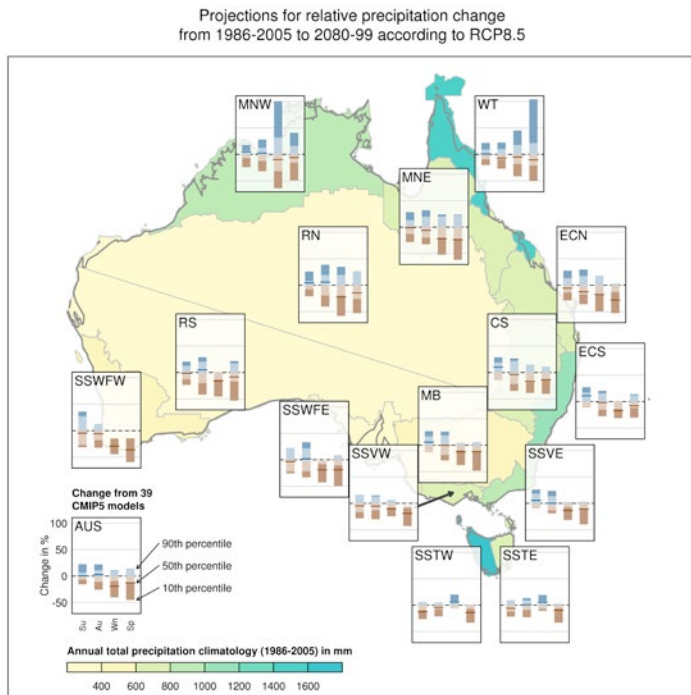
Figure 7.2.2 shows the seasonal variation in the projected rainfall changes for 2030 and 2090 under three emission scenarios, with additional seasonal information in Table 7.2.1. Figure 7.2.2 also contrasts the projected changes with natural variability (with ‘substantial’ changes exceeding natural variability). In all seasons in 2030 under RCP4.5 ranges of change show mostly small differences from the ranges expected from natural variability, and thus represent mostly little change, although a tendency to decrease is present in winter and spring, particularly in Southern Australia (-10 to +5 %). By 2090, winter and spring decreases

are clearly evident throughout Australia under RCP8.5 and also in Southern Australian under RCP4.5. The magnitude of these changes is around -40 % to little change in Southern Australia, and -40 % to +10 % in Eastern Australia and -50 % to +20 % in the Rangelands. Under RCP4.5, the 2090 changes are generally about half as large. The decreases in southern areas also become evident as early as 2050 under RCP8.5 (not shown). By contrast, under RCP4.5 and RCP8.5 in 2090, there is medium to high agreement on little change throughout Australia in autumn, and in Southern Australia and Eastern Australia in summer, but still with some models showing large changes. In the Rangelands and Northern Australia there is low agreement on the direction of summer rainfall change under RCP8.5 with the changes spanning a large range (around -25 to +25 %). Decreases are projected in spring and winter, but rainfall amounts are low in these seasons, particularly winter, so results are not discussed quantitatively.

To illustrate finer spatial variations in projected rainfall change, this Report presents seasonal changes for each of the 15 sub-clusters (Figure 7.2.3 and 7.2.4). To highlight the contrast between areas of projected increase and decrease in rainfall, RCP8.5 and 2090 was chosen as this maximises signal to noise. Figure 7.2.3 show ranges of model results contrasted to natural variability, whereas agreement amongst models on simulated changes is summarised in Figure 7.2.4. The figures show that the Southern and Eastern Australia winter drying is present in all the southern clusters including the southern Rangelands, but is absent in Tasmania where there is a tendency amongst the models for little change or an increase in winter rainfall. This borderline between mainland Australia and Tasmania is consistent with the relative position and projected change in the mean atmospheric circulation. The simulated tendency for spring decrease is present in all clusters except the northern Rangelands and the Top End. All clusters show medium agreement on little change in autumn with only some Queensland clusters showing a slight tendency to decrease. The summer signal is mixed in all areas, except for decrease in western Tasmania. In many of the southern and eastern areas, the range of projected summer change is not much larger than that expected due to natural variability, with the consequence that the result can be characterised there as ‘high agreement on little change’, although a tendency to increase over New South Wales can be noted.

FIGURE 7.2.2: MEDIAN AND 10TH TO 90TH PERCENTILE RANGE OF PROJECTED SEASONAL RAINFALL PERCENT DIFFERENCE FOR FOUR FUTURE TWENTY YEAR PERIODS RELATIVE TO THE 1986–2005 PERIOD (GREY BAR) FOR RCP2.6 (GREEN), RCP4.5 (BLUE) AND RCP8.5 (PURPLE). FINE LINES SHOW THE RANGE OF INDIVIDUAL YEARS AND SOLID BARS FOR TWENTY YEAR RUNNING MEANS. RESULTS ARE SHOWN FOR EASTERN AUSTRALIAN (EA), NORTHERN AUSTRALIAN (NA), RANGELANDS (R) AND SOUTHERN AUSTRALIAN (SA) SUPER-CLUSTERS.





The magnitude of the simulated changes varies substantially between regions, seasons and by model. In this RCP8.5 2090 case changes approach 50 % at the ends of the model range for some regions and seasons (e.g. up to 50 % rainfall reduction in winter and spring in south-western WA). For the tropical clusters, it should be noted, however, that the large spread for the winter season can be explained by the fact that these are relative changes and winter has very low levels of rainfall (i.e. even small absolute changes will result in large percentage changes). In general, the magnitude of the projected change scales down for earlier dates and lower RCPs. An exception is rainfall change over NSW, where the direction of the change under RCP2.6 in summer is opposite to what it is under the other RCPs (not shown). This result is likely to be due to the greater impact of ozone recovery versus increasing greenhouse gas concentrations in the RCP2.6 scenario. As shown by Eyring *et al.* (2013), this scenario leads to a contrary response in the Southern Annular Mode (SAM) compared to the others (implying a westerly anomaly over south-eastern Australia in this season and less rainfall) (Hendon *et al.* 2007).

FIGURE 7.2.3: MEDIAN AND 10TH TO 90TH PERCENTILE RANGE OF PROJECTED SEASONAL RAINFALL CHANGES IN SUB-CLUSTERS FOR 39 CMIP5 GCMS FOR 2080–2099 RELATIVE TO 1986–2005 FOR RCP8.5 (IN PERCENT). BLUE INDICATES INCREASE AND BROWN DECREASE (SEE KEY). THE PALER PORTION OF THE BAR IS THE 10TH TO 90TH PERCENTILE RANGE EXPECTED FROM NATURAL VARIABILITY AND THE DARKER PORTIONS ARE WHERE THE CHANGES ARE LARGER THAN THE 10TH AND 90TH PERCENTILE EXPECTED FROM NATURAL VARIABILITY. THE AUSTRALIAN AVERAGE RESULT IS IN THE BOTTOM LEFT. NOTE THE CHOICE OF A HIGH FORCING CASE (2090 AND RCP8.5) WHICH WAS MADE SO THAT REGIONAL DIFFERENCES COULD BE MORE CLEARLY ILLUSTRATED. FOR QUANTITATIVE CLUSTER PROJECTION INFORMATION FOR OTHER RCPs AND FOR 2030, SEE RELEVANT CLUSTER REPORT.

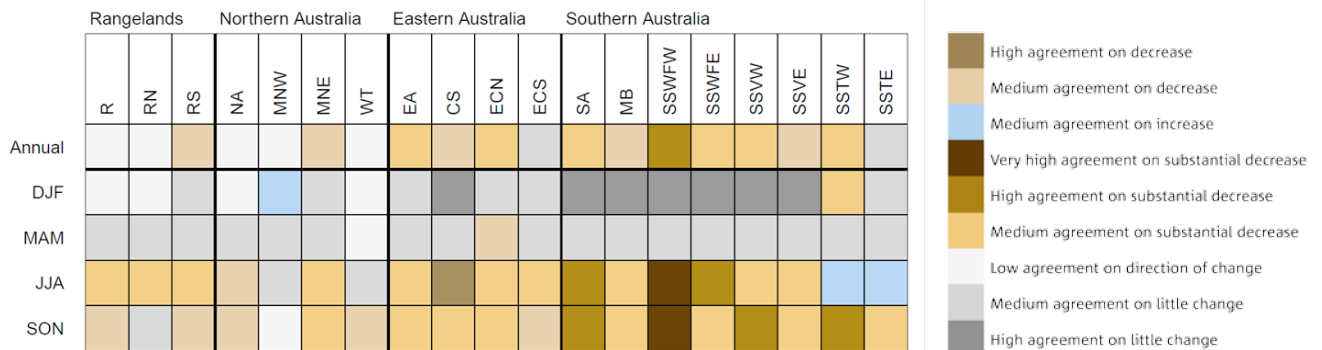


FIGURE 7.2.4: CLUSTER AND SUB-CLUSTER ANALYSIS OF AGREEMENT AMONGST CMIP5 MODELS ON MAGNITUDE AND DIRECTION OF SIMULATED RAINFALL CHANGE IN 2090 UNDER RCP8.5 ('MEDIUM' IS MORE THAN 60 % OF MODELS, 'HIGH' MORE THAN 75 %, 'VERY HIGH' MORE THAN 90%, AND 'SUBSTANTIAL' REPRESENTS A CHANGE OUTSIDE THE 10 TO 90 % RANGE OF MODEL NATURAL VARIABILITY).



In addition to the ranges of rainfall change presented above by region, ranges of rainfall change have also been prepared at the individual grid point level. This uses the same method of producing gridded percentiles of the projected change as was applied in the CSIRO and BOM, (2007) projections (Section 6.2). Maps of the 10th, 50th and 90th percentiles of seasonal rainfall change are shown in Figure 7.2.5 for a case with a global warming of 3.7 °C

(the RCP8.5 2090 mid case – see Chapter 5). Percentiles at the grid point level allow finer spatial details in projected change to be considered. These gridded projected changes can also be used in combination with a high resolution observed baseline to consider projected future climate change in absolute terms. When the 10th percentile annual rainfall change is applied (the driest case) rainfall contours can shift hundreds of kilometres coastward compared to

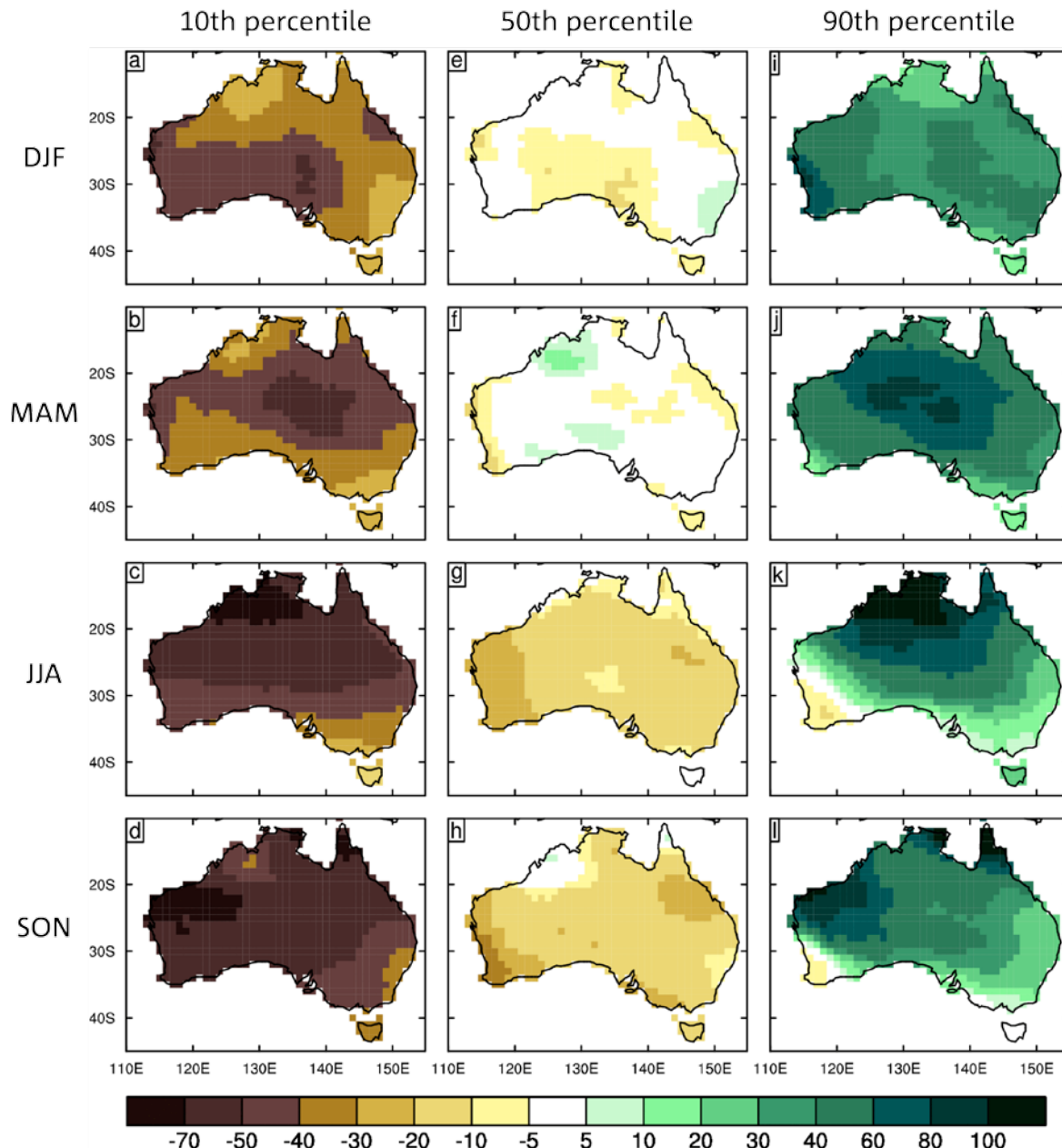


FIGURE 7.2.5: GRIDDED 10TH, 50TH AND 90TH PERCENTILE SEASONAL RAINFALL CHANGES FROM CMIP5, 2090 RCP8.5 (METHOD OF CSIRO AND BOM, 2007).

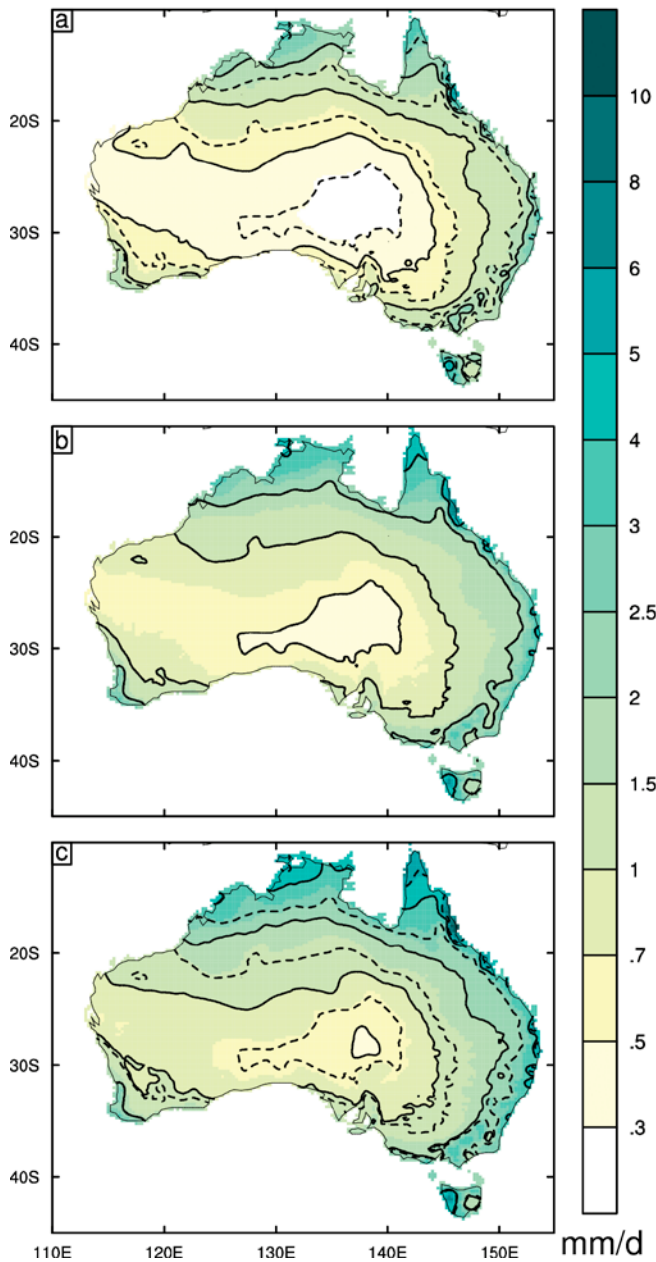


FIGURE 7.2.6: ANNUAL MEAN RAINFALL (AS A RATE IN MM/DAY), FOR THE PRESENT CLIMATE (B), AND FOR DRIER CONDITIONS (A) OR WETTER CONDITIONS (C). THE PRESENT IS USING A BOM DATA SET FOR 1958–2001, ON A 0.25 GRID. THE DRIER/WETTER IS USING THE 10TH AND 90TH PERCENTILE FACTOR FOR % CHANGE AT 2090, UNDER RCP8.5. IN EACH PANEL THE 0.5 MM/DAY, 1 MM/DAY, 2 MM/DAY AND 4 MM/DAY CONTOURS ARE PLOTTED WITH SOLID BLACK LINES. IN (A) AND (C) THE SAME CONTOURS FROM THE ORIGINAL CLIMATE (B) ARE PLOTTED AS DOTTED LINES.

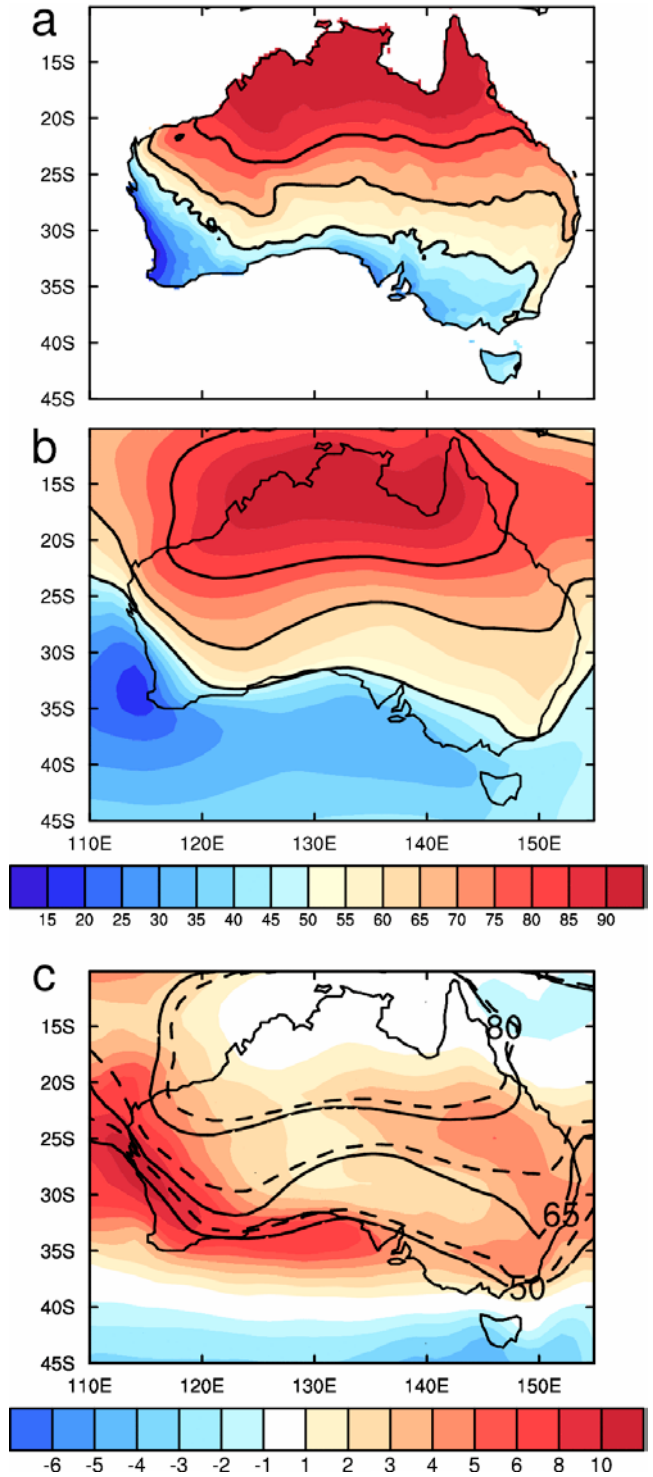


FIGURE 7.2.7: PERCENTAGE OF ANNUAL RAIN THAT FALLS IN THE WARMER SIX MONTHS FROM: (A) BOM 1900–2008, AND (B) CMIP5 40-MODEL MEAN, FOR 1986–2005 (SHOWING 50 %, 65 % AND 80 % CONTOUR LINES). NOTE ALSO THE OBSERVATIONAL DATA SET DOES NOT EXTEND OVER THE OCEAN AREAS IN (A)). (C) CHANGE IN PERCENTAGE OF RAIN IN THE WARMER SIX MONTHS, FROM THE MEAN CHANGES FOR 2080–2099 UNDER RCP8.5, COMPARED TO 1986–2005. THE 50 %, 65 % AND 80 % CONTOUR LINES FROM THE BASE CLIMATE ARE SHOWN AS DASHED LINES, WITH THOSE FOR THE 2080–2099 CLIMATE SHOWN AS SOLID LINES.



present, whereas with the 90th percentile projection (the wettest case) rainfall contours shift a similar distance in the opposite direction (Figure 7.2.6).

Finally, the tendency for winter rainfall decrease combined with a lack of clear change in summer rainfall, implies a projected southward shift of the summer-dominated rainfall zone. This shift is illustrated in Figure 7.2.7. Under an RCP8.5 2090 case, the multi-model mean indicates a southward expansion of the boundary between the summer and winter rainfall zones, which especially affects southern and south-western parts of Australia.

DOWNSCALED CMIP5 RESULTS

This Section examines the projected rainfall changes using two downscaling methods (CCAM and SDM – see Section 6.3) applied to a subset of CMIP5 models. The focus is on differences in the projected changes consistently produced by downscaling compared to the GCMs, either as a difference in the magnitude of change compared to the host models, or a regional difference in the direction of change. We use up to 22 simulations from SDM (all models that provided suitable inputs) and six CCAM simulations

(chosen for their performance over Australia and the globe). Figure 7.2.8 compares the projected rainfall change for Australia from GCMs and the equivalent from downscaling for a common set of five models. It is notable that these five models tend towards rainfall increase in northern Australia.

Downscaling has the potential to show more regional detail in projected changes, especially where finer resolution is a benefit in simulating important fine-scale processes or topographic effects (see Chapter 6.3.5). Where this can be demonstrated, this is termed ‘added value’ in the climate change signal. In these results there are plausible differences between the rainfall projection in eastern and western Tasmania in CCAM in summer, as was found in the Climate Futures for Tasmania project (Grose *et al.* 2013). There is also an indication of difference between east and west Tasmania in winter, especially in the SDM results. There is also a greater projected rainfall decline in western Victoria in autumn in SDM results than the host models (not shown), which is more in line with recent trends. There are some indications of a different projection in the Eastern Seaboard compared to west of the Great Dividing Ranges in summer, but the results are not clear and consistent so remain an ongoing research topic.

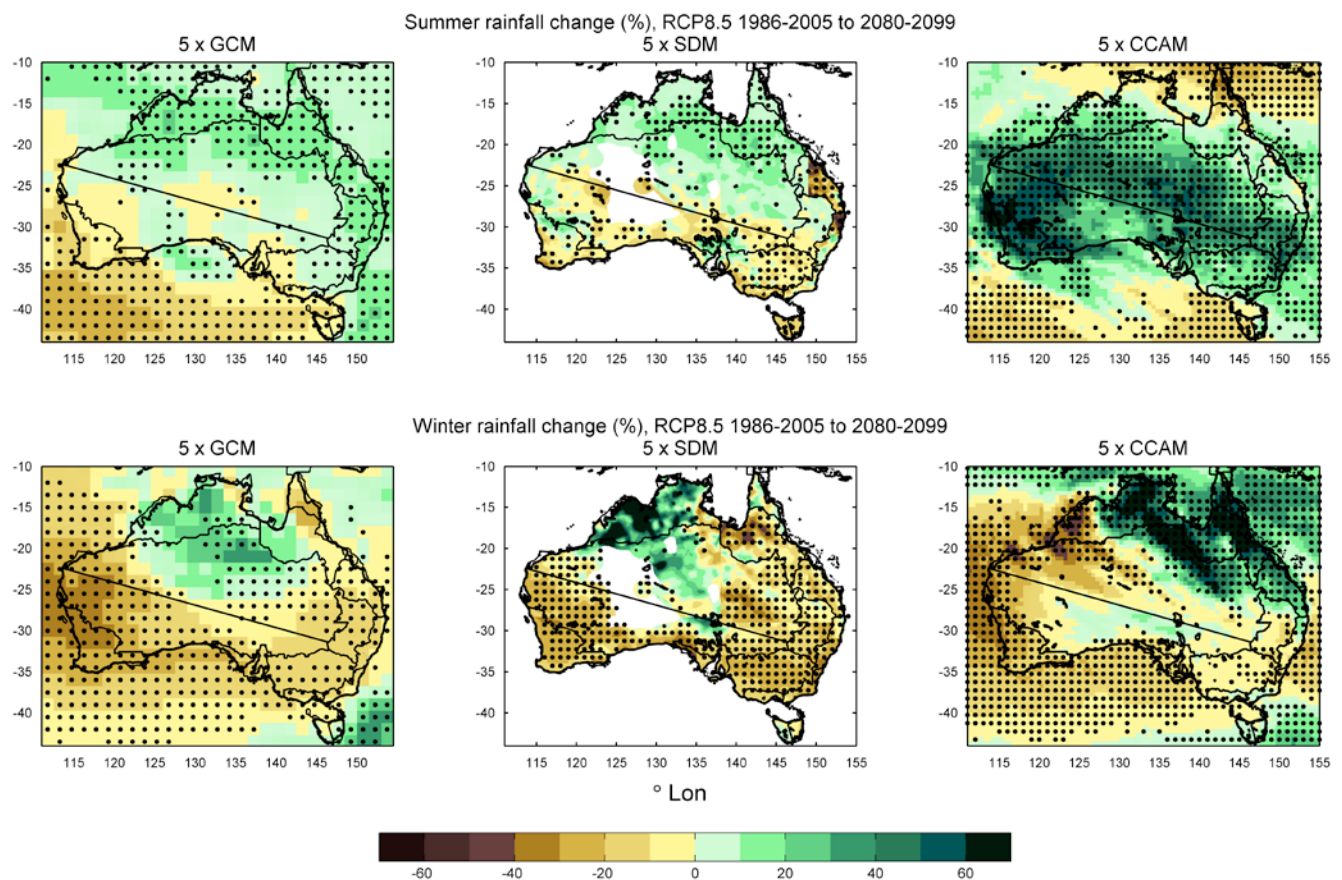


FIGURE 7.2.8: PROJECTED CHANGE IN MEAN RAINFALL FOR RCP8.5 1986–2005 TO 2080–2099 FOR: (TOP ROW) SUMMER AND (BOTTOM ROW) WINTER, IN: (LEFT) FIVE GLOBAL CLIMATE MODELS (GCMs): ACCESS-1.0, CNRM-CM5, MPI-ESM-LR, CCSM4, NORESM1-M, (MIDDLE) BUREAU OF METEOROLOGY STATISTICAL DOWNSCALING USING THE SAME FIVE GCMs AS INPUT, AND (RIGHT) CCAM DYNAMICAL DOWNSCALING ALSO USING THE SAME FIVE GCMs AS INPUT. STIPPLING SHOWS WHERE AT LEAST FOUR OUT OF FIVE SIMULATIONS AGREE ON THE DIRECTION OF CHANGE.

There are other cases where the downscaling produces a different projection to the global climate model but there is not a clear and intuitive link to the resolution of surface effects such as topography. In these instances, the downscaled projection can't be considered a superior projection for a physically plausible reason. However, the results may represent another plausible projection, that could be combined with GCM projections and therefore widen the range of projected change. These cases include a wetter future for many regions of southern and western Australia in summer, shown in both downscaling methods, primarily CCAM (Figure 7.2.8).

There are also cases where downscaling can produce different results from the host model due to the nature of the method or model used. These differences are an unavoidable result of the process and provide important context for interpreting the results. The Bureau of Meteorology statistical downscaling method uses a distinct set of predictors for different climate regions and this can produce regional differences with artificial sharp boundaries, such as in East Coast South and East Coast North in summer (Figure 7.2.8b). Dynamical downscaling such as CCAM can produce different patterns of change at the wider scale since it uses a new atmospheric model with its own model components for simulating the atmosphere.

In these circumstances it is not clear that wider-scale changes from CCAM should be trusted any more than those from the GCM.

In balancing this potential for 'added value' in the regional climate change signal but also the potential for different results due to the method used, this Report examines the regionally-averaged results for downscaling (Figure 7.2.9 and Figure 7.2.10).

Figure 7.2.9 shows projected rainfall changes from 22 of the CMIP5 GCMs downscaled using the SDM compared to the original GCM results for the same set of models. The range of projected changes is very similar to the GCM-based projected ranges in most sub-regions and seasons, but there are some potentially important differences in coastal eastern Australia, namely a markedly stronger decrease in south-western Victoria in summer and autumn, and spring increase as opposed to decrease in south-east Queensland. Differences in the magnitude of changes in eastern Tasmania compared to western Tasmania can be seen in some seasons such as winter. Notably all these differences are in regions with fine-scale and potentially strong topographical influences which would not be well represented in the GCMs. The SDM projects a summer decrease in the clusters on the east coast compared to the slight increase in GCMs however the magnitude of this

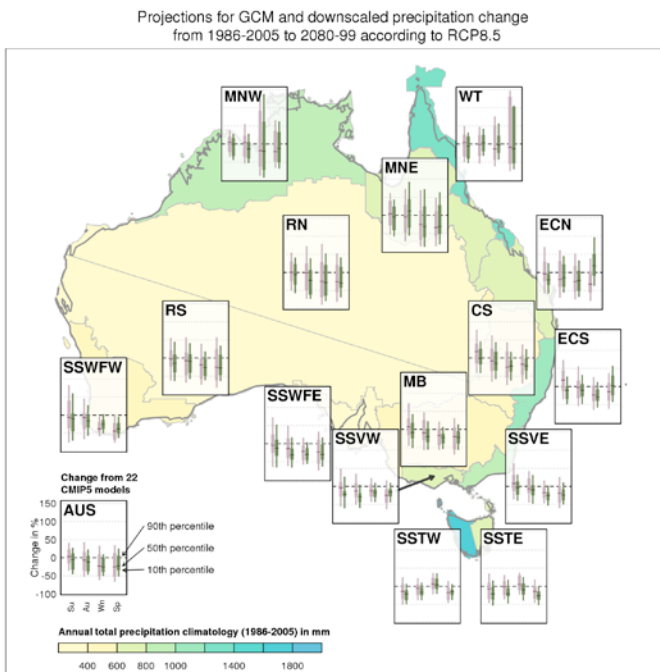


FIGURE 7.2.9: MEDIAN AND 10TH TO 90TH PERCENTILE PROJECTED CHANGES TO RAINFALL IN SUB-CLUSTERS FOR 22 CMIP5 GCMs, AND FOR THE SAME 22 MODELS DOWNSCALED USING THE BOM-SDM DOWNSCALING SYSTEM, FOR 2080–2099 RELATIVE TO 1986–2005 FOR RCP8.5. FINE LINES SHOW THE RANGE OF INDIVIDUAL YEARS AND SOLID BARS FOR TWENTY YEAR RUNNING MEANS. EACH PAIR OF BARS HAS THE CHANGES FROM THE GCMs ON THE LEFT (PURPLE) AND THE CHANGES FROM THE DOWNSCALING ON THE RIGHT (GREEN), EACH AVERAGED OVER THE REGION.

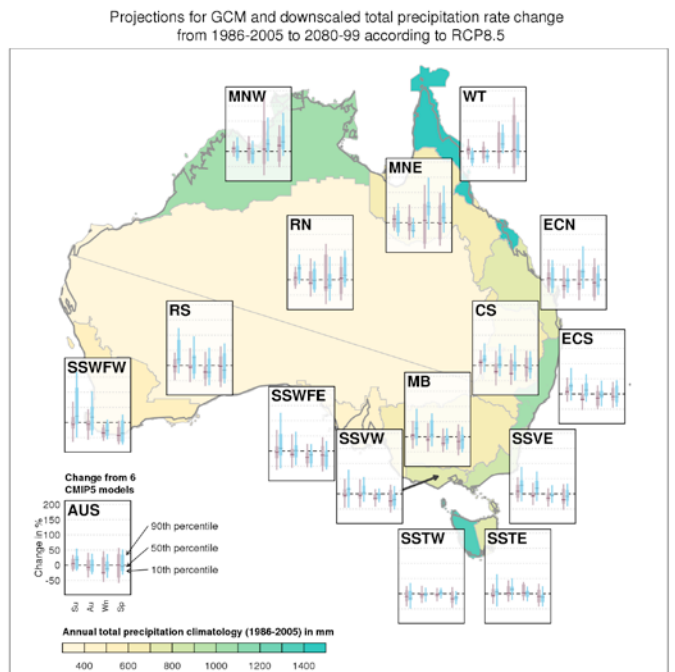


FIGURE 7.2.10: MEDIAN AND 10TH TO 90TH PERCENTILE PROJECTED CHANGES IN RAINFALL IN SUB-CLUSTERS FOR 6 CMIP5 GCMs, AND FOR THE SAME 6 MODELS DOWNSCALED USING THE CCAM DYNAMICAL DOWNSCALING MODEL FOR 2080–2099 RELATIVE TO 1986–2005 FOR RCP8.5. FINE LINES SHOW THE RANGE OF INDIVIDUAL YEARS AND SOLID BARS FOR TWENTY YEAR RUNNING MEANS. EACH PAIR OF BARS HAS THE CHANGES FROM THE GCMs ON THE LEFT (PURPLE) AND THE CHANGES FROM THE DOWNSCALING ON THE RIGHT (BLUE), EACH AVERAGED OVER THE REGION.



change is influenced by the artificial boundaries between regions in this area (see Figure 7.2.8, centre panels).

The case for ‘added value’ in downscaling compared to host models is strengthened if different downscaling methods agree on a particular change and its difference from the host models. However, many of these differences between downscaling and GCM results from the SDM results are not also found in the CCAM downscaled results (Figure 7.2.10). Differences between CCAM and the host GCMs are most evident in the tropics, with the strong indication of summer rainfall decline in wet tropical Queensland (as opposed to a mixed result in the GCMs). Proportional changes in the tropical dry season are less significant in absolute terms. The CCAM comparison is small (six models), and further analysis of these results combined with those from further downscaling, will be needed to properly assess likely rainfall changes in these key coastal regions.

Due to the effect of enhanced resolution of the atmosphere and the additional surface details, downscaled results may show a climate change signal that is different and more physically plausible than that from the host model. This indicates the potential for ‘added value’ in the downscaling and thus may give reason to use this over the GCM alone. However, the lack of consistency between downscaled results in many cases here indicates there are some unresolved questions about what is driving the changes and where the downscaling results provide unambiguous added value. A different direction of change in eastern compared to western Tasmania in some seasons, and a greater autumn rainfall decline in south-east Australia than GCMs project are the two main cases of potential added value from these projections. The results show that one must keep in mind the range of possible climate change, as projected by the GCMs, when using the downscaled data.

PLAUSIBLE PROCESSES AND CONFIDENCE IN RAINFALL PROJECTIONS

This section discusses the plausible processes which are likely to be associated with the CMIP5-simulated rainfall changes for Australia presented in the previous sections. Drawing upon this, and other relevant information, such as downscaling results, model evaluation, and consistency of historical CMIP5 projections with observed trends (Chapter 5), conclusions are drawn on projected rainfall change with associated confidence levels (see Section 6.4). These statements are also presented systematically, along with their rationale in Table 7.2.2. As this discussion focuses on interpreting the regional response and the confidence in it, the evidence used (and presented in Table 7.2.2) is predominantly for the high forcing case (RCP8.5 and 2090) when this response is most evident. The discussion in this section is organised according to the four super-clusters, but clusters and sub-clusters are explicitly discussed where there are notable exceptions at that level. Some further relevant discussion for specific clusters can be found in the Cluster Reports.

SOUTHERN AUSTRALIA (SOUTHERN FLATLANDS, SOUTHERN SLOPES, MURRAY BASIN)

Mean annual rainfall is projected to decrease in southern Australia as a whole over the course of the century, with this being particularly evident in winter and spring (Table 7.2.1). In all seasons by 2030, ranges of change show mostly small differences from the ranges expected from natural variability, although a tendency to decrease is present in winter and spring. By 2090, winter and spring decreases are strongly evident throughout under RCP8.5 and RCP4.5 (Tables 7.2.1 and 7.2.2). There are various lines of evidence that support this.

The future changes of greatest plausibility are the global increase in temperature, specific humidity and, for the Southern Hemisphere, a southward shift and intensification of the westerlies and expansion of the tropics coinciding in an upward trend in the Southern Annular Mode (SAM), and a shift to higher pressures over the Australian region (IPCC, 2013, see also Section 7.3.2). These pressure changes broadly lead to reduced cool season rainfall, which is a projected continuation of a recent trend.

Many regions within southern Australia have experienced declining cool-season rainfall since the 1970s, particularly in late-autumn and early winter (IOCI, 2002, Timbal, 2009, CSIRO, 2012), driven at least in part by changes to large-scale circulation that are projected to continue in the 21st century. These are the intensification and possibly southerly movement of the subtropical ridge (STR) of high pressure, changes in atmospheric blocking, and a poleward movement of the westerly storm tracks (Frederiksen and Frederiksen, 2005, 2007; CSIRO, 2012, Timbal and Drosdowsky, 2013). These trends are discussed further in Section 4.2 and Section 7.3, but are considered here in the context of rainfall projections. Overall the mean meridional (north-south) circulation (MMC) has been observed to widen, a change that is particularly consistent for the Southern Hemisphere across a range of different measures (Lucas *et al.* 2014) and is linked to surface changes observed such as the strengthening and shift of the STR (Nguyen *et al.* 2013). The relationship is significant across the entire cool season from April to October in south-eastern Australia (Timbal and Drosdowsky, 2013).

GCMs consistently project a future increase of the STR intensity and a further southward shift in the region of summer rainfall dominance (Figure 7.2.11 and see Section 7.3.3). In general GCMs capture many of the broad features of the MMC with accuracy, including having the STR broadly in the correct place and with a correct annual cycle (see Section 5.2). However, they can have a poor depiction of the inter-annual STR-rainfall relationship across southern Australia (Kent *et al.* 2013). These biases can be seen in the seasonal cycle of rainfall (see Figure 7.2.7), which shows that the dominance of summer rainfall extends too far south



in the climate model simulations of the present climate. These biases lower the confidence in the magnitude of the models' regional rainfall projections associated with the circulation changes described above. Also, the link to increased STR intensity is weaker in models than observed in the zonal mean (Timbal and Drosowsky, 2013, Whan *et al.* 2014), so the rainfall decrease associated with these projected circulation changes may be underestimated.

There are some regional exceptions to the general projection of drying. Winter rainfall in Tasmania is

projected to experience little change or to increase due to its southern location where it continues to be influenced by the westerlies as they strengthen and changes to the moisture content of air may also play a role (see Figure 7.2.11). The MMC describes changes across the breadth of Australia, however there are also important changes that differ in the west compared to the east of the Australian region that are important to rainfall change. One such change is projected change to atmospheric blocking and associated weather systems (Pook *et al.* 2012, Risbey *et al.* 2013a,b). These studies show that much of the recent rainfall decline in the south-west and south-east is related

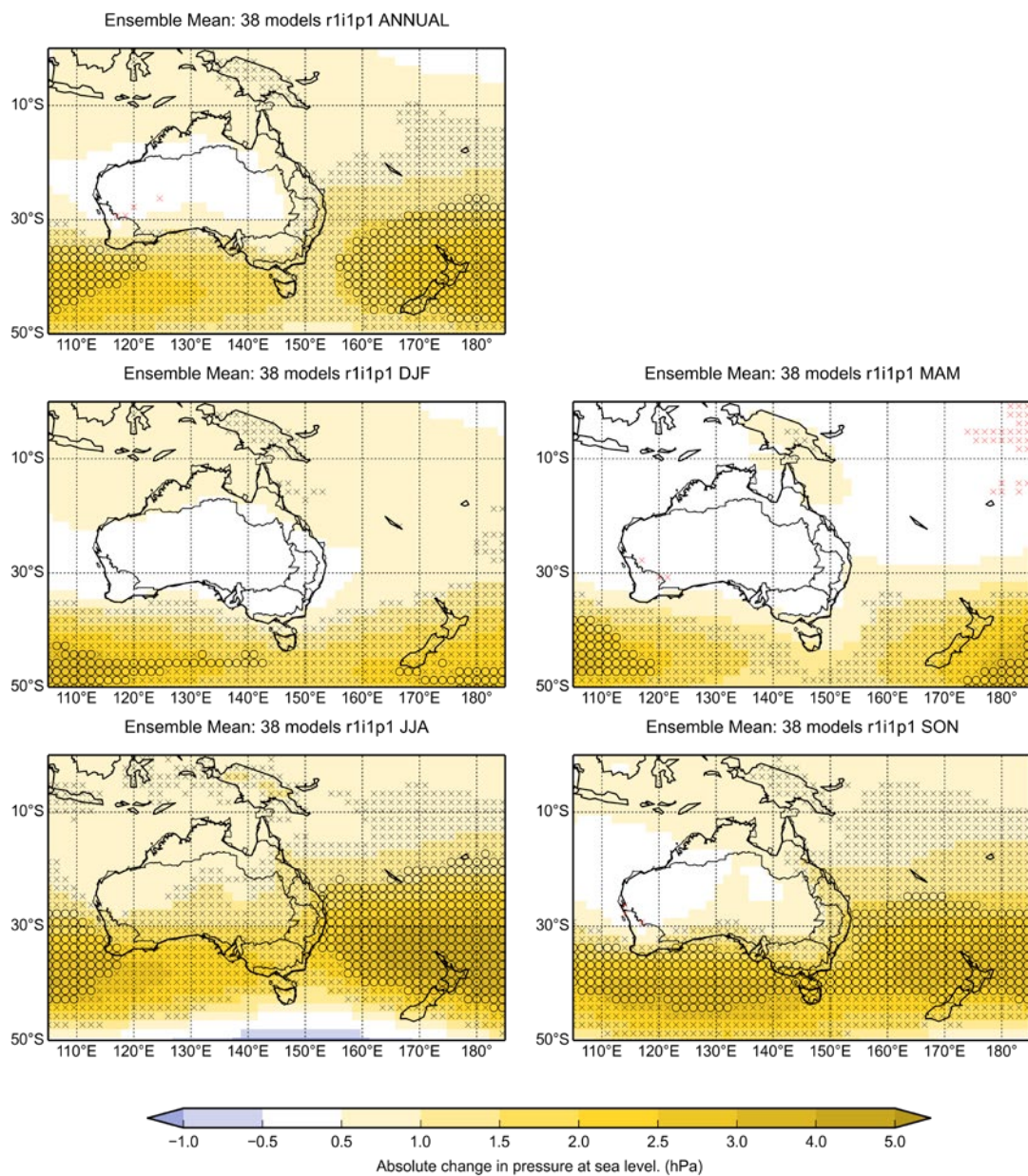


FIGURE 7.2.11: ENSEMBLE MEAN CHANGES IN MEAN SEA LEVEL PRESSURE (IN HPA) UNDER RCP8.5 (PERIOD 2080–99 VERSUS PERIOD 1986–2005) FOR ANNUAL (TOP LEFT) AND THE 4 SEASONS. THE STIPPLING DENOTES MODEL AGREEMENT ON CHANGES GREATER THAN 0.5 HPA (INCREASES OR DECREASES) AT THE LEVEL OF GREATER THAN 90 % (BLACK CIRCLES) OR GREATER THAN 67 % (BLACK CROSSES). THE EQUIVALENT MODEL AGREEMENT ON CHANGES LESS THAN 0.5 HPA (I.E. ESSENTIALLY NO CHANGE) ARE SHOWN IN RED.



to cut-off lows. The variation in rainfall from cut-off lows in turn is driven by longer period shifts in the preferred location and intensity of blocking and the zonally asymmetric circulation. Climate models have difficulty capturing the magnitude and variability of blocking, which is a source of additional uncertainty for rainfall projections for southern Australia.

There is less certainty and more regional variation in the rainfall projections in summer and autumn than for winter and spring (see Table 7.2.2). On average in southern Australia there is at least medium agreement amongst models on little change even under high forcing (2090 and RCP8.5) but the model range indicates that significant changes of either direction are also possible. Regional exceptions in the direction of summer rainfall change include a projected substantial decrease in western Tasmania (*medium confidence* – see Table 7.2.2), which is an expected response to an enhanced easterly regime as SAM shifts to a more positive mode through the century.

There are some regions of complex topography and a diversity of regional climate influences across a relatively small area in southern Australia, including across Tasmania and over the Great Dividing Range. Therefore, downscaling of climate models (see above and Section 6.3) has the potential for producing ‘added value’ in the regional climate change signal for such regions. For example, CCAM projects a rainfall increase in eastern Tasmania in summer and autumn in contrast to the decrease in the west, supporting the results from the Climate Futures for Tasmania project (Grose *et al.* 2013). However these new CCAM projections agree with GCMs for a decrease in spring rainfall in Tasmania which is in contrast to the Climate Futures for Tasmania results. The Bureau SDM (but not CCAM) shows an enhancement of the projected decline in rainfall in south-west Victoria in autumn. This decline is consistent with the observed decline (discussed above) whereas the GCM projections are not (see Section 5.3). Since the SDM more finely resolves the relationship between weather systems and local rainfall for this relatively restricted region, this may be a more physically plausible projection than the GCMs and suggests that the projected cool season decline may have a stronger influence on autumn rainfall than the GCMs results would indicate.

Based on the above considerations, the confidence on projected rainfall change in southern Australia is summarised in Table 7.2.2 for the high forcing case (RCP8.5 and 2090). The high likelihood of a hemispheric circulation response to increasing greenhouse gases resulting in reduced cool season rainfall, along with the consistency between models for projected declines in cool-season (winter and spring) rainfall across southern Australia (and the converse in winter in Tasmania) provide *high confidence* in the cool season rainfall decline across southern Australia (and increase in winter in Tasmania). In general, the direction of change in summer and autumn rainfall

cannot be confidently projected in the region, but there is *medium confidence* in a decrease in south-western Victoria in autumn and in western Tasmania in summer. The cool season rainfall declines are projected to become evident against natural variability as early as 2030 in the Southern and South-western Flatlands and 2050 under RCP4.5 and 8.5 in south-western Victoria.

CENTRAL SLOPES AND EAST COAST

Projections of mean rainfall change in eastern Australia are the most uncertain of any broad region of Australia. Models show a range of projections for mean annual rainfall, from a substantial decrease to a substantial increase. Nevertheless, there is medium agreement in a substantial decrease in rainfall under high forcing (RCP8.5 and 2090) since around half of GCMs show this trend (Table 7.2.1). While the southern Australian climatological features also have an influence in eastern Australia (more particularly in the East Coast sub-cluster and in the inland cluster of Central Slopes), there are several drivers of change in this region that models do not simulate particularly well, such as the rainfall teleconnection to ENSO (Section 5.2.2) and this reduces the level of confidence in projections along with the large model range.

There is a similar level of uncertainty when it comes to seasonal rainfall projections. There is medium agreement amongst the GCMs in substantial rainfall reductions in winter and spring under RCP8.5 and at 2090 (Table 7.2.1 and 7.2.2), and this is the primary factor driving the simulated reduction in annual rainfall. These changes are driven by some physically plausible drivers of change (see below). By contrast, the rainfall projection for summer and autumn is particularly uncertain, with a large model range and numerous processes involved. Changes in all seasons in 2030 are small relative to natural variability (Table 7.2.1).

The projected reduction in winter rainfall over eastern and south-eastern Australia is shown by the GCMs, as well as the SDM. A considerable proportion of the total winter rainfall in the subtropical and temperate regions of eastern Australia is associated with the occurrence of cut-off lows. This proportion rises as the intensity of the rainfall increases, such that a high proportion of the heavy and extreme rainfall events in this region are caused by these systems (Pepler and Rakich, 2010, Dowdy *et al.* 2013b). These low pressure systems are cut off from (i.e. not embedded within) the storm track region that moves with the prevailing westerly wind to the south of the subtropical ridge. Projections based on global climate models suggest that increasing greenhouse gas concentrations towards the end of this century will lead to fewer cut-off lows in the subtropical East Coast region of Australia where these systems are known as East Coast Lows (Dowdy *et al.* 2014). There may also be fewer cut-off lows in the region around Tasmania while noting that the intensity of the systems that do occur could potentially become stronger (Grose



et al. 2012). These results are consistent with an observed trend towards reduced storminess in eastern and southern Australia since 1890 (Alexander *et al.* 2011). Given that these storms are characterised by strong vorticity and baroclinic instability in the upper troposphere (Risbey *et al.* 2009a, Mills *et al.* 2010, Dowdy *et al.* 2013a), changes in their occurrence are likely related to changes in the climatology of a number of related upper-tropospheric phenomena. These phenomena include Rossby waves, atmospheric blocking and a split in the jet-stream over eastern Australia during winter (Freitas and Rao, 2014, Grose *et al.* 2012).

The Great Dividing Range is a topographic feature that may influence regional differences in projected climate change. There could plausibly be a different mean rainfall trend projected for the Eastern Seaboard (East Coast South) compared to inland from the ranges (Central Slopes). Indeed, a tendency for summer increase in Central Slopes contrasts with a decreasing tendency in East Coast North, and the spring decline is stronger in Central slopes than in East Coast South.

The results from the two downscaling techniques show conflicting signals. The SDM results show a rainfall decrease in East Coast South in summer, in contrast to the GCM projected increase, however CCAM results show an even larger rainfall increase than GCMs. CCAM also projects a larger increase than GCMs in both East Coast South and Central Slopes in autumn. CCAM also projects little change in winter rainfall which is in contrast to the GCM results and the SDM. In East Coast North, the SDM projects a rainfall increase in spring which is the opposite of GCMs, however this is not supported by CCAM results. CCAM projects an increase in winter rainfall which is in contrast to GCM results. Results from the forthcoming regional climate change study for the region, the NSW and ACT Regional climate modelling project (NARCLiM) outlined in Evans *et al.* (2014) will also shed light on this issue.

In summary, for the eastern Australian region as a whole under high climate forcing (RCP8.5 and 2090) there is *medium confidence* in a winter rainfall decrease. This relates to the southward retreat and weakening of winter storm systems. There is *high confidence* in this change in the Central Slopes cluster where there is also *medium confidence* in spring decreases (see Central Slopes Cluster Report). There is also *medium confidence* in a winter decrease in East Coast South. Otherwise, there is *low confidence* in projecting the direction of seasonal rainfall change in this region, with strongly contrasting results between both downscaling methods and with the GCMs, particularly in the East Coast cluster. The large uncertainty in this region is likely to be related to the range of rainfall drivers and competing influences on rainfall change. The regional climate change signal in this area is a topic of ongoing research for both global modelling and downscaling. In the near future (2030), there is *high confidence* that natural variability will predominate over trends due to greenhouse gas emissions.

NORTHERN AUSTRALIA

The strong monsoonal climate across tropical Australia has a distinct West-East pattern: north-western Australia is predominantly impacted by the seasonal progression across the equator of the Inter-tropical convergence zone (setting up the background state for the monsoon onset to occur) while north eastern Australia (Gulf region and coastal North-Queensland) has additional impact from the easterly trade wind regime which can bring rainfall even during the monsoon westerly break periods. It therefore makes sense to assess causes and processes for future changes to rainfall across northern Australia with this geographic distinction in mind. Following is a seasonal assessment of the confidence in rainfall projections across tropical Australia. However, since there is only very little climatological rainfall during winter (Jun-Aug is the dry season) across this domain, projected rainfall changes are not very meaningful and are therefore not considered here for this season.

In summer (peak monsoon season), GCM projections for the entire northern Australia region (NA) show low agreement in the direction of change in the high forcing case (2090 and RCP8.5), with both substantial increases and decreases being projected. In 2030, and at 2090 under RCP4.5, there is at least medium agreement amongst models on little change. Notably, the recent wide-spread decadal upward trend (in western parts) and downward trend (in coastal eastern parts) in rainfall is not captured by the models (see Section 5.3.2). Downscaling results are generally very similar (particularly SDM) with some disagreement for CCAM results. Only for the Monsoonal north-west region there is agreement in the GCMs on some increase. In autumn (which includes the transition of the monsoon retreat) GCM projections for the entire NA super-cluster show some agreement on little change under high forcing (RCP8.5 and 2090), although substantial changes are present in a minority of models. SDM and CCAM downscaling show a similar range of results compared to GCMs with some disagreement in the Wet Tropics region. The observed recent upward trend is not captured in the models. In spring (which includes the transition of the monsoon onset), GCM projections for the entire NA super-cluster show some agreement on a decrease under high forcing (RCP8.5 and 2090), with this being more evident in Monsoonal North East. In the near future (2030), there is model agreement on little change. The SDM and CCAM downscaling show very similar changes compared to the GCMs, but the spread in the CCAM downscaling simulations is somewhat smaller.

Changes to rainfall across the Top End of Australia are closely related to two competing processes evolving more strongly under future climate change conditions: (a) increases in atmospheric moisture content due to higher temperatures favours mean rainfall increases



during the wet season; (b) a slowing down of the tropical circulation favours mean rainfall decreases during the wet season. Because both of these processes are simulated with different strength by different models, the resulting projected changes in wet season rainfall carry large uncertainties in either direction. Furthermore, as with the Rangelands, change in the northern warm season can be related to the pattern of equatorial sea surface temperature changes, which differs considerably among the global models (see Section 3.6).

Relevant in the consideration is the observed rainfall trend over the previous forty years in north-west Western Australia. Recent studies have associated this trend with changes to sea surface temperatures either to the north-west (Indian Ocean) (Shi *et al.* 2008) or north-east (Western North Pacific Warm Pool-) of tropical Australia (Li *et al.* 2013). In the latter case, the relationship between the North Pacific Warm Pool and tropical Australia rainfall in the CMIP5 models would be strongly influenced by one of the typical systematic errors seen in current coupled climate models: the “cold tongue” bias in the equatorial Pacific sea surface temperatures. Indeed, most models fail to adequately reproduce the recent rainfall trend in north-west Western Australia (see Section 5.2).

Another consideration in the assessment is the simulation of some of the important processes associated with tropical Australia rainfall during the wet season: the eastward propagation of the MJO (which can trigger the Australian monsoon onset); the diurnal evolution of rainfall and the additional rainfall contributed by tropical cyclones. While CMIP5 models have some skill in capturing these processes, this skill can be low or only seen in a smaller sub-sample of models (see Section 5.2).

In summary (see Table 7.2.2) under high forcing (2090 & RCP8.5) some models show large annual and wet season change, but there is *low confidence* in projecting the direction of that change. Confidence in the projected rainfall changes is low throughout the region in the other seasons (and not relevant in winter when rainfall is very low). In addition to the widely varying direct GCM results, confidence is low because different processes, such as Monsoon onset, MJO and tropical circulation can have different (and opposite in sign) impact on model projected rainfall changes and there is large spread in the skill of models in simulating these processes. Additionally, there is some inconsistency between model results for historical periods and observations. In 2030, the range of projected changes differs little from that expected due to natural variability (*high confidence*).

RANGELANDS

Annually, and in summer and autumn, rainfall averaged across the Rangelands cluster is dominated by similar rain-bringing mechanisms to the northern Australia super-cluster (just discussed) and has similar projected changes from the GCMs. Under high forcing (RCP8.5 and 2090) the change in summer and autumn (and annual) rainfall could be substantial, but confidence in the direction of change is low for similar reasons to those stated for northern Australia.

Changes in winter (and to a lesser extent, spring) are influenced more by southern Australian rainfall processes and projected changes, as discussed above for the Southern Australian super-cluster. This is particularly the case for the southern portion of the cluster (Rangelands South) where rainfall decreases are strongly indicated in winter (associated with the southward retreat the mid-latitude storm systems) and to a lesser extent in spring.

The projections in the Rangelands are not greatly modified by the available downscaling, although the changes in summer simulated by CCAM tend to be more positive. Changes in rainfall associated with tropical cyclones, which can impact parts of the Rangelands, remain uncertain. Changes in all seasons in 2030 are small relative to natural variability (Table 7.2.1). The likely drying in the south, and little change in the north, leads to a likely southward shift across the Rangelands of the dominance of warm season rainfall (Figure 7.2.7).

In summary, decreases in winter rainfall are projected for the south, with *high confidence*, and become evident later in the century, especially under high forcing (2090 and RCP8.5). There is strong model agreement and good understanding of the physical mechanisms driving this change (southward shift of winter storm systems). Decreases are also projected for spring, but with *medium confidence* only. Changes to rainfall in other seasons, and annually, for later in the century are possible and potentially very important for this region, but the direction of change cannot be confidently projected given the spread of model results. In the near future (2030), there is *high confidence* that that natural variability will predominate over trends due to greenhouse gas emissions.

TABLE 7.2.2: SUMMARY OF RATIONALE FOR CONFIDENCE IN REGIONAL AND SUB-REGIONAL RAINFALL CHANGES (NA, EA, R AND SA SUPER-CLUSTERS, AND EXCEPTIONAL SUB-REGIONS), MEDIUM AND HIGH CONFIDENCE IN DECREASE IS INDICATED BY LIGHT AND ORANGE SHADING RESPECTIVELY, MEDIUM CONFIDENCE IN INCREASE WITH BLUE SHADING, MEDIUM CONFIDENCE IN LITTLE CHANGE WITH DARK GREY SHADING AND LOW CONFIDENCE ON THE DIRECTION OF CHANGE WITH LIGHT GREY SHADING. DJF=SUMMER, MAM=AUTUMN, JJA=WINTER, SON=SPRING. WINTER IN NORTHERN AUSTRALIA NOT SHOWN AS IT IS SEASONALLY DRY.

SEASON	SUB-REGIONAL EXCEPTION	2090 RCP85 CMIP5 RANGE OF CHANGE (%)	2090 RCP8.5 CMIP5 MODEL AGREEMENT (PERCENTS ARE FRACTION OF MODELS)	ADDITIONAL EVIDENCE: DOWNSCALING/CONSISTENCY OF OBSERVED TRENDS WITH GCMs	ADDITIONAL EVIDENCE: PLAUSIBLE PROCESSES/MODEL RELIABILITY	AGREEMENT OF MULTIPLE LINES OF EVIDENCE	SUMMARY STATEMENT WITH CONFIDENCE	DO THE GCM RESULTS PROVIDE A RANGE OF CHANGE FOR USE IN APPLICATIONS
SOUTHERN AUSTRALIA								
ANNUAL		-26 to +4	<i>Medium agreement in substantial decrease</i> (69%)	Downscaling generally agrees, obs. trend not inconsistent	Related to cool season circulation change, e.g. well supported southward shift of westerlies, strengthening of subtropical ridge. Relevant GCM processes reasonable	Good	Medium confidence in decrease	Yes
DJF		-13 to +16	<i>High agreement in little change</i> (71%), but also substantial increase (18%) & decrease (11%).	Downscaling generally agrees, obs. trend not inconsistent	Balance of tropical and mid-latitude influences not certain	Good, but process understanding less certain	Medium confidence in little change	Possibly too narrow, less relevant for Western Tasmania
MAM	WESTERN TASMANIA (SSTW)	-26 to +6	<i>Medium agreement in substantial decrease</i> (63%).	Downscaling generally agrees, obs. trend not inconsistent	Region well exposed to SAM-related weakening westerlies Likely difference between east and west Tasmania	Good	Medium confidence in decrease	Yes
		-25 to +13	<i>Medium agreement in little change</i> (57%), but also substantial decrease (28%) & increase (15%).	Statistical downscaled decrease stronger in many subregions. Obs decrease stronger in some regions.	Balance of tropical influences and strength cool season processes uncertain. Statistical downscaling suggests stronger influence of cool season trend than in GCMs.	Some disagreement	Low confidence in direction of change	GCM range may be biased high
	SOUTH-WESTERN VICTORIA (SSVW)	-30 to +15	<i>Medium agreement in little change</i> (52%), but also substantial decrease (35%) & increase (12%).	Downscaling decrease stronger in SW Vic and more consistent with observed drying	Predominance of cool season southward shift of westerlies and increasing intensity of subtropical ridge	Some disagreement	Medium confidence in decrease	GCM range likely to be biased high. SDM downscaling preferable
JJA		-32 to -2	<i>High agreement in substantial decrease</i> (80%).	Downscaling generally agrees, obs. trend not inconsistent	Related to cool season circulation change, e.g. well supported southward shift of westerlies and related storms. Relevant GCM processes reasonable	Good	High confidence in a decrease	Yes, except in Tasmania
	WESTERN TASMANIA (SSTW)	-6 to +20	<i>Medium agreement in increase</i> (64%).	Downscaling generally agrees, obs. trend not inconsistent	Related to strengthening and moistening of westerlies at this latitude (reasonable evidence)	Good	Medium confidence in an increase	Yes
	EASTERN TASMANIA (SSTE)	-11 to +19	<i>Medium agreement in increase</i> (62%).	Downscaling generally agrees, obs. trend not inconsistent	Related to strengthening and moistening of westerlies at this latitude (reasonable evidence)	Good	Medium confidence in increase	Downscaling will better reveal likely east-west contrast
SON		-44 to -3	<i>High agreement in substantial decrease</i> (79%).	Downscaling generally agrees, obs. trend not inconsistent	Related to cool season circulation change, but increasing tropical influences. Shift in IOD would cause drying	Good, but process understanding less certain	High confidence in decrease	Yes



SEASON	SUBREGIONAL EXCEPTION	2090 RCP85 CMIP5 RANGE OF CHANGE (%)	2090, RCP8.5 CMIP5 MODEL AGREEMENT (PERCENTS ARE FRACTION OF MODELS)	ADDITIONAL EVIDENCE: DOWNSCALING/CONSISTENCY OF OBSERVED TRENDS WITH CCMS	ADDITIONAL EVIDENCE: PLAUSIBLE PROCESSES/MODEL RELIABILITY	AGREEMENT OF MULTIPLE LINES OF EVIDENCE	SUMMARY STATEMENT WITH CONFIDENCE	DO THE GCM RESULTS PROVIDE A RELEVANT RANGE OF CHANGE FOR USE IN APPLICATIONS
--------	-----------------------	--------------------------------------	--	---	--	---	-----------------------------------	---

EASTERN AUSTRALIA

ANNUAL		-25 to +12	<i>Med. agreement in substantial decrease</i> (52%), but also substantial increase (2.1%).	Downscaling generally agrees, obs. trend is not strong.	Balance of tropical and mid-latitude influences not certain	Some disagreement	Low confidence in direction of change	Yes
DJF		-16 to +28	<i>Medium agreement in little change</i> (61%), but also substantial increase (27%) & decrease (13%).	Downscaling does not agree, obs. trend is not strong.	GCMs may not adequately represent the influence of Eastern Seaboard topography on the summer trade winds in producing rainfall	Not good agreement	Low confidence in direction of change	Possibly too narrow, with greater positive changes possible
MAM		-33 to +26	<i>Medium agreement in little change</i> (55%), but also substantial decrease (28%) & increase (17%).	Downscaling agrees, obs. trend is not strong.	Projected changes in physical processes are more difficult for 'shoulder seasons' than summer/winter.	Good, but process understanding less certain	Low confidence in direction of change	Yes
JJA		-40 to +7	<i>Medium agreement in substantial decrease</i> (53%).	Downscaling and obs. generally agree.	Related to southward shift of westerlies and fewer East Coast Lows.	Good	Medium confidence in a decrease	Yes
SON		-41 to +8	<i>Medium agreement in substantial decrease</i> (57%).	Downscaling does not agree, obs. trend is not strong.	Projected changes in physical processes are more difficult for 'shoulder seasons' than summer/winter.	Not good agreement	Low confidence in direction of change	Possibly too narrow, with greater positive changes possible
	COASTAL SE QLD (ECN)	-53 to +3	<i>Medium agreement in substantial decrease</i> (64%).	Downscaling does not agree (indicates little change or an increase), obs. trend is not strong.	Projected changes in physical processes are more difficult for 'shoulder seasons' than summer/winter. Projected windspeed increase reduces confidence in rainfall decrease	Not good agreement	Low confidence in direction of change	Possibly too narrow, with greater positive changes possible



SEASON	SUBREGIONAL EXCEPTION	2090 RCP85 CMIP5 RANGE OF CHANGE (%)	2090 RCP8.5 CMIP5 MODEL AGREEMENT (PERCENTS ARE FRACTION OF MODELS)	ADDITIONAL EVIDENCE: DOWNSCALING/CONSISTENCY OF OBSERVED TRENDS WITH GCMs	ADDITIONAL EVIDENCE: PLAUSIBLE PROCESSES/MODEL RELIABILITY	AGREEMENT OF MULTIPLE LINES OF EVIDENCE	SUMMARY STATEMENT WITH CONFIDENCE	DO THE GCM RESULTS PROVIDE A RANGE OF CHANGE FOR USE IN APPLICATIONS
NORTHERN AUSTRALIA								
ANNUAL		-26 to +23	Low agreement in direction of change (51% decrease), but substantial decrease (37%) & increase (32%) possible.	BOM-SDM Statistical Downscaling generally agrees well; CCAM Downscaling disagrees over Wet Tropics (large decreases).	Competing processes with opposite impact on model projected rainfall changes contribute to uncertainty. May also be sensitive to aerosol forcing. Large model spread in skill of simulating processes involved such as Monsoon onset, MJO and tropical circulation. Also, GCMs may not adequately represent the influence of Eastern Seaboard topography on rainfall.	Some disagreement	Low confidence in direction of change	Yes
DJF		-2.4 to +1.8	Low agreement in direction of change (56% of increase), but substantial increase (42%) & decrease (29%) possible.	BOM-SDM Statistical Downscaling generally agrees – CCAM downscaling disagrees in North-east and Wet Tropics. Observed trend is inconsistent or not captured in many GCMs.	Balance of tropical and mid-latitude influences not certain	Good, but process understanding less certain	Medium confidence in little change	Possibly too narrow, less relevant for Western Tasmania
	MONSOONAL NORTH WEST (MNW)	-2.4 to +1.8	Medium agreement in increase (64%).	Both types of Downscaling generally agree. Observed trend is inconsistent or not captured in many GCMs.	As above.	Some disagreement	Low confidence in direction of change	Yes
MAM		-3.0 to +2.6	Medium agreement in little change (37%), but substantial decrease (33%) and increase (31%) possible.	Both Downscaling generally agree in north-west but disagree in North-east and Wet Tropics.	GCMs vary in their response – some favouring an early, other a late monsoon season retreat – depending on each models circulation changes - contributing to spread either side. Also, GCMs may not adequately represent the influence of Eastern Seaboard topography on rainfall.	Some disagreement	Low confidence in direction of change	GCM range may be biased high
SON		-4.4 to +4.4	Medium agreement in decrease (64%).	BOM-SDM Statistical Downscaling generally agrees. Observed trend is inconsistent in many GCMs.	GCMs vary in their response – some favouring an early, other a late monsoon season retreat – depending on each models circulation changes - contributing to spread either side.	Some disagreement	Low confidence in the direction of change	Yes
	MONSOONAL NORTH EAST (MNE)	-6.2 to +2.4	Medium agreement in substantial decrease (53%), but substantial increase is possible (11%).	CCAM downscaling disagrees. Observed trend is inconsistent in many GCMs.	Changes in surface pressure along North-east coastal regions supports changes to easterly trade regime circulation.	Some disagreement	Low confidence in the direction of change	Yes



SEASON	SUBREGIONAL EXCEPTION	2090 RCP85 CMIP5 RANGE OF CHANGE (%)	2090 RCP8.5 CMIP5 MODEL AGREEMENT (PERCENTS ARE FRACTION OF MODELS)	ADDITIONAL EVIDENCE: DOWNSCALING/CONSISTENCY OF OBSERVED TRENDS WITH GCMS	ADDITIONAL EVIDENCE: PLAUSIBLE PROCESSES/MODEL RELIABILITY	AGREEMENT OF MULTIPLE LINES OF EVIDENCE	SUMMARY STATEMENT WITH CONFIDENCE	DO THE GCM RESULTS PROVIDE A RELEVANT RANGE OF CHANGE FOR USE IN APPLICATIONS
RANGELANDS								
ANNUAL		-32 to +18	<i>Low agreement in direction of change</i> (59% decrease), but also substantial decrease (41%) and increase (22%)	Observed northern trends not well explained but indicate substantial changes are possible	Influence of low-latitude sea surface temperatures evident in observed ENSO, and variations in long-term trends among models.	Some disagreement	Low confidence in direction of change	Yes
DJF		-22 to +25	<i>Low agreement in direction of change</i> (52% increase), but also substantial decrease (36%) and increase (33%)	As above	As above	As above	Low confidence in direction of change	Yes
MAM		-42 to +32	<i>Medium agreement in little change</i> (54%), but also substantial increase (28%) and decrease (19%)	As above	As above	As above	Low confidence in direction of change	Yes
JJA		-50 to +18	<i>Medium agreement in substantial decrease</i> (61%), but also substantial increase (14%)	See RS discussion below	See RS discussion below	Good for southern rainfall, although will some variation in modelled cool season circulation trends	Medium confidence in a decrease	Yes
	RANGELANDS (RS)	-46 to +1	<i>Medium agreement on substantial decrease</i> (61%)	Observed trends in south partially attributable to forced change, but also indicate substantial changes are possible,	Potential for cool season retreat of westerlies to drive seasonal rainfall trend in south-west and south-east evident from both observations and model trends.	Good for southern rainfall, although will some variation in modelled cool season circulation trends	High confidence in a decrease	Yes
SON		-50 to +23	<i>Medium agreement in decrease</i> (68%)	Observed changes not inconsistent	Influence of IOD-like trends is evident from both observations and models. Also still some potential for cool season circulation changes affecting the south	Good for southern rainfall, although will some variation in modelled cool season circulation trends	Medium confidence in a decrease	Yes

7.2.2 PROJECTED EXTREME RAINFALL CHANGE

EXTREME RAIN EVENTS ARE PROJECTED TO BECOME MORE INTENSE

Extreme rainfall events (wettest day of the year and wettest day in 20 years) are projected to increase in intensity with *high confidence*. Confidence is reduced to *medium confidence* for south-western Western Australia, where the reduction in mean rainfall may be so strong as to significantly weaken this tendency.

As the atmosphere warms, its capacity to hold moisture increases, enhancing the potential for extreme rainfall events and the risk of flooding and erosion events. However, changes in the atmospheric circulation patterns that trigger heavy rainfall events could also change, thereby either enhancing or partially offsetting this effect. Studies of the observed record of extreme rainfall in Australia show some evidence of an increase in rainfall extremes (see Section 4.2.1).

Various studies prior to CMIP5 have noted a tendency for an increase in the intensity and/or the proportion of rainfall in extreme categories, with this being most strongly evident where mean rainfall is projected to increase, but often also evident elsewhere (Alexander and Arblaster, 2009, Rafter and Abbs, 2009). Fine-scale regional modelling based on CMIP3 GCMs shows a tendency for short duration (sub-daily) rainfall to increase more rapidly than longer duration (daily and multi-day) rainfall (Abbs and Rafter, 2009, IPCC, 2012), indicating an increase in extreme rainfall across Australia, but with only *low confidence*.

The CMIP5 results also simulate a strong tendency for an increase in various indices of extreme rainfall in the Australian region. This Report demonstrates this change using the simulated annual maximum daily rainfall, and the estimate (using GEV analysis) of the 20-year return value of the annual maximum. The latter represents changes to rare extremes, which are particularly relevant to studies of flood occurrence. The results shown are from a subset of twenty-one CMIP5 models for which the relevant data were available. Figures 7.2.12 and 7.2.13 show projected changes in the wettest day in 20 years for 2090 alongside those for annual mean and annual wettest day for three RCPs and the four super-cluster regions (Figure 7.2.12) and for RCP8.5 for each of the sub-regions (Figure 7.2.13). These results were calculated point by point and then area-averaged.

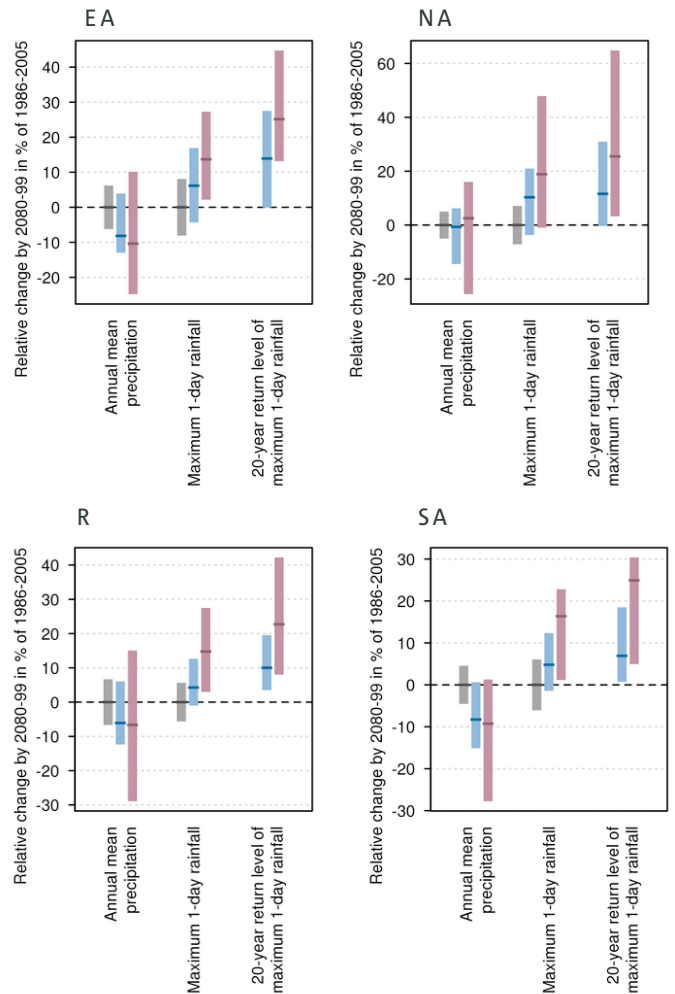


FIGURE 7.2.12: CHANGES TO EXTREME RAINFALL. FOR EACH PANEL FROM LEFT: PROJECTED CHANGE IN 2080–99 FOR ANNUAL MEAN PRECIPITATION, ANNUAL MAXIMUM 1-DAY RAINFALL, AND 20-YEAR RETURN LEVEL OF ANNUAL MAXIMUM 1-DAY RAINFALL IN PERCENT OF THE 1986-2005 AVERAGE. THE HORIZONTAL TICK DENOTES THE MEDIAN AND THE BAR DENOTES THE 10TH TO 90TH PERCENTILES OF THE CMIP5 RESULTS. THE SCENARIOS FROM LEFT TO RIGHT ARE: NATURAL VARIABILITY ONLY (GREY), RCP4.5 (BLUE), AND RCP8.5 (PURPLE). NATURAL VARIABILITY ONLY IS NOT SHOWN FOR THE 20-YEAR RETURN LEVELS. RESULTS ARE SHOWN FOR NORTHERN AUSTRALIAN (NA), EASTERN AUSTRALIAN (EA), RANGELANDS (R) AND SOUTHERN AUSTRALIAN (SA) SUPER-CLUSTERS.



Projections for relative precipitation change from 1986–2005 to 2080–99 according to RCP8.5 for both the annual mean and annual extremes

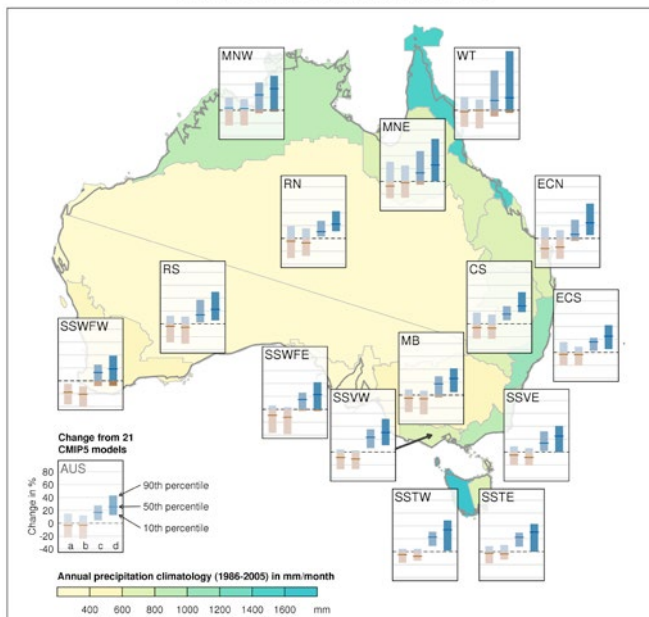


FIGURE 7.2.13: MEDIAN AND 10TH TO 90TH PERCENTILE RANGE OF PROJECTED CHANGE IN DAILY RAINFALL FOR 2080–2099 RELATIVE TO 1986–2005 FOR RCP8.5. SHOWN IN EACH BOX FROM LEFT TO RIGHT IS (A) THE ANNUAL MEAN FOR THE LARGER SET OF 39 MODELS, AS WELL AS (B) THE ANNUAL MEAN RAINFALL, (C) THE ANNUAL WETTEST DAY, AND (D) THE 20 YEAR RETURN LEVEL OF THE ANNUAL WETTEST DAY RAINFALL CALCULATED FROM A CONSISTENT SUBSET OF 21 CMIP5 MODELS. BLUE INDICATES INCREASE AND BROWN DECREASE. THE AUSTRALIAN AVERAGE RESULT IS SHOWN AT BOTTOM LEFT.

The results show a marked tendency for an increase in the annual maximum one day rainfall. This is most evident under high forcing (2090 and RCP8.5), and least evident or absent under RCP2.6 (not shown). The increasing tendency is also present (although small) in 2030 (not shown). The increase under high forcing contrasts markedly with the median change in annual rainfall, which shows little change or a decrease in most cases. Indeed, even in the sub regional analysis (Figure 7.2.13), the median projected change in the annual maximum rainfall is positive in all sub-regions, including sub-regions with a strong decrease in mean rainfall, such as south-west WA.

Projected change in the 20-year return value of the annual maximum rainfall is generally even more consistently positive, and of greater magnitude, than the change in the annual maximum rainfall (Figures 7.2.12 and 7.2.13). Confidence in this result is increased through noting that the full 10th to 90th percentile range of results shows a positive change in many cases. This tendency is more strongly evident in southern Australia and its sub-regions. Increases in the magnitude of this event are around 25 %

under RCP8.5 in 2090. Such increases in the magnitude of 20-year return period events could alternatively be viewed as these events occurring with greater frequency than in the baseline climate.

In summary, the agreement between theoretical expectations, a wealth of previous research and the CMIP5 results means that *high confidence* can be placed in a projection of a future trend toward increases in the intensity of extreme rainfall events (wettest day of the year, on average, and rarer events) throughout most of Australia. Confidence should be reduced to *‘medium confidence’* only for south-west WA, where the reduction in mean rainfall may be so strong as to significantly weaken this tendency. It is also important to note that the interpretation of GCM-based extreme rainfall change in quantitative terms is more problematic because of the very large difference in spatial scale between typical extreme rainfall events in the real world and what the GCMs are able to simulate. This means that the magnitude of regional GCM-based extreme rainfall changes are of *‘low confidence’* and should be treated as indicative only.

7.2.3 DROUGHT

TIME IN DROUGHT IS PROJECTED TO INCREASE IN SOUTHERN AUSTRALIA, WITH A GREATER FREQUENCY OF SEVERE DROUGHTS

The time in drought is projected to increase over southern Australia with *high confidence*, consistent with the projected decline in mean rainfall. Time in drought is projected to increase with *medium* or *low confidence* in other regions. The nature of droughts is also projected to change with a greater frequency of extreme droughts, and less frequent moderate to severe drought projected for all regions (*medium confidence*).

The previous projections using CMIP3 models (CSIRO and BOM, 2007), indicated that more drought (based on annual rainfall below the 5th percentile) would be likely, and occurring over larger areas, in south-west Australia, Victoria and Tasmanian regions, with little detectable change in the other regions (Hennessy *et al.* 2008). Similar results were also found when the projections were based on analyses of exceptionally low soil moisture (Hennessy *et al.* 2008) and an index involving the ratio between rainfall and potential evapotranspiration (Kirono *et al.* 2011b).

To study how drought might change under increasing greenhouse gases, this Report analyses the Standardised Precipitation Index (SPI, see Box 7.2.1), based on monthly rainfall simulated by CMIP5 GCMs. A brief description about the method used to generate the SPI and to define drought events is provided in Box 7.2.1, which also describes the three measures of drought characteristics reported here, namely drought proportion (or time in drought), frequency, and duration.

Figure 7.2.14 shows the regional average of drought proportion, which is a fraction of the time in drought during each 20 year period for each super-cluster region. The multi-model median indicates a drought proportion of around 35 % (in Rangelands and Northern Australia) to 39 % (in Eastern Australia and Southern Australia) during the 20-year period centred on 1995 (1986-2005), and an increase of roughly 5 to 20 % in the future, depending on the RCP. The bars representing the uncertainty range are relatively large, but they tend to be above the baseline level (1995) and hence suggest a high model agreement on the increase especially over the Southern Australia region. Other regions show a larger mix of results (i.e. between increase and decrease).

Regarding the drought frequency, which is the number of drought events in a 20 year period, the models indicate a decrease for moderate and severe drought but an increase for extreme drought in the future (Figure 7.2.15). Noteworthy is the high agreement among models and emission scenarios. In general, similar results are found in all four NRM super-cluster regions, but with the uncertainty range indicating an increase through to little change for extreme drought, except in Southern Australia where all models indicate an increase (not shown).

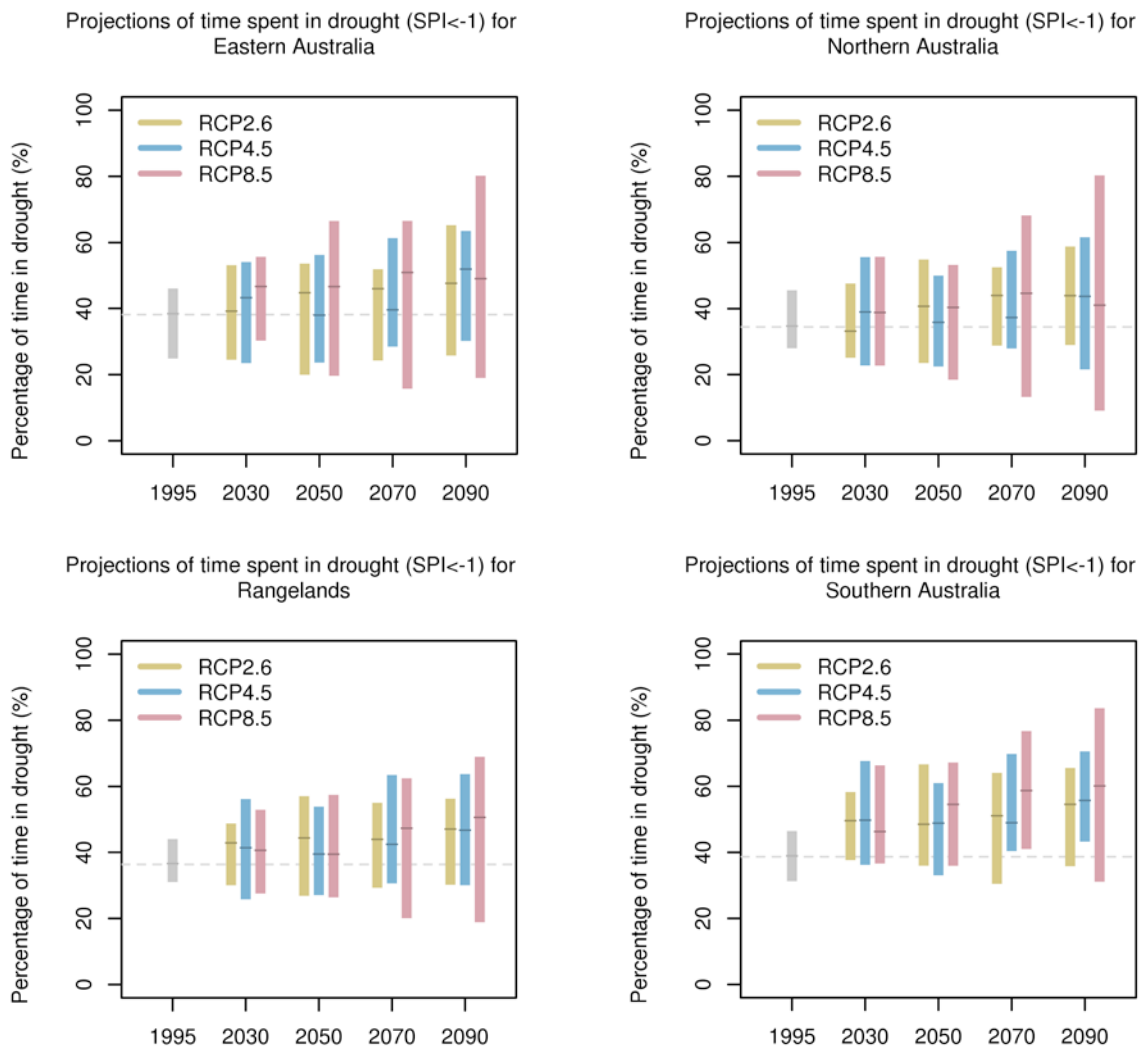


FIGURE 7.2.14: MEDIAN AND 10TH TO 90TH PERCENTILE RANGE IN PROJECTED CHANGE IN PROPORTION OF TIME SPENT IN DROUGHT FOR FIVE 20-YEAR PERIODS. RESULTS ARE SHOWN FOR NATURAL VARIABILITY (GREY), RCP2.6 (GREEN), RCP4.5 (BLUE) AND RCP8.5 (PURPLE) FOR SUPER-CLUSTERS. PROPORTION OF THE TIME IN DROUGHT IS DEFINED AS ANY TIME THE SPI IS CONTINUOUSLY (GREATER THAN OR EQUAL TO 3 MONTHS) NEGATIVE AND REACHES AN INTENSITY OF -1.0 OR LESS AT SOME TIME DURING EACH EVENT (SEE ALSO BOX 7.2.1).



For drought duration, little change is projected in moderate and severe drought but an increase for duration in extreme drought (Figure 7.2.16). For extreme drought, in particular, the multi-model agreement is high, with the largest changes occurring for RCP8.5. Overall, the results for all NRM super-clusters are relatively similar (not shown).

In assessing confidence in these projections, we note that at the global scale the CMIP5 models can reproduce both the observed influence of ENSO on drought over land and the observed global mean aridity trend (Dai, 2013), and that Australia-wide observation-based data always fall within the range of the models' ensemble (Orlowsky and Seneviratne, 2013). The projected increase in time

in drought is consistent with the general tendency for reduced annual rainfall (Section 7.2 and Appendix A), but this tendency is weak in the north. Moreover, there is consistency with the observed increase over the north-east coast, south-east coast and Murray-Darling Basin during 1960-2009 (Gallant *et al.* 2013). The overall increase in the time in drought is also consistent with CMIP3-based studies (Hennessy *et al.* 2008, Kirono *et al.* 2011b). In summary, the drought proportion can be expected with *high confidence* to increase over Southern Australia (and at the cluster level, over SSWF, see Cluster Reports), and with *medium confidence* for the rest of the country except Northern Australia where the increase is with *low confidence*.

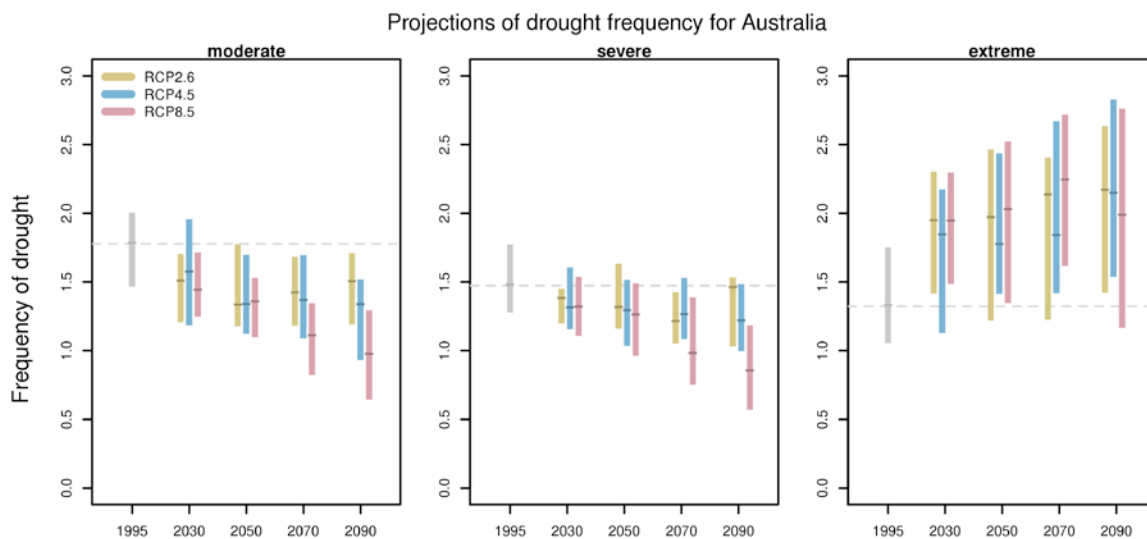


FIGURE 7.2.15: MEDIAN AND 10TH TO 90TH PERCENTILE RANGE OF CHANGE IN AVERAGE DROUGHT FREQUENCY IN AUSTRALIA FOR THREE DROUGHT CATEGORIES AND FOR FIVE 20-YEAR PERIODS. THE DROUGHT FREQUENCY IN A CATEGORY IS THE NUMBER OF EVENTS IN THIS CATEGORY OCCURRING IN THE 20-YEAR PERIOD (SEE ALSO BOX 7.2.1).

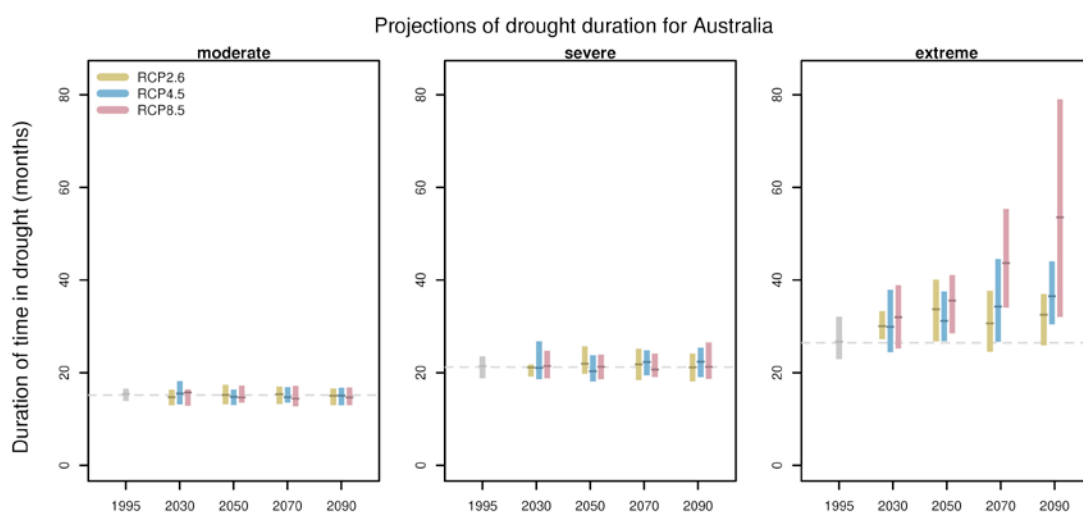


FIGURE 7.2.16: MEDIAN AND 10TH TO 90TH PERCENTILE RANGE OF PROJECTED CHANGE IN THE AVERAGE DURATION OF DROUGHTS IN AUSTRALIA FOR THREE DROUGHT CATEGORIES AND FOR FIVE 20-YEAR PERIODS. DROUGHT DURATION MEASURES THE AVERAGE LENGTH (IN MONTHS) OF A DROUGHT EVENT IN A GIVEN CATEGORY WITHIN A GIVEN 20-YEAR PERIOD (SEE ALSO BOX 7.2.1).

The projections of change to the frequency and duration of drought presented here are consistent with the observed trends as shown in Gallant *et al.* (2013), as well as the indication that ENSO events will intensify as a result of global warming and may cause an intensification of El Niño-driven drying in Australia (Power *et al.* 2013). However, Ault *et al.* (2012) report that CMIP3 and CMIP5 climate models tend to overestimate the magnitude of high frequency fluctuations, and underestimate the risk of future decadal-scale droughts, thus reducing the confidence in projections.

In summary, there is *medium confidence* in less frequent moderate and severe droughts and *medium confidence* in more frequent and longer extreme drought.

Note that this study uses a meteorological drought index which is based on rainfall only. Nicholls (2004) reported the important contribution of temperature (via evaporation) on drought in Australia. Also, see Section 7.7.1 where results demonstrating a decrease in soil moisture due to projected increases in potential evaporation are presented.

BOX 7.2.1: DROUGHT INDEX AND DEFINITION

Drought in general means acute water shortage. The primary cause of any drought is a lack of rainfall over an extended period of time, usually a season or more, resulting in a water shortage for some activities, groups, or sectors. The response of different entities (*e.g.* agricultural and hydrological systems) to water shortage conditions can vary substantially as a function of time scales and other socio-environmental conditions. As such, drought can be experienced and defined in many ways using various indices, which can be classified into meteorological, agricultural, and hydrological drought (Dai, 2011).

Different drought indices give different results so may result in somewhat different change patterns, especially on small scales (Seneviratne, 2012), and drought projections can be dependent on the choice of drought index (Burke and Brown, 2008, Taylor *et al.* 2013). Thus, any drought projection needs to be interpreted cautiously in the context of the drought index being used.

The standardized precipitation index (SPI, McKee *et al.* 1993, Lloyd-Hughes and Saunders, 2002) used in this Report, is based solely on rainfall. It is calculated by fitting a probability density function to the frequency distribution of a long-term (*i.e.* 1900–2005 for this Report) series of rainfall values, summed over the timescale of interest. In this Report, monthly data are used and the timescale of interest is 12 months, which is considered as the time required for water deficit conditions to affect various agricultural and hydrological systems (*e.g.* Szalai and Szinell, 2000, Zargar *et al.* 2011). Thus, each monthly value is the total rainfall for the previous 12 months. Subsequently, the probability distribution is transformed to a standardized normal

distribution. Negative SPI values are indicative of dryness while positive values are indicative of wetness. In addition, the SPI over 1900–2005 has a mean of zero and standard deviation of one, due to the normalisation. Table B7.2.1 provides the classification system to define drought intensities. In this case, a drought event occurs any time the SPI is continuously (greater than or equal to 3 months) negative and reaches an intensity of -1.0 or less at some time during each event (See Figure B7.2.1). The drought begins when the SPI first falls below zero and ends with the first positive value of SPI following a value of -1.0 or less (McKee *et al.* 1993).

This Report describes characteristic of drought for each of the five time periods: 1995 (1986–2005); 2030 (2020–2039); 2050 (2040–2059); 2070 (2060–2079); and 2090 (2080–2099). The characteristics of drought are represented by three measures. The first is drought proportion, which is calculated as the fraction of the time (20-years period) in drought. The second is drought frequency, which is defined as the number of droughts in a given 20-year period. The third, drought duration, measures the average length (in months) of a drought event for the selected period.

TABLE B7.2.1: DROUGHT CATEGORY BASED ON STANDARDISED PRECIPITATION INDEX (MCKEE *ET AL.* 1993, LLOYD-HUGHES AND SAUNDERS, 2002, DAI, 2011).

SPI VALUE	DROUGHT CATEGORY
0 to -0.99	Near normal
-1.00 to -1.49	Moderate
-1.50 to -1.99	Severe
-2 or less	Extreme



BOX 7.2.1 DROUGHT INDEX AND DEFINITION

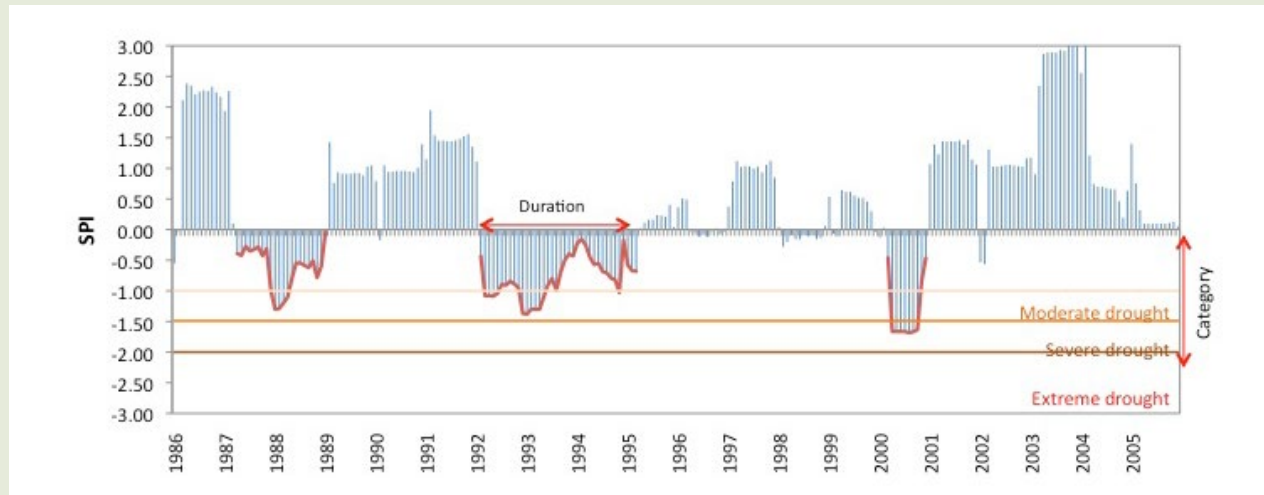


FIGURE B7.2.1: ILLUSTRATION OF A STANDARDISED PRECIPITATION INDEX (SPI) TIME SERIES AND THE ASSOCIATED DROUGHTS (RED-SOLID LINES) FOR A LOCATION WITHIN A 20-YEAR PERIOD. IN THIS EXAMPLE, THE SITE EXPERIENCES: (I) A DROUGHT PROPORTION OF 29 %; (II) TWO MODERATE DROUGHTS (WITH AN AVERAGE DURATION OF 30 MONTHS); AND (III) ONE SEVERE DROUGHT (WITH A DURATION OF 10 MONTHS).

7.2.4 SNOW

SNOWFALL IN THE AUSTRALIAN ALPS IS PROJECTED TO DECREASE, ESPECIALLY AT LOW ELEVATIONS

There is *very high confidence* that as warming progresses there will be a decrease in snowfall, an increase in snowmelt and thus reduced snow cover. These trends will be large compared to natural variability and most evident at low elevations.

The spatial resolution of global climate models is too coarse to represent snow-covered areas in the Australian Alps directly. The highest elevation in CMIP5 models for grid boxes in South-Eastern Australia representative of the Australian Alps is between 290m and 940m (most models' highest elevation is between 450m and 650m); hence no CMIP5 model can represent the snow covered Alpine area. Advanced off-line snow models are required to explore projections of snow conditions across the Australian Alps. These methods provide projections of snow depth, area and duration, and integrate changes in snowfall, melt and ablation (Hennessy *et al.* 2008, Hendrikx *et al.* 2013). Such calculations using the latest climate models dataset (CMIP5) are not available yet.

Projected changes in snowfall have been assessed using statistically downscaled CMIP5 climate model results. Accumulated precipitation falling on days where maximum temperature stays below 2 °C has been used to create an annual total of equivalent snowfall. This has been done using the Bureau of Meteorology analogue-based statistical downscaling approach applied to 22 of the CMIP5 models. The annual equivalent snowfall was computed for two locations: a 5 km grid box (148.40W, 35.95S, elevation 1419m) near Cabramurra (NSW) for which a long-term observed record of annual snow accumulation exists (Davis, 2013), and the highest 5 km grid box (148.40W, 36.15S, elevation 1923m). The two locations provide an insight into future changes in snowfall across a range of elevations spanning the area where snow is currently observed.

At these two locations (Figure 7.2.17), simulated snowfall showed a decline in the last 50 years. This observed snowfall decline is a component of the decline in snow accumulation observed at the Cabramurra station (Davis, 2013). The reduction in simulated snowfall is primarily due to warming rather than a decline in precipitation, *i.e.* an increase in the ratio of rain to snow. Davis (2013) also points to warming as being the primary reason for the observed decline in Cabramurra snow depth.

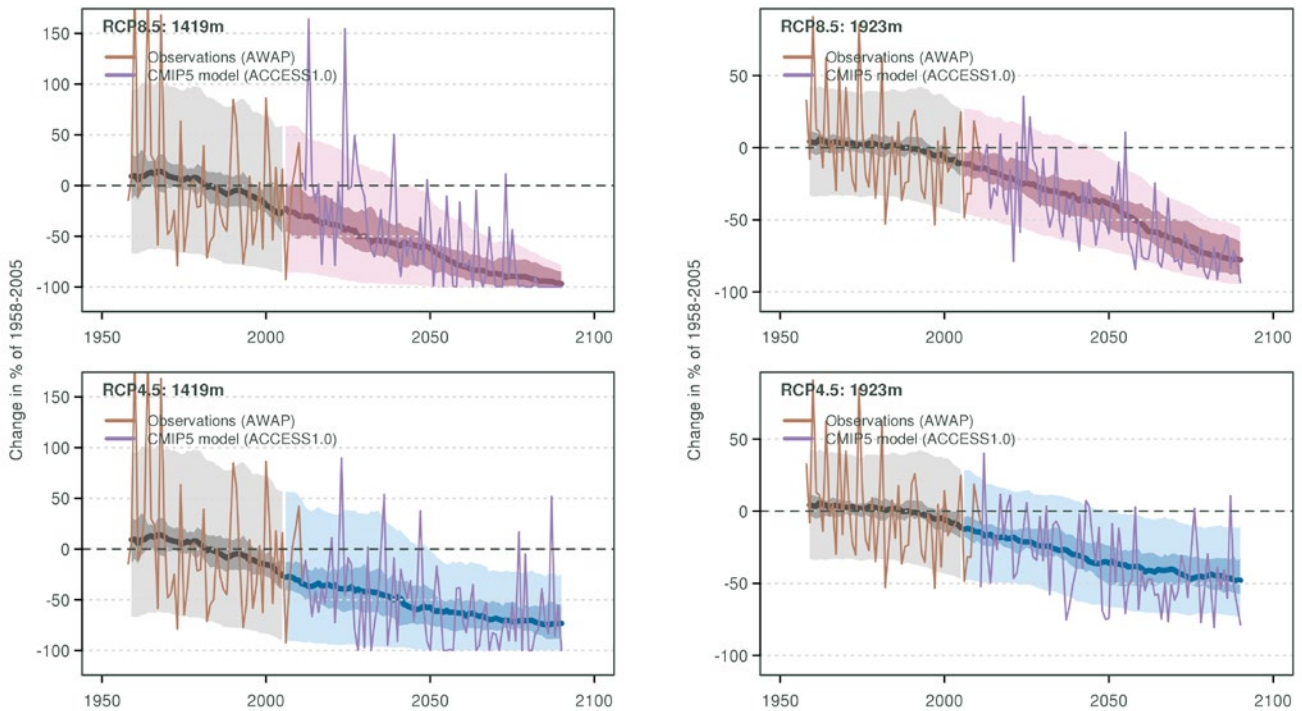


FIGURE 7.2.17: CHANGE IN SNOWFALL FOR TWO LOCATIONS IN THE BUREAU OF METEOROLOGY OPERATIONAL 5-KM GRIDDED OBSERVATIONS CORRESPONDING TO A LOW ELEVATION CONSISTENT WITH THE CURRENT SNOWLINE (LEFT GRAPHS) AND FOR THE HIGHEST ELEVATION IN THE GRIDDED OBSERVATIONS (RIGHT GRAPH). FUTURE PROJECTIONS FROM 2006 ONWARD ARE PROVIDED FOR THE RCP8.5 (TOP GRAPHS) AND RCP4.5 (BOTTOM GRAPH). EACH PANEL SHOWS THE MODEL ENSEMBLE MEDIAN (THICK LINE), THE 10TH TO 90TH PERCENTILE OF ANNUAL SNOWFALL (LIGHT SHADING) AND THE 10TH TO 90TH PERCENTILE OF 20-YEAR MEAN SNOWFALL (DARK SHADING), AWAP OBSERVATIONS (BROWN) AND AN EXAMPLE OF A POSSIBLE FUTURE TIME SERIES (LIGHT PURPLE) FROM A SINGLE MODEL (ACCESS-1.0).

Projections clearly show a continuing reduction in snowfall during the 21st century. The magnitude of decrease depends on the altitude of the region and on the emission scenario (Figure 7.2.17). At the low elevation grid box (1419m), years without snowfall start to be observed from 2030 in some models. By 2090, these years become common with RCP8.5. Figure 7.2.17 displays the result from a single downscaled model (ACCESS 1.0) illustrating how this model depicts interannual variability. It highlights the fact that with RCP4.5, while years without snowfall will become possible, years with normal snowfall (by today's standard) still occur at the end of the 21st century but less frequently. At the high elevation grid box (1923m), the reduction of snowfall is less in percentage terms, averaging about 50 % by 2090 with RCP4.5 and 80 % with RCP8.5.

These projections concern only snowfall, excluding the additional impacts of climate change on snow-melt and ablation. Hence the full picture in terms of snow depth, area and duration is not provided. Such advanced analysis was performed using temperature and precipitation projections from 18 CMIP3 climate models as input to the CSIRO snow model to estimate changes in snow conditions over Victoria for 20-year periods centred on 2020 and 2050, relative to a 20-year period centred on 1990 (Bhend *et al.* 2012). Results were calculated for each climate model for three different IPCC SRES greenhouse gas emissions scenarios: low (B1), medium (A1B) and high (A1FI).

Decreases in maximum snow depth are evident in all these simulations, but there is a wide range of uncertainty due to differences in projections between the 18 climate models

TABLE 7.2.3: SIMULATED ANNUAL-AVERAGE MAXIMUM SNOW-DEPTH (CM) AT FOUR SKI RESORTS FOR 20-YEAR PERIODS CENTRED ON 1990 AND 2050 FOR LOW (B1), MEDIUM (A1B) AND HIGH (A1FI) EMISSION SCENARIOS. THE RANGE OF DEPTHS REPRESENTS THE SPREAD OF RESULTS FROM 18 CMIP3 CLIMATE MODELS. SIMULATED SNOW-DEPTHS HAVE BEEN ROUNDED TO THE NEAREST 5 CM.

SITE	1980-1999	2040-2059		
		LOW EMISSIONS	MED EMISSIONS	HIGH EMISSIONS
FALLS CREEK	150	50-105	30-90	20-80
MT HOTHAM	130	40-95	25-80	15-70
MT BULLER	95	20-60	10-50	5-45
MT BUFFALO	60	10-30	5-25	0-20



(Table 7.2.3). For example, at Falls Creek ski resort, the simulated average maximum depth is 150 cm in the 20-year period centred on 1990. By 2020, the average maximum depth decreases to 80-135 cm for the three different emission scenarios. By 2050, the average maximum depth decreases to 50-105 cm for the low scenario and 20-80 cm for the high scenario. A decline in snow-cover is also simulated. For example, by 2020, the area of Victoria averaging at least 1 day of snow-cover decreases by 10-40 % across the three scenarios. By 2050, the area decreases by 25-55 % for the low scenario and 35-75 % for the high scenario. Across four ski resorts (Falls Creek, Mt Hotham, Mt Buller and Mt Buffalo), by 2020, the average snow season becomes 5-35 days shorter for the three scenarios. By 2050, the average snow season becomes 20-55 days shorter for the low scenario and 30-80 days shorter for the high scenario. Larger changes are likely at lower elevations, such as Mt Baw Baw and Lake Mountain, but projections for these sites were considered to be less robust.

In summary, there is *very high confidence* that as warming progresses there will be very substantial decreases in snowfall, increase in melt and thus reduced snow cover, with these trends being large compared to natural variability, especially under a high emissions scenario.

7.3 WINDS, STORMS AND WEATHER SYSTEMS

7.3.1 MEAN AND EXTREME WINDS

MEAN WIND SPEEDS ARE PROJECTED TO DECREASE IN SOUTHERN MAINLAND AUSTRALIA IN WINTER AND INCREASE IN TASMANIA

By 2030, changes in near-surface wind speeds are projected to be small compared to natural variability (*high confidence*). By 2090, wind speeds are projected to decrease in southern mainland Australia in winter (*high confidence*) and south-eastern mainland Australia in autumn and spring. Winter decreases are not expected to exceed 10 % under RCP8.5. Wind speed is projected to increase in winter in Tasmania. Projected changes in extreme wind speeds are generally similar to those for mean wind.

MEAN WINDS

Wind patterns in Australia are associated with the location and seasonal movement of broad-scale circulation systems, with westerlies south of the subtropical high pressure belt affecting southern Australia in winter, and trade wind south-easterlies to its north, and with monsoonal westerlies over the Top End in summer (Figure 7.3.1). Changes in wind

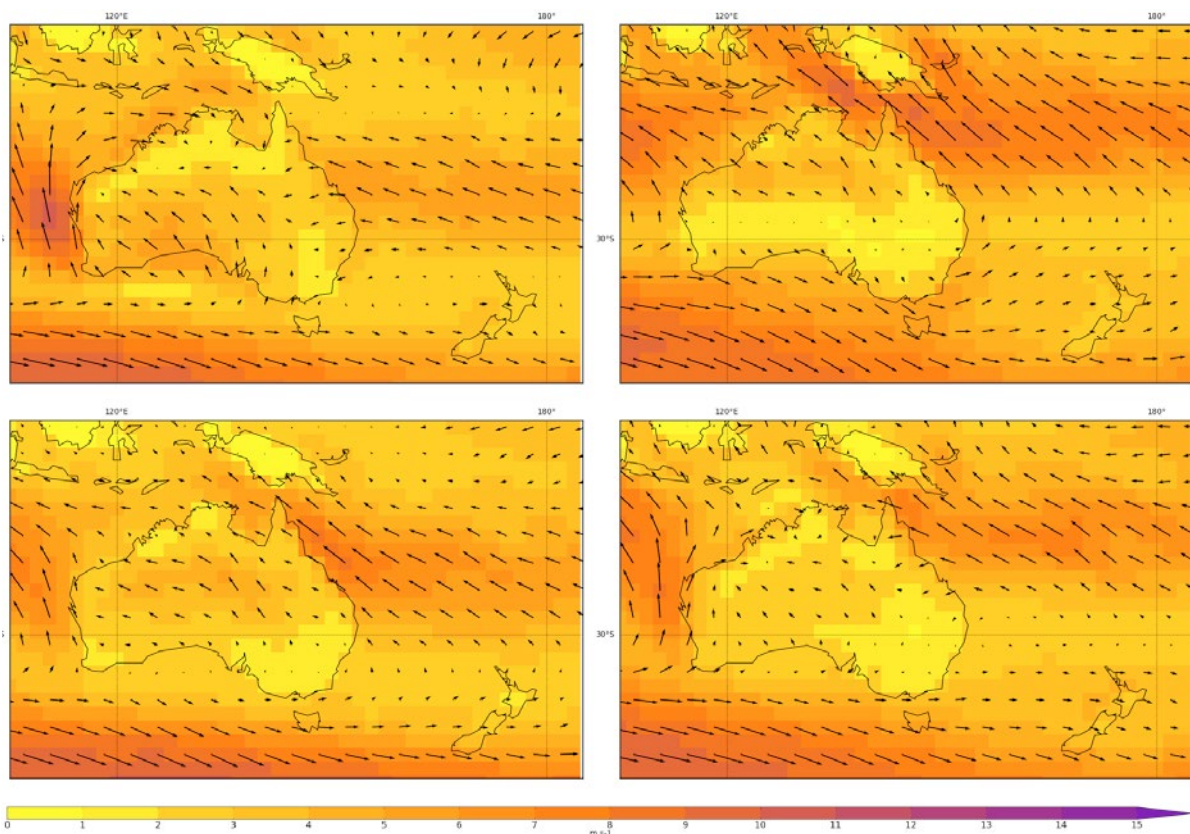


FIGURE 7.3.1: NCEP2 WINDS AVERAGED OVER 1986–2005 FOR SUMMER (DJF), AUTUMN (MAM), WINTER (JJA) AND SPRING (SON). COLOUR SCALE SHOWS WIND SPEED (UNITS ARE M/S) AND VECTOR ARROWS SHOW WIND SPEED AND DIRECTION.

-20° -10° 0° 10° 20° 30° 40° 50°

attributes (e.g. wind speed, direction and extremes) can have large biophysical and societal impacts in both the terrestrial and marine environments. In the terrestrial environment, changes to winds may have potential consequences for the agricultural and energy sectors and building codes. In the marine environment, winds influence waves, currents and coastal sea levels, which in turn affect coastal erosion, sediment transport, inundation and saltwater intrusion into coastal wetlands and aquifers. For example, changes in wind direction and storm-induced wind extremes associated with natural interannual climate cycles affect erosion/accretion patterns along eastern Australian beaches (Harley *et al.* 2010). Wind speeds near the surface undergo strong transition due to frictional effects such as terrain and vegetation (e.g. Troccoli *et al.* 2012, see also Section 4.2). The model-derived surface wind speeds reported in this Section are 10 m above the surface.

Assessment of wind changes in the CMIP5 models involved a smaller set of models than for other variables. This was primarily because wind speed data were not consistently archived by all modelling groups for all time periods required. In addition, inspection of wind speed changes revealed that a small number of models exhibited unusually large increases in some land areas compared to

surrounding areas. Inspection of other model variables suggested that the cause of the wind speed increases were related to large changes in surface roughness across the same small areas of the model. Since these changes were unusual compared to other adjacent regions in the model and compared to the majority of other models assessed, and because these large changes strongly influenced the results of some cluster regions, the particular models concerned were removed from the ensemble. The two models removed were IPSL-CM5A-MR, IPSL-CM5B-LR. This reduced the total number of models assessed for mean winds to 24 models compared with, for example, 39 models for mean rainfall change.

Projected wind speed differences by season in the CMIP5 models are illustrated for the four super-clusters in Figure 7.3.2 for 2030 and 2090 and three RCPs, and for each of the sub-clusters in Figure 7.3.3 for 2090 and RCP8.5. Wind speed differences expected due to natural variability are also indicated in both figures.

In the near future (2030), differences are mostly comparable to those expected due to natural variability, and thus represent little change. This can be seen in Figure 7.3.2 for the super-cluster averages, where these differences are

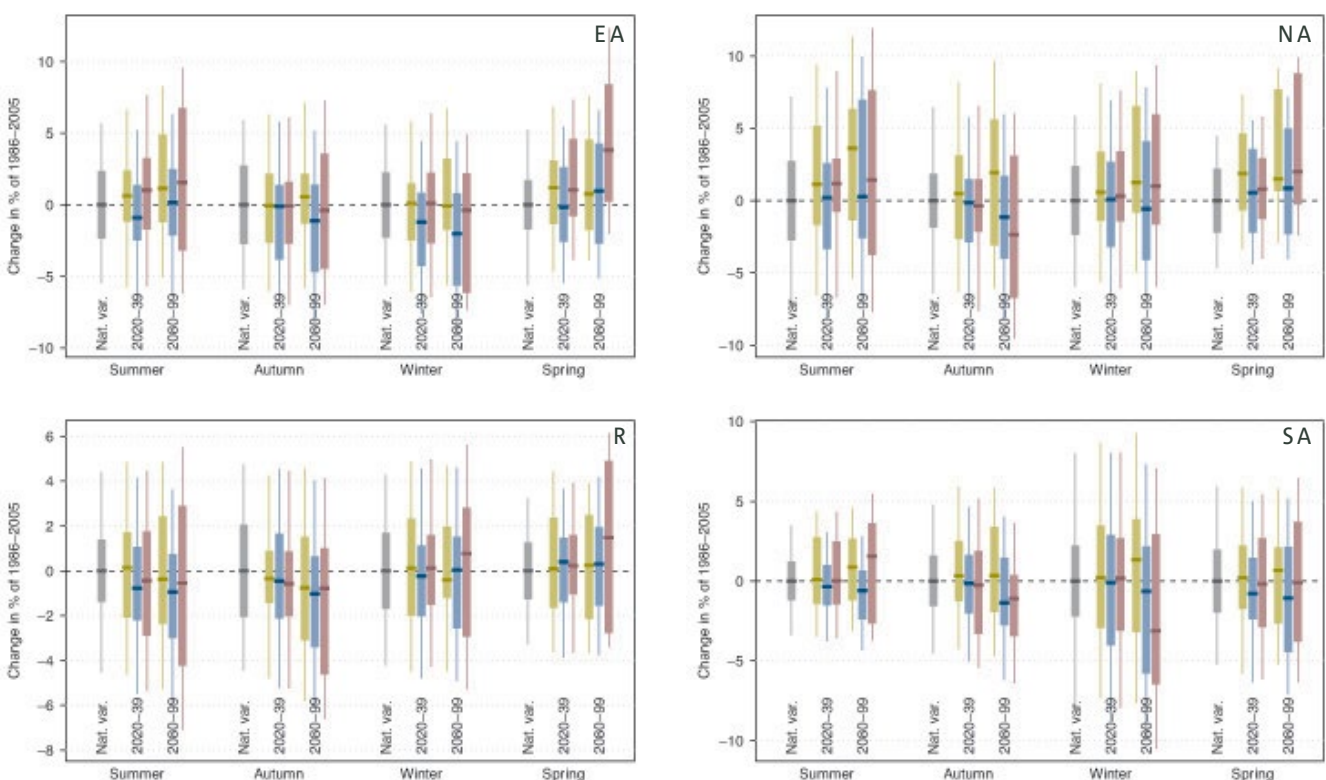


FIGURE 7.3.2: MEDIAN AND 10TH TO 90TH PERCENTILE RANGE OF PROJECTED CHANGE IN SEASONAL WIND SPEED (IN PERCENT) FOR 2020–2039 AND 2080–2099 RELATIVE TO THE 1986–2005 PERIOD (GREY BAR) FOR RCP2.6 (GREEN), RCP4.5 (BLUE) AND RCP8.5 (PURPLE). FINE LINES SHOW THE RANGE OF INDIVIDUAL YEARS AND SOLID BARS FOR TWENTY YEAR RUNNING MEANS. RESULTS ARE SHOWN FOR EASTERN AUSTRALIAN (EA), NORTHERN AUSTRALIAN (NA), RANGELANDS (R) AND SOUTHERN AUSTRALIAN (SA) SUPER-CLUSTERS.

-20° -10° 0° 10° 20° 30° 40° 50°

mostly within $\pm 3\%$, although larger ranges are present at the sub-cluster level (not shown). By late in the century (2090) and under RCP8.5, changes become evident in some models, with greatest consistency on spring increases in Eastern Australia and winter decreases in Southern Australia. Changes at this large-scale exceed 5% in some models. This pattern of change is also clear in the sub-cluster results at 2090 and RCP8.5 (Figure 7.3.3) with the north-eastern cluster regions (MNE, WT, ECN, CS and RN), showing spring increase, and the southern mainland sub-cluster regions (CS, ECS, SSWFE and MB) showing winter decreases. The spring increase in the north extends to winter in MNE and WT. In the mainland south-east (SSWFE, SSVW, SSVE and MB), decreases are present in autumn and spring, as well as in winter. However, further south in the Tasmanian regions of SSTW and SSTE, there is a strong tendency for wind speed to increase in winter. Changes in 2090 under RCP8.5 are mostly in the range of $\pm 10\%$ and often less than $\pm 5\%$.

Projections for relative near-surface wind speed change from 1986–2005 to 2080–99 according to RCP8.5

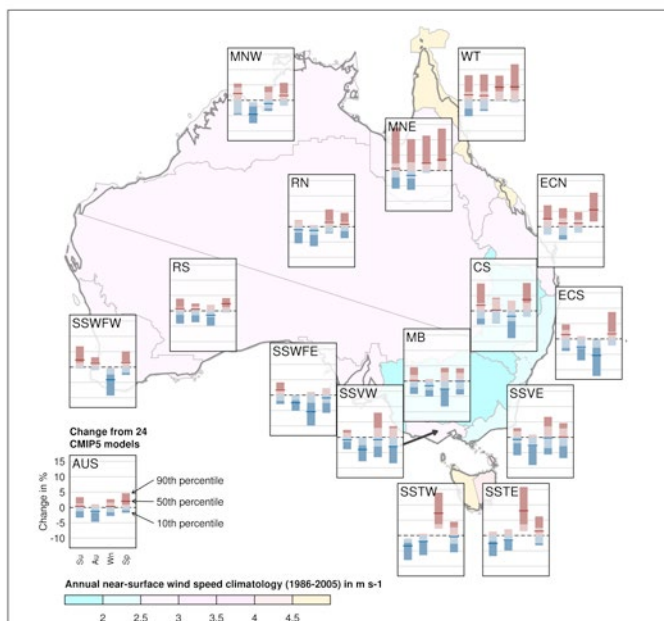


FIGURE 7.3.3: MEDIAN AND 10TH TO 90TH PERCENTILE RANGE OF PROJECTED CHANGE IN SEASONAL 10-M WIND SPEED (PERCENT) ACROSS 24 CMIP5 CLIMATE MODELS FOR EACH SEASON FOR R85 FOR 2080–2099 RELATIVE TO 1986–2005. RED INDICATES INCREASE AND BLUE DECREASE (SEE KEY) AND PALER PORTION OF THE BAR IS THE 10TH TO 90TH PERCENTILE RANGE EXPECTED FROM NATURAL VARIABILITY. THE WIND SPEED CLIMATOLOGY OVER THE 1986–2005 PERIOD IS INDICATED BY THE COLOUR OF THE SHADING ON THE MAP OF AUSTRALIA.

These findings are generally consistent with a previous assessment of wind change in an ensemble of 19 CMIP3 models over the period 2081–2100 relative to 1981–2000 forced by the SRES A1B emissions scenario (McInnes *et al.* 2011). In winter, there was agreement in at least two thirds of models of a general increase in wind speed over the tropical half of mainland Australia north of 30° S, on wind speed decrease between 30 and 40° S and wind speed increase south of 40° S. Overall, these changes were consistent with a projected increase in the trade wind easterlies to the north of 30° S, the southward movement of the subtropical ridge and a strengthening of the mid-latitude westerlies over the Southern Ocean. The seasonal movement of the subtropical ridge southward in summer means that the trade easterlies affect a greater part of the continent during this season (Figure 7.3.1). Future changes to this pattern projected for summer indicate that there was less agreement on the direction of wind speed change between the different models to the north of 30° S, a consistent increase in wind speed over the southern mainland coast and decreases over Tasmania.

In summary, in the near future (2030) changes to mean wind speed are projected to be small compared with natural variability (*high confidence*). However, late in the century under higher RCPs, a pattern of winter wind speed decrease across southern mainland Australia, autumn and spring decrease in south-eastern mainland Australia, and winter increase over Tasmania is projected. These changes are consistent with broad-scale patterns of circulation change and the winter changes are projected with *high confidence*. Earlier studies also pointed to stronger trade winds, but the current results show that tendency primarily in spring. The reason for this spring focus is not clear and this projection is of *low confidence*.

EXTREME WINDS

Extreme winds create hazardous conditions for marine and terrestrial activities and infrastructure. The intensity of extreme winds at the surface is strongly modified by terrain and vegetation, while over the ocean extreme winds lead to high ocean waves which in turn may modify the wind field. GCMs are not able to adequately resolve many small scale meteorological phenomena that contribute to extreme winds such as tropical cyclones, East Coast Lows or thunderstorm downbursts. Therefore, alternative approaches such as downscaling are needed to resolve such systems. This contributes to a general lowering of confidence on extreme wind changes (*e.g.* McInnes *et al.* 2011).

Extreme winds may be characterised by a variety of metrics such as high percentiles or return periods. Here, two extreme wind metrics were calculated; the average of the annual maximum wind speed over the twenty years of data and an estimate of the 20-year return period of the annual maximum calculated using GEV analysis.

Since daily-maximum winds were not available from the CMIP5 archive, extreme wind metrics were evaluated from the daily-averaged wind speed data. Furthermore,

because daily-averaged wind speed was archived in a smaller number of models than daily-averaged zonal and meridional (westerly and northerly) components of wind speed, daily wind speed was recalculated from daily-average wind speed components, so as to make most use of the available the model output. Using the daily averaged wind speed components to produce wind speeds leads to values that are slightly lower than the wind speeds directly output from the model since changes in wind direction through the course of the day tends to reduce the average of the wind speed components. Wind speed values were available for an ensemble of sixteen models, however the two IPSL models were removed for reasons discussed in the previous section leaving only fourteen. Figure 7.3.4 compares the annual changes in the two extremes metrics with changes in the annual mean surface wind. The left-most bar shows the change across the ensemble of 24 models discussed in the previous section while the second bar shows the change just for the 14 models used for the extremes analysis. Comparing these two bars for each sub-cluster region shows that in general, the changes in the average winds across the smaller ensemble are consistent with those from the larger ensemble. The third bar shows the change in the average of the annual maximum wind while the fourth bar shows the 20-year return period wind.

The changes in extreme winds are generally consistent with those seen for mean winds. Across northern Australia there is a tendency for the median wind speed to increase in tropical areas (WT, RN and MNW). Although there is a greater tendency towards an increase in winds in MNE, there is little change in median value. Across south-eastern mainland Australia there is a general tendency towards a decrease across the ensemble in both the annual average and the 20-year wind speed (see results in Figure 7.3.4 for SSWFE, SSVW, MB, ECN, ECS and in CS for the 20-year wind speed only). For SSVE, RS and SSWFW, for annual and 20-year values and CS for annual average only, there is little change in the median value although there is a large spread in the direction and magnitude of change in individual models. Over Tasmania (SSTW and SSTE), median values indicate large increase although again there is a large spread in the direction and magnitude of change in individual models.

The pattern of extreme wind speed change seen here can be compared with the changes reported in McInnes *et al.* (2010) for the CMIP3 model ensemble, although that study characterised extreme winds using the 99th percentile wind speeds (which are less extreme than the annual maximum and 20-year return period values). Changes across the north of the continent consisted mainly of multi-model agreement on small change. Over the southern half of the continent there was multi-model agreement on decreases in extreme winds and over Tasmania, there was multi-model agreement on extreme wind increase, similar to results reported here.

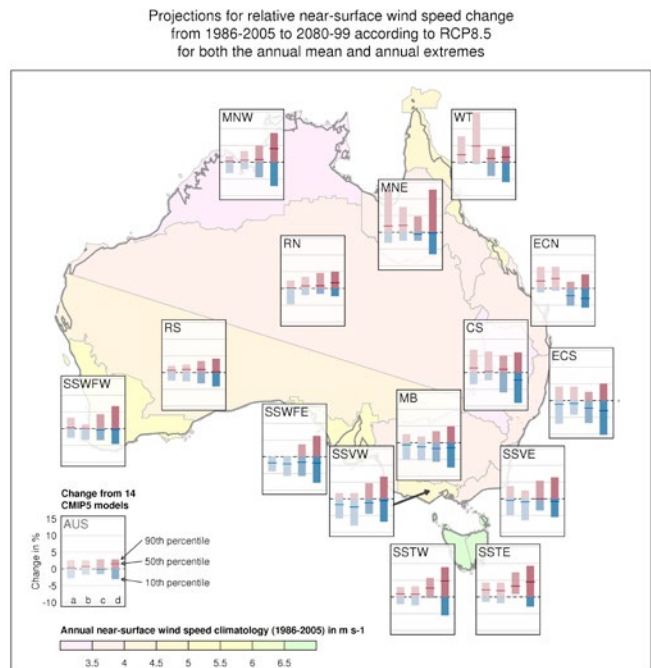


FIGURE 7.3.4: MEDIAN AND 10TH TO 90TH PERCENTILE RANGE OF PROJECTED CHANGE IN ANNUAL MEAN NEAR-SURFACE WIND SPEED IN SUB-CLUSTERS FOR 2080–2099 RELATIVE TO 1986–2005 FOR RCP8.5. SHOWN IN EACH BOX FROM LEFT TO RIGHT IS (A) THE ANNUAL DAILY MEAN NEAR-SURFACE WIND SPEED FOR THE LARGER SET OF 24 MODELS, AS WELL AS (B) THE ANNUAL DAILY MEAN NEAR-SURFACE WIND SPEED, (C) THE ANNUAL WINDIEST DAY, AND (D) THE 20 YEAR RETURN LEVEL OF THE ANNUAL WINDIEST DAY CALCULATED FROM A CONSISTENT SUBSET OF 14 MODELS. RED INDICATES AN INCREASE IN RELATIVE NEAR-SURFACE WIND SPEED AND BLUE A DECREASE.

In summary, changes in extreme winds tend to follow the direction of change indicated for mean winds, with only a few exceptions such as the decrease in extreme winds in the East Coast region during spring. Because of the various shortcomings associated with modelling extremes of near-surface winds, including the inability of models to resolve small scale meteorological systems that contribute to extreme winds such as tropical cyclones, there is generally *low confidence* in wind projections in the tropics. However, there is generally *medium confidence* in decreases in extreme wind speeds over the south of the continent and increases over Tasmania because the changes are consistent with broad-scale changes to circulation in these latitudes and because the scale of the weather systems that are responsible for extreme winds are better characterised by GCMs.

7.3.2 SYNOPTIC SYSTEMS

TROPICAL CYCLONES MAY OCCUR LESS OFTEN, BECOME MORE INTENSE, AND MAY REACH FURTHER SOUTH

Tropical cyclones are projected to become less frequent with a greater proportion of high intensity storms (stronger winds and greater rainfall) (*medium confidence*). A greater proportion of storms may reach south of 25 degrees South (*low confidence*).

MID-LATITUDE WEATHER SYSTEMS ARE PROJECTED SHIFT SOUTH IN WINTER, AND THE TROPICS TO EXPAND SOUTHWARD

The observed intensification of the subtropical ridge and expansion of the Hadley Cell circulation are projected to continue in the 21st century (*high confidence*). Both represent an expansion of the tropics.

In winter, mid-latitude weather systems are projected to shift south and the westerlies are projected to strengthen (*high confidence*). Concurrent and related changes in various measures of mid-latitude circulation are projected, including a more positive Southern Annular Mode, a decrease in the number of deep lows affecting south-west Western Australia and a decrease in the number of fronts in southern Australia.

Synoptic systems are a major cause of severe weather including strong winds and heavy rainfall. It is therefore important to assess how these systems may change in the future. Systems relevant to Australia include tropical cyclones, mid-latitude cyclones and their associated cold fronts.

TROPICAL CYCLONES

Tropical cyclones are phenomena that are a major cause of socio-economic loss and damage for tropical and subtropical Australia. Knutson *et al.* (2010) reviewed the results of a number of studies analysing changes in tropical cyclones by the end of the 21st century. The changes are found to be largely model-dependent but suggest an overall decrease in numbers of tropical cyclones globally. These changes vary between individual ocean basins but the decrease in tropical cyclone activity is most pronounced in the Southern Hemisphere. More recently the IPCC *Fifth Assessment Report* (IPCC, 2013; pg 1220) concludes “it is likely that the global frequency of occurrence of tropical cyclones will either decrease or remain essentially unchanged, concurrent with a likely increase in both global mean tropical cyclone maximum wind speed and precipitation rates. The future influence of climate change on tropical cyclones is likely to vary by region, but the specific characteristics of the changes are not yet well quantified and there is low confidence in region-specific projections of

frequency and intensity.” Most recent global and regional studies are consistent with these findings (*e.g.* Murakami *et al.* 2012, Tory *et al.* 2013b,c, Chattopadhyay and Abbs, 2012). However, Emanuel (2013) downscaled a suite of CMIP5 GCMs, finding an increase in both the frequency and intensity of tropical cyclones in most locations, with the exception of the south-western Pacific region near Australia; it should be noted that these CMIP5 results are found to differ substantially from the application of this downscaling technique to a selection of CMIP3 models.

This Report presents an analysis of projected changes of tropical cyclone frequency and location in the Australian region in CMIP5 models. Although the resolution of the majority of global climate models is coarse, the current generation of GCMs is able to simulate the broad-scale atmospheric conditions associated with tropical cyclone activity and they do produce atmospheric circulations that resemble tropical cyclones with global distributions that generally match the observed tropical cyclone climatology (*e.g.* Camargo *et al.*, 2005). However, they have insufficient temporal and spatial resolution to capture the high wind speeds and other small-scale features associated with observed tropical cyclones.

Three “empirical methods” were used to infer tropical cyclone activity from the large-scale environmental conditions and were applied to the outputs of CMIP5 GCMs. These three schemes are known as the Genesis Potential Index (GPI) (Emanuel and Nolan, 2004), the Murakami modification of the GPI (GPI-M) (Murakami and Wang, 2010) and the Tippett Index (Tippett *et al.* 2011). Two “direct detection” schemes were applied to the outputs from a subset of CMIP5 GCM model outputs: these are the CSIRO Direct Detection (CDD) scheme which is a modified version of the Nguyen and Walsh (2001) detection scheme coupled with the tracking scheme of Hart (2003), and the Okubo-Weiss-Zeta Parameter (OWZP) of Tory *et al.* (2013 a,b,c). Projections from the CDD and OWZP only consider GCMs which reproduced a tropical cyclone climatology with annual tropical cyclone numbers within $\pm 50\%$ of that observed.

These methods were applied to a selection of CMIP5 models to investigate changes in the frequency of tropical cyclones at the end of the 21st century under the RCP8.5 emissions scenario relative to the historical run. The analysis was performed over both the north-east (0-40 °S; 130-170 °E) and north-west (0-40 °S; 90-130 °E) of the continent.

Over both regions, results indicate a general decrease in tropical cyclone genesis (formation) frequency (Figures 7.3.5 and 7.3.6), although the five methods show different results across the different models. Using the direct detection methodologies (OWZP or CDD), a little over a half of projected changes are for a decrease in genesis frequency of between 15 to 35 % in the eastern region whereas in the west, the majority of models (around 85 %) project a decrease. The three empirical techniques assess changes in the main atmospheric conditions known to be



necessary for tropical cyclone formation. About two-thirds of models suggest the conditions for tropical cyclone formation will become less favourable in both regions with about one third of projected changes being for a decrease of between 5 and 30 %. There is *medium confidence* for this projection. Further analysis of the CDD results shows negligible changes in genesis latitude and storm duration for the Australian region; importantly a larger proportion of storms are projected to decay south of 25 °S in the late 21st century. This projected southward movement in the decay location of tropical cyclones is consistent with the observed migration of tropical cyclone activity away from the tropics (Kossin *et al.* 2014).

To enable changes in intensity, size and rainfall to be captured, it is necessary to use some form of downscaling. Downscaling studies of tropical cyclones affecting the Australian and south-west Pacific (Lavender and Walsh, 2011, Abbs and Rafter, 2012, Abbs *et al.* 2014) consistently project an increase in the proportion of high intensity (high windspeed, low minimum pressure) storms, a corresponding decrease in the proportion of mid-range intensity storms and an increase in the rainfall close to the storm centre; in particular the increase is largest in the most intense tropical cyclones. In summary, based on global and regional studies, tropical cyclones are projected to become less frequent with a greater proportion of high intensity storms (stronger winds and greater rainfall) (*medium confidence*); a greater proportion of storms may reach south of 25 degrees south (*low confidence*).

EXTRA-TROPICAL CYCLONES AND STORM TRACKS

The mean transport of energy via the Hadley Cell from the tropics to the subtropical ridge transfers energy away from the tropics. This large-scale climatological feature has impacts on the weather of southern Australia (see Section 4.1.2). Over the last 30 years the Hadley Cell has been expanding poleward (Lucas *et al.* 2012), although not all climate models capture the magnitude of this trend (Nguyen *et al.* 2013). CMIP3 climate model simulations generally indicate a poleward expansion of the Hadley circulation of a further 1 to 2 ° of latitude (approximately 100 to 200 km) by the end of the 21st century, and an associated expansion of the subtropical dry zone (Previdi and Liepert, 2007). In response to the Hadley circulation broadening, climate models project an increase in the subtropical ridge intensity over the 21st century in the vicinity of Australia and a southward movement of its mean position (Kent *et al.* 2013; see also Figure 7.2.11). These projected changes are likely to contribute to reductions in storminess and rainfall over southern Australia. However, it is important to note that most CMIP3 climate models failed to adequately reproduce the correlation between the subtropical ridge intensity and south-eastern Australian rainfall which lowers the confidence in GCM rainfall projections for southern Australia (Kent *et al.* 2013).

The number of extra-tropical cyclones impacting Australia is expected to decline, as indicated by the changes projected in the large-scale climate features described

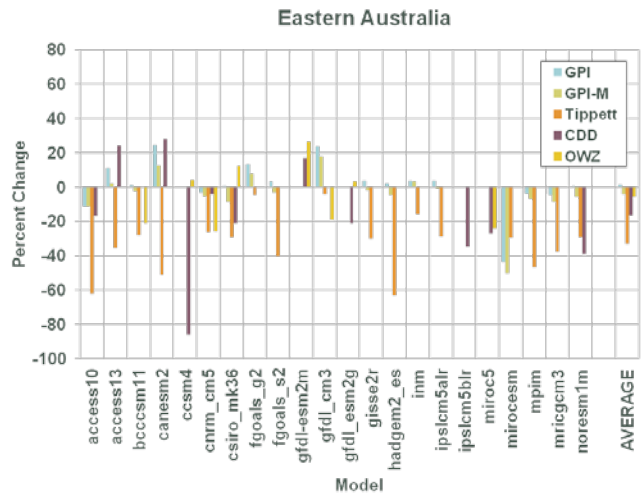


FIGURE 7.3.5: PROJECTED PERCENTAGE CHANGE IN THE FREQUENCY OF TROPICAL CYCLONE FORMATION FOR EASTERN AUSTRALIA (0-40°S; 130 °E -170 °E) FOR 22 CMIP5 CLIMATE MODELS, BASED ON FIVE METHODS (SEE TEXT FOR DEFINITIONS), FOR 2080–2099 RELATIVE TO 1980–1999 FOR RCP8.5.

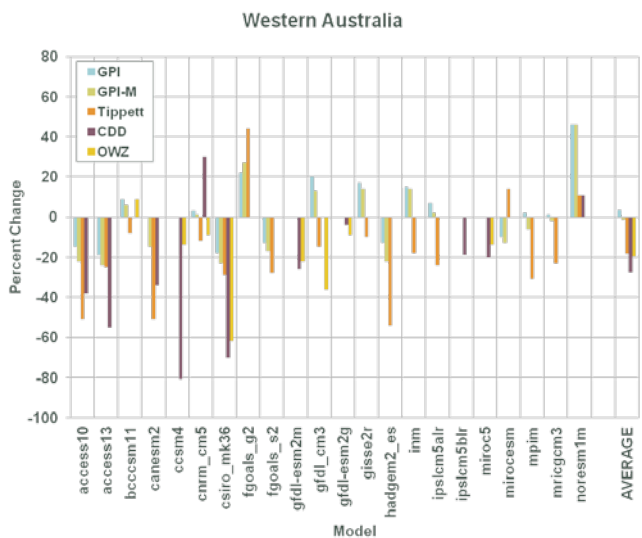


FIGURE 7.3.6: AS FOR FIG 7.3.5 FOR WESTERN AUSTRALIA (0-40 °S; 90-130 °E).

above. A decrease in the number of winter deep low pressure systems impacting south-west Western Australia is projected through this century by a number of CMIP3 models under the A2 scenario (Hope *et al.* 2006). That study showed fewer weather disturbances. This aligns with the atmosphere in the region becoming increasingly stable through this century as shown by Frederiksen *et al.* (2011). There is a projected decrease in the number of fronts across most models in the south and an associated decrease in frontal rainfall, particularly in the south-west by 2090 (Catto *et al.* 2013). In summer, the results are less clear, as the interactions between frontal systems and the continent



are markedly different due to a stronger thermal contrast between the land and the ocean. For example, Hasson *et al.* (2009) found that intense frontal systems affecting south-eastern Australia associated with extreme winds and dangerous fire weather will increase strongly by end of the 21st century although this increase is strongly dependent on the emission scenario considered for the projections. Cut-off lows are also important rain-bearing low pressure systems across southern and eastern Australia (Risbey *et al.* 2009a, Pook *et al.* 2012). In CCAM and an example CMIP3 model these are projected to decline (Grose *et al.* 2012).

In eastern Australia, cut-off lows are often termed East Coast Lows and are very important for rainfall (Pepler and Rakich, 2010, Dowdy *et al.* 2013b). These and other types of cut-off lows in Australia are influenced by blocking in the Tasman Sea (Pook *et al.* 2013). Throughout the 21st century, climate models project a continuation of the decreasing trend in East Coast Low occurrence that has been observed over the last 30 years (Dowdy *et al.* 2013c, Dowdy *et al.* 2014). The projected trend results in an approximately 30 % reduction in East Coast Low formation in the late 21st century compared to the late 20th century. The changes in intensity of cut-off lows have been investigated for Tasmania in CCAM downscaling of CMIP3 models and there is some indication that the most severe cut-off lows could increase in their severity (Grose *et al.* 2012).

In summary, mid-latitude weather systems are projected to shift south and the westerlies are projected to strengthen (*high confidence*). Concurrent and related changes in various measures of mid-latitude circulation are projected, including an increase in the Southern Annular Mode, a decrease in the number of deep lows affecting south-west Western Australia and a decrease in the number of fronts in southern Australia.

7.4 SOLAR RADIATION

MORE SUNSHINE IN WINTER AND SPRING

There is *high confidence* in little change in solar radiation over Australia in the near future (2030). Late in the century (2090), there is *medium confidence* in an increase in winter and spring in southern Australia. The increases in southern Australia may exceed 10 % by 2090 under RCP8.5.

Changes in solar radiation would have impacts on many sectors including agriculture and livestock, health, ecosystems and energy. The CMIP5 simulations indicate that, as in the case of rainfall, natural variability in solar radiation remains large compared to the greenhouse gas induced climate signal over time (Figure 7.4.1). Annual results (not shown) indicate generally little change in Northern Australia and Rangelands, whereas increases are

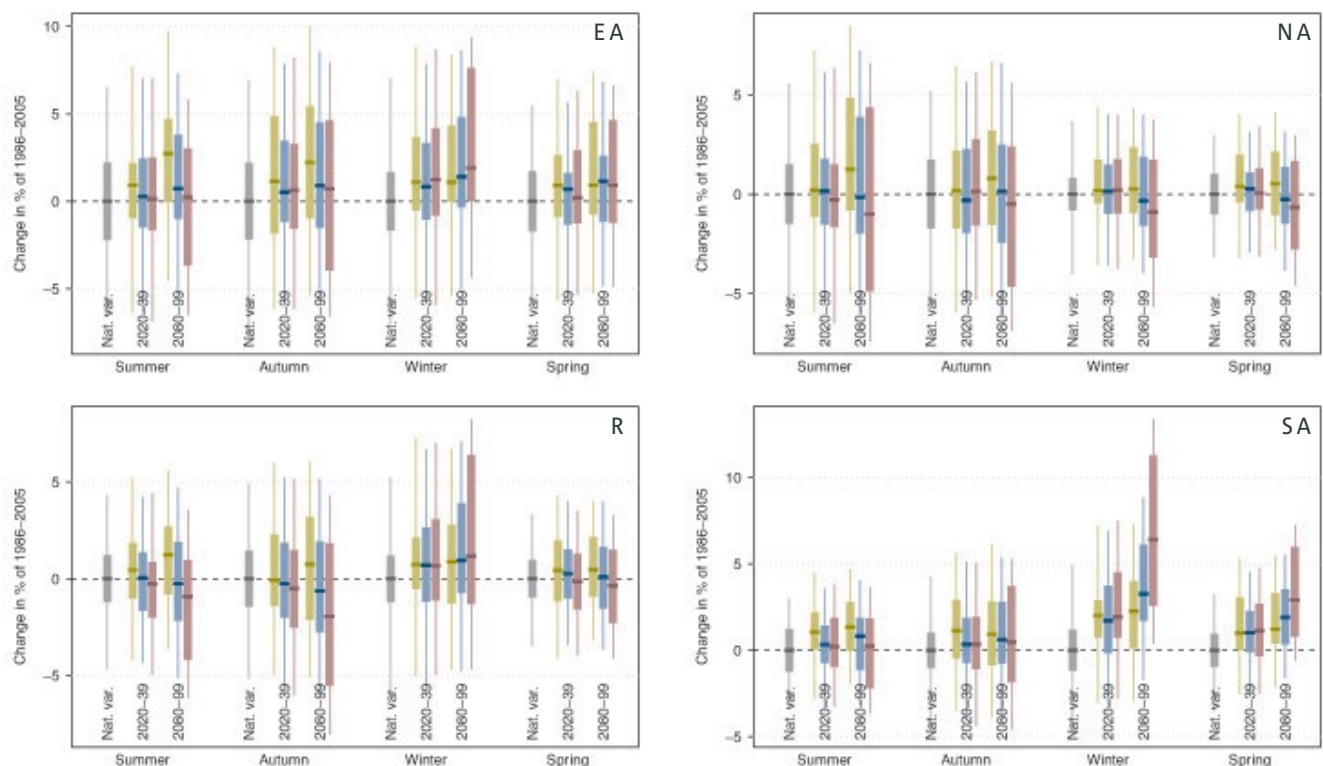


FIGURE 7.4.1: MEDIAN AND 10TH TO 90TH PERCENTILE RANGE OF PROJECTED SEASONAL SOLAR RADIATION CHANGE FOR 2020–2039 AND 2080–2099 RELATIVE TO THE 1986–2005 PERIOD (GREY BAR) FOR RCP2.6 (GREEN), RCP4.5 (BLUE) AND RCP8.5 (PURPLE) FOR FOUR SUPER-CLUSTER REGIONS. FINE LINES SHOW THE RANGE OF INDIVIDUAL YEARS AND SOLID BARS FOR TWENTY YEAR RUNNING MEANS.

-20° -10° 0° 10° 20° 30° 40° 50°

evident in Southern and Eastern Australia, consistent with previous projections (CSIRO and BOM, 2007). The increases for Southern Australia are generally less than 3% even by 2090 under RCP8.5. The results by season (Figure 7.4.1) show that the southern Australian increase is primarily in winter and spring. For other regions, the signal is mixed although the median values indicate a small increase in Eastern Australia and Rangelands, and a small decrease in Northern Australia. In summer and autumn in 2090, the median values indicate a small increase in all regions for RCP2.6 scenario, and no-change or small decrease for RCP4.5 and RCP8.5, although changes outside that expected due to natural variability are simulated by some models. In general, the pattern of the change is the opposite to that of rainfall (Section 7.2).

Projections for relative surface downwelling shortwave radiation change from 1986-2005 to 2080-99 according to RCP8.5

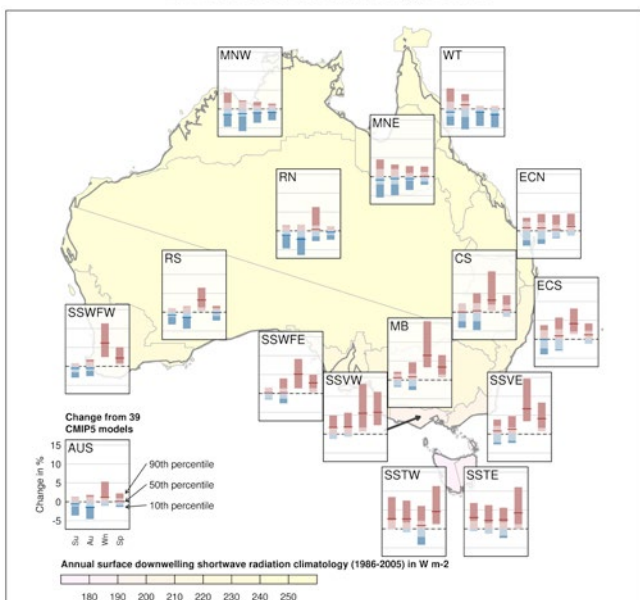


FIGURE 7.4.2: MEDIAN AND 10TH TO 90TH PERCENTILE RANGE OF PROJECTED CHANGES IN SEASONAL SOLAR RADIATION FOR 2080–2099, RELATIVE TO 1986–2005, FOR RCP8.5 FOR 20-YEAR MEANS IN SUB-CLUSTERS. RED INDICATES INCREASE AND BLUE DECREASE (SEE KEY) AND PALER PORTION OF THE BAR IS THE 10TH TO 90TH PERCENTILE RANGE EXPECTED FROM NATURAL VARIABILITY. THE SOLAR RADIATION CLIMATOLOGY OVER THE 1986–2005 PERIOD IS INDICATED BY THE COLOUR OF THE SHADING ON THE MAP OF AUSTRALIA.

Examining finer spatial variations in projected solar radiation change (Figure 7.4.2), it can be seen that the increases in winter and spring under high forcing (2090 and RCP8.5) are present in all the southern regions, whereas a decrease is evident over the Monsoonal North. The summer and autumn signal is mixed in almost all southern regions, except for increases in Tasmania and south-west Victoria. Again, the direction of changes in radiation is in general negatively related to changes in rainfall (Section 7.2), since less/more rainfall often means more/less radiation. A further comparison also reveals that overall the projected change in radiation is the opposite to that of the cloud condensed water content, a measure of the mass of water in cloud in a specified amount of dry air (not shown).

To a large extent, these new projections are consistent with the previous ones (CSIRO and BOM, 2007), particularly for summer and autumn, and the increase for winter and spring. Compared to CMIP3, CMIP5 generally suggests a larger decrease and a lesser increase over the north (See Appendix A).

In summary, annual radiation observations in Australia show a high year to year variability with no significant long-term change (only a very weak increase) during the latter half of the 20th century (Chapter 4). Such high variability remains strong compared to the greenhouse gas induced climate change signal out to 2100. On a seasonal basis, there are variations in magnitude of changes for the near future and late in the century and across regions. Overall, the new projected changes are consistent with the observed trends and with the 2007 projections. However, an Australian wide model evaluation suggests that not all models can reproduce the climatology of solar radiation reasonably well (Chapter 5), while a global study has shown that as with CMIP3, CMIP5 models underestimate the observed trends in some regions in the world due to an underestimation of aerosol direct radiative forcing and/or a deficient aerosol emission inventories (Allen *et al.* 2013). Nevertheless, there is *high confidence* in little change in solar radiation over Australia in the near future (2030). Late in the century (2090), there is *medium confidence* in a small increase in winter and spring in southern Australia.

7.5 HUMIDITY

LOWER RELATIVE HUMIDITY

Relative humidity is projected to decline in inland regions and where rainfall is projected to decline. By 2030, the decreases are relatively small (*high confidence*). By 2090, there is *high confidence* that humidity will decrease in winter and spring as well as annually, and there is *medium confidence* in declining relative humidity in summer and autumn.

Water vapour (humidity), at the surface, has a role in many hydrometeorological and ecological processes (*e.g.* hydrology, atmospheric heat transport, cloud formation, human comfort and plant transpiration).

Unlike other atmospheric variables, humidity can be measured in different ways. Relative humidity and specific humidity are the common ones, describing the degree of saturation of the air and the amount of water in the air, respectively. Through the Clausius-Clapeyron relation, if relative humidity is constant then specific humidity increases close to exponentially with temperature. Another common measure is the dewpoint temperature which is the temperature to which the air needs to be cooled to allow condensation to occur. The closer the dew point temperature is to the current air temperature, the higher the relative humidity of the air. Chapter 4 describes historical humidity variability based on the observations in Australia.

The new CMIP5 model results for relative humidity show a tendency for a decrease across Australia and in all seasons. This is large compared to natural variability mainly in winter and spring in southern Australia, and especially at 2090 under RCP8.5 (Figure 7.5.1). The magnitude of changes depends on time frame and RCP, but even under RCP8.5 the seasonal changes are generally not outside the range of +1 to -6 %. In the near future (2030), the corresponding range is +1 to -3 %. Increases are present in some models, especially in summer and autumn and in regions other than southern Australia, but in no case does the model median show increase.

Figure 7.5.2 shows seasonal changes for each of the fifteen sub-regions in 2090 under RCP8.5. It is notable here that the magnitude of the decrease has the potential to be larger in the regions with a large inland component and smaller in the more coastally oriented regions, particularly southern ones, such as southern Victorian and Tasmania.

These results are relatively similar to those of CMIP3 (see Appendix A). They are also consistent with the tendency for relative humidity to decline over land with increasing temperature. This has been noted globally in observations and in CMIP5 results and is related to the land warming faster than the neighbouring ocean. This means that moisture laden air moving from oceans to land encounters warmer land than was previously the case, resulting in reduced relative humidity (Simmons *et al.* 2010, IPCC,

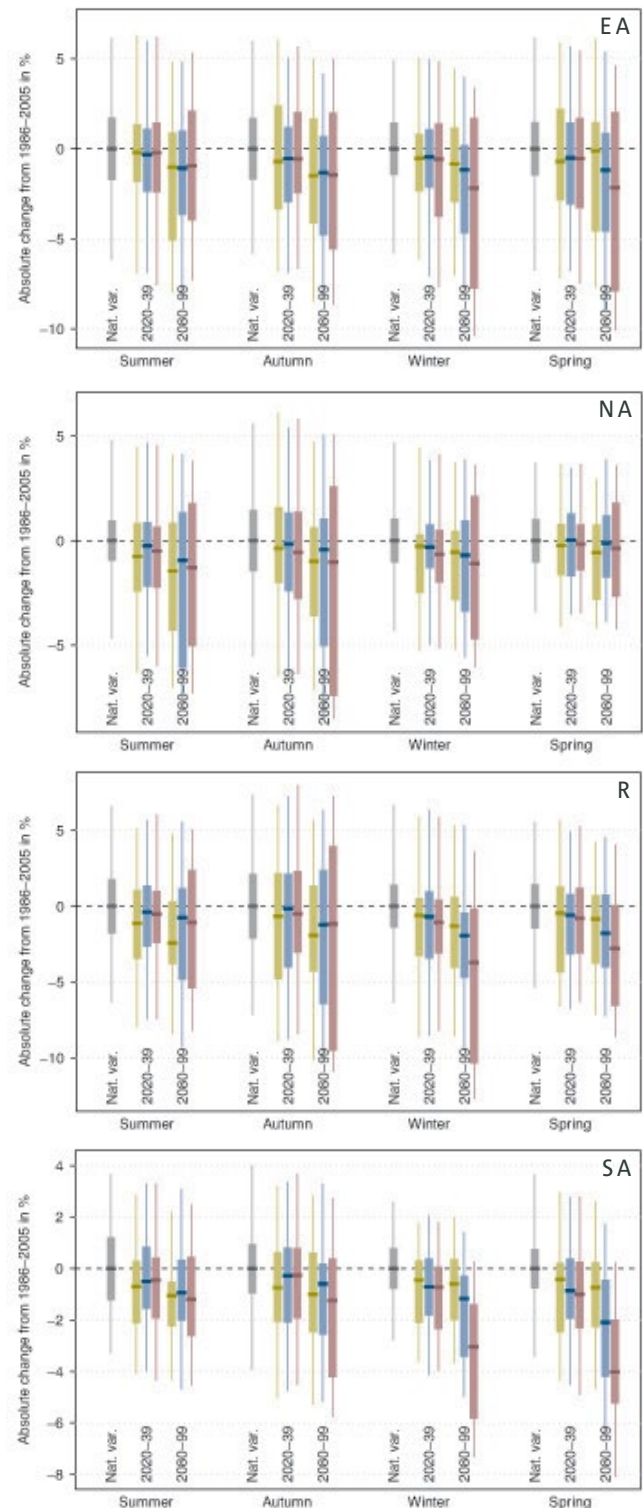


FIGURE 7.5.1: MEDIAN AND 10TH TO 90TH PERCENTILE RANGE OF PROJECTED SEASONAL RELATIVE HUMIDITY CHANGE FOR 2020–2039 AND 2080–2099 RELATIVE TO THE 1986–2005 PERIOD (GREY BAR) FOR RCP2.6 (GREEN), RCP4.5 (BLUE) AND RCP8.5 (PURPLE) FOR FOUR SUPER-CLUSTER REGIONS. FINE LINES SHOW THE RANGE OF INDIVIDUAL YEARS AND SOLID BARS FOR TWENTY YEAR RUNNING MEANS.

2013, Chapter 12). The stronger tendency is for a decrease in southern areas (including coastal areas) in winter and spring, and is clearly related to the simulated reduction in rainfall in those regions and seasons (Section 7.2).

In summary, the pattern of change simulated in CMIP5 is consistent with a general tendency for reduced relative humidity over land and in regions where rainfall is projected to decline. Australia-wide annual humidity observations also show a weak long-term drying – at roughly the same rate as that identified globally (e.g. (Dai, 2006, Simmons *et al.* 2010), although it is unclear whether the Australian observed changes are due to an anthropogenic cause (see Chapter 4). It may also be noted that CMIP3 model results have been shown to simulate climatological means and interannual variability of humidity characteristics well compared to the observations (Willett *et al.* 2010). It is concluded that there is a *high confidence* that humidity will decrease in winter and spring as well as annually, and there is a *medium confidence* of a decline in summer and autumn in 2090. In the near future (2030) the decreases are relatively small (i.e. less than 3%), thus there is a *high confidence* in modest change in the near future.

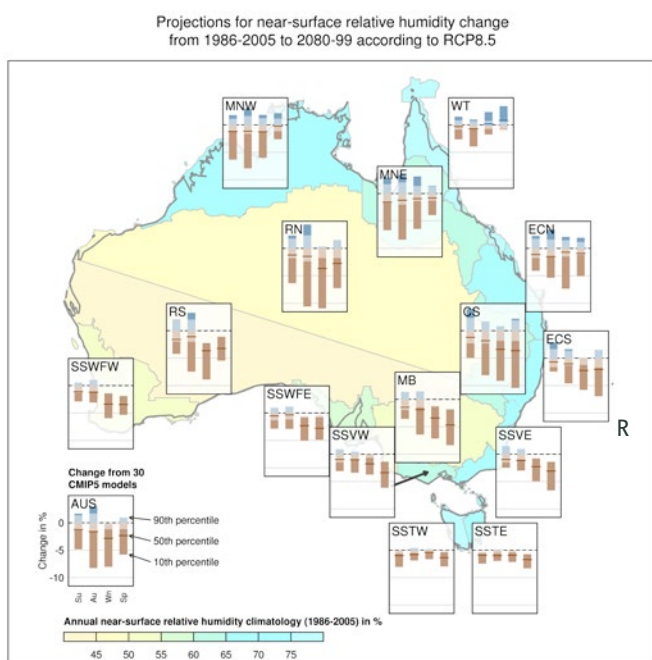


FIGURE 7.5.2: MEDIAN AND 10TH TO 90TH PERCENTILE RANGE OF PROJECTED SEASONAL RELATIVE HUMIDITY CHANGES FROM CMIP5 MODELS FOR 2080–2099 RELATIVE TO 1986–2005 FOR RCP8.5 FOR 20-YEARS MEANS IN SUB-CLUSTERS. THE BARS FOR 15 REGIONS OVERLIE A MAP WITH EACH REGION COLOURED TO INDICATE ITS BASE MODEL CLIMATE AVERAGE. BLUE INDICATES INCREASE AND BROWN DECREASE (SEE KEY) AND PALER PORTION OF THE BAR IS THE 10TH TO 90TH PERCENTILE RANGE EXPECTED FROM NATURAL VARIABILITY. THE RELATIVE HUMIDITY CLIMATOLOGY OVER THE 1986–2005 PERIOD IS INDICATED BY THE COLOUR OF THE SHADING ON THE MAP OF AUSTRALIA.

7.6 POTENTIAL EVAPOTRANSPIRATION

HIGHER EVAPORATION RATES

There is *high confidence* in increasing potential evapotranspiration (atmospheric moisture demand) closely related to local warming, although there is only *medium confidence* in the magnitude of change.

Evapotranspiration is a collective term for the transfer of water vapour to the atmosphere from both vegetated and unvegetated land surfaces. It is a key component in the water balance of a system such as a landscape, catchment or irrigation region. In practice, actual evapotranspiration is rather difficult to measure and its estimate is often based on information about potential evapotranspiration and soil moisture. Potential evapotranspiration is often regarded as the maximum possible evaporation rate that would occur under given meteorological conditions if water sources were available. It is commonly estimated through pan evaporation, that gives a measure of potential evaporation over a small open water body, or alternatively it is estimated using a formulation which considers meteorological variables affecting evapotranspiration (see McMahon *et al.* (2013) for a detailed practical guide).

Generally, it is expected that potential evapotranspiration will increase with increasing temperatures and an intensifying hydrologic cycle (Huntington, 2006). The previous projections, based on CMIP3 models, of annual potential evapotranspiration indicated increases over Australia (CSIRO and BOM, 2007). The multi-model median estimates in 2070 under the high emission scenario (A1FI) were six percent in the south and west, and ten percent in the north and east.

Those estimates are based on the *Morton model* (Morton, 1983), which has been widely used in Australia including in constructing Australia's evaporation atlas (BOM, 2001) and in the hydrological impact of climate change on major Sustainable Yields assessment projects in Australia (e.g. Chiew *et al.* 2008). The Morton model requires input of air temperature, relative humidity and downward solar radiation at the surface, but not the wind speed. It parameterises the vapour transfer coefficient which is dependent on atmospheric pressure, but not directly on wind speed. This approach was found to have a small mean annual error (i.e. less than 2.5% of mean annual rainfall) (Hobbins *et al.* 2001). Also, the method compares favourably with other methods for calculating potential evaporation in rainfall-runoff modelling (Chiew and McMahon, 1991) and is strongly correlated to the pan evaporation observations (Kirono *et al.* 2009). This provides confidence in the use of the Morton method in Australia. When applied to the CMIP3 model data, the Morton model results reproduce the spatial distribution of the observed annual mean and coefficient of variation, but show less skill in reproducing the linear trends (Kirono and Kent, 2011).

For this Report, potential evapotranspiration is calculated using the Morton model using the CMIP5 model data. There are three types of evaporation generated using the model, i.e. point potential evapotranspiration, areal potential evapotranspiration and actual evapotranspiration. This Report focuses on the areal potential evapotranspiration, which is also known as wet-environment areal evapotranspiration (McMahon *et al.* 2013). Unlike pan evaporation that represents evaporation occurring from a small area of water surface only, areal potential evapotranspiration represents potential evapotranspiration (from soil, vegetation, and water surfaces) that would occur when moisture supply was not limited over a large area (greater than 1km²) (BOM, 2001). The climatology over Australia indicates that both point and areal potential evapotranspiration have similar spatial patterns, but the average areal potential evapotranspiration is lower than the point value (www.bom.gov.au). As in the CMIP3 case, the CMIP5 modelled results reproduce the spatial distribution and annual cycle of the observed climatology (not shown here).

The simulated potential evapotranspiration change for 2030 and 2090 for different emission scenarios (Figure 7.6.1) show a strong tendency for increases throughout Australia in all four seasons. This is also true for annually averaged projections (results not shown). In 2030 the increases are already large compared to natural variability (although

less than 5% in magnitude), and are very marked in 2090 under RCP8.5 (around 10-20% increase seasonally as well as annually). In percentage terms, the largest increase is projected in autumn and winter while the smallest is in summer and spring, although in absolute terms (not shown) the summer changes are the largest. The seasonal changes for each of the 15 sub-regions in 2090 under RCP8.5 (Figure 7.6.2) show a similar pattern at the sub-regional level, although the relative increase in winter is particularly noticeable in the south-east of the continent.

In summary, an increase in areal potential evapotranspiration can be projected with *high confidence*. The increasing trend emerges even in the near future (2030). This increase agrees with theoretical expectations, and is consistent amongst almost all CMIP5 models (and CMIP3 models). However, *medium confidence* is placed on the magnitude of the increase. This is due to there being no clear changes observed in pan evaporation across Australia in data available since 1970 (Section 4.2) (although it is noted that pan evaporation is a different measure to areal evapotranspiration). Also, it has been shown that some CMIP3 GCMs have a tendency to not reproduce the historical linear trends (Kirono and Kent, 2011).

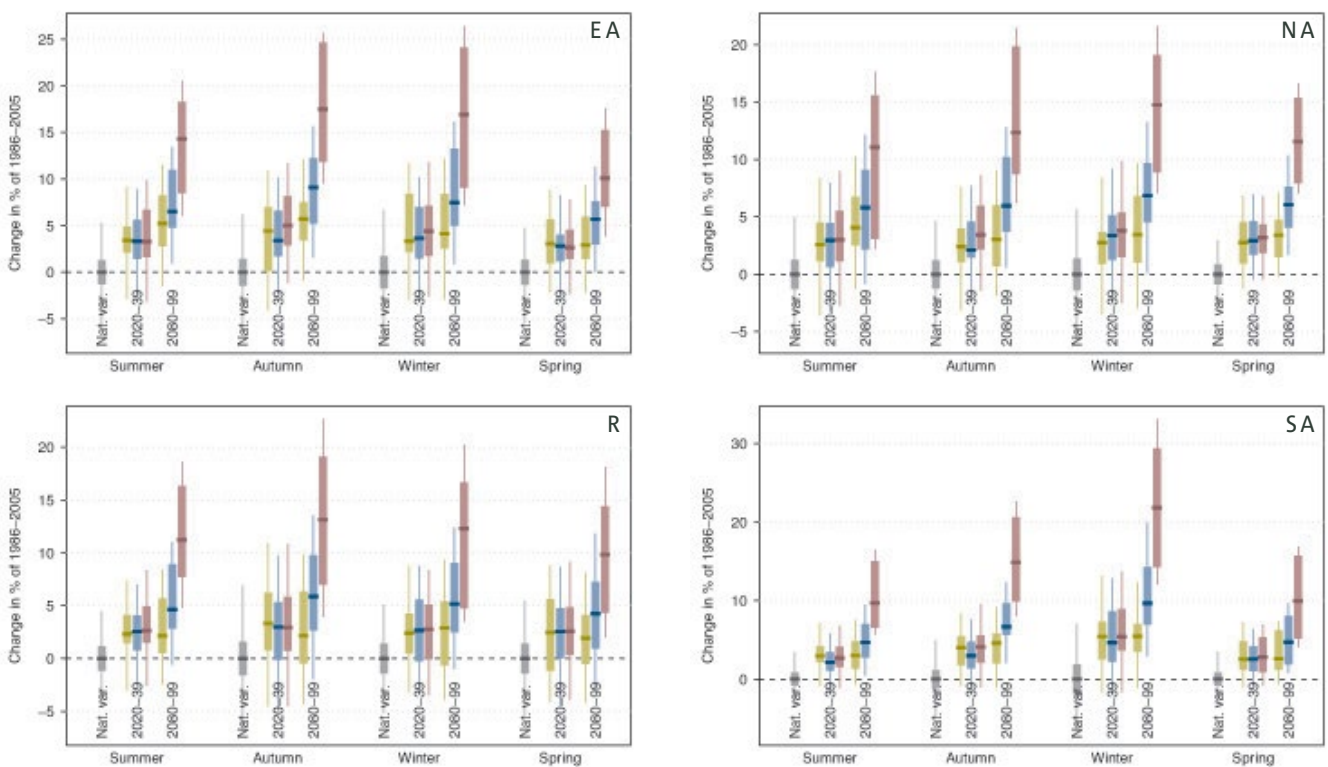


FIGURE 7.6.1: MEDIAN AND 10TH TO 90TH PERCENTILE RANGE OF PROJECTED CHANGE IN SEASONAL POTENTIAL EVAPOTRANSPIRATION FOR 2020–2039 AND 2080–2099 RELATIVE TO THE 1986–2005 PERIOD (GREY BAR) FOR RCP2.6 (GREEN), RCP4.5 (BLUE) AND RCP8.5 (PURPLE) FOR FOUR SUPER-CLUSTER REGIONS. FINE LINES SHOW THE RANGE OF INDIVIDUAL YEARS AND SOLID BARS FOR TWENTY YEAR RUNNING MEANS.

Projections for relative wet-environment potential evapotranspiration change from 1986-2005 to 2080-99 according to RCP8.5

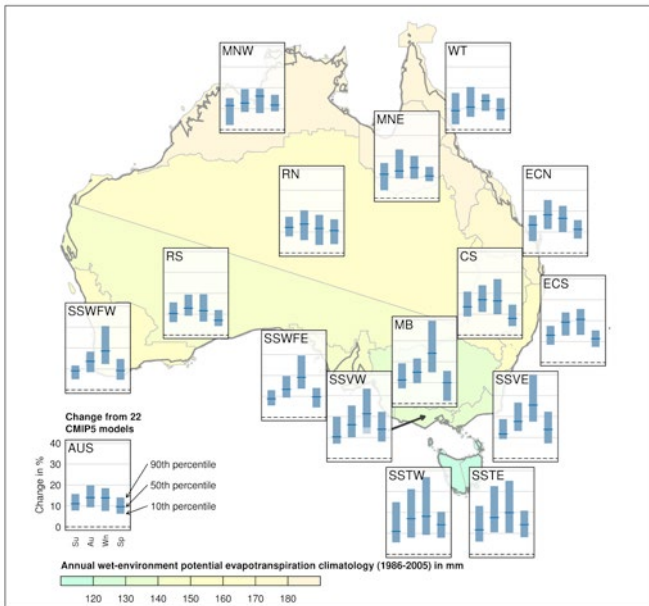


FIGURE 7.6.2 MEDIAN AND 10TH TO 90TH PERCENTILE RANGE OF PROJECTED CHANGE IN SEASONAL WET-ENVIRONMENTAL POTENTIAL EVAPOTRANSPIRATION FOR 2080–2099 RELATIVE TO 1986–2005 FOR RCP8.5 FOR 20-YEAR MEANS IN SUB-CLUSTERS. BLUE INDICATES INCREASE (SEE KEY) AND PALER PORTION OF THE BAR IS THE 10TH TO 90TH PERCENTILE RANGE EXPECTED FROM NATURAL VARIABILITY. THE POTENTIAL EVAPOTRANSPIRATION CLIMATOLOGY OVER THE 1986–2005 PERIOD IS INDICATED BY THE COLOUR OF THE SHADING ON THE MAP OF AUSTRALIA. THE AUSTRALIAN RESULT IS IN THE BOTTOM LEFT.

7.7 SOIL MOISTURE AND RUNOFF

SOIL MOISTURE IS PROJECTED TO DECREASE AND FUTURE RUNOFF WILL DECREASE.

There is *high confidence* in decreasing soil moisture in the southern regions (particularly in winter and spring) driven by the projected decrease in rainfall and higher evaporative demand. There is *medium confidence* in decreasing soil moisture elsewhere in Australia where evaporative demand is projected to increase but the direction of rainfall change is uncertain.

Decreases in runoff are projected with *high confidence* in south-western Western Australia and southern South Australia, and with *medium confidence* in far south-eastern Australia, where future rainfall is projected to decrease. The direction of change in future runoff in the northern half of Australia cannot be confidently projected because of the uncertainty in the direction of rainfall change.

Runoff is the water that flows into rivers and water bodies. Soil moisture is the water stored in the soil. Broadly, runoff follows the same pattern as rainfall over Australia, with the far north and parts of Tasmania having the highest runoff. Due to the high potential evapotranspiration, and modest or low rainfall (see Section 7.6), most of continental Australia has low mean annual runoff, with little to no runoff in most of interior Australia. Runoff can be highly seasonal, particularly to the north, with most regions having 95 % or more of their runoff occurring during the wet season. These moisture variables are difficult to simulate in GCMs where, due to their relatively coarse resolution, the models cannot simulate much of the rainfall and land surface detail that is important to key hydrological processes. For such reasons, and for consistency with many previous studies, we do not present directly simulated GCM runoff and soil moisture, but rather examine results of hydrological models forced by rainfall and potential evapotranspiration from the same GCMs shown elsewhere in this Report.

7.7.1 PROJECTED CHANGES IN SOIL MOISTURE

Various studies project a wide range of significant changes in soil moisture, driven by changes in rainfall and higher evaporative demand (Chiew, 2006; Hennessy *et al.* 2008). Future soil moisture will decrease where rainfall decreases, and increase where rainfall increases significantly. Where there is a small increase in rainfall, the direction of soil moisture change will depend on the compensating effect of the higher rainfall and higher evaporative demand.

The soil moisture changes reported here are estimated using a dynamic hydrological model based on an extension of the Budyko framework (Zhang *et al.* 2008), forced by monthly rainfall and potential evaporation from the CMIP5 GCMs. Projected change in seasonal average soil-moisture



for 2020-39 and 2080-99 with respect to 1986-2005, under RCP4.5 and RCP8.5, are shown in Figure 7.7.1 (left hand column). Soil moisture, at the broad-scale as presented for Northern Australia, Eastern Australia, the Rangelands and the Southern Australia super-clusters, generally reflects the time lag of rainfall accumulated over several months. Different approaches should therefore generally show similar results, reflecting the changes in the seasonal rainfall inputs and higher potential evapotranspiration (from higher future temperatures). In all time frames, regions and emission scenarios in Figure 7.7.1 a decreasing tendency is evident. In 2030 this is mostly small compared to natural variability, but not in winter in Eastern Australia and the Rangelands, nor in winter and spring in Southern Australia. Changes are larger in 2090, with simulated decreases of up to 15 % in winter in Southern Australia. Figure 7.7.2 shows the projected changes in seasonal average soil moisture for 2080-2099 relative to 1986-2005 for RCP8.5 for each cluster region (detailed discussion can be found in respective Cluster Reports).

In summary, the simulated changes to soil moisture are influenced by the projected changes in rainfall (Section 7.2) and the higher evaporative demand (Section 7.6). There is *high confidence* in decreased soil moisture in the southern regions (particularly in winter and spring) driven by the projected decrease in rainfall and higher evaporative demand. There is *medium confidence* in decreased soil moisture elsewhere in Australia where evaporative demand will increase but the direction of rainfall change is uncertain.

7.7.2 PROJECTED CHANGES IN RUNOFF

Future runoff is strongly influenced by future rainfall, with the percentage change in annual rainfall in Australia generally amplified 2-3 times in the percentage change in annual runoff (Chiew, 2006). Runoff is also influenced by temperature, and the higher potential evaporation associated with each 1 °C increase in temperature will reduce annual runoff by 2–5 % (although some studies report bigger reductions) (Chiew, 2006, Cai and Cowan, 2008, Potter *et al.* 2008).

Reported here are projections of annual runoff estimated using the empirical Budyko energy and water balance relationship (Teng *et al.* 2012). The Budyko relationship is used here because it is simple and can provide estimates of changes in long-term average runoff resulting from changes in long-term average rainfall and potential evapotranspiration. As the Budyko relationship applies to long-term water and energy balances, the runoff projection plots show 30-year moving averages and the 20-year results presented here also come from these 30-year running means.

The projected range of change in annual runoff in the four broad regions across Australia are shown above in Figure 7.7.1 (right hand column), for 2020-39 and 2080-2099 relative to the present, under RCP4.5 and RCP8.5. The range of future runoff projections is large, mainly because of the uncertainty in the rainfall projections. The median runoff

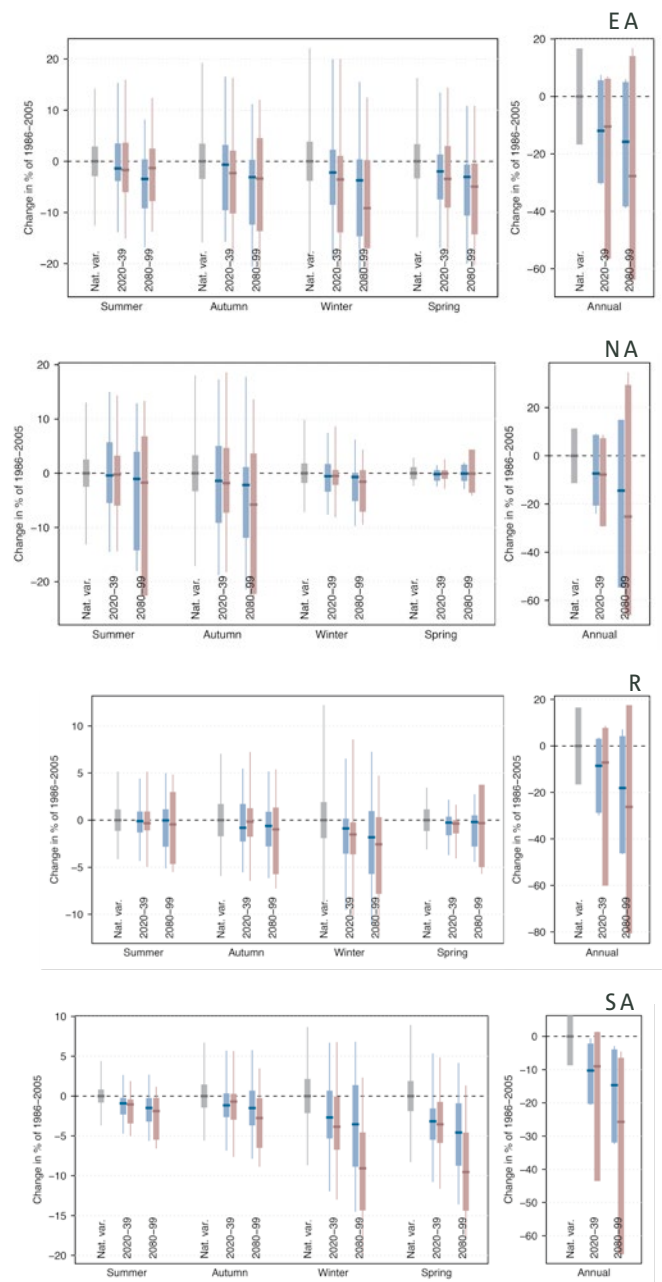


FIGURE 7.7.1: MEDIAN AND 10TH TO 90TH PERCENTILE RANGE OF PROJECTED CHANGE IN SEASONAL SOIL MOISTURE (LEFT COLUMN) AND ANNUAL RUNOFF (RIGHT COLUMN) FOR 2020-39 AND 2080-99 WITH RESPECT TO 1986-2005 ASSOCIATED WITH NATURAL VARIABILITY ONLY (GREY), RCP4.5 (BLUE) AND RCP8.5 (PURPLE). FINE LINES SHOW THE RANGE OF INDIVIDUAL YEARS AND SOLID BARS FOR TWENTY YEAR RUNNING MEANS.

projections show a general decrease. In Southern Australia practically all models show a decrease by 2090, ranging from around zero to -30 % and zero to -60 % under RCP4.5 and RCP8.5, respectively. Model median results are similar in the Rangelands, Eastern Australia, and Northern Australia although increase is evident in some models (a range of around +10 to -40 % for RCP4.5 and +30 to -70 % for RCP8.5). Results vary somewhat amongst individual cluster regions (Figure 7.7.2) with much stronger consistency for a decrease in south-west Western Australia.

It should be noted that the Budyko relationship does not take into account the influence of other climate factors on runoff, such as potential changes in seasonal rainfall and high intensity rainfall. The former is important in regions like south-east Australia where rainfall in many catchments is relatively uniform through the year while most of the runoff occurs in winter. The future annual runoff is therefore more dependent on changes in the cool season rainfall than the summer or annual rainfall. Future projections indicate a likely decline in winter rainfall (with less agreement in the direction of change in summer rainfall) in far southern Australia, and by not taking this into account, the Budyko relationship will overestimate future runoff (or underestimate the decline in future runoff).

By contrast, extreme high rainfall is likely to be more intense in the future (Section 7.2). As a significant amount of runoff is generated during high rainfall events and multi-day rainfall events, by not taking this into account, the Budyko relationship will underestimate future runoff (or underestimate the increase in regions where higher future runoff is projected, or overestimate the decline in regions where lower future runoff is projected). In addition, projections into the more distant future will need to also consider potential changes in the climate-runoff relationship and vegetation characteristics in a significantly warmer and higher CO₂ world. This explains why the runoff projections shown here may be different to those obtained from detailed hydrological modelling or directly from global climate models.

The range of potential change in long-term average runoff presented here is useful for broad-scale or initial assessment of climate change impacts on the many sectors affected by water. For more detailed impact assessment and adaptation studies, hydrological modelling with appropriate downscaled and regional climate scenarios can provide more reliable estimates of future average runoff and other runoff characteristics (Chiew *et al.* 2009b, CSIRO, 2012).

There are a number of larger regional hydrological modelling studies reporting projections of future runoff. These include the CSIRO Sustainable Yields projects (Chiew *et al.* 2009a for Murray-Darling Basin, Charles *et al.* 2010 for far south-west Australia, Petheram *et al.* 2009 for northern Australia, and Post *et al.* 2009 for Tasmania), South Eastern Australian Climate Initiative (Post *et al.* 2012) and Vaze and Teng (2011) for New South Wales. These studies differ in the choice of hydrological models, method used to construct future climate scenarios and the range of global climate models used (typically CMIP3), but the broad projections in long-term average annual runoff are consistent to those presented here.

In summary, the simulated changes in runoff are strongly influenced by the projected changes in rainfall and their uncertainties (Section 7.2). Decreases in runoff are projected with *high confidence* in the Southern and South-western Flatlands region (Southern Australia and south-western Western Australia), where the decrease in rainfall is most strongly indicated, and with *medium confidence* in far south-eastern Australian, where rainfall is also projected to decrease. The direction of change in runoff in the northern half of Australia is less certain because of the uncertainty in the direction of rainfall change.

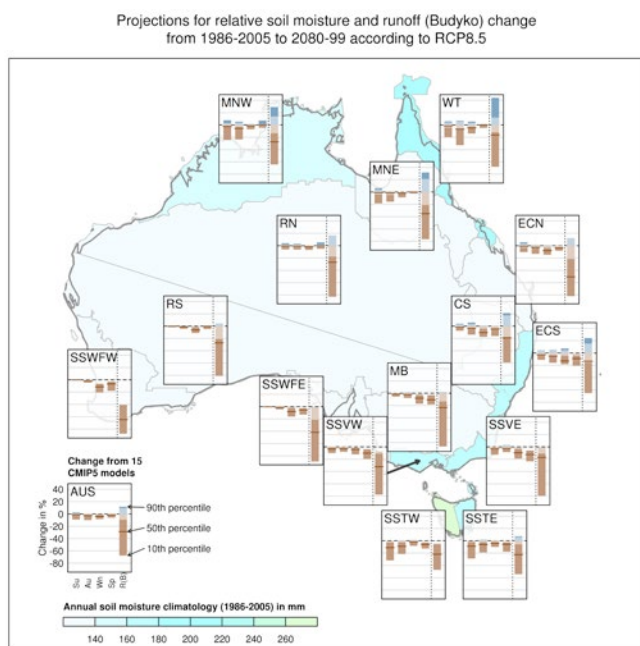


FIGURE 7.7.2: MEDIAN AND 10TH TO 90TH PERCENTILE RANGE OF PROJECTED CHANGES IN SEASONAL AVERAGE SOIL-MOISTURE (LEFT PANEL) AND ANNUAL RUNOFF (R(B): RIGHT PANEL) FOR 2080–2099 RELATIVE TO 1986–2005 FOR RCP8.5 (IN PERCENT) FOR SUB-CLUSTERS. BLUE INDICATES INCREASE AND BROWN DECREASE (SEE KEY) AND PALER PORTION OF THE BAR IS THE 10TH TO 90TH PERCENTILE RANGE EXPECTED FROM NATURAL VARIABILITY. IN THE BACKGROUND IS CLIMATOLOGICAL ANNUAL AVERAGE SOIL-MOISTURE SIMULATED FROM OBSERVED RAINFALL AND POTENTIAL EVAPORATION (SILO GRIDDED DATASETS).



7.8 FIRE WEATHER

SOUTHERN AND EASTERN AUSTRALIA ARE PROJECTED TO EXPERIENCE HARSHER FIRE WEATHER; CHANGES ELSEWHERE ARE LESS CERTAIN

Projected warming and drying in southern and eastern Australia will lead to fuels that are drier and more ready-to-burn, with increases in the average forest fire danger index and a greater number of days with severe fire danger (*high confidence*).

There is *medium confidence* that there will be little change in fire frequency in tropical and monsoonal northern Australia. There is *low confidence* in projections of fire risk in the arid inland areas where fire risk is dependent on availability of fuel, which is driven by episodic rainfall.

Bushfire occurrence at a given place depends on four ‘switches’: 1.) ignition, either human-caused or from natural sources like lightning; 2.) fuel abundance or load – a sufficient amount of fuel must be present; 3.) fuel dryness, where lower moisture contents are required for fire, and; 4.) suitable weather conditions for fire spread, generally hot, dry and windy (Bradstock, 2010). The settings of the switches depend on meteorological conditions across a variety of time scales, particularly the fuel conditions. Given this strong dependency on the weather, climate change will have a significant impact on future fire weather (e.g. Hennessy *et al.* 2005, Lucas *et al.* 2007, Williams *et al.* 2009, Clarke *et al.* 2011a, Grose *et al.* 2014b).

Fire weather is estimated here using the McArthur Forest Fire Danger Index (FFDI; McArthur, 1967), which captures two of the four switches. The fuel dryness is summarised by the drought factor (DF) component of FFDI, a metric ranging from 0 to 10, that indicates the fuel’s readiness to burn. The DF varies in response to both long-term and short-term rainfall. See Lucas (2010b) for an example of these dependencies. The FFDI also captures the ability of a fire to spread, as the temperature, relative humidity and wind speed are direct inputs into the calculation. Fuel abundance is not measured by FFDI, but does depend on rainfall to first order. Higher rainfall totals generally result in a larger fuel load, particularly in regions dominated by grasslands. The FFDI does not consider ignitions.

A set of eight CMIP5 models were selected for the provision of application-ready data, based on current climate performance, data availability and adequate representation of the span of projected climate change in CMIP5 (See Box 9.2 in Chapter 9). Due to the specific data format requirements of the fire weather assessment, and project resource limitations, it was only possible to use a sample of three of these eight CMIP5 GCMs (GFDL-ESM2M, MIROC5 and CESM-CAM5). Despite the use of a small sample and regional variation, representation of the range of future climates is reasonable, with MIROC5 and CESM-CAM5

generally in the middle to the wetter end of the range of rainfall projections and GFDL-ESM2M toward or at the dry end (see the model distribution of projected rainfall changes in Figures 9.9 and 9.10 in Chapter 9).

From these models, monthly-mean changes to maximum temperature, rainfall, relative humidity and wind speed were calculated for each sub-cluster over 30 year time-slices centred on 2030, 2050, 2070 and 2090. Following Hennessy *et al.* (2005) and Lucas *et al.* (2007), the mean changes from these models were applied to observation-based high-quality historical fire weather records (Lucas, 2010b). Generally, these stations are the same as those selected for the study of Clarke *et al.* (2013). A period centred on 1995 (*i.e.* 1981–2010) was chosen as the baseline. The observed station records of maximum temperature, relative humidity, rainfall and wind speed were modified using the model-derived changes for each time-slice and emission scenario. From these adjusted records, future fire weather was estimated using the FFDI. Severe fire weather occurs when the FFDI exceeds 50, the level where the human impacts of bushfire rapidly increase (e.g. Bianchi *et al.* 2010). Being based on observed records, this methodology maintains the observed variability of past fire weather, preserving the relationship between the variables and avoiding potential issues of model bias. However, by fixing this variability, any future changes that may be important to future fire weather, such as a change in the frequency of El Niño events, will not be captured; the observed interannual and decadal variability is not changed. This approach is good at capturing the mean changes to FFDI, while approaches based on direct use of climate model output (Clarke *et al.* 2011a) or dynamical downscaling (Grose *et al.* 2014b) may better capture changes to the extremes and overall variability of fire weather.

In southern and eastern Australia, significant fire activity occurs primarily in areas characterised by forests and woodlands; fuel is abundant and the ‘weather switch’, well-characterised by FFDI, is key to fire occurrence. The results show the future as having a harsher annual-mean fire weather climate in these areas (Table 7.8.1). In both super-clusters, the simulations suggest progressively warmer and drier future climates. In Southern Australia, the results from the models used suggest a 15–25 % reduction in rainfall on average, particularly focused on the Murray Basin. The average decline is 10–15 % in Eastern Australia, with large declines in south-east Queensland in particular (see further discussion of projected rainfall change in Section 7.2). The simulated reduction in rainfall leads to higher drought factors (DF), which implies drier, more ready-to-burn fuels. Simulations also indicate a greater number of ‘severe’ fire danger days. Across both super-clusters, these number of severe days increases by up 160–190 % in the worst case 2090 scenario (driest model, RCP8.5), nearly a threefold increase. Increases of 30–35 % in annual total FFDI (\sum FFDI from July to June) are also simulated by 2090 in the worst case, indicating a broad increase in fire weather conditions.

–20° –10° 0° 10° 20° 30° 40° 50°

Many stations in these two super-clusters overlap with those used by Lucas *et al.* (2007). The 2050 RCP8.5 estimates from this study (not shown) are similar to the high global warming results shown in Lucas *et al.* (2007), although individual stations may be different.

There is also sub-regional uncertainty in the projections, largely driven by the spread in rainfall projections amongst the models. For instance, the considerably drier GFDL-ESM2M model results in a harsher fire weather climate than what is reflected by the average values shown here. As shown in the Cluster Reports, changes to Σ FFDI are upwards of 50 % at many stations in the worst case, indicating higher trends than the average. However, it should also be noted that Section 7.2, based on a range of evidence additional to the full range of GCM results, concluded that a decrease in rainfall in eastern Australia could only be confidently projected in winter (although confidence in southern Australian decreases was much higher). Nevertheless, models projecting greater rainfall may reduce the size of the change in FFDI, but probably not its direction. Hence, there is *high confidence* placed in the

direction of change (i.e. harsher fire weather climates) in southern and eastern Australia, but less on the magnitude of the future change.

In Northern Australia and the Rangelands, the weather conditions are often conducive to fire activity, and the limiting switch in these regions is fuel availability (*e.g.* Williams *et al.* 2009). In this case FFDI is not as relevant to understanding future fire activity. In Northern Australia, bushfire is frequent, occurring on an annual basis in some areas, as abundant wet season rainfall drives vegetation growth that dries and eventually burns during the following dry season. Moving southward into the Rangelands, the average rainfall amount declines, vegetation becomes sparser and bushfire is correspondingly rarer. In more arid regions, the rainfall is subject to higher interannual variability, driven by tropical cyclones, the position of the monsoon trough and large-scale factors like the El Niño-Southern Oscillation. If there are more extended wet periods, then fuel becomes more abundant and fire risk increases, while more dry periods would lower fuel loads and reduce fire risk.

TABLE 7.8.1: MEAN ANNUAL VALUES OF MAXIMUM TEMPERATURE (T; °C), RAINFALL (R; MM), DROUGHT FACTOR (DF; NO UNITS), THE NUMBER OF SEVERE FIRE DANGER DAYS (SEV; FFDI GREATER THAN 50; DAYS PER YEAR) AND CUMULATIVE ANNUAL FFDI (CUM. FFDI; NO UNITS) FOR THE 1995 BASELINE AND PROJECTIONS FOR 2030 AND 2090 RCP4.5 AND RCP8.5 SCENARIOS. RESULTS ARE ORGANISED BY SUPER-CLUSTER; ALL STATIONS AND THE RESULTS FOR THE THREE MODELS USED WITHIN THE SUPER-CLUSTER ARE AVERAGED FOR EACH TIME-SLICE AND SCENARIO.

SUPER CLUSTER	VARIABLE	1995 BASELINE	2030 RCP4.5	2030 RCP8.5	2090 RCP4.5	2090 RCP8.5
SOUTHERN AUSTRALIA	T	21.1	22.3	22.2	23.2	24.8
	R	614	507	521	509	468
	DF	6.4	6.7	6.6	6.8	7.3
	SEV	2.8	3.6	3.4	3.8	5.3
	cum. FFDI	2772	3043	2978	3132	3638
EASTERN AUSTRALIA	T	25.0	26.1	26.4	27.3	29.0
	R	968	856	830	828	809
	DF	6.4	6.6	6.7	6.8	7.1
	SEV	1.2	1.5	1.8	1.9	3.2
	cum. FFDI	2692	2859	3037	3103	3584
NORTHERN AUSTRALIA	T	30.3	31.2	31.5	32.3	33.8
	R	1235	1193	1194	1256	1217
	DF	7.2	7.3	7.3	7.2	7.3
	SEV	2.5	3.1	3.4	3.6	5.3
	cum. FFDI	3568	3726	3762	3829	4168
RANGELANDS	T	28.4	29.8	29.9	30.8	32.7
	R	318	273	293	293	285
	DF	8.6	8.8	8.7	8.8	8.9
	SEV	12.7	18.6	17.1	18.8	27.6
	cum. FFDI	6949	7784	7530	7763	8709



Section 7.2 and the Cluster Reports for the Wet Tropics and the Monsoonal North indicate *low confidence* in the direction of rainfall change, although rainfall declines are more likely in the inland and southern parts of these clusters. In the Rangelands, the spread of model results is quite large, and reductions are greater in the southern sub-cluster of the Rangelands.

In both Northern Australia and the Rangelands, when and where fire occurs there is *high confidence* that fire behaviour will be more extreme, the result of higher temperatures and a relatively greater number of 'severe' fire danger days. However, projecting specific changes in future fire frequency from the information used in this evaluation is difficult and the projections are limited to general tendencies. In areas where copious amounts of rain already fall, the projected changes in the rainfall are unlikely to have a significant impact on fire frequency; even in the drier GFDL model simulations, there is still a 'wet season' that results in significant rain and the growth of vegetation, leading to bushfire. Thus there is *medium confidence* that there will be comparatively little change in fire frequency in these regions (Top End, Kimberley, Wet Tropics). In southern and inland regions of Monsoon North, the future fire frequency is less clear. If rainfall-producing weather events occur more often (i.e. a change in the frequency of wet years), then more frequent fire activity could be expected. This uncertainty in the future is even larger in the Rangelands, where sufficient rainfall to drive adequate fuel growth for bushfire is very episodic and even more sensitive to the interannual variability that is not suitably accounted for in this analysis. Consequently, there is *low confidence* for fire projections in the Rangelands. Additionally, changes to the vegetation type from the introduction of exotic species and the higher CO₂ background should also be considered. More detailed modelling efforts encompassing these effects are required to address future fire activity.

CHAPTER EIGHT

PROJECTIONS (AND RECENT TRENDS): MARINE AND COASTS



SUNSHINE COAST, QUEENSLAND, ISTOCK

-20° -10° 0° 10° 20° 30° 40° 50°



CHAPTER 8 PROJECTIONS (AND RECENT TRENDS): MARINE AND COASTS

Changes in sea levels and their extremes, sea surface temperatures and ocean pH that have the potential to affect both the coastal terrestrial and marine environments are discussed in this Section. The impact of sea level rise and changes to the frequency of extreme sea levels will be felt through coastal flooding and erosion, and through resulting changes in coastal vegetation (e.g. salt marshes, mangroves and other coastal wetlands). For the adjacent marine environment, increases in ocean temperatures and decreases in pH have the potential to alter the distribution of marine vegetation (e.g. sea grass and kelp forests), increase coral bleaching and mortality, and affect coastal fisheries.

8.1 SEA LEVEL RISE

8.1.1 FACTORS CONTRIBUTING TO SEA LEVEL CHANGE

Global mean sea level (GMSL) changes as a result of changes in the density of the ocean (ocean thermal expansion or contraction) and/or changes in the mass of the ocean through exchanges with the cryosphere (glaciers and ice sheets) and the terrestrial environment (soil moisture, terrestrial reservoirs, lakes, ground water, Etc.). In addition to the global averaged change, changes in relative sea level (i.e. the changes in sea level relative to the land) vary regionally as a result of changes in ocean dynamics (changes in ocean currents related to changes in surface winds, air-sea fluxes of heat and freshwater and internal variability), changes in the Earth's gravitational field as a result of changes in the distribution of water on the Earth, and vertical motion of the land (Church *et al.* 2013, Church *et al.* 2011a, Slangen *et al.* 2012, Church *et al.* 2014).

8.1.2 HISTORICAL GLOBAL MEAN SEA LEVEL CHANGE

Over time scales of hundreds of thousands of years, sea level has varied by over 100 m as the mass of ice sheets (particularly over north America and northern Europe and Asia) waxed and waned through glacial cycles (Foster and Rohling, 2013, Rohling *et al.* 2009). At the time of the last interglacial (129 to 116 thousand years ago), sea level was likely between 5 and 10 m higher than present (Kopp *et al.* 2009, Dutton and Lambeck, 2012, Kopp *et al.* 2013). These higher sea levels occurred under different orbital (solar) forcing and when global averaged temperature was up to 2 °C warmer than preindustrial values and high latitude temperatures were more than 2 °C warmer for several thousand years (IPCC, 2013). Over the following 100,000 years sea level fell as major ice sheets formed over northern America, Europe and Asia.

Since the peak of the last ice age, sea level has risen by more than 120 m (Lambeck *et al.* 2002), mostly from about 20 to 6 thousand years ago, after which contributions from the decaying ice sheets reduced considerably. Over the

last several thousand years, sea levels were comparatively steady with fluctuation in sea level not exceeding 0.25 m on time scales of a few hundred years (Woodroffe *et al.* 2012, Masson-Delmotte *et al.* 2014). Estimates of relative sea level from salt marshes (Gehrels and Woodworth, 2013) and the available long tide gauge records (Jevrejeva *et al.* 2008, Woodworth, 1999) indicate a transition from these low rates of sea level change (order tenths mm yr⁻¹) to 20th century rates (order mm yr⁻¹) in the late 19th to early 20th century.

Between 1900 and 2010, the available tide gauge estimates of GMSL (Church and White, 2006, Church and White, 2011, Jevrejeva *et al.* 2006, Jevrejeva *et al.* 2008, Ray and Douglas, 2011) indicate a rate of rise of 1.7 ± 0.2 mm/yr. All of these analyses indicate significant changes in the rate of rise during the 20th century with the largest rates since 1993 and also in the 1920 to 1950 period. The larger rate of rise since 1993 is also confirmed by the satellite altimeter data (Church *et al.* 2011b, Masters *et al.* 2012 and references therein). The Church *et al.* and the Jevrejeva *et al.* analyses indicate an acceleration (about 0.01 mm yr⁻²) in the rate of sea level rise from the start of the analysis in the late 19th century. However, Ray and Douglas (2011) found no significant acceleration for the 20th century alone.

The large transfer of mass from the ice sheets to the ocean changes the surface loading of the Earth and induces an ongoing response of the viscous mantle of the Earth. As a result, relative sea level has been falling in locations of former ice sheets, rising at faster than the global average rates in the immediately adjacent regions (for example New York) and rising slightly less than the global average in many locations distant from the locations of former ice sheets. For Australia, this means that sea level (compared to present day sea levels) was around a metre or more higher in some parts of Australia several thousand years ago and that the ongoing response of the Earth (Glacial Isostatic Adjustment, GIA) means that relative sea level around Australia is rising about 0.3 mm yr⁻¹ less than it otherwise would (Lambeck, 2002).



8.1.3 THE AUSTRALIAN COASTLINE

A number of studies of the regional distribution of 20th century sea level rise have been completed over recent years, for example the North Sea (Wahl *et al.* 2013), British Isles (Woodworth *et al.* 2009), the English Channel (Haigh *et al.* 2009), the German Bight (Wahl *et al.* 2011), Norwegian and Russian coasts (Henry *et al.* 2012), the Mediterranean (Tsimplis *et al.* 2011, Calafat and Jorda, 2011), USA (Snay *et al.* 2007, Sallenger *et al.* 2012), and New Zealand (Hannah and Bell, 2012). The Australian region is perhaps the best instrumented southern hemisphere location for a comparable assessment (Burgette *et al.* 2013, White *et al.* 2014, whose results are quoted extensively here). However, to date, no coherent and robust global pattern in a regional distribution of sea level rise has been agreed for the 20th century or recent decades, other than that associated with GIA.

Sea level measurements began in Australia with the first sea level benchmark at Port Arthur (Tasmania) in about 1840 (Hunter *et al.* 2003), followed by the installation of tide gauges in Fort Denison (Sydney) and Fremantle (Western Australia). Indeed, Australia has the two longest sea level records in the southern hemisphere; Fort Denison from

1886 and Fremantle from 1897. The number of tide gauges around the Australian coast increased slowly until the mid 1960s. After 1966, there were 16 tide gauges along the Australian coastline (Figure 8.1.1), with at least one gauge in most sections of coast. Since 1993, high quality satellite altimeter data are also available for the surrounding oceans.

There is significant variability in sea level from year to year (Figure 8.1.2) and a single mode represents about 70 % of the total low-frequency variance (White *et al.* 2014). This variability is strongly correlated with the Southern Oscillation Index and propagates through the Indonesian Archipelago to north-western Australia and then propagates anticlockwise around Australia, decreasing in magnitude with distance from Darwin. Removing the signal associated with this mode of variability improves the agreement between long-term records (Figure 8.1.3). These results demonstrate the value of considering regional (spatial scales of order of 1000 km) signals and observations from several tide gauges (rather than just local measurements from a single gauge) when considering sea level variability and change (White *et al.* 2014). Over 1966 to 2009, the average of the relative tide gauge trends is

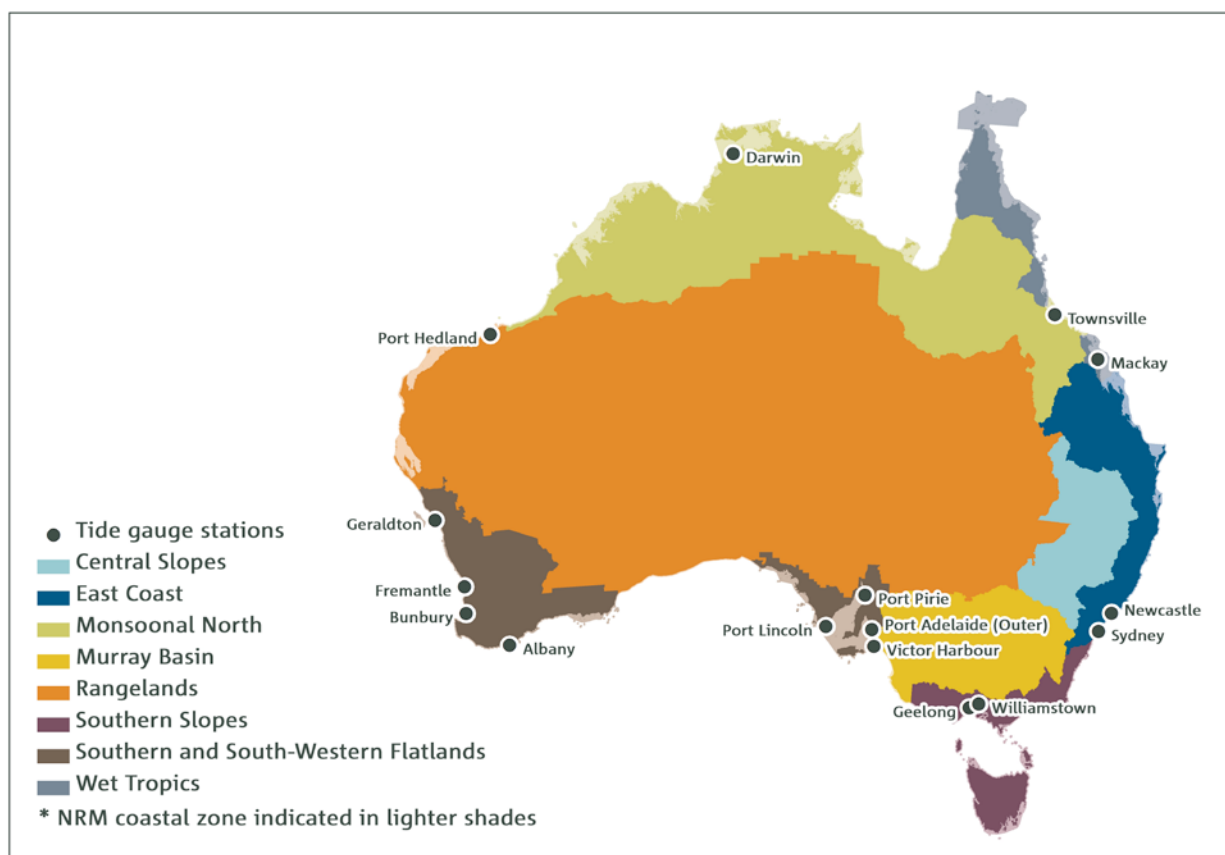


FIGURE 8.1.1: LOCATIONS ALONG THE AUSTRALIAN COASTLINE OF 16 STATIONS WITH NEAR CONTINUOUS TIDE GAUGE RECORDS AVAILABLE FOR THE PERIOD 1966 TO 2010 (SOURCE: WHITE *ET AL.* 2014).



$1.4 \pm 0.2 \text{ mm yr}^{-1}$, ranging from 0.8 mm yr^{-1} at Fort Denison and Victor Harbour to 2.6 mm yr^{-1} at Darwin. When the signal related to the Southern Oscillation Index is removed, the average trend is $1.6 \pm 0.2 \text{ mm yr}^{-1}$. This average is less than the global mean trend of $2.0 \pm 0.3 \text{ mm yr}^{-1}$ over the same period because the land is rising from GIA and atmospheric pressure is increasing at a number of locations in Australia (White *et al.* 2014). If it were not for these factors, the Australian average trend would be larger at 2.1 mm yr^{-1} , ranging from 1.3 mm yr^{-1} at Sydney to 3.0 mm yr^{-1} at Darwin (Figure 8.1.3).

The number of gauges increased further during the late 1980s to early 1990s. For 1993 to 2009, the corresponding average Australian trend in relative mean sea level change

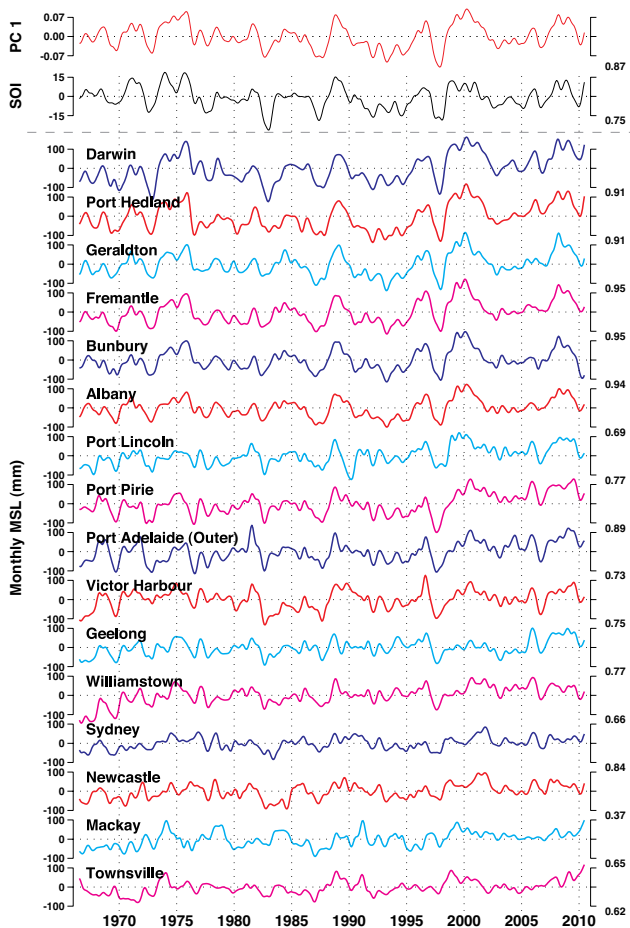


FIGURE 8.1.2: LOW-PASSED RELATIVE MEAN SEA LEVEL FOR THE 16 NEAR CONTINUOUS RECORDS AVAILABLE FOR THE PERIOD 1966 TO 2010, FROM DARWIN IN THE NORTH, ANTICLOCKWISE TO TOWNSVILLE IN THE NORTH-EAST. THE LOW-PASSED SOUTHERN OSCILLATION INDEX AND THE AMPLITUDE (PC1) OF THE SEA LEVEL VARIABILITY REPRESENTING 70% OF THE TOTAL VARIANCE ARE ALSO SHOWN. NOTE THAT THE RECORDS AT PORT ADELAIDE AND NEWCASTLE ARE AFFECTED BY LOCAL LAND SUBSIDENCE (SOURCE: WHITE *ET AL.* 2014).

is $4.5 \pm 1.3 \text{ mm yr}^{-1}$, but 2.7 mm yr^{-1} after the signal correlated with the Southern Oscillation Index is removed, and 3.1 mm yr^{-1} after allowance for GIA and atmospheric pressure changes are also included. The GMSL trend estimated from tide gauge records is 2.0 and 2.8 mm yr^{-1} over 1966 to 2009 and 1993 to 2009, respectively (White *et al.* 2014), and 3.4 mm yr^{-1} as estimated from satellite altimeters over 1993 to 2009 (and 3.2 mm yr^{-1} to December 2013). That is, after correcting for GIA and atmospheric pressure changes, the average of the Australian tide gauge trends are similar to and show a similar increase in rate as the trend in GMSL. At least part of the reason for the spatial and temporal variability in trends around Australia relates to decadal and natural variability.

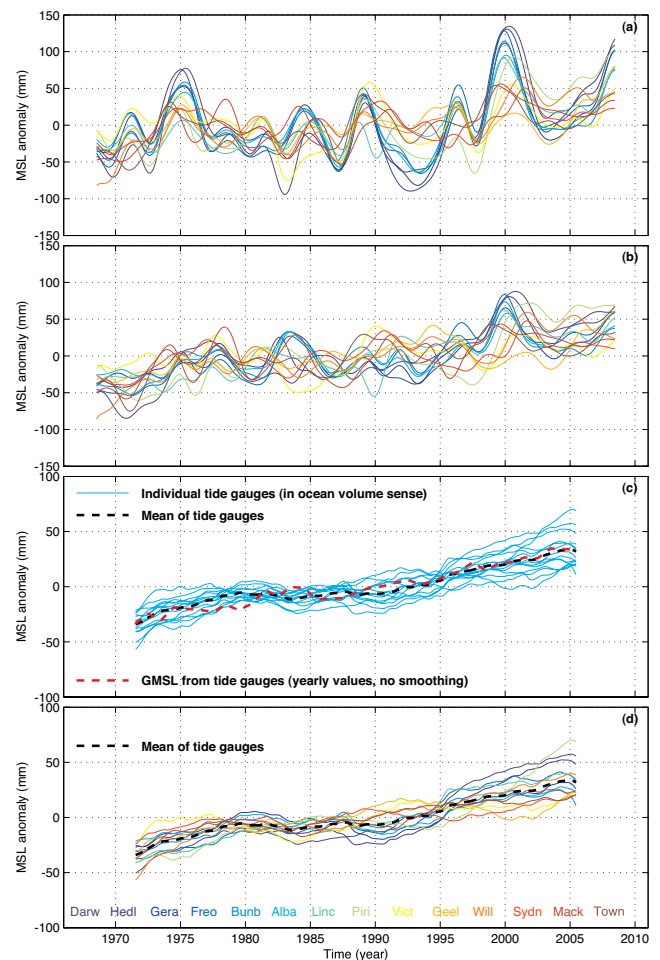


FIGURE 8.1.3: (A) LOW-PASSED RELATIVE MEAN SEA LEVELS FOR THE 14 RECORDS AVAILABLE FOR 1966 TO 2010 THAT ARE USEFUL FOR CALCULATING LONG-TERM TRENDS, AND (B) AFTER THE COMPONENT OF VARIABILITY RELATED TO ENSO HAS BEEN REMOVED. IN (C), THE DATA SMOOTHED WITH A TEN YEAR RUNNING AVERAGE AND CORRECTED FOR GIA AND COMPARED WITH THE AVERAGE OF THE RECORDS AND THE GLOBAL MEAN SEA LEVEL FROM CHURCH AND WHITE (2011). (D) AS IN (C), BUT WITH 14 TIDE GAUGE RECORDS PLOTTED IN DIFFERENT COLOURS TO AID DISTINCTION (SOURCE: WHITE *ET AL.* 2014).

The rates of sea level rise are not uniform around Australia. Over the period from 1993 when satellite altimeter data are available, the sea level trends are larger than the GMSL trend in northern Australia and similar to the GMSL trend in southern Australia (Figure 8.1.4; White *et al.* 2014). The tide gauge and altimeter trends are generally similar, with several exceptions: the tide gauge rates at Hillary's (northern Perth) and Adelaide are larger because of downward land motion; at the Gold Coast Seaway there is an instrumental issue; and the gauges at Eden and Bunbury have trends that are anomalous compared with nearby locations to the north and south that may be related to unresolved datum or vertical land motion issues. Off south-eastern Australia, the altimeter shows a larger trend offshore than the tide gauge trends. This is thought to be associated with a strengthening of the ocean circulation in the South Pacific Ocean and southward extension of the East Australian Current (Hill *et al.* 2011, Deng *et al.* 2010), resulting in lower trends at the coast compared with offshore. The larger rates in northern Australia are largely associated with interannual variability and these larger rates are not representative of a longer term trend (Zhang and Church, 2012, White *et al.* 2014).

The two longest Australian sea level records from Fort Denison Sydney and Fremantle extend back to the late 19th century. The Sydney record appears to contain some anomalous data between 1910 and 1940, with falling sea level near the start of the period and rapidly rising sea level

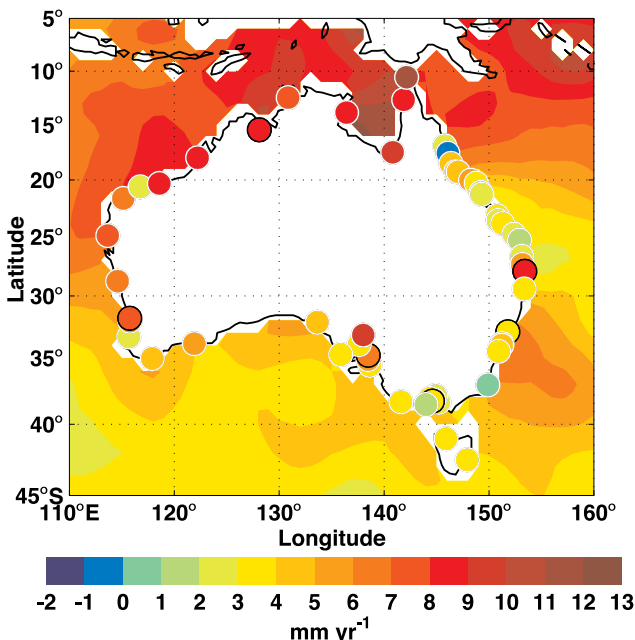


FIGURE 8.1.4: SEA LEVEL TRENDS FROM JANUARY 1993 TO DECEMBER 2010 FROM SATELLITE ALTIMETERS (COLOUR CONTOURS) AND TIDE GAUGES (COLOURED DOTS), BOTH AFTER CORRECTION FOR GLACIAL ISOSTATIC ADJUSTMENT (GIA). THE RED DOT ON THE EAST COAST AT 28 °S IS GOLD COAST SEAWAY.

near the end of this period (White *et al.* 2014). Over the full record from 1886 to 2010, the relative sea level trend at Sydney is $0.65 \pm 0.05 \text{ mm yr}^{-1}$, slightly less than the trend of 0.8 mm yr^{-1} over 1966 to 2010. When this latter period is corrected for GIA and atmospheric pressure changes, the trend is 1.3 mm yr^{-1} , less than the global average trend over 1966 to 2009 of 2.0 mm yr^{-1} . At Fremantle, the relative sea level trend over 1897 to 2010 is $1.6 \pm 0.1 \text{ mm yr}^{-1}$, with a trend of 2.2 mm yr^{-1} over 1920 to 1960, little trend from 1960 to 1990 and 4 mm yr^{-1} over the last two decades.

8.1.4 GLOBAL PROJECTIONS

Ocean thermal expansion and glaciers and ice caps are the main contributors to global mean sea level change during the 20th century and are expected to be the major contributors during the 21st century (see below), with additional contributions from the loss of mass from ice sheets, and changes in the mass of water stored on land.

The methods of Church *et al.* (2014) are used to project future sea level changes by combining projected changes in sea level related to changes in ocean density and circulation (available directly from available CMIP5 GCMs) with contributions derived from purpose-built models designed to estimate additional sea level contributions. These additional contributions are the loss of mass from glaciers, the surface mass balance and the dynamic response of the Greenland and Antarctic ice sheets, changes in land water storage, the mass redistribution from glacier and ice sheet loss and its gravitational response on the ocean, and GIA.

Time series for individual contributions to global mean sea level projections are displayed in Figure 8.1.5. How these contributions and associated uncertainties are combined to form global mean sea level can be found in the supplementary materials of chapter 13 of the IPCC *Fifth Assessment Report* and will not be repeated here.

As in Church *et al.* (2014), global mean sea level change for various contributions under four different RCPs is given in Table 8.1.1. Projected changes for 2090 (the average over 2080 to 2100) compared to 1986–2005 range from 26–55 cm for RCP2.6 (strong mitigation scenario) to 45–82 cm for RCP8.5 (high emissions scenario), where the range represents 90 percent of the model range. Ocean thermal expansion and melting glaciers and ice caps are the main contributors to global mean sea level change. The IPCC *Fifth Assessment Report* concluded that the global mean sea level change was likely to be in the 5-95th percentile range of model results. However, because of uncertainties in climate sensitivity and other parameters, this range is considered to be the likely range covering 66 % of possibilities. It is possible that a larger global mean sea level rise could occur prior to 2100 as a result of an instability of the marine based West Antarctic Ice Sheet, but there is currently insufficient scientific evidence to assign a specific likelihood to values larger than the above likely range. Any additional contribution from the potential collapse of the marine-based sector of the Antarctic Ice Sheet, if initiated, was



assessed not to exceed several tenths of a metre of sea level rise by 2100 (Church *et al.* 2014).

Ocean thermal expansion, glaciers and ice caps are the main contributors to global mean sea level change (about 35 to 45 and 25 to 26 percent of the total, respectively) by

2090 across all RCPs. For RCP8.5 and 6.0, the rate of rise for both contributions increases throughout the 21st century, whereas for RCP2.6 and 4.5, the rate of rise decreases after about 2030 and 2070, respectively (Church *et al.* 2014).

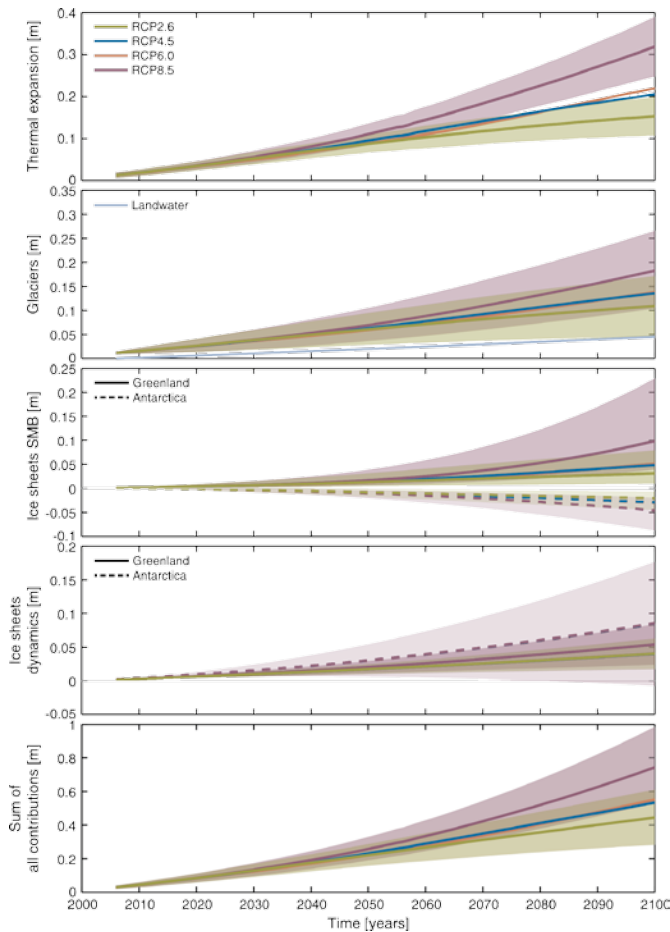
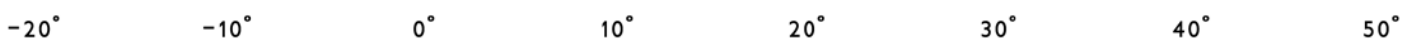


FIGURE 8.1.5: CONTRIBUTIONS (THICK COLOURED LINES) TO 21ST CENTURY SEA LEVEL RISE IN METRES CALCULATED USING THE RESULTS OF INDIVIDUAL GCMS FOR ALL RCPs. (A) GLOBAL AVERAGED OCEAN THERMAL EXPANSION. (B) GLACIER MASS LOSS. (C) CHANGES IN THE SURFACE MASS BALANCE OF THE GREENLAND AND ANTARCTIC ICE SHEETS, (D) ICE SHEET DYNAMICAL CONTRIBUTIONS (E) THE SUM OF ALL CONTRIBUTIONS. FOR RCP8.5 AND RCP2.6 THE MULTI-MODEL MEAN VALUES WITH 5 TO 95 PERCENT UNCERTAINTY RANGES (SHADED AREAS) ARE SHOWN. FOR RCP6.0 AND RCP4.5, ONLY THE MULTI-MODEL MEAN VALUES ARE SHOWN. THE CONTRIBUTION FROM CHANGES IN TERRESTRIAL STORAGE IS NOT SHOWN. NOTE THAT THE RANGES OF SEA LEVEL RISE SHOULD BE CONSIDERED LIKELY (66TH PERCENTILE RANGE) AND THAT IF A COLLAPSE IN THE MARINE BASED SECTORS OF THE ANTARCTIC ICE SHEET WERE INITIATED, THESE PROJECTIONS COULD BE SEVERAL TENTHS OF A METRE HIGHER BY LATE IN THE CENTURY.

TABLE 8.1.1: MEDIAN VALUES AND LIKELY RANGES EXPRESSED IN METRES FOR PROJECTIONS OF GLOBAL AVERAGE SEA LEVEL RISE AND ITS COMPONENTS IN 2081 TO 2100 RELATIVE TO 1986 TO 2005 UNDER FOUR RCPs (BASED ON TABLE 13.5 OF THE IPCC FIFTH ASSESSMENT REPORT). THESE RANGES ARE BASED ON THE 5 TO 95 % RANGE OF MODEL RESULTS FOR SEA LEVEL RISE BUT SHOULD ONLY BE CONSIDERED LIKELY (GREATER THAN 66 % PROBABILITY). IF A COLLAPSE IN THE MARINE BASED SECTORS OF THE ANTARCTIC ICE SHEET WERE INITIATED, THESE PROJECTIONS COULD BE SEVERAL TENTHS OF A METRE HIGHER BY LATE IN THE CENTURY.

	RCP2.6	RCP4.5	RCP6.0	RCP8.5
THERMAL EXPANSION	0.14 (0.10 to 0.18)	0.19 (0.14 to 0.23)	0.19 (0.15 to 0.24)	0.27 (0.21 to 0.33)
GLACIERS	0.10 (0.04 to 0.16)	0.12 (0.06 to 0.19)	0.12 (0.06 to 0.19)	0.16 (0.09 to 0.23)
GREENLAND ICE SHEET SMB	0.03 (0.01 to 0.07)	0.04 (0.01 to 0.09)	0.04 (0.01 to 0.09)	0.07 (0.03 to 0.16)
ANTARCTIC ICE SHEET SMB	-0.02 (-0.04 to 0.00)	-0.02 (-0.05 to -0.01)	-0.02 (-0.05 to -0.01)	-0.04 (-0.07 to -0.01)
GREENLAND ICE SHEET RAPID DYN	0.04 (0.01 to 0.06)	0.04 (0.01 to 0.06)	0.04 (0.01 to 0.06)	0.05 (0.02 to 0.07)
ANTARCTIC ICE SHEET RAPID DYN	0.07 (-0.01 to 0.16)	0.07 (-0.01 to 0.16)	0.07 (-0.01 to 0.16)	0.07 (-0.01 to 0.16)
LAND WATER STORAGE	0.04 (-0.01 to 0.08)	0.04 (-0.01 to 0.08)	0.04 (-0.01 to 0.08)	0.04 (-0.01 to 0.08)
SEA LEVEL RISE IN 2081-2100	0.40 (0.26 to 0.55)	0.47 (0.32 to 0.63)	0.47 (0.33 to 0.63)	0.62 (0.45 to 0.82)



8.1.5 REGIONAL PROJECTIONS FOR AUSTRALIA FOR THE 21ST CENTURY

SEA LEVELS WILL CONTINUE TO RISE THROUGHOUT THE 21ST CENTURY AND BEYOND.

In line with global mean sea level, Australian sea levels are projected to rise through the 21st century (very high confidence), and are very likely to rise at a faster rate during the 21st century than over the past four decades, or the 20th century as a whole, for the range of RCPs considered (*high confidence*). Sea level projections for the Australian coastline by 2090 (the average of 2080 to 2100) are comparable to, or slightly larger than (by up to about 6 cm) the global mean sea level projections of 26-55 cm for RCP2.6 and 45-82 cm in RCP8.5 (*medium confidence*). These ranges of sea level rise are considered likely (at least 66 % probability), and that if a collapse in the marine based sectors of the Antarctic ice sheet were initiated, the projections could be up to several tenths of a metre higher by late in the century. Regional projections for 2100 (a single year) are not given because of the effect of interannual to decadal variability on regional sea levels. However, for all scenarios, global averaged sea level in 2100 will be higher than in 2090 and sea level is projected to continue to rise beyond 2100.

To determine the regional changes in sea level around the Australian coastline, the approach of Church *et al.* (2011a) and Slangen *et al.* (2012) is used. This involved combining the dynamic ocean sea level distribution (changes in sea level from ocean circulation changes) with the regional changes associated with contemporary changes in mass of glaciers and ice sheets and its gravitational response in the ocean, and an ongoing GIA from the viscoelastic response of the Earth (movement in the mantle) to the redistribution of ice sheet mass since the last glacial maximum.

Each of the components associated with a change in mass implies changes in the Earth's gravitational field and vertical movement of the crust (sea level fingerprints). This analysis used the fingerprints calculated by Mitrovica *et al.* (2011). The glacier fingerprints were based on the loss of

mass during the latter half of the 20th century, as estimated by Cogley (2009). While the 21st century pattern of glacier mass loss may differ from that assumed by Mitrovica *et al.* (2011), the resultant changes in the Australian region are likely to be small. The Greenland fingerprint is insensitive to details of the exact location of mass loss on the Greenland Ice Sheet. Lacking more detailed information, for Antarctica, the mass gain from increased accumulation of snow is assumed uniformly distributed over the continent whereas the dynamic loss is expected to be from the West Antarctic Ice Sheet. The projected small changes in the mass of water stored on land in reservoirs and aquifers are here assumed to result in a uniform change in sea level around the globe.

For the GIA, the sea level projections presented here use results from the pseudo-spectral algorithm of Kendall *et al.* (2005) which takes into account time varying shorelines, changes in the geometry of grounded marine-based ice, and the feedback into sea level of Earth's rotation changes. The ice load history is based on the ICE-5G model of Peltier (2004).

The regional distribution in sea level change for projections for 2081 to 2100 compared to 1986 to 2005 for each of the four scenarios is shown in Figure 8.1.6. For all scenarios, the rate of rise is larger during the 21st century is faster than over the past four decades, or the 20th century as a whole, for the range of emissions scenarios considered (*high confidence*). The amount of regional sea level rise is largest for RCP8.5 and smallest for RCP2.6, with RCP4.5 and 6.0 being similar. On the larger scale, the CMIP3 climate model simulations assessed in the IPCC Fourth Assessment (Sen Gupta and England, 2006, Hall and Visbeck, 2002) indicate a robust southward shift of the Antarctic Circumpolar Current (ACC) associated with an intensification of the circumpolar circulation (Wang and Cai, 2013). This change is reflected in high sea level anomalies north of the axis of the ACC, with low anomalies to the south. The East Australian Current (EAC) and associated sea level anomalies also show intensification likely due to a strengthening of the subtropical gyre circulation coupled to ACC changes as shown by Zhang *et al.* (2013) for CMIP3 simulations.



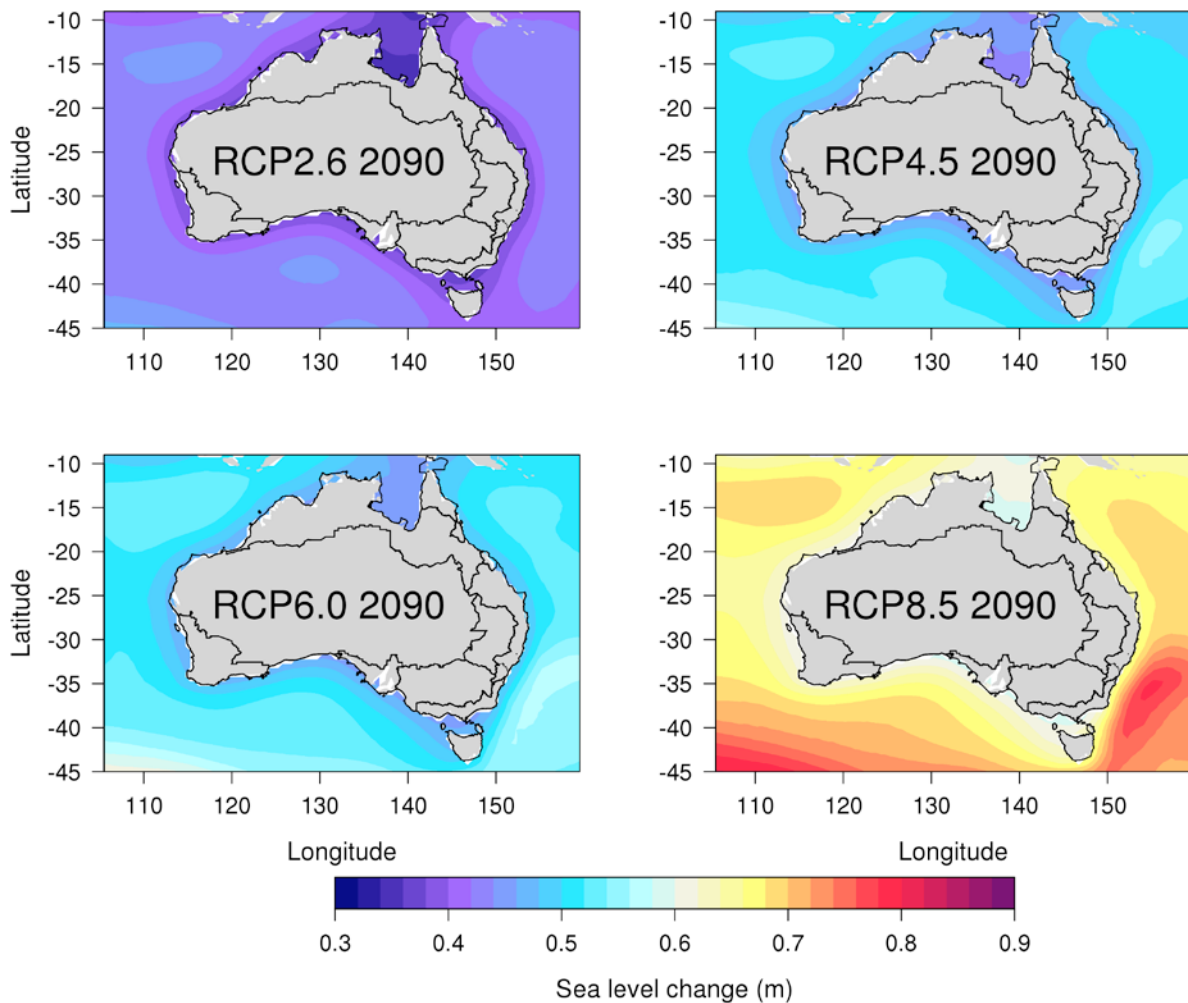


FIGURE 8.1.6: THE REGIONAL DISTRIBUTION IN SEA LEVEL CHANGE IN METRES FOR PROJECTIONS FOR 2090 (THE AVERAGE OF 2080 TO 2100) COMPARED TO 1986 TO 2005 MEAN LEVEL FOR EACH OF THE FOUR SCENARIOS. THE REGIONAL SEA LEVEL PROJECTIONS (SHADINGS) AND UNCERTAINTIES (SOLID LINES) COMBINE CONTRIBUTIONS FROM THE OCEAN DYNAMICAL RESPONSE WITH CHANGES IN MASS OF GLACIERS AND ICE SHEETS AND ITS GRAVITATIONAL RESPONSE ON THE OCEAN, AND AN ONGOING GLACIAL ISOSTATIC ADJUSTMENT (GIA). THE REGIONAL DISTRIBUTIONS IN SEA LEVEL RISE PROJECTIONS ARE CONSIDERED LIKELY. HOWEVER, IF A COLLAPSE IN THE MARINE BASED SECTORS OF THE ANTARCTIC ICE SHEET WERE INITIATED, THE PROJECTIONS COULD BE SEVERAL TENTHS OF A METRE HIGHER BY LATE IN THE CENTURY.

The projections indicate that around the Australian Coast, the rate of sea level rise during the 21st century will be larger than the average rate during the 20th century as radiative forcing from increasing greenhouse gas emissions continues (Figure 8.1.7). This result applies even for the lowest emission scenario, RCP2.6, which would require significant mitigation measures. For the first decades of the 21st century the projections are almost independent of the RCP chosen (Table 8.1.2), but they begin to separate significantly from about 2050. For higher emissions, particularly for RCP8.5, the rate of rise continues to increase through the 21st century and results in sea level rise about

30 percent higher than RCP4.5 and 6.0 levels by 2100. Strengthening of the subtropical gyre circulation of the South Pacific Ocean is projected to lead to a larger rise off the south-eastern Australian coastline; however the current low resolution models may not adequately represent how these higher offshore sea levels are expressed at the coast. This pattern intensifies with higher emissions. Sea level projections for the Australian coastline (Table 8.1.2) are comparable to or slightly larger (by up to about 0.06 m) than the GMSL projections (*medium confidence*).

TABLE 8.1.2: MEDIAN VALUES AND LIKELY RANGES FOR PROJECTIONS OF REGIONAL SEA LEVEL RISE (IN METRES) RELATIVE TO 1986 TO 2005 UNDER ALL RCP EMISSION SCENARIOS FOR LOCATIONS ALONG THE AUSTRALIAN COASTLINE OF 16 STATIONS WITH NEAR CONTINUOUS TIDE GAUGE RECORD AVAILABLE FOR THE PERIOD 1966 TO 2010. HOWEVER, NOTE THAT THE CURRENT LOW RESOLUTION MODELS MAY NOT ADEQUATELY REPRESENT HOW OFFSHORE SEA LEVELS (PARTICULARLY THE HIGHER SEA LEVELS OFFSHORE FROM SOUTH-EASTERN AUSTRALIA) ARE EXPRESSED AT THE COAST. NOTE ALSO THAT THESE RANGES ARE BASED ON THE 5 TO 95 % RANGE OF MODEL RESULTS FOR SEA LEVEL RISE BUT SHOULD ONLY BE CONSIDERED LIKELY (GREATER THAN 66 % PROBABILITY). IF A COLLAPSE IN THE MARINE BASED SECTORS OF THE ANTARCTIC ICE SHEET WERE INITIATED, THESE PROJECTIONS COULD BE SEVERAL TENTHS OF A METRE HIGHER BY LATE IN THE CENTURY.

STATIONS	SCENARIOS	2030	2050	2070	2090
DARWIN	RCP2.6	0.12(0.07-0.16)	0.21(0.13-0.28)	0.30(0.18-0.42)	0.38(0.22-0.55)
	RCP4.5	0.12(0.08-0.16)	0.22(0.14-0.30)	0.34(0.22-0.46)	0.46(0.29-0.65)
	RCP6.0	0.11(0.07-0.15)	0.21(0.14-0.28)	0.33(0.21-0.45)	0.47(0.30-0.65)
	RCP8.5	0.13(0.08-0.17)	0.25(0.17-0.33)	0.41(0.28-0.56)	0.62(0.41-0.85)
PORT HEDLAND	RCP2.6	0.11(0.07-0.16)	0.20(0.13-0.28)	0.29(0.18-0.42)	0.38(0.22-0.55)
	RCP4.5	0.12(0.07-0.16)	0.22(0.14-0.30)	0.33(0.21-0.46)	0.46(0.28-0.64)
	RCP6.0	0.11(0.07-0.15)	0.21(0.13-0.28)	0.32(0.21-0.45)	0.47(0.29-0.65)
	RCP8.5	0.12(0.08-0.17)	0.24(0.16-0.33)	0.41(0.27-0.55)	0.61(0.40-0.84)
GERALDTON	RCP2.6	0.12(0.07-0.17)	0.21(0.13-0.29)	0.30(0.18-0.42)	0.39(0.22-0.56)
	RCP4.5	0.12(0.07-0.16)	0.22(0.14-0.30)	0.34(0.21-0.47)	0.46(0.28-0.65)
	RCP6.0	0.11(0.06-0.16)	0.21(0.13-0.29)	0.33(0.20-0.45)	0.47(0.29-0.65)
	RCP8.5	0.13(0.08-0.17)	0.24(0.16-0.33)	0.41(0.27-0.56)	0.61(0.40-0.85)
FREMANTLE	RCP2.6	0.12(0.07-0.16)	0.21(0.13-0.29)	0.30(0.18-0.42)	0.39(0.22-0.56)
	RCP4.5	0.12(0.07-0.16)	0.22(0.14-0.30)	0.33(0.21-0.46)	0.46(0.28-0.65)
	RCP6.0	0.11(0.06-0.16)	0.21(0.13-0.29)	0.32(0.20-0.45)	0.47(0.29-0.65)
	RCP8.5	0.12(0.08-0.17)	0.24(0.16-0.33)	0.41(0.26-0.56)	0.61(0.39-0.84)
BUNBURY	RCP2.6	0.12(0.07-0.17)	0.21(0.13-0.29)	0.30(0.18-0.43)	0.40(0.23-0.57)
	RCP4.5	0.12(0.07-0.17)	0.22(0.14-0.30)	0.34(0.21-0.47)	0.47(0.29-0.65)
	RCP6.0	0.11(0.07-0.16)	0.21(0.13-0.29)	0.33(0.21-0.46)	0.47(0.30-0.66)
	RCP8.5	0.13(0.08-0.18)	0.25(0.16-0.34)	0.41(0.27-0.56)	0.62(0.40-0.85)
ALBANY	RCP2.6	0.12(0.08-0.17)	0.22(0.14-0.30)	0.31(0.20-0.44)	0.41(0.24-0.58)
	RCP4.5	0.13(0.08-0.17)	0.23(0.15-0.31)	0.35(0.23-0.48)	0.48(0.31-0.66)
	RCP6.0	0.12(0.07-0.17)	0.22(0.14-0.30)	0.34(0.22-0.47)	0.49(0.31-0.67)
	RCP8.5	0.13(0.09-0.18)	0.26(0.17-0.34)	0.43(0.29-0.57)	0.64(0.43-0.87)
PORT LINCOLN	RCP2.6	0.12(0.07-0.16)	0.21(0.13-0.28)	0.30(0.18-0.42)	0.38(0.23-0.55)
	RCP4.5	0.12(0.08-0.16)	0.22(0.14-0.30)	0.33(0.21-0.46)	0.45(0.28-0.63)
	RCP6.0	0.11(0.07-0.16)	0.21(0.13-0.29)	0.32(0.20-0.45)	0.46(0.29-0.64)
	RCP8.5	0.13(0.08-0.17)	0.24(0.16-0.33)	0.40(0.27-0.55)	0.60(0.39-0.83)
PORT PIRIE	RCP2.6	0.12(0.07-0.16)	0.21(0.13-0.28)	0.30(0.18-0.42)	0.38(0.23-0.55)
	RCP4.5	0.12(0.08-0.16)	0.22(0.14-0.30)	0.33(0.21-0.46)	0.45(0.28-0.63)
	RCP6.0	0.11(0.07-0.16)	0.21(0.13-0.29)	0.32(0.20-0.45)	0.46(0.29-0.64)
	RCP8.5	0.13(0.08-0.17)	0.24(0.16-0.33)	0.40(0.27-0.55)	0.60(0.39-0.83)
PORT ADELAIDE (OUTER)	RCP2.6	0.12(0.07-0.16)	0.21(0.13-0.29)	0.30(0.19-0.42)	0.39(0.23-0.55)
	RCP4.5	0.12(0.08-0.16)	0.22(0.14-0.30)	0.33(0.21-0.46)	0.46(0.29-0.63)
	RCP6.0	0.11(0.07-0.16)	0.21(0.13-0.29)	0.33(0.20-0.45)	0.46(0.29-0.65)
	RCP8.5	0.13(0.08-0.17)	0.25(0.16-0.33)	0.41(0.27-0.56)	0.61(0.40-0.84)



STATIONS	SCENARIOS	2030	2050	2070	2090
VICTOR HARBOUR	RCP2.6	0.12(0.07-0.16)	0.21(0.13-0.28)	0.30(0.18-0.42)	0.38(0.23-0.55)
	RCP4.5	0.12(0.08-0.16)	0.22(0.14-0.30)	0.33(0.21-0.46)	0.45(0.28-0.63)
	RCP6.0	0.11(0.07-0.16)	0.21(0.13-0.29)	0.32(0.20-0.45)	0.46(0.28-0.64)
	RCP8.5	0.13(0.08-0.17)	0.24(0.16-0.33)	0.40(0.26-0.55)	0.60(0.39-0.83)
GEELONG	RCP2.6	0.11(0.07-0.16)	0.20(0.12-0.28)	0.29(0.18-0.41)	0.37(0.22-0.53)
	RCP4.5	0.12(0.07-0.16)	0.21(0.13-0.29)	0.32(0.20-0.45)	0.44(0.27-0.62)
	RCP6.0	0.11(0.06-0.16)	0.20(0.12-0.28)	0.31(0.19-0.44)	0.45(0.27-0.63)
	RCP8.5	0.12(0.08-0.17)	0.24(0.15-0.33)	0.40(0.26-0.54)	0.59(0.38-0.82)
WILLIAMSTOWN	RCP2.6	0.11(0.07-0.16)	0.20(0.12-0.28)	0.29(0.17-0.40)	0.37(0.22-0.53)
	RCP4.5	0.11(0.07-0.16)	0.21(0.13-0.29)	0.32(0.20-0.45)	0.44(0.27-0.62)
	RCP6.0	0.11(0.06-0.16)	0.20(0.12-0.28)	0.31(0.19-0.44)	0.45(0.27-0.63)
	RCP8.5	0.12(0.08-0.17)	0.24(0.15-0.32)	0.39(0.25-0.54)	0.59(0.38-0.81)
SYDNEY	RCP2.6	0.13(0.09-0.18)	0.22(0.14-0.29)	0.30(0.19-0.42)	0.38(0.22-0.54)
	RCP4.5	0.13(0.09-0.18)	0.24(0.16-0.31)	0.35(0.24-0.48)	0.47(0.30-0.65)
	RCP6.0	0.13(0.08-0.17)	0.22(0.15-0.30)	0.34(0.23-0.46)	0.48(0.32-0.65)
	RCP8.5	0.14(0.10-0.19)	0.27(0.19-0.36)	0.44(0.31-0.59)	0.66(0.45-0.88)
NEWCASTLE	RCP2.6	0.13(0.09-0.18)	0.22(0.14-0.30)	0.30(0.19-0.42)	0.38(0.22-0.54)
	RCP4.5	0.14(0.09-0.18)	0.24(0.16-0.32)	0.36(0.24-0.48)	0.47(0.31-0.65)
	RCP6.0	0.13(0.08-0.17)	0.22(0.15-0.30)	0.34(0.23-0.46)	0.48(0.32-0.66)
	RCP8.5	0.14(0.10-0.19)	0.27(0.19-0.36)	0.45(0.31-0.59)	0.66(0.46-0.88)
MACKAY	RCP2.6	0.13(0.08-0.17)	0.21(0.14-0.29)	0.30(0.19-0.42)	0.38(0.22-0.55)
	RCP4.5	0.13(0.09-0.17)	0.23(0.16-0.31)	0.35(0.23-0.47)	0.47(0.30-0.64)
	RCP6.0	0.12(0.08-0.17)	0.22(0.15-0.29)	0.34(0.23-0.45)	0.48(0.31-0.65)
	RCP8.5	0.14(0.09-0.18)	0.26(0.18-0.35)	0.43(0.30-0.57)	0.64(0.44-0.87)
TOWNSVILLE	RCP2.6	0.13(0.08-0.17)	0.21(0.14-0.29)	0.30(0.19-0.42)	0.38(0.23-0.54)
	RCP4.5	0.13(0.09-0.17)	0.23(0.16-0.31)	0.35(0.23-0.47)	0.47(0.30-0.64)
	RCP6.0	0.12(0.08-0.16)	0.22(0.15-0.29)	0.34(0.22-0.45)	0.47(0.31-0.65)
	RCP8.5	0.13(0.09-0.18)	0.26(0.18-0.34)	0.43(0.30-0.57)	0.64(0.44-0.86)

-20° -10° 0° 10° 20° 30° 40° 50°

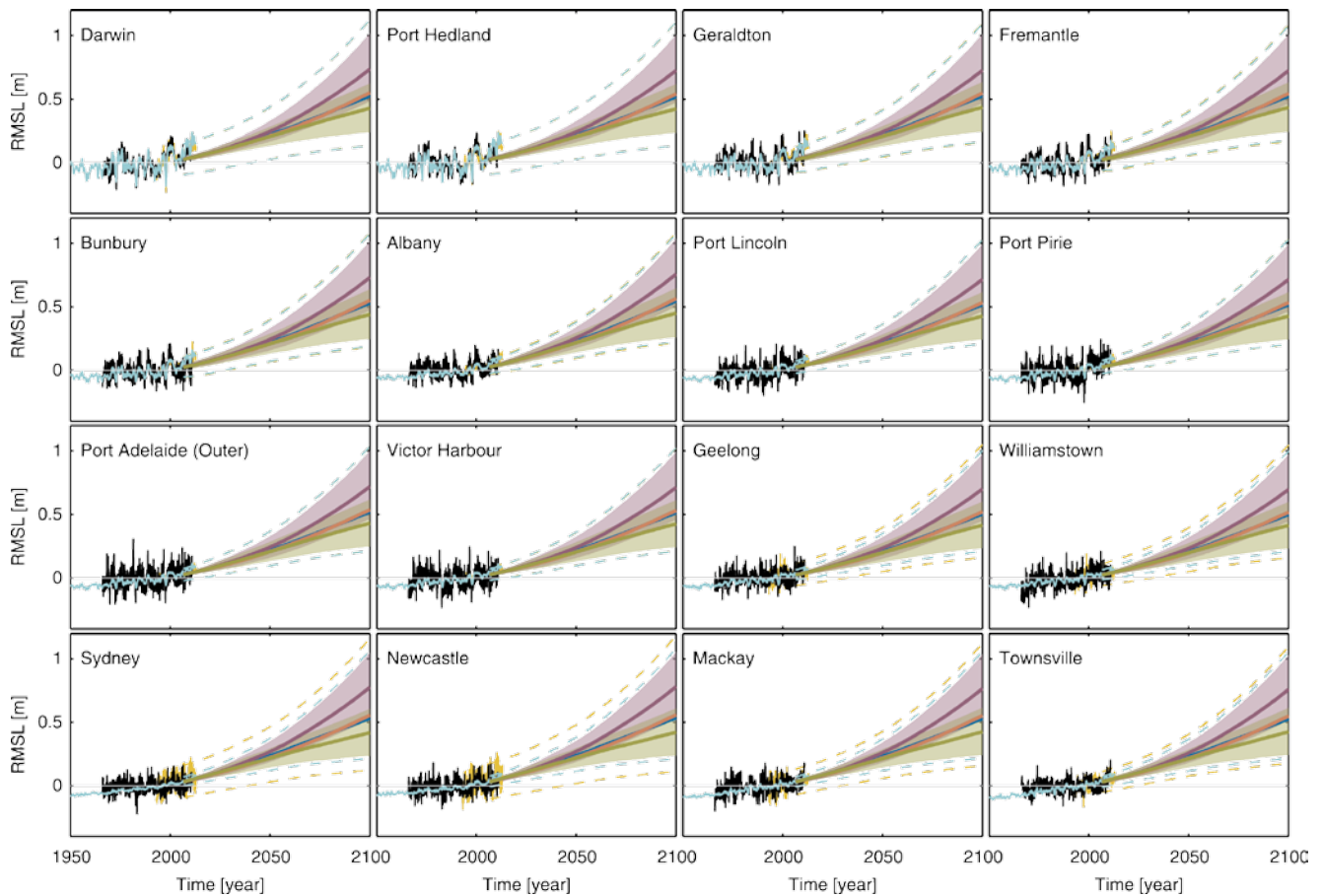


FIGURE 8.1.7: OBSERVED AND PROJECTED RELATIVE SEA LEVEL CHANGE IN METRES FOR THE 16 NEAR CONTINUOUS RECORDS AVAILABLE FOR THE PERIOD 1966 TO 2010, FROM DARWIN IN THE NORTH, ANTICLOCKWISE TO TOWNSVILLE IN THE NORTH-EAST. THE OBSERVED TIDE GAUGE RELATIVE SEA LEVEL RECORDS ARE INDICATED IN BLACK, WITH THE SATELLITE RECORD (SINCE 1993) IN MUSTARD AND TIDE GAUGE RECONSTRUCTION (WHICH HAS LOWER VARIABILITY) IN CYAN. MULTI-MODEL MEAN PROJECTIONS SHOWN AS THICK LINES (RCP8.5 PURPLE, RCP6.0 ORANGE, RCP4.5 BLUE AND RCP2.6 OLIVE) WITH LIKELY UNCERTAINTY RANGE FOR THE RCP8.5 AND RCP2.6 EMISSIONS SCENARIOS SHOWN BY THE PURPLE AND OLIVE SHADED REGIONS FROM 2006 TO 2100. THE MUSTARD AND CYAN DASHED LINES ARE AN ESTIMATE OF INTERANNUAL VARIABILITY IN SEA LEVEL DERIVED FROM OBSERVED ALTIMETER AND TIDE GAUGE RECONSTRUCTION RECORDS (LIKELY UNCERTAINTY RANGE ABOUT THE PROJECTIONS) AND INDICATE THAT INDIVIDUAL MONTHLY AVERAGES OF SEA LEVEL CAN BE ABOVE OR BELOW LONGER TERM AVERAGES. NOTE THAT THESE RANGES ARE BASED ON THE 5 TO 95 % RANGE OF MODEL RESULTS FOR SEA LEVEL RISE BUT SHOULD ONLY BE CONSIDERED LIKELY (GREATER THAN 66 % PROBABILITY). IF A COLLAPSE IN THE MARINE BASED SECTORS OF THE ANTARCTIC ICE SHEET WERE INITIATED, THESE PROJECTIONS COULD BE SEVERAL TENTHS OF A METRE HIGHER BY LATE IN THE CENTURY.

Significant interannual variability of monthly sea level records (Figure 8.1.2) has been effectively removed in forming the ensemble average projections. However, the interannual variability will continue through the 21st century and beyond. An indication of its magnitude is given by the dotted lines plotted above the top and below the bottom of the projections in Figure 8.1.7, indicating the 5 to 95 percent uncertainty range of the detrended historical records.

8.1.6 CAVEATS

Changes in local winds, ocean currents and changes in seawater density on the continental shelves contribute to the variability and trends of sea level along the coast. However, due to their coarse resolution (spatial resolution of order 1° of lat/lon), GCMs do not accurately represent the details of ocean currents such as the East Australian Current, are not eddy resolving and do not completely represent deep ocean and continental shelf interactions or local coastal processes resulting in changes of coastlines. As a result, the coastal response of sea level to climate change contains additional uncertainties to those represented in GCMs. These additional uncertainties are not expected to



change the large-scale results qualitatively but may result in slightly higher or lower sea levels than reported here. Also, GCMs do not represent processes such as fluvial and wave erosion, sediment transport or land subsidence. Local geological effects could lead to significant departure from the modelled local sea level changes. Compaction of sediments in deltaic regions and reclaimed land from the sea for infrastructure developments, subsidence exacerbated by ground water extraction, and changes in sediment supply to the coast as rivers become more managed, may quantitatively increase sea level change projections at some locations.

Note the regional projections included here are slightly different to those in Church *et al.* (2013). Here, the projections only include any changes in mean sea level averaged over 20 years. The interannual variability in sea level is assumed approximately constant and is indicated by the dashed lines in Figure 8.1.7. In contrast, in Church *et al.* (2013), the regional projections include the year to year variability in sea level. Other minor differences in the way regional sea levels are computed result in only trivial differences in the projections.

8.1.7 BEYOND 2100

At the end of the 21st century, sea level is continuing to rise in all scenarios, with the rate in the high emission scenario equivalent to the average rate experienced during the deglaciation of the Earth following the last glacial maximum. Global mean and Australian sea levels will continue to increase beyond 2100, with thermal expansion contributions continuing to rise for many centuries proportional to the degree of warming. In contrast, mountain glacier contributions per degree of warming show a tendency to slow as the amount of glacier ice available to melt decreases. Surface melting of the Greenland ice sheet is projected to continue. It is not yet possible to quantify the timing or amount of a multi-century contribution from the dynamic response of the Antarctic ice sheet to ocean and atmosphere future warming. Longer term sea level rise will depend on future emissions.

8.2 EXTREME SEA LEVELS

EXTREME SEA LEVELS WILL RISE

Taking into account uncertainty in sea level rise projections and nature of extreme sea levels along the Australian coastline, an indicative extreme sea level 'allowance' is calculated. This allowance is the minimum distance required to raise an asset to maintain current frequency of breaches under projected sea level rise. Along the Australian coast, these allowances are comparable to the upper end of the range of the respective sea level projections (*medium confidence*). The main contribution to increasing extreme sea levels is from the rise in mean sea level (*medium confidence*). Contributions to extreme sea levels from

changes in weather events are projected to be small or negative (*low confidence*).

Extreme coastal sea levels arise from the combination of factors including astronomical tides, storm surges and wind waves. Storm surges can arise from the passage of weather systems and their associated strong surface winds and falling atmospheric pressure. Sea levels increase at a rate of approximately 1 cm per hPa fall in local air pressure (the so-called inverse barometer effect) and wind stress directed onshore increases the water level against the coast (wind setup), while offshore winds reduce coastal sea levels (referred to as wind setdown). Along mid-latitude coastlines, sustained longshore wind stress can also alter coastal sea levels. In the Southern Hemisphere, anticlockwise/clockwise flow around a coastline leads to elevated/lowered coastal sea levels through Earth rotation effects that deflect the induced longshore current to the left of the direction of flow (often referred to as current setup/setdown). For example, along the south coast of Australia, the majority of storm surges have been found to occur in response to westerly to south-westerly winds that accompany strong cold fronts, which are most common during the colder months of the year from about April to October (McInnes and Hubbert, 2003).

The term storm tide refers to the combination of storm surge and astronomical tides. Wave breaking in the surf zone can further increase coastal sea levels through wave setup and wave runup, the first of which is the temporary elevation in sea levels due to the cumulative effect of wave breaking, and the second of which is the maximum elevation up the shore that is reached by an individual wave breaking. In general, storm surges tend to be higher in coastal regions with relatively wide and shallow continental shelves compared to narrow shelf regions. In Australia, such regions include the tropical regions, Bass Strait and the Great Australian Bight. On the other hand, higher wave energy can reach the coast in regions where the continental shelf is narrower such as the coastlines of the Southern and South-Western flatlands west, Murray Basin and the East Coast South.

Other factors such as ocean currents and climate variability can also contribute to variations in coastal sea levels on different timescales. For example, on the south-west Western Australia coastline, the stronger southward flow of the Leeuwin Current in winter compared to summer leads to sea levels that are about 0.2 m higher at the coast due to current setup (Pattiaratchi and Eliot, 2008). Over the East Coast region, warm and cool eddies from the East Australian Current can also contribute to local sea level changes of similar magnitudes.

Haigh *et al.* (2014) simulated the extreme sea levels arising from weather and tides over the period 1949 to 2009 using 6-hourly meteorological forcing obtained from the NCEP reanalyses. Extreme sea level data were found to be well represented by a particular extreme value distribution (the Gumbel distribution). Fitting the 61 years of modelled data



to this distribution enabled return periods of storm tides to be estimated. The 1-in-100 year storm tide level is shown in Figure 8.2.1. This is the height that has a 1 per cent chance of occurring in any given year. The heights vary around the coastline according to both the tidal range and the magnitude of storm surges that can occur along a section of coast due to the coastline features and the prevailing meteorology of the region. The highest storm tides occur on the north-west shelf due to the large tidal range and the fact that large storm surges can occur over the wide shelf region. Lower storm tides occur on the coastlines of the southern and SW flatlands west, Murray Basin and East Coast South due to the narrower continental shelf and smaller tidal range.

Under future climate conditions, extreme sea levels are expected to change due to increases in regional sea level (Section 8.1) and changes in climate and meteorological events (Section 7.3). To account for the projected increase in mean sea levels and associated uncertainties, Hunter (2012) developed an allowance, based on the range of sea level rise projections and the behaviour of extreme sea levels, which provides guidance on the amount of sea level rise that should be considered for future planning and adaptation activities. The method estimates the minimum height that structures would need to be raised in a future period so that the expected number of exceedences of that height would remain the same as those expected under present sea level conditions (see also Hunter *et al.* 2013).

The allowance accounts not only for the uncertainty in the sea level rise projections but also the characteristics of extreme sea level events in the coastal location of interest. In this method it is assumed that extreme sea level return periods follow a simple Gumbel distribution and that the uncertainty in future sea level rise can be approximated using a normal distribution.

The allowance is given by $A = \Delta z + (\sigma^2/2\lambda)$ where Δz is the mid-range sea level rise scenario, σ is the standard deviation of the sea level rise projection uncertainty, and λ is the Gumbel scale parameter. This scale parameter describes the degree of stretching of the extreme sea level distribution where a larger scale parameter describes a distribution with a heavier tail and hence a greater probability of extreme events occurring.

The allowances were calculated using the regional sea level rise projections presented in Section 8.1 and the scale parameters generated by Haigh *et al.* (2014). Values for 2030 and 2090 (relative to 1986 to 2005) under RCP4.5 and 8.5 are shown in Figure 8.2.2. Selected allowance values around Australia are also provided in Table 8.2.1. These allowances show that when the uncertainty on sea level rise projections is small, as is the case for 2030, the allowances are close to the median sea level rise scenario. For example, for both Townsville and Albany the allowances for RCP4.5 are calculated to be 0.13 m, the same as the median sea level rise scenarios in these locations (Table 8.1.2). However as the uncertainty becomes larger, as is the case for 2090,

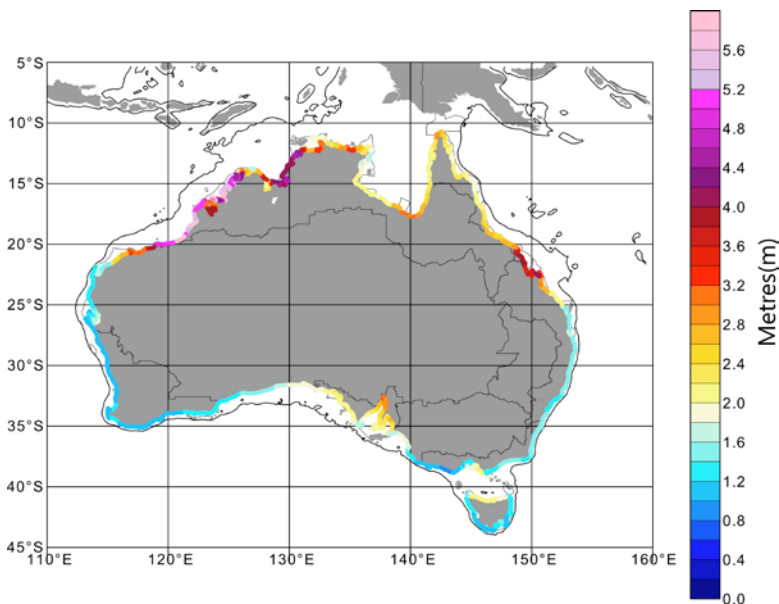


FIGURE 8.2.1: THE 1-IN-100 YEAR STORM TIDE HEIGHT IN METRES (COLOURED DOTS) RELATIVE TO MEAN SEA LEVEL CALCULATED FROM A HYDRODYNAMICAL MODEL OF STORM TIDES FROM 1949 TO 2009 USING 6-HOURLY METEOROLOGICAL FORCING FROM THE NCEP REANALYSES AND TIDAL FORCING FROM THE TPX07.2 TIDAL MODEL. ALSO SHOWN IS THE 150 M ISOBATH. RETURN PERIODS OF STORM TIDES WERE ESTIMATED BY FITTING A GUMBEL DISTRIBUTION TO THE MODELLED ANNUAL MAXIMUM SEA LEVELS OVER THE 61-YEAR PERIOD.

the allowances become larger and tend to lie between the median and 95th percentile sea level rise projection. For example, for Townsville and Albany under RCP8.5, the allowances become 0.74 and 0.81 m respectively, which lie between the median and 95th percentile projections of both locations i.e. 0.64 [0.44-0.86] and 0.64 [0.43-0.87] respectively.

The relatively higher allowance at Albany compared to Townsville is because the allowances are also dependent on the current nature of extreme sea levels, which are characterised by the steepness of the extreme sea level return period curves. In areas that do not experience large sea level extremes, a given sea level rise will more dramatically increase the frequency of extreme sea levels occurring than a location with a greater propensity for extreme sea levels. For example, in Albany, extreme sea levels tend to be less extreme leading to a less steep return period curve compared to Townsville. Consequently the sea level allowance for Albany is higher than that for Townsville.

Extreme sea levels may also change in the future due to changes in weather systems. Colberg and McInnes (2012) examined the changes to annual maximum sea levels along the coastline of southern Australia and Tasmania over the period 2080 to 2099 compared to 1980 to 1999 in four climate model simulations under the SRES A2 emission scenario (Nakicenovic and Swart, 2000). Changes were found to be small, amounting to at most a few centimetres (typically at least an order of magnitude smaller than the projected sea level rise for that scenario). They were also mostly negative (i.e. leading to a reduction in extreme sea levels) along the south coast with small increases occurring in eastern Bass Strait and parts of Tasmania, mostly in winter and spring. The changes were consistent with the southward movement of the subtropical ridge bringing weaker winds to the south coast but stronger winds and higher variability over Tasmania. The change to storm tides arising from a projected increase of cyclone intensity has been investigated along the Queensland east coast using synthetic cyclone modelling approaches. Results reported

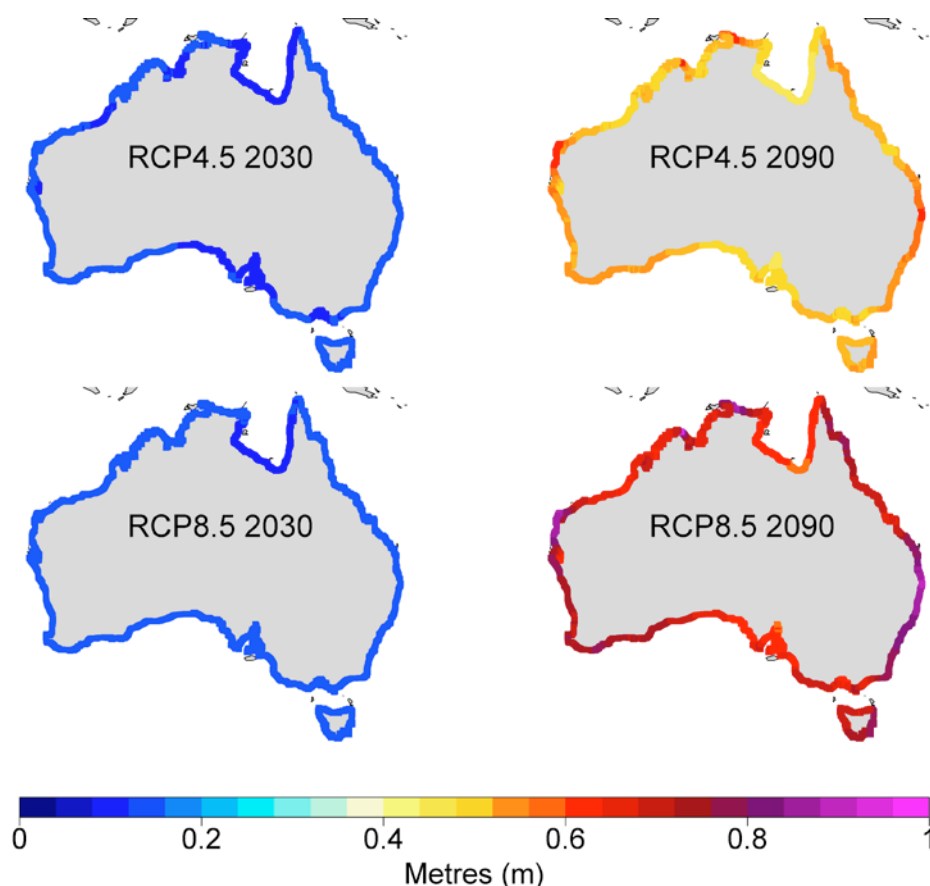


FIGURE 8.2.2: THE ALLOWANCE OR THE VERTICAL DISTANCE THAT AN ASSET NEEDS TO BE RAISED UNDER A RISING SEA LEVEL SO THAT THE PRESENT LIKELIHOOD OF FLOODING DOES NOT INCREASE. VALUES ARE SHOWN FOR RCP4.5 AND RCP8.5 ASSUMING THE PROJECTED SEA LEVEL INCREASE FOR 2030 AND 2090, THE UNCERTAINTY IN THOSE PROJECTIONS AND AN ESTIMATE OF EXTREME SEA LEVEL FREQUENCY AND HEIGHTS BASED ON SEA LEVELS OVER THE PERIOD 1949–2009.

TABLE 8.2.1: THE ALLOWANCE, OR MINIMUM HEIGHT (IN METRES) THAT STRUCTURES WOULD NEED TO BE RAISED FOR THE FUTURE PERIOD SO THAT THE EXPECTED NUMBER OF EXCEEDENCES OF THAT HEIGHT WOULD REMAIN THE SAME AS FOR THE 1986-2005 AVERAGE SEA LEVEL CONDITIONS. EXAMPLES ARE SELECTED FOR A SUBSET OF LOCATIONS GIVEN IN TABLE 8.1.2.

STATIONS	SCENARIOS	2030	2050	2070	2090
DARWIN	RCP2.6	0.12	0.21	0.32	0.43
	RCP4.5	0.12	0.23	0.36	0.52
	RCP6.0	0.12	0.22	0.35	0.53
	RCP8.5	0.13	0.26	0.45	0.71
PORT HEDLAND	RCP2.6	0.12	0.21	0.32	0.43
	RCP4.5	0.12	0.23	0.36	0.52
	RCP6.0	0.11	0.22	0.35	0.52
	RCP8.5	0.13	0.26	0.44	0.70
GERALDTON	RCP2.6	0.12	0.22	0.35	0.49
	RCP4.5	0.12	0.24	0.39	0.57
	RCP6.0	0.12	0.23	0.38	0.58
	RCP8.5	0.13	0.27	0.48	0.78
FREMANTLE	RCP2.6	0.12	0.22	0.34	0.47
	RCP4.5	0.12	0.24	0.38	0.56
	RCP6.0	0.12	0.22	0.37	0.56
	RCP8.5	0.13	0.26	0.47	0.76
BUNBURY	RCP2.6	0.12	0.22	0.34	0.47
	RCP4.5	0.12	0.24	0.38	0.55
	RCP6.0	0.12	0.23	0.37	0.56
	RCP8.5	0.13	0.27	0.47	0.75
ALBANY	RCP2.6	0.13	0.24	0.36	0.50
	RCP4.5	0.13	0.25	0.40	0.59
	RCP6.0	0.13	0.24	0.39	0.60
	RCP8.5	0.14	0.28	0.50	0.81
PORT ADELAIDE (INNER)	rcp25	0.13	0.24	0.36	0.50
	RCP4.5	0.13	0.25	0.40	0.59
	RCP6.0	0.13	0.24	0.39	0.60
	RCP8.5	0.14	0.28	0.50	0.81
VICTOR HARBOUR	rcp25	0.12	0.21	0.32	0.43
	RCP4.5	0.12	0.22	0.35	0.50
	RCP6.0	0.11	0.21	0.34	0.51
	RCP8.5	0.13	0.25	0.44	0.69
SYDNEY	RCP2.6	0.14	0.24	0.35	0.48
	RCP4.5	0.14	0.26	0.41	0.59
	RCP6.0	0.13	0.24	0.40	0.60
	RCP8.5	0.15	0.30	0.52	0.84

STATIONS	SCENARIOS	2030	2050	2070	2090
NEWCASTLE	RCP2.6	0.14	0.24	0.36	0.49
	RCP4.5	0.14	0.26	0.42	0.60
	RCP6.0	0.13	0.25	0.40	0.61
	RCP8.5	0.15	0.30	0.53	0.86
MACKAY	RCP2.6	0.13	0.22	0.33	0.43
	RCP4.5	0.14	0.24	0.38	0.53
	RCP6.0	0.13	0.23	0.36	0.53
	RCP8.5	0.14	0.28	0.47	0.73
TOWNSVILLE	RCP2.6	0.13	0.23	0.33	0.44
	RCP4.5	0.13	0.24	0.38	0.53
	RCP6.0	0.13	0.23	0.37	0.54
	RCP8.5	0.14	0.28	0.47	0.74

in Harper *et al.* (2009) showed that a 10 % increase in tropical cyclone intensity produced only a small increase in the 1-in-100 year storm tide, although larger increases were apparent for longer return periods (*e.g.* 1-in-1000 year storm tides). Such changes have not been incorporated in the allowances presented using the method of Hunter (2012).

In summary, the projected sea level allowances provide guidance on the amount of sea level rise that should be considered for future planning and adaptation activities to ensure that the frequency of extreme sea level exceedences in the future will remain unchanged from present conditions. For 2030, the current rate of sea level exceedences can be preserved by adopting a median sea level rise scenario, but by 2090 a value higher than the median sea level rise projection will be necessary (*high confidence*). However, only *medium confidence* is given to the actual allowance values provided since their calculation has utilised modelled extreme sea level data, which contains uncertainties, and because the allowances have not taken into account possible changes in the behaviour of extreme sea levels in the future. Although future changes in weather conditions may also contribute to changes in future extreme sea levels, the hydrodynamic downscaling studies that investigate such changes are few and of limited regional extent, which leads to *low confidence* in their projected changes at this time. However, the studies that have been undertaken suggest that the influence of such changes on the 1-in-100 year storm tide may be small for parts of Australia's coastline.

8.3 SEA SURFACE TEMPERATURE

OCEANS AROUND AUSTRALIA WILL WARM

There is very *high confidence* that sea surface temperatures around Australia will rise, with the magnitude of the warming dependent on the RCP. Near-coastal sea surface temperature rise around Australia is typically around 0.4-1.0 °C by 2030 and around 2-4 °C by 2090 under RCP8.5 compared to current (1986–2005).

Sea surface temperature (SST), the temperature measured in the upper ocean (from the surface down to 20 m), has significantly warmed globally over the last five decades (*e.g.* Levitus *et al.* 2000). SST is key variable in controlling the temperature of the land surface as well as the productivity of the marine environment. SSTs vary spatially around Australia, between 9 °C in the far south and 29 °C in the north (Locarnini *et al.* 2010), but these can be higher close to land. SST varies on interannual, seasonally and diurnal timescales. Analysis of the last 30 years shows warming along more than 70 % of the world's coastlines, with an earlier onset of the warm season although the rates of change are highly heterogeneous (Lima and Wethey, 2012). An example of this is the unprecedented ocean temperatures that were recorded along the Western Australian coast during the austral summer of 2010/2011, with near shore temperatures peaking at about 5 °C above average (Pearce and Feng, 2013, also see Section 4.2). This event is associated a long-term SST increase off the Western Australian Coast (Leeuwin Current) that has intensified post 1980 (Zinke *et al.* 2014). There has also been a warming of western boundary currents, such as off the east of Australia and Tasmania (Holbrook and Bindoff, 1997) where the



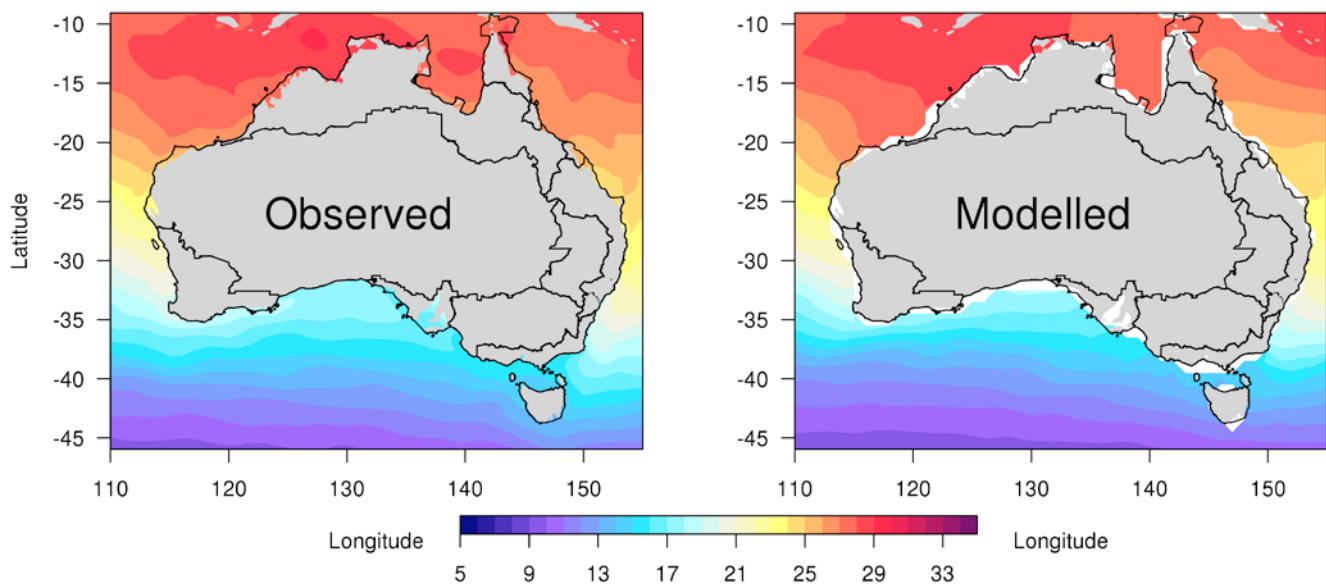


FIGURE 8.3.1: (A) OBSERVED SEA SURFACE TEMPERATURE (CARS; RIDGWAY *ET AL.* 2002) AND (B) SIMULATED SEA SURFACE TEMPERATURE 1986–2005 (°C); THE SIMULATION REPRESENTS THE MEDIAN OF 14 CMIP5 MODELS.

warming has been 2 to 3 times faster than the global mean (Wu *et al.* 2012). In the future, sea surface temperatures are projected to continue to increase (*e.g.* Knutti and Sedláček, 2013) although the impacts on the coastal ocean, where local processes and hydrodynamics can play a key role are not resolved in climate models.

Figure 8.3.1 compares observed *in situ* SSTs with those of the simulated mean over the 1986 to 2005 period. Overall the spatial pattern of SST is well represented, with the north to south gradient captured well in the simulations. However the SST is slightly warmer in the simulations with the isotherms shifted southwards and this is more evident along the southern coastline of Australia.

Under all emissions scenarios, a sea surface temperature increase around Australia is projected (Figure 8.3.2). All emissions scenarios show that the smallest increases in SST occur in southern Australia, while the largest warming occurs along the north-west coast of Australia, southern Western Australia, and along the east coast of Tasmania. The magnitude of this warming depends on the emissions scenario, with the largest increases in SST under RCP8.5. Generally warming is around (0.4–1.0 °C) in 2030 (under RCP 4.5), but is typically around 2–4 °C under RCP8.5 in 2090. Along the east coast of Tasmania in particular, very large changes are seen, with median changes as large as

4 °C projected under RCP8.5, and greater than 6 °C in the 90th percentile. The 10th and 90th percentiles of RCP8.5 show the same spatial pattern as the 50th percentile but with different magnitudes, which indicates a robust spatial warming pattern. The magnitude of the large-scale increases in SST may be much larger along the coast (*e.g.* Lima and Wetthey, 2012) and modulated by processes such as local hydrodynamics and processes that are not well resolved in climate models (Matear *et al.* 2013). Nevertheless, this large-scale warming projected under RCP4.5 and RCP8.5 indicates that around Australia marine biodiversity is likely to be impacted through southward shifts in some marine species (to cooler regions) and local extinction for others (Wernberg *et al.* 2011), as well as threatening the long-term viability of key habitats such as coral reefs *e.g.* Frieler *et al.* (2012) and Hoegh-Guldberg *et al.* (2007). There is *very high confidence* that the oceans around Australia will warm in the future, and the magnitude of this warming will be dependent on the RCP, but only *medium confidence* in the coastal projections of this warming.



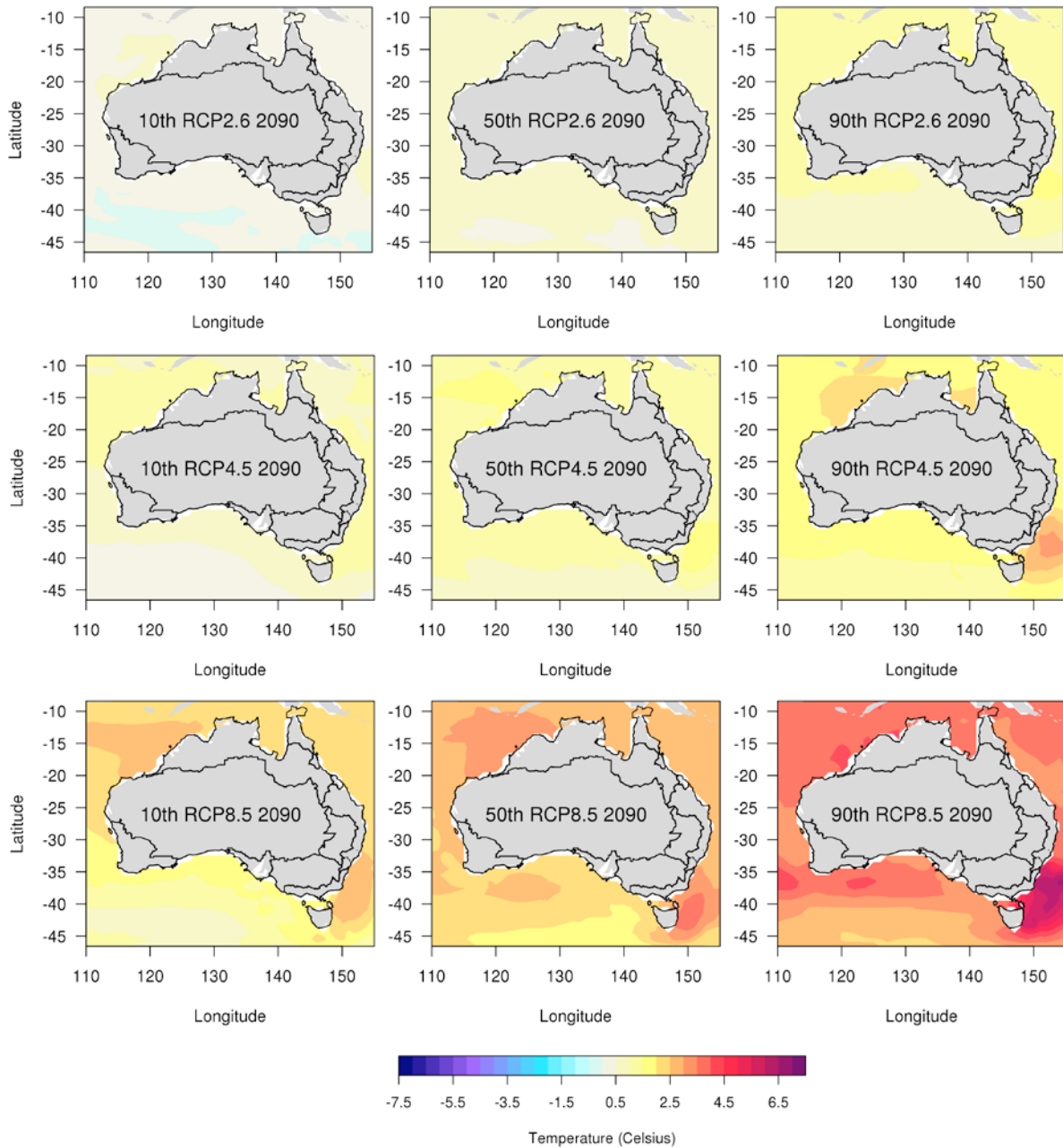


FIGURE 8.3.2: THE PERCENTILE CHANGES IN SEA SURFACE TEMPERATURE (°C) FOR 2080–2099 RELATIVE TO THE PERIOD 1986–2005 FOR RCP2.6 (TOP), RCP4.5 (MIDDLE) AND RCP8.5 (LOWER). SHOWN IN EACH ROW ARE THE (LEFT) 10TH PERCENTILE, (MIDDLE) 50TH PERCENTILE AND (RIGHT) 90TH PERCENTILE OF 14 CMIP5 MODELS.

-20° -10° 0° 10° 20° 30° 40° 50°

8.4 SEA SURFACE SALINITY

OCEAN SALINITY MAY CHANGE

Changes in sea surface salinity reflect changes in rainfall and may affect ocean circulation and mixing. A net reduction in the salinity of Australian coastal waters is projected, but this projection is of *low confidence*. For some southern regions, models indicate an increase in sea surface salinity, particularly under higher emissions.

Salinity is an important gauge to help understand how the water cycle is changing due to climate change and changes in salinity are likely to have local impacts on estuaries and riverine environments. Over the last 50 years the sea surface salinity around Australia has changed, becoming more saline in southern and south-eastern Australia and less saline in northern Australia (Ridgway, 2007, Durack and Wijffels, 2010). These changes are associated with changes in the hydrological cycle and strengthening of the East Australian Current (EAC); the increase in salinity in Southern Australia can be attributed to a decrease in precipitation. These changes in precipitation and the EAC have been attributed to a strengthening of the Southern Annular Mode (SAM) over this period (e.g. Hendon *et al.* 2007, and see Section 4.2). In northern Australia there has been an increase in precipitation (e.g. Josey *et al.* 1998) leading to a decrease in salinity. In the future the hydrological cycle is expected to continue to undergo significant changes (Held and Soden, 2006, Knutti and Sedláček, 2013). In projecting changes in sea surface salinity it is important to note that in the coastal ocean local processes such as river input and

hydrodynamics can play a key role, but these processes are not well resolved (or even necessarily represented) in current GCMs.

Figure 8.4.1 compares the observed sea surface salinity (CARS; Ridgway *et al.* 2002) with the median of 14 CMIP5 models. Overall there are large biases; the models show significantly less salinity than observed. These biases are most pronounced in north-western Australia where the changes are up to 2 units lower, in the Coral Sea, and on the boundary of the Southern Ocean. The differences in northern Australia are likely associated with errors in simulating tropical precipitation, e.g. Lee and Wang (2014) while in southern Australia the explanation of the model biases is not well known.

All emissions scenarios show that in the 10th percentile and median case there is a net reduction in sea surface salinity around Australia. However in some areas, particularly under RCPs 8.5 and 4.5, there is an increase in sea surface salinity e.g. Tasmania and south-west Western Australia. The 90th percentile suggests an increase in surface salinity around all of Australia, and some large changes in Torres Strait and along the east coast of Australia. The large-scale pattern is consistent across all emission scenarios (Figure 8.4.2) with the strength of the change proportional to the emission scenario. The pattern of sea surface salinity changes is related to both changes in precipitation (see Section 7.2) and evaporation, the latter of which is expected to increase as the ocean warms. These changes will impact ocean circulation and mixing around Australia.

A net reduction in the salinity of Australian coastal waters is projected with *low confidence*, as some regions may show an increase in sea surface salinity, particularly under higher emissions.

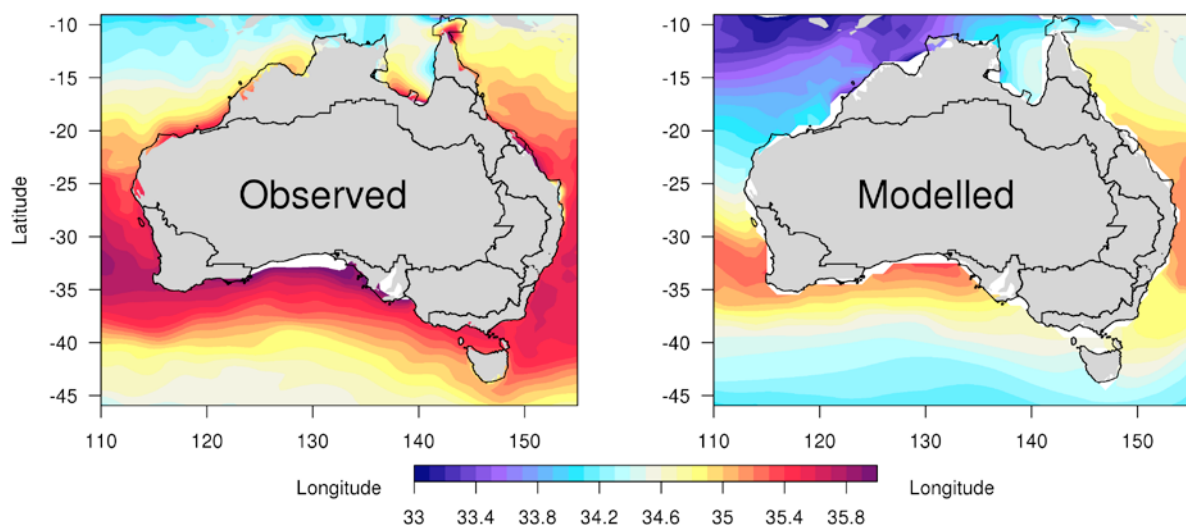


FIGURE 8.4.1: (A) OBSERVED SEA SURFACE SALINITY (CARS; RIDGWAY *ET AL.* 2002) AND (B) SIMULATED SEA SURFACE SALINITY 1986–2005; THE SIMULATION REPRESENTS THE MEDIAN OF 14 CMIP5 MODELS.



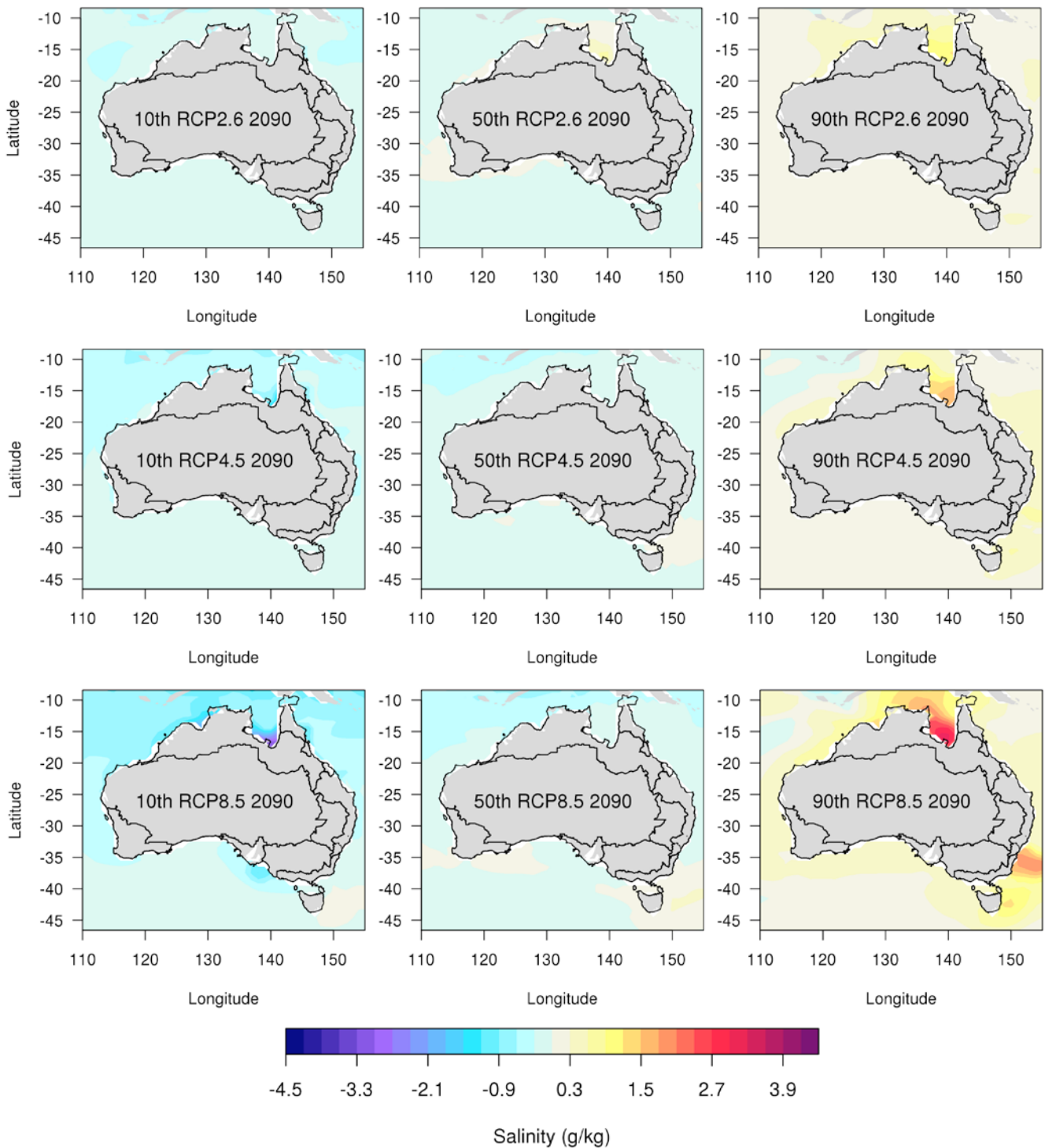


FIGURE 8.4.2: THE PERCENTILE CHANGES IN SEA SURFACE SALINITY FOR 2080–2099 RELATIVE TO THE PERIOD 1986–2005 FOR RCP2.6 (TOP), RCP4.5 (MIDDLE) AND RCP8.5 (LOWER). IN EACH ROW SHOWN IS THE 10TH (LEFT), 50TH (CENTRE) AND 90TH (RIGHT) OF 14 CMIP5 MODELS.

-20° -10° 0° 10° 20° 30° 40° 50°

8.5 OCEAN ACIDIFICATION

OCEANS AROUND AUSTRALIA WILL BECOME MORE ACIDIC

There is *very high confidence* that around Australia the ocean will become more acidic, with a net reduction in pH. There is also *high confidence* that the rate of ocean acidification will be proportional to the carbon dioxide emissions. There is *medium confidence* that long-term viability of corals will be impacted under RCP8.5 and RCP4.5, and that there will be harm to marine ecosystems from the large reduction in pH under RCP8.5.

The oceans play a key role in reducing the rate of global climate change as they have absorbed nearly 30 % of the anthropogenic CO₂ emitted over the last 200 years (Ciais *et al.* 2013 and references therein), and at present take up more than 25 % of current annual CO₂ emissions (Le Quéré *et al.* 2013). When CO₂ is dissolved at the sea surface it reacts with the seawater to form carbonate, bicarbonate and hydrogen ions (a small proportion remains as dissolved

CO₂). As CO₂ enters the ocean it changes the equilibrium between these ions, leading to a net reduction in carbonate concentration and a reduction in the seawater pH. These two changes are collectively known as ocean acidification. Ocean acidification is a predictable and measurable consequence of rising atmospheric CO₂ and therefore the rate of future ocean acidification will be determined mainly by its future concentration.

Over the past 200 years, there has been a 0.1 unit change in the ocean's surface water pH, representing a 26 % increase in the concentration of hydrogen ions in seawater (Raven *et al.* 2005). These changes in ocean pH in the global ocean have been extensively observed (Feely *et al.* 2009). Ocean acidification is likely to impact the entire marine ecosystem from plankton at the base to fish at the top. Factors that can be impacted include reproductive health, organism growth and physiology, species composition and distributions, food web structure and nutrient availability (Fabry *et al.* 2008, Iglesias-Rodriguez, *et al.* 2008, Munday *et al.* 2009, 2010). Carbonate is used (together with calcium) in the form of aragonite by corals to form hard reef structures and by other invertebrate organisms such as oysters, clams, lobsters, crabs and starfish and some plankton (*e.g.* pteropods, coccolithophores, foraminifera) to make their

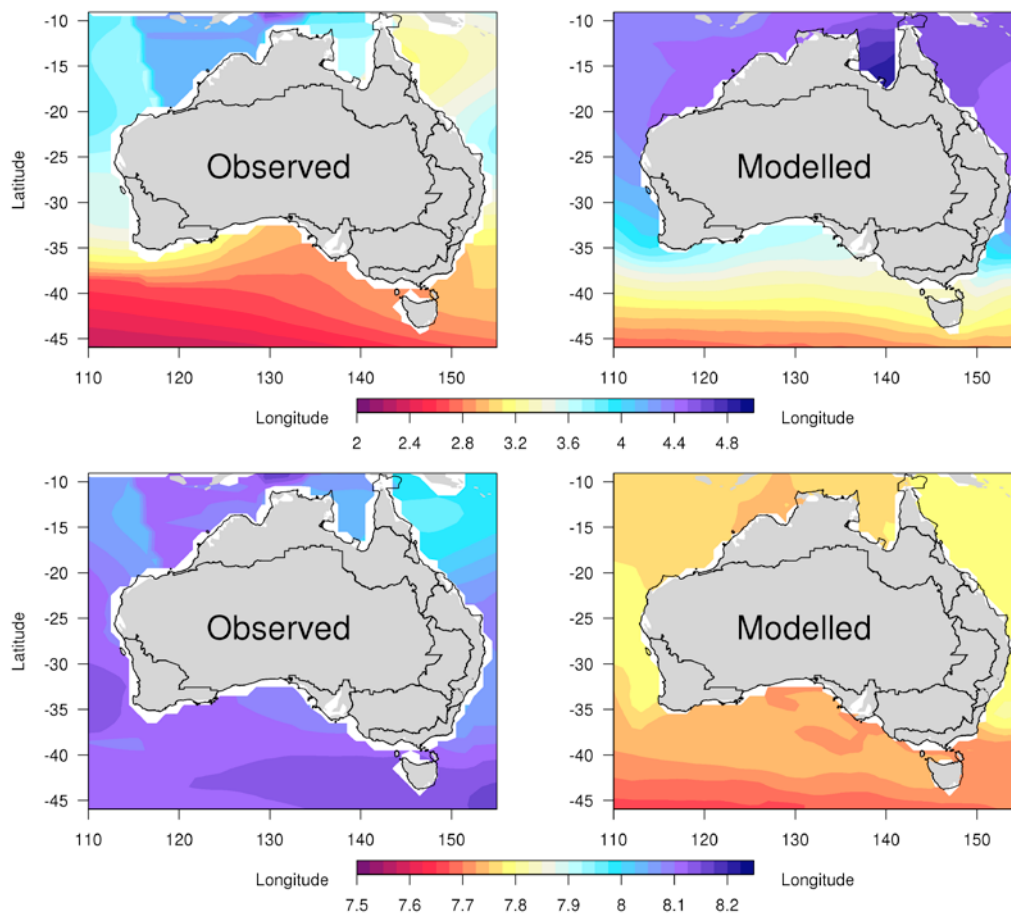


FIGURE 8.5.1: (TOP) ARAGONITE SATURATION STATE AND (BOTTOM) PH FOR THE YEAR 1995, WITH (LEFT) OBSERVED AND (RIGHT) SIMULATED. THE SIMULATION REPRESENTS THE MEDIAN OF SIX CMIP5 MODELS.



models suggest that the values of ΩA and pH are higher than observed. Conversely along the north-West coastline, the values of ΩA and pH are lower than observed. However in these two regions the observations are very sparse. The other major difference occurs along the northern edge of the Southern Ocean where the models suggest that the values ΩA and pH are higher than observed. These differences are potentially due to both limited observations and model biases (Bopp *et al.* 2013). It is important to note

that many of the impacts of ocean acidification will be felt along the coastlines, which are not well resolved in the relatively coarse climate models.

Under all emission scenarios a net decrease in pH and ΩA occurs, with the largest changes associated with the highest atmospheric CO₂ levels (Figures 8.5.2 and 8.5.3. Around Australia the largest decreases occur along the mid-latitude and northern Australia coast with the largest median drop

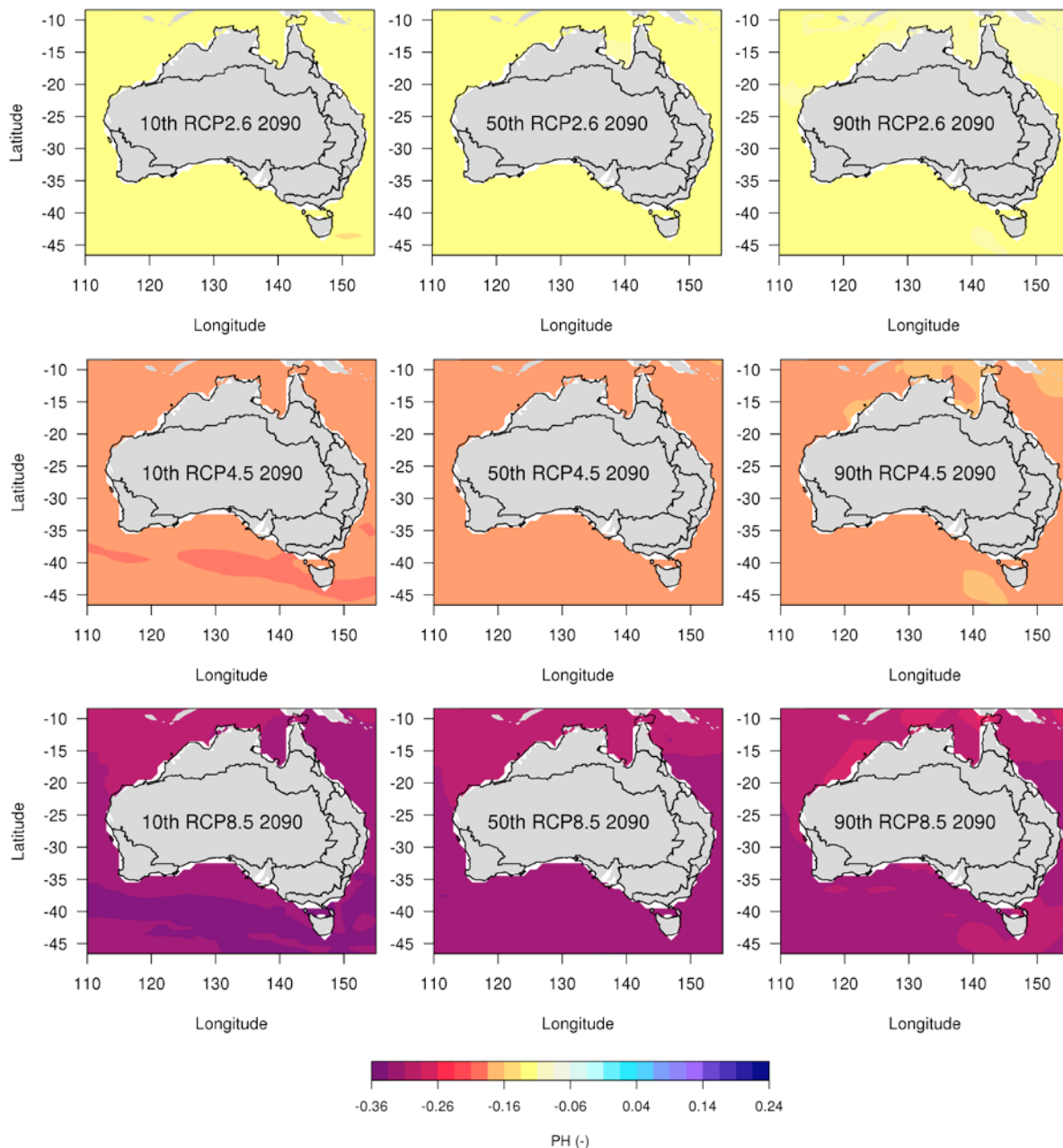


FIGURE 8.5.3: THE SIMULATED CHANGE IN PH FOR 2080–2099 WITH REFERENCE TO THE PERIOD 1986–2005 FOR RCP2.6 (TOP), RCP4.5 (MIDDLE) AND RCP8.5 (LOWER). IN EACH ROW IS SHOWN THE (LEFT) 10TH PERCENTILE, (MIDDLE) 50TH PERCENTILE (MEDIAN), AND (RIGHT) THE 90TH PERCENTILE FROM AN ENSEMBLE OF SIX CMIP5 MODELS.



in Ω_A of 1.5 under RCP8.5. Such a decrease would mean that values of Ω_A are lower than those at which corals are historically found. These changes are expected to have significant negative impacts on the long-term health, diversity and viability of corals (Fabricius *et al.* 2011) and aquaculture. In southern Australia, the changes in pH and Ω_A are smaller than at mid-latitudes and northern Australia, but these changes are significant because their values in the present day are lower. This means impacts of ocean acidification are expected sooner. For example the values of Ω_A under RCP8.5 by 2090 are close to or less than 1, meaning that the waters will no longer be super-saturated with respect to Ω_A and dissolution of calcium carbonate will begin to occur. Such changes will have serious impacts on key marine species, *e.g.* pteropods at the base of the food web (*e.g.* Orr *et al.* 2005), as well as on aquaculture (*e.g.* Feely *et al.* 2008) and other industries.

There is *very high confidence* that around Australia as atmospheric CO_2 levels continue to rise the oceans will become more acidic, showing a net reduction in aragonite saturation state and pH. There is also *high confidence* that the rate and magnitude of ocean acidification will be dependent on RCP followed. Under high and medium emissions (RCP8.5 and RCP4.5) there is *medium confidence* that long-term viability of corals will be impacted. There is also *medium confidence* under high emissions (RCP8.5) that there will be negative impacts on the marine ecosystem from the large projected reduction in pH.

CHAPTER NINE

USING CLIMATE CHANGE DATA IN IMPACT ASSESSMENT AND ADAPTATION PLANNING

BANANA PLANTATION AFTER CYCLONE YASI, QUEENSLAND, ISTOCK

-20° -10° 0° 10° 20° 30° 40° 50°

CHAPTER 9 USING CLIMATE CHANGE DATA IN IMPACT ASSESSMENT AND ADAPTATION PLANNING

Climate change data provide an essential input to the impact assessment process. Methods for generating, presenting and selecting data are described in this chapter, along with information to help users find data and research tools. This includes a decision tree to guide users to the most relevant material; report-ready images and tables; climate change data (such as a 10 percent decrease in rainfall relative to 1986-2005); and application-ready data (where projected changes have been applied to observed data for use in detailed impact assessments). Links are provided to other projects that supply climate change information.

9.1 INTRODUCTION

In Chapters 6, 7 and 8, climate projections derived from CMIP5 modelling experiments were evaluated and presented. Chapter 9 describes how to apply these projections in impact assessments that will inform regional NRM planning in Australia. This builds on information contained in Chapter 6 of the 2007 *Climate Change in Australia* technical report (CSIRO and BOM, 2007).

It is useful to distinguish between two broad types of projection information; *scientific knowledge* about the range of plausible climate change and *datasets for use in applications*. Chapters 7 and 8 of this Report include qualitative statements as well as some quantitative ranges of change, with confidence levels, about projected climate change which is represented by the path on the left of Figure 9.1. The path on the right of the figure, datasets for applications, is the focus of this chapter. The scientific knowledge product can potentially synthesise a broader range of relevant evidence than the application datasets product.

The provision of application-ready datasets is usually designed to assist users in undertaking impact assessment. It draws on similar material to the scientific knowledge product, but is restricted to modelling techniques and approaches that produce projection datasets in a form suitable for use in applications. Typically this results in only a subset of the ranges of plausible future climate change being considered. A subset may be required if users require downscaled climate data (available from limited models) or if a small number of multivariate scenarios are required (best served by single climate models).

Application-ready datasets do not always represent all changes provided by global climate models. As such, a key challenge is to ensure that application-ready data used in impact assessment are as representative as possible of current knowledge of climate change (described by the yellow arrow in Figure 9.1). Researchers should use scientific knowledge about plausible climate change (Chapters 7 and 8) in conjunction with application-ready data.

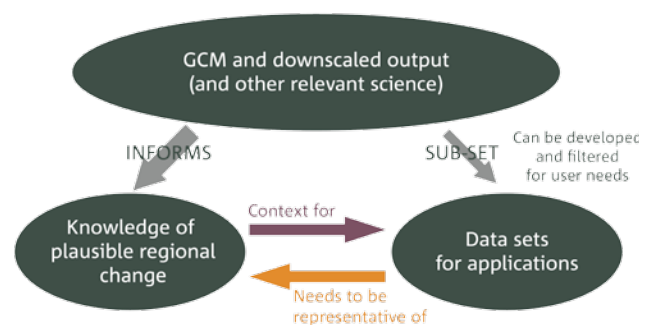


FIGURE 9.1: THE RELATIONSHIP BETWEEN THE CLIMATE PROJECTION INFORMATION PRESENTED IN CHAPTERS 7 AND 8 AND THE DATASETS FOR IMPACT ASSESSMENT APPLICATIONS DESCRIBED IN THIS CHAPTER. INFORMATION FROM GLOBAL CLIMATE MODELS (GCMs) AND DOWNSCALED OUTPUT AND OTHER SOURCES (TOP ELLIPSE) CAN BE DRAWN UPON TO INFORM OUR KNOWLEDGE OF PLAUSIBLE REGIONAL CHANGES TO CLIMATE (ELLIPSE IN THE LOWER LEFT) AND ALSO FOR USE IN IMPACT ASSESSMENTS WHERE APPLICATION OF THE INFORMATION IS REQUIRED (ELLIPSE IN THE LOWER RIGHT). THE KNOWLEDGE OF THE PLAUSIBLE REGIONAL CHANGE PROVIDES CONTEXT FOR THE DATASETS FOR APPLICATIONS, BEARING IN MIND THESE DATASETS NEED TO BE REPRESENTATIVE OF THE KNOWLEDGE.

A process for undertaking a climate change *impact assessment* is described in Section 9.2. The series of steps in Figure 9.2 describe a robust approach to this including; *establishing the context* (scope and audience), *identifying the known risks* (within the current climate) and *risk analysis* (current practices and newly identified risks). These first three steps require climate information as an input. The *evaluation of risks* phase ranks severity and identifies areas for further analysis (not addressed in this Chapter). During *risk treatment* decisions are made, and emphasis should be placed on continuous monitoring of their effectiveness and reviewing lessons from the process. Other frameworks exist, but have many similarities to this simple process.

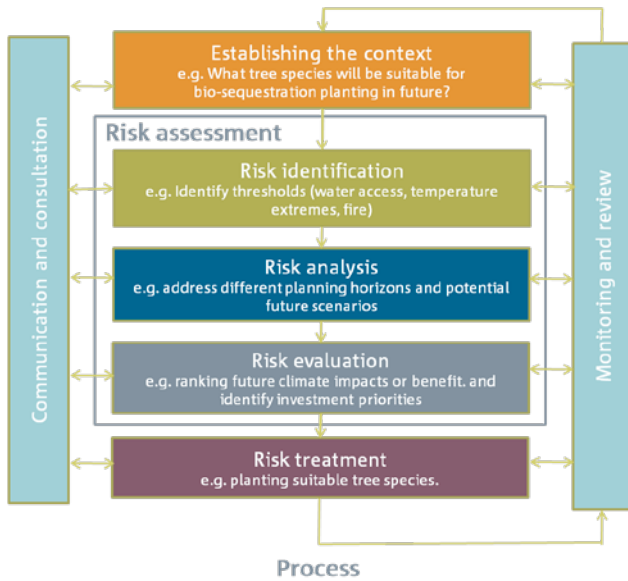
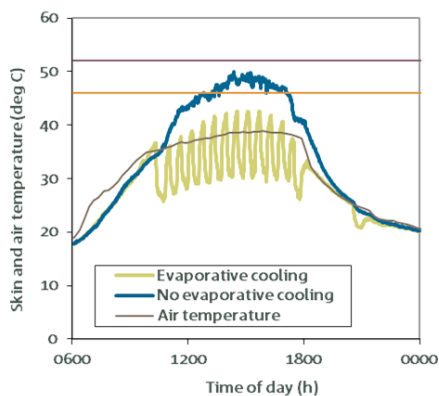


FIGURE 9.2 STEPS INVOLVED IN UNDERTAKING A CLIMATE CHANGE IMPACT ASSESSMENT (ADAPTED FROM STANDARDS AUSTRALIA, 2009).

The *Climate Futures* framework has been developed by CSIRO to assist decision-makers in understanding the range and likelihood of future climates when conducting their impact assessment (Whetton *et al.* 2012). An associated web-tool, *Australian Climate Futures* (Box 9.1), provides Australian climate change projections in a user-friendly format. Section 9.3 provides a description of this and other data, tools or resources from the Climate Change in Australia body of work.

It is important to recognise that climate change scenarios can meet some, but not all, of the needs of future planning (Wilby *et al.* 2009). Other factors that are also changing, such as population, socio-economic status, infrastructure and markets, can have a large influence on future planning. Decision-makers should also consider the implications of non-climatic changes.



9.2 CONDUCTING A CLIMATE CHANGE IMPACT ASSESSMENT

9.2.1 ESTABLISHING THE CONTEXT

The approach to undertaking an impact assessment will vary, depending on the context. Therefore it is essential to establish the context. This requires a definition of the scope of the assessment, a clarification of the objectives, and identification of the stakeholders and their objectives and concerns. It is also important to establish success criteria against which risks to the objectives can be evaluated. Relevant climate change scenarios can then be identified.

9.2.2 RISK IDENTIFICATION

Current risks are affected by current climate variability, especially extreme events. For example, railway lines are sensitive to buckling on extremely hot days (McEvoy *et al.* 2012), while the timing of grape maturity is sensitive to growing season temperature and soil moisture status (Webb *et al.* 2012), and urban flooding may be influenced by extreme daily rainfall. Small changes in average climate underpin larger changes in extreme weather phenomena such as heatwaves, frosts, floods, cyclones, storm surges, tornadoes and hail.

Some impact assessments require information about a single climate variable, such as temperature. However, combinations of variables are required to quantify factors such as fire weather (temperature, humidity, wind and rain), snow cover (precipitation and temperature) and soil moisture (rainfall and evaporation) (Willows and Connell, 2003).

In an impact assessment, it is important to understand the relevant temporal scales. For some studies, it is necessary to assess hourly climate data, while for others monthly or seasonal averages can be sufficient. In many situations it is the intensity, frequency and duration of a weather event that can significantly affect risk, as illustrated in Figure 9.3. In other cases, it is the sequence of events that is important, such as consecutive or clustered occurrences, or coincident events involving two or more climate variables (Leonard *et al.* 2013).



FIGURE 9.3: (LEFT) DAILY TEMPERATURE VARIABILITY AND THRESHOLD EXCEEDANCE AND THE EFFECT OF EVAPORATIVE COOLING ON SKIN TEMPERATURE OF ROYAL GALA APPLE; (RIGHT) EFFECT OF EXTREME TEMPERATURES ON ROYAL GALA APPLE.



The spatial scale required in an impact assessment will vary depending on the proposed project outcome. For example, a study on pome fruit used data from a single location in the relevant horticultural regions to describe reductions in accumulated annual chilling (exposure to cold temperatures required to break dormancy) in future climates (Darbyshire *et al.* 2013), whereas catchment scale information is often required in hydrological studies (CSIRO, 2008). Local government area (LGA) climate data can also be useful to align with other inputs such as population data (*e.g.* Baynes *et al.* 2013). Sometimes, even broader-scale data are sufficient for national assessments.

9.2.3 RISK ANALYSIS

The risk analysis stage includes a review of current management regimes and an analysis of the new levels of risk for different climate scenarios (Australian Greenhouse Office, 2006, Dunlop *et al.* 2013).

PLANNING HORIZONS

As mentioned above, changes in intensity, frequency, duration and timing are relevant across a range of temporal and spatial scales. Decisions made today will have consequences for many decades in future with regard to regional planning, land use, infrastructure investments, etc. The planning horizon will vary for different sectors. For example, when planning forest plantings for bio-sequestration of carbon emissions, the trees will be exposed to the climate in 2030 and beyond, so it is important to consider climate change projections (Figure 9.4).

CLIMATE CHANGE DATA SOURCES

Climate change projection data are usually based on output from climate models driven by various scenarios of greenhouse gas emissions, aerosols and land-use change (see Chapters 3, 7 and 8). Data can be accessed via a range of providers, such as national weather services, government departments, non-governmental organisations, academic institutions or research organisations. Identifying an appropriate dataset for use in impact assessment requires a good understanding of the pros and cons of different methods and data products (Wilby *et al.* 2009, Ekström *et al.* accepted).

The CMIP5 climate model simulations described in this Report have been undertaken using four concentration pathways, called RCP8.5, RCP6.0, RCP4.5 and RCP2.6 (Moss *et al.* 2010, van Vuuren *et al.* 2011) (see Section 3.2). Data from 16 to 39 CMIP5 models (Table 3.3.2) have been assessed and they produce a range of different projections². Users of climate projections are strongly advised to represent a range of climate model results in their studies and reports, rather than simply using the multi-model median change or results from a single model. CSIRO's *Climate Futures* approach has been developed to simplify communication and use of climate projections and to help capture the range of projection results relevant to a specified region (Whetton *et al.* 2012). This enables a large amount of climate model output (for a particular time period and emissions scenario) to be summarised by grouping it into a small number of categories, each of which is defined by a range of change in two climate variables such as temperature and rainfall. It is supported by the *Australian Climate Futures* web-tool (Box 9.1).

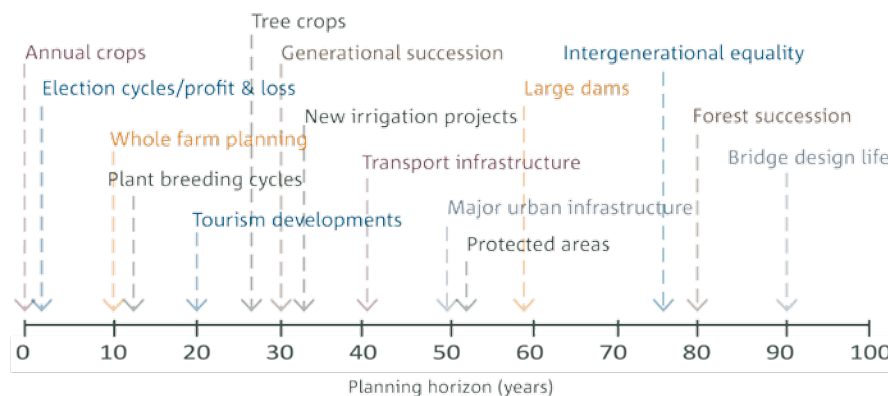


FIGURE 9.4: TYPICAL PLANNING HORIZONS (YEARS) FROM DIFFERENT SECTORS (SOURCE: JONES AND MCINNES, 2004).

2 NB: When conducting an impact assessment where more than one climate variable is relevant, it is inappropriate to mix projections from different models, *e.g.* a temperature projection from model A and a rainfall projection from model B. Only values obtained from a single model have internal consistency and are considered physically plausible.

BOX 9.1: AUSTRALIAN CLIMATE FUTURES

Australian Climate Futures is a free web-based tool that provides regional climate projections for Australia (Clarke *et al.* 2011b, Whetton *et al.* 2012). It includes projections from the global climate modelling experiments that informed the IPCC's *Fourth Assessment Report* (CMIP3) (IPCC, 2007) and *Fifth Assessment Report* (CMIP5) (IPCC, 2013) as well as a range of dynamically and statistically downscaled projections. These can be explored for up to 13 future time periods (2030, 2035, 2040..., 2085, 2090) and seven emissions scenarios (SRES: B1, A1B and A2; RCP: 2.6, 4.5, 6.0 and 8.5).

Users can explore projections for different averaging periods (e.g. monthly, seasonal, annual) and a range of climate variables for their region of interest, including:

- mean temperature
- maximum temperature
- minimum temperature
- rainfall
- downward solar radiation
- relative humidity
- areal potential evapotranspiration
- drought
- extreme daily rainfall (1 in 20 yr event)
- wind-speed

Projected changes from all available climate models are classified into broad categories defined by two climate variables, e.g. the change in annual mean temperature and rainfall. Thus, model results can be sorted into different categories or 'climate futures', such as '*warmer and wetter*' or '*hotter and much drier*'. The Australian Climate Futures web-tool produces a colour-coded matrix (Figure B9.1) which shows the spread and clustering in all the model results across different climate change categories, and allows users to explore how this changes under different RCPs and time periods.

Users can identify cases of particular relevance to their impact assessment, such as 'best case' and 'worst' case climate futures. In addition, it is often possible to identify

a 'maximum consensus' climate future in which most climate model results reside. For example, consider a study into the possible impacts of climate change on the incidence of mosquito-borne diseases in the sub-tropics. In this example, the worst case is likely to be the climate future with the greatest increase in rainfall and temperature. In Figure B9.1, the worst case is the 'Much Hotter – Wetter' climate future, which has low model consensus (only 2 out of 30 models) but it is a possible future that should be considered. The best case may be regarded as the '*hotter – drier*' climate future. The maximum consensus is the '*hotter – little change*' future.

A range of regional breakdowns, including three levels of detail based on Australia's natural resource management regions, are available in the tool, allowing exploration of the climate futures at this scale. For example, the division of Australia into four large super-clusters allows generation of broad-scale, multi-purpose projections. In contrast, the sub-cluster boundaries allow generation of regionally relevant projections for specific purposes.

Importantly, the tool is underpinned by comprehensive climate model evaluation (Chapter 5). This ensures only those models that were found to perform satisfactorily over the Australian region are included. A few of these models were found to have limitations in particular regions only. The tool brings this information to the attention of users when relevant, and provides the opportunity to exclude those results if desired.

A key feature of Australian Climate Futures is the Representative Model Wizard. This identifies a suitable subset of models that can be used to represent the selected climate futures, e.g. a model to represent a 'worst' case future, one to represent a 'best' case future and one to represent the 'maximum consensus' future. For those with limited resources, this feature reduces the effort involved in analysing model data in impact studies.



BOX 9.1 AUSTRALIAN CLIMATE FUTURES

		Annual surface temperature (°C)			
		Slightly warmer 0 to +0.5	Warmer +0.5 to 1.5	Hotter +1.5 to +3.0	Much hotter > +3.0
Annual rainfall (%)	Much wetter > +15.0				
	Wetter +5.0 to +15.0		2 of 30 GCMs	9 of 30 GCMs 1 of 6 DS	2 of 30 GCMs
	Little change -5.0 to +5.0			13 of 30 GCMs 4 of 6 DS	2 of 30 GCMs
	Drier -15.0 to -5.0			2 of 30 GCMs 1 of 6 DS	
	Much drier < -15.0				

FIGURE B9.1: EXAMPLE DISPLAY OF PROJECTIONS FROM THE AUSTRALIAN CLIMATE FUTURES TOOL. THESE ARE CLASSIFIED BY ANNUAL AVERAGE CHANGES IN SURFACE TEMPERATURE AND RAINFALL, AND INCLUDE RESULTS FROM GLOBAL CLIMATE MODELS (GCMs) AND DOWNSCALING (DS). IN THIS EXAMPLE, COLOUR SHADINGS INDICATE DEGREE OF CONSENSUS AMONG THE GCM RESULTS ONLY. SOURCES OF DOWNSCALED RESULTS DISPLAYED WILL VARY WITH REGION.

The tool is fully integrated with the *Climate Change in Australia* website, greatly simplifying the process of displaying and downloading of datasets, GIS layers, maps and figures from the selected models.

The complete list of projections results that can be explored using the web-tool are shown in Table B9.1.

TABLE B9.1: PROJECTIONS RESULTS REPRESENTED IN THE AUSTRALIAN CLIMATE FUTURES WEB TOOL.

PROJECTIONS DATA	TYPE	COVERAGE
CMIP5	GCM	Australia-wide
CMIP3	GCM	Australia-wide
CCAM 50km	Dynamically downscaled from CMIP5	Australia-wide
BoM Analogue 5 km	Statistically downscaled from CMIP5	Australia-wide
NARcliM 10 km	Dynamically downscaled from CMIP3	NSW & ACT

METHODS FOR CREATING DATASETS FOR USE IN IMPACT ASSESSMENTS

For simple impact assessments, it may be sufficient to provide qualitative information about the direction of future climate change. For example, warmer with more droughts, heavier daily rainfall, higher sea level, fewer but stronger cyclones, and more ocean acidification. This could facilitate a high-level scoping process, such as a workshop discussion, that identifies potential impacts and prioritises elements that may need further quantification.

Other impact assessments need quantitative information. In many cases, projected changes (relative to some reference period) are required for different years, emissions scenarios, climate variables and regions. In other cases, application-ready datasets are needed. Various methods are available for producing application-ready datasets. The choice of method must be matched to the intended application, taking into account constraints of time, resources, human capacity and supporting infrastructure (Wilby *et al.* 2009). A summary of some common methods for creating application-ready datasets follows, with advantages and disadvantages presented in Table 9.1.

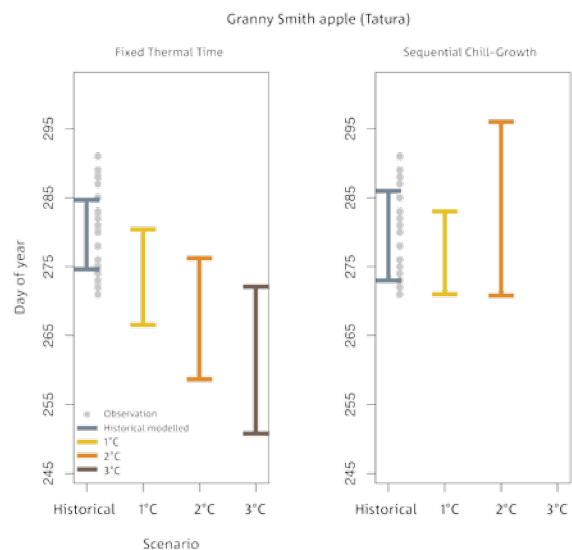


FIGURE 9.5: FUTURE FULL BLOOM TIMING (DAY OF YEAR (DOY) OF GRANNY SMITH APPLE AFTER A WARMING OF 1, 2 OR 3 °C USING TWO DIFFERENT MODELLING METHODS, FIXED THERMAL TIME AND SEQUENTIAL CHILL GROWTH. NB. MODELLING THAT INCORPORATED CHANGES TO CHILLING ACCUMULATION (SEQUENTIAL CHILL GROWTH) INDICATED CHILL REQUIREMENTS WERE NOT FULFILLED SO NO PROJECTED FLOWERING TIMING COULD BE ESTIMATED (SOURCE: DARBYSHIRE *ET AL.* 2014).



Sensitivity analysis. This entails running a climate impact model with observed climate data to establish a baseline level of risk, then re-running the model with the same input data, modified by selected changes in climate (e.g. a warming of 1, 2 or 3 °C). This simple methodology has been effectively used to demonstrate climate change impacts in the agricultural sector (Figure 9.5) (Cullen *et al.* 2012, Darbyshire *et al.* 2014).

Delta change or perturbation method. The projected changes in mean climate, as simulated by a climate model, are applied to observed climate data. This may be in the form an additive or multiplicative factor depending on the variable, with Figure 9.6 giving an example for temperature. This approach is often used in impact assessments (Webb *et al.* 2008). Some modifications to this method may incorporate projected changes in daily climate variability using quantile scaling. This technique was used in a study on future population heat exposure (Baynes *et al.* 2013).

Climate analogues. Historical climate data are used as an analogue for the future. The analogue may correspond to a different climate in time or space, such as a past climate anomaly that may occur more often in future in a particular region, or a location that currently has a climate similar to that expected in another region in the future (see section 9.3.4).

Weather generation. This involves the use of a statistical model that simulates time series of weather data, with statistical properties similar to observed weather data. These properties can be modified for future climates using information from climate models.

Statistical downscaling. A method that utilises a statistical relationship between the local-scale variable of interest and larger-scale atmospheric fields from global climate models (Charles *et al.* 1999, Timbal and McAvaney, 2001, Kokic *et al.* 2011). This is achieved through regression methods (e.g. multiple regression statistics, principal component, canonical correlation analysis, neural networks), weather typing or through the use of weather generators calibrated to the larger-scale atmospheric fields (see Section 6.3). To implement this technique, high-quality observed data are required for a number of decades to calibrate the statistical model.

Dynamical downscaling. This involves the use of a finer resolution atmospheric climate model, driven by output from a global climate model (Figure 9.7 and Section 6.3). This provides better representation of topography and associated effects on local climate, such as rainfall in mountainous regions, as well as the potential to better simulate extreme weather features, such as tropical cyclones. However, this method is computationally intensive and the results are strongly dependent on the choice of both global climate model and fine resolution atmospheric model. Furthermore, results from dynamically downscaled regional climate models are required to be bias-corrected (using statistical techniques) before they are suitable for use in climate change impact assessments. This method has been used in a study of impacts on agriculture reported through the *Climate Futures for Tasmania* initiative (Holz *et al.* 2010).

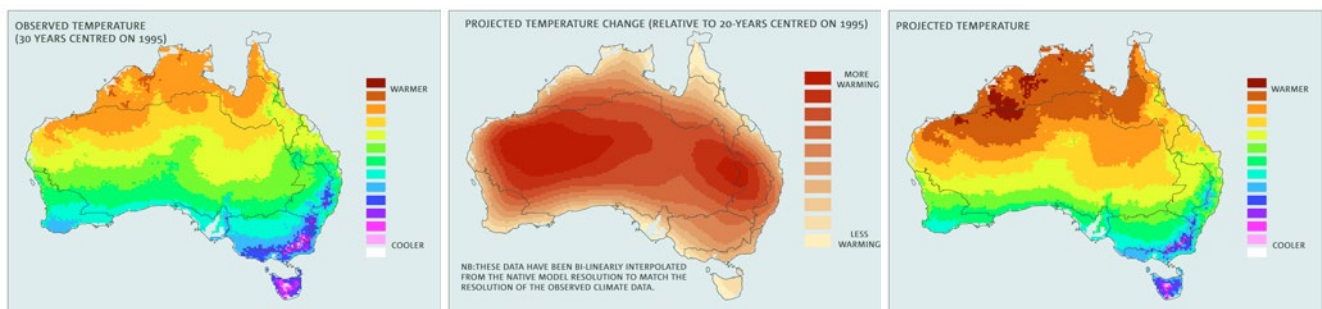


FIGURE 9.6: FUTURE TEMPERATURE INFORMATION (RIGHT) IS CREATED BY ADDING PROJECTED TEMPERATURE CHANGE FROM A CLIMATE MODEL (MIDDLE) TO OBSERVED DATA (LEFT). THIS IS AN EXAMPLE OF THE 'DELTA CHANGE' OR 'PERTURBATION METHOD'.



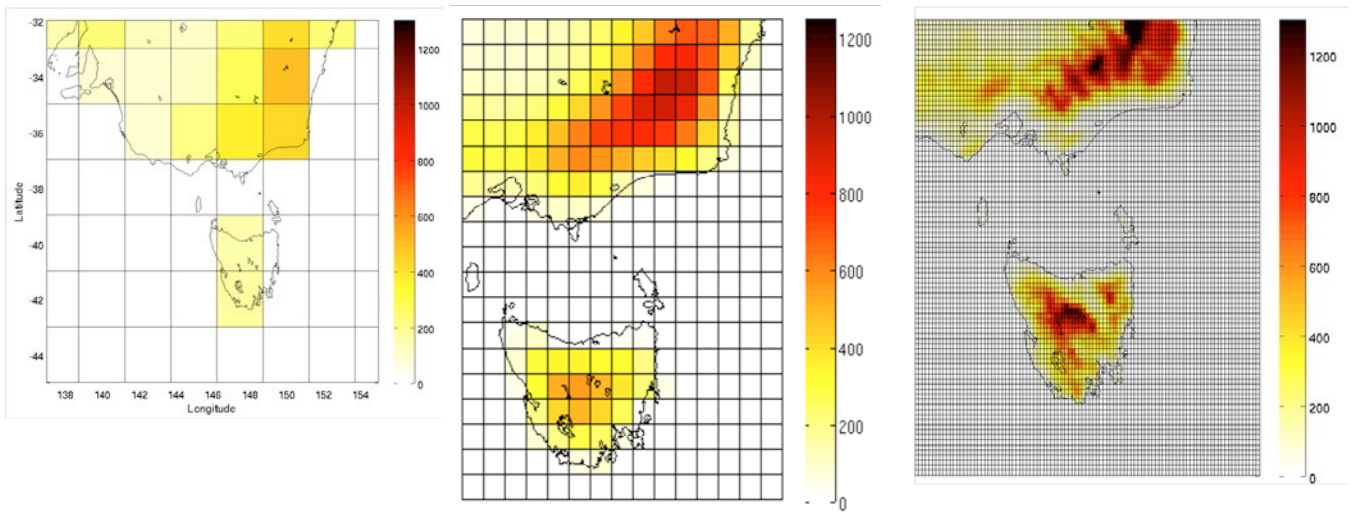


FIGURE 9.7: THE GRID SPACING AND REPRESENTATION OF TOPOGRAPHY OF TASMANIA IN A TYPICAL CMIP3 GLOBAL CLIMATE MODEL (LEFT) COMPARED TO THAT USED IN DYNAMICAL DOWNSCALING FOR THE *CLIMATE FUTURES FOR TASMANIA* PROJECT (HOLZ *ET AL.* (2010): INTERMEDIATE (MIDDLE) AND FINE (RIGHT) GRIDS FROM THE CCAM REGIONAL CLIMATE MODELS. THE COLOUR SCALE INDICATES SURFACE HEIGHT (M).

The application-ready data (described in Section 9.3.3) employed the delta change method for all variables (Section 6.3). Quantile scaling was used to create daily rainfall data that include projected changes in variance. Where appropriate, statistically and dynamically downscaled data are also accessible (see Section 9.6.1).

TABLE 9.1: SUMMARY OF TYPICAL CHARACTERISTICS ASSOCIATED WITH METHODS FOR APPLICATION OF CLIMATE PROJECTIONS. COLOUR CODING INDICATES EASE OF USE WITH BLUE BEING EASIER AND ORANGE BEING MORE DIFFICULT (SOURCE: WILBY *ET AL.* (2009) AND EKSTRÖM *ET AL.* (ACCEPTED)).

METHOD	ADVANTAGES AND DISADVANTAGES (IN ITALICS)
SENSITIVITY ANALYSIS	Requires no future climate change information. Shows most important variables/system thresholds. Allows comparisons between studies. <i>Impact model uncertainty seldom reported or unknown.</i> <i>May not be OK near complex topography and coastlines.</i> <i>Change in mean only.</i> OK for some applications but not others. Represents range of change if benchmarked to other scenarios.
WEATHER GENERATORS	Provide daily or sub-daily weather variables. Preserve relationships between weather variables. Already in widespread use for simulating present climate. <i>Needs high quality observational data for calibration and verification.</i> Assumes a constant relationship between large-scale circulation patterns and local weather. Scenarios are sensitive to choice of predictors and quality of GCM output. Scenarios are typically time-slice rather than transient. <i>Difficulty reproducing inter-annual variability (e.g. due to ENSO) and tropical weather phenomena such as monsoons and tropical cyclones.</i>
DELTA CHANGE METHOD	Simple to implement and suitable for many applications. Facilitates assessment of outputs from a large number of GCMs <i>Limited applicability where changes in variance are important.</i> <i>May not capture projected climate behaviour around complex topography.</i>
DELTA CHANGE METHOD (INCLUDING FUTURE CHANGES TO VARIABILITY, E.G. QUANTILE SCALING)	Suitable for many applications Includes changes in variability that may be important for adequately simulating extreme events <i>Requires statistical expertise to implement</i> <i>May not capture projected climate behaviour around complex topography.</i>
STATISTICAL DOWNSCALING	Good for many applications, but restricted by availability of relevant variables. Site-specific time-series and other statistics, e.g. extreme event frequencies. Good near high topography. <i>Requires high quality observational data over a number of decades for calibration and verification.</i> <i>Assumes a constant relationship between large-scale circulation patterns and local weather.</i> <i>Scenarios are sensitive to choice of forcing factors and host GCM or RCM.</i> <i>Choice of host GCM or RCM constrained by archived outputs.</i> <i>Hard to choose from the large variety of methods, each with pros and cons.</i> <i>Need to be aware of any shortcomings of the particular method chosen.</i>
DYNAMICAL DOWNSCALING WITH BIAS CORRECTION	Provides regional climate scenarios at 10-60 km resolution. Reflects underlying land-surface controls and feedbacks. Preserves relationships between weather variables. Often gives better representation of coastal and mountain effects, and extreme weather events. Simulations with bias-corrected SSTs should make the present-climate simulation more realistic than the host GCM. <i>Requires high quality observational data for model verification.</i> <i>Should not be assumed that the dynamically downscaled projections are necessarily more reliable than projections based on the host model.</i> <i>High computational demand.</i> <i>Projections are sensitive to choice of host GCM and RCM.</i>
DYNAMICAL DOWNSCALING CHANGE FACTOR METHOD APPLIED TO HIGH RES. OBS.	As for dynamical downscaling with bias correction. This technique is suitable for many agricultural and biodiversity applications.



9.2.4 RISK EVALUATION AND RISK TREATMENT

After risks have been analysed, it is important to rank the risks in terms of their severity. In some cases it is possible to screen out minor risks that can be set aside and identify those risks for which more detailed analysis is recommended (Australian Greenhouse Office, 2006). This should include social and economic analysis. Risk treatment is the identification of relevant options to manage the risks and their consequences, selecting the best options for incorporating into forward plans, and implementing them (Australian Greenhouse Office, 2006).

9.3 INFORMATION PRODUCTS FOR RISK IDENTIFICATION AND ANALYSIS

9.3.1 CLIMATE CHANGE IN AUSTRALIA WEBSITE

The *Climate Change in Australia* website, produced in parallel with this Report, provides users with extensive access to information on climate change science, climate projections, data sources and regional impacts and adaptation resources.

The website includes broad narratives about Australia's future climate, information resources (such as downloadable reports, videos and images), guidance on using climate change projections for research, tips for users who are involved in communicating about climate change within regional communities, tools to support planning and climate decision making, and data mining interfaces to enhance the discoverability of national and regional climate change projections.

Several web interfaces allow users to search for additional climate change projection information that is not described in this Report. This is particularly relevant to users who want to explore alternative time slices, require more information about changes to a variable of interest, or require access to the underpinning climate data. Data exploration interfaces include the ability to look at selected climate thresholds, regional climate analogues, data tables, map-based information, as well as the opportunity to download climate change data (relative to a 'present' baseline) and application-ready data for impact studies.

As described in Chapter 2, the regionalisation scheme used to develop narratives and deliver data has been tailored to Australia's natural resource management (NRM) sector. The website also utilises this scheme and provides access to regional climate change impacts and adaptation information through linking with relevant Australian research projects. These projects are focused on providing resources to assist in the development of natural resource management plans.

9.3.2 DECISION TREE

A decision tree underlies the architecture of the *Climate Change in Australia* website, and allows users to find the type of climate change information appropriate to their impact assessment (Figure 9.8). Through this mechanism users are led to sources of data, reports, background information and guidance material that may be useful in undertaking an impact assessment. This type of tool has been used successfully in the UK (Street *et al.* 2009, Steynor *et al.* 2012).

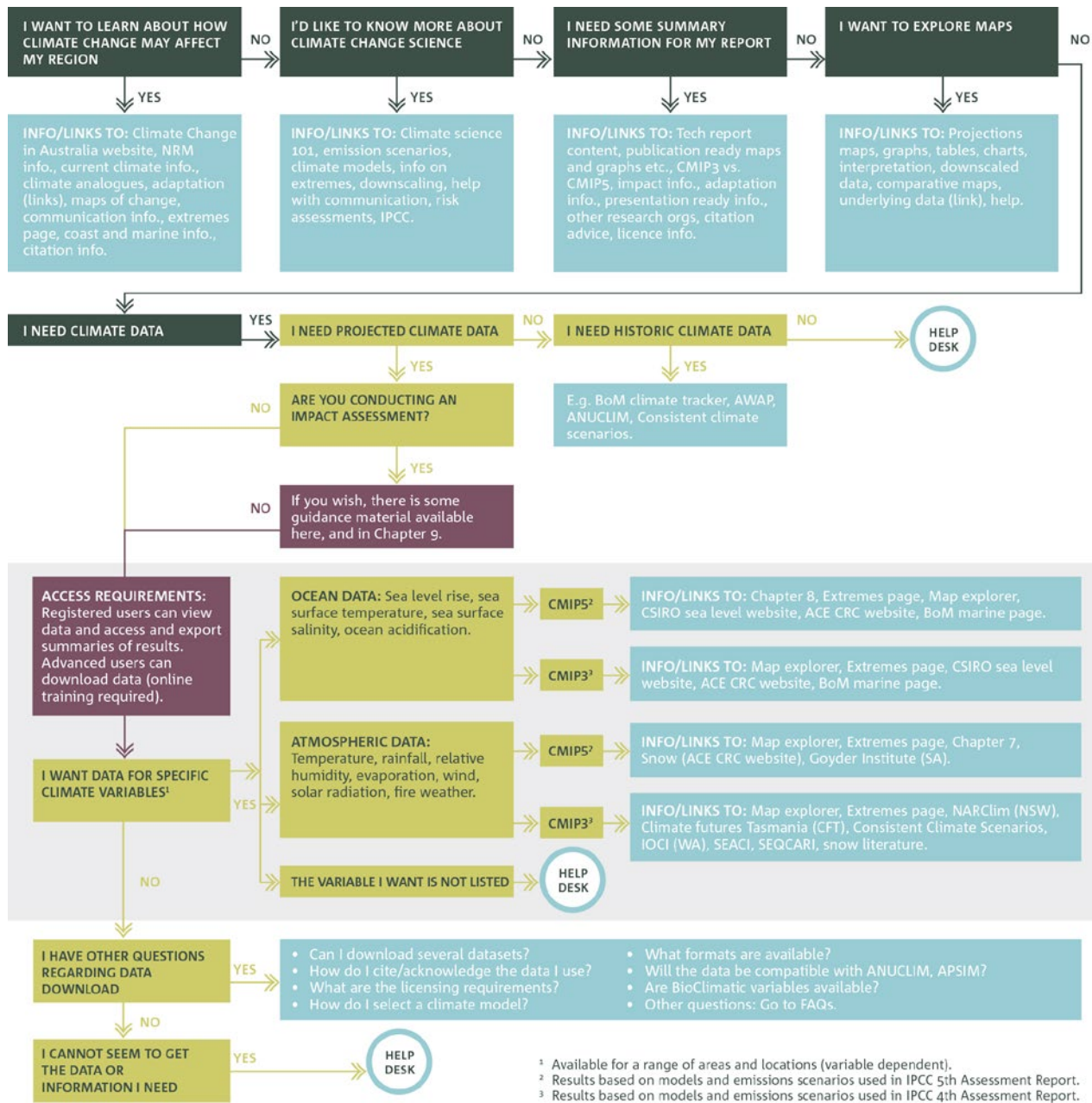


FIGURE 9.8: DECISION TREE AVAILABLE ON THE CLIMATECHANGEINAUSTRALIA.GOV.AU WEBSITE, WITHIN WHICH THE MAP EXPLORER PROVIDES A PATHWAY TO THE DOWNLOADABLE DATA PROVIDED FOR THE NRM PROJECT. PALE GREY BOX INDICATES REGISTRATION REQUIREMENT FOR ACCESS TO DATA AND INFORMATION.



9.3.3 REPORT-READY PROJECTED CHANGE INFORMATION

In many cases, simple figures and tables are all that might be required for insertion into a report, or for a presentation. Along with figures for model specific results for all of the variables, time periods and spatial scales, images and tables are also provided for ensembles of models, indicating ranges of projected change for regional averages. Images for model-specific results are also provided for all of the variables, time periods and spatial scales described in Tables 9.2 and 9.3, along with supporting text.

9.3.4 CLIMATE DATA

Two types of data are delivered to users:

- Projected climate changes (relative to the IPCC reference period 1986–2005);
- Application-ready future climate data (where projected climate changes are applied to 30 years' of observed data).

Data are provided in varying levels of spatial detail to suit different purposes: Area averaged data are provided for the NRM domains (super-clusters, clusters and sub-clusters); nation-wide gridded data; and point data for selected localities. The CMIP5 models used in this assessment have an average spatial resolution (spacing between data points) of approximately 180km (ranging from 67km to 333km). The projected change data are available at the original grid resolution for each model. For application-ready data, bi-linear interpolation has been used to produce finer 5 km gridded resolution data to align with the grid resolution of the AWAP baseline climate dataset. Although these data look more detailed when re-gridded to a finer scale, the process of bi-linear interpolation does not add extra information, and therefore is not more accurate than the coarser resolution data.

PROJECTED CLIMATE CHANGE DATA

Projected climate change data are informative for impact assessment and are made available as described in Table 9.2. The changes are relative to 1986-2005, and based on CMIP5 global climate models and downscaling where appropriate. Annual, seasonal and monthly changes are supplied for 20-year periods centred on 2030, 2050, 2070 and 2090 for most variables and RCPs.

APPLICATION-READY DATA

Application-ready data are synthetic future data, generated by combining projected changes with observed data. These data can be used in detailed impact assessments when appropriate observed climate data are available (having sufficient quality and duration). Projected climate changes derived from eight CMIP5 models (see Box 9.2 and Figures 9.9 and 9.10) have been applied to 30-year observed datasets centred on 1995 (1981-2010)³ using the delta change method described in Section 9.2.3 for most variables.

The daily rainfall time series produced for the NRM project, however, uses a multi-timeframe quantile-quantile (MQQ) scaling approach. Using this technique, a change to daily rainfall variability, as well as the mean, is produced. Changes at longer timeframes are also of interest to many applications, such as year to year variability. The MQQ method allows the projected changes in variability (over different time-scales) as indicated by climate model outputs to be expressed in the dataset by calculating eleven distinct change factors between the baseline and future period. A unique change factor is calculated for each of eleven time-windows examined in a wavelet multi-resolution decomposition (Percival and Mofjeld, 1997, Li *et al.* 2012). These change factors are then applied to the observed dataset to scale up or down at each of these different timeframes.

Application-ready data include averages and time series over a range of spatial scales, as shown in Table 9.3, and they can be accessed through a range of 'interfaces' with guidance available via the decision tree (Figure 9.8).

Engagement with NRM sector professionals and researchers led to recommendations for delivery of data that would align with various ecological and plant production modelling tools. Bioclimatic model developers identified a number of data requirements that have been addressed to maximise the integration with the climate projections products. In response to this engagement, monthly climate projection data for 'Bioclim' variables (Sutherst *et al.* 2007), ANUCLIM compatibility (Xu and Hutchinson, 2011) and text file format suitable for use in impacts modelling *e.g.* the crop modelling package APSIM (McCown *et al.* 1996) were recognised as a useful addition to the outputs from this project.

³ To minimise the influence of natural variability on observed climate averages over the baseline period, for example the recent south-east Australian drought, a 30-year baseline dataset is used, i.e. an extended period centred on 1995.

TABLE 9.2: PROJECTED CHANGE DATA FOR DIFFERENT CLIMATE VARIABLES AND A VARIETY OF TEMPORAL AND SPATIAL SCALES, FOR 20-YEAR PERIODS CENTRED ON 2030, 2050, 2070 AND 2090, RELATIVE TO A 20-YEAR PERIOD CENTRED ON 1995 (1986-2005). GRIDDED CHANGES ARE AVAILABLE FOR INDIVIDUAL CLIMATE MODELS, FOR ALL FOUR RCPs WHERE POSSIBLE, ON THE ORIGINAL CLIMATE MODEL GRID. GREEN = AVAILABLE, GOLD = INFORMATION IN TECHNICAL AND CLUSTER REPORTS, WHITE = NOT AVAILABLE.

VARIABLE	ANNUAL		SEASONAL		MONTHLY	
	GRIDDED	AREA AVG.	GRIDDED	AREA AVG.	GRIDDED	AREA AVG.
MEAN TEMPERATURE ^A						
MAXIMUM DAILY TEMPERATURE ^A						
MINIMUM DAILY TEMPERATURE ^A						
RAINFALL ^A						
RELATIVE HUMIDITY ^A						
WET AREAL EVAPOTRANSPIRATION ^A						
SOLAR RADIATION ^A						
WIND-SPEED ^A						
EXTREME RAINFALL (INTENSITY OF 1 IN 20 YR EVENT) ^{B,C,G}						
EXTREME WIND (INTENSITY OF 1 IN 20 YR EVENT) ^G						
DROUGHT (SPI-BASED ^D , DURATION, FREQUENCY, % TIME)						
FIRE ^E						
SEA LEVEL RISE (MEAN AND EXTREME) ^{F,H}						
SEA SURFACE TEMPERATURE ^H						
SEA SURFACE SALINITY ^H						
OCEAN ACIDIFICATION (ARAGONITE SATURATION) ^{G,H}						
TROPICAL CYCLONE FREQUENCY/LOCATION						
TROPICAL CYCLONE INTENSITY						
SNOW						
RUNOFF AND SOIL MOISTURE						

A Gridded changes will be available for individual climate models on the original climate model grid.

B Event is defined as 24-hour total rainfall.

C These data are considered an interim product and will be updated using higher resolution models and reported in the Australian rainfall and runoff (ARR) handbook (anticipated 2015).

D Standardised Precipitation Index, a probability index that considers precipitation only. Drought projections available for 20 models (RCP4.5 and RCP8.5) and 13 models for RCP2.6 (see McKee *et al.*, 1993 for a description of the method for calculation of the SPI).

E Fire-weather data are supplied at 39 sites for three models (see Data Delivery Brochure).

F Data for 16 tide gauge sites (see Data Delivery Brochure), not for individual models but for a multi-model range defined by the 5th to 95th percentile.

G Event is defined as 24-hour total rainfall.

H No data for individual models but for a multi-model range defined by the 5th to 95th percentile.



TABLE 9.3: ‘APPLICATION-READY’ FUTURE CLIMATE DATA FOR DIFFERENT CLIMATE VARIABLES AND A VARIETY OF TEMPORAL AND SPATIAL SCALES, FOR 30-YEAR PERIODS CENTRED ON 1995, 2030, 2050, 2070 AND 2090. THIS INCLUDES GRIDDED DATA AND DATA FOR CITIES AND TOWNS. DATA FOR CITIES ARE LIMITED BY AVAILABILITY OF A RELIABLE BASELINE DATASET. PROJECTIONS ARE BASED ON CHANGES FROM EIGHT CLIMATE MODELS, AND DOWNSCALING WHERE APPROPRIATE. GREEN = DATA AVAILABLE, WHITE = DATA NOT AVAILABLE.

TEMPORAL SCALE	ANNUAL				SEASONAL				MONTHLY				DAILY	
	GRIDDED		CITY/TOWN ^c		GRIDDED		CITY/TOWN ^c		GRIDDED		CITY/TOWN ^c		GRIDDED	CITY/TOWN ^c
SPATIAL SCALE														
CLIMATE VARIABLE	AVERAGES	TIME-SERIES	AVERAGES	TIME-SERIES	AVERAGES	TIME-SERIES	AVERAGES	TIME-SERIES	AVERAGES	TIME-SERIES	AVERAGES	TIME-SERIES	TIME-SERIES	TIME-SERIES
Mean temperature (°C) ^e	Green	Green	Green	Green	Green	Green	Green	Green	Green	Green	Green	Green	Green	Green
Maximum daily temperature ^e	Green	Green	Green	Green	Green	Green	Green	Green	Green	Green	Green	Green	Green	Green
Minimum daily temperature ^e	Green	Green	Green	Green	Green	Green	Green	Green	Green	Green	Green	Green	Green	Green
Days above/below/between temperature thresholds ^{a,e}	Green	Green	Green	Green	Green	Green	Green	Green	Green	Green	Green	Green	Green	Green
Rainfall (mm) ^e	Green	Green	Green	Green	Green	Green	Green	Green	Green	Green	Green	Green	Green	Green
Relative humidity (%) ^h	Green	Green	Green	Green	Green	Green	Green	Green	Green	Green	Green	Green	Green	Green
Point potential evapotranspiration ^{d,j}	Green	Green	Green	Green	Green	Green	Green	Green	Green	Green	Green	Green	Green	Green
Wet areal evapotranspiration (mm) ^f	Green	Green	Green	Green	Green	Green	Green	Green	Green	Green	Green	Green	Green	Green
Mean wind-speed (ms ⁻¹) ^c	Green	Green	Green	Green	Green	Green	Green	Green	Green	Green	Green	Green	Green	Green
Solar radiation (Wm ⁻²) ⁱ	Green	Green	Green	Green	Green	Green	Green	Green	Green	Green	Green	Green	Green	Green
Fire weather ^b	Green	Green	Green	Green	Green	Green	Green	Green	Green	Green	Green	Green	Green	Green
Fire weather days above/below/between thresholds ^b	Green	Green	Green	Green	Green	Green	Green	Green	Green	Green	Green	Green	Green	Green

- A Thresholds presented in days per year above ‘XX’ °C (days), for example.
- B Forest Fire Danger Index (FFDI) for 39 sites. Also see Data Delivery Brochure.
- C For availability of data for cities and towns see Data Delivery Brochure.
- D Proxy for Pan Evaporation.

Baseline datasets (1981–2010)

- E Australian Water Availability Project (AWAP) time series data (0.05° grid) (Jones *et al.*, 2009).
- F CSIRO Land and Water dataset (Morton, 1983, Teng *et al.*, 2012) (0.05° grid).
- G ERA interim reanalysis (0.75° grid), but daily gridded wind data have quality control problems (Dee *et al.*, 2011). High quality daily wind speed data used in fire weather analysis were sourced from 39 sites—see Data Delivery Brochure.
- H ERA interim reanalysis (0.75° grid), but daily humidity data at cities/towns have quality control problems (Dee *et al.*, 2011).
- I ERA interim reanalysis (0.75° grid), but daily solar radiation data at cities/towns have quality control problems (Dee *et al.*, 2011).
- J Bureau of Meteorology high quality monthly pan-evaporation dataset (see Jovanovic *et al.* 2008).



BOX 9.2: MODEL SELECTION FOR APPLICATION-READY DATA

Eight of the 40 CMIP5 models assessed in this project have been selected for use in provision of application-ready data. This facilitates efficient exploration of climate projections for Australia.

A number of steps were considered in the model selection process:

- Rejection of models that were found to have a low performance ranking across a number of metrics in Chapter 5 and in some other relevant assessments, e.g. *Pacific Climate Change Science Program* (Grose *et al.* 2014a), ENSO evaluation (Cai *et al.* 2014).
- Selection of models for which projection data were available for climate variables commonly used in impact assessments, for at least RCP4.5 and RCP8.5. Projections for other RCPs are included where possible.
- Amongst these, identification of models that are representative of the range of seasonal temperature and rainfall projections for a climate centred on 2050

and 2090 and RCP4.5 and RCP8.5 using the *Australian Climate Futures* software (see Figure B9.1 from this chapter and Whetton *et al.* (2012).

- Projections for wind were assessed separately from temperature and rainfall to ensure the CMIP5 range was captured. This is because the direction and magnitude of wind projections are not necessarily correlated with the temperature and/or rainfall projections.
- Availability of corresponding statistical or dynamical downscaled data.
- Consideration of the independence of the models (Knutti *et al.* 2013).

The eight models and the reasons for their inclusion are shown in Table B9.4. Their results are shown in context of the 40 models for temperature and rainfall over the four NRM super-clusters (see Figure 2.3) for 2050 and 2090 (Figure 9.10 and 9.11).

TABLE B9.4: SELECTED CMIP5 MODELS AND REASONS FOR THEIR INCLUSION.

SELECTED MODELS	CLIMATE FUTURES	WIND	OTHER
ACCESS1.0	Maximum consensus for many regions.		The model exhibited a high skill score with regard to historical climate.
CESM1-CAM5	Hotter and wetter, or hotter and least drying		This model was representative of a low change in an index of the Southern Annular Mode (per degree global warming). Further, the model has results representing all RCPs.
CNRM-CM5	Hot /wet end of range in Southern Australia		This model was representative of low warming/dry SST modes as described in Watterson (2012) (see Section 3.6). It also has a good representation of extreme El Niño in CMIP5 evaluations (see Cai <i>et al.</i> (2014)).
GFDL-ESM2M	Hotter and drier model for many clusters	Greatest increase	This model was representative of the hot/dry SST mode as described in (Watterson, 2012) (see Section 3.6). It also has a good representation of extreme El Niño in CMIP5 evaluations (see Cai <i>et al.</i> (2014)). Further, the model has results representing all RCPs.
HadGEM2-CC	Maximum consensus for many regions.	Greatest reduction	This model has good representation of extreme El Niño in CMIP5 evaluations (see Cai <i>et al.</i> (2014)
CanESM2			This model was representative of the hot/wet SST mode as described in Watterson (2012) (Section 3.6). It also has a high skill score with regard to historical climate and it increased representation of the spread in genealogy of models (Knutti <i>et al.</i> , 2013). It also has good representation of extreme El Niño in CMIP5 evaluations (Cai <i>et al.</i> , 2014).
MIROC5 (non-commercial use only)	Low warming wetter model		This model was representative of a higher change in an index of the Southern Annular mode (per degree global warming). It also has good representation of extreme El Niño in CMIP5 evaluations (see Cai <i>et al.</i> (2014)). Further, the model has results representing all RCPs.
NorESM1-M	Low warming wettest representative model	No wind data	This model was representative of the low warming/wet SST mode as described in Watterson (2012) (see Section 3.6). The model also has results representing all RCPs.



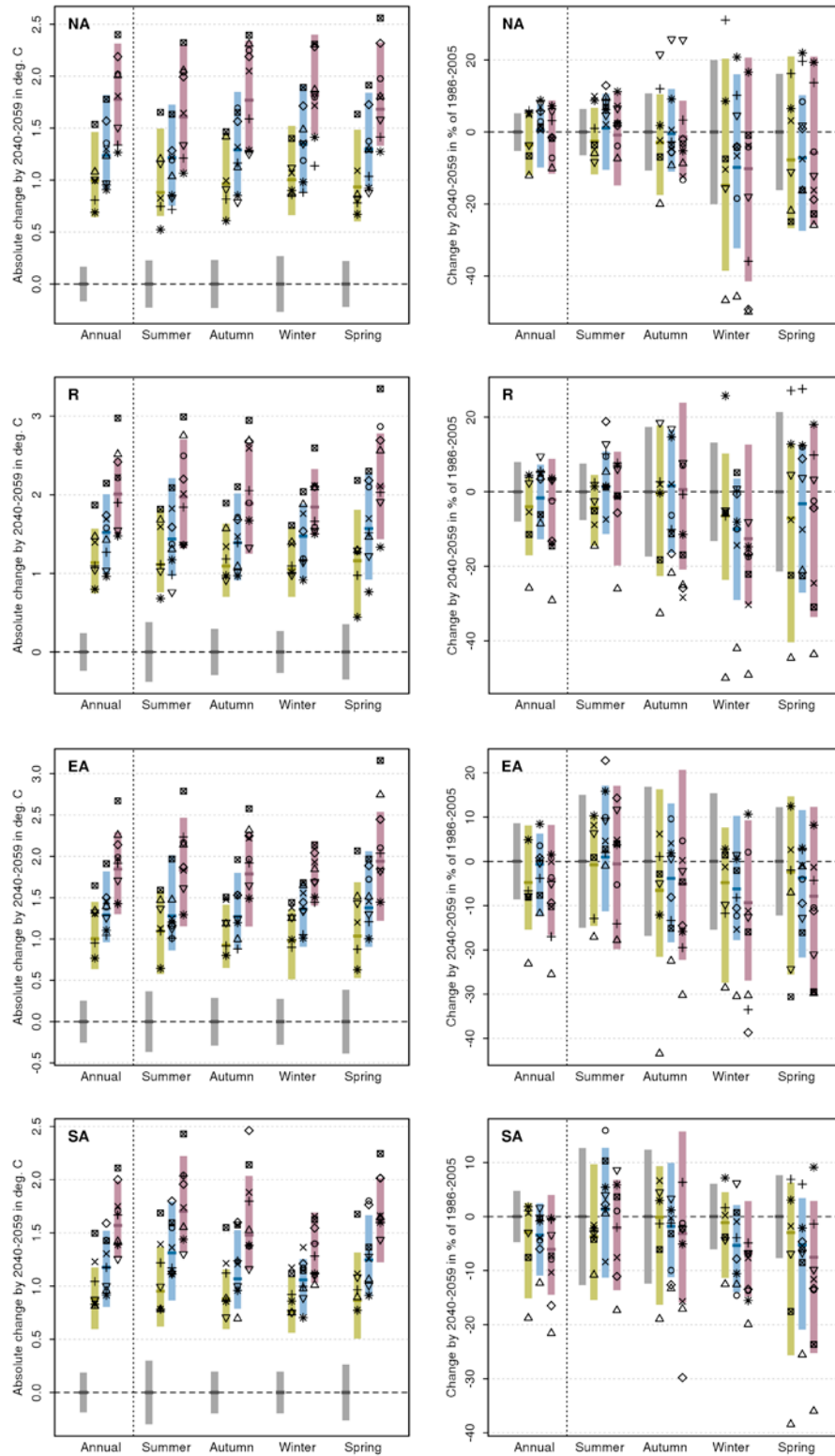


FIGURE 9.9: MID CENTURY (2050) PROJECTED TEMPERATURE CHANGE ($^{\circ}\text{C}$, LEFT), RAINFALL RELATIVE PERCENT CHANGE (RIGHT) FOR, FROM TOP TO BOTTOM, NORTHERN AUSTRALIA, RANGELANDS, EASTERN AUSTRALIA, AND SOUTHERN AUSTRALIA SUPER-CLUSTERS. DATA FOR ANNUAL, SUMMER (DJF), AUTUMN (MAM), WINTER (JJA) AND SPRING (SON) ARE PLOTTED FROM LEFT TO RIGHT IN EACH GRAPH. BAR RANGES INDICATE 10TH TO 90TH PERCENTILE OF 20-YEAR RUNNING MEAN OF 40 CMIP5 MODELS: HISTORICAL (GREY), RCP2.6 (GREEN), RCP4.5 (BLUE) AND RCP8.5 (PURPLE). SUPERIMPOSED ON THE BARS ARE RESULTS FOR EIGHT SELECTED MODELS: ACCESS1.0 (CIRCLE), GFDL-ESM2M (TRIANGLE-UP), CNRM-CM5 (PLUS), CESM1-CAM5 (CROSS), HADGEM2-CC (DIAMOND), MIROC5 (TRIANGLE-DOWN), CANESM2 (SQUARE), AND NORESM1-M (STAR).

-20° -10° 0° 10° 20° 30° 40° 50°

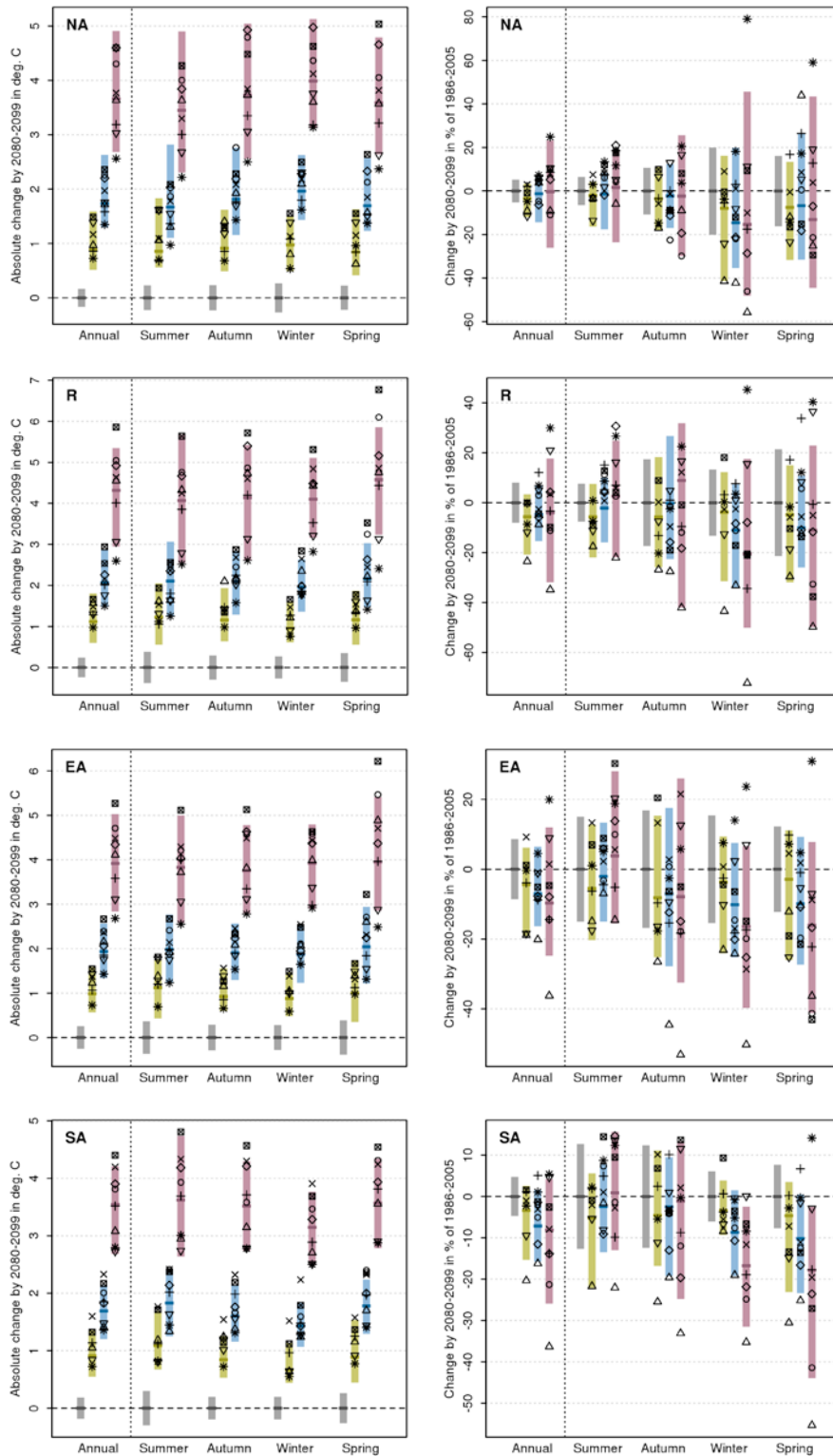


FIGURE 9.10: AS FOR FIGURE 9.9 BUT FOR THE END OF THE CENTURY (2090).



9.3.5 CLIMATE ANALOGUE TOOL

Identification of areas that experience similar climatic conditions, but which may be separated in space or time (i.e. with past or future climates) can be helpful when starting to consider adaptation strategies to a changing climate. Locating areas where the current climate is similar to the projected future climate of a place of interest (e.g. what will the future climate of Melbourne be like?) is a simple method for visualising and communicating the impact of projected changes (Hallegatte *et al.* 2007, Whetton *et al.* 2013).

The climate analogue tool available on the website is based on the approach used by Whetton *et al.* (2013), which matches annual average rainfall and maximum temperature (within set tolerances). This approach was also used to generate the analogue cases presented as examples in each of the Cluster Reports. These results should capture sites of broadly similar annual maximum temperature and water balance, but ignores potentially important seasonal differences in rainfall occurrences and other factors. The online tool has additional features that give the user the potential to refine the search for analogues by including measures of rainfall seasonality (per cent of annual rainfall that falls in summer) and temperature seasonality (difference in summer and winter temperature). Figure 9.11 depicts analogues after a 3 °C increase in annual maximum temperature and a 15 percent decrease in annual rainfall, e.g. where Melbourne's future climate matches the current climate in Dubbo (NSW). Nevertheless we note that other potentially important aspects of local climate are still not matched with this approach, such as frost days or other local climate influences, and for agriculture applications, solar radiation and soils are not considered. Thus we advise against the analogues being used directly in adaptation planning without considering more detailed information.

9.3.6 LINKS TO OTHER PROJECTS

Links to other CMIP3 based projects and sources of data are available through the website.

Information portals and State Government initiatives include:

- Climate Futures for Tasmania: This project details the general impacts of climate change in Tasmania over the 21st century, with a description of past and present climate and projections for the future. It assesses how water will flow through various Tasmanian water catchments and into storage reservoirs under different climate scenarios. It also assesses specific climate indicators most important for productivity in several key agricultural groups. Working with emergency service agencies, the project identifies the climate variables of greatest concern to emergency managers (<http://www.acecrc.org.au/Research/Climate%20Futures>).

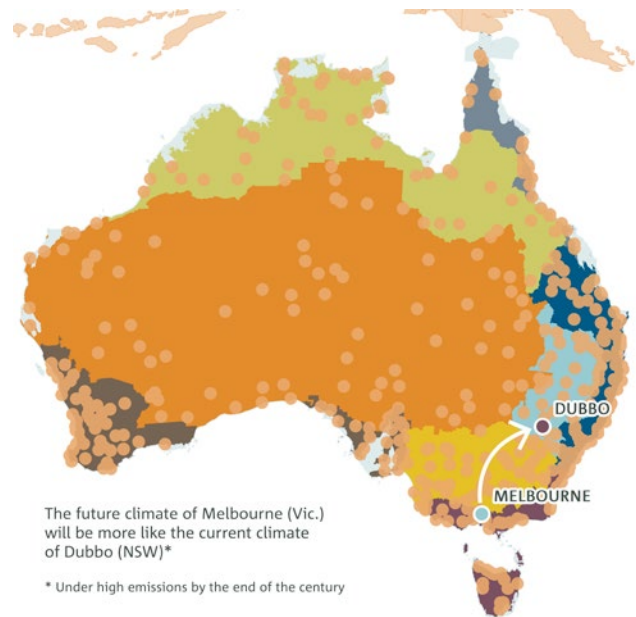


FIGURE 9.11: CLIMATE ANALOGUE EXAMPLE (MELBOURNE, +3 °C AND -15 % RAINFALL).

- South Eastern Australian Climate Initiative: This program was established in 2005 to improve understanding of the nature and causes of climate variability and change in south-eastern Australia in order to better manage climate impacts. It concluded in September 2012 (<http://www.seaci.org/>).
- Indian Ocean Climate Initiative: This program investigated the causes of climate change in Western Australia and developed regional projections. It ended in 2013 (www.ioici.org.au).
- The Goyder Institute for Water Research: This program was established in 2010 to support the security and management of South Australia's water supply and contribute to water reform in Australia. CMIP5 data are used in this project. (<http://goyderinstitute.org/>).
- South East Queensland Climate Adaptation Research Initiative: This program provides access to information on climate projections and adaptation options for settlements in South-east Queensland. It ended in November 2012. (<http://www.griffith.edu.au/environment-planning-architecture/urban-research-program/research/south-east-queensland-climate-adaptation-research-initiative>)

DATA PORTALS

- James Cook University Tropical Data Hub: a research data repository (<https://eresearch.jcu.edu.au/tdh>)
- NSW and ACT Regional Climate Modelling (NARcliM): This project is producing an ensemble of regional climate projections for south-east Australia in collaboration with the NSW Government. This ensemble is designed to provide robust projections that span the range of likely future changes in climate. A wide variety of climate variables will be available at high temporal and spatial resolution for use in impacts and adaptation research (<http://www.ccrcc.unsw.edu.au/NARcliM/>).
- The Consistent Climate Scenarios Project: This project provides Australia-wide projections data for 2030 and 2050 as daily time-series in a format suitable for most biophysical models. It includes daily projections of rainfall, evaporation, minimum and maximum temperature, solar radiation and vapour pressure deficit for individual locations. Projections data were also developed on a 5 km grid across Australia. (<http://www.longpaddock.qld.gov.au/climateprojections>)
- CliMond: This is a set of free climate data products consisting of high resolution interpolated surfaces of recent historical climate and relevant future climate data. These are available at monthly time-scales, for 35 Bioclim variables, in CLIMEX format, and as the Köppen-Geiger climate classification scheme (<https://www.climond.org/>).
- Climate Futures for Tasmania: This project included a data portal (<https://dl.tpac.org.au/tpacportal/>).



CHAPTER TEN

RESEARCH DIRECTIONS



WIND FARM, WESTERN AUSTRALIA, ISTOCK

-20° -10° 0° 10° 20° 30° 40° 50°

CHAPTER 10 RESEARCH DIRECTIONS

The projections presented in this Report are the most comprehensive and broadly based ever produced for Australia. This has been made possible by Australian scientists working to make significant advances in our observational networks, understanding of regional climate drivers and how these may change in the future, analysis of climate model simulations, and consultation with end-users. There has been substantial leveraging of the Australian Climate Change Research Program. Australia's participation in global fora, such as the fifth Climate Model Intercomparison Project (CMIP5), has enabled the projections and underpinning research to benefit from improved international scientific understanding of the global climate system, as represented in the recent reports of the IPCC.

Future research directions to allow for the continued improvement of Australian climate projections include:

- increasing our understanding of the drivers of regional climate and extremes, such as the El Niño-Southern Oscillation and the Indian Ocean Dipole, and how they are likely to change in the future
- maintaining and enhancing an extensive observational network, to detect climate variability and change and track atmospheric and ocean processes that influence major climate drivers
- developing capability in multi-year and decadal predictions
- enhancing downscaling techniques
- ongoing participation in international modelling comparisons, to enable continued leveraging of extensive global research into model development
- support for end-users of projections, including targeted support, communication products and tailored projections for specific sectors of the community, government or economy.

10.1 UNDERSTANDING CLIMATIC VARIABILITY AND MONITORING CHANGE

It is through weather and climate extremes that most of us experience the impacts caused by climate change. Advances in our ability to estimate 21st century climate will come from improving our capacity to understand how important phenomena that influence variability and extremes, such as the El Niño-Southern Oscillation and the Indian Ocean Dipole, are likely to change in future. This will allow for improved projections of likely changes to droughts, floods, frosts, heatwaves, fires, hailstorms, extreme winds, tropical cyclones and the monsoon.

The Senate Inquiry into “Recent trends in and preparedness for extreme weather events” made ten recommendations, two of which were:

- a. The committee recommends that the Bureau of Meteorology and CSIRO continue to improve projections and forecasts of extreme weather events at a more local level
- b. The committee notes the linkage between climate change and extreme weather events and recommends that the Bureau of Meteorology and CSIRO conduct further research to increase understanding in the areas of:
 - i. the interaction between large-scale natural variations, climate change and extreme weather events;
 - ii. the impacts of climate change on rainfall patterns and tropical cyclones;
 - iii. that Australia cooperatively engage, where appropriate, with international research initiatives in these areas

Multi-year and decadal predictions (2-10 years) are becoming a focus for international climate science efforts. Critical drivers of our climate such as the El Niño-Southern Oscillation often operate on multi-year to decadal scales. Planning and risk management decisions for many sectors are also made on these timescales. Researchers need to identify the variables that can be skilfully predicted and how far into the future some predictive skill remains evident. It is likely that near-term predictability will vary by region, so specific Australian studies continue to be needed.

Observational networks continue to provide vital information for detecting and attributing change, for undertaking process studies and for improving near-term predictions and long-term projections. The Bureau of Meteorology's observational network is an important national resource, providing the long-term and high quality data needed for climate research. The network is also monitoring variables for which we have little information, such as wind speed and evapotranspiration.

Ocean observational networks are also critical to understanding the storage and distribution of global heat and the drivers of our regional climate. Australia's investment in ocean monitoring is targeting areas of importance to Australia, including the Southern Ocean and tropics, while contributing to and benefiting from the global effort (*e.g.* Ocean Observations Panel for Climate, Global Ocean Observing System and Global Climate



Observing System). Extensive ocean observations and their assimilation into models will be essential for multi-year and decadal predictions.

Ocean observations are also important to understanding and projecting sea level rise, alterations to wave patterns, variations in regional sea level and investigating extreme events such as storm surges. Australia is particularly vulnerable to sea level rise and this remains an important area of further research.

10.2 NEW CLIMATE MODEL ENSEMBLES

The international research community is commencing the latest round of climate model comparisons: the Coupled Model Intercomparison Project phase 6 (CMIP6), run under the auspices of the World Climate Research Programme. By participating in these model intercomparisons, Australia has access to substantial research outputs from the global climate science community. The ACCESS model is used in Australia for weather and seasonal forecasting as well as longer-term climate projections, and our participation in global activities enables improved modelling capacity on all time scales. Australia needs to expand its data storage and analysis infrastructure to ensure we benefit from this research.

There is also a need to improve downscaling techniques. While a number of dynamical and statistical options exist, each has pros and cons. A more thorough assessment of the reliability of these techniques is needed in order to extract the greatest benefit.

10.3 TARGETED PROJECTION PRODUCTS AND COMMUNICATION

Research and experience overseas indicate that ongoing support from science agencies is required for users to effectively apply climate projections. Well-resourced climate projection support services are needed to meet the growing demand from researchers, planners and decision-makers to assess potential impacts, explore management options and implement effective adaptation strategies. The WMO Global Framework for Climate Services provides guidance on how this might be done. Vaughan and Desai (2014) review institutional arrangements of selected emerging climate services across local, national, regional, and international scales.

Some sectors require specific projection products to answer important questions. For example, further research on runoff is needed if researchers are to reliably translate projected rainfall changes into likely changes to soil moisture, run-off and river flows. More detailed modelling of fire weather, fuel and ignition is needed to understand how climate change will affect fire frequency, duration and intensity.

This Australian projections program has involved strong linkages between development of climate change products and their application by the NRM community. As well as

continuing to strengthen these linkages, this integrated approach could be applied productively in other important sectors, such as for cities, agriculture, coastal communities, disaster management, energy and mining.

People sometimes require information tailored for their specific context. To maximise the impact of the new projections, they could readily be regionalised in ways beyond the eight natural resource management clusters that are addressed in this Report. State-based projections could be developed and communicated, as has been done by the NSW/ACT Regional Climate Modelling project (NARClm), the Victorian Climate Initiative (VicCI) and the Goyder Institute (for South Australia). Projections for Australia's big cities could be prepared and supported.

The extensive stakeholder interactions undertaken by climate change researchers in this program, and in the allied impacts and adaptation program, highlight the need for regular provision of a wide range of communication products, support and training. There is demand for general information on climate change and its causes, as well as specific information on the likely regional changes and adaptation and mitigation options. It is evident that there is demand to build capability in understanding and applying climate science information by institutions, communities and decision-makers. Climate researchers need to further build their capability and capacity to support this interaction.

A growing body of evidence from social scientists demonstrates that some communication methods and approaches work far better than others. Social science needs to continue to inform the way in which we communicate climate information.

10.4 CONCLUSIONS

Australia now has arguably the world's most comprehensive and up to date climate change projections. These projections provide an excellent basis for adaptation and risk management activities.

There is clear community demand for support in interpreting and applying the projections. This is a demand that is likely to exceed the agencies' ability and resources to respond. There are a number of other communication products that could be readily produced with modest additional resources, such as separate State and Territory projections, sector-specific information and projections for Australia's major urban areas.

The reality of climate change means that observations of the land, atmosphere and oceans must continue in order to track the extent of the changes. A focus on changes to weather and climate extremes will help target adaptation work, as it is these extremes that produce the greatest impacts on many sectors. Multi-year to decadal predictions that account for both climatic variability and the underpinning climate change will be valuable for near-term decision making and investments.

APPENDIX A COMPARISON OF CMIP3 AND CMIP5 CHANGES OVER AUSTRALIA

A.1 INTRODUCTION

This Appendix compares projected changes based on CMIP5 with those based on CMIP3, as used for Climate Change in Australia (CSIRO and BOM, 2007). In 2007, the range of change in each variable was presented in a probabilistic form, with the change at each location, for a given scenario and time in the future, being represented as a probability density function (PDF). The method used relies on the pattern scaling approximation, as described in section 6.2, with further details given by Watterson (2008). In order to derive comparable results the method is applied again using CMIP5 data. The range in the PDFs allows for both the uncertainty in the global warming and in the local response to it (or 'change per degree'), with both factors based on the ensemble of models. For CMIP3, 23 models were used, while suitable data are available from up to 40 CMIP5 models (Section 3.3.1). For some variables, the local response factors were derived from fewer models, as noted below. The model change per degree data are first interpolated to a common one-degree grid of points at which the local changes are calculated.

The scaling approximation is very helpful for this comparison, as results can be presented for the same standard case as considered in the earlier sections. This was for the change in 2080-2099 relative to 1986-2005 under the RCP8.5 scenario, for which the best (or median) estimate of global warming is 3.7 °C. Given that the mean global sensitivity of the CMIP3 models is very similar to that of CMIP5 (see section 3.6), scaling the 2007 PDFs to this same median global warming gives an indication of projections based on CMIP3 model responses for this case. The 2007 projections focused on the SRES A1B scenario, and the time 2070, when the median global warming was 2.1 °C. Only the A1FI scenario produced a warming as large as 3.7 °C within the 21st century (consistent with Figure 3.2.2).

Results are presented here for six surface variables that are important to climate impacts. The focus is on the Australian maps of annual changes for three percentiles, the median, denoted P50, and the P10 and P90 values representing the upper and lower values across the likely range. Some seasonal results from CMIP5 are shown in the sections for each variable in chapter 7, and brief comparisons are made. Note that the P10 to P90 ranges are larger than they would be for a specific global warming of 3.7 °C because the uncertainty in global sensitivity is also included. As noted in Section 3.6, the uncertainty in global warming, relative to the mean, is similar in the two ensembles. Thus we can attribute the differences in the final PDFs from CMIP3 and CMIP5 largely to the local response factors. The relative comparisons may hold also for the change around 2030, from both the 2007 and new projections, given that the global warming in 2030 for the various scenarios

is approximately 0.8 to 1 °C. However, details may differ, particularly for changes (shown earlier) that are based directly on the CMIP5 simulations. Changes forced by aerosols and ozone are not well represented in these scaled results.

A.2 TEMPERATURE

The P10, P50 and P90 results for the annual temperature case from both CMIP3 and CMIP5 are shown in Fig. A.1. The percentile values are similar in CMIP3 and CMIP5, although the north-west is notably less warm in CMIP5. Averaged over Australia the best estimate of the warming from CMIP5 is 4.2 °C, 0.2 °C smaller than in CMIP3, in this case. Changes for the four seasonal cases in CMIP3 are also similar to those for CMIP5 shown in Section 7.1.

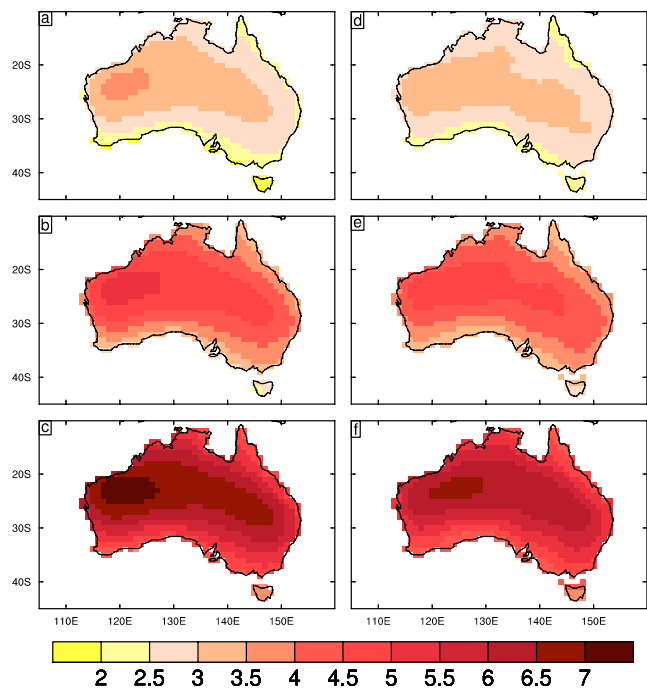


FIGURE A.1: CHANGES IN TEMPERATURE (IN °C) FOR THE ANNUAL, STANDARD CASE, FROM CMIP3 (LEFT) AND CMIP5 (RIGHT). THE MIDDLE PANELS (B, E) ARE THE MEDIAN RESULT. THE TOP PANELS (A, D) ARE THE 10TH PERCENTILE RESULT AND BOTTOM PANELS (C, F) ARE THE 90TH PERCENTILE RESULT.

In both ensembles, there is a consistent increase in warming from the coast to the interior. This is partly a result of the maritime influence along the coast, as the warming for model ocean points is slower. In these results, and also for rainfall, only data from model land points are used. In the CMIP5 calculations for temperature, precipitation and land surface variables, values are extrapolated across each model coastline to ensure that the full ensemble of models is used at each (actual) land grid point shown.



A.3 RAINFALL

The PDFs for rainfall (precipitation) at each point have been calculated using the same method as for CMIP3, using local responses expressed as percentages of the model base climate. Following Watterson (2008), for positive local responses, the global warming factor (centred on 3.7 °C in the standard case) is combined in the usual linear way. However, negative responses are applied in a compounding way, which prevents the net change exceeding an unrealistic -100 %. The changes for the annual case are shown in Figure A.2. Decreases occur for much of the continent in the P50 result, but there is little change in part of the north and also in NSW in the CMIP5 case. In fact, the all-Australia average is now -4.5 %, compared to -11.8 % for CMIP3. Decreases remain large in the south-west. At all points, however, there is a wide range of change, with P90 being positive, except in the far south-west. The percentiles from CMIP5 for changes in each season are shown in Section 7.2. Again, in CMIP5 there are fewer declines, with a slight increase for NSW now extending from summer into autumn.

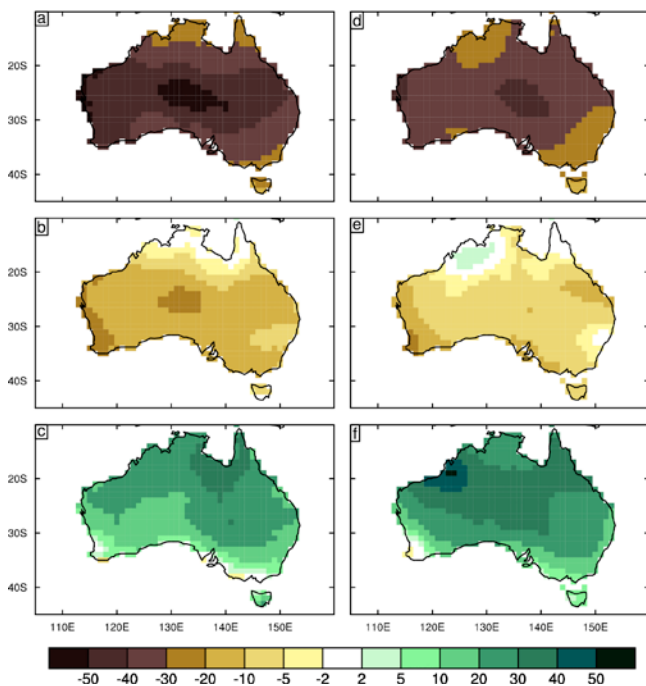


FIGURE A.2: CHANGES IN RAINFALL (IN %) FROM CMIP3 (LEFT) AND CMIP5 (RIGHT). THREE PERCENTILES OF THE LOCAL PDFS FOR CHANGE ARE SHOWN: (A, D) 10TH, (B, E) 50TH AND (C, F) 90TH.

A.4 SOLAR RADIATION

For both CMIP3 (20 models) and CMIP5 (38 models) the median estimate for annual solar radiation (downwards at surface) is for little change over Australia (Figure A.3), except for a small increase in the south, particularly Victoria. The changes range typically from -10 W m^{-2} to 10 W m^{-2} , with considerable regional variation. For CMIP5, the rise in radiation at P90 is smaller in the north-west than elsewhere, and a decrease is more likely there. Throughout the north a considerable decline is possible at P10. The positive median change in the south is consistent with a general decrease in cloudiness in mid-latitudes. However, the changes in cloud (not shown), like those in rainfall, differ between models.

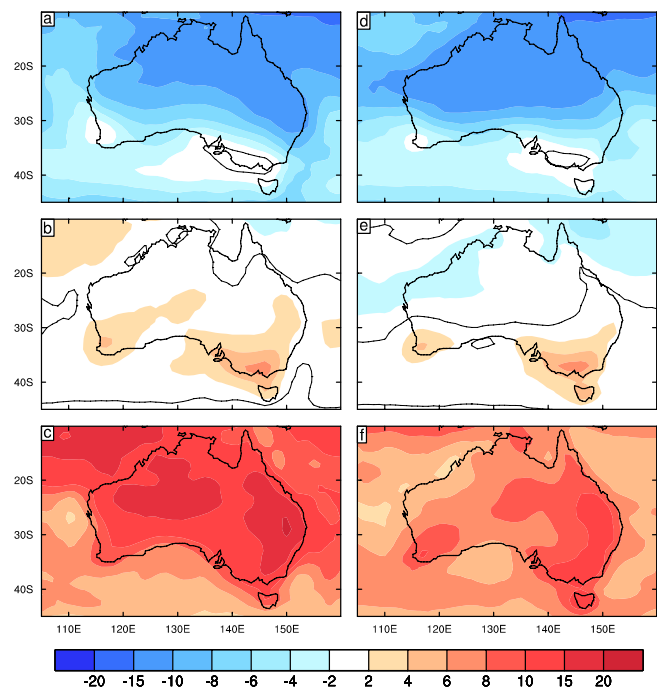


FIGURE A.3: CHANGES IN SOLAR RADIATION (IN W M^{-2}) FROM CMIP3 (LEFT) AND CMIP5 (RIGHT) FOR THE STANDARD CASE. THREE PERCENTILES OF THE LOCAL PDFS FOR CHANGE, ANNUAL CASE, ARE SHOWN: (A, D) 10TH, (B, E) 50TH AND (C, F) 90TH. THE ZERO LINE IS DRAWN.

A.5 RELATIVE HUMIDITY

Changes in (near-surface) relative humidity also differ much more across the percentiles than between CMIP3 (14 models) and CMIP5 (29 models), as seen in Figure A.4. In both ensembles, the median change is for a small decline, around 2 to 3 % (of the saturation value), in humidity except over Tasmania and some mainland coasts. Over most of the regional ocean, there is some chance of a small increase, except to the south-east of Australia. In *Climate Change in Australia* (CSIRO and BOM, 2007), it was stated that humidity changes were broadly consistent with rainfall. In CMIP5 for P50, declines are more widespread in humidity than in rainfall, however. This difference may be associated with the representation of land surface characteristics. As is evident in the maps, changes over the ocean in relative humidity are smaller.

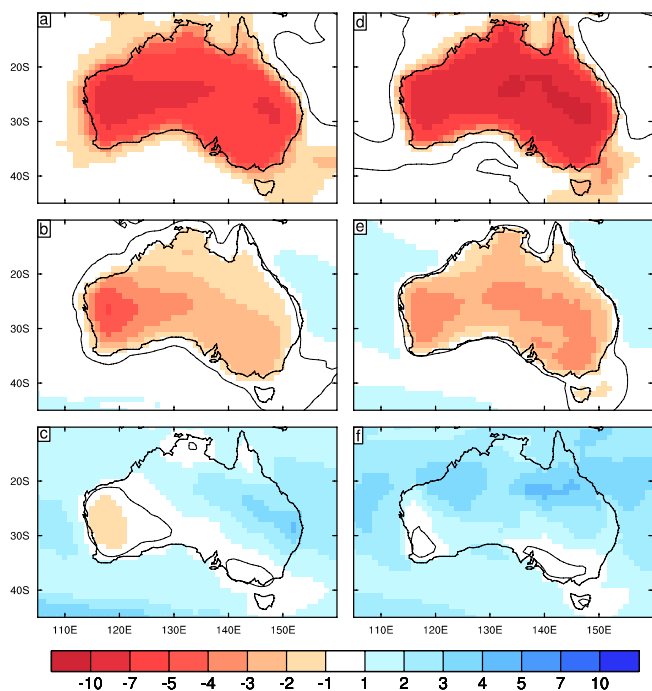


FIGURE A.4: CHANGES IN HUMIDITY (IN % OF SATURATION) FROM CMIP3 (LEFT) AND CMIP5 (RIGHT) FOR THE STANDARD CASE. THREE PERCENTILES OF THE LOCAL PDFS FOR CHANGE, ANNUAL CASE, ARE SHOWN: (A, D) 10TH, (B, E) 50TH AND (C, F) 90TH. THE ZERO LINE IS DRAWN.

A.6 SURFACE WIND SPEED

Most models in CMIP5 have provided data for the true mean speed (at the 10 m height), averaged from speeds during the model simulation (which was not available from CMIP3). Changes calculated using the PDF method for the annual case are shown in Figure A.5, using change per degree data from 19 models. Note that the changes in speed have been converted to a percentage using the 1986-2005 multi-model mean. The range over the PDF is from substantial decreases to increases, over nearly all of Australia. The pattern of change for P50 is quite similar to the results presented in 2007, despite those being calculated using speeds from monthly mean wind components. However, for P90 the changes over the surrounding ocean seem more moderate in CMIP5, and with fewer areas with an increase.

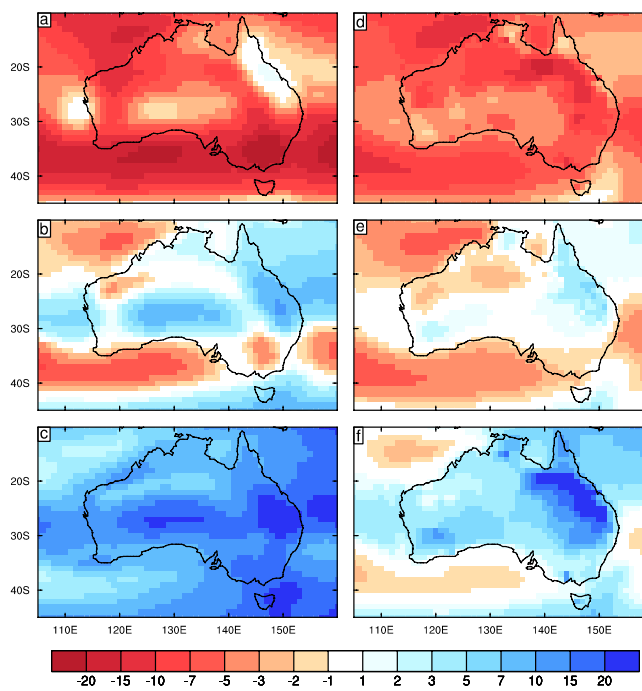


FIGURE A.5: CHANGES IN WIND SPEED (IN % OF THE BASE PERIOD MULTI-MODEL MEAN) FROM CMIP3 (LEFT) AND CMIP5 (RIGHT) FOR THE STANDARD CASE. THREE PERCENTILES OF THE LOCAL PDFS FOR CHANGE, ANNUAL CASE, ARE SHOWN: (A, D) 10TH, (B, E) 50TH AND (C, F) 90TH.

A.7 POTENTIAL EVAPOTRANSPIRATION

The potential evapotranspiration' has been evaluated for CMIP5 (using 22 models), similarly to CMIP3 (14 models) – see Section 7.6. The fields calculated using the scaling approach also very similar over Australian land (Figure A.6). All changes in the P10, P50 and P90 fields are increases. The mean P50 for the standard case is 11 % for each ensemble.

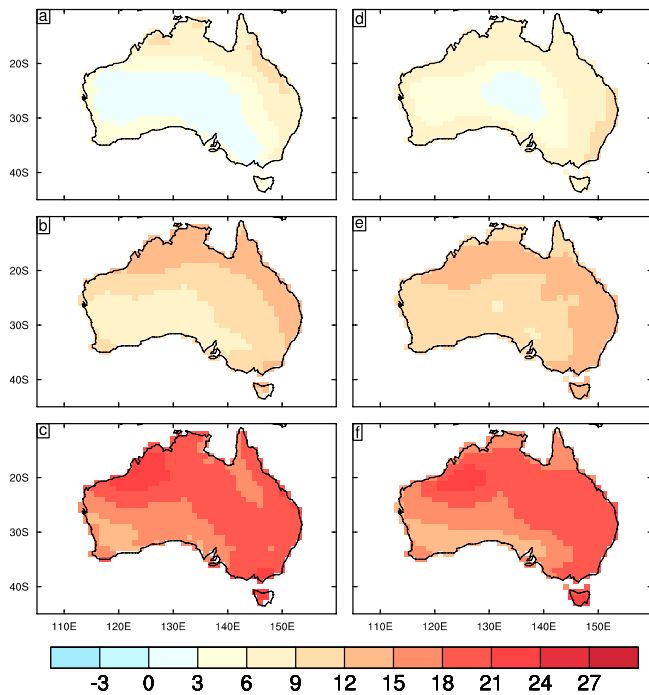


FIGURE A.6: CHANGES IN POTENTIAL EVAPOTRANSPIRATION (IN % OF THE BASE PERIOD MULTI-MODEL MEAN) FROM CMIP3 (LEFT) AND CMIP5 (RIGHT) FOR THE STANDARD CASE. THREE PERCENTILES OF THE LOCAL PDFS FOR CHANGE, ANNUAL CASE, ARE SHOWN: (A, D) 10TH, (B, E) 50TH AND (C, F) 90TH.

A.8 SUMMARY

In conclusion, the comparisons show that for a scenario with a large global warming towards the end of the century, the pattern of simulated change in these six surface variables is generally similar in the CMIP3 and CMIP5 ensembles. This applies to both the median estimate of change and to the range of changes, as estimated using the pattern scaling approach. However, there are some differences, attributable to small differences in local response to global warming. Scaled to the standard case, with a median estimate for global warming of 3.7 °C, the mean warming over Australia is typically 5 % less in CMIP5. The reduction is consistent with a less negative rainfall change in the median change field for CMIP5, although the P50 rainfall change remains near-zero in the north. Humidity and solar radiation decrease slightly in the south in both ensembles. The best estimate for wind speed is still for little change. However, all these variables still have a considerable range of change as depicted in the 10th and 90th percentile fields. At many locations, the range spans both signs, except for temperature and potential evapotranspiration.

REFERENCES

- ABBS, D. & RAFTER, A. 2009. Impact of Climate Variability and Climate Change on Rainfall Extremes in Western Sydney and Surrounding Areas: Component 4 - Dynamical Downscaling. Report to the Sydney Metro Catchment Management Authority and Partners. Melbourne: CSIRO.
- ABBS, D. J. & RAFTER, A. S. 2012. Tropical cyclone projections for the west Australian region. Indian Ocean Climate Initiative (2012) Western Australia's Weather and Climate: A Synthesis of Indian Ocean Climate Initiative Stage 3 Research. Australia: CSIRO and BOM. p. 93-95.
- ABBS, D. J., LAVENDER, S. L., RAFTER, A. S. & ROUBICEK, A. J. 2014. Projected changes in SW Pacific Tropical Cyclones by the late 21st Century: Results based on direct detection in and downscaling of CMIP5 model outputs. CSIRO Climate Adaptation Flagship report. 19pp.
- ADLER, R. F., HUFFMAN, G. J., CHANG, A., FERRARO, R., XIE, P. P., JANOWIAK, J., RUDOLF, B., SCHNEIDER, U., CURTIS, S., BOLVIN, D., GRUBER, A., SUSSKIND, J., ARKIN, P. & NELKIN, E. 2003. The version-2 global precipitation climatology project (GPCP) monthly precipitation analysis (1979–present). *Journal of Hydrometeorology*, v. 4, p. 1147-1167.
- AUSTRALIAN GREENHOUSE OFFICE, 2006. Climate Change Impacts & Risk Management. A Guide for Business and Government. Broadleaf Capital International, Marsden Jacob Associates, For the Department of the Environment and Heritage.
- ALEXANDER, L. V., ZHANG, X., PETERSON, T. C., CAESAR, J., GLEASON, B., KLEIN TANK, A. M. G., HAYLOCK, M., COLLINS, D., TREWIN, B., RAHMIZADEH, F., TAGIPOUR, A., RUPA KUMAR, K., REVADEKAR, J., GRIFFITHS, G., VINCENT, L., STEPHENSON, D. B., BURN, J., AQUILAR, E., BRUNET, M., TAYLOR, M., NEW, M., ZHAI, P., RUSTICUCCI, M. & VAZQUEZ-AGUIRRE, J. L. 2006. Global observed changes in daily climate extremes of temperature and precipitation. *Journal of Geophysical Research*, 111, D05109.
- ALEXANDER, L., WANG, X., WAN, H. & TREWIN, B. 2011. Significant decline in storminess over southeast Australia since the late 19th century. *Australian Meteorological and Oceanographic Journal*, 61, 23-30.
- ALEXANDER, L. V. & ARBLASTER, J. M. 2009. Assessing trends in observed and modelled climate extremes over Australia in relation to future projections. *International Journal of Climatology*, 29, 417-435.
- ALLAN, R. & ANSELL, T. 2006. A new globally complete monthly historical gridded mean sea level pressure dataset (HadSLP2): 1850-2004. *Journal of Climate*, 19, 5816-5842.
- ALLEN, R., SHERWOOD, S., NORRIS, J. & ZENDER, C. 2012. Recent Northern Hemisphere tropical expansion primarily driven by black carbon and tropospheric ozone. *Nature*, 485, 350-U93.
- ALLEN, R. J., NORRIS, J. R. & WILD, M. 2013. Evaluation of multidecadal variability in CMIP5 surface solar radiation and inferred underestimation of aerosol direct effects over Europe, China, Japan, and India. *Journal of Geophysical Research-Atmospheres*, 118, 6311-6336.
- ANDERSSON, A., FENNIG, K., KLEPP, C., BAKAN, S., GRAßL, H. & SCHULZ, J. 2010. The Hamburg Ocean Atmosphere Parameters and Fluxes from Satellite Data - HOAPS-3. *Earth System Science Data*, 2, 215-234.
- ANTHONY, K. R., KLINE, D. I., DIAZ-PULIDO, G., DOVE, S. & HOEGH-GULDBERG, O. 2008. Ocean acidification causes bleaching and productivity loss in coral reef builders. *Proceedings of the National Academy of Sciences*, 105, 17442-17446.
- ARBLASTER, J. & MEEHL, G. 2006. Contributions of external forcings to southern annular mode trends. *Journal of Climate*, 19, 2896-2905.
- AULT, T. R., COLE, J. E. & GEORGE, S. S. 2012. The amplitude of decadal to multidecadal variability in precipitation simulated by state-of-the-art climate models. *Geophysical Research Letters*, 39.
- AUSTRALIAN BUREAU OF STATISTICS. 2013. Census 2011: Mesh Block Counts [Online]. Available: www.abs.gov.au/websitedbs/censushome.nsf/home/meshblockcounts?opendocument&navpos=269
- BARNES, E. A. & POLVANI, L. 2013. Response of the midlatitude jets, and of their variability, to increased greenhouse gases in the CMIP5 models. *Journal of Climate*, 26, 7117-7135.
- BAYNES, T., HERR, A., LANGSTON, A., COLLINS, K., CLARKE, J. & WEBB, L. 2013. Coastal Climate Risk Project Milestone 1 Technical Annex. CSIRO.
- BECK, C., GRIESER, J. & RUDOLPH, B. 2005. A new monthly precipitation climatology for the global land areas for the period 1951 to 2000. *Geophysical Research Abstracts*, 7, 07154.
- BEDNARŠEK, N., TARLING, G., BAKKER, D., FIELDING, S., JONES, E., VENABLES, H., WARD, P., KUZIRIAN, A., LEZE, B. & FEELY, R. 2012. Extensive dissolution of live pteropods in the Southern Ocean. *Nature Geoscience*, 5, 881-885.
- BERRY, G., REEDER, M. & JAKOB, C. 2011. A global climatology of atmospheric fronts. *Geophysical Research Letters*, 38.
- BHEND, J., BATHOLS, J. & HENNESSY, K. 2012. Climate change impacts on snow in Victoria. CSIRO report for the Victorian Department of Sustainability and Environment 42 pp. www.climatechange.vic.gov.au/home/climate-change-impacts-on-snow-in-victoria,-2013
- BHEND, J. & WHETTON, P. 2013. Consistency of simulated and observed regional changes in temperature, sea level pressure and precipitation. *Climatic Change*, 118, 799-810.

- BINDOFF, N. L., STOTT, P. A., ACHUTARAO, K.M., ALLEN, M.R., GILLET, N., GUTZLER, D., HANSINGO, K., HEGERL, G., HU, Y., JAIN, S., MOKHOV, I.I., OVERLAND, J., PERLWITZ, J., SEBBARI, R. & ZHANG, X. 2013. Detection and Attribution of Climate Change: from Global to Regional. In: *Climate Change 2013: The Physical Science Basis. Contribution of Working Group I to the Fifth Assessment Report of the Intergovernmental Panel on Climate Change* [STOCKER, T. F., QIN, D., PLATTNER, G.-K., TIGNOR, M., ALLEN, S.K., BOSCHUNG, J., NAUELS A., XIA, Y., BEX, V. & MIDGLEY, P.M. (eds.)]. Cambridge University Press, Cambridge, United Kingdom and New York, NY, USA. www.climatechange2013.org and www.ipcc.ch
- BLANCHI, R., LUCAS, C., LEONARD, J. & FINKELE, K. 2010. Meteorological conditions and wildfire-related house loss in Australia. *International Journal of Wildland Fire*, 19, 914-926.
- BOM 2001. *Climatic Atlas of Australia - Evapotranspiration*. Australian Bureau of Meteorology.
- BOM 2013a. Special Climate Statement 43 – Extreme heat in January 2013. www.bom.gov.au/climate/current/statements/scs43e.pdf
- BOM 2013b. Bureau of Meteorology, Climate Change Tracker. Commonwealth of Australia. www.bom.gov.au/climate/
- BOM 2014a. State of the climate. Bureau of Meteorology. Commonwealth of Australia.
- BOM 2014b. Annual climate statement 2013. Bureau of Meteorology. Commonwealth of Australia.
- BOPP, L., RESPLANDY, L., ORR, J., DONEY, S., DUNNE, J., GEHLEN, M., HALLORAN, P., HEINZE, C., ILYINA, T. & SÉFÉRIAN, R. 2013. Multiple stressors of ocean ecosystems in the 21st century: projections with CMIP5 models. *Biogeosciences*, 10, 6225-6245.
- BRACEGIRDLE, T. & STEPHENSON, D. 2012. Higher precision estimates of regional polar warming by ensemble regression of climate model projections. *Climate Dynamics*, 39, 2805-2821.
- BRADSTOCK, R. A. 2010. A biogeographic model of fire regimes in Australia: current and future implications. *Global Ecology and Biogeography*, 19, 145-158.
- BRAGANZA, K., POWER, S., TREWIN, B., ARBLASTER, J., TIMBAL, B., HOPE, P., FREDERIKSEN, C., MCBRIDE, J., JONES, D. & PLUMMER, N. 2011. Update on the state of the climate, long-term trends and associated causes. In: KEENAN, T. D. & CLEUGH, H. A. (eds.). Canberra, Australia: Centre for Australian Weather and Climate Research. 106pp
- BROHAN, P., KENNEDY, J. J., HARRIS, I., TETT, S. F. B. & JONES, P. D. 2006. Uncertainty estimates in regional and global observed temperature changes: a new dataset from 1850. *Journal of Geophysical Research*, 111, D12106
- BURGESS, S., RICKETTS, J., PANJKOV, A., CARTER, J. & DAY, K. 2012. Consistent Climate Scenarios Project User Guide: 'Change factor' and 'Quantile-matching' based climate projections data. Queensland Department of Science, Information Technology, Innovation and the Arts.
- BURGETTE, R. J., WATSON, C. S., CHURCH, J. A., WHITE, N. J., TREGONING, P. & COLEMAN, R. 2013. Characterizing and minimizing the effects of noise in tide gauge time series: relative and geocentric sea level rise around Australia. *Geophysical Journal International*, 194, 719-736.
- BURKE, E. J. & BROWN, S. J. 2008. Evaluating uncertainties in the projection of future drought. *Journal of Hydrometeorology*, 9, 292-299.
- BUSER, C. M., KUNSCH, H. R., LUTHI, D., WILD, M. & SCHAR, C. 2009. Bayesian multi-model projection of climate: bias assumptions and interannual variability. *Climate Dynamics*, 33, 849-868.
- CAI, W., BORLACE, S., LENGAIGNE, M., VAN RENSCH, P., COLLINS, M., VECCHI, G., TIMMERMANN, A., SANTOSO, A., MCPHADEN, M., WU, L., ENGLAND, M., WANG, G., GUILYARDI, E. & JIN, F. 2014. Increasing frequency of extreme El Niño events due to greenhouse warming. *Nature Climate Change*, 4, 111-116.
- CAI, W. & COWAN, T. 2006. SAM and regional rainfall in IPCC AR4 models: Can anthropogenic forcing account for southwest Western Australian winter rainfall reduction? *Geophysical Research Letters*, 33.
- CAI, W. & COWAN, T. 2008. Dynamics of late autumn rainfall reduction over southeastern Australia. *Geophysical Research Letters*, 35.
- CAI, W. & COWAN, T. 2013. Why is the amplitude of the Indian Ocean Dipole overly large in CMIP3 and CMIP5 climate models? *Geophysical Research Letters*, 40, (6), 1200-1205.
- CAI, W., ZHENG, X.-T., WELLER, E., COLLINS, M., COWAN, T., LENGAIGNE, M., YU, W. & YAMAGATA, T. 2013. Projected response of the Indian Ocean Dipole to greenhouse warming. *Nature Geoscience*, 6, 999-1007.
- CAI, W., SULLIVAN, A. & COWAN, T. 2009. Rainfall Teleconnections with Indo-Pacific Variability in the WCRP CMIP3 Models. *Journal of Climate*, 22, 5046-5071.
- CAI, W., SULLIVAN, A., COWAN, T., RIBBE, J. & SHI, G. 2011. Simulation of the Indian Ocean Dipole: A relevant criterion for selecting models for climate projections. *Geophysical Research Letters*, 38, L03704.
- CALAFAT, F. M. & JORDA, G. 2011. A Mediterranean sea level reconstruction (1950-2008) with error budget estimates. *Global and Planetary Change*, 79, 118-133.
- CALLAGHAN, J. & POWER, S. 2010. A reduction in the frequency of severe land-falling tropical cyclones over eastern Australia in recent decades. *Clim Dynam.* doi:10.1007/s00382-010-0883-2.
- CAMARGO, S. J., BARNSTON, A. G. & ZEBIAK, S. E. 2005. A statistical assessment of tropical cyclone activity in atmospheric general circulation models. *Tellus A*, 57, 589-604.
- CATTO, J., JAKOB, C. & NICHOLLS, N. 2013. A global evaluation of fronts and precipitation in the ACCESS model. *Australian Meteorological and Oceanographic Journal*, 63, 191-203.

- CATTO, J., NICHOLLS, N. & JAKOB, C. 2012a. North Australian Sea Surface Temperatures and the El Niño-Southern Oscillation in Observations and Models. *Journal of Climate*, 25, 5011-5029.
- CATTO, J., NICHOLLS, N. & JAKOB, C. 2012b. North Australian Sea Surface Temperatures and the El Niño-Southern Oscillation in the CMIP5 Models. *Journal of Climate*, 25, 6375-6382.
- CHANDLER, R. E. 2013. Exploiting strength, discounting weakness: combining information from multiple climate simulators. *Philosophical Transactions of the Royal Society A: Mathematical, Physical and Engineering Sciences*, 371 (1991). 20120388
- CHARLES, S., BARI, M., KITSIOS, A. & BATES, B. 2007. Effect of GCM bias on downscaled precipitation and runoff projections for the Serpentine catchment, Western Australia. *International Journal of Climatology*, 1673-1690.
- CHARLES, S. P., BATES, B. C. & HUGHES, J. P. 1999. A spatiotemporal model for downscaling precipitation occurrence and amounts. *Journal of Geophysical Research: Atmospheres* (1984–2012), 104, 31657-31669.
- CHARLES, S., SILBERSTEIN, R., TENG, J., FU, G., HODGSON, G., GABROVSEK, C., CRUTE, J., CHIEW, F., SMITH, I. & KIRONO, D. 2010. Climate analyses for south-west Western Australia. A report to the Australian Government from the CSIRO South-West Western Australia Sustainable Yields Project. CSIRO, Australia. 83 pp.
- CHATTOPADHYAY, M. & ABBS, D. 2012. On the variability of projected tropical cyclone genesis in GCM ensembles. *Tellus Series a-Dynamic Meteorology and Oceanography*, 64 18696.
- CHIEW, F. 2006. Estimation of rainfall elasticity of streamflow in Australia. *Hydrological Sciences Journal- Journal Des Sciences Hydrologiques*, 51, 613-625.
- CHIEW, F., TENG, J., KIRONO, D., FROST, A., BATHOLS, J., VAZE, J., VINEY, N., HENNESSY, K. & CAI, W. 2008. Climate data for hydrologic scenario modelling across the Murray-Darling Basin. A Report to the Australian Government from the CSIRO Murray-Darling Basin Sustainable Yields Projects. Australia.
- CHIEW, F. H. S., KIRONO, D. G. C., KENT, D. & VAZE, J. 2009a. Assessment of rainfall simulations from global climate models and implications for climate change impact on runoff studies. 18th World IMACS/MODSIM Congress. Cains, Australia: <http://mssanz.org.au/modsim09>
- CHIEW, F. H. & MCMAHON, T. A. 1991. The Applicability of Morton's and Penman's Evapotranspiration Estimates in Rainfall-Runoff Modeling. *JAWRA Journal of the American Water Resources Association*, 27, 611-620.
- CHIEW, F. H. S., TENG, J., VAZE, J. & KIRONO, D. G. C. 2009b. Influence of global climate model selection on runoff impact assessment. *Journal of Hydrology*, 379, 172-180.
- CHRISTENSEN, J., KJELLSTROM, E., GIORGI, F., LENDERINK, G. & RUMMUKAINEN, M. 2010. Weight assignment in regional climate models. *Climate Research*, 44, 179-194.
- CHRISTENSEN, J. H., RUMMUKAINEN, M. & LENDERINK, G. 2009. Formulation of very-high-resolution climate model ensembles for Europe. In: VAN DER LINDEN, P. & MITCHELL, J. F. B. (eds.) *ENSEMBLES: Climate Change and its Impacts: Summary of research and results from the ENSEMBLES project*. Exeter EX1 3PB, UK: Met Office Hadley Centre.
- CHRISTIDIS, N., STOTT, P., KAROLY, D. & CIAVARELLA, A. 2013. An attribution study of the heavy rainfall over eastern Australia in March 2012 [in "Explaining extreme events of 2012 from a climate perspective"]. *Bull. Amer. Meteor. Soc*, 94, S58-S60.
- CHURCH, J., GREGORY, J., WHITE, N., PLATTEN, S. & MITROVICA, J. 2011a. Understanding and Projecting Sea Level Change. *Oceanography*, 24, 130-143.
- CHURCH, J. A., WHITE, N. J., KONIKOW, L. F., DOMINGUES, C. M., COGLEY, J. G., RIGNOT, E., GREGORY, J. M., VAN DEN BROEKE, M. R., MONAGHAN, A. J. & VELICOGNA, I. 2011b. Revisiting the Earth's sea-level and energy budgets from 1961 to 2008. *Geophysical Research Letters*, 38, L18601.
- CHURCH, J., WHITE, N. & ARBLASTER, J. 2005. Significant decadal-scale impact of volcanic eruptions on sea level and ocean heat content. *Nature*, 438, 74-77.
- CHURCH, J. A., CLARK, P. U., CAZENAVE, A., GREGORY, J. M., JEVREJEVA, S., LEVERMANN, A., MERRIFIELD, M. A., MILNE, G. A., NEREM, R. S., NUNN, P. D., PAYNE, A. J., PFEFFER, W. T., STAMMER, D. & UNNIKRISHNAN, A. S. 2014. Sea Level Change. In: STOCKER, T. F., D. QIN, G.-K. PLATTNER, M. TIGNOR, S. K. ALLEN, J. BOSCHUNG, A. NAUELS, Y. XIA, V. BEX AND P. M. MIDGLEY (ed.) *Climate Change 2013: The Physical Science Basis. Contribution of Working Group I to the Fifth Assessment Report of the Intergovernmental Panel on Climate Change*.
- CHURCH, J. A. & WHITE, N. J. 2006. A 20th century acceleration in global sea-level rise. *Geophysical Research Letters*, 33.
- CHURCH, J. A. & WHITE, N. J. 2011. Sea-Level Rise from the Late 19th to the Early 21st Century. *Surveys in Geophysics*, 32, 585-602.
- CHURCH, J. A., WHITE, N. J., DOMINGUES, C. M., MONSELESAN, D. P. & MILES, E. R. 2013. Sea-Level and Ocean Heat-Content Change. 103, 697-725.
- CIAIS, P., SABINE, C., BALA, G., BOPP, L., BROVKIN, V., CANADELL, J., CHHABRA, A., DEFRIES, R., GALLOWAY, J., HEIMANN, M., JONES, C., LE QUÉRÉ, C., MYNENI, R. B., PIAO, S. & THORNTON, P. 2013. Carbon and Other Biogeochemical Cycles. Contribution of Working Group I to the Fifth Assessment Report of the Intergovernmental Panel on Climate Change. In: STOCKER, T. F., D. QIN, G.-K. PLATTNER, M. TIGNOR, S.K. ALLEN, J. BOSCHUNG, A. NAUELS, Y. XIA, BEX, V. & MIDGLEY, P. M. (eds.) *Climate Change 2013: The Physical Science Basis*. Cambridge, United Kingdom and New York, NY, USA: Cambridge University Press.
- CLARKE, H., LUCAS, C. & SMITH, P. 2013. Changes in Australian fire weather between 1973 and 2010. *International Journal of Climatology*, 33, 931-944.

- CLARKE, H., SMITH, P. & PITMAN, A. 2011a. Regional signatures of future fire weather over eastern Australia from global climate models. *International Journal of Wildland Fire*, 20, 550-562.
- CLARKE, J. M., WHETTON, P. H. & HENNESSY, K. J. 2011b. Providing Application-specific Climate Projections Datasets: CSIRO's Climate Futures Framework. In: CHAN, F., MARINOVA, D. & ANDERSSON, R. S. (eds.) MODSIM2011, 19th International Congress on Modelling and Simulation. Perth, Western Australia: Modelling and Simulation Society of Australia and New Zealand.
- COELHO, C. & GODDARD, L. 2009. El Niño-Induced Tropical Droughts in Climate Change Projections. *Journal of Climate*, 22, 6456-6476.
- COGLEY, J. G. 2009. Geodetic and direct mass-balance measurements: comparison and joint analysis. *Annals of Glaciology*, 50, 96-100.
- COLBERG, F. & MCINNES, K. 2012. The impact of future changes in weather patterns on extreme sea levels over southern Australia. *Journal of Geophysical Research-Oceans*, 117, (C8).
- COLMAN, R., MOISE, A. & HANSON, L. 2011. Tropical Australian climate and the Australian monsoon as simulated by 23 CMIP3 models. *Journal of Geophysical Research-Atmospheres*, 116.
- COOLEY, S. R., KITE-POWELL, H. L. & DONEY, S. C. 2009. Ocean acidification's potential to alter global marine ecosystem services. *Oceanography* 22(4) 172-181.
- CSIRO 1992. Climate change scenarios for the Australian region. Melbourne: CSIRO Division of Atmospheric Research.
- CSIRO 1996. Climate change scenarios for the Australian region. Melbourne: CSIRO Division of Atmospheric Research.
- CSIRO 2001. Climate change projections for Australila. Aspendale: CSIRO.
- CSIRO 2008. Murray-Darling Basin Sustainable Yields Project. A report to the Australian Government from the CSIRO.
- CSIRO 2012. Climate and water availability in south-eastern Australia – A synthesis of findings from Phase 2 of the South Eastern Australian Climate Initiative (SEACI). CSIRO, September.
- CSIRO AND BOM 2007. Climate change in Australia: technical report, Aspendale, Australia, CSIRO Marine and Atmospheric Research.
- CULLEN, B. R., ECKARD, R. J. & RAWNSLEY, R. P. 2012. Resistance of pasture production to projected climate changes in south-eastern Australia. *Crop and Pasture Science*, 63, 77-86.
- DAI, A. 2006. Recent climatology, variability, and trends in global surface humidity. *Journal of Climate*, 19, 3589-3606.
- DAI, A. 2011. Drought under global warming: a review. *Wiley Interdisciplinary Reviews: Climate Change*, 2, 45-65.
- DAI, A. 2013. Increasing drought under global warming in observations and models. *Nature Climate Change*, 3, 52-58.
- DARBYSHIRE, R., WEBB, L., GOODWIN, I. & BARLOW, S. 2013. Evaluation of recent trends in Australian pome fruit spring phenology. *International Journal of Biometeorology*, 57, 409-421.
- DARBYSHIRE, R., WEBB, L., GOODWIN, I. & BARLOW, S. 2014. Challenges in predicting climate change impacts on pome fruit phenology. *International Journal of Biometeorology*, 58, 1119-1133.
- DAVIS, C. J. 2013. Towards the development of long-term winter records for the Snowy Mountains. *Australian Meteorological and Oceanographic Journal*, 63, 303-313.
- DEE, D., UPPALA, S., SIMMONS, A., BERRISFORD, P., POLI, P., KOBAYASHI, S., ANDRAE, U., BALMASEDA, M., BALSAMO, G. & BAUER, P. 2011. The ERA-Interim reanalysis: Configuration and performance of the data assimilation system. *Quarterly Journal of the Royal Meteorological Society*, 137, 553-597.
- DENG, X., GRIFFIN, D. A., RIDGWAY, K. R., CHURCH, J. A., FEATHERSTONE, W. E., WHITE, N. & CAHILL, M. 2010. Chapter 18: Satellite altimetry for geodetic, oceanographic and climate studies in the Australian region. In: VIGNUDELLI, S., KOSTIANOV, A., CIPOLLINI, P. & BENVENISTE, J. (eds.) *Coastal Altimetry*. Berlin Heidelberg: Springer-Verlag.
- DEPARTMENT OF AGRICULTURE. 2013. Natural resource management [Online]. Commonwealth of Australia. Available: www.nrm.gov.au/about/nrm/regions/
- DEPARTMENT OF THE ENVIRONMENT. 2013. Australia's bioregions (IBRA) [Online]. Available: www.environment.gov.au/topics/land/national-reserve-system/science-maps-and-data/australias-bioregions-ibra
- DESER, C., KNUTTI, R., SOLOMON, S. & PHILLIPS, A. S. 2012a. Communication of the role of natural variability in future North American climate. *Nature Climate Change*, 2, 775-779.
- DESER, C., PHILLIPS, A., BOURDETTE, V. & TENG, H. 2012b. Uncertainty in climate change projections: the role of internal variability. *Climate Dynamics*, 38, 527-546.
- DONAT, M., ALEXANDER, L., YANG, H., DURRE, I., VOSE, R. & CAESAR, J. 2013a. Global Land-Based Datasets for Monitoring Climatic Extremes. *Bulletin of the American Meteorological Society*, 94, 997-1006.
- DONAT, M., ALEXANDER, L., YANG, H., DURRE, I., VOSE, R., DUNN, R., WILLETT, K., AGUILAR, E., BRUNET, M., CAESAR, J., HEWITSON, B., JACK, C., TANK, A., KRUGER, A., MARENGO, J., PETERSON, T., RENOM, M., ROJAS, C., RUSTICUCCI, M., SALINGER, J., ELRAYAH, A., SEKELE, S., SRIVASTAVA, A., TREWIN, B., VILLARROEL, C., VINCENT, L., ZHAI, P., ZHANG, X. & KITCHING, S. 2013b. Updated analyses of temperature and precipitation extreme indices since the beginning of the twentieth century: The HadEX2 dataset. *Journal of Geophysical Research-Atmospheres*, 118, 2098-2118.

- DONEY, S. C., FABRY, V. J., FEELY, R. A. & KLEYPAS, J. A. 2009. Ocean Acidification: The Other CO₂ Problem. *Annu. Rev. Mar. Sci.*, 1, 169-92.
- DOWDY, A., MILLS, G. & TIMBAL, B. 2013a. Large-scale diagnostics of extratropical cyclogenesis in eastern Australia. *International Journal of Climatology*, 33, 2318-2327.
- DOWDY, A., MILLS, G., TIMBAL, B., GRIFFITHS, M. & WANG, Y. 2013b. Understanding rainfall projections in relation to extratropical cyclones in eastern Australia. *Australian Meteorological and Oceanographic Journal*, 63, 355-364.
- DOWDY, A., MILLS, G., TIMBAL, B. & WANG, Y. 2013c. Changes in the Risk of Extratropical Cyclones in Eastern Australia. *Journal of Climate*, 26, 1403-1417.
- DOWDY, A., MILLS, G., TIMBAL, B. & WANG, Y. 2014. Fewer large waves projected for eastern Australia due to decreasing storminess. *Nature Climate Change*, 4, 283-286.
- DOWDY, A. J. 2014. Long-term changes in Australian tropical cyclone numbers. *Atmospheric Science Letters*, doi: 10.1002/asl2.502.
- DROSDOWSKY, W. 2005. The latitude of the subtropical ridge over eastern Australia: The L index revisited. *International Journal of Climatology*, 25, 1291-1299.
- DUNLOP, M., PARRIS, H., RYAN, P. & KROON, F. 2013. Climate-ready conservation objectives: a scoping study. National Climate Change Adaptation Research Facility, Gold Coast. Available: http://apo.org.au/files/docs/Dunlop-Climate-ready-conservation-objectives_0.pdf.
- DUNN-SIGOUIN, E. & SON, S. 2013. Northern Hemisphere blocking frequency and duration in the CMIP5 models. *Journal of Geophysical Research-Atmospheres*, 118, 1179-1188.
- DURACK, P. J. & WIJFFELS, S. E. 2010. Fifty-year trends in global ocean salinities and their relationship to broad-scale warming. *Journal of Climate*, 23, 4342-4362.
- DURACK, P., WIJFFELS, S. & MATEAR, R. 2012. Ocean Salinities Reveal Strong Global Water Cycle Intensification During 1950 to 2000. *Science*, 336, 455-458.
- DUTTON, A. & LAMBECK, K. 2012. Ice volume and sea level during the last interglacial. *Science*, 337, 216-9.
- EKSTRÖM, M., GROSE, M. R. & WHETTON, P. H. submitted. An appraisal of downscaling methods used in climate change research. *WIREs Climate Change*.
- EMANUEL, K. A. 2013. Downscaling CMIP5 climate models shows increased tropical cyclone activity over the 21st century. *Proceedings of the National Academy of Sciences*, 110.
- EMANUEL, K. A. & NOLAN, D. 2004. Tropical cyclone activity and the global climate system. Preprints, 26th Conf. on Hurricanes and Tropical Meteorology, Miami, FL, Amer. Meteor. Soc. A, 2004. [Æftp://texmex.mit.edu/pub/emanuel/PAPERS/em_nolan_extended_2004.pdf](http://texmex.mit.edu/pub/emanuel/PAPERS/em_nolan_extended_2004.pdf)
- ENGLAND, M. H., MCGREGOR, S., SPENCE, P., MEEHL, G. A., TIMMERMANN, A., CAI, W., GUPTA, A. S., MCPHADEN, M. J., PURICH, A. & SANTOSO, A. 2014. Recent intensification of wind-driven circulation in the Pacific and the ongoing warming hiatus. *Nature Climate Change*, 4, 222-227.
- ENGLAND, M., UMMENHOFER, C. & SANTOSO, A. 2006. Interannual rainfall extremes over southwest Western Australia linked to Indian ocean climate variability. *Journal of Climate*, 19, 1948-1969.
- EVANS, J. & BOYER-SOUCHET, I. 2012. Local sea surface temperatures add to extreme precipitation in northeast Australia during La Niña. *Geophysical Research Letters*, 39.
- EVANS, J. P. 2011. CORDEX - An international climate downscaling initiative. MODSIM2011. Perth, Australia.
- EVANS, J., JI, F., LEE, C., SMITH, P., ARGÜESO, D. & FITA, L. 2014. Design of a regional climate modelling projection ensemble experiment-NARCLiM. *Geoscientific Model Development*, 7, 621-629.
- EYRING, V., ARBLASTER, J. M., CIONNI, I., SEDLÁČEK, J., PERLWITZ, J., YOUNG, P. J., BEKKI, S., BERGMANN, D., CAMERON-SMITH, P., COLLINS, W. J., FALUVEGI, G., GOTTSCHALDT, K. D., HOROWITZ, L. W., KINNISON, D. E., LAMARQUE, J. F., MARSH, D. R., SAINT-MARTIN, D., SHINDELL, D. T., SUDO, K., SZOPA, S. & WATANABE, S. 2013. Long-term ozone changes and associated climate impacts in CMIP5 simulations. *Journal of Geophysical Research: Atmospheres*, 118, 5029-5060.
- FABRICIUS, K. E., LANGDON, C., UTHICKE, S., HUMPHREY, C., NOONAN, S., DE'ATH, G., OKAZAKI, R., MUEHLEHNER, N., GLAS, M. S. & LOUGH, J. M. 2011. Losers and winners in coral reefs acclimatized to elevated carbon dioxide concentrations. *Nature Climate Change*, 1, 165-169.
- FABRY, V. J., SEIBEL, B. A., FEELY, R. A. & ORR, J. C. 2008. Impacts of ocean acidification on marine fauna and ecosystem processes. *ICES Journal of Marine Science: Journal du Conseil*, 65, 414-432.
- FAWCETT, R., TREWIN, B., BRAGANZA, K., SMALLEY, R., JOVANOVIĆ, B., JONES, D. A. 2012. On the sensitivity of Australian temperature trends and variability to analysis methods and observation networks. *CAWCR Research Report 50*, Bureau of Meteorology, Melbourne, 66 pp.
- FAWCETT, R., TREWIN, B., R SMALLEY, R., and BRAGANZA, K. 2013. On the changing nature of Australian monthly and daily temperature anomalies. In *proceedings of the Australian Meteorological and Oceanographic Society Annual Conference*, Melbourne, 2013.
- FEELY, R. A., SABINE, C. L., HERNANDEZ-AYON, J. M., IANSON, D. & HALES, B. 2008. Evidence for upwelling of corrosive "acidified" water onto the continental shelf. *Science*, 320, 1490-1492.
- FEELY, R. A., DONEY, S. C. & COOLEY, S. R. 2009. Ocean acidification: present conditions and future changes in a high-CO₂ world. *Oceanography* 22 (4) 36-47.



- FENNIG, K., ANDERSSON, A., BAKAN, S., KLEPP, C. & SCHROEDER, M. 2012. Hamburg Ocean Atmosphere Parameters and Fluxes from Satellite Data - HOAPS 3.2 - Monthly Means / 6-Hourly Composite. (electronic publication). Satellite Application Facility on Climate Monitoring. www.hoaps.zmaw.de/index.php?id=pub
- FESER, F., ROCKEL, B., VON STORCH, H., WINTERFELDT, J. & ZAHN, M. 2011. Regional Climate Models Add Value to Global Model Data: A Review and Selected Examples. *Bulletin of the American Meteorological Society*, 92, 1181-1192.
- FLATO, G., MAROTZKE, J., ABIODUN, B., BRACONNOT, P., CHOU, S., COLLINS, W., COX, P., DRIOUECH, F., EMORI, S. & EYRING, V. 2013. Evaluation of climate models. *Climate change*, 741-866.
- FISCHER, E. & KNUTTI, R. 2014. Detection of spatially aggregated changes in temperature and precipitation extremes. *Geophysical Research Letters*, 41, 547-554.
- FOLEY, A. M. 2010. Uncertainty in regional climate modelling: A review. *Progress in Physical Geography*, 34, 647-670.
- FOSTER, G. L. & ROHLING, E. J. 2013. Relationship between sea level and climate forcing by CO₂ on geological timescales. *Proc Natl Acad Sci U S A*, 110, 1209-14.
- FOWLER, H. & WILBY, R. 2007. Beyond the downscaling comparison study. *International Journal of Climatology*, 27, 1543-1545.
- FREDERIKSEN, J. S. & FREDERIKSEN, C. S. 2005. Decadal Changes in Southern Hemisphere Winter Cyclogenesis. Published, Aspendale, Victoria: CSIRO Marine and Atmospheric Research Paper No. 002, 35pp
- FREDERIKSEN, J. S. & FREDERIKSEN, C. S. 2007. Inter-decadal Changes in Southern Hemisphere Winter Storm Track Modes. *Tellus A*, 59A, 599-617.
- FREDERIKSEN, C. S., FREDERIKSEN, J. S., SISSON, J. M. & OSBROUGH, S. L. 2011. Changes and projections in Australian winter rainfall and circulation: Anthropogenic forcing and internal variability. 2, 143-162. FREITAS, A. C. V. & RAO, V. B. 2014. Global changes in propagation of stationary waves in a warming scenario. *Quarterly Journal of the Royal Meteorological Society*, 140, 364-383.
- FRIEDLINGSTEIN, P., MEINSHAUSEN, M., ARORA, V. K., JONES, C. D., ANAV, A., LIDDICOAT, S. K. & KNUTTI, R. 2014. Uncertainties in CMIP5 climate projections due to carbon cycle feedbacks. *Journal of Climate* 27(2) 511-526.
- FRIELER, K., MEINSHAUSEN, M., GOLLY, A., MENGEL, M., LEBEK, K., DONNER, S. & HOEGH-GULDBERG, O. 2012. Limiting global warming to 2 [thinsp][deg] C is unlikely to save most coral reefs. *Nature Climate Change*, 3, 165-170.
- GALLANT, A., HENNESSY, K. & RISBEY, J. 2007. Trends in rainfall indices for six Australian regions: 1910-2005. *Australian Meteorological Magazine*, 223-239.
- GALLANT, A. J. E. & KAROLY, D. J. 2010. A Combined Climate Extremes Index for the Australian Region. *Journal of Climate*, 23, 6153-6165.
- GALLANT, A., KAROLY, D. & GLEASON, K. 2014. Consistent Trends in a Modified Climate Extremes Index in the United States, Europe, and Australia. *Journal of Climate*, 27, 1379-1394.
- GALLANT, A. J. E., REEDER, M. J., RISBEY, J. S. & HENNESSY, K. J. 2013. The characteristics of seasonal-scale droughts in Australia, 1911-2009. *International Journal of Climatology*, 33, 1658-1672.
- GEHRELS, W. R. & WOODWORTH, P. L. 2013. When did modern rates of sea-level rise start? *Global and Planetary Change*, 100, 263-277.
- GILLETT, N. & THOMPSON, D. 2003. Simulation of recent Southern Hemisphere climate change. *Science*, 302, 273-275.
- GIORGI, F. & MEARNS, L. O. 1999. Introduction to special section: Regional climate modeling revisited. *J. Geophys. Res.*, 104, 6335-6352.
- GLECKLER, P., TAYLOR, K. & DOUTRIAUX, C. 2008. Performance metrics for climate models. *Journal of Geophysical Research-Atmospheres*, 113.
- GRAINGER, S., FREDERIKSEN, C. & ZHENG, X. 2013. Modes of interannual variability of Southern Hemisphere atmospheric circulation in CMIP3 models: assessment and projections. *Climate Dynamics*, 41, 479-500.
- GRAINGER, S., FREDERIKSEN, C. S. & ZHENG, X. 2014. Assessment of modes of interannual variability of Southern Hemisphere atmospheric circulation in CMIP5 models *Journal of Climate*, (accepted).
- GROSE, M., CORNEY, S., KATZFEY, J., BENNETT, J., HOLZ, G., WHITE, C. & BINDOFF, N. 2013. A regional response in mean westerly circulation and rainfall to projected climate warming over Tasmania, Australia. *Climate Dynamics*, 40, 2035-2048.
- GROSE, M. R., BROWN, J. N., NARSEY, S., BROWN, J. R., MURPHY, B. F., LANGLAIS, C., GUPTA, A. S., MOISE, A. F. & IRVING, D. B. 2014a. Assessment of the CMIP5 global climate model simulations of the western tropical Pacific climate system and comparison to CMIP3. *International Journal of Climatology*, 34 (12), 3382-3399.
- GROSE, M., POOK, M., MCINTOSH, P., RISBEY, J. & BINDOFF, N. 2012. The simulation of cutoff lows in a regional climate model: reliability and future trends. *Climate Dynamics*, 39, 445-459.
- GROSE, M. R., BARNES-KEOGHAN, I., CORNEY, S., WHITE, C., HOLZ, G., BENNETT, J., GAYNOR, S. & BINDOFF, N. 2010. Climate Futures for Tasmania: general climate impacts technical report, Hobart, Antarctic Climate & Ecosystems Cooperative Research Centre.
- GROSE, M. R., FOX-HUGHES, P., HARRIS, R. M. & BINDOFF, N. L. 2014b. Changes to the drivers of fire weather with a warming climate—a case study of southeast Tasmania. *Climatic Change*, 1-15.
- GUILYARDI, E., WITTENBERG, A., FEDOROV, A., COLLINS, M., WANG, C., CAPOTONDI, A., VAN OLDENBORGH, G. J. & STOCKDALE, T. 2009. Understanding El Niño in ocean-atmosphere general circulation models: progress and challenges. *Bulletin of the American Meteorological Society*, 90, 325-340.

- HAIGH, I., NICHOLLS, R. & WELLS, N. 2009. Mean sea level trends around the English Channel over the 20th century and their wider context. *Continental Shelf Research*, 29, 2083-2098.
- HAIGH, I., WIJERATNE, E., MACPHERSON, L., PATTIARATCHI, C., MASON, M., CROMPTON, R. & GEORGE, S. 2014. Estimating present day extreme water level exceedance probabilities around the coastline of Australia: tides, extra-tropical storm surges and mean sea level. *Climate Dynamics*, 42, 121-138.
- HALL, A. & VISBECK, M. 2002. Synchronous variability in the southern hemisphere atmosphere, sea ice, and ocean resulting from the annular mode. *Journal of Climate*, 15, 3043-3057.
- HALLEGATTE, S., HOURCADE, J. & AMBROSI, P. 2007. Using climate analogues for assessing climate change economic impacts in urban areas. *Climatic Change*, 82, 47-60.
- HANNAH, J. & BELL, R. G. 2012. Regional sea level trends in New Zealand. *Journal of Geophysical Research-Oceans*, 117.
- HANSEN, J., RUEDY, R., SATO, M., & LO, K. 2010. Global surface temperature change. *Reviews in Geophysics*, 48, RG4004.
- HANSEN, J., SATO, M. & RUEDY, R. 2012. Perception of climate change. *Proceedings of the National Academy of Sciences of the United States of America*, 109, E2415-E2423.
- HARLEY, M., TURNER, I., SHORT, A. & RANASINGHE, R. 2010. Interannual variability and controls of the Sydney wave climate. *International Journal of Climatology*, 30, 1322-1335.
- HARPER, B., HARDY, T., MASON, L. & FRYAR, R. 2009. Developments in storm tide modelling and risk assessment in the Australian region. *Natural hazards*, 51, 225-238.
- HARRIS, I., JONES, P., OSBORN, T. & LISTER, D. 2013. Updated high-resolution grids of monthly climatic observations—the CRU TS3. 10 Dataset. *International Journal of Climatology*, 34, 623-642.
- HART, R. 2003. A cyclone phase space derived from thermal wind and thermal asymmetry. *Monthly Weather Review*, 131, 585-616.
- HASSON, A., MILLS, G., TIMBAL, B. & WALSH, K. 2009. Assessing the impact of climate change on extreme fire weather events over southeastern Australia. *Climate Research*, 39, 159-172.
- HAWKINS, E. & SUTTON, R. 2009. The Potential to Narrow Uncertainty in Regional Climate Predictions. *Bulletin of the American Meteorological Society*, 90, 1095-1107.
- HELD, I. M. & SODEN, B. J. 2006. Robust responses of the hydrological cycle to global warming. *Journal of Climate*, 19, 5686-5699.
- HENDON, H., LIM, E., ARBLASTER, J. & ANDERSON, D. 2014. Causes and predictability of the record wet east Australian spring 2010. *Climate Dynamics*, 42, 1155-1174.
- HENDON, H., THOMPSON, D. & WHEELER, M. 2007. Australian rainfall and surface temperature variations associated with the Southern Hemisphere annular mode. *Journal of Climate*, 2452-2467.
- HENDRIKX, J., ZAMMIT, C., HREINSSON, E. & BECKEN, S. 2013. A comparative assessment of the potential impact of climate change on the ski industry in New Zealand and Australia. *Climatic Change*, 119, 965-978.
- HENNESSY, K. J., WHETTON, P., SMITH, I., BATHOLS, J., HUTCHINSON, M. & SHARPLES, J. 2003. The impact of climate change on snow conditions in mainland Australia, CSIRO Atmospheric Research Aspendale, 47 p.
- HENNESSY, K., FAWCETT, R., KIRONO, D., MPELASOKA, F., JONES, D., BATHOLS, J., WHETTON, P., STAFFORD-SMITH, M., HOWDEN, M., MITCHELL, C. & PLUMMER, N. 2008. An assessment of the impact of climate change on the nature of frequency of exceptional climatic events. A Report to the Australian Government. Australia.
- HENNESSY, K., LUCAS, C., NICHOLLS, N., BATHOLS, J., SUPPIAH, R. & RICKETTS, J. 2005. Climate change impacts on fire-weather in south-east Australia. Consultancy report by CSIRO Marine and Atmospheric Research, Bureau of Meteorology and Bushfire CRC for the New South Wales Greenhouse Office, Victorian Department of Sustainability and Environment, ACT Government, Tasmanian Department of Primary Industries, Water and Environment and the Australian Greenhouse Office. Victoria
- HENRY, O., PRANDI, P., LLOVEL, W., CAZENAVE, A., JEVREJEVA, S., STAMMER, D., MEYSSIGNAC, B. & KOLDUNOV, N. 2012. Tide gauge-based sea level variations since 1950 along the Norwegian and Russian coasts of the Arctic Ocean: Contribution of the steric and mass components. *Journal of Geophysical Research-Oceans*, 117.
- HEGERL, G. C., ZWIERS, F. W., BRACONNOT, P., GILLET, N.P., LUO, Y., MARENGO ORSINI, J.A. NICHOLLS, N., PENNER, J.E. & STOTT, P.A. 2007. Understanding and Attributing Climate Change. In: *Climate Change 2007: The Physical Science Basis*. Contribution of Working Group I to the Fourth Assessment Report of the Intergovernmental Panel on Climate Change [Solomon, S., D. Qin, M. Manning, Z. Chen, M. Marquis, K.B. Averyt, M. Tignor and H.L. Miller (eds.)]. Cambridge University Press, Cambridge, United Kingdom and New York, NY, USA.
- HILL, K. L., RINTOUL, S. R., RIDGWAY, K. R. & OKE, P. R. 2011. Decadal changes in the South Pacific western boundary current system revealed in observations and ocean state estimates. *Journal of Geophysical Research-Oceans*, 116.
- HOBBINS, M. T., RAMIREZ, J. A., BROWN, T. C. & CLAESSENS, L. 2001. The complementary relationship in estimation of regional evapotranspiration: The Complementary Relationship Areal Evapotranspiration and Advection-Aridity models. *Water Resources Research*, 37, 1367-1387.
- HOEGH-GULDBERG, O., MUMBY, P., HOOTEN, A., STENECK, R., GREENFIELD, P., GOMEZ, E., HARVELL, C., SALE, P., EDWARDS, A. & CALDEIRA, K. 2007. Coral reefs under rapid climate change and ocean acidification. *Science*, 318, 1737-1742.

-20° -10° 0° 10° 20° 30° 40° 50°



- HOLBROOK, N. J. & BINDOFF, N. L. 1997. Interannual and decadal temperature variability in the southwest Pacific Ocean between 1955 and 1988. *Journal of Climate*, 10, 1035-1049.
- HOLZ, G. K., GROSE, M. R., BENNETT, J. C., CORNEY, S. P., WHITE, C. J., PHELAN, D., POTTER, K., KRITICOS, D. J., RAWNSLEY, R., PARSONS, D., LISSON, S., GAYNOR, S. M. & BINDOFF, N. L. 2010. Climate Futures for Tasmania: impacts on agriculture technical report. Hobart, Tasmania: Antarctic Climate and Ecosystems Cooperative Research Centre.
- HOPE, P., DROSDOWSKY, W. & NICHOLLS, N. 2006. Shifts in the synoptic systems influencing southwest Western Australia. *Climate Dynamics*, 26, 751-764.
- HOPE, P., TIMBAL, B. & FAWCETT, R. 2010. Associations between rainfall variability in the southwest and southeast of Australia and their evolution through time. *International Journal of Climatology*, 30, 1360-1371.
- HU, Y., TAO, L. & LIU, J. 2013. Poleward expansion of the Hadley circulation in CMIP5 simulations. *Advances in Atmospheric Sciences*, 30, 790-795.
- HUFFMAN, G. J., ADLER, R. F., BOLVIN, D. T. & GU, G. 2009. Improving the global precipitation record: GPCP Version 2.1. *Geophysical Research Letters*, 36, L17808.
- HUNG, M., LIN, J., WANG, W., KIM, D., SHINODA, T. & WEAVER, S. 2013. MJO and Convectively Coupled Equatorial Waves Simulated by CMIP5 Climate Models. *Journal of Climate*, 26, 6185-6214.
- HUNTER, J. 2012. A simple technique for estimating an allowance for uncertain sea-level rise. *Climatic Change*, 113, 239-252.
- HUNTER, J. R., CHURCH, J. A., WHITE, N. J. & ZHANG, X. 2013. Towards a global regionally varying allowance for sea-level rise. *Ocean Engineering* 71, 17-27.
- HUNTER, J., COLEMAN, R. & PUGH, D. 2003. The sea level at Port Arthur, Tasmania, from 1841 to the present. *Geophysical Research Letters*, 30.
- HUNTINGTON, T. G. 2006. Evidence for intensification of the global water cycle: Review and synthesis. *Journal of Hydrology*, 319, 83-95.
- IGBP (International Geosphere-Biosphere Programme), 2010. IGBP Global Change magazine, 75, June 2010 www.igbp.net/publications/globalchangemagazine/globalchangemagazine/75.5.1b8ae20512db692f2a6800010715.html
- IGLESIAS-RODRIGUEZ, M. D., HALLORAN, P. R., RICKABY, R. E., HALL, I. R., COLMENERO-HIDALGO, E., GITTINS, J. R., GREEN, D. R., TYRRELL, T., GIBBS, S. J. & VON DASSOW, P. 2008. Phytoplankton calcification in a high-CO₂ world. *Science*, 320, 336-340.
- IHARA, C., KUSHNIR, Y. & CANE, M. A. 2008. Warming trend of the Indian Ocean SST and Indian Ocean dipole from 1880 to 2004. *Journal of Climate*, 21, 2035-2046.
- INNESS, P., SLINGO, J., GUILYARDI, E. & COLE, J. 2003. Simulation of the Madden-Julian oscillation in a coupled general circulation model. Part II: The role of the basic state. *Journal of Climate*, 16, 365-382.
- IOCI 2002. Climate variability and change in south west Western Australia. Technical Report, Indian Ocean Climate Initiative Panel. Perth, Australia.
- IPCC 1995 Climate change 1995: the science of climate change. Contribution of Working Group I to the Second Assessment of the Intergovernmental Panel on Climate Change. In: HOUGHTON, J. T., MEIRA FILHO, L., CALLENDER, B., HARRIS, N., KATTENBERG, A. & MASKELL, K. (eds.). Cambridge University Press Cambridge, United Kingdom.
- IPCC 2001. Climate Change 2001: The Scientific Basis. In: HOUGHTON, J. T., DING, Y., GRIGGS, D. J., NOGUER, M., VAN DER LINDEN, P. J., DALI, X., MASKELL, K. & JOHNSON, C. (eds.). Cambridge: Cambridge University Press.
- IPCC 2007. Climate Change 2007: The Physical Science basis: Working group I contribution to the Fourth Assessment report of the IPCC. In: SOLOMON, S. (ed.). Cambridge: Cambridge University Press.
- IPCC 2012. Summary for Policymakers. In: Managing the risks of extreme events and disasters to advance climate change adaptation. In: FIELD CB, V. B., TF STOCKER, D QIN, DJ DOKKEN, KL EBI, MD MASTRANDEA, KJ MARCH, GK PLATTNER, SK ALLEN, M TIGNOR, AND PM MIDGLEY (EDS) (ed.) Special Report of Working Groups I and II of the Intergovernmental Panel on Climate Change. Cambridge, UK, and New York, NY, USA: Cambridge University Press.
- IPCC 2013. Climate Change 2013: The Physical Science Basis. Contribution of Working Group I to the Fifth Assessment Report of the Intergovernmental Panel on Climate Change. In: STOCKER, T. F., D. QIN, G.-K. PLATTNER, M. TIGNOR, S. K. ALLEN, J. BOSCHUNG, A. NAUELS, Y. XIA, V. BEX AND P. M. MIDGLEY (ed.).
- IPCC 2014. Climate Change 2014: Mitigation of Climate Change. Contribution of Working Group III to the Fifth Assessment Report of the Intergovernmental Panel on Climate Change In: EDENHOFER, O., R. PICHES-MADRUGA, Y. SOKONA, E. FARAHANI, S. KADNER, K. SEYBOTH, A. ADLER, I. BAUM, S. BRUNNER, P. EICKEMEIER, B. KRIEMANN, J. SAVOLAINEN, S. SCHLÖMER, C. VON STECHOW, T. ZWICKEL & MINX, J. C. (eds.). Cambridge, United Kingdom and New York, NY, USA.: Cambridge University Press.
- JAKOB, D. 2010. Challenges in developing a high-quality surface wind-speed data-set for Australia. *Australian Meteorological Magazine*, 60, 227-236.
- JEVREJEVA, S., GRINSTED, A., MOORE, J. C. & HOLTGATE, S. 2006. Nonlinear trends and multiyear cycles in sea level records. *Journal of Geophysical Research*, 111.
- JEVREJEVA, S., MOORE, J. C., GRINSTED, A. & WOODWORTH, P. L. 2008. Recent global sea level acceleration started over 200 years ago? *Geophysical Research Letters*, 35.
- JIANG, X., MALONEY, E., LI, J. & WALISER, D. 2013. Simulations of the Eastern North Pacific Intraseasonal Variability in CMIP5 GCMs. *Journal of Climate*, 26, 3489-3510.

- JONES, R. & MCINNES, K. 2004. A scoping study on impact and adaptation strategies for climate change in Victoria. CSIRO Atmospheric Research, Melbourne, Australia: Report to the Greenhouse unit of the Victorian department of sustainability and environment.
- JONES, D. A., WANG, W. & FAWCETT, R. 2009a. High-quality spatial climate data-sets for Australia. *Australian Meteorological and Oceanographic Journal*, 58, 233-248.
- JONES, G., STOTT, P. & CHRISTIDIS, N. 2013. Attribution of observed historical near-surface temperature variations to anthropogenic and natural causes using CMIP5 simulations. *Journal of Geophysical Research-Atmospheres*, 118, 4001-4024.
- JONES, J., FOGT, R., WIDMANN, M., MARSHALL, G., JONES, P. & VISBECK, M. 2009b. Historical SAM Variability. Part I: Century-Length Seasonal Reconstructions. *Journal of Climate*, 22, 5319-5345.
- JOSEY, S. A., KENT, E. C. & TAYLOR, P. K. 1998. The Southampton Oceanography Centre (SOC) ocean-atmosphere heat, momentum and freshwater flux atlas, Southampton Oceanography Centre Southampton, UK.
- JOURDAIN, N. C., GUPTA, A. S., TASCHETTO, A. S., UMMENHOFER, C. C., MOISE, A. F. & ASHOK, K. 2013. The Indo-Australian monsoon and its relationship to ENSO and IOD in reanalysis data and the CMIP3/CMIP5 simulations. *Climate Dynamics*, 41, 3073-3102.
- JOVANOVIĆ, B., COLLINS, D., BRAGANZA, K., JAKOB, D. & JONES, D. 2011. A high-quality monthly total cloud amount dataset for Australia. *Climatic Change*, 108, 485-517.
- JOVANOVIĆ, B., JONES, D. & COLLINS, D. 2008. A high-quality monthly pan evaporation dataset for Australia. *Climatic Change*, 87, 517-535.
- KALNAY, E., KANAMITSU, M., KISTLER, R., COLLINS, W., DEAVEN, D., GANDIN, L., IREDELL, M., SAHA, S., WHITE, G., WOOLLEN, J., ZHU, Y., CHELLIAH, M., EBISUZAKI, W., HIGGINS, W., JANOWIAK, J., MO, K. C., ROPELEWSKI, C., WANG, J., LEETMAA, A., REYNOLDS, R., JENNE, R. & JOSEPH, D. 1996. The NCEP/NCAR 40-year reanalysis project. *Bulletin of the American Meteorological Society*, 77, 437-471.
- KANAMITSU, M., EBISUZAKI, W., WOOLLEN, J., YANG, S., HNILO, J., FIORINO, M. & POTTER, G. 2002. NCEP-DOE AMIP-II reanalysis (R-2). *Bulletin of the American Meteorological Society*, 83, 1631-1643.
- KARL, T. R., NICHOLLS, N. & GHAZI, A. 1999. Clivar/GCOS/WMO workshop on indices and indicators for climate extremes workshop summary. *Weather and Climate Extremes*. Springer.
- KAROLY, D. & BRAGANZA, K. 2005. Attribution of recent temperature changes in the Australian region. *Journal of Climate*, 18, 457-464.
- KENDALL, R. A., MITROVICA, J. X. & MILNE, G. A. 2005. On post-glacial sea level - II. Numerical formulation and comparative results on spherically symmetric models. *Geophysical Journal International*, 161, 679-706.
- KENDON, E., JONES, R., KJELLSTROM, E. & MURPHY, J. 2010. Using and Designing GCM-RCM Ensemble Regional Climate Projections. *Journal of Climate*, 23, 6485-6503.
- KENT, D., KIRONO, D., TIMBAL, B. & CHIEW, F. 2013. Representation of the Australian subtropical ridge in the CMIP3 models. *International Journal of Climatology*, 33, 48-57.
- KEY, R. M., KOZYR, A., SABINE, C. L., LEE, K., WANNINKHOF, R., BULLISTER, J. L., FEELY, R. A., MILLERO, F. J., MORDY, C. & PENG, T. H. 2004. A global ocean carbon climatology: Results from Global Data Analysis Project (GLODAP). *Global Biogeochemical Cycles*, 18.
- KING, A. D., S. C. LEWIS, S. E. PERKINS, L. V. ALEXANDER, M. G. DONAT, D. J. KAROLY & M. T. BLACK 2013. Limited Evidence of Anthropogenic Influence on the 2011-12 Extreme Rainfall over Southeast Australia. In 'Explaining Extreme Events of 2012 from a Climate Perspective'. *Bull. Amer. Meteor. Soc.*, 94, S55-S58.
- KIM, D., SOBEL, A., DEL GENIO, A., CHEN, Y., CAMARGO, S., YAO, M., KELLEY, M. & NAZARENKO, L. 2012. The Tropical Subseasonal Variability Simulated in the NASA GISS General Circulation Model. *Journal of Climate*, 25, 4641-4659.
- KIM, D., SPERBER, K., STERN, W., WALISER, D., KANG, I., MALONEY, E., WANG, W., WEICKMANN, K., BENEDICT, J., KHAIROUTDINOV, M., LEE, M., NEALE, R., SUAREZ, M., THAYER-CALDER, K. & ZHANG, G. 2009. Application of MJO Simulation Diagnostics to Climate Models. *Journal of Climate*, 22, 6413-6436.
- KIRONO, D. G. C., HENNESSY, K., MPELASOKA, F. & KENT, D. 2011a. Approaches for generating climate change scenarios for use in drought projections - a review. *CAWCR Technical report No 034*.
- KIRONO, D. G. C., JONES, R. N. & CLEUGH, H. A. 2009. Pan-evaporation measurements and Morton-point potential evaporation estimates in Australia: are their trends the same? *International Journal of Climatology*, 29, 711-718.
- KIRONO, D. G. C. & KENT, D. M. 2011. Assessment of rainfall and potential evaporation from global climate models and its implications for Australian regional drought projection. *International Journal of Climatology*, 31, 1295-1308.
- KIRONO, D. G. C., KENT, D. M., HENNESSY, K. J. & MPELASOKA, F. 2011b. Characteristics of Australian droughts under enhanced greenhouse conditions: Results from 14 global climate models. *Journal of Arid Environments*, 75, 566-575.
- KNUTSON, T., MCBRIDE, J., CHAN, J., EMANUEL, K., HOLLAND, G., LANDSEA, C., HELD, I., KOSSIN, J., SRIVASTAVA, A. & SUGI, M. 2010. Tropical cyclones and climate change. *Nature Geoscience*, 3, 157-163.
- KNUTTI, R., FURRER, R., TEBALDI, C., CERMAK, J. & MEEHL, G. 2010. Challenges in Combining Projections from Multiple Climate Models. *Journal of Climate*, 23, 2739-2758.
- KNUTTI, R., MASSON, D. & GETTELMAN, A. 2013. Climate model genealogy: Generation CMIP5 and how we got there. *Geophysical Research Letters*, 40, 1194-1199.

- KNUTTI, R. & SEDLÁČEK, J. 2013. Robustness and uncertainties in the new CMIP5 climate model projections. *Nature Climate Change*, 3, 369-373.
- KOKIC, P., CRIMP, S. & HOWDEN, M. 2011. Forecasting climate variables using a mixed-effect state-space model. *Environmetrics*, 22, 409-419.
- KOPP, R. E., SIMONS, F. J., MITROVICA, J. X., MALOOF, A. C. & OPPENHEIMER, M. 2009. Probabilistic assessment of sea level during the last interglacial stage. *Nature*, 462, 863-7.
- KOPP, R. E., SIMONS, F. J., MITROVICA, J. X., MALOOF, A. C. & OPPENHEIMER, M. 2013. A probabilistic assessment of sea level variations within the last interglacial stage. *Geophysical Journal International*, 193, 711-716.
- KOSSIN, J. P., EMANUEL, K. A. & VECCHI, G. A. 2014. The poleward migration of the location of tropical cyclone maximum intensity. *Nature*, 509, 349-352.
- KUHLBRODT, T. & GREGORY, J. 2012. Ocean heat uptake and its consequences for the magnitude of sea level rise and climate change. *Geophysical Research Letters*, 39.
- KULESHOV, Y., FAWCETT, R., QI, L., TREWIN, B., JONES, D., MCBRIDE, J. & RAMSAY, H. 2010. Trends in tropical cyclones in the South Indian Ocean and the South Pacific Ocean. *Journal of Geophysical Research-Atmospheres*, 115.
- LAMBECK, K. 2002. Sea Level Change from Mid Holocene to Recent Time: an Australian Example With Global Implications. *Ice Sheets, Sea Level and the Dynamic Earth*. *Geodynamics Science* 29, 33-50.
- LAMBECK, K., ESAT, T. M. & POTTER, E. K. 2002. Links between climate and sea levels for the past three million years. *Nature*, 419, 199-206.
- LANGENBRUNNER, B. & NEELIN, J. 2013. Analyzing ENSO Teleconnections in CMIP Models as a Measure of Model Fidelity in Simulating Precipitation. *Journal of Climate*, 26, 4431-4446.
- LARGE, W. G. & YEAGER, S. 2004. Diurnal to decadal global forcing for ocean and sea-ice models: the data sets and flux climatologies. *CGD Division of the National Center for Atmospheric Research, NCAR Technical Note: NCAR/TN-460+STR*.
- LARGE, W. G. & YEAGER, S. 2009. The global climatology of an interannually varying air-sea flux data set. *Climate Dynamics*, 33, 341-364.
- LAVENDER, S. & WALSH, K. 2011. Dynamically downscaled simulations of Australian region tropical cyclones in current and future climates. *Geophysical Research Letters*, 38.
- LE QUÉRÉ, C., PETERS, G., ANDRES, R., ANDREW, R., BODEN, T., CIAIS, P., FRIEDLINGSTEIN, P., HOUGHTON, R., MARLAND, G., MORIARTY, R., SITCH, S., TANS, P., ARNETH, A., ARVANITIS, A., BAKKER, D. C. E., BOPP, L., CANADELL, J. G., CHINI, L. P., DONEY, S. C., HARPER, A., HARRIS, I., HOUSE, J. I., JAIN, A. K., JONES, S. D., KATO, E., KEELING, R. F., KLEIN GOLDEWIJK, K., KÖRTZINGER, A., KOVEN, C., LEFÈVRE, N., MAIGNAN, F., OMAR, A., ONO, T., PARK, G.-H., PFEIL, B., POULTER, B., RAUPACH, M. R., REGNIER, P., RÖDENBECK, C., SAITO, S., SCHWINGER, J., SEGSCHNEIDER, J., STOCKER, B. D., TAKAHASHI, T., TILBROOK, B., VAN HEUVEN, S., VIOVY, N., WANNINKHOF, R., WILTSHIRE, A. & ZAEHLE, S. 2013. Global carbon budget 2013. *Earth System Science Data Discussions*, 6, 689-760.
- LEE, J.-Y. & WANG, B. 2014. Future change of global monsoon in the CMIP5. *Climate Dynamics*, 42, 101-119.
- LEONARD, M., WESTRA, S., PHATAK, A., LAMBERT, M., VAN DEN HURK, B., MCINNES, K., RISBEY, J., SCHUSTER, S., JAKOB, D. & STAFFORD-SMITH, M. 2013. A compound event framework for understanding extreme impacts. *Wiley Interdisciplinary Reviews: Climate Change* 5(1) 113-128.
- LEVITUS, S., ANTONOV, J., BOYER, T. & STEPHENS, C. 2000. Warming of the world ocean. *Science*, 287, 2225-2229.
- LEWIS, S. & KAROLY, D. 2013. Anthropogenic contributions to Australia's record summer temperatures of 2013. *Geophysical Research Letters*, 40, 3705-3709.
- LEWIS, S. C. & KAROLY, D. J. 2014. The role of anthropogenic forcing in the record 2013 Australia-wide annual and spring temperatures. *Bulletin of the American Meteorological Society*, (in press).
- LI, X.-F., YU, J. & LI, Y. 2013. Recent Summer Rainfall Increase and Surface Cooling over Northern Australia since the Late 1970s: A Response to Warming in the Tropical Western Pacific. *Journal of Climate*, 26, 7221-7239.
- LI, Y., LI, J. & FENG, J. 2012. A Teleconnection between the Reduction of Rainfall in Southwest Western Australia and North China. *Journal of Climate*, 25, 8444-8461.
- LIMA, F. & WETHEY, D. 2012. Three decades of high-resolution coastal sea surface temperatures reveal more than warming. *Nature Communications*, 3.
- LIN, J., KILADIS, G., MAPES, B., WEICKMANN, K., SPERBER, K., LIN, W., WHEELER, M., SCHUBERT, S., DEL GENIO, A., DONNER, L., EMORI, S., GUEREMY, J., HOURDIN, F., RASCH, P., ROECKNER, E. & SCINOCCA, J. 2006. Tropical intraseasonal variability in 14 IPCC AR4 climate models. Part I: Convective signals. *Journal of Climate*, 19, 2665-2690.
- LIU, L., YU, W. & LI, T. 2011. Dynamic and Thermodynamic Air-Sea Coupling Associated with the Indian Ocean Dipole Diagnosed from 23 WCRP CMIP3 Models. *Journal of Climate*, 24, 4941-4958.
- LLOYD-HUGHES, B. & SAUNDERS, M. A. 2002. A drought climatology for Europe. *International Journal of Climatology*, 22, 1571-1592.

- LOCARNINI, R. A., MISHONOV, A. V., ANTONOV, J. I., BOYER, T. P. & GARCIA, H. E., BARANOVA, O. K., ZWENG, M. M. & JOHNSON, D. R. 2010. World Ocean Atlas 2009, Volume 1: Temperature. In: S. LEVITUS (ed.). NOAA Atlas NESDIS 68, U.S. Government Printing Office, Washington, D.C., 184 pp ftp://ftp.nodc.noaa.gov/pub/WOA09/DOC/wao09_vol1_text.pdf
- LUCAS, C., HENNESSY, K., MILLS, G. & BATHOLS, J. 2007. Bushfire Weather in Southeast Australia: Recent Trends and Projected Climate Change Impacts. Consultancy Report prepared for The Climate Institute of Australia. Bush fire Cooperative Research Centre: Victoria
- LUCAS, C. 2010a. A high-quality historical humidity database for Australia. Australia: CAWCR Tehnical Report No 024.
- LUCAS, C. 2010b. On developing a historical fire weather data-set for Australia. Australian Meteorological and Oceanographic Journal, 60, 1-13.
- LUCAS, C., NGUYEN, H. & TIMBAL, B. 2012. An observational analysis of Southern Hemisphere tropical expansion. Journal of Geophysical Research-Atmospheres, 117.
- LUCAS, C., TIMBAL, B. & NGUYEN, H. 2014. The expanding tropics: a critical assessment of the observational and modeling studies. Wiley Interdisciplinary Reviews: Climate Change 5(1) 89-112.
- MADDEN, R. A. & JULIAN, P. R. 1972. Description of global-scale circulation cells in the tropics with a 40-50 day period. Journal of the Atmospheric Sciences, 29, 1109-1123.
- MADDEN, R. A. & JULIAN, P. R. 1994. Observations of the 40-50-day tropical oscillation-A review. Monthly Weather Review, 122, 814-837.
- MARAUN, D., WETTERHALL, F., IRESON, A., CHANDLER, R., KENDON, E., WIDMANN, M., BRIENEN, S., RUST, H., SAUTER, T. & THEMEßL, M. 2010. Precipitation downscaling under climate change: recent developments to bridge the gap between dynamical models and the end user. Reviews of Geophysics, 48, (3).
- MARSHALL, G. 2007. Half-century seasonal relationships between the Southern Annular Mode and Antarctic temperatures. International Journal of Climatology, 27, 373-383.
- MASSON-DELMOTTE, V., SCHULZ, M., ABE-OUCHI, A., BEER, J., GANOPOLSKI, A., GONZÁLEZ-ROUCO, J.-E., JANSEN, E., LAMBECK, K., LUTERBACHER, J., NAISH, T., OSBORN, T., OTTO-BLIESNER, B., QUINN, T., RAMESH, R., ROJAS, M., SHAO, X. & TIMMERMANN, A. 2014. Chapter 5: Information from the Paleoclimate Archives. In: STOCKER, T. F., D. QIN, G.-K. PLATTNER, M. TIGNOR, S. K. ALLEN, J. BOSCHUNG, A. NAUELS, Y. XIA, V. BEX AND P. M. MIDGLEY (ed.) Climate Change 2013: The Physical Science Basis. Contribution of Working Group I to the Fifth Assessment Report of the Intergovernmental Panel on Climate Change.
- MASTRANDREA, M. D., FIELD, C. B., STOCKER, T. F., EDENHOFER, O., EBI, K. L., FRAME, D. J., HELD, H., KRIEGLER, E., MACH, K. J. & MATSCHOSS, P. R. 2010. Guidance note for lead authors of the IPCC fifth assessment report on consistent treatment of uncertainties. Intergovernmental Panel on Climate Change (IPCC).
- MASTERS, D., NEREM, R. S., CHOE, C., LEULIETTE, E., BECKLEY, B., WHITE, N. & ABLAIN, M. 2012. Comparison of Global Mean Sea Level Time Series from TOPEX/Poseidon, Jason-1, and Jason-2. Marine Geodesy, 35, 20-41.
- MATEAR, R., CHAMBERLAIN, M., SUN, C. & FENG, M. 2013. Climate change projection of the Tasman Sea from an Eddy-resolving Ocean Model. Journal of Geophysical Research: Oceans, 118, 2961-2976.
- MAXINO, C., MCAVANEY, B., PITMAN, A. & PERKINS, S. 2008. Ranking the AR4 climate models over the Murray-Darling Basin using simulated maximum temperature, minimum temperature and precipitation. International Journal of Climatology, 1097-1112.
- MCARTHUR, A. G. 1967. Fire behaviour in Eucalypt forests. Leaflet. Forestry Timber Bureau Australia, 35-35.
- MCBRIDE, J. L. & NICHOLLS, N. 1983. Seasonal relationships between Australian rainfall and the Southern Oscillation. Monthly Weather Review, 111, 1998-2004.
- MCCOWN, R. L., HAMMER, G. L., HARGREAVES, J. N. G., HOLZWORTH, D. P. & FREEBAIRN, D. M. 1996. APSIM: A Novel Software System for Model Development, Model Testing, and Simulation in Agricultural Research. Agricultural Systems, 50, 255-271.
- MCEVOY, D., AHMED, I. & MULLETT, J. 2012. The impact of the 2009 heat wave on Melbourne's critical infrastructure. Local Environment, 17, 783-796.
- MCGRATH, G. S., SADLER, R., FLEMING, K., TREGONING, P., HINZ, C. & VENEKLAAS, E. J. 2012. Tropical cyclones and the ecohydrology of Australia's recent continental-scale drought. Geophysical Research Letters, 39.
- MCGREGOR, J. L. & DIX, M. R. 2008. An updated description of the conformal-cubic atmospheric model. High resolution numerical modelling of the atmosphere and ocean, Springer: 51-76.
- MCINNES, K., ERWIN, T. & BATHOLS, J. 2011. Global Climate Model projected changes in 10 m wind speed and direction due to anthropogenic climate change. Atmospheric Science Letters, 12, 325-333.
- MCINNES, K. & HUBBERT, G. 2003. A numerical modelling study of storm surges in Bass Strait. Australian Meteorological Magazine, 52, 143-156.
- MCINNES, K., HUBBERT, G., ABBS, D. & OLIVER, S. 2002. A numerical modelling study of coastal flooding. Meteorology and Atmospheric Physics, 80, 217-233.
- MCKEE, T. B., DOESKEN, N. J. & KLEIST, J. 1993. The relationship of drought frequency and duration to time scales. Proceedings of the 8th Conference on Applied Climatology, American Meteorological Society Boston, MA, 179-183.

- MCMAHON, T. A., PEEL, M. C., LOWE, L., SRIKANTHAN, R. & MCVICAR, T. R. 2013. Estimating actual, potential, reference crop and pan evaporation using standard meteorological data: a pragmatic synthesis. *Hydrology and Earth System Sciences*, 17, 1331-1363.
- MCVICAR, T., RODERICK, M., DONOHUE, R., LI, L., VAN NIEL, T., THOMAS, A., GRIESER, J., JHAJHARIA, D., HIMRI, Y., MAHOWALD, N., MESCHERSKAYA, A., KRUGER, A., REHMAN, S. & DINPASHOH, Y. 2012. Global review and synthesis of trends in observed terrestrial near-surface wind speeds: Implications for evaporation. *Journal of Hydrology*, 416, 182-205.
- MCVICAR, T., VAN NIEL, T., LI, L., RODERICK, M., RAYNER, D., RICCIARDULLI, L. & DONOHUE, R. 2008. Wind speed climatology and trends for Australia, 1975-2006: Capturing the stilling phenomenon and comparison with near-surface reanalysis output. *Geophysical Research Letters*, 35.
- MEARNS, L. O., GUTOWSKI, W., JONES, R., LEUNG, R., MCGINNIS, S., NUNES, A. & QIAN, Y. 2009. A regional climate change assessment program for North America. *Eos, Transactions American Geophysical Union*, 90, 311-311.
- MEEHL, G., ARBLASTER, J., MATTHES, K., SASSI, F. & VAN LOON, H. 2009. Amplifying the Pacific Climate System Response to a Small 11-Year Solar Cycle Forcing. *Science*, 325, 1114-1118.
- MEEHL, G. A., COVEY, C., TAYLOR, K. E., DELWORTH, T., STOUFFER, R. J., LATIF, M., MCAVANEY, B. & MITCHELL, J. F. B. 2007. THE WCRP CMIP3 Multimodel Dataset: A New Era in Climate Change Research. *Bulletin of the American Meteorological Society*, 88, 1383-1394.
- MEINSHAUSEN, M., SMITH, S., CALVIN, K., DANIEL, J., KAINUMA, M., LAMARQUE, J., MATSUMOTO, K., MONTZKA, S., RAPER, S., RIAHI, K., THOMSON, A., VELDEERS, G. & VAN VUUREN, D. 2011. The RCP greenhouse gas concentrations and their extensions from 1765 to 2300. *Climatic Change*, 109, 213-241.
- MEYERS, G., MCINTOSH, P., PIGOT, L. & POOK, M. 2007. The years of El Niño, La Niña, and interactions with the tropical Indian ocean. *Journal of Climate*, 20, 2872-2880.
- MILLS, G. 2005. A re-examination of the synoptic and mesoscale meteorology of Ash Wednesday 1983. *Australian Meteorological Magazine*, 54, 35-55.
- MILLS, G. A., WEBB, R., DAVIDSON, N. E., KEPERT, J., SEED, A. & ABBS, D. 2010. The Pasha Bulker east coast low of 8 June 2007. Centre for Australian Weather and Climate Research, Australia, CAWCR Technical Report 23.
- MIN, S., SIMONIS, D. & HENSE, A. 2007. Probabilistic climate change predictions applying Bayesian model averaging. *Philosophical Transactions of the Royal Society a-Mathematical Physical and Engineering Sciences*, 365, 2103-2116.
- MITCHELL, R., FORGAN, B., CAMPBELL, S. & QIN, Y. 2013. The climatology of Australian tropical aerosol: Evidence for regional correlation. *Geophysical Research Letters*, 40, 2384-2389.
- MITROVICA, J. X., GOMEZ, N., MORROW, E., HAY, C., LATYCHEV, K. & TAMISIEA, M. E. 2011. On the robustness of predictions of sea level fingerprints. *Geophysical Journal International*, 187, 729-742.
- MIZUTA, R., YOSHIMURA, H., MURAKAMI, H., MATSUEDA, M., ENDO, H., OSE, T., KAMIGUCHI, K., HOSAKA, M., SUGI, M., YUKIMOTO, S., KUSUNOKI, S. & KITO, A. 2012. Climate Simulations Using MRI-AGCM3.2 with 20-km Grid. *Journal of the Meteorological Society of Japan*, 90A, 233-258.
- MOISE, A., COLMAN, R. & BROWN, J. 2012. Behind uncertainties in projections of Australian tropical climate: Analysis of 19 CMIP3 models. *Journal of Geophysical Research-Atmospheres*, 117.
- MOISE, A. & HUDSON, D. 2008. Probabilistic predictions of climate change for Australia and southern Africa using the reliability ensemble average of IPCC CMIP3 model simulations. *Journal of Geophysical Research-Atmospheres*, 113 (D15).
- MORICE, C. P., KENNEDY, J. J., RAYNER, N. A. & JONES, P. D. 2012. Quantifying uncertainties in global and regional temperature change using an ensemble of observational estimates: The HadCRUT4 data set. *Journal of Geophysical Research: Atmospheres* (1984–2012), 117.
- MÖRNER, N.-A. & ETIOPE, G. 2002. Carbon degassing from the lithosphere. *Global and Planetary Change*, 33, 185-203.
- MORTON, F. I. 1983. Operational estimates of areal evapotranspiration and their significance to the science and practice of hydrology. *Journal of Hydrology*, 66, 1-76.
- MOSS, R., EDMONDS, J., HIBBARD, K., MANNING, M., ROSE, S., VAN VUUREN, D., CARTER, T., EMORI, S., KAINUMA, M., KRAM, T., MEEHL, G., MITCHELL, J., NAKICENOVIC, N., RIAHI, K., SMITH, S., STOUFFER, R., THOMSON, A., WEYANT, J. & WILBANKS, T. 2010. The next generation of scenarios for climate change research and assessment. *Nature*, 463, 747-756.
- MOY, A. D., HOWARD, W. R., BRAY, S. G. & TRULL, T. W. 2009. Reduced calcification in modern Southern Ocean planktonic foraminifera. *Nature Geoscience*, 2, 276-280.
- MUNDAY, P. L., DIXSON, D. L., MCCORMICK, M. I., MEEKAN, M., FERRARI, M. C. & CHIVERS, D. P. 2010. Replenishment of fish populations is threatened by ocean acidification. *Proceedings of the National Academy of Sciences*, 107, 12930-12934.
- MUNDAY, P. L., DONELSON, J. M., DIXSON, D. L. & ENDO, G. G. 2009. Effects of ocean acidification on the early life history of a tropical marine fish. *Proceedings of the Royal Society B: Biological Sciences*, 276, 3275-3283.
- MURAKAMI, H. & WANG, B. 2010. Future Change of North Atlantic Tropical Cyclone Tracks: Projection by a 20-km-Mesh Global Atmospheric Model. *Journal of Climate*, 23, 2699-2721.

- MURAKAMI, H., MIZUTA, R. & SHINDO, E. 2012. Future changes in tropical cyclone activity projected by multi-physics and multi-SST ensemble experiments using the 60-km-mesh MRI-AGCM. *Climate Dynamics*, 39 (9-10), 2569-2584.
- MURPHY, B. & TIMBAL, B. 2008. A review of recent climate variability and climate change in southeastern Australia. *International Journal of Climatology*, 28, 859-879.
- MYHRE, G., MYHRE, C., SAMSET, B. & STORELVMO, T. 2013. Aerosols and their Relation to Global Climate and Climate Sensitivity. *Nature Education Knowledge*, 4, 7.
- NAKIĆENOVIĆ, N. & SWART, R. (eds.) 2000. Special Report on Emissions Scenarios. A Special Report of Working Group III of the Intergovernmental Panel on Climate Change, Cambridge, United Kingdom and New York, NY, USA: Cambridge University Press.
- NEELIN, J., CHOU, C. & SU, H. 2003. Tropical drought regions in global warming and El Niño teleconnections. *Geophysical Research Letters*, 30.
- NEELIN, J. D. 2007. Moist dynamics of tropical convection zones in monsoons, teleconnections, and global warming. In: T. SCHNEIDER & A. SOBEL (eds.) *Moist dynamics of tropical convection zones in monsoons, teleconnections and global warming*. Princeton: Princeton University Press.
- NGUYEN, H., EVANS, A., LUCAS, C., SMITH, I. & TIMBAL, B. 2013. The Hadley Circulation in Reanalyses: Climatology, Variability, and Change. *Journal of Climate*, 26, 3357-3376.
- NGUYEN, K. & WALSH, K. 2001. Interannual, decadal, and transient greenhouse simulation of tropical cyclone-like vortices in a regional climate model of the South Pacific. *Journal of Climate*, 14, 3043-3054.
- NICHOLLS, N. 2004. The changing nature of Australian droughts. *Climatic Change*, 63, 323-336.
- NICHOLLS, N. 2010. Local and remote causes of the southern Australian autumn-winter rainfall decline, 1958-2007. *Climate Dynamics*, 34, 835-845.
- NUNEZ, M. & LI, Y. 2008. A cloud-based reconstruction of surface solar radiation trends for Australia. *Theoretical and Applied Climatology*, 91, 59-75.
- O'GORMAN, P. & SCHNEIDER, T. 2009. The physical basis for increases in precipitation extremes in simulations of 21st-century climate change. *Proceedings of the National Academy of Sciences of the United States of America*, 106, 14773-14777.
- ONOGI, K., TSUTSUI, J., KOIDE, H., SAKAMOTO, M., KOBAYASHI, S., HATSUSHIKA, H., MATSUMOTO, T., YAMAZAKI, N., KAMAHORI, H., TAKAHASHI, K., KADOKURA, S., WADA, K., KATO, K., OYAMA, R., OSE, T., MANNOJI, N. & TAIRA, R. 2007. The JRA-25 Reanalysis. *Journal of the Meteorological Society of Japan*. Ser. II, 86, (3), 369-432.
- ORLOWSKY, B. & SENEVIRATNE, S. I. 2013. Elusive drought: uncertainty in observed trends and short- and long-term CMIP5 projections. *Hydrology and Earth System Sciences*, 17, 1765-1781.
- ORR, J. C., FABRY, V. J., AUMONT, O., BOPP, L., DONEY, S. C., FEELY, R. A., GNANADESIKAN, A., GRUBER, N., ISHIDA, A. & JOOS, F. 2005. Anthropogenic ocean acidification over the twenty-first century and its impact on calcifying organisms. *Nature*, 437, 681-686.
- OTTO, F., MASSEY, N., VAN OLDENBORGH, G., JONES, R. & ALLEN, M. 2012. Reconciling two approaches to attribution of the 2010 Russian heat wave. *Geophysical Research Letters*, 39.
- PAETH, H. & MANNIG, B. 2013. On the added value of regional climate modeling in climate change assessment. *Climate Dynamics*, 41, 1057-1066.
- PAGE, C. M. & JONES, D. 2001. OzClim: The development of a climate scenario generator for Australia. In: ZERGER, A. & ARGENT, R. M. (eds.) *MODSIM 2001 International Congress on Modelling and Simulation*. Modelling and Simulation Society of Australia and New Zealand.
- PARKER, W. S. 2013. Ensemble modeling, uncertainty and robust predictions. *Wiley Interdisciplinary Reviews: Climate Change*, 4, 213-223.
- PATTIARATCHI, C. & ELIOT, M. 2008. Sea level variability in south-west Australia: from hours to decades. *Proceedings of the 31st ASCE International Conference on Coastal Engineering (Hamburg, Germany)*.
- PEARCE, A. F. & FENG, M. 2013. The rise and fall of the "marine heat wave" off Western Australia during the summer of 2010/2011. *Journal of Marine Systems*, 111, 139-156.
- PELTIER, W. R. 2004. GLOBAL GLACIAL ISOSTASY AND THE SURFACE OF THE ICE-AGE EARTH: The ICE-5G (VM2) Model and GRACE. *Annual Review of Earth and Planetary Sciences*, 32, 111-149.
- PEPLER, A., COUTTS-SMITH, A. & TIMBAL, B. 2014. The role of East Coast Lows on rainfall patterns and inter-annual variability across the East Coast of Australia. *International Journal of Climatology*, 34, 1011-1021.
- PEPLER, A. S. & RAKICH, C. S. 2010. Extreme inflow events and synoptic forcing in Sydney catchments. *IOP Conference Series: Earth and Environmental Science*, 2010. IOP Publishing, 012010.
- PERCIVAL, D. B. & MOFJELD, H. O. 1997. Analysis of subtidal coastal sea level fluctuations using wavelets. *Journal of the American Statistical Association*, 92, 868-880.
- PERKINS, S., ALEXANDER, L. & NAIRN, J. 2012. Increasing frequency, intensity and duration of observed global heatwaves and warm spells. *Geophysical Research Letters*, 39.
- PERKINS, S., PITMAN, A. & SISSON, S. 2009. Smaller projected increases in 20-year temperature returns over Australia in skill-selected climate models. *Geophysical Research Letters*, 36.
- PERKINS, S. E., PITMAN, A. J., HOLBROOK, N. J. & MCANENEY, J. 2007. Evaluation of the AR4 climate models' simulated daily maximum temperature, minimum temperature, and precipitation over Australia using probability density functions. *Journal of Climate*, 20, 4356-4376.

-20° -10° 0° 10° 20° 30° 40° 50°



- PETHERAM, C., RUSTOMJI, P. & VLEESHOUWER, J. 2009. Rainfall-runoff modelling across northern Australia. A report to the Australian Government from the CSIRO Northern Australia Sustainable Yields Project. CSIRO Water for a Healthy Country Flagship, Australia.
- PHILANDER, G. (ed.) 1990. *El Niño, La Niña, and the Southern Oscillation*, San Diego, CA: Academic Press.
- PITMAN, A. J., NARISMA, G. T., PIELKE, R. & HOLBROOK, N. 2004. Impact of land cover change on the climate of southwest Western Australia. *Journal of Geophysical Research: Atmospheres* (1984–2012), 109, 1-12.
- PITMAN, A. & PERKINS, S. 2008. Regional Projections of Future Seasonal and Annual Changes in Rainfall and Temperature over Australia Based on Skill-Selected AR4 Models. *Earth Interactions*, 12(12), 1-50.
- POLVANI, L., WAUGH, D., CORREA, G. & SON, S. 2011. Stratospheric Ozone Depletion: The Main Driver of Twentieth-Century Atmospheric Circulation Changes in the Southern Hemisphere. *Journal of Climate*, 24, 795-812.
- POOK, M. & GIBSON, T. 1999. Atmospheric blocking and storm tracks during SOP-1 of the FROST Project. *Australian Meteorological Magazine*, 51-60.
- POOK, M., RISBEY, J., MCINTOSH, P., UMMENHOFER, C., MARSHALL, A. & MEYERS, G. 2013. The Seasonal Cycle of Blocking and Associated Physical Mechanisms in the Australian Region and Relationship with Rainfall. *Monthly Weather Review*, 141, 4534-4553.
- POOK, M. J., RISBEY, J. S. & MCINTOSH, P. C. 2012. The synoptic climatology of cool-season rainfall in the Central Wheatbelt of Western Australia. *Monthly Weather Review*, 140, 28-43.
- POST, D., CHIEW, F., TENG, J., VAZE, J., MPELASOKA, F., SMITH, I., KATZFEY, J., MARSTON, F., MARVANEK, S. & KIRONO, D. 2009. Production of climate scenarios for Tasmania.: a report to the Australian Government from the CSIRO Tasmania Sustainable Yields Project. CSIRO Water for Healthy Country Flagship, Australia. 49.
- POST, D. A., CHIEW, F. H. S., TENG, J., WANG, B. & MARVANEK, S. 2012. Projected changes in climate and runoff for south-eastern Australia under 1 °C and 2 °C of global warming. A SEACI Phase 2 special report Australia: CSIRO.
- POTTER, N. J., CHIEW, F. H. S., FROST, A. J., SRIKANTHAN, R., MCMAHON, T. A., PEEL, M. C. & AUSTIN, J. M. 2008. Characterisation of recent rainfall and runoff in the Murray-Darling Basin. A report to the Australian Government from the CSIRO Murray-Darling Basin Sustainable Yields Project. CSIRO, Australia.
- POWER, S., CASEY, T., FOLLAND, C., COLMAN, A. & MEHTA, V. 1999. Inter-decadal modulation of the impact of ENSO on Australia. *Climate Dynamics*, 15, 319-324.
- POWER, S. & COLMAN, R. 2006. Multi-year predictability in a coupled general circulation model. *Climate Dynamics*, 26, 247-272.
- POWER, S., DELAGE, F., CHUNG, C., KOCIUBA, G. & KEAY, K. 2013. Robust twenty-first-century projections of El Niño and related precipitation variability. *Nature*, 502, 541-545.
- POWER, S., HAYLOCK, M., COLMAN, R. & WANG, X. 2006. The predictability of interdecadal changes in ENSO activity and ENSO teleconnections. *Journal of Climate*, 19, 4755-4771.
- PREVIDI, M. & LIEPERT, B. 2007. Annular modes and Hadley cell expansion under global warming. *Geophysical Research Letters*, 34.
- RAFTER, A. & ABBS, D. 2009. An analysis of future changes in extreme rainfall over Australian regions based on GCM simulations and Extreme Value Analysis. In: SANDERY, P. A., LEEUWENBURG, T., WANG, G. & HOLLIS, A. J. (eds.) *CAWCR Research Letters*, Issue 3. Melbourne: CSIRO.
- RAHMSTORF, S. & COUMOU, D. 2011. Increase of extreme events in a warming world. *Proceedings of the National Academy of Sciences of the United States of America*, 108, 17905-17909.
- RANDALL, D. A., WOOD, R. A., BONY, S., COLMAN, R., FICHEFET, T., FYFE, J., KATTSOV, J., PITMAN, A., SHUKLA, J., SRINIVASAN, J., STOUFFER, R. J., SUMI, A. & TAYLOR, K. E. 2007. *Climate Models and Their Evaluation*. In: *Climate Change 2007: The Physical Science Basis*. Contribution of Working Group I to the Fourth Assessment Report of the Intergovernmental Panel on Climate Change [Solomon, S., D. Qin, M. Manning, Z. Chen, M. Marquis, K.B. Averyt, M.Tignor and H.L. Miller (eds.)]. Cambridge University Press, Cambridge, United Kingdom and New York, NY, USA.
- RAPHAEL, M. & HOLLAND, M. 2006. Twentieth century simulation of the southern hemisphere climate in coupled models. Part 1: large scale circulation variability. *Climate Dynamics*, 26, 217-228.
- RAUPACH, M., BRIGGS, P., HAVERD, V., KING, E., PAGET, M. & TRUDINGER, C. 2009. Australian Water Availability Project (AWAP). Canberra, Australia.(www.csiro.au/awap): CSIRO Marine and Atmospheric Research, Component: Final Report for Phase 3. CAWCR Technical Report No. 013.
- RAUPACH, M., BRIGGS, P., HAVERD, V., KING, E., PAGET, M. & TRUDINGER, C. 2012. Australian Water Availability Project. Canberra, Australia: CSIRO Marine and Atmospheric Research. www.csiro.au/awap
- RAVEN, J., CALDEIRA, K., ELDERFIELD, H., HOEGH-GULDBERG, O., LISS, P., RIEBESELL, U., SHEPHERD, J., TURLEY, C. & WATSON, A. 2005. Ocean acidification due to increasing atmospheric carbon dioxide, The Royal Society.
- RAY, R. D. & DOUGLAS, B. C. 2011. Experiments in reconstructing twentieth-century sea levels. *Progress in Oceanography*, 91, 496-515.

- RAYNER, N. A., PARKER, D. E., HORTON, E. B., FOLLAND, C. K., ALEXANDER, L. V., ROWELL, D. P., KENT, E. C. & KAPLAN, A. 2003. Global analyses of sea surface temperature, sea ice, and night marine air temperature since the late nineteenth century. *Journal of Geophysical Research: Atmospheres*, 108, D1.
- REINECKER, M. M., SUAREZ, M. J., GELARO, R., TODLING, R., BACMEISTER, J., LIU, E., BOSILOVICH, M. G., SCHUBERT, S. D., TAKACS, L., KIM, G.-K., BLOOM, S., CHEN, J., COLLINS, D., CONATY, A., DA SILVA, A., GU, W., JOINER, J., KOSTER, R. D., LUCCHESI, R., MOLOD, A., OWENS, T., PAWSON, S., PEGION, P., REDDER, C. R., REICHLE, R., ROBERTSON, F. R., RUDDICK, A. G., SIENKIEWICZ, M. & WOOLLEN, J. 2011. MERRA: NASA's Modern-Era Retrospective Analysis for Research and Applications. *Journal of Climate*, 24, 3624–3648.
- RICKETTS, J. & PAGE, C. M. 2007. A web based version of OzClim for exploring climate change impacts and risks in the Australian region. In: OXLEY, L. & KULASIRI, D. (eds.) MODSIM 2007 International Congress on Modelling and Simulation. Modelling and Simulation Society of Australia and New Zealand.
- RIDGWAY, K. 2007. Long-term trend and decadal variability of the southward penetration of the East Australian Current. *Geophysical Research Letters*, 34 (13), L13613.
- RIDGWAY, K., DUNN, J. & WILKIN, J. 2002. Ocean interpolation by four-dimensional weighted least squares-application to the waters around Australasia. *Journal of Atmospheric and Oceanic Technology*, 19, 1357-1375.
- RISBEY, J., KAROLY, D., REYNOLDS, A. & BRAGANZA, K. 2003. Global warming signature in Australia's worst drought. 16, 6-11.
- RISBEY, J., MCINTOSH, P. & POOK, M. 2013a. Synoptic components of rainfall variability and trends in southeast Australia. *International Journal of Climatology*, 33, 2459-2472.
- RISBEY, J., POOK, M. & MCINTOSH, P. 2013b. Spatial trends in synoptic rainfall in southern Australia. *Geophysical Research Letters*, 40, 3781-3785.
- RISBEY, J., POOK, M., MCINTOSH, P., UMMENHOFER, C. & MEYERS, G. 2009a. Characteristics and variability of synoptic features associated with cool season rainfall in southeastern Australia. *International Journal of Climatology*, 29, 1595-1613.
- RISBEY, J., POOK, M., MCINTOSH, P., WHEELER, M. & HENDON, H. 2009b. On the Remote Drivers of Rainfall Variability in Australia. *Monthly Weather Review*, 137, 3233-3253.
- ROGELJ, J., MEINSHAUSEN, M. & KNUTTI, R. 2012. Global warming under old and new scenarios using IPCC climate sensitivity range estimates. *Nature Climate Change*, 2, 248-253.
- ROHLING, E. J., GRANT, K., BOLSHAW, M., ROBERTS, A. P., SIDDALL, M., HEMLEBEN, C. & KUCERA, M. 2009. Antarctic temperature and global sea level closely coupled over the past five glacial cycles. *Nature Geoscience*, 2, 500-504.
- ROPELEWSKI, C. F. & HALPERT, M. 1989. Precipitation patterns associated with the high index phase of the Southern Oscillation. *Journal of Climate*, 2, 268-284.
- RUDOLF, B., BECK, C., GRIESER, J. & SCHNEIDER, U. 2005. Global Precipitation Analysis Products. Global Precipitation Climatology Centre (GPCC), DWD, Internet publication, 1-8. www.gewex.org/PAN-GEWEX-MTG/Pan-GEWEX_GPCC-2006.pdf
- RUMMUKAINEN, M. 2010. State-of-the-art with regional climate models. *Wiley Interdisciplinary Reviews: Climate Change*, 1, 82-96.
- SAHA, S., MOORTHY, S., PAN, H.-L., WU, X., WANG, J., NADIGA, S., TRIPP, P., KISTLER, R., WOOLLEN, J., BEHRINGER, D., LIU, H., STOKES, D., GRUMBINE, R., GAYNO, G., WANG, J., HOU, Y.-T., CHUANG, H.-Y., JUANG, H.-M. H., SELA, J., IREDELL, M., TREADON, R., KLEIST, D., VAN DELST, P., KEYSER, D., DERBER, J., EK, M., MENG, J., WEI, H., YANG, R., LORD, S., VAN DEN DOOL, H., KUMAR, A., WANG, W., LONG, C., CHELLIAH, M., XUE, Y., HUANG, B., SCHEMM, J.-K., EBISUZAKI, W., LIN, R., XIE, P., CHEN, M., ZHOU, S., HIGGINS, W., ZOU, C.-Z., LIU, Q., CHEN, Y., HAN, Y., CUCURULL, L., REYNOLDS, R. W., RUTLEDGE, G. & GOLDBERG, M. 2010. The NCEP Climate Forecast System Reanalysis. *Bulletin of the American Meteorological Society*, 91, 1015–1057.
- SAJI, N., GOSWAMI, B., VINAYACHANDRAN, P. & YAMAGATA, T. 1999. A dipole mode in the tropical Indian Ocean. *Nature*, 401, 360-363.
- SAJI, N., XIE, S. & YAMAGATA, T. 2006. Tropical Indian Ocean variability in the IPCC twentieth-century climate simulations. *Journal of Climate*, 19, 4397-4417.
- SALLENGER, A. H., DORAN, K. S. & HOWD, P. A. 2012. Hotspot of accelerated sea-level rise on the Atlantic coast of North America. *Nature Climate Change*, 2, 884-888.
- SANTOSO, A., MCGREGOR, S., JIN, F.-F., CAI, W., ENGLAND, M. H., AN, S.-I., MCPHADEN, M. J. & GUILYARDI, E. 2013. Late-twentieth-century emergence of the El Niño propagation asymmetry and future projections. *Nature*, 504, 126-130.
- SEN GUPTA, A. & ENGLAND, M. H. 2006. Coupled Ocean–Atmosphere–Ice Response to Variations in the Southern Annular Mode. *Journal of Climate*, 19, 4457-4486.
- SCAIFE, A. A., COPSEY, D., KENDON, L., VIDALE, P.-L., MARTIN, G. M., MILTON, S., MOUFOUMA-OKIA, W., ROBERTS, M. J., PALMER, WALTERS, D. N. & WILLIAMS, K. 2011. Final Report of the CAPTIVATE model development project. Deliverable D3.2.7 (Internal Report), Met. Office Hadley Centre.
- SENEVIRATNE, S. I. 2012. CLIMATE SCIENCE Historical drought trends revisited. *Nature*, 491, 338-339.
- SEWPA. 2013. Australia's Ecoregions [Online]. Department of Sustainability, Environment, Water, Populations and Communities. Available: <http://www.environment.gov.au/parks/nrs/science/bioregion-framework/terrestrial-habitats.html>

- SHI, G., CAI, W., COWAN, T., RIBBE, J., ROTSTAYN, L. & DIX, M. 2008. Variability and trend of North West Australia rainfall: observations and coupled climate modeling. *Journal of Climate*, 21, 2938-2959.
- SILVERMAN, J., LAZAR, B., CAO, L., CALDEIRA, K. & EREZ, J. 2009. Coral reefs may start dissolving when atmospheric CO₂ doubles. *Geophysical Research Letters*, 36.
- SIMMONDS, I. & KEAY, K. 2000. Mean Southern Hemisphere extratropical cyclone behavior in the 40-year NCEP-NCAR reanalysis. *Journal of Climate*, 13, 873-885.
- SIMMONDS, I., KEAY, K. & BYE, J. 2012. Identification and Climatology of Southern Hemisphere Mobile Fronts in a Modern Reanalysis. *Journal of Climate*, 25, 1945-1962.
- SIMMONS, A., WILLET, K., JONES, P., THORNE, P. & DEE, D. 2010. Low-frequency variations in surface atmospheric humidity, temperature, and precipitation: Inferences from reanalyses and monthly gridded observational data sets. *Journal of Geophysical Research-Atmospheres*, 115.
- SLANGEN, A. B. A., KATSMAN, C. A., VAN DE WAL, R. S. W., VERMEERSEN, L. L. A. & RIVA, R. E. M. 2012. Towards regional projections of twenty-first century sea-level change based on IPCC SRES scenarios. *Climate Dynamics*, 38, 1191-1209.
- SMITH, I. & CHANDLER, E. 2010. Refining rainfall projections for the Murray Darling Basin of south-east Australia--the effect of sampling model results based on performance. *Climatic Change*, 102, 377-393.
- SMITH, R. L., TEBALDI, C., NYCHKA, D. & MEARN, L. O. 2009. Bayesian Modeling of Uncertainty in Ensembles of Climate Models. *Journal of the American Statistical Association*, 104, 97-116.
- SNAY, R., CLINE, M., DILLINGER, W., FOOTE, R., HILLA, S., KASS, W., RAY, J., ROHDE, J., SELLA, G. & SOLER, T. 2007. Using global positioning system-derived crustal velocities to estimate rates of absolute sea level change from North American tide gauge records. *Journal of Geophysical Research-Solid Earth*, 112.
- SODEN, B., WETHERALD, R., STENCHIKOV, G. & ROBOCK, A. 2002. Global cooling after the eruption of Mount Pinatubo: A test of climate feedback by water vapor. *Science*, 296, 727-730.
- SON, S., GERBER, E., PERLWITZ, J., POLVANI, L., GILLETT, N., SEO, K., EYRING, V., SHEPHERD, T., WAUGH, D., AKIYOSHI, H., AUSTIN, J., BAUMGAERTNER, A., BEKKI, S., BRAESICKE, P., BRUHL, C., BUTCHART, N., CHIPPERFIELD, M., CUGNET, D., DAMERIS, M., DHOMSE, S., FRITH, S., GARNY, H., GARCIA, R., HARDIMAN, S., JOCKEL, P., LAMARQUE, J., MANCINI, E., MARCHAND, M., MICHOU, M., NAKAMURA, T., MORGENSTERN, O., PITARI, G., PLUMMER, D., PYLE, J., ROZANOV, E., SCINOCCA, J., SHIBATA, K., SMALE, D., TEYSSERE, H., TIAN, W. & YAMASHITA, Y. 2010. Impact of stratospheric ozone on Southern Hemisphere circulation change: A multimodel assessment. *Journal of Geophysical Research-Atmospheres*, 115.
- SPERBER, K. & ANNAMALAI, H. 2008. Coupled model simulations of boreal summer intraseasonal (30-50 day) variability, Part 1: Systematic errors and caution on use of metrics. *Climate Dynamics*, 31, 345-372.
- SPERBER, K., ANNAMALAI, H., KANG, I., KITO, A., MOISE, A., TURNER, A., WANG, B. & ZHOU, T. 2013. The Asian summer monsoon: an intercomparison of CMIP5 vs. CMIP3 simulations of the late 20th century. *Climate Dynamics*, 41, 2711-2744.
- SPERBER, K. & KIM, D. 2012. Simplified metrics for the identification of the Madden-Julian oscillation in models. *Atmospheric Science Letters*, 13, 187-193.
- STANDARDS AUSTRALIA. 2009. ISO 31000:2009 Australian/New Zealand Standard. Sydney Australia. <http://sherq.org/31000.pdf>
- STERN, H., DE HOEDT, G. & ERNST, J. 2000. Objective classification of Australian climates. *Australian Meteorological Magazine*, 49, 87-96.
- STEYNOR, A., GAWITH, M. & STREET, R. 2012. Engaging users in the development and delivery of climate projections: the UKCIP experience of UKCP09. UKCIP, Oxford.
- STONE, D. A., ALLEN, M. R., STOTT, P. A., PALL, P., MIN, S. K., NOZAWA, T. & YUKIMOTO, S. 2009. The Detection and Attribution of Human Influence on Climate. *Annual Review of Environment and Resources*, 34, 1-16.
- STOTT, P., GILLETT, N., HEGERL, G., KAROLY, D., STONE, D., ZHANG, X. & ZWIERS, F. 2010. Detection and attribution of climate change: a regional perspective. *Wiley Interdisciplinary Reviews-Climate Change*, 1, 192-211.
- STOTT, P. A., STONE, D. A. & ALLEN, M. R. 2004. Human contribution to the European heatwave of 2003. *Nature*, 432, 610-614.
- STREET, R. B., STEYNOR, A., BOWYER, P. & HUMPHREY, K. 2009. Delivering and using the UK climate projections 2009. *Weather*, 64, 227-231.
- STURMAN, A. P. & TAPPER, N. J., 2006. *The weather and climate of Australia and New Zealand*, Oxford University Press Melbourne.
- SUPPIAH, R., HENNESSY, K., WHETTON, P. H., MCINNES, K., MACADAM, I., BATHOLS, J., RICKETTS, J. & PAGE, C. M. 2007. Australian climate change projections derived from simulations performed for the IPCC 4th Assessment Report. *Australian Meteorological Magazine*, 56, 131-152.
- SUTHERST, R., MAYWALD, G. & KRITICOS, D. 2007. CLIMEX Version 3: User's Guide. Hearne Scientific Software Pty Ltd.
- SZALAI, S. & SZINELL, C. 2000. Comparison of two drought indices for drought monitoring in Hungary – a case study. Dordrecht: Kluwer.
- TAYLOR, I. H., BURKE, E., MCCOLL, L., FALLOON, P. D., HARRIS, G. R. & MCNEALL, D. 2013. The impact of climate mitigation on projections of future drought. *Hydrology and Earth System Sciences*, 17, 2339-2358.

- TAYLOR, K. 2001. Summarizing multiple aspects of model performance in a single diagram. *Journal of Geophysical Research-Atmospheres*, 106, 7183-7192.
- TAYLOR, K. E., STOUFFER, R. J. & MEEHL, G. A. 2012. An overview of CMIP5 and the experiment design. *Bulletin of the American Meteorological Society*, 93, 485-498.
- TEBALDI, C., SMITH, R. L., NYCHKA, D. & MEARN, L. O. 2005. Quantifying uncertainty in projections of regional climate change: A Bayesian approach to the analysis of multimodel ensembles. *Journal of Climate*, 18, 1524-1540.
- TENG, J., CHEW, F., VAZE, J., MARVANEK, S. & KIRONO, D. 2012. Estimation of Climate Change Impact on Mean Annual Runoff across Continental Australia Using Budyko and Fu Equations and Hydrological Models. *Journal of Hydrometeorology*, 13, 1094-1106.
- THOMPSON, D. & SOLOMON, S. 2002. Interpretation of recent Southern Hemisphere climate change. *Science*, 296, 895-899.
- THOMPSON, D., SOLOMON, S., KUSHNER, P., ENGLAND, M., GRISE, K. & KAROLY, D. 2011. Signatures of the Antarctic ozone hole in Southern Hemisphere surface climate change. *Nature Geoscience*, 4, 741-749.
- THOMPSON, D. & WALLACE, J. 2000. Annular modes in the extratropical circulation. Part I: Month-to-month variability. *Journal of Climate*, 13, 1000-1016.
- TIMBAL, B. 2009. The continuing decline in South-East Australian rainfall – Update to May 2009. *CAWCR Research Letters*, 2, 4-11.
- TIMBAL, B. & ARBLASTER, J. M. 2006. Land cover change as an additional forcing to explain the rainfall decline in the south west of Australia. *Geophysical Research Letters*, 33, L07717.
- TIMBAL, B., ARBLASTER, J., BRAGANZA, K., FERNANDEZ, E., HENDON, H., MURPHY, B., RAUPACH, M., RAKICH, C., SMITH, I. & WHAN, K. 2010. Understanding the anthropogenic nature of the observed rainfall decline across South Eastern Australia, Centre for Australian Weather and Climate Research. Technical Report No. 026 www.cawcr.gov.au/publications/technicalreports/CTR_026.pdf
- TIMBAL, B. & DROSDOWSKY, W. 2013. The relationship between the decline of South Eastern Australia rainfall and the strengthening of the subtropical ridge. *International Journal of Climatology*, 33, 1021-1034.
- TIMBAL, B. & FAWCETT, R. 2013. A Historical Perspective on Southeastern Australian Rainfall since 1865 Using the Instrumental Record. *Journal of Climate*, 26, 1112-1129.
- TIMBAL, B., FERNANDEZ, E. & LI, Z. 2009. Generalization of a statistical downscaling model to provide local climate change projections for Australia. *Environmental Modelling & Software*, 24, 341-358.
- TIMBAL, B. & HENDON, H. 2011. The role of tropical modes of variability in recent rainfall deficits across the Murray-Darling Basin. *Water Resources Research*, 47 (12).
- TIMBAL, B. & MCAVANEY, B. J. 2001. An Analogue based method to downscale surface air temperature: Application for Australia. *Climate dynamics*, 17, 947-963.
- TIMBAL, B., WANG, Y., EVANS, A., CHAN, F., MARINOVA, D. & ANDERSSON, R. 2011. Downscaling climate change information: an essential ingredient to incorporate uncertainties into adaptation policies. 19th International Congress on Modelling and Simulation (Modsim2011), 115-126.
- TIPPETT, M., CAMARGO, S. & SOBEL, A. 2011. A Poisson Regression Index for Tropical Cyclone Genesis and the Role of Large-Scale Vorticity in Genesis. *Journal of Climate*, 24, 2335-2357.
- TORY, K., CHAND, S., DARE, R. & MCBRIDE, J. 2013a. An Assessment of a Model-, Grid-, and Basin-Independent Tropical Cyclone Detection Scheme in Selected CMIP3 Global Climate Models. *Journal of Climate*, 26, 5508-5522.
- TORY, K., CHAND, S., DARE, R. & MCBRIDE, J. 2013b. The Development and Assessment of a Model-, Grid-, and Basin-Independent Tropical Cyclone Detection Scheme. *Journal of Climate*, 26, 5493-5507.
- TORY, K., CHAND, S., MCBRIDE, J., YE, H. & DARE, R. 2013c. Projected Changes in Late-Twenty-First-Century Tropical Cyclone Frequency in 13 Coupled Climate Models from Phase 5 of the Coupled Model Intercomparison Project. *Journal of Climate*, 26, 9946-9959.
- TRENBERTH, K., STEPANIAK, D. & CARON, J. 2000. The global monsoon as seen through the divergent atmospheric circulation. *Journal of Climate*, 13, 3969-3993.
- TREWIN, B. 2002. Charts from the past—24 May, 1994. *Bull. Aust. Meteor. Ocean. Soc.*, 17, 74.
- TREWIN, B. 2010. Exposure, instrumentation, and observing practice effects on land temperature measurements. *Wiley Interdisciplinary Reviews-Climate Change*, 1, 490-506.
- TREWIN, B. 2013. A daily homogenized temperature data set for Australia. *International Journal of Climatology*, 33, 1510-1529.
- TREWIN, B. & VERMONT, H. 2010. Changes in the frequency of record temperatures in Australia, 1957-2009. *Australian Meteorological and Oceanographic Journal*, 60, 113-119.
- TREWIN, B. & SMALLEY, R. 2013. Changes in extreme temperatures in Australia, 1910 to 2011. In proceedings of the Australian Meteorological and Oceanographic Society Annual Conference, Melbourne, 2013. 11-13.
- TROCCOLI, A., MULLER, K., COPPIN, P., DAVY, R., RUSSELL, C. & HIRSCH, A. 2012. Long-Term Wind Speed Trends over Australia. *Journal of Climate*, 25, 170-183.
- TSIMPLIS, M., SPADA, G., MARCOS, M. & FLEMMING, N. 2011. Multi-decadal sea level trends and land movements in the Mediterranean Sea with estimates of factors perturbing tide gauge data and cumulative uncertainties. *Global and Planetary Change*, 76, 63-76.
- UMMENHOFER, C., ENGLAND, M., MCINTOSH, P., MEYERS, G., POOK, M., RISBEY, J., GUPTA, A. & TASCHETTO, A. 2009. What causes southeast Australia's worst droughts? *Geophysical Research Letters*, 36.

- UPPALA, S., KALLBERG, P., SIMMONS, A., ANDRAE, U., BECHTOLD, V., FIORINO, M., GIBSON, J., HASELER, J., HERNANDEZ, A., KELLY, G., LI, X., ONOGI, K., SAARINEN, S., SOKKA, N., ALLAN, R., ANDERSSON, E., ARPE, K., BALMASEDA, M., BELJAARS, A., VAN DE BERG, L., BIDLOT, J., BORMANN, N., CAIRES, S., CHEVALLIER, F., DETHOF, A., DRAGOSAVAC, M., FISHER, M., FUENTES, M., HAGEMANN, S., HOLM, E., HOSKINS, B., ISAKSEN, L., JANSSEN, P., JENNE, R., MCNALLY, A., MAHFOUF, J., MORCLETTE, J., RAYNER, N., SAUNDERS, R., SIMON, P., STERL, A., TRENBERTH, K., UNTCH, A., VASILJEVIC, D., VITERBO, P. & WOOLLEN, J. 2005. The ERA-40 re-analysis. *Quarterly Journal of the Royal Meteorological Society*, 131, 2961-3012.
- VAN HAREN, R., VAN OLDENBORGH, G., LENDERINK, G., COLLINS, M. & HAZELEGER, W. 2012. SST and circulation trend biases cause an underestimation of European precipitation trends. *Climate Dynamics*, 1-20.
- VAN OLDENBORGH, G. J., DRIJFHOUT, S., VAN ULDEN, A., HAARSMA, R., STERL, A., SEVERIJNS, C., HAZELEGER, W. & DIJKSTRA, H. 2009. Western Europe is warming much faster than expected. *Climate of the Past*, 5, 1-12.
- VAN OLDENBORGH, G. J., REYES, F. D., DRIJFHOUT, S. & HAWKINS, E. 2013. Reliability of regional climate model trends. *Environmental Research Letters*, 8, 014055.
- VAN VUUREN, D. P., EDMONDS, J., KAINUMA, M., RIAHI, K., THOMSON, A., HIBBARD, K., HURTT, G. C., KRAM, T., KREY, V. & LAMARQUE, J.-F. 2011. The representative concentration pathways: an overview. *Climatic Change*, 109, 5-31.
- VAUGHAN, C. & DESSAI, S. 2014. *Climate services for society: origins, institutional arrangements, and design elements for an evaluation framework*. Wiley Interdisciplinary Reviews: Climate Change, 5, (5), 587-603.
- VAUTARD, R., CATTIAUX, J., YIOU, P., THEPAUT, J. & CIAIS, P. 2010. Northern Hemisphere atmospheric stilling partly attributed to an increase in surface roughness. *Nature Geoscience*, 3, 756-761.
- VAZE, J. & TENG, J. 2011. Future climate and runoff projections across New South Wales, Australia: results and practical applications. *Hydrological Processes*, 25, 18-35.
- VAZE, J., TENG, J. & CHIEW, J. H. S. 2011. Assessment of GCM simulations of annual and seasonal rainfall and daily rainfall distribution across south-east Australia. *Hydrological Processes*, 25, 1486-1497.
- VERDON-KIDD, D. C. & KIEM, A. S. 2009. On the relationship between large-scale climate modes and regional synoptic patterns that drive Victorian rainfall. *Hydrology and Earth System Sciences*, 13, 467-479.
- WAHL, T., HAIGH, I. D., WOODWORTH, P. L., ALBRECHT, F., DILLINGH, D., JENSEN, J., NICHOLLS, R. J., WEISSE, R. & WOPPELMANN, G. 2013. Observed mean sea level changes around the North Sea coastline from 1800 to present. *Earth-Science Reviews*, 124, 51-67.
- WAHL, T., JENSEN, J., FRANK, T. & HAIGH, I. D. 2011. Improved estimates of mean sea level changes in the German Bight over the last 166 years. *Ocean Dynamics*, 61, 701-715.
- WALISER, D., JIN, K., KANG, I., STERN, W., SCHUBERT, S., WU, M., LAU, K., LEE, M., KRISHNAMURTHY, V., KITOH, A., MEEHL, G., GALIN, V., SATYAN, V., MANDKE, S., WU, G., LIU, Y. & PARK, C. 2003. AGCM simulations of intraseasonal variability associated with the Asian summer monsoon. *Climate Dynamics*, 21, 423-446.
- WALISER, D., SPERBER, K., HENDON, H., KIM, D., WHEELER, M., WEICKMANN, K., ZHANG, C., DONNER, L., GOTTSCHALCK, J., HIGGINS, W., KANG, I., LEGLER, D., MONCRIEFF, M., VITART, F., WANG, B., WANG, W., WOOLNOUGH, S., MALONEY, E., SCHUBERT, S., STERN, W. & OSCILLATION, C. M.-J. 2009. MJO Simulation Diagnostics. *Journal of Climate*, 22, 3006-3030.
- WANG, B. & DING, Q. 2008. Global monsoon: Dominant mode of annual variation in the tropics. *Dynamics of Atmospheres and Oceans*, 44, 165-183.
- WANG, C., PICAUT, J., WANG, C., XIE, S. & CARTON, J. 2004a. Understanding ENSO physics - A review. *Earth's Climate: the Ocean-Atmosphere Interaction*, 147, 21-48.
- WANG, G. & CAI, W. 2013. Climate-change impact on the 20th-century relationship between the Southern Annular Mode and global mean temperature. *Sci Rep*, 3, 2039.
- WANG, Y., LEUNG, L. R., MCGREGOR, J. L., LEE, D.-K., WANG, W.-C., DING, Y. & KIMURA, F. 2004b. Regional climate modeling: progress, challenges and prospects. *Journal of the Meteorological Society of Japan*, 82, 1599-1628.
- WATANABE, M., KUG, J., JIN, F., COLLINS, M., OHBA, M. & WITTENBERG, A. 2012. Uncertainty in the ENSO amplitude change from the past to the future. *Geophysical Research Letters*, 39.
- WATTERSON, I. 1996. Non-dimensional measures of climate model performance. *International Journal of Climatology*, 16, 379-391.
- WATTERSON, I. 2009. Components of precipitation and temperature anomalies and change associated with modes of the Southern Hemisphere. *International Journal of Climatology*, 29, 809-826.
- WATTERSON, I. 2010. Relationships between southeastern Australian rainfall and sea surface temperatures examined using a climate model. *Journal of Geophysical Research-Atmospheres*, 115.
- WATTERSON, I. 2012. Understanding and partitioning future climates for Australian regions from CMIP3 using ocean warming indices. *Climatic Change*, 111, 903-922.
- WATTERSON, I., BATHOLS, J. & HEADY, C. 2013a. What influences the skill of climate models over the continents? *Bulletin of the American Meteorological Society*, 95, 689-700.
- WATTERSON, I., HIRST, A. & ROTSTAYN, L. 2013b. A skill score based evaluation of simulated Australian climate. *Australian Meteorological and Oceanographic Journal*, 63, 181-190.

- WATTERSON, I., MCGREGOR, J. & NGUYEN, K. 2008. Changes in extreme temperatures of Australasian summer simulated by CCAM under global warming, and the roles of winds and land-sea contrasts. *Australian Meteorological Magazine*, 57, 195-212.
- WATTERSON, I. G. 2008. Calculation of probability density functions for temperature and precipitation change under global warming. *Journal of Geophysical Research*, 113, D12106.
- WATTERSON, I. G. & WHETTON, P. H. 2011. Distributions of decadal means of temperature and precipitation change under global warming. *Journal of Geophysical Research: Atmospheres* (1984–2012), 116.
- WATTERSON, I. G. & WHETTON, P. H. 2013. Probabilistic projections of regional temperature and precipitation extending from observed time series. *Climatic Change*, 1-15.
- WEBB, L., WHETTON, P. & BARLOW, E. W. R. 2008. Climate change and wine grape quality in Australia. *Climate Research*, 36, 99-111.
- WEBB, L. B., WHETTON, P. H., BHEND, J., DARBYSHIRE, R., BRIGGS, P. R. & BARLOW, E. W. R. 2012. Earlier wine-grape ripening driven by climatic warming and drying and management practices. *Nature Climate Change*, 2, 259-264.
- WEIGEL, A. P., KNUTTI, R., LINIGER, M. A. & APPENZELLER, C. 2010. Risks of Model Weighting in Multimodel Climate Projections. *Journal of Climate*, 23, 4175-4191.
- WELLER, E. & CAI, W. 2013a. Asymmetry in the IOD and ENSO Teleconnection in a CMIP5 Model Ensemble and Its Relevance to Regional Rainfall. *Journal of Climate*, 26, 5139-5149.
- WELLER, E. & CAI, W. 2013b. Realism of the Indian Ocean Dipole in CMIP5 Models: The Implications for Climate Projections. *Journal of Climate*, 26, 6649-6659.
- WENTZ, F., RICCIARDULLI, L., HILBURN, K. & MEARS, C. 2007. How much more rain will global warming bring? *Science*, 317, 233-235.
- WERNBERG, T., RUSSELL, B. D., THOMSEN, M. S., GURGEL, C. F. D., BRADSHAW, C. J. A., POLOCZANSKZ, E. S. & CONNELL, S. D. 2011. Seaweed Communities in Retreat from Ocean Warming. *Current Biology* 21, 1828–1832.
- WHAN, K., TIMBAL, B. & LINDESAY, J. 2014. Linear and nonlinear statistical analysis of the impact of subtropical ridge intensity and position on south-east Australian rainfall. *International Journal of Climatology*, 34, 326-342.
- WHEELER, M., HENDON, H., CLELAND, S., MEINKE, H. & DONALD, A. 2009. Impacts of the Madden-Julian Oscillation on Australian Rainfall and Circulation. *Journal of Climate*, 22, 1482-1498.
- WHETTON, P., HENNESSY, K., CLARKE, J., MCINNES, K. & KENT, D. 2012. Use of Representative Climate Futures in impact and adaptation assessment. *Climatic Change*, 115, 433-442.
- WHETTON, P. H., KAROLY, D., WATTERSON, I. G., WEBB, L., DROST, F., KIRONO, D. & MCINNES, K. 2013. Australia's Climate in a Four Degree World. In: CHRISTOFF, P. (ed.) *Four Degrees of Global Warming. Australia in a hot world*. London: Earthscan/Routledge.
- WHITE, N. J., HAIGH, I. D., CHURCH, J. A., KEON, T., WATSON, C. S., PRITCHARD, T., WATSON, P. J., BURGETTE, R. J., ELIOT, M., MCINNES, K. L., YOU, B., ZHANG, X. & TREGONING, P. 2014. Australian Sea Levels - Trends, regional variability and Influencing Factors. *Earth Science Reviews*, 136, 155-174.
- WILBY, R. L., TRONI, J., BIOT, Y., TEDD, L., HEWITSON, B. C., SMITH, D. M. & SUTTON, R. T. 2009. A review of climate risk information for adaptation and development planning. *International Journal of Climatology*, 29, 1193-1215.
- WILLETT, K. M., JONES, P. D., THORNE, P. W. & GILLETT, N. P. 2010. A comparison of large scale changes in surface humidity over land in observations and CMIP3 general circulation models. *Environmental Research Letters*, 5.
- WILLIAMS, R. J., BRADSTOCK, R. A., CARY, G. J., ENRIGHT, N., GILL, A., LIEDLOFF, A., LUCAS, C., WHELAN, R., ANDERSEN, A. & BOWMAN, D. 2009. Interactions between climate change, fire regimes and biodiversity in australia-a preliminary assessment. Report to the Department of Climate Change and Department of the Environment, Water, Heritage and Arts. Canberra.
- WILLOWS, R. I. & CONNELL, R. K. 2003. *Climate adaptation: Risk, uncertainty and decision-making*. UKCIP, Oxford: UKCIP Technical Report.
- WOODROFFE, C. D., MCGREGOR, H. V., LAMBECK, K., SMITHERS, S. G. & FINK, D. 2012. Mid-Pacific microatolls record sea-level stability over the past 5000 yr. *Geology*, 40, 951-954.
- WOODWORTH, P. L. 1999. High waters at Liverpool since 1768: the UK's longest sea level record. *Geophysical Research Letters*, 26, 1589-1592.
- WOODWORTH, P. L., TEFERLE, F. N., BINGLEY, R. M., SHENNAN, I. & WILLIAMS, S. D. P. 2009. Trends in UK mean sea level revisited. *Geophysical Journal International*, 176, 19-30.
- WU, L., CAI, W., ZHANG, L., NAKAMURA, H., TIMMERMANN, A., JOYCE, T., MCPHADEN, M. J., ALEXANDER, M., QIU, B. & VISBECK, M. 2012. Enhanced warming over the global subtropical western boundary currents. *Nature Climate Change*, 2, 161-166.
- XAVIER, P. 2012. Intraseasonal Convective Moistening in CMIP3 Models. *Journal of Climate*, 25, 2569-2577.
- XAVIER, P., DUVEL, J., BRACONNOT, P. & DOBLAS-REYES, F. 2010. An Evaluation Metric for Intraseasonal Variability and its Application to CMIP3 Twentieth-Century Simulations. *Journal of Climate*, 23, 3497-3508.
- XIE, P. & ARKIN, P. A. 1997. Global Precipitation: A 17-Year Monthly Analysis Based on Gauge Observations, Satellite Estimates, and Numerical Model Outputs. *Bulletin of the American Meteorological Society*, 78, 2539–2558.

- XU, T. & HUTCHINSON, M. 2011. ANUCLIM version 6.1 user guide. Canberra: The Australian National University Fenner School of Environment and Society.
- YAMAGATA, T., BEHERA, S., LUO, J., MASSON, S., JURY, M., RAO, S., WANG, C., XIE, S. & CARTON, J. 2004. Coupled ocean-atmosphere variability in the tropical Indian ocean. *Earth's Climate: the Ocean-Atmosphere Interaction*, 147, 189-211.
- YOUNG, I., ZIEGER, S. & BABANIN, A. 2011. Global Trends in Wind Speed and Wave Height. *Science*, 332, 451-455.
- ZARGAR, A., SADIQ, R., NASER, B. & KHAN, F. I. 2011. A review of drought indices. *Environmental Reviews*, 19, 333-349.
- ZHANG, L., POTTER, N., HICKEL, K., ZHANG, Y. & SHAO, Q. 2008. Water balance modeling over variable time scales based on the Budyko framework – Model development and testing. *Journal of Hydrology*, 360, 117-131.
- ZHANG, X. & CHURCH, J. A. 2012. Sea level trends, interannual and decadal variability in the Pacific Ocean. *Geophysical Research Letters*, 39 (21).
- ZHANG, X., CHURCH, J. A., PLATTEN, S. M. & MONSELESAN, D. 2013. Projection of subtropical gyre circulation and associated sea level changes in the Pacific based on CMIP3 climate models. *Climate Dynamics*, 43 131-144.
- ZHANG, X. B., ZWIERS, F. W., HEGERL, G. C., LAMBERT, F. H., GILLET, N. P., SOLOMON, S., STOTT, P. A. & NOZAWA, T. 2007. Detection of human influence on twentieth-century precipitation trends. *Nature*, 448, 461-U4.
- ZHENG, F., LI, J., CLARK, R. T. & NNAMCHI, H. C. 2013. Simulation and projection of the Southern Hemisphere annular mode in CMIP5 models. *Journal of Climate*, 26, 9860-9879.
- ZINKE, J., ROUNTREY, A., FENG, M., XIE, S.-P., DISSARD, D., RANKENBURG, K., LOUGH, J. & MCCULLOCH, M. 2014. Corals record long-term Leeuwin current variability including Ningaloo Niño/Niña since 1795. *Nature Communications*, 5, 3607.

NRM GLOSSARY OF TERMS

Adaptation	<p>The process of adjustment to actual or expected climate and its effects. Adaptation can be autonomous or planned.</p> <p><i>Incremental adaptation</i> Adaptation actions where the central aim is to maintain the essence and integrity of a system or process at a given scale.</p> <p><i>Transformational adaptation</i> Adaptation that changes the fundamental attributes of a system in response to climate and its effects.</p>
Aerosol	A suspension of very small solid or liquid particles in the air, residing in the atmosphere for at least several hours.
Aragonite saturation state	The saturation state of seawater with respect to aragonite (Ω) is the product of the concentrations of dissolved calcium and carbonate ions in seawater divided by their product at equilibrium: $([Ca^{2+}] \times [CO_3^{2-}]) / [CaCO_3] = \Omega$
Atmosphere	The gaseous envelope surrounding the Earth. The dry atmosphere consists almost entirely of nitrogen and oxygen, together with a number of trace gases (e.g. argon, helium) and greenhouse gases (e.g. carbon dioxide, methane, nitrous oxide). The atmosphere also contains aerosols and clouds.
Carbon dioxide	A naturally occurring gas, also a by-product of burning fossil fuels from fossil carbon deposits, such as oil, gas and coal, of burning biomass, of land use changes and of industrial processes (e.g. cement production). It is the principle anthropogenic greenhouse gas that affects the Earth's radiative balance.
Climate	The average weather experienced at a site or region over a period of many years, ranging from months to many thousands of years. The relevant measured quantities are most often surface variables such as temperature, rainfall and wind.
Climate change	A change in the state of the climate that can be identified (e.g. by statistical tests) by changes in the mean and/or variability of its properties, and that persists for an extended period of time, typically decades or longer.
Climate feedback	An interaction in which a perturbation in one climate quantity causes a change in a second, and that change ultimately leads to an additional (positive or negative) change in the first.
Climate projection	A climate projection is the simulated response of the climate system to a scenario of future emission or concentration of greenhouse gases and aerosols, generally derived using climate models. Climate projections are distinguished from climate predictions by their dependence on the emission/concentration/radiative forcing scenario used, which in turn is based on assumptions concerning, for example, future socioeconomic and technological developments that may or may not be realised.
Climate scenario	A plausible and often simplified representation of the future climate, based on an internally consistent set of climatological relationships that has been constructed for explicit use in investigating the potential consequences of anthropogenic climate change, often serving as input to impact models.
Climate sensitivity	The effective climate sensitivity (units; °C) is an estimate of the global mean surface temperature response to doubled carbon dioxide concentration that is evaluated from model output or observations for evolving non-equilibrium conditions.
Climate variability	Climate variability refers to variations in the mean state and other statistics (such as standard deviations, the occurrence of extremes, etc.) of the climate on all spatial and temporal scales beyond that of individual weather events. Variability may be due to natural internal processes within the climate system (internal variability), or to variations in natural or anthropogenic external forcing (external variability).
Cloud condensation nuclei	Airborne particles that serve as an initial site for the condensation of liquid water, which can lead to the formation of cloud droplets. A subset of aerosols that are of a particular size.



CMIP3 and CMIP5	Phases three and five of the Coupled Model Intercomparison Project (CMIP3 and CMIP5), which coordinated and archived climate model simulations based on shared model inputs by modelling groups from around the world. The CMIP3 multi-model dataset includes projections using SRES emission scenarios. The CMIP5 dataset includes projections using the Representative Concentration Pathways (RCPs).
Confidence	The validity of a finding based on the type, amount, quality, and consistency of evidence (e.g. mechanistic understanding, theory, data, models, expert judgment) and on the degree of agreement
Decadal variability	Fluctuations, or ups-and-downs of a climate feature or variable at the scale of approximately a decade (typically taken as longer than a few years such as ENSO, but shorter than the 20–30 years of the IPO)
Detection and attribution	Detection of change is defined as the process of demonstrating that climate or a system affected by climate has changed in some defined statistical sense, without providing a reason for that change. An identified change is detected in observations if its likelihood of occurrence by chance due to internal variability alone is determined to be small, for example, less than 10 per cent. Attribution is defined as the process of evaluating the relative contributions of multiple causal factors to a change or event with an assignment of statistical confidence.
Downscaling	Downscaling is a method that derives local to regional-scale information from larger-scale models or data analyses. Different methods exist: e.g. dynamical, statistical and empirical downscaling.
El Niño Southern Oscillation (ENSO)	A fluctuation in global scale tropical and subtropical surface pressure, wind, sea surface temperature, and rainfall, and an exchange of air between the south-east Pacific subtropical high and the Indonesian equatorial low. Often measured by the surface pressure anomaly difference between Tahiti and Darwin or the sea surface temperatures in the central and eastern equatorial Pacific. There are three phases: neutral, El Niño and La Niña. During an El Niño event the prevailing trade winds weaken, reducing upwelling and altering ocean currents such that the eastern tropical surface temperatures warm, further weakening the trade winds. The opposite occurs during a La Niña event.
Emissions scenario	A plausible representation of the future development of emissions of substances that are potentially radiatively active (e.g. greenhouse gases, aerosols) based on a coherent and internally consistent set of assumptions about driving forces (such as demographic and socioeconomic development, technological change) and their key relationships.
Extreme weather	An extreme weather event is an event that is rare at a particular place and time of year. Definitions of rare vary, but an extreme weather event would normally be as rare as or rarer than the 10th or 90th percentile of a probability density function estimated from observations.
Fire weather	Weather conditions conducive to triggering and sustaining wild fires, usually based on a set of indicators and combinations of indicators including temperature, soil moisture, humidity, and wind. Fire weather does not include the presence or absence of fuel load.
Global Climate Model or General Circulation Model (GCM)	A numerical representation of the climate system that is based on the physical, chemical and biological properties of its components, their interactions and feedback processes. The climate system can be represented by models of varying complexity and differ in such aspects as the spatial resolution (size of grid-cells), the extent to which physical, chemical, or biological processes are explicitly represented, or the level at which empirical parameterisations are involved.
Greenhouse gas	Greenhouse gases are those gaseous constituents of the atmosphere, both natural and anthropogenic, that absorb and emit radiation at specific wavelengths within the spectrum of terrestrial radiation emitted by the Earth's surface, the atmosphere itself, and by clouds. Water vapour (H ₂ O), carbon dioxide (CO ₂), nitrous oxide (N ₂ O), methane (CH ₄) and ozone (O ₃) are the primary greenhouse gases in the Earth's atmosphere.
Hadley cell/circulation	A direct, thermally driven circulation in the atmosphere consisting of poleward flow in the upper troposphere, descending air into the subtropical high-pressure cells, return flow as part of the trade winds near the surface, and with rising air near the equator in the so-called Inter-Tropical Convergence zone.

Indian Ocean Dipole (IOD)	Large-scale mode of interannual variability of sea surface temperature in the Indian Ocean. This pattern manifests through a zonal gradient of tropical sea surface temperature, which in its positive phase in September to November shows cooling off Sumatra and warming off Somalia in the west, combined with anomalous easterlies along the equator.
Inter-decadal Pacific oscillation	A fluctuation in the sea surface temperature (SST) and mean sea level pressure (MSLP) of both the north and south Pacific Ocean with a cycle of 15–30 years. Unlike ENSO, the IPO may not be a single physical ‘mode’ of variability, but be the result of a few processes with different origins. The IPO interacts with the ENSO to affect the climate variability over Australia. A related phenomena, the Pacific Decadal Oscillation (PDO), is also an oscillation of SST that primarily affects the northern Pacific
Jet stream	A narrow and fast-moving westerly air current that circles the globe near the top of the troposphere. The jet streams are related to the global Hadley circulation. In the southern hemisphere the two main jet streams are the polar jet that circles Antarctica at around 60 °S and 7–12 km above sea level, and the subtropical jet that passes through the mid-latitudes at around 30 °S and 10–16 km above sea level.
Madden Julian Oscillation (MJO)	The largest single component of tropical atmospheric intra-seasonal variability (periods from 30 to 90 days). The MJO propagates eastwards at around 5 m s ⁻¹ in the form of a large-scale coupling between atmospheric circulation and deep convection. As it progresses, it is associated with large regions of both enhanced and suppressed rainfall, mainly over the Indian and western Pacific Oceans.
Monsoon	A monsoon is a tropical and subtropical seasonal reversal in both the surface winds and associated rainfall, caused by differential heating between a continental-scale land mass and the adjacent ocean. Monsoon rains occur mainly over land in summer.
Percentile	A percentile is a value on a scale of one hundred that indicates the percentage of the data set values that is equal to, or below it. The percentile is often used to estimate the extremes of a distribution. For example, the 90th (or 10th) percentile may be used to refer to the threshold for the upper (or lower) extremes.
Radiative forcing	Radiative forcing is the change in the net, downward minus upward, radiative flux (expressed in W m ⁻²) at the tropopause or top of atmosphere due to a change in an external driver of climate change, such as a change in the concentration of carbon dioxide or the output of the Sun.
Representative Concentration Pathways (RCPs)	Scenarios that include time series of emissions and concentrations of the full suite of greenhouse gases and aerosols and chemically active gases, as well as land use/ cover. The word representative signifies that each RCP provides only one of many possible scenarios that would lead to the specific radiative forcing characteristics.
Return period	An estimate of the average time interval between occurrences of an event (e.g. flood or extreme rainfall) of a defined size or intensity.
Risk	The potential for consequences where something of value is at stake and where the outcome is uncertain. Risk is often represented as a probability of occurrence of hazardous events or trends multiplied by the consequences if these events occur.
Risk assessment	The qualitative and/or quantitative scientific estimation of risks.
Risk management	The plans, actions, or policies implemented to reduce the likelihood and/or consequences of risks or to respond to consequences.
Subtropical ridge (STR)	The subtropical ridge runs across a belt of high pressure that encircles the globe in the middle latitudes. It is part of the global circulation of the atmosphere. The position of the subtropical ridge plays an important part in the way the weather in Australia varies from season to season.
Southern Annular Mode (SAM)	The leading mode of variability of Southern Hemisphere geopotential height, which is associated with shifts in the latitude of the mid-latitude jet.



SAM index	The SAM Index, otherwise known as the Antarctic Oscillation Index (AOI) is a measure of the strength of SAM. The index is based on mean sea level pressure (MSLP) around the whole hemisphere at 40 °S compared to 65 °S. A positive index means a positive or high phase of the SAM, while a negative index means a negative or low SAM. This index shows a relationship to rainfall variability in some parts of Australia in some seasons.
SRES scenarios	SRES scenarios are emissions scenarios developed by Nakićenović and Swart (2000) and used, among others, as a basis for some of the climate projections shown in Chapters 9 to 11 of IPCC (2001) and Chapters 10 and 11 of IPCC (2007).
Uncertainty	A state of incomplete knowledge that can result from a lack of information or from disagreement about what is known or even knowable. It may have many types of sources, from imprecision in the data to ambiguously defined concepts or terminology, or uncertain projections of human behaviour. Uncertainty can therefore be represented by quantitative measures (e.g. a probability density function) or by qualitative statements (e.g. reflecting the judgment of a team of experts).
Walker circulation	An east-west circulation of the atmosphere above the tropical Pacific, with air rising above warmer ocean regions (normally in the west), and descending over the cooler ocean areas (normally in the east). Its strength fluctuates with that of the Southern Oscillation.

GLOSSARY REFERENCES

- BOM (Australian Bureau of Meteorology). www.bom.gov.au/watl/about-weather-and-climate/australian-climate-influences.shtml (cited August 2014)
- IPCC *Fourth Assessment Report*. 2007. www.ipcc.ch/pdf/glossary/ar4-wg1.pdf (cited August 2014)
- IPCC *Fifth Assessment Report*. 2013. http://ipcc-wg2.gov/oeAR5/images/uploads/WGIIAR5-Glossary_FGD.pdf (cited August 2014)
- MUCCI, A. 1983. The solubility of calcite and aragonite in seawater at various salinities, temperatures, and one atmosphere total pressure *American Journal of Science*, 283 (7), 780-799.
- NAKIĆENOVIĆ, N. & SWART, R. (eds.) 2000. *Special Report on Emissions Scenarios. A Special Report of Working Group III of the Intergovernmental Panel on Climate Change*, Cambridge, United Kingdom and New York, NY, USA: Cambridge University Press.
- STURMAN, A. P. & TAPPER, N. J., 2006. *The weather and climate of Australia and New Zealand*, Oxford University Press Melbourne.



MACDONNELL RANGES, NORTHERN TERRITORY, ISTOCK

-20° -10° 0° 10° 20° 30° 40° 50°



WWW.CLIMATECHANGEINAUSTRALIA.GOV.AU

-20° -10° 0° 10° 20° 30° 40° 50°